Platelet extracellular vesicles and the transfer of microRNA in atherosclerosis

Thesis submitted for the degree of
Doctor of Philosophy
at the University of Leicester

by

Ashley Robert Ambrose BSc, MSc
Department of Cardiovascular Sciences
University of Leicester

2016

Abstract

On activation, platelets release two types of extracellular vesicle (EV); procoagulant microvesicles and exosomes. Platelets contain abundant microRNAs which can be packaged into EV and released into the blood, making a significant contribution to circulating microRNA. We aimed to characterise the EV released from platelets, profile their microRNA content and then identify and observe the effects of the EV microRNA on targets in monocytes.

Washed platelets from healthy subjects were maximally stimulated with agonists specific for GPVI (CRP-XL), PAR1 (SFFLRN), PAR4 (AYGPKF), P2Y1/P2Y12 (ADP). Released EVs isolated by differential centrifugation were characterised by size (Nanosight), the exosome-specific markers CD63 & HSP70 (western blotting), and the procoagulant characteristics of microvesicles (Annexin-V binding and thrombin generation). RNA was isolated from EV populations, reverse transcribed, amplified, and the microRNA profiled on TaqMan microRNA microarrays. Targets for platelet-derived EV (pdEV) were then identified using a detailed bioinformatic approach, and the effect of the pdEV on the protein expression of these targets in monocytes was investigated.

Stimulation through GPVI was the most potent generator of pdEV and produced a mixed population of exosomes and microvesicles. Stimulation at the PAR and P2Y receptors resulted in predominantly exosome production. Degradation of ADP with apyrase, significantly reduced both microvesicles and exosome production following stimulation with all agonists. The pdEVs contained between 57-79 different miRNA with a core of 45 miRNA observed throughout.

From these 45 microRNA we identified 3592 predicted targets and 811 previously validated targets. Incorporation of platelet-monocyte interaction transcriptome datasets identified 34 targets in monocytes with strong evidence for regulation by pdEV microRNA. Addition of pdEV to whole blood revealed that they were preferentially targeted to monocytes and incubating them with primary monocytes and THP-1 cells demonstrated their uptake (flow cytometry and confocal microscopy) and the transfer of their microRNA cargo (RT-PCR). Critically, the delivery of microRNA via pdEV caused reduced protein expression of two selected targets; the haematopoietic transcription factor LMO2 and the scavenger receptor SCARB1 in culture.

Together, these results indicate that platelets produce EV in an agonist-dependent manner which is reliant on secondary ADP signalling. The microRNA profile released is consistent regardless of agonist and comprises a group of microRNA with many potential interactions in monocytes. The pdEV are preferentially taken up by monocytes in the blood where they are able to alter protein expression of targets such as SCARB1, which has potential implications in the development of atherosclerosis.

Acknowledgements

Table of Contents

Table of tables

Table of figures

Publications and presentations arising from this thesis

Published abstracts

ASHLEY R AMBROSE, MUHAMMED IMRAN ASLAM, J HOWARD PRINGLE, ALISON H GOODALL. 2013. Profiling the microRNA content of platelets, platelet-derived exosomes and plasma. UK Platelet Meeting; September 2013. *(Poster presentation)*

ASHLEY R. AMBROSE, MUHAMMED I. ASLAM, J. H. PRINGLE AND ALISON H. GOODALL. 2014. Profiling the microRNA content of platelets, platelet derived exosomes and plasma. 2014. Abstracts from the Third International Meeting of ISEV 2014 Rotterdam, The Netherlands, April 30(th) - May 3(rd), 2014. J Extracell Vesicles, 3, 24214. *Abstract O8C-335 (Oral presentation)*

AMBROSE, A. R., KRISHNAN, U., HAMBY, S. E., SAMANI, N. J. & GOODALL, A. H. 2014. Investigating the Potential Effects of Platelet-Derived Exosomal microRNA on Monocyte Gene Expression. Atherosclerosis, 237, E4-E4. *(Poster presentation at the British Atherosclerosis society, autumn meeting 2014)*

ASHLEY R AMBROSE, J H PRINGLE, ALISON H GOODALL. 2015. Platelets release extracellular vesicles in an agonist dependent manner but release a consistent profile of microRNA. Special Issue: Abstracts of the XXV Congress of the International Society on Thrombosis and Haemostasis, June 20-25, 2015 Abstracts. J Thromb Haemost, 13. *Abstract AS041 (Oral presentation)*

ASHLEY R AMBROSE, J H PRINGLE, ALISON H GOODALL. 2016. Platelet-derived extracellular vesicles act as an intercellular communication mechanism with monocytes. Abstracts of papers presented at the 2015 UK Platelet Meeting held at the University of Leicester, 15-16 September 2015. Platelets, 27, 2-25. *Abstract P36 (Poster presentation)*

ASHLEY R AMBROSE, J H PRINGLE, ALISON H GOODALL. Platelet-derived extracellular vesicles act as an intercellular communication mechanism with monocytes. M5 Flow Cytometry Meeting; December 15th 2015. *Abstract 4 (Poster presentation)*

Manuscripts in preparation

AMBROSE AR, PRINGLE J. H, GOODALL A. H. *Profiling the characteristics and microRNA contents of extracellular vesicles released from platelets by different agonists.*

AMBROSE A. R, PRINGLE J. H, GOODALL A. H. *Platelet-derived extracellular vesicles act as an intercellular communication mechanism with monocytes.*

Abbreviations

Abbreviation	Description
ABC	ATP binding cassette
ACD	Acid citrate dextrose
ADAM9	ADAM Metallopeptidase Domain 9
ADP	Adenosine di-phosphate
ANOVA	Analysis of variance
APS	Ammonium persulphate
ARNTL	Aryl Hydrocarbon Receptor Nuclear Translocator–Like
ASA	Acetylsalicylic acid
ATP	Adenosine tri-phosphate
BCL2	B–Cell CLL/Lymphoma 2
BP	Biological process
BSA	Bovine serum albumin
CAD	Coronary artery disease
CBFB	Core–Binding Factor, Beta Subunit
CC	Cellular component
CCND1	Cyclin D1
CCNE1	Cyclin E1
CD	Cluster of differentiation
CDC37L1	Cell Division Cycle 37–Like 1
CDKN1A	Cyclin–Dependent Kinase Inhibitor 1A
CERP	Cholesterol efflux regulatory protein
COX	Cyclooxygenase
CPDB	Consensus pathway database
CRP-XL	Collagen related peptide cross linked
CT	Cycle threshold
CTI	Corn trypsin inhibitor
CVD	Cardiovascular disease
DAG	Diacylglycerol

DAPI	4',6-Diamidino-2-Phenylindole
DC	Detergent compatible
DCAF12	DDB1 and CUL4 Associated Factor 12
DMSO	Dimethyl sulphoxide
DNA	Deoxyribose nucleic acid
dNTP	Deoxynucleotide triphosphate
dTTP	Deoxythymidine triphosphate
E2F1	E2F Transcription Factor 1
E2F5	E2F Transcription Factor 5
EDTA	Ethylenediaminetetraacetic acid
EIF2S2	Eukaryotic Translation Initiation Factor 2 Subunit Beta
ELISA	Enzyme-linked immunosorbant assay
EPB41L3	Erythrocyte Membrane Protein Band 4.1–Like 3
ESCRT	Endosomal sorting complex required for transport
ESR1	Estrogen Receptor 1
ETP	Endogenous thrombin potential
EV	Extracellular vesicles
FBS	Foetal bovine serum
FBXW7	F–Box and WD Repeat Domain Containing 7
FC	Fold change
Fc	Fragment crystallisable
FDR	False discovery rate
FITC	Fluorescein isothiocyanate
FS	Formyl saline
FSc	Forward scatter
GO	Gene ontology
GP	Glycoprotein
GPCR	G-protein coupled receptor
HBS	HEPES buffered saline pH7.4
HBS.Ca	HEPES buffered saline with Calcium
HBS.pH6	HEPES buffered saline pH6

HDL	High density lipoprotein
HDL-C	High-density lipoprotein cholesterol
HHEX	Haematopoietically Expressed Homeobox
HRP	Horseradish peroxidase
HSP	Heat Shock Protein
HSP90B1	Heat Shock Protein 90kDa Beta Member 1
JAM-C	Junction adhesion molecule C
ICAM-1	Intercellular Adhesion Molecule 1
Ig	Immunoglobulin
IL-1β	Interleukin-1 beta
IP$_3$	Inositol triphosphate
ISEV	International Society on Extracellular Vesicles
ITAM	Immune tyrosine-based activation motif
kDa	Kilodalton
KIF5A	Kinesin Family Member 5A
LDL	Low-density lipoprotein
LFA-1	Lymphocyte function-associated antigen 1
LMO2	LIM Domain Only 2
MAC-1	Macrophage-1 antigen
M-CSF	Macrophage-colony stimulating factor
MFI	Median fluorescence intensity
MI	Myocardial infarction
MPL	Myeloproliferative leukaemia protein
mRNA	messenger RNA
MVB	Multivesicular body
MW	Molecular weight
MYLIP	Myosin regulatory light chain interacting protein
NAGK	N-Acetyl glucosamine Kinase
NKG2D	Natural killer cell receptor 2D
NTA	Nano-particle Tracking Analysis
oxLDL	Oxidised low-density lipoprotein

PAGE	Polyacrylamide gel electrophoresis
PANTHER	Protein ANnotation THrough Evolutionary Relationship
PAR	Protease activated receptor
PBMC	Peripheral blood mononuclear cell
PBS	Phosphate buffered saline
PCR	Polymerase chain reaction
pdEV	Platelet-derived extracellular vesicles
PF4	Platelet factor 4
PFA	Paraformaldehyde
PGI_2	Prostacyclin I_2
PIP_2	Phosphatidylinositol 4,5-bisphosphate
PLC	Phospholipase C
PLSCR4	Phospholipid Scramblase 4
PMA	Phorbol 12-Myristate 13-Acetate
PPP	Platelet poor plasma
PriMo	Primary human monocyte
PROM1	Prominin 1
PRP	Platelet rich plasma
PS	Phosphatidylserine
PSGL-1	P-selectin glycoprotein ligand 1
PTEN	Phosphatase and Tensin Homolog
PTH	Parathyroid Hormone
PTHLH	Parathyroid Hormone-like hormone
PVDF	Polyvinylidene difluoride
RAC1	Ras–Related C3 Botulinum Toxin Substrate 1
RBL2	Retinoblastoma–Like 2
RE	Relative expression
REEP3	Receptor Accessory Protein 3
RHOB	Ras Homolog Family Member B
RISC	RNA-induced silencing complex
RNA	Ribonucleic acid

RT	Room temperature
RT-PCR	Real time polymerase chain reaction
RTr	Reverse transcription
SCARB1	Scavenger Receptor Class B Member 1
SD	Standard deviation
SDS	Sodium dodecylsulphate
SEM	Standard error of the mean
SSc	Side scatter
TBS	Tris-buffered-saline
TEMED	N,N,N',N'-Tetramethylethylenediamine
TF	Tissue factor
TFPI	Tissue factor pathway inhibitor
TG	Thrombin generation
TPA	Tissue plasminogen activator
TRAP	Thrombin receptor activating peptide
ttpeak	Time to peak
UPA	Urokinase plasminogen activator
USP3	Ubiquitin Specific Peptidase 3
UTR	Untranslated region
UV	Ultraviolet
VCAM-1	Vascular cell adhesion molecule 1
VEGFA	Vascular Endothelial Growth Factor A
VitaminD3	1α,25-Dihydroxyvitamin-D3
vs	Versus
vWf	von Willebrand factor
WGA	Wheatgerm agglutinin
ZFPM2	Zinc Finger Protein FOG Family Member 2
ZNF367	Zinc Finger Protein 367
+ve	Positive
-ve	Negative

Chapter 1

Introduction

1 Introduction

1.1 Cardiovascular Disease

Cardiovascular Disease (CVD) is the single largest cause of mortality worldwide and recent data indicates that it is responsible for 30% of all deaths. Whilst the overall pattern of disease affecting the world has shifted over the last 20 years the threat to health posed by CVD remains constant (Lozano et al., 2013). Due to its prevalence in all countries, regardless of their industrial and economic status, high rates of CVD is a trend that is predicted to continue (Lopez et al., 2006, Mathers and Loncar, 2006, Deaton et al., 2011). It has been well established that CVD is heavily influenced by issues such as poor diet and a lack of exercise but despite their modifiable nature the global mortality and morbidity of CVD has not decreased (Kelly et al., 2012, Roger et al., 2012). The lack of CVD reduction through the modification of risk factors means that research into the disease mechanisms, potential therapies and diagnostic tools is necessary to identify those at risk and reduce the burden of CVD on global health and finances (Deaton et al., 2011).

CVD is a broad class of conditions involving disease of the heart such as heart failure and myocardial infarction (MI; heart attacks) and those affecting the peripheral circulation, e.g. stroke and deep vein thrombosis. A pathology underlying many of these diseases is atherosclerosis, a chronic condition which causes narrowed and hardened arteries that can potentially trigger more severe acute events (Hansson, 2005).

1.1.1 Atherosclerosis

Atherosclerosis is the formation of fatty plaques in artery walls that reduce the size of the vessel lumen and stiffen the vasculature, due to loss of elasticity. Atherosclerosis progresses with age and is thought to be present in all adults, it takes decades of continual development before there is any clinical manifestation (Ross, 1999). The development of this condition is outlined in Figure 1.1 which demonstrates progression from fatty streaks (A) to advanced lesions (E). The extent and rate of development of an individual's atherosclerotic burden can be influenced by environmental and genetic risk factors. Smoking, consumption of alcohol and a poor diet, in tandem with a sedentary lifestyle, can lead to increased circulating cholesterol, hypertension, diabetes and obesity which all increase the incidence of atherosclerosis (Howard et al., 1998, Kadoglou et al., 2008a, Kadoglou et al., 2008b, Creager et al., 2003, Mokdad et al., 2001). Alongside lifestyle factors, inherited conditions such as hypercholesterolemia, where circulating low-density lipoproteins (LDL) is raised lead to increased atherosclerotic progression (Goldstein and Brown, 1985, Tousoulis et al., 2003).

The fatty streaks begin with an accumulation of LDL within the endothelium of the vasculature, possibly initiated through endothelial damage, the LDL is then oxidised (oxLDL) (Figure 1.1B). This triggers the expression of receptors such as vascular cell adhesion molecule 1 (VCAM-1) and P-selectin on the luminal side of the vessel endothelium and release of factors, such as Macrophage Colony Stimulating Factor (M-CSF) within the plaque or vessel wall which leads to the recruitment and infiltration of monocytes (Figure 1.1G) (Moore and Tabas, 2011, Gebuhrer et al., 1995, Ley et al., 2011). P-selectin is a cell adhesion molecule found in endothelial cells and platelets, it is stored in granules which are translocated to the membrane, leading to surface expression following activation through inflammatory cytokines or agonists such as thrombin. Platelets are also attracted to these sites of endothelial damage and act to facilitate monocyte accumulation through P-selectin to P-selectin glycoprotein ligand 1 (PSGL-1) interactions making them an important factor in plaque development (Kuckleburg et al., 2011, Furman et al., 1998, Huo et al., 2003, Ley et al., 2011, Nofer et al., 2010).

Once monocytes are present within the plaque they differentiate into macrophages in response to M-CSF and phagocytose the oxidized-LDL through scavenger receptors. The oxLDL is hydrolysed to form cholesterol which the macrophages either exocytose or retain as lipid droplets within cytoplasmic vesicles (Brown et al., 1980). As the macrophages become laden with cholesterol they become larger and their morphology alters leading to them being described as foam cells (Figure 1.1C/G-ii) (Maxfield and Tabas, 2005). Eventually the foam cells become overloaded with cholesterol and combined with their pro-inflammatory environment they undergo apoptosis which further increases the inflammatory status of the fatty plaque (Tabas, 2010, Tabas et al., 2010).

The combination of apoptotic cells, cholesterol deposition and inflammatory signals lead to the proliferation of smooth muscle cells in the media layer of arteries, and eventually the permeation of these into the plaque region. The development of a necrotic core follows, and unless smooth muscle cell proliferation is prevented through nitric oxide signalling from the endothelium resulting in the clearance of apoptotic cells then the plaque will continue to develop (Palmer et al., 1987, Furchgott and Zawadzki, 1980). At this stage the plaque is still stable and in most cases will have no clinical presentation, although large stable plaques can present as angina pectoris.
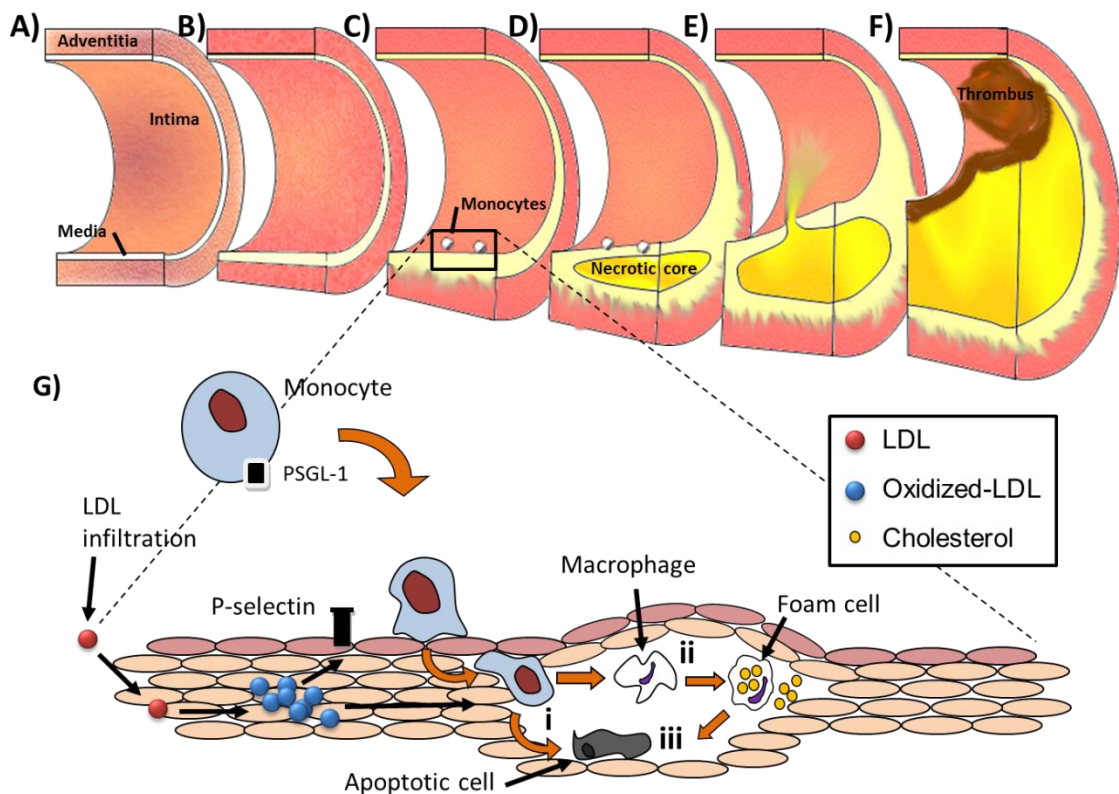
Figure 1.1 – The development of atherosclerosis A) shows the elements of a healthy artery wall under physiological conditions, B) demonstates the intial phase of atherosclerosis whereby LDL accumulates in the vessel wall and is oxidised to oxLDL. C) Monocytes are attracted to the area of endothelial damage and there is further accumaltion of LDL/oxLDL. D) Further monocyte accumulation, which differentiate to macrophages and phagocytose the LDL to form foam cells. There is also apoptosis and cholesterol deposition contributing to the formation of a necrotic core. E) Plaque rupture and F) thrombus formation in response to plaque rupture, causing vessel occlusion and tissue ischaemia. G) The involvement of monocytes; LDL infiltrates the damaged endothelium, is hydrolysed to oxLDL leading to endothelium expression of P-selectin which attracts monocytes and these move into the vessel wall where they become macrophages and then foam cells (ii) through the ingestion of cholesterol. Based on work by (Libby, 2001).

Atherosclerotic plaques such as these most frequently develop at artery bifurcations or other areas of non-laminar flow which reduces nitric oxide levels in the endothelium making endothelial cells more prone to activation (Zand et al., 1999, Asakura and Karino, 1990, Liao, 2013, Gimbrone et al., 1997). The development of advanced lesions within the coronary arteries, termed coronary artery disease (CAD), triggers reduced blood flow, starving the myocardium of oxygen and essential nutrients. As this becomes more severe it presents as chest pain, termed angina pectoris. However in some situations the first indication of CAD will be a MI where a coronary artery becomes completely occluded triggering myocardial ischaemia. Total occlusion is an acute event that is initiated by plaque rupture, which occurs when plaques become unstable, or the cap of the plaque is eroded, and the contents of the plaque come into direct contact with the blood, leading to the development of a thrombus which can completely block the artery (Virmani et al., 1999).

1.2 Haemostasis

The blood is essential for the transport of nutrients to, and waste products away from the organs and tissues of the body and it has crucial roles in the immune response, homeostasis and haemostasis (Alberts et al., 2008). Blood is a complex mix of cells, plasma, extracellular vesicles (EVs), lipoproteins, proteins, lipids and small molecules such as glucose (Basu and Kulkarni, 2014). Each of these has a specific function that is dependent on effective communication between all components of the blood and vasculature. This communication is reliant upon a diverse network of signals, and dysfunction of the network has the potential to cause disease (Chesney et al., 1997, Kozek-Langenecker et al., 2003).

The maintenance of the blood in a fluid state within the vasculature is termed haemostasis and involves equilibrating three key factors that if unbalanced result in thrombosis. The three factors make up Virchow's triad and are defined as; blood flow stasis, injury to the vascular endothelium and the ease of blood clotting (Chung and Lip, 2003). Divergence from the conserved equilibrium can be triggered by interrupted or slowed blood flow, damaged endothelial cells as a result of altered shear stress or hypertension, and hypercoagulability as seen following trauma, or in conditions such as cancer or inherited defects in specific elements of the coagulation cascade. Maintenance of haemostasis involves a complex network of factors in the circulation that include platelets, the vascular endothelium, microvesicles and coagulation factors (Rasche, 2001). There are many events that can lead to deviation from haemostasis, for example endothelial injury triggers clot formation to prevent blood leaving the vessel.

The process of forming a clot results in the blood transitioning from a liquid to a solid, gel-like state through a controlled, localised response. Injured endothelial cells expose the blood to constituents of the underlying extracellular matrix such as von Willebrand factor (vWf) and collagen. An interaction between the exposed vWf and the glycoprotein (GP) Ib/V/IX complex on platelets tethers platelets to the damaged endothelium, but this is a transient interaction which results in the platelets rolling. If the level of endothelial damage and therefore exposed vWf is high enough then the platelet rolling will be slow allowing for the formation of stronger attachments (van Gils et al., 2009). Stable attachment is then achieved through two receptors; GPVI and GPIa-IIa, which bind to the exposed collagen. The interaction though GPVI propagates calcium signalling, triggering platelet activation and granule secretion which releases secondary mediators such as adenosine diphosphate (ADP) into the local environment.

These secondary mediators feed back onto the platelets and cause platelet shape change and membrane protein transformation including activation of integrins such as the GPIaIIa and

5

GPIIb-IIIa complexes. The GPIIb-IIIa complex promotes platelet recruitment and clot stabilisation through binding to fibrinogen (Versteeg et al., 2013, Vine, 2009, Roberts et al., 2004). Further clot growth and stabilisation occurs through platelet recruitment of monocytes via specific surface receptor interactions; critically the interaction of P-selectin with PSGL-1. In parallel the coagulation cascade triggers the cleavage by Factor-Xa, of prothrombin to thrombin, which converts fibrinogen to fibrin, an insoluble protein that is cross-linked by Factor-XIIIa and in doing so stabilises the clot.

In conjunction with intercellular communication and negative feedback loops clots are able to successfully form appropriately sized and stable haemostatic plugs that prevent blood leaving the vessel but do not cause complete occlusion (Davie, 1995). This is a multi-modal process and involves inhibitory factors such as tissue factor pathway inhibitor (TFPI), Protein-C and antithrombin that inhibit coagulation and limit thrombus growth, as well as fibrinolytic factors such as plasminogen, which when converted to plasmin can break down the fibrin clot. Protein-C is activated through the binding of Protein-C and thrombin to the thrombomodulin receptor on the surface of endothelial cells, activated Protein-C then degrades Factor-Va and Factor-VIIIa, thereby inhibiting the coagulation cascade (Dahlback and Villoutreix, 2005). Antithrombin is a constitutively active serine protease inhibitor (serpin) found in the plasma that binds to, and blocks the active sites of the serine proteases; FIXa, FXa, FXIa, and FXIIa. The affinity of antithrombin for these factors is significantly enhanced by the presence of heparin sulfates or clinical administration of heparin (Blajchman, 1994). In addition, as the clot grows over intact, healthy endothelium it encounters PGI_2 released from endothelial cells. This triggers cAMP production in platelets, which inhibits calcium flux and therefore reduces activation (Stitham et al., 2011). Alongside the mechanisms acting to reduce platelet activation, fibrinolysis also occurs, preventing excessive clot growth. Plasminogen is a circulating enzyme that binds to fibrin in the clot and is converted to plasmin by Tissue Plasminogen Activator (TPA) and urokinase (UPA), which are slowly released from damaged endothelium. Plasmin then acts to lyse the thrombus through cleavage of the fibrin mesh, thereby removing the clot from the healing endothelium (Chapin and Hajjar, 2015).

In response to atypical pathologies such as atherosclerotic plaque rupture, clot formation is not as well controlled and can become overwhelmed by the release of large amounts of prothrombotic material such as collagen and tissue factor (TF)+ve microvesicles. This prevents normal regulation of the haemostatic processes and can lead to total vessel occlusion, resulting in acute events such as MI or stroke (Jackson, 2011). As platelets are the central player in thrombosis, patients who survive the acute events of strokes and MI are treated with anti-

platelet drugs to prevent reoccurrences. These therapies include the widely used cyclooxygenase (COX) inhibitor, aspirin (acetylsalicylic acid (ASA)) (Campbell et al., 2007), ADP receptor antagonists such as clopidogrel, prasugrel and ticagrelor (Wijeyeratne and Heptinstall, 2011) and risk factor controllers such as statins (e.g. atorvastatin) which lower cholesterol (Stancu and Sima, 2001) thereby reducing plaque growth. However these treatments are ordinarily used to slow atherosclerotic progress or following acute events to prevent secondary occurrences; research into the mechanisms driving the disease, including platelet-monocyte crosstalk is required to allow intervention before acute events.

1.3 Platelets

1.3.1 Structure, formation and function

Anucleate platelets have a circular, biconvex morphology, a diameter between 2-3μm and under physiological conditions humans have ~250 million/mL of blood. Platelets are released into the circulation following budding from megakaryocytes in a process known as thrombopoiesis that occurs in the bone marrow. Platelets are produced when mature megakaryocytes form pseudopodal processes, called pro-platelet elongations, in a microtubule driven process (Michelson, 2007). These elongations project into the vasculature of the bone marrow sinusoids and twisting of the proplatelets microtubules under the shear stress in the vessel causes individual pre-platelets to break off and then mature into platelets in the circulation (Thon and Italiano, 2010, Thon et al., 2010). Each megakaryocyte fragments into ~8000 platelets, which circulate for ~10 days before being phagocytosed in the spleen or liver (Kaplan and Saba, 1978).

Platelet formation is regulated by the circulating levels of thrombopoietin, a growth factor that stimulates megakaryocytes via its specific receptor, the myeloproliferative leukaemia protein (MPL). Circulating levels of thrombopoietin is regulated by platelets which also express MPL; platelets bind thrombopoietin and degrade it, therefore when platelet concentrations are low there is increased circulating thrombopoietin resulting in increased stimulation of thrombopoiesis. Recent evidence suggests that thrombopoiesis may also be controlled by microRNA expression, for example miR-150-5p promotes megakaryocyte differentiation and platelet production (Barroga et al., 2008).

As mentioned previously, platelets are central to the process of thrombosis and haemostasis but they also have many other biologically significant roles (Jacoby et al., 2001). Platelets localise to sites of inflammation and infection, and through the release of the many chemokines and cytokines they contain, and through their interactions with leukocytes they mediate the

inflammatory response (Smyth et al., 2009, Semple et al., 2011, Gawaz et al., 2005). Activated platelets also contribute to angiogenesis in normal vessels and tumours, and to atherosclerosis through interactions with leukocytes (Egan et al., 2011, Sabrkhany et al., 2011, Battinelli et al., 2011). This suggests that platelets have the potential to modify a variety of disease pathologies and so understanding their role in intercellular communication and diseases such as atherosclerosis and cancer is crucial to the development of new therapeutic targets and improving clinical outcomes (Semple et al., 2011, Jackson and Schoenwaelder, 2003).

1.3.2 Platelet activation

Many platelet functions require activation and this can be triggered by a number of different stimuli, resulting in dramatic shape change from a plate-like morphology to a sphere with a multitude of pseudopodal extensions, followed by aggregation and degranulation. Clot formation and the platelet activation involved in this process incorporates a number of signalling cascades that act through membrane receptors. Platelets express a wide variety of receptors on their surface that fall largely into two categories (Figure 1.2). Firstly, receptors that respond to agonists; predominantly G-protein coupled receptors (GPCRs) and immunoreceptor tyrosine-based activation motif (ITAM) receptors, and secondly, adhesion receptors that are mainly integrins. These receptors all have roles within the platelet and act, to various degrees, through a variety of intercellular signalling pathways.
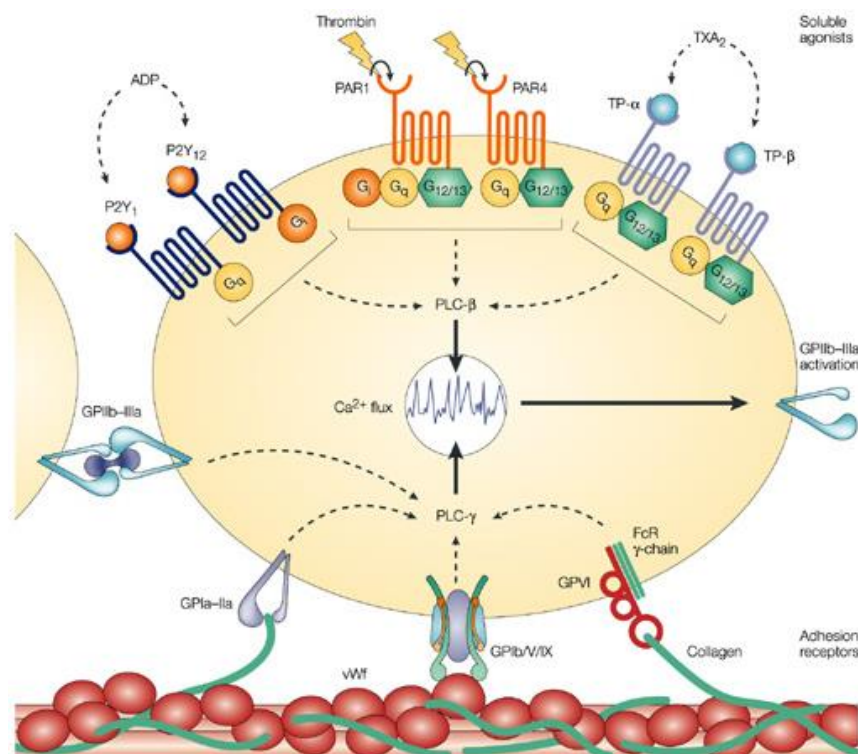
Figure 1.2 – Adhesion and agonist receptors on the platelet surface A schematic of a platelet showing the main platelet receptors, their agonists and the phospholipase C pathways that they signal through. Figure adapted from (Jackson and Schoenwaelder, 2003).

1.3.2.1   Pathways of activation

A key point in these agonist evoked pathways is signalling through phospholipase C (PLC), which initiates calcium signalling, leading to platelet activation and functional effects, such as shape change or granule secretion. PLC catalyses the reaction that transforms Phosphatidylinositol 4,5-bisphosphate (PIP_2) to Inositol 1,4,5-trisphosphate (IP_3) and Diacylglycerol (DAG) and this triggers the release of calcium from intracellular stores (Szumilo and Rahden-Staron, 2008, Williams, 1999). There are two variants of PLC in platelets, PLC-γ and PLC-β, each of which functions downstream of a distinct set of receptors (Figure 1.2).

1.3.2.1.1   PLC-γ

PLC-γ is found downstream of many of the GP receptors that are associated with clot formation through binding, adhesion and stabilisation of a clot and it's structure (Jackson and Schoenwaelder, 2003). The initial interaction occurs through GPVI and GPIb/V/IX which induce the activation of integrins such as GPIa-IIa and GPIIb-IIIa, resulting in the formation of a firm platelet clot. GPVI is a platelet specific member of the immunoglobulin superfamily of type 1 transmembrane glycoproteins and it forms complexes with the dimeric, ITAM-containg fragment crystallisable (Fc) receptor γ-chain. GPVI is the primary activation receptor for collagen on platelets and is required for adhesion to collagen (Nieswandt et al., 2001b, Nieswandt and Watson, 2003).

The GPVI receptor recognises the glycine-proline-hydroxyproline sequence present on triple helical collagens, which are shared by a cross-linked collagen related peptide (CRP-XL) and convulxin, a toxin in snake venom (Asselin et al., 1997, Morton et al., 1995, Jandrot-Perrus et al., 1997, Atkinson et al., 2001). Binding of any of these results in the cross-linking of adjacent GPVI receptors, which triggers tyrosine phosphorylation by Src kinases within the ITAM (Asselin et al., 1999). Subsequently, signalling through Src and Syk proteins leads to the activation of PLC-γ2 which cleaves PIP_2 to IP_3 and DAG causing the release of intracellular calcium through the calcium channel ORAI1 (Feske et al., 2006, Williams, 1999, Szumilo and Rahden-Staron, 2008). Activation of GPVI with the specific agonists CRP-XL or convulxin leads to rapid aggregation and degranulation of platelets in an ADP- and thromboxaneA$_2$-independent response. However activation following binding of collagen is slower and requires the release and feedback of ADP and thromboxaneA$_2$ to achieve a full response (Quinton et al., 2002, Atkinson et al., 2001, Nieswandt et al., 2001a).

The GPIb/V/IX complex is a four subunit glycoprotein comprised of GPIbα, GPIbβ, GPIX and GPV in a 1:2:1:1 ratio. GPIbα binds to vWf although the complex also has binding sites for thrombin,

macrophage-1 antigen (MAC-1; $\alpha_m\beta_2$) and P-selectin. Its interaction with vWf is important for the initiation of platelet adhesion. This is a transient interaction, which causes the rolling of platelets until stable adhesion through other platelet glycoproteins is achieved (Marchese et al., 1999, Nieswandt and Watson, 2003). Recent evidence suggests that there is a mechanosensing domain in the GPIbα receptor which unfolds when GPIbα is bound to vWf in a high shear stress environment and this leads to changes in GPIbβ and GPIX triggering platelet signalling, however the role of this complex in the initiation and propagation of platelet activation is still under debate (Zhang et al., 2015b).

The integrin GPIa-IIa ($\alpha_2\beta_1$) is also a collagen receptor on platelets that binds to monomeric type1 collagen and is important for adhesion. The strength of this interaction is dependent on activation of the integrin via secondary signals through other pathways such as GPVI, ADP and thromboxaneA$_2$ (Moroi et al., 2000). The downstream signalling from GPIa-IIa through PLC-γ is important for platelet spreading and thrombus stabilisation (Suzuki-Inoue et al., 2001, Inoue et al., 2003).

GPIIb-IIIa ($\alpha_{IIb}\beta_3$) is an integrin complex which acts as a receptor for fibrinogen and vWf, and leads to firm adhesion of platelets to fibrinogen resulting in clot stabilisation and growth (Savage et al., 1996). The GPIIb-IIIa complex is one of the most abundant platelet receptors but under normal conditions it has low binding affinity for its ligands vWf and fibrinogen. However, when platelets are activated the inside-out signalling triggers a conformational change that significantly increases the receptors binding capacity for vWf and fibrinogen leading to fibrinogen-mediated platelet activation (Shattil, 2006, Shattil, 1999, French and Seligsohn, 2000).

1.3.2.1.2 PLC-β

PLC-β transduces signals from GPCRs and is critical in the recruitment of further platelets to the clot, platelet shape change, platelet secretion and aggregation. The GPCRs are reactive to soluble mediators that are released by platelets into the local environment of a clot following GPVI activation (Offermanns, 2006).

ADP is released from platelet dense granules or cells of the damaged vasculature. It acts on the P2Y1 and P2Y12 purinoceptors that are coupled to G_q and G_i G-proteins respectively. These G-proteins function to activate PLC-β signalling resulting in sustained platelet activation and procoagulant activity. In addition, platelet response to low levels of thrombin, collagen and thromboxane are reliant on secondary ADP signalling (Murugappa and Kunapuli, 2006, Gachet, 2006, Gachet et al., 2006). ADP is known to have different functions via the P2Y1 and P2Y12

receptors; stimulation at P2Y1 triggers the principal but weak and reversible activation, which is sustained by subsequent stimulation at P2Y12 receptors, but P2Y12 activation cannot occur without P2Y1 priming (Gachet, 2008). In addition, there are data that suggests that these receptors may have separate roles in EV production, procoagulant activity and Rac activation (Soulet et al., 2005, Leon et al., 2003, Kahner et al., 2008).

Thrombin is a major platelet activator, which acts through the protease activated receptors (PAR) 1 and 4. It is formed through activation of the coagulation cascade by the cleavage of prothrombin by Factor-Xa; a process that is amplified by the tenase and prothrombinase complexes that form on cell surfaces, including those of activated platelets and microvesicles (Heemskerk et al., 2002). Thrombin activity at PAR receptors functions through multiple G-proteins including G_q/G_{12}/G_{13} and G_I leading to platelet activation and degranulation. Low doses of thrombin have been shown to act at PAR1 alone and in humans, high concentrations can also signal through PAR4. There are specific peptides that target PAR1 (Ser-Phe-Leu-Leu-Arg-Asn-NH_2) and PAR4 (Ala-Tyr-Pro-Gly-Lys-Phe-NH_2) that can be used as receptor-specific agonists (Kahn et al., 1998, Offermanns et al., 1994).

The third major group of platelet GPCRs are the TP receptors for thromboxane, which is a short-lived agonist synthesised from arachidonic acid by COX-1. Activation of the TP receptors leads to platelet activation via G_q and $G_{12/13}$ G-proteins, triggering platelet activation through the PLC-β pathway (Heemskerk et al., 2002). Inhibition of thromboxane activity leads to prolonged bleeding times and unstable thrombi in mice (Thomas et al., 1998). As well as ADP, thrombin and thromboxane there are several other platelet agonists that act at GPCRs stimulating or potentiating activation through the PLC-β pathway, these include epinephrine and serotonin which are weak agonists and require secondary mediators to truly activate platelets (Hjemdahl et al., 1994, King et al., 2009, Li et al., 1997).

1.3.3 Platelet-releasate

As listed above, there are a number of different stimuli that trigger platelet activation resulting in dramatic shape change, degranulation, increased procoagulant activity and aggregation. A slice through a platelet 'at rest' is shown in Figure 1.3, it contains a large number of vesicles and secretable factors that are released following activation. Platelets have been shown to directly secrete in excess of 300 molecules following activation from intracellular storage granules and as EV and their cargo (Coppinger et al., 2004, Pienimaeki-Roemer et al., 2014).
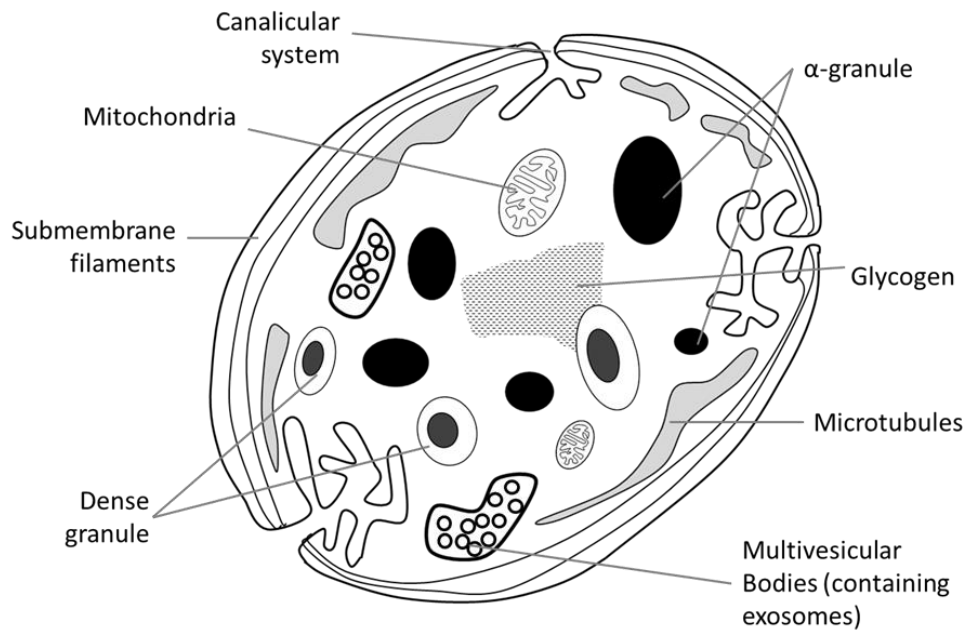
Figure 1.3 – Platelet structure *A simplistic cut-through of a platelet depicting its structure and the presence of internal granules and organelles.*

There are three types of intracellular storage granules found in platelets; α-granules, dense granules and lysosomes, which release their contents directly into the extracellular environment. The α-granules are unique to platelets, although similar to the Weibel Palade bodies of endothelial cells. They contain the largest population of releasable molecules and include factors involved in haemostasis (e.g. vWf and Factor-V), angiogenesis (e.g. Vascular endothelial growth factor (VEGF)), anti-angiogenesis (e.g. angiostatin), growth factors, proteases, cytokines and necrotic factors (Coppinger et al., 2004, Coppinger et al., 2007, Gawaz et al., 2005). The dense granules, also known as γ-granules, are unique to platelets in mammals but are similar to acidocalsisomes found in bacteria and unicellular eukaryotes (Ruiz et al., 2004). Dense granules contain smaller secretable molecules such as calcium, histamine, serotonin, polyphosphate, adenosine-triphosphate (ATP) and ADP. Their main roles are in cell signalling and haemostasis (King et al., 2009). Lysosomes are structurally similar to α-granules and are predominantly responsible for the secretion of digestive enzymes (Rendu and Brohard-Bohn, 2001).

1.4 Extracellular vesicles

In addition to releasing their granule contents platelets release several types of membranous EV; specifically microvesicles, and exosomes. EVs are released by most cell types into bodily fluids such as the blood, saliva, urine and cerebrospinal fluid (Zlotogorski-Hurvitz et al., 2015, Ashcroft et al., 2012, Oosthuyzen et al., 2013, Quinn et al., 2015). Platelet-derived EV (pdEV) were first mentioned in the literature in 1946 (Chargaff and West, 1946) but it took until 1999

for both microvesicles and exosomes to be characterised as being released from platelets (Heijnen et al., 1999). Research into EVs has expanded exponentially over the last 2 decades due to the recognition of their roles in intercellular communication, and their potential to act as readily accessible biomarkers of a diverse array of diseases (Yanez-Mo et al., 2015).

Despite the attention the field has received there are still fundamental questions over how the EV subtypes are defined and in isolating separate EV populations, which has led to difficulties in determining specific markers or functions (van der Pol et al., 2016). Many of the problems have been caused by EV isolation techniques that attempt to, but are ultimately unsuccessful in isolating discrete EV subtypes, such as ultracentrifugation (Taylor et al., 2011, Taylor and Shah, 2015, Tauro et al., 2012). Such studies then attribute their findings to a single EV subtype despite the EV population being heterogeneous. Notwithstanding the confusion there are some generally accepted characteristics of microvesicles and exosomes, shown in Figure 1.4.

Microvesicles are larger EV, ranging between ~100-1000nm although microvesicles larger than 400nm are rarely found in the blood (Mathivanan et al., 2010, Gyorgy et al., 2011b). The main cellular sources of microvesicles in the circulation are platelets, megakaryocytes, erythrocytes and leukocytes, particularly monocytes, but almost all cells can release them (Arraud et al., 2014, Berckmans et al., 2001, Ashcroft et al., 2012, Flaumenhaft et al., 2009). Ordinarily they are released following cellular activation, however low constitutive release is also observed (Cauwenberghs et al., 2006).

Microvesicles are formed through the activity of the lipid transporter enzymes; Aminophospholipid Translocase P type ATPase, ATP-Binding Cassette (ABC) transporters and Transmembrane protein 16F that were originally identified as flippase, floppase and scrambalase, respectively. The flippase enzymes target the external phospholipids (phosphatidylcholine/sphingomyelin) for internalisation, whilst the floppases target internal phospholipids (phosphatidylserine (PS)/phosphatidylethanolamine) for externalisation in an ATP dependent event. Scramblases promote the switching of the phospholipids and do this in a calcium-dependent manner (Aye et al., 2009). In addition, increased calcium activates phosphatases such as calpain which degrade the cytoskeletal proteins e.g. actin (Piccin et al., 2007, Morel et al., 2011). Taken together these changes result in membrane budding/blebbing, as shown in Figure 1.4 (Hugel et al., 2005, Pegtel, 2014).

Microvesicles

- 100-1000nm
- Negatively charged phospholipid exposure, predominantly Phosphatidylserine (PS)
- Procoagulant
- Bud directly from the plasma membrane
- Carry markers of their cell-of-origin
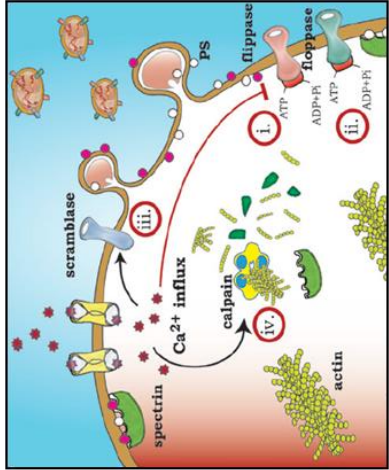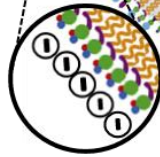
Exosomes

- ~40-100nm
- Membrane rich in cholesterol
- Form in multivesicular bodies
- Contain proteins and mainly microRNA
- Markers include tetraspanins (e.g. CD63 & CD81), HSP70, Alix, TSG101 etc
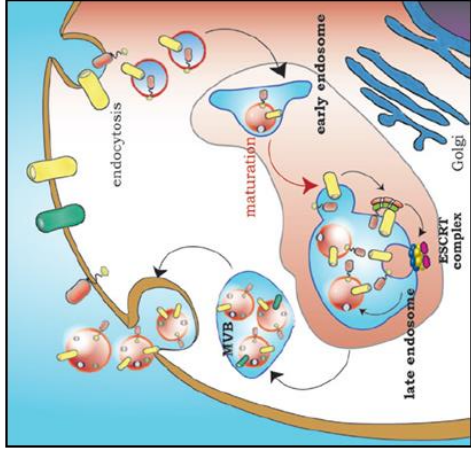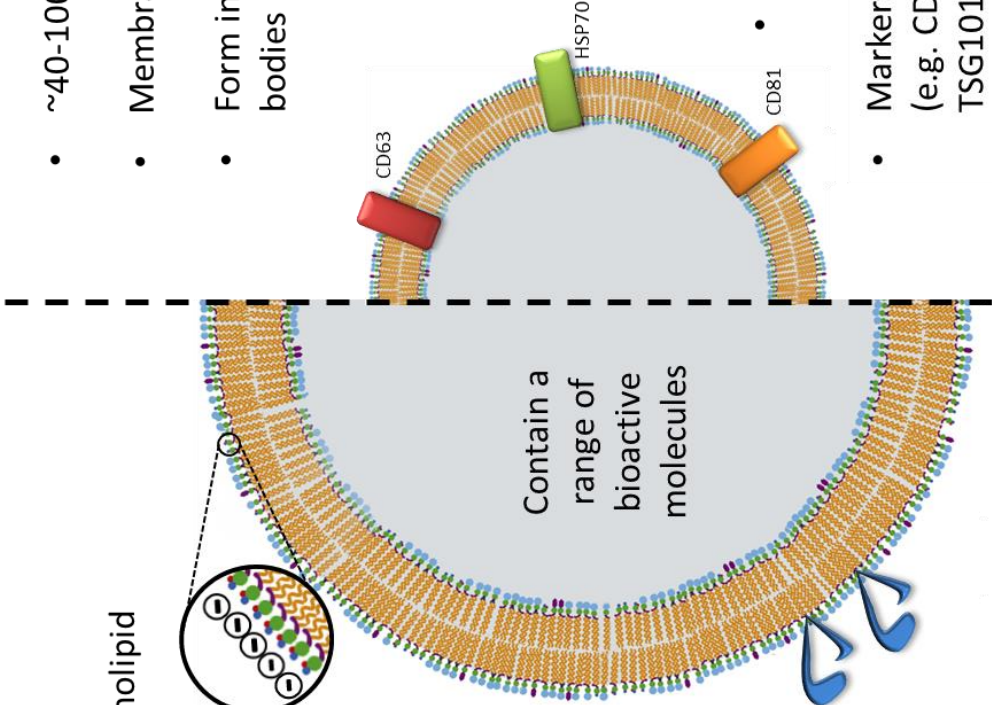
Contain a range of bioactive molecules

CD63

HSP70

CD81

endocytosis

maturation

early endosome

Golgi

ESCRT complex

MVB

late endosome

PS

flippase

floppase

ATP

ADP+Pi

ATP

ADP+Pi

i.

ii.

scramblase

iii.

Ca²⁺ influx

calpain

iv.

spectrin

actin

Figure 1.4 – Characteristics of extracellular vesicles Attributes used to distinguish microvesicles and exosomes including inset figures on their biogenesis adapted from (Pegtel, 2014).

The overall structure of microvesicles is a phospholipid bilayer vesicle with a high level of negatively-charged phospholipid, predominantly PS, on the outer leaflet. This provides one of the major functional characteristics of microvesicles, the support of blood coagulation. Platelet microvesicles are highly pro-coagulant and have been implicated in disease with evidence suggesting that they may play a role in tumour metastasis and angiogenesis (Hugel et al., 2005, Zhang and Yang, 2012). The outer membrane is also comprised of antigens characteristic of platelets e.g. CD61. Microvesicles have also been shown to contain over 500 different proteins, (Janowska-Wieczorek et al., 2005, Smalley et al., 2008) including those involved in coagulation (e.g. fibrinogen), transport (e.g. VAMP8) and intracellular signalling (e.g. PKC, SRC) (Garcia et al., 2005, Jin et al., 2005). This combination of contents makes microvesicles extremely effective intercellular signallers.

Exosomes are smaller than microvesicles, ~40-100nm and have also been heavily investigated. The understanding of roles for exosomes began with their identification as vesicles removing unwanted proteins from reticulocytes in 1987 (Johnstone et al., 1987). Shortly after their discovery it was observed that B-lymphocytes released vesicles into the body that were antigen presenting, thereby demonstrating an immunological role for exosomes (Raposo et al., 1996). Exosomes are released from cells when multi-vesicular bodies (MVBs) fuse with the plasma membrane (Keller et al., 2006, Thery et al., 2009). This is illustrated in Figure 1.4 and occurs either constitutively, or as a result of stimulation, from a variety of cells such as macrophages, platelets and endothelial cells (Denzer et al., 2000, Bhatnagar et al., 2007, Saunderson et al., 2008).

Exosomes form within MVBs through inward budding of the MVBs membrane, a process that is mediated by the Endosomal Sorting Complex Required for Transport (ESCRT) and Rab-GTPases (Ludwig and Giebel, 2012, Vlassov et al., 2012, Pegtel, 2014). Some MVBs are delivered to the lysosomes for degradation whilst others are recycled back to the plasma membrane where they release exosomes. The mechanisms that govern MVBs fate are poorly understood but an abundance of the sphingolipid, ceramide, within the MVB's membrane is thought to lead to exosome budding into the MVB. This is due to endosomal micro-domain fusion and directs the MVB to the cell membrane rather than lysosomes (Trajkovic et al., 2008).

The molecular composition of released exosomes is determined by their cellular origin as this influences the membrane composition and vesicle contents. Unlike microvesicles the exosomal membrane does not fully represent the membrane of their cell of origin and due to their intracellular creation exosomes have a distinct membrane signature, expressing tetraspanins at

significantly greater levels than normal membranes (Stoorvogel et al., 2002, Conde-Vancells et al., 2008). Tetraspanins are a family of transmembrane proteins which localise to microdomains where they stabilise and modulate the function of other transmembrane proteins. Through this function they have been shown to be critical in cellular adhesion and fusion with demonstrable roles in egg-spermatozoa fusion and viral entry (Thali, 2009, Rubinstein et al., 2006a, Peng et al., 2011, Li et al., 2014). These known actions, coupled with their enrichment on exosomes, have been investigated to demonstrate their roles in exosome targeting, uptake, cargo recruitment and biogenesis (Rana et al., 2012, Hemler, 2005, Morelli et al., 2004).

Proteomic analysis of medulloblastoma-derived exosomes only identified a limited proteome of ~150 proteins (Epple et al., 2012). However they do contain RNA, with exosomes being particularly abundant in microRNA from their cell of origin (Valadi et al., 2007, Diehl et al., 2012, Kosaka et al., 2013a). Recent evidence suggests that exosomes are the most concentrated source of microRNA in the circulation, which would explain the observed stability of microRNA in the blood and provide these EVs with a mechanism to significantly influence target cells (Gallo et al., 2012). Exosomes contain the necessary machinery, such as the Dicer and Argonaute 2 complexes, to process and facilitate the activity of their RNA content, suggesting that exosomes are an integral part of the communication and regulation systems of the entire body (Landry et al., 2009, Jaiswal et al., 2012).

As well as the physiological roles of EVs there are also pathological roles. Many researchers have attributed these to specific EV subtypes but as mentioned previously experimental limitations mean that these findings can only really be attributed to EV as a whole. For example exosomes released from tumours can transport molecules to suppress the immune system, such as NK Cell Receptor D (NKG2D) ligands which reduce the toxicity of natural killer cells, thereby enhancing tumour survival (Ashiru et al., 2010). However in this study cellular debris was removed with a 10,000g centrifugation followed by pelleting of exosomes at 100,000g; a process that would not remove microvesicles and that would also co-isolate extra protein complexes and lipoproteins.

Whilst EVs have been shown to be secreted from almost all cells of the body, it is platelets that are their most significant source in the blood. Up to 50% of EVs in the circulation of healthy individuals originate from platelets and the number of exosomes that can be released from a platelet is also exceptionally high suggesting an important role for EVs derived from platelets (Heijnen et al., 1999, Berckmans et al., 2001). Exosomes can fuse with target cells and shed their contents, potentially through a tetraspanin driven mechanism, thereby directly affecting the gene expression of that cell (Montecalvo et al., 2012, Risitano et al., 2012).

1.5 microRNA

microRNAs are non-coding RNAs comprised of ~22 nucleotides that are conserved across the majority of animal and plant species. To date the human genome is reported to contain between 1000-2000 different microRNA (Lee and Ambros, 2001, Ambros et al., 2003, Mendell and Olson, 2012). Over 60% of the protein coding genes in humans are thought to be modulated by microRNAs although this figure may be as high as 92% (Bartel, 2004, Friedman et al., 2009). MicroRNAs are negative regulators of gene translation that fine-tune protein expression via their interaction with mRNAs (Baek et al., 2008). MicroRNA transcription is a result of co-expression with nearby 'host' genes, or following methylation of their promoter sequences by transcription factors. Once transcribed they regulate protein expression at a post-transcriptional level through imperfect base pairing to complementary mRNA sequences (O'Donnell et al., 2005, Winter et al., 2009).

MicroRNA biogenesis is a multi-step process shown in Figure 1.5, briefly, microRNA is transcribed by RNA polymerase II creating a hairpin-looped pri-microRNA. This is cleaved by Drosha to a pre-microRNA which leaves the nucleus in an Exportin-5/Ran-GTP-mediated process, the pre-microRNA is then cleaved to mature microRNAs by Dicer. Pri- and Pre-microRNA have hairpin structures that can become 2 separate, mature microRNAs known as the guide (-5p) and passenger (-3p) strands. The guide and passenger strand from each pre-microRNA duplex can have separate fates and will either be incorporated into the mRNA binding RNA-induced silencing complex (RISC) or degraded (Winter et al., 2009). Several factors influence whether a strand is incorporated into the RISC; firstly, the thermodynamic stability of the molecule, generally the least stable molecule will integrate with the RISC and the most stable is degraded although it is also possible for both strands to be functional (Krol et al., 2010, Khvorova et al., 2003). Secondly, cell type; recent evidence suggests that one strand from the pre-microRNA may be degraded in a certain cell whilst the inverse may occur in another cell (Liu and Abraham, 2013). A third possible factor is the environment, for example some microRNAs may have specific roles in development, but not in any processes beyond (Ro et al., 2007). Both the secondary and tertiary factors are likely to be significantly influenced by the mRNA milieu of a particular cell, which may define how these mRNA interact with the microRNA (Seitz, 2009).
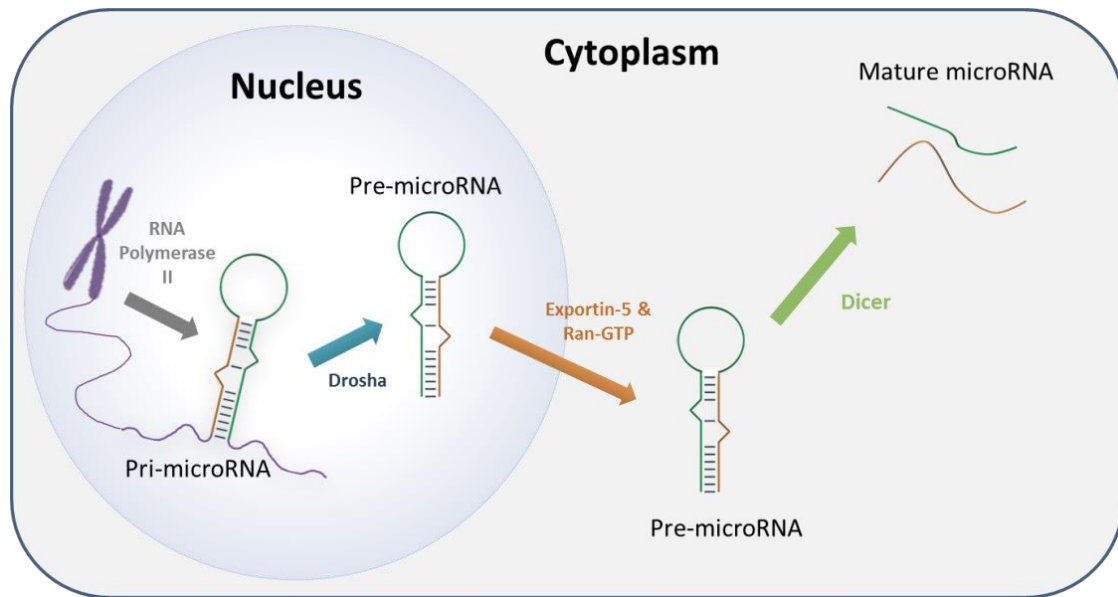
Figure 1.5 – MicroRNA biogenesis *A schematic of microRNA biogenesis, pri-microRNA is transcribed by RNA polymerase II, pri-microRNA is cleaved to pre-microRNA by Drosha and then exported from the cell in an Exportin-5 and Ran-GTP driven process. Once outside the nucleus the pre-microRNA is cleaved to mature microRNA by Dicer and then incorporates into the RISC for functional activity.*

The effectiveness of protein repression by microRNA is highly variable, with most interactions causing less than 50% reduction. Binding of microRNA to target sequences on mRNAs predominantly occurs in the microRNAs seed region which is comprised of 6-8 nucleotides at the 5' end of the microRNA (nucleotides ~2-8). Binding is also observed at nucleotides 13-16, although this is considered to be a secondary site (Grimson et al., 2007). Binding to mRNA follows microRNA incorporation into the RISC, which requires microRNA to bind to the RISCs Argonaute protein. The complex triggers target protein repression, microRNA can cause mRNA degradation as a result of perfect binding of the microRNA to its target. This is a phenomenon normally observed in plants however (Voinnet, 2009). In animals the usual outcome is translational repression due to imperfect binding (Bartel, 2009, Hoy and Buck, 2012).

Each microRNA can target hundreds of genes that are often in related biological pathways, and individual genes can be targeted by multiple microRNAs. Much of our current knowledge about microRNA interactions is based upon computer generated predictions and so our understanding of the role microRNA play in normal and disease states is far from complete (Baek et al., 2008, Lee et al., 2008).
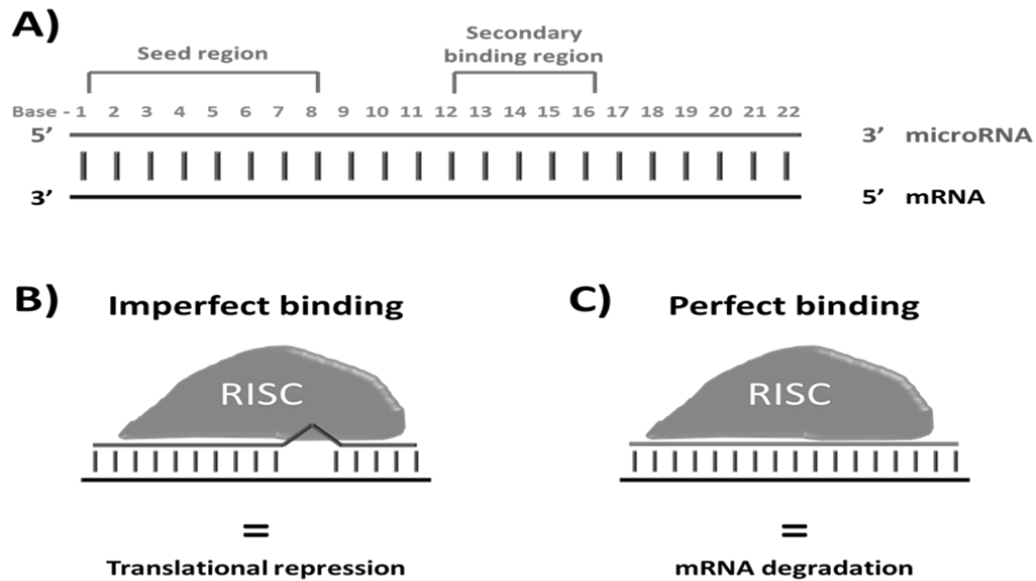
Figure 1.6 – MicroRNA binding *MicroRNA are incorporated into the RISC and then bind to complimentary bases in the 3'-UTR of mRNA. The most important binding region is the seed region as binding here can only tolerate 1 mismatch and normally comprises of binding between 6-8 pairs of nucleotides. Following binding at the seed region, binding spreads to other regions which are more tolerant of mismatches. A) Shows the structure of an individual microRNA binding to an mRNA with the specific binding regions highlighted. B) If the microRNA binds to the mRNA imperfectly then translation of the mRNA is repressed (animals). C) If the microRNA binds to the target mRNA perfectly then the mRNA will be degraded (plants).*

MicroRNAs are likely to influence almost every pathway and function within the human body to some extent and validating these interactions experimentally has proved challenging. This makes it difficult to link specific targets to individual microRNA, but many studies have identified microRNAs essential to specific functions. For example miR-181a-5p was shown to be involved in haematopoietic differentiation, driving haematopoietic progenitor cells towards a B-lymphocyte fate (Cheng et al., 2010). MiR-494 mediates apoptosis and reduces expression of activating transcription factor 3, potentially implicating it in acute kidney injury (Lan et al., 2012). Recent studies have also found that specific microRNA are essential to the biogenesis and physiological function of platelets, as well as diseases involving them such as Polycythaemia Vera, examples are listed in Table 1.1 (Bruchova et al., 2008, Opalinska et al., 2010, Edelstein and Bray, 2011, Dangwal and Thum, 2012, Dahiya et al., 2015, McManus and Freedman, 2015).

Table 1.1 – Platelet associated microRNA Details of microRNA which have been identified as functionally important in platelet production or function and several microRNA expressed in platelets which have shown correlation to disease.

microRNA	Proposed role	Reference
Platelet Biogenesis		
miR-146a-5p	Decreased megakaryocytopoeisis by targeting CXCR4	(Labbaye et al., 2008)
miR-10a-5p	Decreased megakaryocytopoeisis via HOXA1 targeting	(Garzon et al., 2006)
miR-34a-5p	Increased megakaryocyte differentiation through targeting MYB	(Navarro et al., 2009)
miR-155-5p	Inhibits megakaryocytopoeisis by targeting ETS-1 and MEIS-1	(Edelstein and Bray, 2011)
miR-150-5p	Enhances megakaryocyte differentiation by targeting c-MYB	(Edelstein and Bray, 2011)
miR-130a-3p	Decreased megakaryocytopoeisis through targeting of MAFB	(Stakos et al., 2012)
Platelet Function		
miR-223-3p	Platelet activation through P2Y12 receptor expression downregulation	(Landry et al., 2009)
miR-200b-3p	Platelet hyperreactivity through downregulation of PRKAR2B	(Nagalla et al., 2011)
miR-107-3p	Platelet hyperreactivity through downregulation of CLOCK	(Nagalla et al., 2011)
miR-96-5p	Platelet granule exocytosis through downregulating VAMP8	(Kondkar et al., 2010)
miR-495-3p	Platelet hyperreactivity through targeting KLHL5 for downregulation	(Stakos et al., 2012)
Disease associated biomarkers		
miR-26b-5p	Polycythaemia Vera	(Bruchova et al., 2008)
miR-340-3p and miR-624-5p	Increased in platelets of patients with premature coronary artery disease	(Sondermeijer et al., 2011)
miR-490-5p/-3p	Increased expression in platelets of patients with essential thrombocytopenia	(Xu et al., 2012)

Researchers have taken two approaches to studying microRNAs in disease; understanding the functional role of microRNA at a molecular level to identify therapeutic targets, and observing microRNA expression in disease to identify potential biomarkers. Investigations of the role of microRNA in disease initially centred on cancer, but now extend to almost all diseases (Kaudewitz et al., 2016, Kannan et al., 2009, Chen et al., 2008, Li et al., 2011). There are numerous studies exploring the role and diagnostic potential of microRNA as biomarkers in CVD and the extent of this research suggests that there is great potential for clinical applications (Latronico et al., 2007, D'Alessandra et al., 2010, D'Alessandra et al., 2012, Dimmeler and Zeiher, 2010, Fichtlscherer et al., 2011, Gupta et al., 2010, Kukreja et al., 2011)

Studies of different CVD conditions have already yielded results, with both biomarkers and functional microRNAs being identified, and in some cases validated using animal models. For

example, miR-24-3p is elevated under the hypoxic conditions observed in some CVD, and has been shown to modulate vascular regeneration following MI in zebrafish (Fiedler et al., 2011). MiR-92a-3p is part of the microRNA-17/92 cluster that is upregulated in several tumours and studies in mice observed that it was influential in the recovery of ischaemic tissue (Bonauer et al., 2009). Recently miR-590-5p and miR-199a-5p were shown to promote re-entry to the cell cycle of ex-vivo cardiomyocytes in rats, suggesting a potential mechanism for heart tissue repair (Eulalio et al., 2012). In addition to these studies in animal models, data from studies in human blood have identified miR-126-3p as a positive indicator of future MI and miR-223-3p and miR-197-5p showing negative correlation with future MI, suggesting these microRNAs could be used as readily accessible biomarkers. An additional but significant finding of these studies was that the microRNA of platelets and pdEV had a huge influence on the microRNA in the blood (Latronico et al., 2007, Zampetaki et al., 2012).

Previous studies have highlighted the importance of platelets and the microRNA they release via EVs on the microRNA profile of the blood. This is an area that has attracted a lot of attention over the last few years. Landry et al. were the first group to profile microRNA in human platelets using a real-time polymerase chain reaction (RT-PCR) approach, and subsequent studies have used several different polymerase chain reaction (PCR) and microarray-based methods to profile platelet microRNA (Landry et al., 2009, Nagalla et al., 2011, Sondermeijer et al., 2011, Osman and Falker, 2011, Stratz et al., 2012, Xu et al., 2012). To date the parity between these datasets has not be analysed, but comparisons of microRNA profiling techniques suggest that there may be differences, indicating that differences between experimental approaches have a significant impact on microRNA profiling (Meyer et al., 2012, Mestdagh et al., 2014, Chugh and Dittmer, 2012, Jensen et al., 2011). There are currently no studies that have produced a detailed profile of the microRNA released from platelets, but microRNA within EV from the plasma and other cells have been studied as potential biomarkers of disease, and as agents of intercellular communication (Valadi et al., 2007, Collino et al., 2010).

The transfer of microRNA and its functional effects within other cells are areas that warrant thorough investigation. Studies in vitro have shown that microRNA can be transferred via exosomes and that this microRNA remains functional following transfer due to the protection from RNAse in the blood conveyed by the EV (Fevrier and Raposo, 2004, Montecalvo et al., 2012, Stoorvogel, 2012, Laffont et al., 2015). There is still debate over the mechanism by which microRNA is carried in the blood and microvesicles, exosomes, apoptotic bodies, Argonaute complexes and lipoproteins all being suggested as potential vehicles. Increasingly the evidence

suggests that exosomes are the predominant carrier (Zernecke et al., 2009, Arroyo et al., 2011, Vickers et al., 2011, Gallo et al., 2012).

The mechanism by which platelets release microRNA has not, to date, been studied systematically. EVs have been shown to contain large amounts of microRNA but studies from other cell types suggests that the microRNA profile of exosomes may not reflect the microRNA profile of the cell of origin (Mittelbrunn et al., 2011, Guduric-Fuchs et al., 2012, Pigati et al., 2010). Investigating pdEVs specifically is important due to their high proportion in the blood, contributing up to 50% of circulating EVs and with this the released platelet microRNA makes a significant contribution to the population of circulating microRNA (Arraud et al., 2014). In addition, exosomes represent an opportunity for these packages of microRNA to be targeted at other cells due to the enrichment of fusogenic tetraspanins in their membranes (Takeda et al., 2003, Zhu et al., 2002, Rubinstein et al., 2006a, Li et al., 2014). A cell that has been shown to interact with platelets in the circulation, in both homeostatic and pathological processes is the monocyte, and in particular, the interaction of platelets with monocytes is important in their activation and recruitment to sites of inflammation.

1.6 Platelet-Monocyte crosstalk

The intercellular communication between platelets and monocytes can occur through different mechanisms; direct interaction, soluble mediators, lipid intermediates and EV transfer (Figure 1.7) (Freedman and Loscalzo, 2002, Cerletti et al., 1999, Baltus et al., 2005, Mause et al., 2005). Direct interaction is the most frequently studied and has been shown to play a role in monocyte recruitment into the thrombus and atheroslerotic plaques. The initial attachments via P-selectin and PSGL-1 trigger secondary interactions between GPs and integrins such as platelet GPIb, GPIIb-IIIa and Junction Adhesion Molecule C (JAM-C) binding to MAC-1 on monocytes. Interaction between CD40L on platelets and CD40 on monocytes also forms, triggering intercellular signalling which propogates signalling between the cells by upregulating monocyte integrin expression e.g. MAC-1 (van Gils et al., 2009).

Attachment of platelets to monocytes is seen in the circulation and the number of these aggregates has been correlated with disease including CAD (Furman et al., 1998), MI (Michelson et al., 2001) and stroke (Smout et al., 2009). The formation of these circulating aggregates also leads to monocyte activation which causes increases in PSGL-1 and integrins such as MAC-1. This strengthens the monocyte-platelet interaction, increases binding to the endothelium (Alonso-Lebrero et al., 2000, Snapp et al., 2002) and upregulation of inflammatory signalling through

interleukin-1β (IL-1β) release and CD40 expression (Weyrich et al., 1995, Weyrich et al., 1996, Zimmerman et al., 1996) potentially driving further inflammation at sites of interaction.
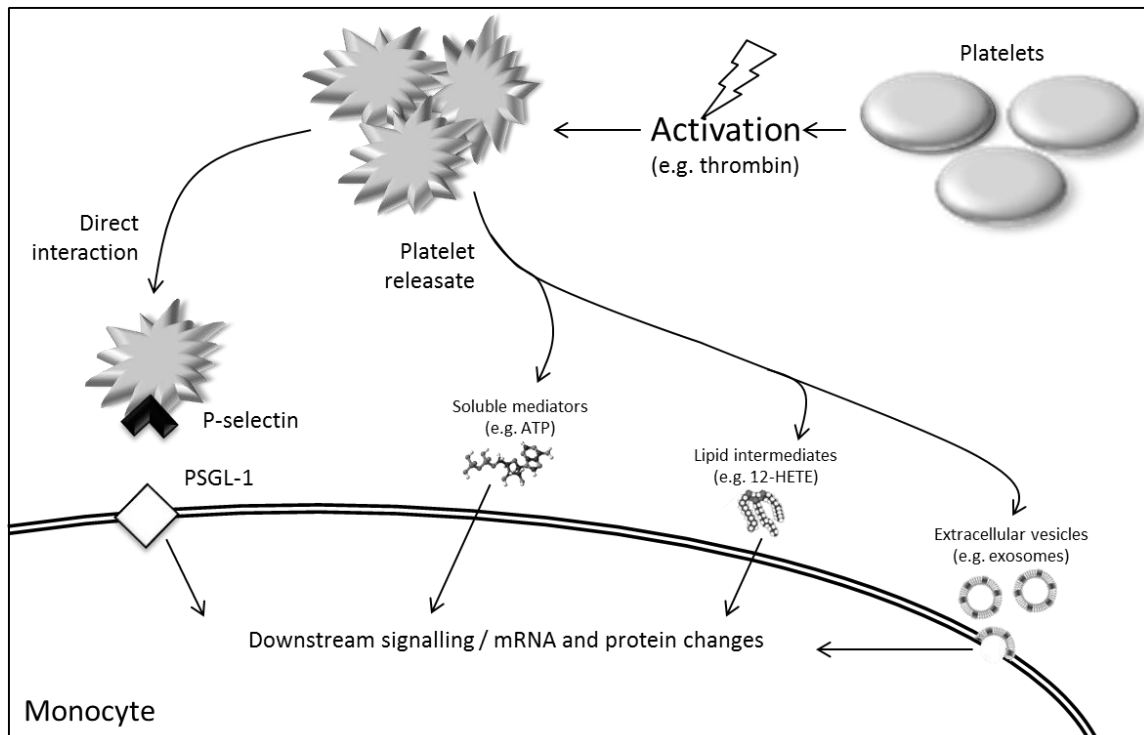
Figure 1.7 – Platelet-Monocyte interactions Diagram of the interactions of platelets and monocytes following platelet activation including direct interaction or signalling through secondary mediators and EV released from platelets.

These direct interactions occur in the circulation and following monocyte recruitment into inflammatory environments such as the thrombus. The attachments position monocytes and platelets directly next to each other which increases the ability of platelets to communicate with monocytes via alternative mechanisms such as soluble mediators and lipid intermediates. When platelets are activated they degranulate which causes the release of α- and dense-granules containing a multitude of proteins that can act on nearby cells (Senzel et al., 2009, Coppinger et al., 2004). The chemokine, CXCL4/Platelet Factor 4 (PF4) is released in large quantities from α-granules and drives monocyte survival and differentiation into macrophages (Sachais et al., 2002, Scheuerer et al., 2000). IL-1β is released from platelets and when this acts on monocytes it triggers cholesterol retention through inhibition of the Cholesterol Efflux Regulatory Protein (CERP), which can trigger foam cell formation and therefore contribute to CAD and related pathologies (de Villiers and Smart, 1999, Lindemann et al., 2001, He et al., 2015).

In addition, EVs provide a mechanism for cell-cell communication, both in an acute setting, following platelet activation, or due to their constitutive release as a steady-state communication mechanism. PdEVs can function over greater distances and potentially target specific cells due to the protective environment that they provide and the specific receptors on

their membrane (Aatonen et al., 2012, Cauwenberghs et al., 2006). Microvesicles have been shown to enhance monocyte adhesion to the endothelium as a result of inflammation (Barry et al., 1998, Mause et al., 2005) whilst in-vitro experiments have shown the delivery of pdEV microRNA to macrophages (Laffont et al., 2015). Taken together these studies demonstrate that EV communication between platelets and monocytes is an important axis of interaction that warrants further investigation. In addition, circulating pdEV have an abundance of microRNA which can significantly alter the function and fate of target cells, which presents a real opportunity to identify new therapeutic targets and improve our understanding of intercellular communication between these cell types.

1.7 Aims and objectives

This introduction has highlighted several areas of unmet research and the experimental work in this thesis aimed to address some of these. We hypothesise that platelets release and deliver microRNA to monocytes via EV (predominantly in exosomes), resulting in altered protein expression in the monocytes, and that this interaction plays a role in the development of atherosclerosis/CAD. These questions are addressed in four interlinked studies, each of which is presented in a separate chapter.

Chapter 2 describes an investigation into the pattern of EV release from platelets following stimulation with different agonists by systematically characterising the EVs released to address two related questions; whether different EV populations were generated by specific agonists, and whether there were stimuli that resulted in the release of a pure population of exosomes. The studies included the use of specific platelet inhibitors to elucidate the secondary signalling pathways leading to release of exosomes and microvesicles.

Chapter 3 compared the profiles of microRNA released from platelets following stimulation with different agonists with that of the parent platelets to determine whether there was any preferential release of specific microRNAs, and to identify potential microRNA biomarkers of platelet activation.

Chapter 4 utilised the pdEV microRNA profiles to explore their potential targets in monocytes developing a novel, in-depth approach using multiple datasets.

Chapter 5 aimed to observe the transfer of microRNA from platelets to monocytes via pdEV and attempted to identify the functional effects of this transfer on potential targets identified in Chapter 4.

Chapter 2

Characterising platelet-derived
Extracellular Vesicles

2 Characterising platelet-derived Extracellular Vesicles

2.1 Introduction

As already discussed, EV are rapidly growing in significance in areas ranging from drug delivery to biomarker identification (Yanez-Mo et al., 2015). However there are still large gaps in our knowledge surrounding their normal function within the body and the state of the field is constantly shifting (van der Pol et al., 2012a). Debate continues to surround the nomenclature used, characteristics of the different EV subpopulations, isolation techniques and their functional role (van der Pol et al., 2016).

Throughout this thesis the term EV has been used as an umbrella term for all vesicles. Two further terms have been used to refer to EV subtypes; microvesicles and exosomes, with microvesicles referred to larger EV (~>100nm) that expose negatively charged phospholipids, such as PS and exosomes being defined as smaller EV (~<100nm) that display markers such as CD63 and HSP70 (Boilard et al., 2015). These terms are in line with current guidelines from the International Society on Extracellular Vesicles (ISEV) but they are not yet used throughout the literature, making some comparisons difficult (Arraud et al., 2014, Yanez-Mo et al., 2015).

Many techniques have been utilised for EV isolation; various centrifugation approaches (density-gradient (Aatonen et al., 2014), ultracentrifugation (Taylor et al., 2011) and differential centrifugation (Thery et al., 2006)) as well as filtration (Lobb et al., 2015), size exclusion chromatography (Welton et al., 2015, de Menezes-Neto et al., 2015) and immune-capture (Tauro et al., 2013), with each technique having its own advantages and disadvantages. Along with the range of isolation techniques, the methods to characterise EV have also grown. The standard methods include flow cytometry, dynamic light scatter, electron microscopy and proteomics, but more recent approaches have included Raman spectroscopy, surface plasmon resonance, RNA-sequencing, resistive pulse sensing, Nano-particle Tracking Analysis (NTA), thrombin generation (TG) assays and atomic force microscopy (van der Pol et al., 2016, Gardiner et al., 2013). This provides researchers with a wealth of tools with which to characterise EV, meaning that more information is available about the different subtypes. However this is currently leading to less, rather than more consensus.

Many of these issues need to be resolved before a true understanding of the importance of EVs in a mechanistic and clinical setting can be truly exploited. Increasingly, elevated levels of EV

have been identified in many disease states such as acute myocardial infarction (Stepien et al., 2012, Jung et al., 2012, Boulanger et al., 2001), acute ischemic stroke (Simak et al., 2006), unstable plaques (Sarlon-Bartoli et al., 2013) and type 2 diabetes (Koga et al., 2005a). They have also been shown to confer functional effects on the cells that take them up including calcification of vascular smooth muscle cells (Kapustin et al., 2015), increased leukocyte adherence (Cai et al., 2015) and cell cycle arrest (Burger et al., 2011). EVs are found in extracellular environments throughout the body; from spinal fluid to the blood. Platelets have been shown to be responsible for up to 50% of the total EV population in blood, meaning that understanding these EV has important implications for intercellular communication in the circulation and for potential clinical applications such as utilisation for drug delivery or biomarkers (Melo et al., 2015, Kwekkeboom et al., 2014, Ailawadi et al., 2015, Arraud et al., 2014).

Platelets have many biological roles in haemostasis, development and immunity and platelet-derived EV (pdEV) contain a variety of cargo with which these tasks can be achieved. Platelets release both microvesicles and exosomes upon activation. This heterogeneity was first reported in 1999 (Heijnen et al., 1999), although pdEV had been observed as early as 1967 when they were described as 'platelet dust' (Wolf, 1967) and their thrombotic potential was described in 1946 (Chargaff and West, 1946). EV release from platelets is constitutive (Cauwenberghs et al., 2006) and is enhanced by shear stress or activation through specific receptors (Aatonen et al., 2012, Kahner et al., 2008). Studies have been conducted to characterise EV production from platelets but this has so far predominantly utilised proteomics and flow cytometry (Aatonen et al., 2014, Garcia et al., 2005, Jin et al., 2005, Xiao et al., 2002).

Despite a lack of clarity on the basic characteristics of pdEV, many studies have focused on their interactions with other cells. They have been shown to interact with endothelial cells (Huber and Holvoet, 2015, Laffont et al., 2013), neutrophils (Duchez et al., 2015), monocytes (Losche et al., 2004, Setzer et al., 2006) and macrophages (Laffont et al., 2015, Sadallah et al., 2011). In interacting with other cells pdEV have been implicated in a variety of processes including apoptosis (Gambim et al., 2007, Janiszewski et al., 2004), inflammation (Hulsmans and Holvoet, 2013), platelet aggregation (Xiao et al., 2002), monocyte recruitment (Mause et al., 2005) and have been shown to transfer RNA (Risitano et al., 2012),. In addition to these physiological functions, pdEV have also been implicated in pathological processes, for example in cardiovascular diseases (Danielson and Das, 2014). Causing endothelial dysfunction following MI (Boulanger et al., 2001), and pdEV from septic shock patients have been reported to induce myocardial dysfunction (Azevedo et al., 2007).

Taken together, this body of work demonstrates the critical function that pdEV have to play in a variety of elements of health and disease. Whilst current research is piecing together some of the functional effects, we still know very little about the pdEV characteristics and their release mechanisms, or whether widely used anti-platelet therapy has a significant effect on their release. The work in this chapter aims to provide a fuller picture on the characteristics of EV released from platelets that have been activated by different agonists and examine whether any of these stimuli generated a pure population of exosomes. Therefore, as detailed in Table 2.1, platelets were stimulated with agonists directed against the GPVI receptor (CRP-XL), the PAR-1 and PAR-4 thrombin receptors (PAR1-AP, PAR4-AP and thrombin), and the P2Y1 and P2Y12 receptors (ADP) to stimulate the release of EV which were then characterised by flow cytometry, NTA, the TG assay and western blotting. Concentrations of all agonists were selected by titration.

Table 2.1 – Agonists used to stimulate platelet activation *The table lists the agonists used for platelet stimulation in this chapter. The targeted receptors are listed alongside the agonist used, agonist concentration and the PLC pathways activated through that receptor.*

Agonist	Receptor(s)	PLC pathway	Agonist Concentration
CRP-XL (Collagen mimetic peptide (GCO-[GPO]$_{10}$GCOG-NH$_2$))	GPVI	Gamma	2μg/mL
PAR1-AP (SFLLRN)	PAR1	Beta	10μM
PAR4-AP (AYGPKF)	PAR4-AP	Beta	200μM
ADP (Adenosine di-phosphate)	P2Y1/P2Y12	Beta	50μM
thrombin (Factor 2)	PAR1/PAR4	Beta	0.32U/mL

2.2 Aims

To characterise the pdEV released in response to different agonists and to determine the effects of platelet inhibitors on pdEV release to determine whether any specific pathway could produce an EV population comprised solely of exosomes.

2.3 Materials and methods

All reagents purchased from Sigma-Aldrich, Gillingham, England unless otherwise stated.

2.3.1 Blood collection

Blood was collected from healthy volunteers who had provided written consent based on ethical approval from the University of Leicester Ethical Practices Committee (ref: ahg5-97b2). Experienced phlebotomists collected blood using a BD Vacutainer Safety-Lok™ Blood Collection Set. To prevent platelet activation due to venous stasis the tourniquet was removed following successful venepuncture.

Blood was collected through a 21 butterfly gauge needle into Vacutainers; the first 1mL was collected into a Vacutainer tube containing EDTA (5.4mg) and additional blood was collected in 4.5mL aliquots into Vacutainers containing sodium citrate (0.105M, 3.2%) up to a total volume of 45mL. The EDTA anticoagulated blood was used to perform a full cell count using a Beckmann Coulter AcTdiff haematology analyser.

2.3.2 Preparation of Platelet Poor Plasma (PPP)

Citrated whole blood was centrifuged at 1800g for 30minutes at RT. The upper layer, of PPP was aspirated taking care not to disturb the lower layers.

2.3.3 Preparation of pooled plasma

Pooled plasma was prepared from 20-25 healthy donors to use as a standard reagent in the TG assay. Six tubes of citrated blood were collected simultaneously from each donor, as described above. Corn Trypsin Inhibitor (CTI) (Cambridge Biosciences, Cambridge, UK) was immediately added to each blood tube (18.3µg/mL), which were centrifuged at 1800g for 30minutes at room temperature (RT). PPP was carefully collected from blood tubes and pooled into a single batch and 1mL aliquots stored at -80°C. All samples were collected and processed within 2hours.

2.3.4 Preparation of serum

Whole blood was collected into serum separator tubes (BD) containing silica which activated the clotting of the blood. Once the blood was taken into the tube it was inverted 6 times and left for 30minutes at RT. The tubes were then centrifuged at 2000g for 15minutes and the supernatant above the acrylic gel retained as serum.

2.3.5 Preparation of washed platelets

Acid-citrate-dextrose (ACD) (0.085M tri-sodium citrate, 0.071M citric acid, 0.11M glucose) was added to each citrated sample of whole blood at a ratio of 1:6 (v/v) and then centrifuged at 160g for 20minutes at RT with slow acceleration and deceleration. This separated the whole blood into an upper layer of platelet rich plasma (PRP), a thin central layer, the buffy coat, containing the white blood cells and a lower layer predominantly of red blood cells. The PRP layer was removed using Pasteur pipettes and transferred into LP4 tubes, taking extra care to leave ~500μl as a buffer above the buffy coat to prevent the PRP being contaminated with leukocytes. Freshly prepared Prostacyclin (PGI$_2$, Enzo Lifesciences, Exeter, UK) at a concentration of 200μg/mL was added to the PRP to a final concentration of 200ng/mL. The tubes of PRP were centrifuged at 600g at RT for 20minutes to pellet platelets, the supernatant was discarded and the pellet re-suspended in 1mL HEPES buffered saline pH6 (HBS.pH6) (150mM NaCl, 5mM KCl, 1mM MgSO4, 10mM HEPES – 0.22μm filtered and taken to pH6 with 2M HCl), before making up to 3mL with HBS.pH6 and adding freshly prepared PGI$_2$ (200ng/mL). The platelets were again sedimented by centrifugation at 600g at RT for 20minutes and platelets re-suspended in 1mL HBS pH7.4 (HBS) (as HBS.pH6 but balanced to pH7.4). Following this final wash step the concentration of the re-suspended platelets was measured using the Beckmann Coulter AcTdiff haematology analyser and diluted using HBS to the required platelet concentration; typically 250x10^3/μl unless stated otherwise.

2.3.6 Activation of washed platelets

For platelet activation platelets were resuspended in HBS.Ca (HBS supplemented with 2mM CaCl$_2$). Platelets were then incubated with CRP-XL (2μg/mL, Professor Richard Farndale, Department of Biochemistry, the University of Cambridge), PAR1-AP (10μM, SFLLRN), PAR4-AP (200μM, AYGPKF), ADP (50μM), thrombin (0.32U/mL) or in the absence of any agonist either individually or in combination for 10minutes at 37°C. The concentrations for platelet agonists were determined by titration; carried out with samples from at least 3 separate blood donors, a titration of PAR4-AP is detailed in Figure 2.1.

2.3.6.1 Titration of PAR4-AP
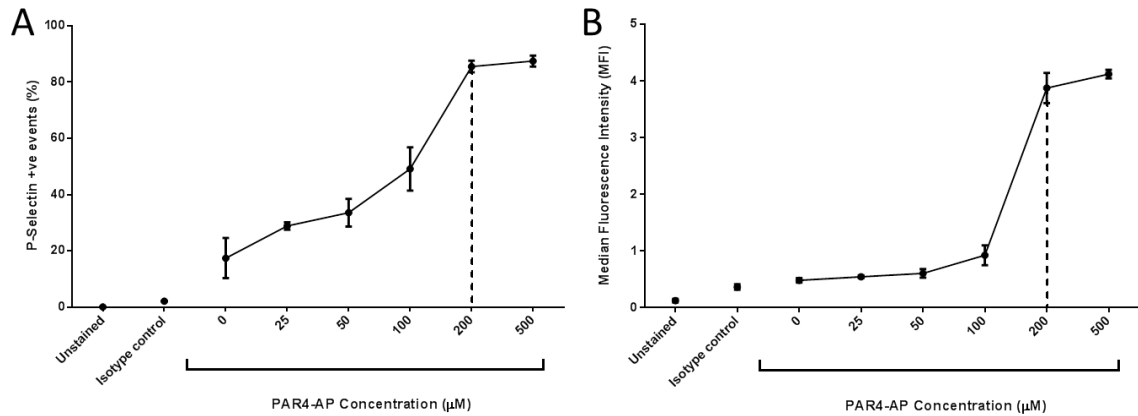
Figure 2.1 – Titration of PAR4-AP (AYGPKF) *To ensure that agonists were used at optimal concentrations they were titrated; washed platelets were activated with increasing concentrations of PAR4-AP and the activation of platelets was measured via P-selectin expression using flow cytometry. An unstained sample and a sample containing an isotype antibody were used as controls. A) Shows the percentage of P-selectin positive platelets with each agonist concentration and B) shows the median fluorescence intensity at each concentration, the selected concentration of 200µM is indicated with a dotted line (n=3±SD).*

2.3.7 Inhibition of washed platelets

In experiments where platelets were inhibited, washed platelets in HBS.Ca were incubated with Apyrase (80µg/mL), Hirudin (10U/mL), aspirin (500µM) or the in-house CD61 monoclonal antibody RFGP56 (500ng/mL) (Watkins et al., 2002) for 15 minutes prior to activation. All inhibitors were titrated to achieve maximal inhibition.

2.3.8 Platelet-releasate

2.3.8.1 Isolation of platelet-releasate following activation of washed platelets

Samples of activated washed platelets were immediately centrifuged twice at 2500g for 15minutes at RT. The EV-rich supernatant was retained after each spin and transferred to a clean Eppendorf tube and used immediately for future experiments or frozen in 1mL aliquots at -80°C.

2.3.8.2 Isolating Extracellular Vesicles using ExoQuick

A second technique to isolate EV from fluids utilised the commercial product ExoQuick (System Biosciences). ExoQuick uses polyethylene glycol to precipitate EV from solution and allowed the formation of an EV pellet using low speed centrifugation. Isolation of EV from the releasate of activated washed platelets was carried out according to the manufacturer's protocol. Briefly, 240µl of ExoQuick solution was added to the EV rich supernatant. The mixture was then vortexed and incubated for 24hours at 4°C. The samples were then centrifuged at 1500g for 30minutes at 4°C, the supernatant was carefully removed and the remaining pellet centrifuged at 1500g for 5minutes. Any remaining supernatant was aspirated and the pellet of EV was gently re-suspended in of 0.1µm filtered HBS.

2.3.9 Flow cytometry

2.3.9.1   Detection of degranulated platelets

An LP3 tube was setup for each sample containing 42µL of HBS and 2µL of Anti-hP-selectin – Fluorescein (R&D Systems, MN, USA) [clone: 9e1] antibody. Washed platelets (5µl), either unactivated or following agonist stimulation were added and the tubes incubated at RT for 20minutes. Following incubation, sample tubes were diluted with 450µl of 0.2% Formyl Saline (FS) (0.2% Formaldehyde in 0.85% (w/v) NaCl) following the 20minute incubation and then incubated for a further 20minutes. A 50µl aliquot was taken and diluted in 450µl HBS and then run on a Gallios flow cytometry system (Beckmann Coulter).

Two controls were used for each experiment; firstly a tube containing HBS and unactivated platelets and secondly an isotype control, 2µl of Mouse IgG1 Fluorescein isotype (R&D Systems) [clone: 11711] instead of Anti-hP-selectin – Fluorescein. The tube without antibodies was used to identify the platelet on the basis of Forward Scatter (FSc) and Side Scatter (SSc) and the isotype control was used to set the background fluorescence.
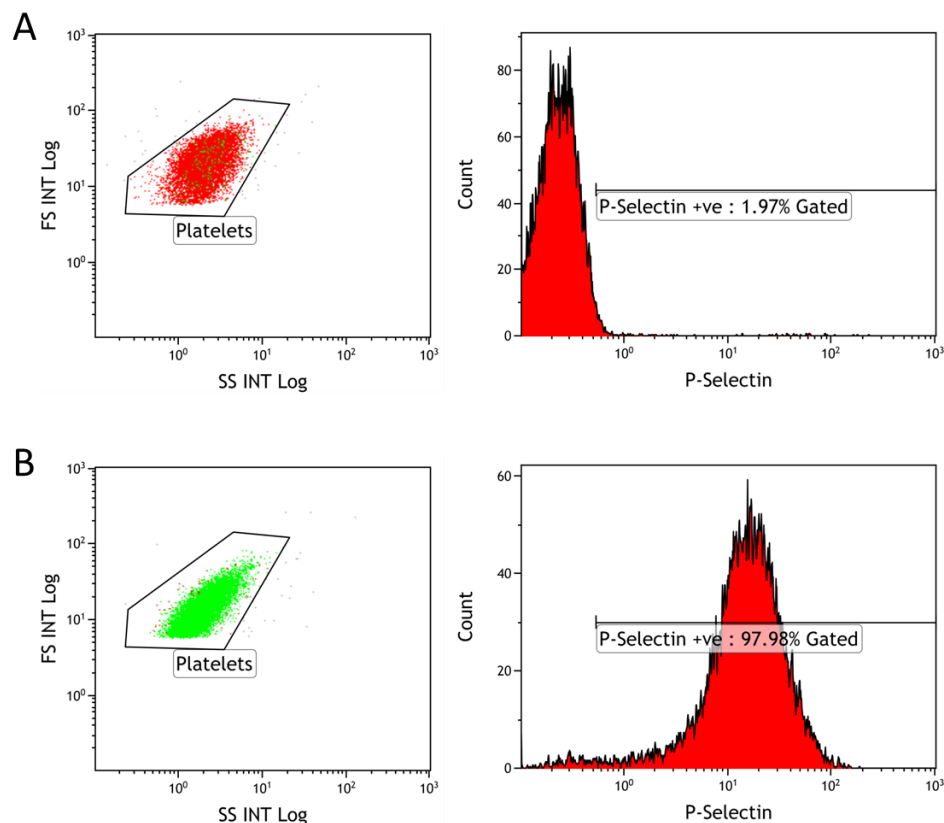
Figure 2.2 – Representative flow analysis of P-selectin expression *Above is an example of a negative (A) and positive (B) analysis of washed platelets for P-selectin using flow cytometry. Platelets were identified using an FSc (Log) vs SSc (Log) plot and the platelet population was gated. The platelets were then analysed for P-selectin expression on the FL1 channel using a histogram. Isotype controls were set at ~2%+ve events and then positive events were detected as events within this gate.*

All antibodies and fluorescent proteins were titrated, using the same conditions as in experiments. Briefly, up to 10 doses of antibody were tested alongside corresponding doses of isotype control to achieve optimal separation between positive and negative events, testing both the percentage of positive cells and median fluorescent intensity. An example titration is shown for Annexin-V FITC in Figure 2.3.
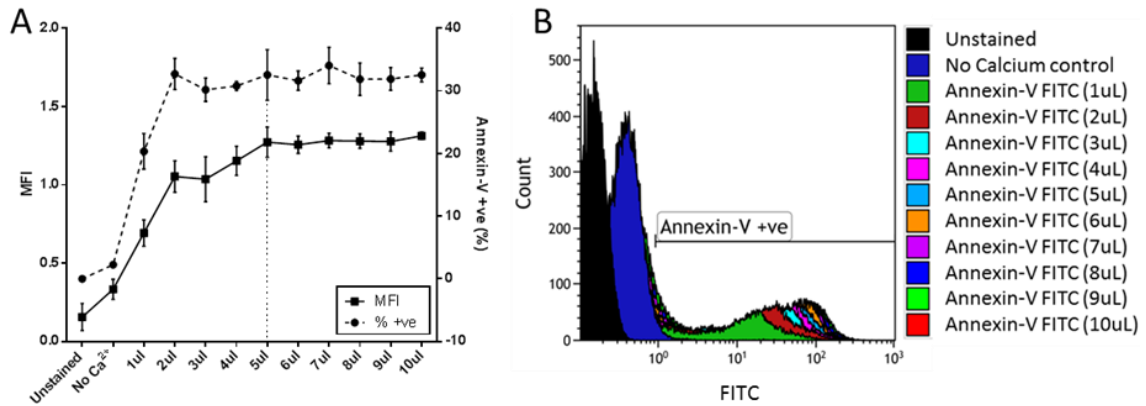
Figure 2.3 – Annexin-V FITC titration *As with agonists, all antibodies and fluorescent reagents for flow cytometry were titrated to achieve optimal doses. Above is an example using the Annexin-V FITC fluorescent protein; increasing concentrations of Annexin-V were used to detect microvesicles released from washed platelets. An unstained and no-calcium condition were used as controls. A) shows the median fluorescence intensity (MFI) on the left axis and percentage of Annexin-V positive events on the right axis for all tested conditions (n=3±SD) and B) shows the overlaid histograms from all experimental conditions.*

2.3.9.2   Detection of microvesicles released from washed platelets

For each sample a tube was set up containing 40µL of HBS.Ca and 5µL of Annexin-V-FITC (Becton Dickinson and Co., NJ, USA). There were 2 controls, one containing 45µL of HBS.Ca and no Annexin-V-FITC and secondly a tube with 40µL of HBS and 5µL of Annexin-V-FITC. This second tube lacked calcium, which is required for Annexin-V to bind, so served as a negative control. Washed platelets (5µ), either unactivated or following agonist stimulation were added to each tube and the tubes incubated at RT for 10minutes. Samples were diluted with 450µl of HBS.Ca (or HBS without calcium for the negative control) after which a 50µl aliquot was taken and diluted in 450µl HBS.Ca (or HBS for the control) and run on the flow cytometer. The tube without antibodies was used to set up the FSc vs SSc gate and the tube without calcium was used to set the fluorescence gating for Annexin-V positive events.
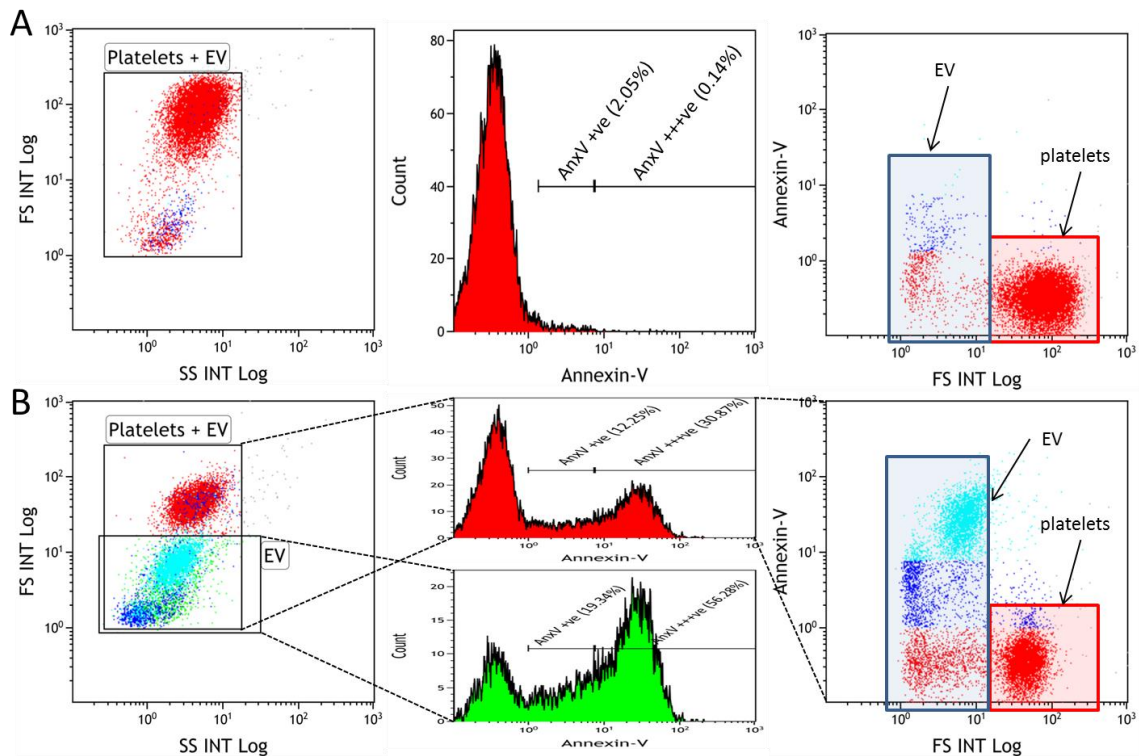
Figure 2.4 – Representative flow cytometry analysis of Annexin-V binding An example of a negative, without calcium (A) and positive, with calcium (B) analysis of washed platelets and their EV for Annexin-V binding using flow cytometry. Platelets and their EV were identified using an FSc (Log) vs SSc (Log) plot with flow cytometer laser settings optimised for small particle detection. The platelets and EV were gated and then analysed for Annexin-V binding on the FL1 channel using a histogram. Isotype controls were set at ~2%+ve events and then actual positive events were detected as events within this gate. The final plot shows how the different sized (FSc) populations stain differently for Annexin-V. Plot (B) also shows an alternate gating strategy used to analyse EV alone. The FSc vs Annexin-V plots are annotated to identify the platelet and EV populations. On the FSc vs SSc or Annexin-V plots, red events indicate Annexin-V negative vesicles or cells, dark blue events bind low amounts of Annexin-V and light blue events represent vesicles or cells with high Annexin-V binding.

2.3.10   Nano-particle Tracking Analysis (NTA)

The size and concentration of EV was measured in the platelet-releasate using a Nanosight NS500 (Malvern Instruments, Malvern, UK). Samples were diluted, using 0.1μm filtered HBS, so that each video recorded between 500-1000 tracks. The Nanosight tracks each visible particle in the sample individually and determines size using the principal of Brownian motion. It then compiles data from all of the particles tracked in the video. The output appeares as a trace (Figure 2.5) which provides smoothed information of the concentration of particles at 1nm size intervals. It is possible to determine the mode particle size (highest peak) and particle concentration (area under the curve) from these traces.
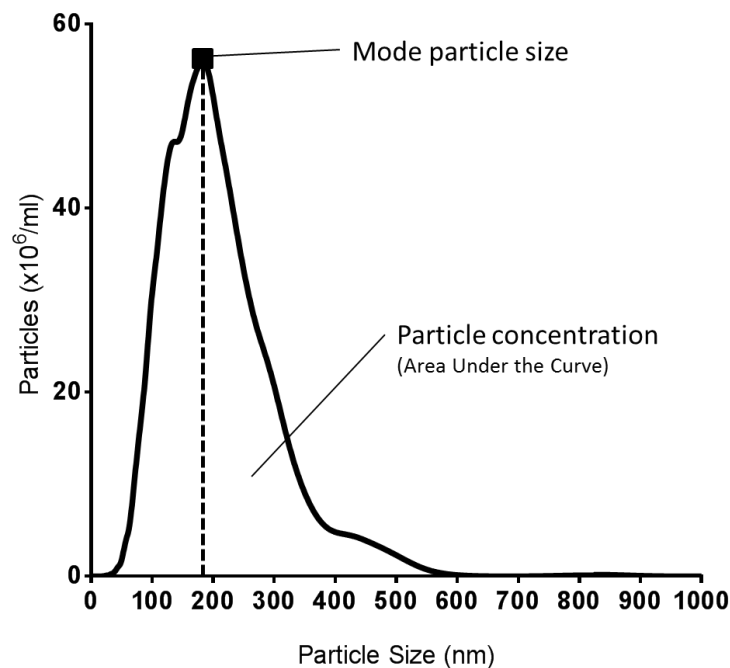
Figure 2.5 – Example NTA trace NTA provided information on the size distribution and concentration of EV populations, this graph shows an example trace from the Nanosight. The Nanosight plots particle concentration (particles x10^6/mL) against particle size (nm) from which it is possible to determine the overall concentration of particles using the area under the curve and the mode particle size.

Prior to running samples, experiments were carried out to identify the optimum settings for the instrument. It was possible to change acquisition of data through alterations in camera level which modified the camera gain (camera sensitivity) and camera shutter speed (amount of light captured). Analysis of the data could be altered through changes to the detection threshold which determined the minimum characteristics for an observed item to be deemed a particle and therefore be tracked in the analysis. Optimisation experiments were first carried out using standard polystyrene beads and then with pdEV. Briefly; 100nm, 200nm and 400nm polystyrene beads and CRP-XL stimulated platelet-releasate were analysed using camera levels 6, 8, 10 and

12 (plus 14 and 16 for beads). The mode particle size, total particle concentration and concentration of particles <120nm were recorded. The results are illustrated in Figure 2.6.

Graph A show that 400nm particles displayed variation in size, which did not correlate with the camera level, and that the concentration detected increased slightly at camera level 16, which may suggest an increase in background detection.

Graph B shows that for 200nm polystyrene beads the size recorded did not vary across any of the camera levels, apart from a slight rise at level 16, but the recorded concentration fell as the camera level increased.

Graph C demonstrates the results for 100nm beads; their recorded size did not change across camera levels 6-14 but these beads were undetectable at level 16, and their measured concentration was significantly reduced at camera levels above 12. As the predominant particle size in platelet-releasate is known to be between 100-200nm the experiment looking at pdEV samples focused on camera levels 6-12 as there was no loss in the detected number of the 100 and 200mm polystyrene beads at these camera levels.

Analysis of the pdEV is shown in graph D, the mode particle size was consistent at all camera levels and the concentration was highest at camera level 12. Therefore camera level 12 was selected for carrying out NTA experiments with pdEVs.

The effects of changing the detection threshold are shown for 100nm beads in part E and pdEV in part F. With 100nm beads there were no differences between any detection threshold settings, however with the pdEV, increases in the detection threshold caused decreases in the particle concentration and mode particle size. At detection thresholds higher than 10 the mode particle size stabilised but the concentration continued to decrease. Therefore the detection threshold was set at 10 for all subsequent experiments to ensure that less bright particles were not missed.
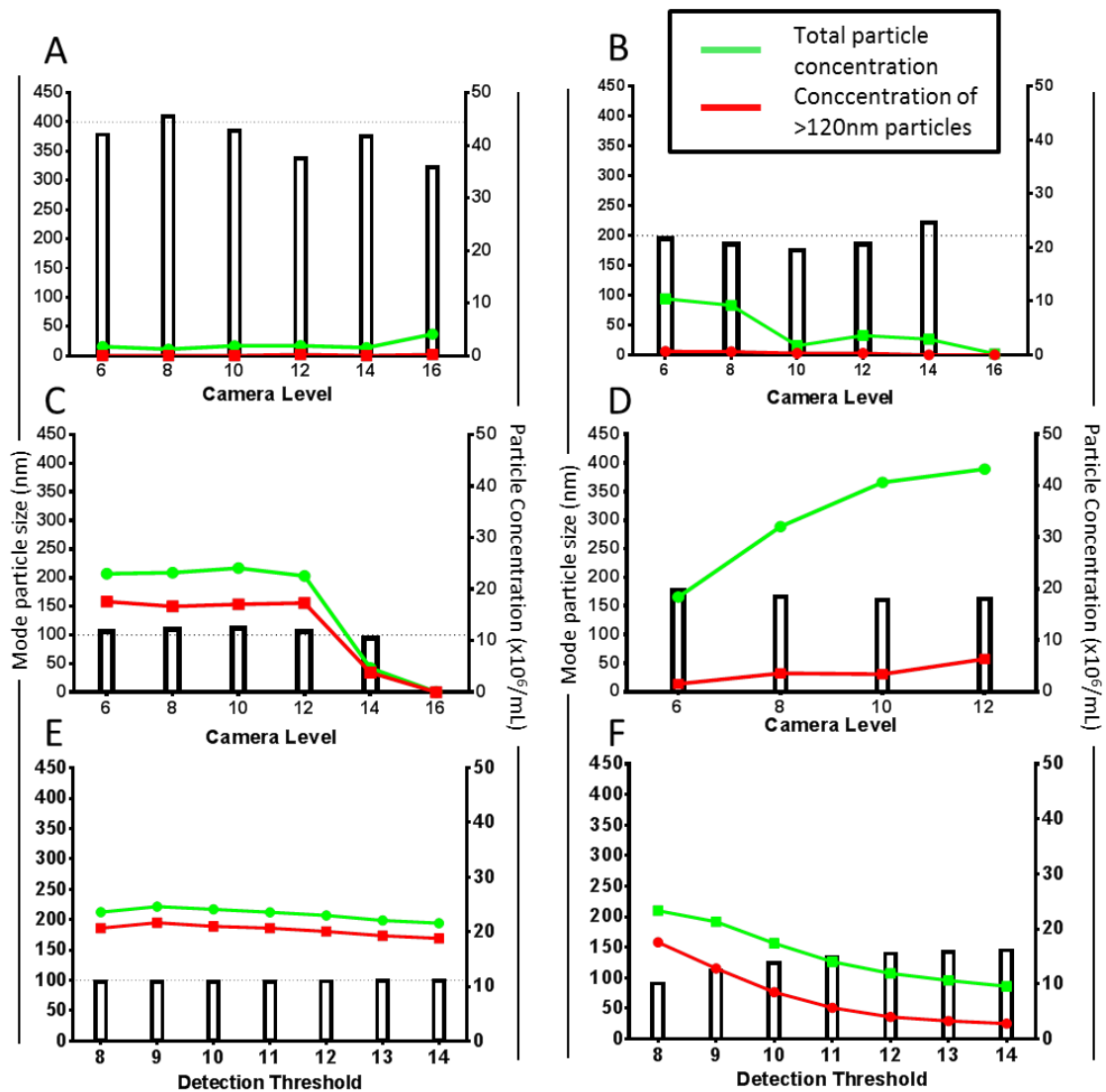
Figure 2.6 – Optimisation of Nanosight instrument settings *The Nanosight NS500 instrument has an array of settings which can be adjusted to optimise sample collection and analysis. Before collecting results from samples these settings were optimised. The effects of camera level (changes in camera shutter speed and camera gain) were tested using 400nm (A), 200nm (B) and 100nm (C) polystyrene beads as well as EV from washed platelets (D). In addition the detection threshold was tested using 100nm beads (E) and platelet-derived EV (F) (n=3 throughout).For all graphs the mode particle size (left Y axis) is shown by the black bars and the particle concentration (right Y axis) is represented by the green line (total particle concentration) and red line (concentration of >120nm particles).*

Based on these preliminary experiments it is clear that biological samples are more sensitive to changes to Nanosight instrument settings making the selection of a single setting difficult. These experiments also demonstrate the difficulty of using beads for the optimisation of biological samples due to the differences in their refractive index (Gardiner et al., 2014, van der Pol et al., 2014, Varga et al., 2014). However ensuring that the machine settings were standardised was important to allow for direct comparisons between samples. Therefore all biological samples were processed at 25°C using camera level 12 (Camera shutter–600, Camera gain–350) and all samples were processed using a script to ensure they were treated uniformly. The script loaded the sample, recorded 3 x 60 second videos and advanced the sample between each recording,

meaning each video recorded a different section of sample. Data was then analysed using the NTA 2.3 software and the standard settings (detection threshold-10 / Blur–Auto / Minimum expected particle size–auto) and results for each sample were an average of the 3 videos. Samples were diluted so that each 60 second video recorded between 500 and 1000 events.

2.3.11   Thrombin generation

TG was used to assess the thrombin-producing potential of the EV samples, to allow differentiation between procoagulant microvesicles and exosomes in the samples. EV preparations were spiked into pooled plasma (2.3.3) and TG was triggered by the PRP reagent (1pM TF). To prevent the concentration of EV in each sample confounding the results, samples were first analysed using NTA and diluted to equalise the EV concentration in all samples. Samples that had been incubated with platelet inhibitors were diluted using the same factor as the matched uninhibited sample.

EVs, prepared as described in 2.3.8.1, were spiked into pooled plasma at a ratio of 1:5 and 80µL of this was added to 20µL of the PRP trigger reagent in a well of a 96-well plate. Each sample was analysed in triplicate and normalised against an additional well of the same pooled plasma using the thrombin calibration reagent which prevented the effects of donor-to-donor variation. Once the plate was loaded with trigger reagent and sample the plate was inserted into a Fluoroscan Ascent (Thermo Labsystems, Waltham, USA). The instruments tubing was flushed with wash solution (HBS with 100mM $CaCl_2$) and then the FluoCa Kit reagents (were mixed (1:40 substrate solution to buffer) (Fluo-Buffer [HBS and 0.1M CaCl2] and the Fluo-Substrate [2.5mM Z-Gly-Gly-Arg-AMC in DMSO]) and loaded into the dispenser in the instrument. Thrombin generation was initiated by the addition of 25µL of the FluoCa kit mixed reagent to each well.

The fluorescence was measured every 20seconds for 1hour; the fluorogenic substrate in the FluoCa kit reagent is broken down in the presence of thrombin resulting in fluorescence that is directly proportional to the amount of thrombin being generated. The software used the recorded values to produce a trace of TG and allowed the assessment of several variables, as shown in Figure 2.7; Lag time – the time taken for TG to start, time to peak (ttPeak) – the time taken before thrombin production was at its peak rate, peak thrombin – the peak rate of thrombin production and Endogenous Thrombin Potential (ETP) – the total thrombin produced by the sample.
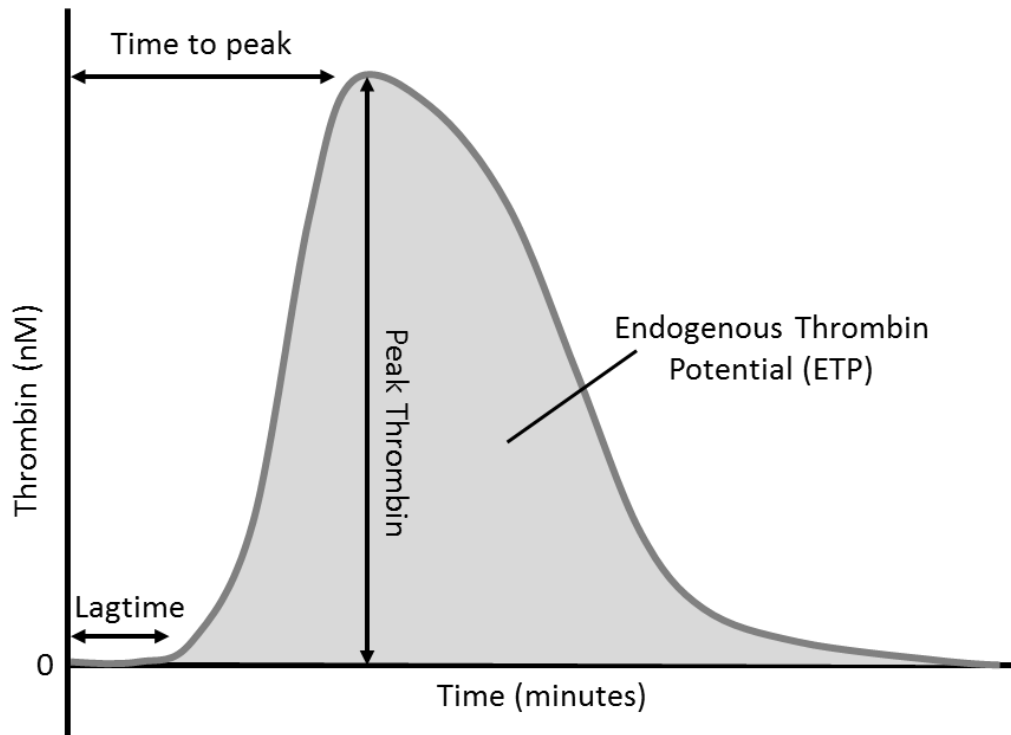
Figure 2.7 – Example of a TG assay trace *TG measures the amount of thrombin produced by a sample over time. From the trace generated by the assay it is possible to gain information on 4 metrics which are sensitive to different things in the assay. The time taken for TG to initiate is termed 'Lag Time', the time taken to reach maximal TG is 'Time to peak' (or ttPeak), the maximal thrombin generated in a single measurement is the 'Peak thrombin' and the total thrombin produced, as represented by the area under the curve is the ETP.*

2.3.12 Western blotting

2.3.12.1 Protein extraction, concentration and quantification

2.3.12.1.1 Protein Extraction with RIPA buffer

RIPA buffer (50mM Tris, 150mM NaCl, 0.5% Sodium Deoxycholate, 0.1% sodium dodecylsulphate (SDS) and 1% Triton X-100) was supplemented with protease (P8340) and phosphatase inhibitor cocktails (P5726) and then either added to liquid samples containing EV in a 1:1 ratio, or directly onto cell pellets. The samples were vortexed and placed on a rocker at 4°C for 30minutes. Samples were mixed thoroughly by pipetting and then centrifuged at 12000g for 15minutes (4°C). The supernatant was retained and stored at -20°C in fresh Eppendorf tubes.

2.3.12.1.2 Concentration of protein with ethanol

Samples of extracted protein were thawed and 100% cold ethanol was added in a 5:1 ratio (v/v). The mixture was placed at -20°C for 2hours and then centrifuged at 15000g for 15minutes (4°C). The supernatant was carefully removed and the pellet was air dried. The pellet was then re-suspended in 90% cold ethanol and centrifuged at 15000g for 15minutes (4°C). The supernatant was removed and the pellet air dried to remove any ethanol. Once all ethanol had evaporated,

the pellet was re-suspended in 50μL 1% SDS in HBS, using a heat block at 50°C if necessary. The re-suspended samples were centrifuged at 10000g for 10minutes to pellet any residual particulate matter. The supernatant, comprising the concentrated protein was then stored at -20°C.

2.3.12.1.3 Protein quantification with the Detergent Compatible (DC) protein assay

The concentration of protein in the samples was quantified using the DC protein assay (Bio-Rad, Hercules, California, USA). Samples were thawed and 4μL diluted with 12μL HBS. A series of standards were prepared by diluting BSA (Thermo Fisher, Waltham, USA (A4503)) in 1% SDS in HBS (1.5, 1.25, 1.0, 0.75, 0.5, 0.25, 0 mg/mL). A 5μL aliquot of sample or standard was added to each well of a 96 well plate with each sample measured in triplicate. To each well 25μL of working reagent A' was added (20μL reagent S in 1000μL reagent A) and then 200μL of reagent B. The plate was gently agitated to mix, incubated at RT for 15minutes and then read in a Novostar microplate reader (BMG Labtech, Cary, North Carolina, USA) at 688nm. The protein standard samples were used to create a standard curve in GraphPad Prism 6. The unknown sample concentrations were interpolated from the standard curve and these values were then normalised for dilution.

2.3.12.2 Polyacrylamide Gel Preparation

Polyacrylamide gels for protein separation were prepared by hand-casting 10% (w/v) gels. Briefly 7mL of resolving gel solution (mixing 5.53mL MilliQ water, 7.5mL 1M Tris-HCl pH 8.8, 6.67mL 30% Acrylamide/Bis-solution (29:1), 200μL 10% (w/v) SDS, 100μL 10% (w/v) ammonium persulphate (APS) and 10μL N,N,N',N'-Tetramethylethylenediamine (TEMED)) was poured between a 1.5mm glass spacer plate and plain glass plate secured in a gel casting frame. Isopropanol (1mL) was poured on top to ensure a level finish and the gel was left to set (~1hour). Once the resolving gel was set, the isopropanol was poured off and washed away with MilliQ water and a 4% (w/v) stacking gel solution (7.35mL MilliQ water, 1.25mL 1M Tris-HCl pH 6.8, 1.33mL 30% Acrylamide/Bis-solution (29:1), 100μL 10% (w/v) SDS, 50μL 10% (w/v) APS and 10μL TEMED) was made up and poured on top of the resolving gel until the glass plates were completely filled. A 1.5mm well comb with either 10 or 15 wells was then inserted into the gel while it set. The combs were removed and the wells washed with MilliQ water, the finished gels were either used immediately or stored in a sealed polythene bag at 4°C overnight.

2.3.12.3 Sample preparation

25μg of sample was run per well, the volume required for this was determined by the protein concentration resulting from the DC protein assay. The sample was diluted with 5x loading

buffer (0.31M Tris-HCl pH6.8, 350mM SDS, 50% Glycerol, 0.05% Bromophenol Blue in MilliQ water) and a total volume of 40µL (10 well gel) or 25µL (15 well gel) was achieved by dilution with MilliQ water. Once the solution of sample, loading buffer and MilliQ water was mixed it was heated at 95°C for 5minutes to denature the proteins.

2.3.12.4 Gel Electrophoresis

Gels were assembled into the electrophoresis tank which was then filled with ~1 Litre 1x SDS PAGE running buffer, dilute from 5x running buffer (125mM Tris-Base, 1M Glycine, 15mM SDS in MilliQ water). The wells were loaded with denatured protein sample and 5µL of the protein standard ladder (PageRuler Plus 10-250kDa, Thermo Fisher Scientific) was added to the end well of each gel. The lid and power apparatus were hooked up to the electrophoresis tank and the gel was electrophoresed at 100v for 15minutes and then at 120v for 90-120minutes or until the samples had run to the end of the gel.

2.3.12.5 Membrane transfer

The transfer of each gel required 1 gel holder cassette, 2 fibre pads, 4 filter papers (7cm x 9cm) and 1 polyvinylidene difluoride (PVDF) membrane (7cm x 9cm) (GE Healthcare). 10minutes before the gel finished running the PVDF membrane was soaked in methanol for 20seconds, then MilliQ water for 2minutes and finally transfer buffer (25mM Tris-Base, 200mM Glycine, 10% Methanol in MilliQ water) for 5minutes. Simultaneously the filter paper and fibre pads were soaked in transfer buffer for 5minutes.

After the gel had finished running the front glass plate was removed and the stacking gel section was discarded. The resolving gel was rinsed in transfer buffer and the transfer apparatus was setup within the cassette. From the bottom upwards; transfer cassette, fibre pad, 2 x filter paper, polyacrylamide gel, PVDF membrane, 2 filter papers, fibre pad and the other side of the transfer cassette. After the second set of filter papers were added the apparatus was gently rolled to remove any air bubbles. The completed cassette was loaded into the transfer apparatus ensuring that the current would run from the polyacrylamide gel towards the PVDF membrane. The tank was filled with ~1litre transfer buffer and the apparatus was run at 63v for 75minutes. Whilst running the transfer apparatus was kept cool with an ice pack.

2.3.12.6 Immunodetection

Following transfer, the PVDF membrane was washed in Tris-buffered saline with tween (TBS.Tween) (25mM Tris-Base, 0.14M NaCl, 2.5mM KCl and 0.1% Tween 20 (Polyoxyethylene sorbitan monolaurate) in MilliQ water) and then transferred to blocking buffer (TBS.Tween and

5% (w/v) Marvel milk powder (Premier International Foods Ltd, Long Sutton, UK)). The membrane was incubated overnight in the blocking solution at 4°C and then rinsed in TBS.Tween, followed by a 15minute wash on a shaker and 2x10minute washes in TBS.Tween. Primary antibodies to CD63 (in-house monoclonal, antibody culture supernatant used at 1:5 dilution) [Clone: RFAC4] and Heat-shock protein 70 (HSP70) (System Biosciences, used at a 1:1000 dilution) were prepared through dilution in blocking buffer to a total volume of 15mL per membrane. The primary antibody solution was added to the membrane and incubated at RT for 1hour.

The membrane was rinsed twice in TBS.Tween and then washed twice for 15minutes and twice for 5minutes in TBS.Tween on a shaker at RT. During the final wash the secondary antibodies were prepared, a Sheep Anti-Mouse IgG, Horseradish Peroxidase (GE Healthcare, Little Chalfont, UK, used at a 1:7500 dilution) [clone: NA931] for the CD63 primary antibody (Chronos et al., 1993) and Goat anti-Rabbit IgG, Horseradish peroxidase (System Biosciences, used at a 1:20000 dilution) for the HSP70 primary antibody, in a total volume of 15mL of blocking buffer. The secondary antibody was then added to the PVDF membrane and incubated for 1hour at RT. Following incubation the membrane was rinsed twice in TBS.Tween and then washed twice for 15minutes and 4x5minutes in TBS.Tween on a shaker at RT.

While the last wash was being carried out the chemiluminescent western blotting detection reagent (Amersham ECL Prime Western Blotting detection reagent, GE Healthcare) was prepared. Once the washing was complete each membrane was incubated with 2mL of the detection reagent for 1minute. The excess solution was then removed and the membrane was placed between 2 polythene sheets and excess solution gently rolled out. The membrane was immediately imaged on an ImageQuant Las 4000 (GE Healthcare) using the chemiluminescence setting and an exposure time appropriate for the membrane.

2.3.12.7 Secondary only controls

An extra two lanes containing 5μL of protein standard ladder (PageRuler Plus, 10-250kDa) and 25μg of platelet protein (extracted with RIPA buffer from the platelet pellets of 12 pooled samples) were run where appropriate to act as a secondary only control. These were transferred onto the same PVDF membrane and then cut away. They were treated identically except for the primary antibody stage where they were incubated in blocking solution without antibody instead of with a primary antibody. They were developed at the same time and this allowed the identification of non-specific binding.

2.4 Results

2.4.1 Preliminary results

Initial experiments were carried out to optimise protocols for flow cytometry, NTA and the use of ExoQuick to isolate EV. Washed platelets were stimulated with CRP-XL, thrombin and PAR1-AP alone or in combination and then analysed. Flow cytometry was used to observe platelet degranulation and PS exposure on EV and NTA to determine EV size distribution and concentration.

2.4.1.1 Flow cytometry and NTA

Preliminary experiments confirmed that the protocol used to wash platelets, as outlined in 2.3.5, yielding unactivated platelets that were able to respond to stimulation with agonists. Figure 2.8 shows that only 5.3% of platelets were activated during isolation, as determined by flow cytometric detection of P-selectin, and there was no increase in Annexin-V binding beyond the isotype control. In addition only low levels of constitutive EV release were observed by NTA.

Figure 2.8A also demonstrates that platelets activated with CRP-XL (2µg/mL), thrombin (0.32U/mL) and PAR1-AP (10µM) became activated, as indicated by significantly increased P-selectin expression due to degranulation. Over 85% of platelets expressed P-Selectin when stimulated with these concentrations of agonists demonstrating that they caused maximal activation. Activation with CRP-XL also generated significantly more microvesicles, as measured by Annexin-V binding to EV, compared to resting samples (28.2% vs 2.96%; p=<0.0001) (Figure 1.8B), or compared with stimulation with PAR1-AP or thrombin (28.2% vs 6.18% and 7.5% respectively; p=<0.0001 for both). However stimulation with thrombin or PAR1-AP resulted in the release of significantly more Annexin-V binding microvesicles than in resting samples (6.18% and 7.5% vs 2.96%,p=<0.001 and p=<0.01 respectively).

NTA analysis also revealed differences between the EV released through stimulation of the GPVI receptor by CRP-XL and those released in response to PAR activation, Figure 2.8C. PAR1-AP stimulation resulted in the highest concentrations of vesicle release and had a mode particle size of ~200nm. However in response to stimulation with thrombin the concentration of EV released was almost 60% less than that with CRP-XL, and the mode particle size was significantly lower at ~100nm. When the agonists were used in combination; CRP-XL + PAR1-AP resulted in EV release that was very similar to that seen with either agonist alone, however the addition of thrombin to CRP-XL or PAR1-AP resulted in a vesicle population resembling that observed with thrombin alone. These experiments suggest that platelets release different populations of EV in

response to stimulation with different agonists. Further experiments were carried out to define the contribution of microvesicles and exosomes to these different populations.
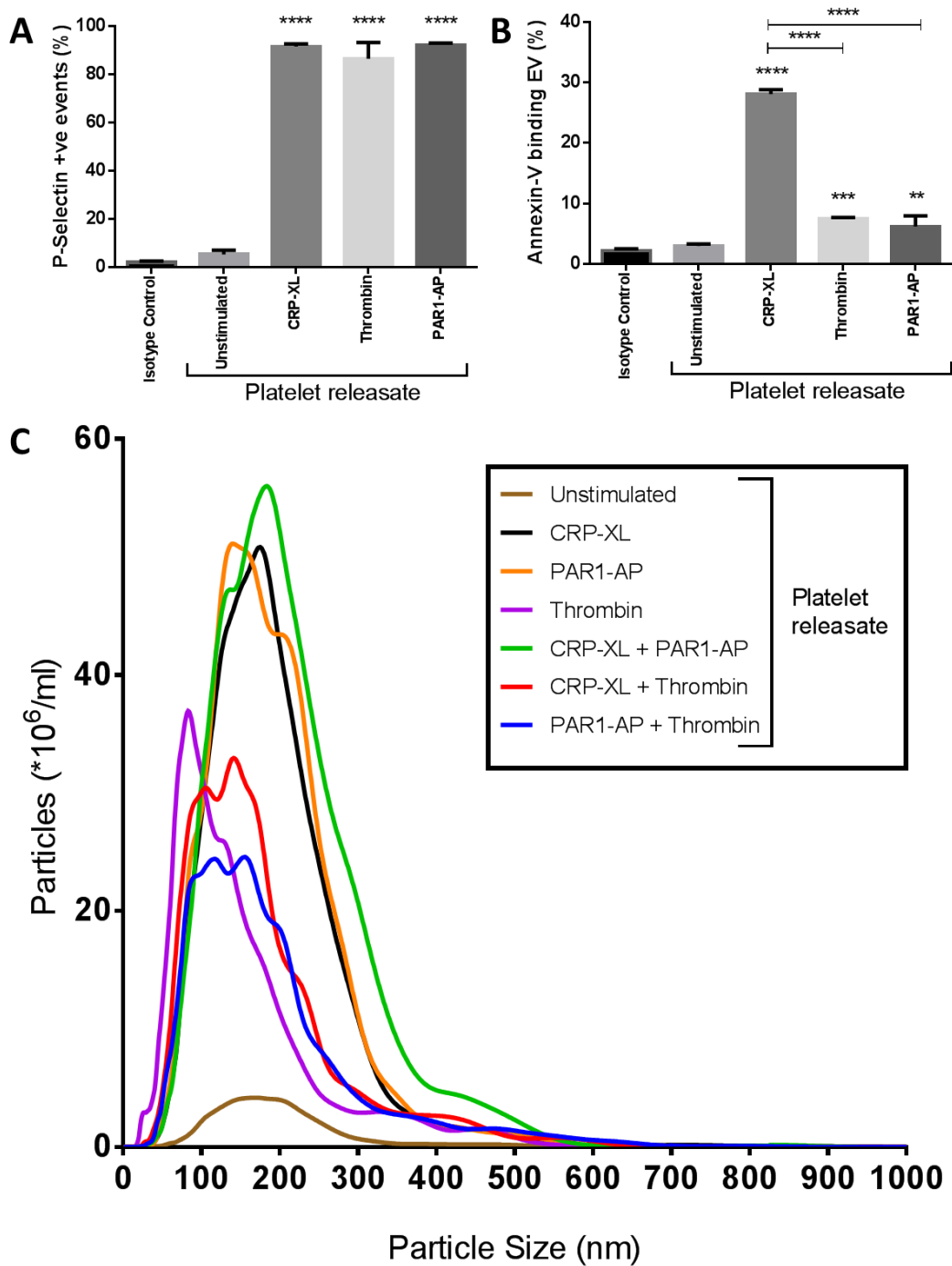
Figure 2.8 – Flow cytometry and NTA data from preliminary EV experiments Washed platelets (250 x 10³/µL) were activated with CRP-XL (2µg/mL), PAR1-AP (10µM) and thrombin (0.32U/mL), alone and in combination. A) Platelet activation was measured via P-selectin using flow cytometry (n=5+/-SD, One Way ANOVA with Tukey's correction), B) Annexin-V expressing microvesicles were detected with flow cytometry using Annexin-V binding (n=5+/-SD, One Way ANOVA with Tukey's correction) and C) the size distribution and concentration of the pdEV were measured using NTA (n=6) (* p=<0.05, ** p=<0.01, *** p=<0.001, **** p=<0.0001).

2.4.1.2   Using ExoQuick to isolate EV

An initial aim was to determine the localisation of microRNA within EV populations and this required the separate isolation of exosomes from microvesicles. ExoQuick is a reagent that isclaimed to specifically isolate exosomes from solutions such as plasma using a proprietary polymer (Taylor and Shah, 2015) without the need for ultracentrifugation. The data in Figure 2.9 demonstrates the use of ExoQuick and its effect on EV size and concentration.
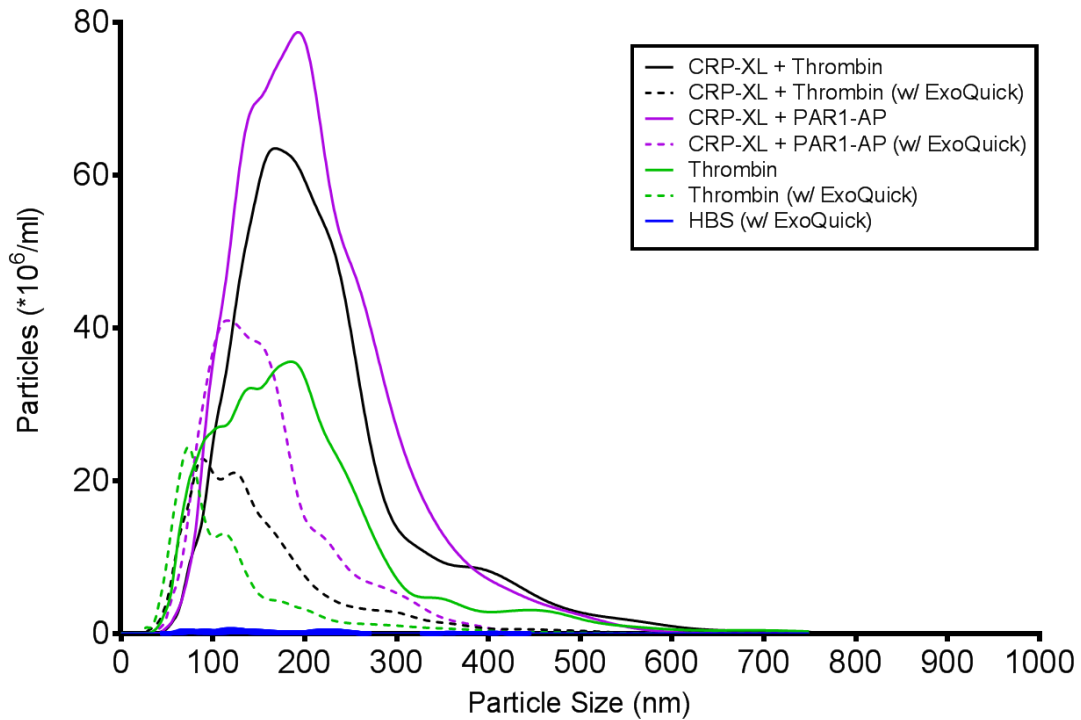
Figure 2.9 – Nanosight traces of EV before and after treatment with ExoQuick Washed platelets (250 x 10^3/µL) were activated with CRP-XL (2µg/mL) + thrombin (0.32U/mL), CRP-XL (2µg/mL) + PAR1-AP (10µM) or thrombin (0.32U/mL) alone and then incubated in buffer or ExoQuick overnight. The resulting EV population was measured using NTA (n=4).

Samples of pdEV rich supernatant were incubated overnight with ExoQuick at 4°C, and then centrifuged to pellet exosomes captured by ExoQuick (2.3.8.2). The pellet was re-suspended in HBS and analysed alongside an identical sample that had not been treated with ExoQuick using NTA. Samples of exosomes isolated with ExoQuick showed a reduction in mode EV size and a substantial reduction in concentration compared to the untreated samples. The pdEV generated by thrombin or by CRP-XL + thrombin and incubated with ExoQuick appeared similar; both had mode vesicle sizes of 89nm and the NTA traces showed almost identical EV size distribution. pdEV generated using CRP-XL + PAR1-AP also changed following incubation with ExoQuick but compared to samples generated with thrombin or CRP-XL + thrombin the mode EV size was larger (121nm), and EV concentration was significantly higher but with a similar size distribution. This suggested that ExoQuick was able to effectively isolate exosome sized vesicles from samples

generated through platelet activation with thrombin or thrombin + CRP-XL, but not PAR1-AP + CRP-XL but the specificity of this was not checked with exosomal markers.

2.4.2 Further characterisation of EV

Following these initial studies it appeared that different agonists may be able to trigger the release of different EV populations, making this a plausible method for separate isolation of microvesicles and exosomes. Thrombin caused the release of smaller EVs, suggesting it was potentially a trigger for exosome production; thrombin acts at the PAR1 and 4 receptors and to explore this in further experiments platelets were stimulated through each of these receptors using specific peptides (PAR1-AP and PAR4-AP). CRP-XL was used to target the GPVI receptor and ADP was introduced to activate platelets via the P2Y1 and P2Y12 receptors.
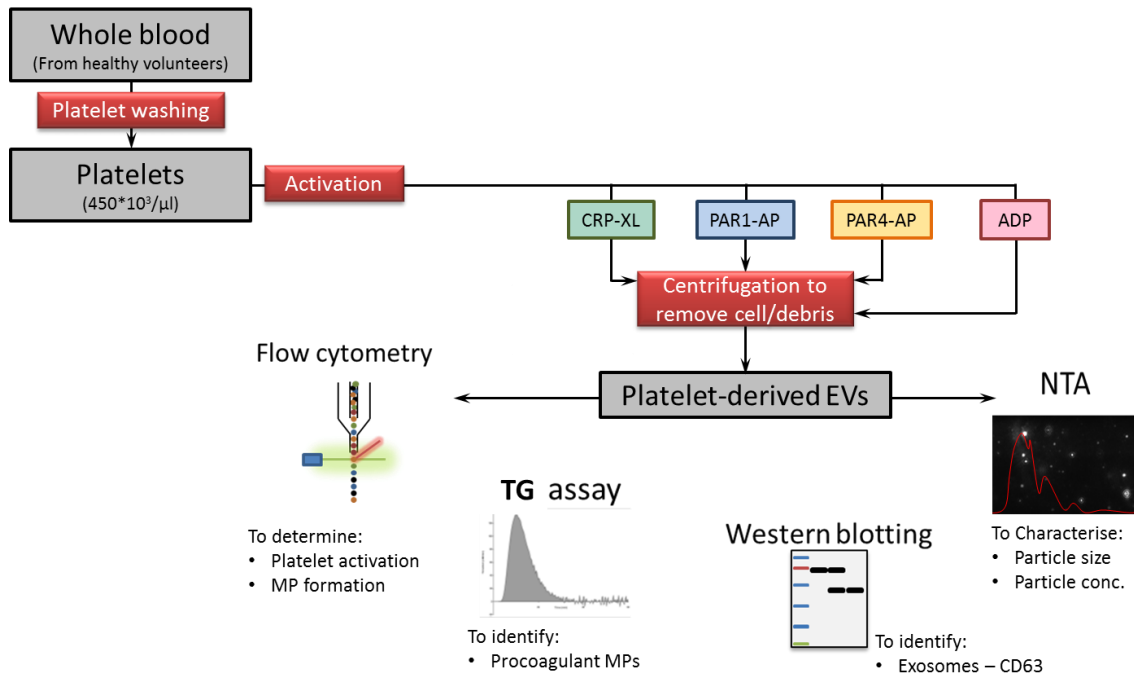
Figure 2.10 – Extracellular vesicle generation, isolation and characterisation workflow *A schematic to show the steps taken to produce and characterise EV. Platelets were isolated from whole blood and then activated with a variety of agonists. Differential centrifugation was used to remove platelets and cell debris before EV samples were analysed using flow cytometry, the TG assay, Western blotting and NTA.*

The overall workflow for the characterisation of pdEV is shown in Figure 2.10. In brief, platelets were isolated from healthy volunteers using the protocol outlined in 2.3.5. The washed platelets were made up at $450 \times 10^3/\mu L$ and then activated with the selected agonists for 10minutes at 37^oC to trigger EV release. The resulting samples were centrifuged as described in 2.3.8.1, and the EV rich supernatant was characterised. Flow cytometry was used to identify Annexin-V binding microvesicles, the TG assay was used to detect procoagulant microvesicles, western blotting to identify the exosomal markers CD63 and HSP70 and NTA to quantify EV size distribution and concentration.

2.4.2.1 Flow Cytometry

2.4.2.1.1 P-Selectin expression on activated platelets
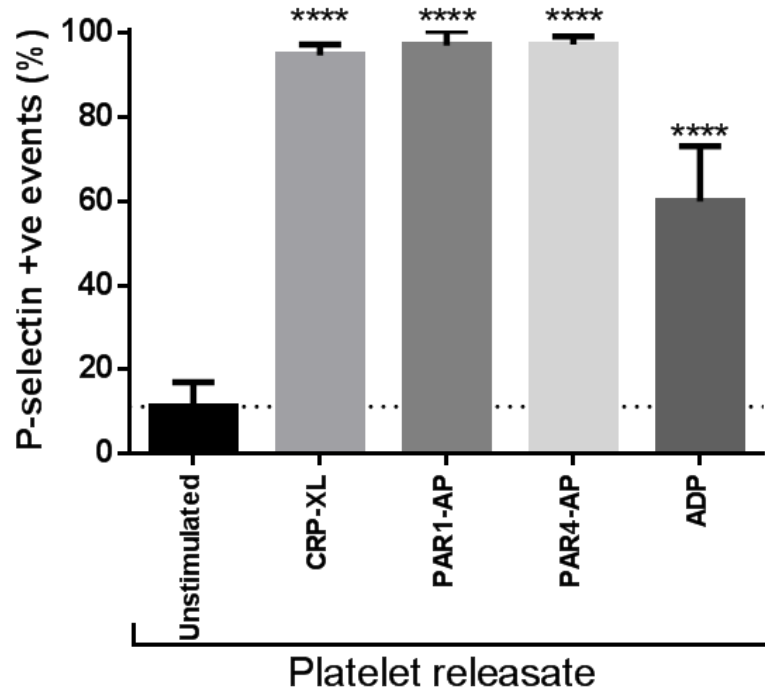
Figure 2.11 – P-selectin expression on platelets following activation *Washed platelets (250 x 10³/µL) were activated with CRP-XL (2µg/mL), PAR1-AP (10µM), PAR4-AP (200µM), ADP (50µM) or left unstimulated and then analysed for P-selectin expression using flow cytometry (n=6+/-SD, One Way ANOVA with Tukey's correction) (* p=<0.05, ** p=<0.01, *** p=<0.001, **** p=<0.0001).*

P-Selectin was measured by flow cytometry as previously described, 2.3.9.1. The data in Figure 2.11 indicates that for this experiment the isolation of platelets from whole blood did not cause significant activation or degranulation with only 11.2% of resting platelets positively expressing P-Selectin. Over 90% of isolated platelets stimulated with CRP-XL, PAR1-AP and PAR4-AP expressed P-selectin whilst 60% of platelets stimulated with ADP positively expressed P-selectin. Agonists were titrated for optimal activation, therefore these values represent maximal P-selectin expression in response to each agonist. ADP is a weaker platelet agonist and, as has been previously shown, generates lower levels of P-selectin expression in response to platelet stimulation (Janes et al., 1994).

2.4.2.1.2 Annexin-V binding to microvesicles

In the absence of activation only 4% of released EV were found to be Annexin-V binding microvesicles exposing negatively charged phospholipids. When platelets were stimulated through GPCRs with PAR1-AP, PAR4-AP or ADP that activate the platelets through the PLC-β pathway, there was no significant change in the number of Annexin-V+ve events. However when

platelets were stimulated via the GPVI receptor with CRP-XL, which acts through the PLC γ pathway, there was a significant release of platelet-derived microvesicles that bound Annexin-V. Over 42% of the EV released from platelets stimulated with CRP-XL were Annexin-V positive, which was a significant increase over the resting platelets ($p = <0.01$) and all other agonists ($p = <0.05$). This demonstrated that stimulation with CRP-XL produced significantly more Annexin-V+ve microvesicles than all other agonists.
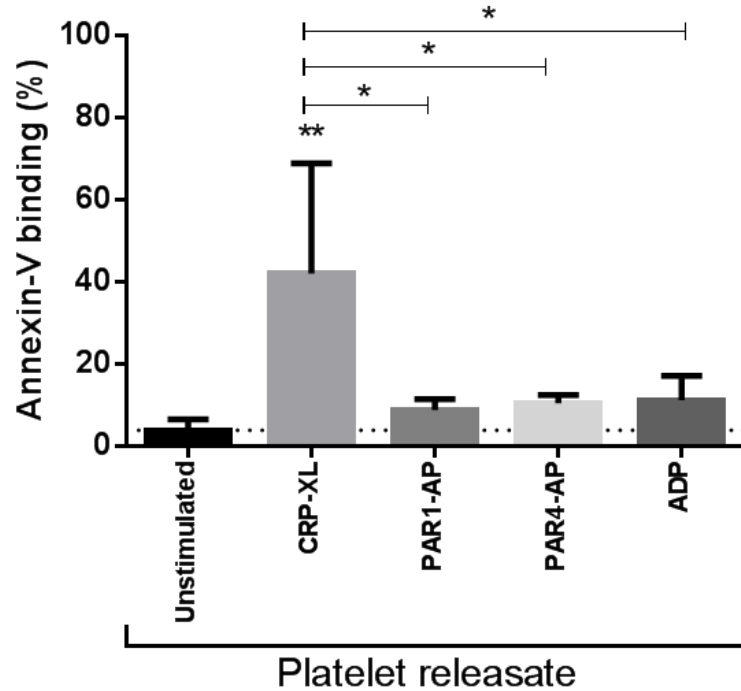
Figure 2.12 – Annexin-V binding to EV generated by stimulating platelets Washed platelets (250 x 10^3/µL) were activated with CRP-XL (2µg/mL), PAR1-AP (10µM), PAR4-AP (200µM), ADP (50µM) or left unstimulated and then analysed using flow cytometry. EV were gated and Annexin-V binding was measured by flow cytometry (n=5+/-SD, One Way ANOVA with Tukey's correction) (* $p = <0.05$, ** $p = <0.01$, *** $p = <0.001$, **** $p = <0.0001$).

2.4.2.2 Analysis of pdEV by NTA

NTA was used to determine the concentration and size distribution of EV released from platelets. Samples were diluted to optimal concentrations and then measured using the Nanosight NS500, as described in 2.3.10. Figure 2.13A shows that CRP-XL caused the release of significantly more EV than resting platelets and an observable but not significant increase beyond the other agonists. PAR1-AP, PAR4-AP and ADP did not have a significant effect on EV release beyond the control. Figure 2.13B shows that almost all samples had a similar mode EV size to resting platelet samples. The only agonist that appeared to show a change from the normal mode vesicle size was ADP; however this was a variable and therefore not significant,

the extent of this is shown in Figure 2.13C. The large SD bars for the vesicle concentration and mode size demonstrated the variability between individual donors particularly with reference to the response to CRP-XL. This probably reflects the known inter-individual differences in GPVI response related to genetic polymorphisms (Jones et al., 2009, Joutsi-Korhonen et al., 2003). Overall the Nanosight data showed that there was a clear increase in the number of EV released following platelet stimulation, but the size profile of these EV was not agonist dependent. However pdEV concentration did vary between agonists, with a significantly higher number observed following stimulation with CRP-XL. However this technique did not allow for the observation of differences between microvesicle and exosome contributions to each agonist's pdEV population.
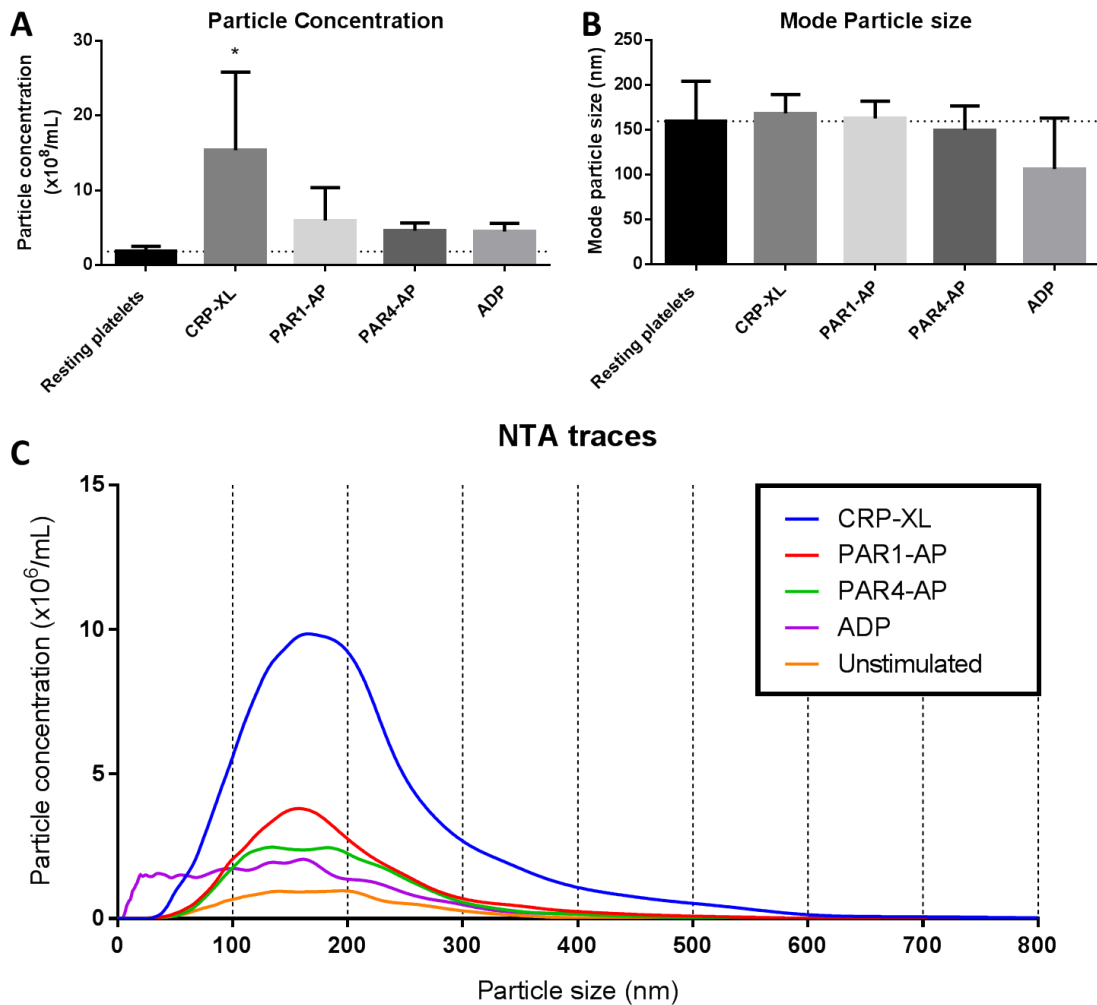
Figure 2.13 – NTA of pdEV *Washed platelets (250 x 10³/μL) were activated with CRP-XL (2μg/mL), PAR1-AP (10μM), PAR4-AP (200μM), ADP (50μM) or left unstimulated and resulting samples were differentially centrifuged to produce an EV rich supernatant which was measured using NTA and measurements corrected for sample dilutions. A) Extracellular Vesicle concentration (n=5+/-SD, One Way ANOVA with Tukey's correction) and B) mode particle size were measured using NTA (n=5+/-SD, One Way ANOVA with Tukey's correction) (* p=<0.05, ** p=<0.01, *** p=<0.001, **** p=<0.0001). C) Shows the average size distribution in all samples (n=5).*

2.4.2.3   Analysis of the thrombin generating potential of pdEV

The TG assay was used to observe the amount of procoagulant microvesicles in pdEV samples. The PRP reagent was used to trigger TG in the assay; it contains TF but minimal amounts of phospholipid meaning the generation of thrombin is reliant on the negatively charged phospholipids exposed on the membranes of microvesicles. EV concentrations were measured using the Nanosight and the samples were standardised by diluting with PBS to 2×10^8 EV/mL for each sample. This ensured that any observed changes were due to differences in the presence of microvesicles and the associated negatively charged phospholipids rather than the total number of EV in the sample. The assay measured the amount of thrombin generated over time and this is plotted as a curve in Figure 2.14E. From the trace the samples relative attributes (as outlined in Figure 2.7) can be determined (Figure 2.14A-D).

Microvesicle detection using the PRP reagent is most sensitive to the peak thrombin (Figure 2.14A) and ETP (Figure 2.14D) metrics. The peak thrombin showed a pattern very similar to that observed with the Annexin-V binding assay (Figure 2.12). All agonists gave a significantly higher peak thrombin value than the resting platelet control (CRP-XL – 161.47nM, PAR1-AP – 50.90nM, PAR4-AP – 35.24nM and ADP – 67.20nM vs resting – 19.83nM, p=<0.0001 for all) but CRP-XL generated significantly more thrombin than the other agonists (p=<0.0001). This pattern was similar for the ETP data, however the differences in ETP between the different agonists were not as marked (CRP-XL – 2084nM/min, PAR1-AP – 1207nM/min, PAR4-AP – 730nM/min and ADP – 1455nM/min vs resting – 410nM/min, p=<0.0001 for all). Despite their insensitivity to the presence of differences in phospholipid the ttPeak (CRP-XL – 14.24min vs resting – 17.14minutes, p=<0.0001) and lag time (CRP-XL – 6.23min vs resting – 7.34minutes, p=<0.0001) showed a significant reduction with the CRP-XL stimulated EV and a slight but not significant increase with PAR1-AP and PAR4-AP.

The TG assay data again showed that pdEV generated with all agonists contain microvesicles that express negatively charged phospholipids on their surface. However, CRP-XL produced significantly more microvesicles than the other agonists.
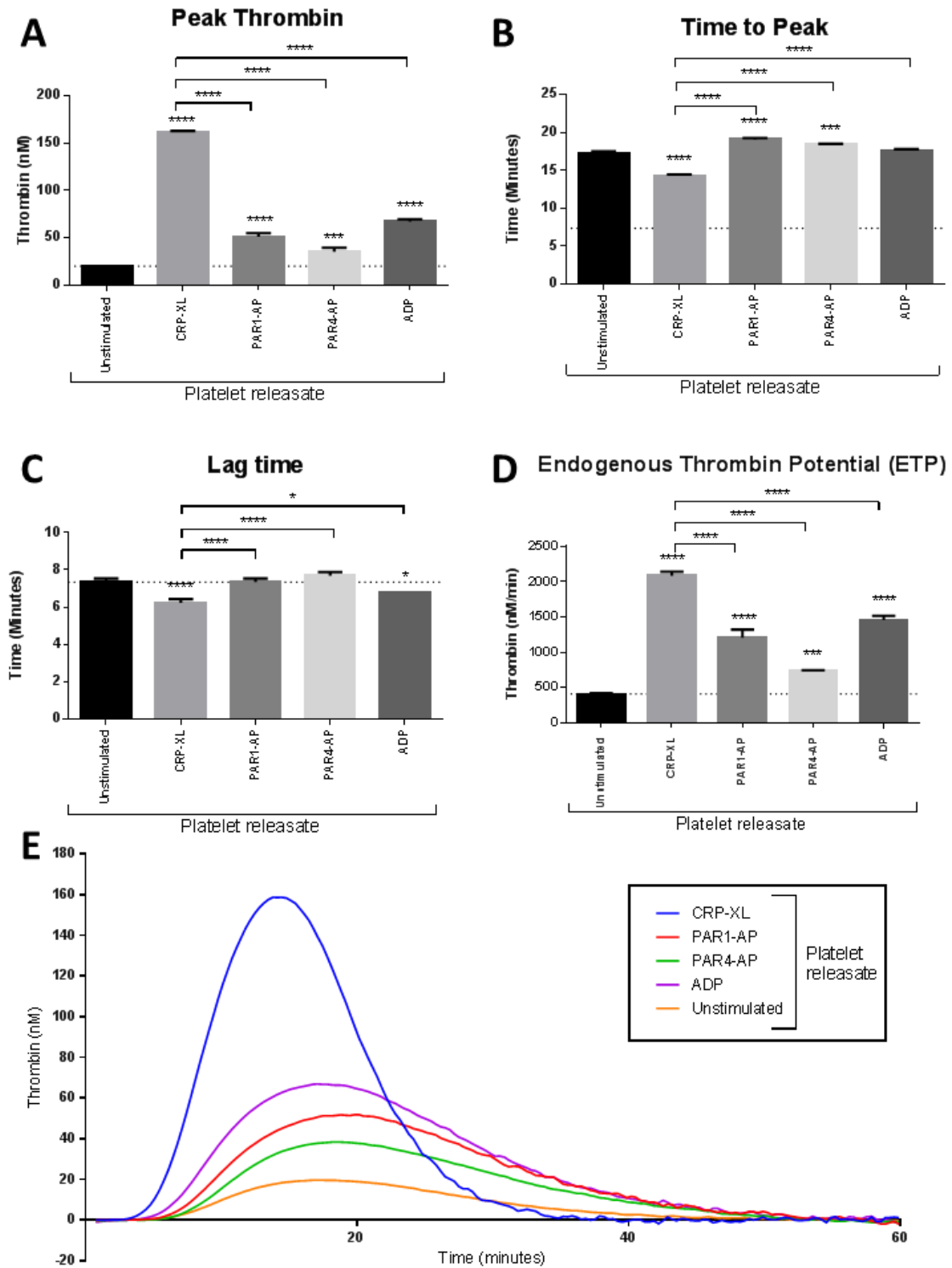
Figure 2.14 – TG assay analysis of pdEV Washed platelets (250 x 10^3/μL) were activated with CRP-XL (2μg/mL), PAR1-AP (10μM), PAR4-AP (200μM), ADP (50μM) or left unstimulated and then EV were isolated using differential centrifugation. Phosphatidylserine exposing microvesicles were measured using the TG assay to identify A) the peak thrombin, B) the ttpeak thrombin, C) the lag time and D) the ETP (n=5+/-SD, One Way ANOVA with Tukey's correction) (* p=<0.05, ** p=<0.01, *** p=<0.001, **** p=<0.0001). E) Shows the average TG trace for each sample.

2.4.2.4   Western blotting for exosomal markers in pdEV

Western blotting was used to detect the exosomal marker, CD63. Protein lysates from pdEV samples were prepared as described in 2.3.12.1 and then Western Blotting was performed as described in 2.3.12. The results in Figure 2.15 demonstrate the presence of CD63 in pdEV samples generated by all tested agonists. The smeared band in all lanes was typical of western blotting for CD63 as it has 3 N-linked glycosylation sites which can be differentially glycosylated. The concentration of CD63 detected in the samples is highest in the EV derived from platelets stimulated with CRP-XL with platelets showing the next highest concentration and PAR1-AP, PAR4-AP and ADP having very similar concentrations.

The second blot showed the absence of the CD63 monoclonal primary antibody. This blot acted as a control to ensure the protein detected on the first blot is specifically the secondary antibody bound to the CD63 primary antibody and not just non-specific binding of the secondary antibody. There was no non-specific binding and therefore the protein detected by the primary antibody in the first blot is CD63. This data indicates that all of the pdEV samples were positive for the exosomal marker CD63, and therefore contained exosomes. Although only partially quantitative there appeared to be greater numbers of CD63+ve EVs (i.e. exosomes) released in response to CRP-XL than to the other agonists, and that ADP was more effective at generating exosomes than either PAR-AP on its own.
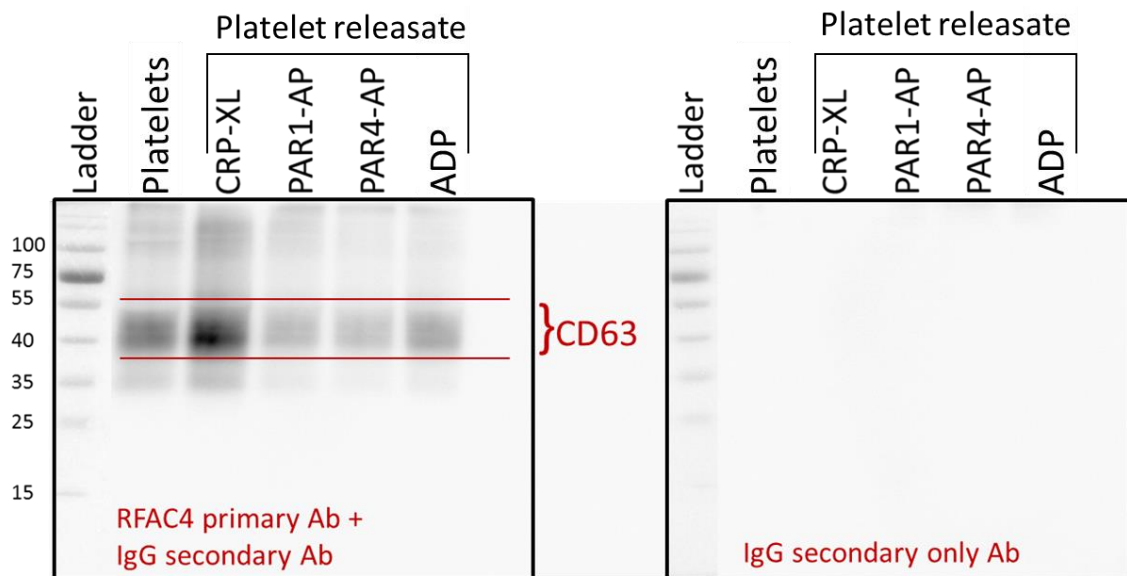
Figure 2.15 – Western Blot for CD63 on pdEV *Washed platelets (450 x 10^3/µL) were activated with CRP-XL (2µg/mL), PAR1-AP (10µM), PAR4-AP (200µM) or ADP (50µM) and then EV were isolated using differential centrifugation. The exosomal marker CD63 was detected using Western Blotting with 25µg of protein from each condition and whole platelet lysate (representative of multiple blots).*

2.4.3 Effects of anti-platelet agents on EV release from platelets

Following the characterisation of pdEV generated with different agonists the results showed that different activation pathways lead to the release of different EV populations. All agonists were found to stimulate the release of both procoagulant microvesicles and exosomes; CRP-XL released the highest concentration of both and caused significantly greater procoagulant activity whilst the other agonists released populations predominantly comprised of exosomes. In these previous experiments there was no control of secondary pathways such as the ADP released from platelets upon activation which may feed back onto the cells. Therefore, to dissect the EV release pathways more precisely, specific inhibitors were utilised to isolate parts of the activation pathway that may be influencing the release of EVs. Figure 2.16 details the anti-platelet agents used and their targets; hirudin to inhibit thrombin, apyrase to inhibit ADP, aspirin to inhibit thromboxane and RFGP56 to inhibit outside-in signalling through the GPIIb-IIIa receptor.
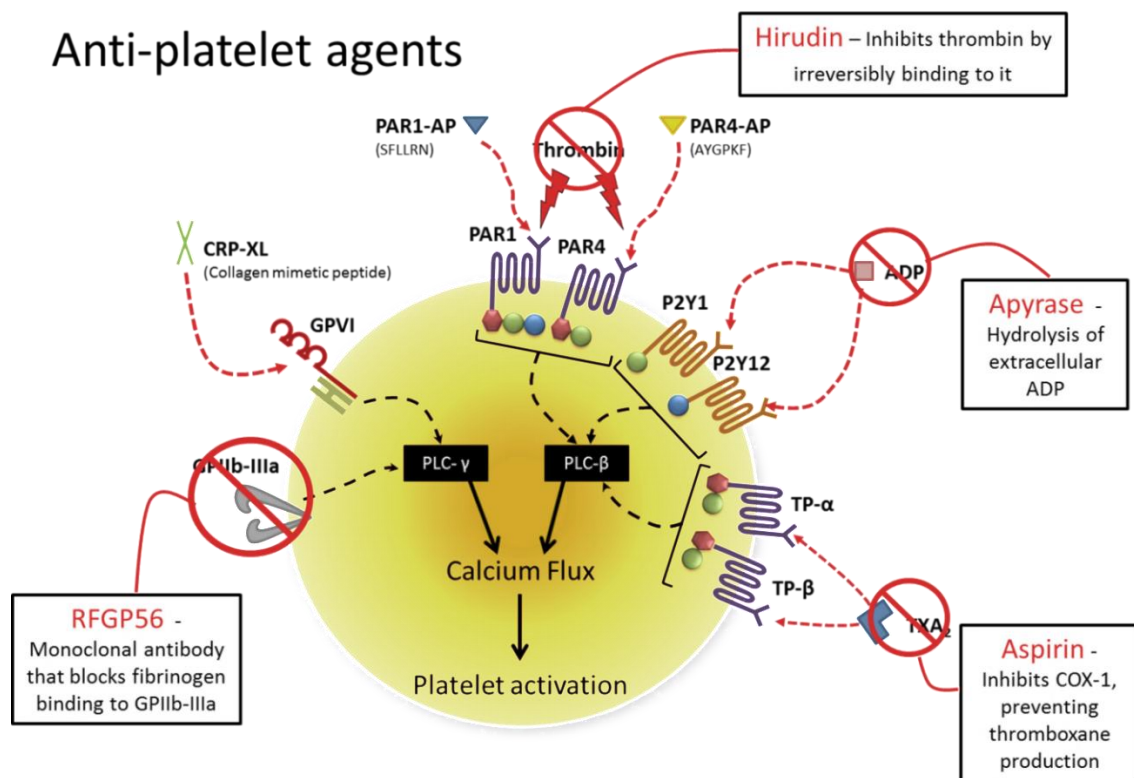
Figure 2.16 – Anti-platelet agents used to investigate the release of EV from platelets A representation of the platelet receptors targeted by the agonists and inhibitors used in proceeding experiments.

The inhibitors were used alongside the previously used agonists and the resulting EV samples were characterised as before. This allowed for the characterisation of both microvesicles and exosomes and any differences that might occur due to the use of the inhibitors. The results for inhibition with aspirin and apyrase are shown in detail below in Figures 1.16 to 1.22. There were

no effects with Hirudin or RFGP56 but the results for these are shown in the summary table (Table 2.2).

2.4.3.1 Flow cytometry of pdEV samples with inhibitors present

2.4.3.1.1 P-Selectin expression

Platelet activation with CRP-XL was not significantly affected by aspirin or apyrase, although apyrase did cause a 20% reduction in P-selectin exposure (Figure 2.17). Inhibition with aspirin caused no change in platelet activation following stimulation with PAR1-AP, however apyrase caused a significant reduction in P-selectin expression (58%, p=<0.01). The inhibitors demonstrated a very similar pattern of effect on platelets stimulated with PAR4-AP; aspirin had no effect and apyrase caused a 59% reduction (p=<0.001). When platelets were stimulated with ADP, apyrase unsurprisingly caused a significant reduction in P-selectin expression, 75% (p=<0.0001). There was also a noticeable reduction of 27% when the platelets were inhibited with aspirin. Overall apyrase caused significant reductions in P-selectin expression against the weaker agonists (PAR1-AP, PAR4-AP and ADP), but the effect was marginal when platelets were stimulated with CRP-XL.

Figure 2.17 – Relative change in P-selectin expression following inhibition of platelets Washed platelets (250x10³/µL) were activated with CRP-XL (2µg/mL), PAR1-AP (10µM), PAR4-AP (200µM), ADP (50µM) or left unstimulated in buffer or in the presence of aspirin (500µM) or apyrase (80µg/mL). Platelet activation was measured via P-selectin expression using flow cytometry, results were normalised by agonist to the uninhibited sample and are shown as a relative change from the uninhibited samples (n=6+/-SD, Plotted as a Min to Max box and whisker plot with median, One Way ANOVA with Tukey's correction) (* p=<0.05, ** p=<0.01, *** p=<0.001, **** p=<0.0001).

2.4.3.1.2 Annexin-V binding

Platelets stimulated with CRP-XL had previously been shown to release the highest concentration of Annexin-V binding microvesicles (Figure 2.12) and inhibition with apyrase

before activation with CRP-XL resulted in a 59% reduction in microvesicle release (p=<0.001). But microvesicle release was not significantly reduced by apyrase in platelets stimulated with PAR1-AP, PAR4-AP and ADP. The concentration of microvesicles released by PAR1-AP, PAR4-AP and ADP without inhibitors was lower than with CRP-XL as shown in Figure 2.12 suggesting that a reduction from this baseline would be difficult to detect. The release of Annexin-V binding microvesicles from activated platelets was not inhibited by aspirin.
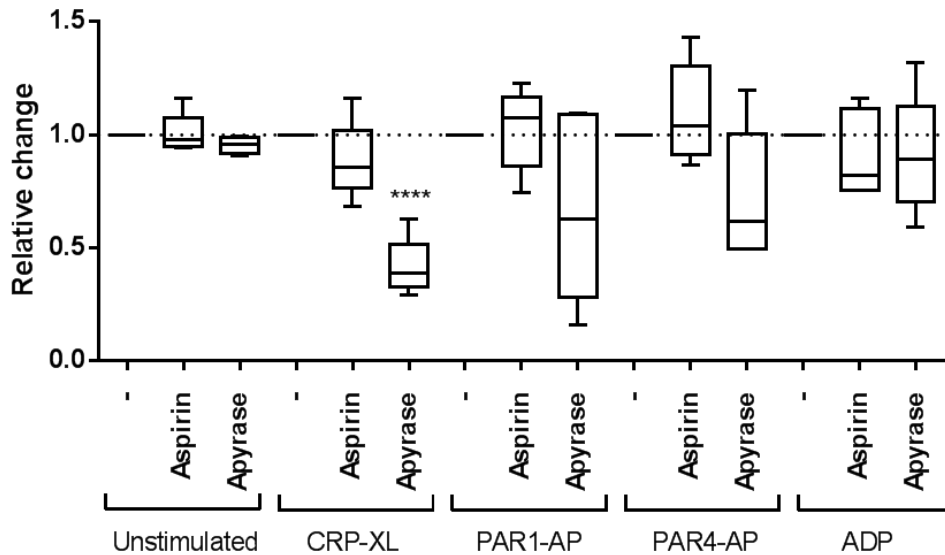
Figure 2.18 – Relative changes in Annexin-V binding on platelet-derived Extracellular vesicles inhibited with apyrase or aspirin Washed platelets (250x10³/μL) were activated with CRP-XL (2μg/mL), PAR1-AP (10μM), PAR4-AP (200μM), ADP (50μM) or left unstimulated in buffer or in the presence of aspirin (500μM) or apyrase (80μg/mL). Microvesicle formation was then measured via Annexin-V binding using flow cytometry, results were normalised by agonist to the uninhibited sample and are shown as a relative change from the uninhibited samples (n=6+/-SD, Plotted as a Min to Max box and whisker plot with median, One Way ANOVA with Tukey's correction) (* p=<0.05, ** p=<0.01, *** p=<0.001, **** p=<0.0001).

2.4.3.2   NTA of pdEV samples with inhibitors present

The NTA results in Figure 2.19 demonstrate the effects of aspirin and apyrase on EV concentration (Figure 2.19A) and mode EV size (Figure 2.19B). EV generated following platelet stimulation with CRP-XL had a consistent mode particle size regardless of inhibition. Aspirin caused a slight, but variable, 15% reduction in EV concentration and apyrase caused a 63% reduction (p=<0.0001). EV from PAR1-AP stimulated platelets showed no change in mode size following aspirin inhibition whilst apyrase caused a 25% reduction (p=<0.05) but there was no significant effect on pdEV concentration. Following PAR4-AP stimulation inhibition with aspirin had no effect on mode particle size or concentration. However apyrase caused a significant reduction in EV concentration, 26% (p=<0.05) but no change in mode EV size (9%). EVs generated by ADP saw no change in mode EV size or concentration with aspirin but apyrase caused a

significant reduction in EV concentration (43%, p=<0.01), there was no effect on the mode vesicle size.

These results are also shown as Nanosight traces in Figure 2.19; clear reductions in EV concentration were caused by apyrase (dotted lines) with all agonists except PAR4-AP and the pdEV size distribution was consistent regardless of agonist and inhibitor combination. The NTA data did not reveal any clear information on the relative amounts of exosomes or microvesicles in the samples.
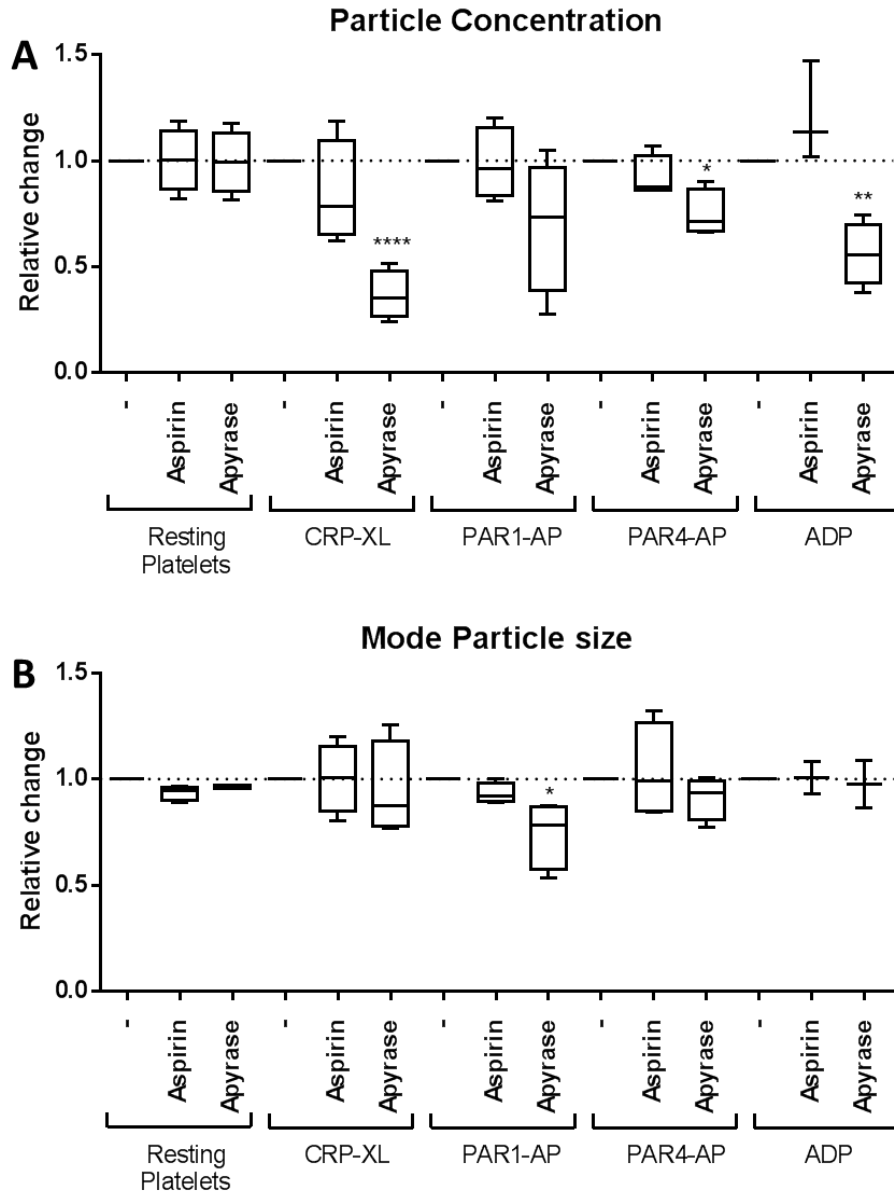
Figure 2.19 – Relative change in mode vesicle size and vesicle concentration of pdEV in response to aspirin and apyrase determined by NTA Washed platelets (250x10³/µL) were activated with CRP-XL (2µg/mL), PAR1-AP (10µM), PAR4-AP (200µM), ADP (50µM) or left unstimulated in buffer or in the presence of aspirin (500µM) or apyrase (80µg/mL). EV were then isolated via differential centrifugation and analysed for mode particle size (A) and concentration (B) using NTA, results were normalised by agonist to the uninhibited sample and are shown as a relative change from the uninhibited samples (n=6+/-SD, Plotted as a Min to Max box and whisker plot with median, One Way ANOVA with Tukey's correction) (* p=<0.05, ** p=<0.01, *** p=<0.001, **** p=<0.0001).
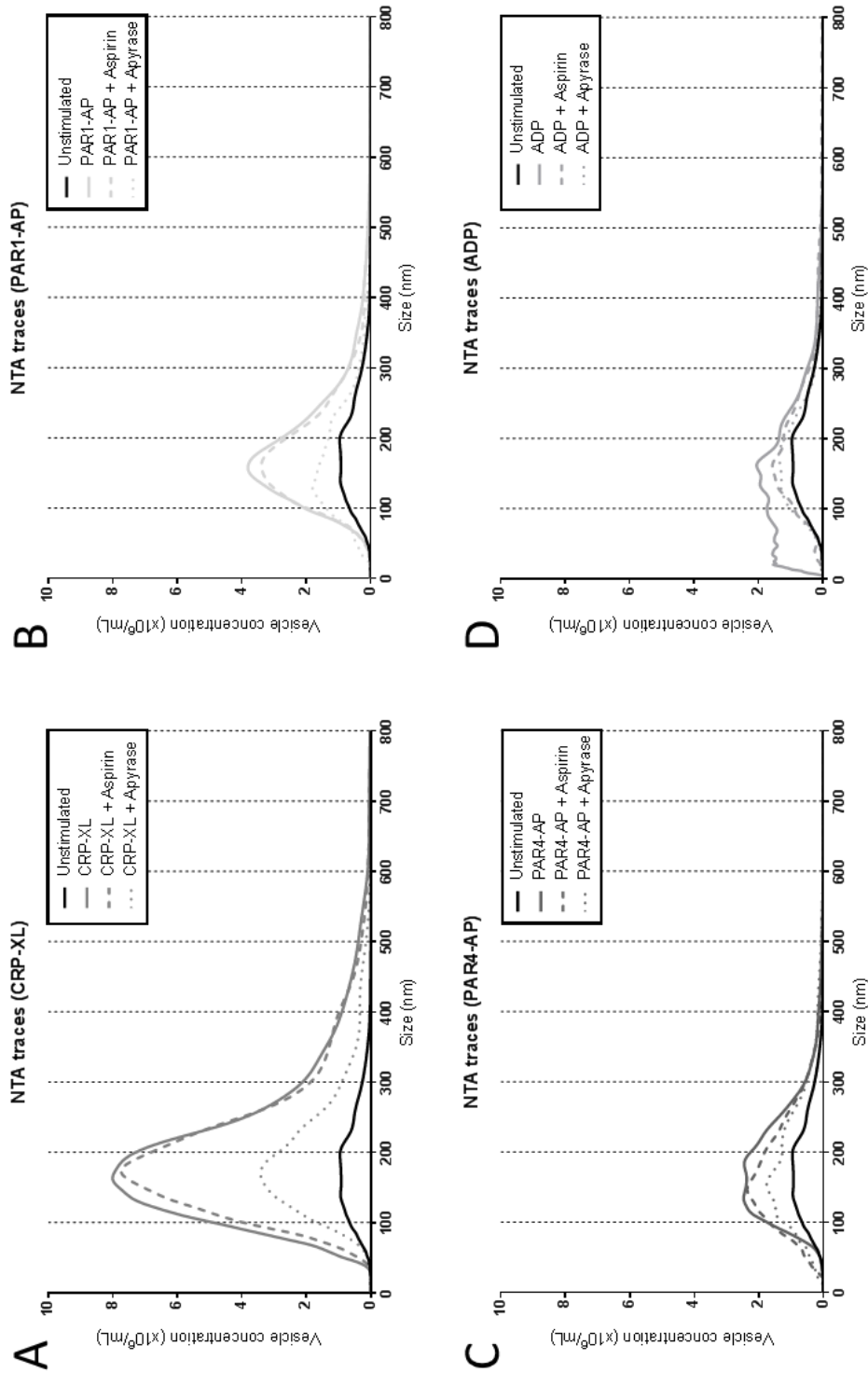
Figure 2.20 – Nanosight traces from pdEV in the presence of apyrase and aspirin *Washed platelets ($250x10^3/\mu L$) were activated with CRP-XL ($2\mu g/mL$), PAR1-AP ($10\mu M$), PAR4-AP ($200\mu M$), ADP ($50\mu M$) or left unstimulated in buffer or in the presence of aspirin ($500\mu M$) or apyrase ($80\mu g/mL$). EV were then isolated via differential centrifugation and analysed for using NTA, traces are shown for each agonist with or without inhibitors; CRP-XL (A), PAR1-AP (B), PAR4-AP (C) and ADP (D) (n=6).*

2.4.3.3   Thrombin Generation of pdEV samples with inhibitors present

The TG assay indicated that TG supported by CRP-XL generated pdEV was altered in the presence of both inhibitors. Aspirin caused significantly increased lag time (+10%, p=<0.05) and ttpeak (+21%, p=<0.0001) and decreased ETP (-6%) and peak thrombin (-37%, p=<0.0001). Apyrase caused increases in lag time and ttpeak (-19% and -32% respectively, p=<0.0001 for both) and significant reductions in peak thrombin (-65%, p=<0.0001) and ETP (-38%, p=<0.0001). These results demonstrate a significant reduction in the production of procoagulant microvesicles from CRP-XL stimulated platelets inhibited with both aspirin and apyrase.

The peak thrombin and ETP of PAR1-AP pdEV were significantly reduced with apyrase (-27% and -35% respectively, both p=<0.0001) and aspirin (-18%, p=<0.01 and -23%, p=<0.0001). There was no significant change to lag time but a significant reduction in ttpeak was observed with both inhibitors (aspirin; -6%, p=<0.01 and apyrase; -9%, p=<0.0001). PAR4-AP generated pdEV had no noticeable change in lag time, ETP and peak thrombin following inhibition with aspirin or apyrase. However ttpeak showed a significant reduction with apyrase, 7% (p=<0.001) but no change with aspirin. ADP generated pdEV were unaffected by aspirin inhibition but apyrase caused significant reductions in ETP, -42% (p=<0.0001) and peak thrombin (-41%, p=<0.0001). These results show that aspirin and apyrase caused some small but significant reductions in procoagulant microvesicle production from platelets stimulated with PAR1-AP, PAR4-AP and ADP. As with the previous assays, apyrase caused the most significant reduction in procoagulant microvesicles and the changes caused by the inhibitors were greater than observed with flow cytometry reflecting the ability of TG to analyse the full sample through changes in activity rather than analysing only detectable particles.
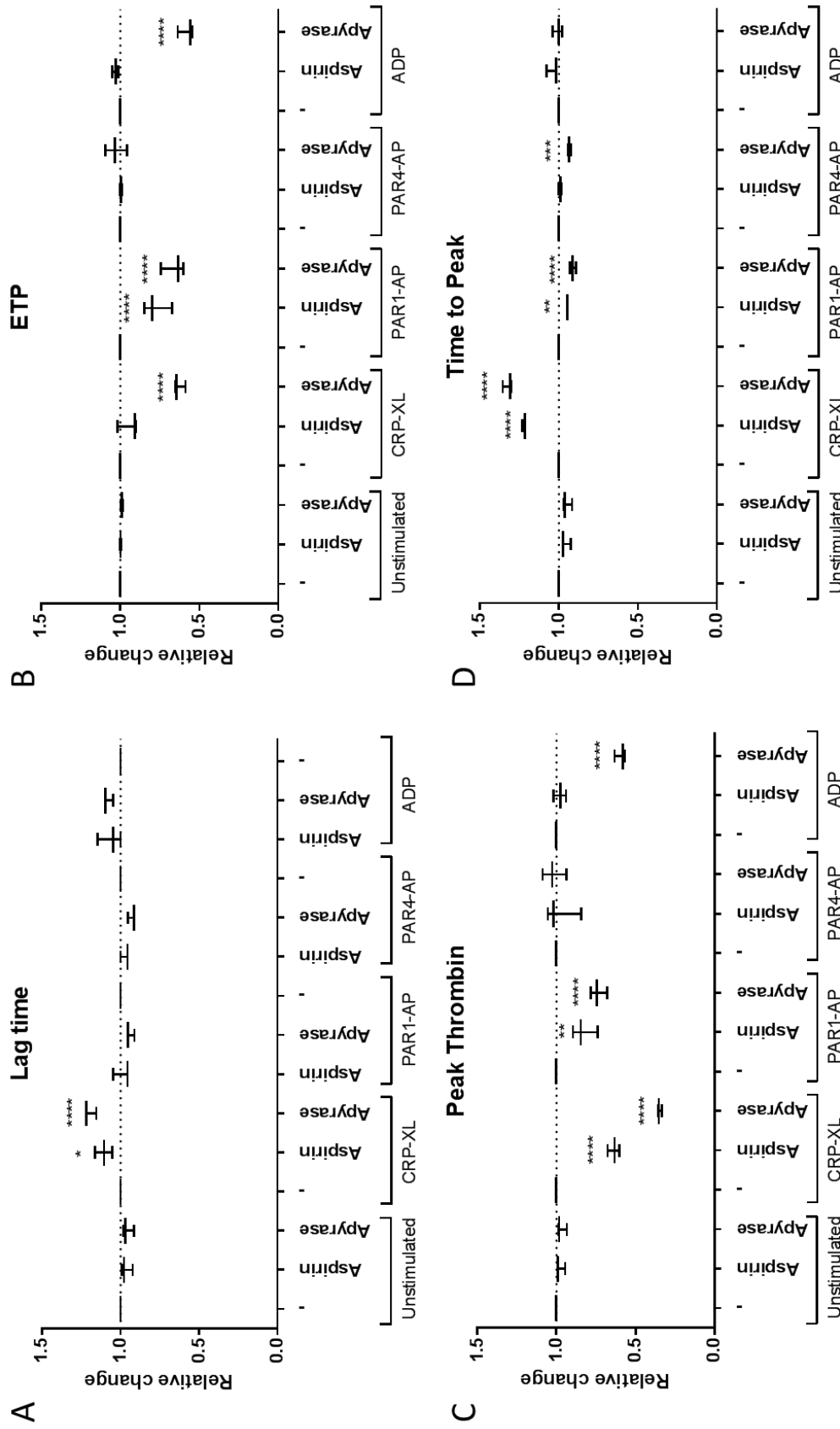
Figure 2.21 – Relative change in thrombin generating ability of platelet-derived EV due to platelet inhibition with aspirin and apyrase Washed platelets (250x10³/µL) were activated with CRP-XL (2µg/mL), PAR1-AP (10µM), PAR4-AP (200µM), ADP (50µM) or left unstimulated in buffer or in the presence of aspirin (500µM) or apyrase (80µg/mL). EV were then isolated via differential centrifugation and analysed using the TG assay, results were normalised by agonist to the uninhibited sample and are shown as a relative change from the uninhibited samples; A) lag time, B) ETP, C) peak thrombin and D) ttpeak thrombin (n=3+/-SD, Plotted as a Min to Max box and whisker plot with median, One Way ANOVA with Tukey's correction) (* p=<0.05, ** p=<0.01, *** p=<0.001, **** p=<0.0001).

2.4.3.4   Western Blotting of pdEV samples with inhibitors present

Of the inhibitors, apyrase had consistently exhibited the strongest effect on the pdEV populations whereas aspirin had only caused significant effects in the TG assay. Therefore apyrase treated samples were analysed by western blotting for the exosomal markers CD63 (Figure 2.22) and HSP70 (Figure 2.23).

2.4.3.4.1   Western blotting for CD63

CD63 appeared as a smear on the western blot (Figure 2.22A) due to the differential glycosylation of the protein, but the main band was consistently found at ~40kDa. The apyrase treated and control samples for each protein were run in adjacent lanes and this clearly showed that apyrase caused reductions in CD63. Protein levels, determined by densitometry, are shown in B and the normalised values for each agonist in C. CRP-XL samples contained the most CD63 with slightly less observed in samples released from PAR agonist stimulated samples and the level of CD63 in pdEV following ADP stimulation was the lowest and was comparable to the level observed following apyrase inhibition of the other agonists. From the normalised data it is clear that apyrase caused a significant reduction in CD63 expression in pdEV samples with all agonists (CRP-XL; -78% (p=0.0048), PAR1-AP; -86% (p=0.0109), PAR4-AP; -87% (p=0.0030) and ADP; -65% (p=0.00007). The ~75% reduction in CD63 expression suggests that there were significantly less exosomes released from platelets inhibited with apyrase. The data from platelet lysate, when compared to EV samples, suggests that CD63 was concentrated in EV, although without a housekeeping control protein for normalisation this was not conclusive.

2.4.3.4.2   Western blotting for HSP70

The main band on the blot (Figure 2.23A) was found at ~70kd which was consistent with the proteins expected location and the band was more distinct than that of CD63, making differences easier to quantify. The amount of protein was quantified with densitometry (B) and normalised (C). The blot shows that there was an obvious difference between the level of HSP70 in the apyrase and control samples and this was confirmed by the densitometry data which showed that the samples run on the blot in Figure 2.23A were reduced following inhibition (CRP-XL; -30%, PAR1-AP; -60%, PAR4-AP; -86% and ADP; -36%). Overall this demonstrated that there was a large reduction in the production of exosomes following inhibition with apyrase.
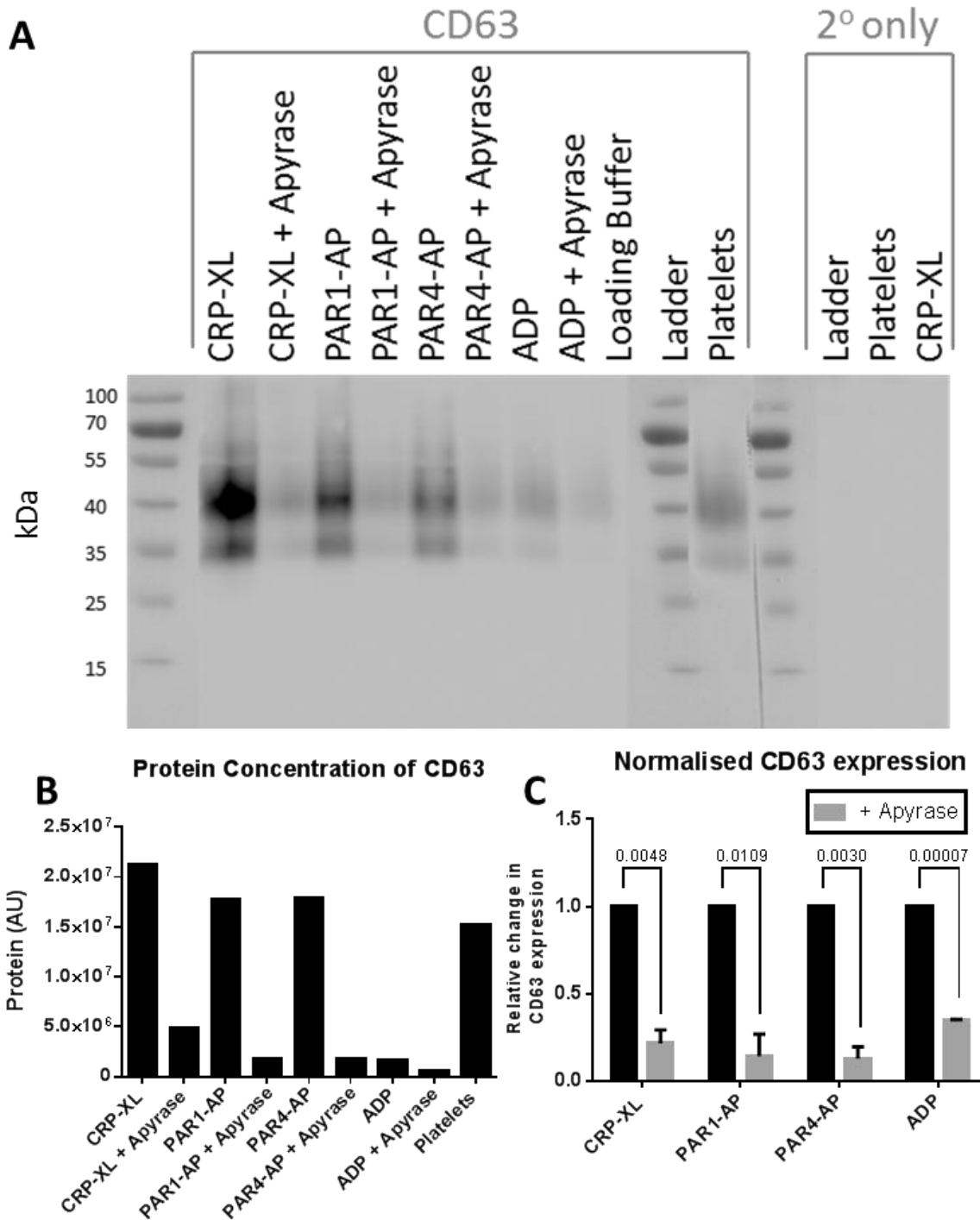
Figure 2.22 – A western blot to detect CD63 in pdEV samples generated in the presence of apyrase *Washed platelets (250x10³/μL) were activated with CRP-XL (2μg/mL), PAR1-AP (10μM), PAR4-AP (200μM) or ADP (50μM) in buffer or in the presence of apyrase (80μg/mL). A) EV were isolated via differential centrifugation and 25μg of protein was analysed by Western blotting for the exosomal marker CD63 [~40kDa] (representative of 3 blots), B) protein expression was quantified using densitometry (representative of blot shown in A) and C) the results from 3 blots were normalised for each inhibitor to show the effect of apyrase on exosome production (n=3+/-SD, Multiple t-test using the Holm-Sidak method).*
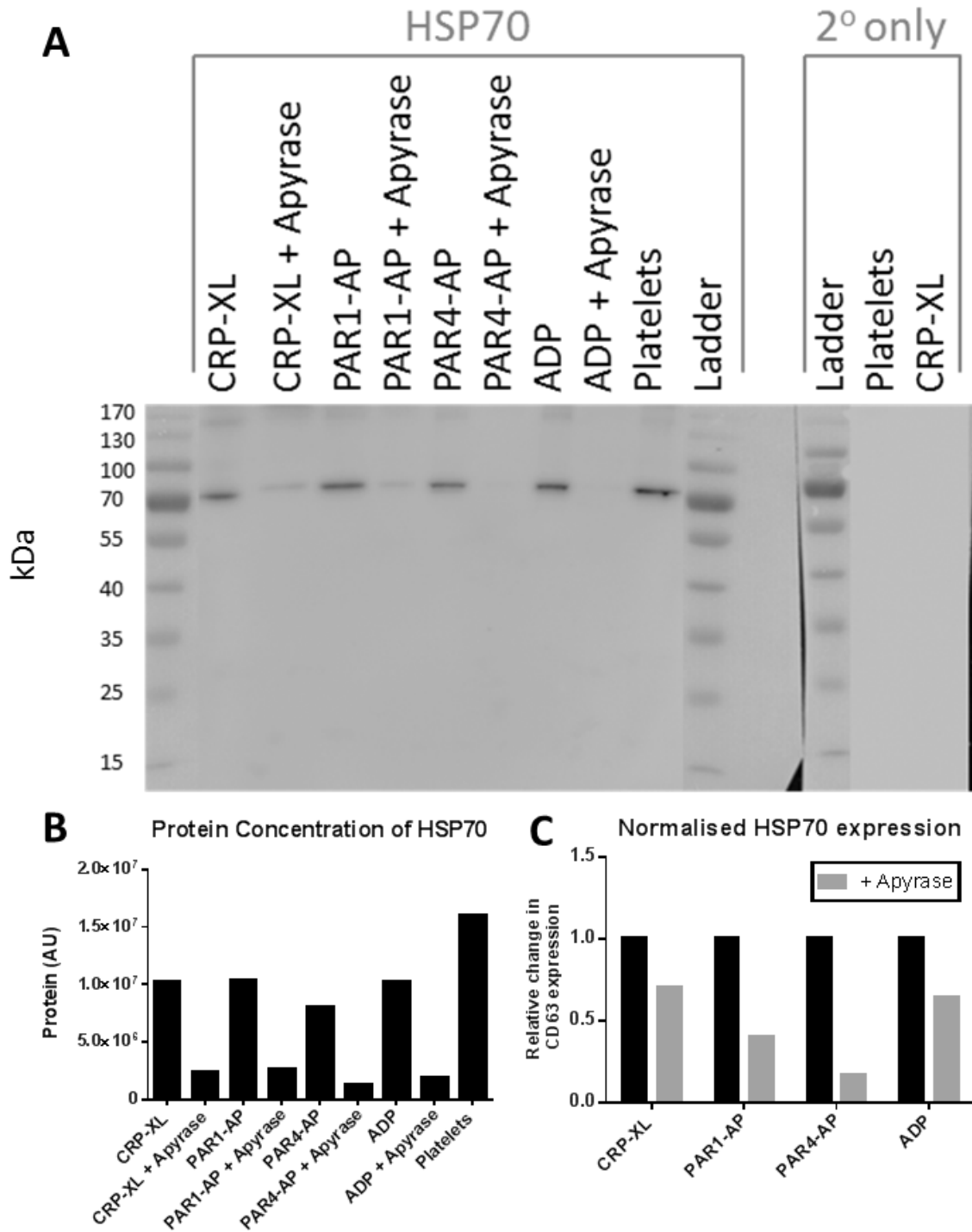
Figure 2.23 – A western blot showing the protein expression of HSP70 in pdEV samples and the effect of apyrase on this expression Washed platelets (250x10³/µL) were activated with CRP-XL (2µg/mL), PAR1-AP (10µM), PAR4-AP (200µM) or ADP (50µM) in buffer or in the presence of apyrase (80µg/mL). A) EV were isolated via differential centrifugation and 25µg of protein was analysed by Western blotting for the exosomal marker HSP70 [~70kDa] (representative of 2 blots), B) protein expression was quantified using densitometry (representative of blot shown in A) and C) the results from 2 blots were normalised for each inhibitor to show the effect of apyrase on exosome production (n=2).

2.4.3.5 Summary of platelet-derived EV inhibition

The effects of anti-platelet agents on EV release from platelets are summarised in Table 2.2. Aspirin had only minor effects on the characteristics of the EV population released from platelets compared to uninhibited samples. The only significant effect was that PAR1-AP and CRP-XL generated EV with a reduced ability to generate procoagulant microvesicles, as measured by the TG assay. However inhibition with apyrase caused significant reductions in both microvesicle and exosome production as evidenced by results from flow cytometry, the TG assay, western blotting and NTA. Table 2.2 also summarises the results from the same experiments using hirudin and RFGP56. In these experiments there were no significant changes observed demonstrating that the inhibition of extracellular thrombin or fibrinogen does not affect pdEV release in this model.

Table 2.2 – A summary of the changes in EV characteristics caused by anti-platelet agents *The results from experiments characterising the effects of aspirin and apyrase on platelet-derived EV (Figures 1.17 to 1.23) are summarised in the upper table. In the lower table are the results of experiments looking at the effect of platelet inhibition with hirudin and the monoclonal antibody RFGP56 on platelet-derived EV.*

Colour key: **green** = No change observed; **yellow** = Non-significant reduction; **light orange** = Significant reduction P<0.01; **orange** = Significant reduction P<0.001; **red** = Significant reduction P<0.0001; **grey** = Experiment not conducted.

Technique		Aspirin				Apyrase			
		CRP-XL	PAR1-AP	PAR4-AP	ADP	CRP-XL	PAR1-AP	PAR4-AP	ADP
Flow Cytometry	P-Selectin (Platelet degranulation)	green	green	green	yellow	yellow	orange	orange	red
	Annexin-V (procoagulant microparticles)	green	green	green	yellow	orange	yellow	yellow	yellow
TG Assay	ETP	green	red	green	green	red	red	green	red
	Peak Thrombin	red	orange	green	green	red	green	green	red
Western Blotting	CD63	grey	grey	grey	grey	orange	orange	green	yellow
	HSP70	grey	grey	grey	grey	yellow	yellow	green	green
Nanosight Tracking Analysis	Vesicle Concentration	yellow	green	green	yellow	red	yellow	orange	orange
	Vesicle size	green	green	green	green	green	green	green	green

Technique		Hirudin				RFGP56			
		CRP-XL	PAR1-AP	PAR4-AP	ADP	CRP-XL	PAR1-AP	PAR4-AP	ADP
Flow Cytometry	P-Selectin (Platelet degranulation)	yellow	yellow	green	green	green	green	green	green
	Annexin-V (procoagulant microparticles)	green	green	green	green	green	green	green	green
TG Assay	ETP	green	green	green	green	green	green	green	green
	Peak Thrombin	green	green	green	green	green	green	green	green
Nanosight Tracking Analysis	Vesicle Concentration	green	green	green	green	green	green	green	green
	Vesicle size	yellow	yellow	yellow	yellow	green	green	green	green

Vs Uninhibited sample — No change observed | Non-significant reduction | Significant reduction P<0.01 | Significant reduction P<0.001 | Significant reduction P<0.0001 | Experiment not conducted

2.5 Discussion

The role of EV as intercellular communicators (Ludwig and Giebel, 2012, Loyer et al., 2014), diagnostic markers (Vlassov et al., 2012, Gaceb et al., 2014, Willeit et al., 2013) or as therapeutic delivery vehicles (Ailawadi et al., 2015, Shtam et al., 2013, Johnsen et al., 2014) has been well established. However there still remains confusion in the field as to how the different subtypes of EV are defined, the best methods to isolate and characterise them and how each subtype contributes to the roles of EVs (van der Pol et al., 2016).

The interchangeable use of the terms exosomes and microvesicles to describe all EV within a population, or the use of alternative terms such as oncosomes (Di Vizio et al., 2012), ectosomes (Sadallah et al., 2011), and nanovesicles (Srivastava et al., 2015) significantly complicates the current literature. There is also a lack of consistency in techniques used to characterise EV subtypes, with many studies using a single technique, such as flow cytometry to define their EV populations. Together these factors mean that understanding the role of EVs, particularly specific functions of EV subtypes is challenging.

An example of the confusion caused is determining the localisation of microRNA in the circulation; both exosomes (Cheng et al., 2014, McDonald et al., 2013) and microvesicles (Loyer et al., 2014) are reported as the source of circulating cell-free microRNA. However the use of the term exosomes in these studies did not refer to a pure population as they used simple ultracentrifugation methods. For example Cheng *et al.* used a low speed 11,000g centrifugation to remove cellular debris and then a single 100,000g centrifugation for 90minutes to pellet all EV meaning that they were unable to effectively separate exosomes from microvesicles, while the study by Loyer *et al.* used the term microvesicles as an umbrella term for all EV, meaning this question remains unanswered.

We defined microvesicles by their larger size >100nm and their procoagulant activity; a result of surface expression of the negatively charged phospholipid, PS, which was identified by their ability to bind Annexin-V, as measured by flow cytometry and their ability to generate thrombin, measured in the TG assay. Exosomes were defined by their smaller size, ~<100nm as measured by NTA and enrichment for tetraspanins, as determined by Western blotting for the exosomal markers CD63 and HSP70 (Boilard et al., 2015, van der Pol et al., 2016).

It is known that platelets release both exosomes and microvesicles (Heijnen et al., 1999, Boilard et al., 2015, Aatonen et al., 2014), and that stimulation of platelets by CRP-XL, through the ITAM receptor, GPVI, is the most potent stimulus for procoagulant microvesicle generation (Aatonen

et al., 2014). pdEV are significant contributors to the EV population in the circulation (Arraud et al., 2014) making platelets an ideal cell type to identify which EV populations released into the circulation contain microRNA. Currently our understanding of the EV populations released from platelets with different agonists is limited and the research that has been carried out is confounded by inconsistent application of EV terminology. We therefore explored whether it was possible to generate a population comprised solely of exosomes through the characterisation of pdEV released with different agonists and with the addition of specific inhibitors.

2.5.1 Release of pdEV

Detailed characteristic profiles of pdEV from CRP-XL, PAR1-AP, PAR4-AP and ADP stimulated platelets were established. We observed that the agonists separated into 2 groups; firstly, CRP-XL, which generated a mixed population of EV containing both microvesicles and exosomes. The number of procoagulant microvesicles was significantly greater with CRP-XL than all other agonists, as demonstrated by Annexin-V binding (Figure 2.11) and measures of procoagulant activity (Figure 2.14). However, alongside microvesicles, CRP-XL also generated significant numbers of exosomes, as evidenced by the presence of smaller EV (>100nm) (Figure 2.13) and the identification of the exosome marker, CD63 (Figure 2.15). The second group of agonists; PAR1-AP, PAR4-AP and ADP directed at GPCRs all generated significantly fewer EVs overall and markedly less Annexin-V binding microvesicles (Figure 2.12). The consequences of this would be a reduced thrombotic potential (Figure 2.14). However the samples still contained smaller EV (Figure 2.13) and the exosome markers CD63 (Figure 2.15/Figure 2.22) and HSP70 (Figure 2.23).

These data suggested that there are discreet activation pathways that trigger the release of microvesicles and exosomes from platelets. CRP-XL triggered the release of both procoagulant microvesicles and exosomes whereas the other agonists predominantly released exosomes. Interestingly the separation of these groups matched the separation of the PLC pathways through which these agonists signal; CRP-XL activates the PLC-γ pathway and PAR1-AP, PAR4-AP and ADP utilise the PLC-β pathway. PLC acts to transform PIP_2 to IP_3 and DAG which triggers release of intracellular calcium and PKC activation. PLC-β is found downstream of the GPCRs for soluble agonists such as ADP and thrombin and PLC-γ is the pathway downstream from receptors such as GPVI and GPIIb-IIIa, and whilst PLCs have been identified in pdEV, their specific role in pdEV release is yet to be elucidated (Garcia et al., 2005, Nonne et al., 2005).

The effect of the two groups of agonists triggering different pathways is shown in Figure 2.24. This difference in response to different agonists suggests that microvesicles and exosomes may

have distinct roles to play in the circulation, although this is speculative and interpreting this through current data would be a challenge due to the remaining confusion in EV terminology (van der Pol et al., 2016).
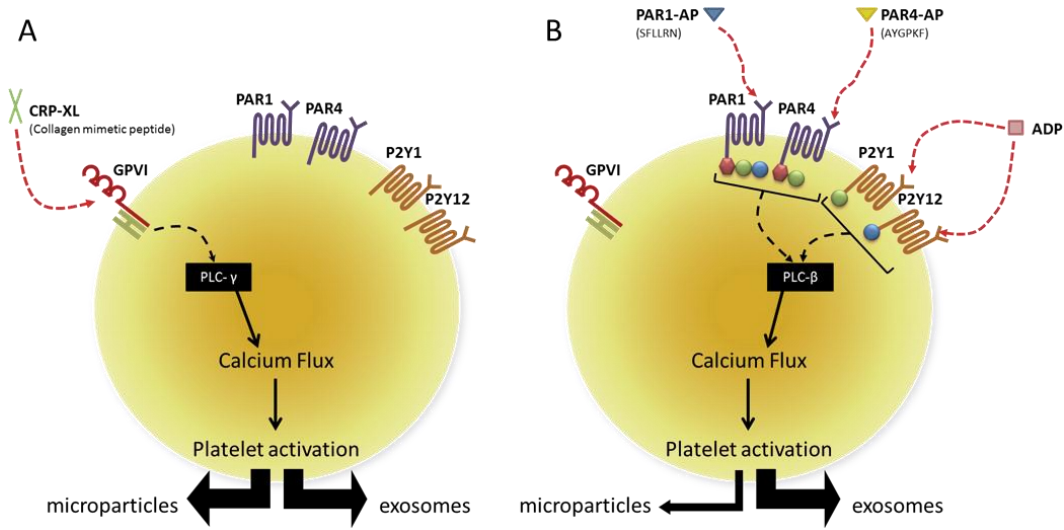
Figure 2.24 – Proposed differential EV release in response to different agonists A) CRP-XL acts on platelets to signal through the PLC-γ pathway, resulting in the release of microvesicles and exosomes. B) PAR1-AP, PAR4-AP and ADP signal through PLC-β and this results in the release of a predominantly exosomal EV population.

The role of the two PLC pathways was further investigated through the use of anti-platelet agents. Blocking secondary pathways of platelet activation with hirudin, aspirin, apyrase and the monoclonal antibody RFGP56 allowed for the analysis of secondary signalling pathways in response to CRP-XL, PAR1-AP, PAR4-AP and ADP. Inhibition with aspirin caused some changes to the procoagulant activity of released pdEV and apyrase caused significant changes to the characteristics of released pdEV. Apyrase caused reductions in the number of microvesicles and exosomes produced and therefore demonstrated that extracellular ADP had a crucial role within pdEV release and a potential mechanism for this is shown in Figure 2.25.
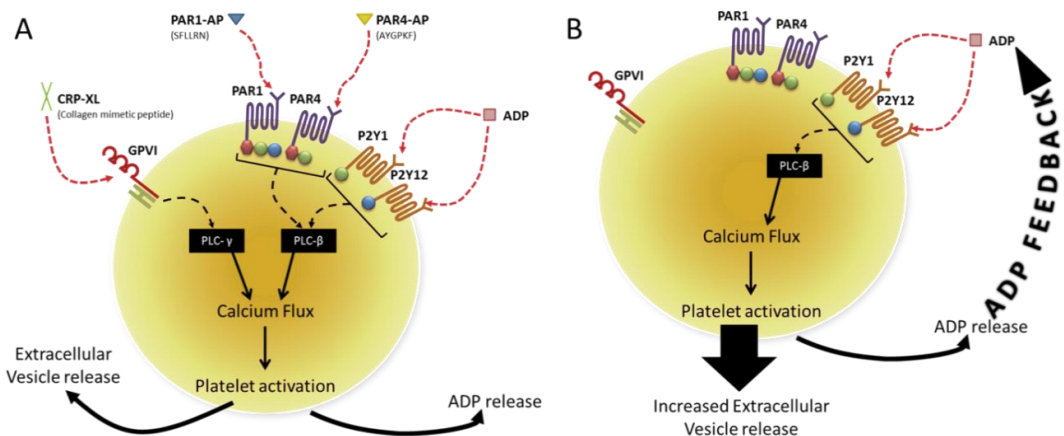
Figure 2.25 – Proposed role of ADP in EV release from platelets ADP is critical to EV release, as evidence by EV release inhibition in the presence of apyrase. We theorise that A) ADP is released from the platelet granules following stimulation and B) this extracellular ADP feeds back onto platelets to increase EV release.

The role of ADP as a secondary mediator of platelet activation and function is not a new concept; ADP plays a role in aggregation, and at high concentrations (>0.5µM) induces two phases of aggregation, although the secondary phase is predominantly due to thromboxaneA$_2$ production with a contribution from the release of further ADP (Smith, 1981). In addition, aggregation in response to weak agonists (e.g. serotonin or epinephrine) is potentiated by secondary ADP release (Mustard and Packham, 1970, Hjemdahl et al., 1994). This response is also observed with low doses of collagen or CRP-XL, however at higher concentrations these agonists overcome the need for secondary ADP for platelet activation (Quinton et al., 2002, Atkinson et al., 2001). This is demonstrated in the P-selectin data (Figure 2.17) that shows apyrase was unable to cause reduced platelet activation in response to CRP-XL stimulation. However apyrase did inhibit EV release following CRP-XL stimulation suggesting that pdEV release is still dependent on secondary ADP release and this secondary ADP signal is triggered by platelet degranulation, as ADP is stored within the platelet dense granules (King et al., 2009, Rendu and Brohard-Bohn, 2001). ADP is known to act through two separate purinergic receptors; P2Y1 and P2Y12. Previous studies have shown that these two receptors have differential functions in TG and signalling pathways (Soulet et al., 2005, Leon et al., 2003). It is therefore possible that only one of these receptors may be required for EV release and some initial work has been carried out in this area which suggests that the P2Y12 receptor is the primary ADP receptor that promotes EV release (Kahner et al., 2008).

The ADP released from platelet granules could work in two ways to induce increased EV release; it could act on adjacent platelets and increase the overall level of platelet activation, resulting in more pdEV release. Alternatively the initial stimulus from the agonists could act as a priming stimulus and then the secondary ADP may cause EV release beyond that observed constitutively. There is some evidence to support the first theory; apyrase prevents complete activation of platelets with CRP-XL, PAR1-AP, PAR4-AP and ADP (Figure 2.17), thereby preventing EV release. This suggests that the ADP released from stimulated platelets acts in an autocrine and paracrine way to trigger EV release from further platelets, thereby potentiating the initial stimulus. However there is not enough evidence in this work to conclude that this is the mechanism by which ADP is critical to EV release.

In comparison to the effects of apyrase the other inhibitors demonstrated significantly less, if any, effect on EV release. The lack of response to aspirin is supported by other studies, although this was only a secondary observation or whilst using lower doses of aspirin (100mg compared to 450mg here) (Lubsczyk et al., 2010, Pfister, 2004). However this does not explain the effect of aspirin on the thrombotic potential of pdEV generated with CRP-XL and PAR1-AP. It is possible

that aspirin caused a slight reduction in the production of microvesicles which was not observed through flow cytometry due to size limitations, but could be seen in the functional TG assay. This small effect would need further investigation but could have important clinical implications due to the widespread use of aspirin (Campbell et al., 2007).

Unlike aspirin and apyrase, there were no significant effects on the characteristics of pdEV released in response to any agonist following inhibition with hirudin or RFGP56. The lack of effect with hirudin suggests that in this isolated system that additional thrombin following a primary stimulus does not play a role in EV release and having observed the same results for PAR1-AP and PAR4-AP there seems to be no differential response between the receptors that thrombin stimulates. However there is evidence that PAR4, rather than PAR1 stimulation triggers ceramide synthesis in platelets (Chen et al., 2013). The sphingolipid, ceramide, is present in the membrane of multivesicular bodies and has been shown to be critical for the production of exosomes. It induces endosomal micro-domain merging which leads to domain budding into the MVBs and results in formation of exosomes (Trajkovic et al., 2008). This suggests that you would expect to see greater exosome production in PAR4-AP stimulated samples but the results cannot confirm this theory.

RFGP56 is directed against GPIIb-IIIa and blocks fibrinogen from binding and consequently prevents platelet aggregation. There is currently limited evidence on EV release following activation at this receptor, although it has been reported that it may play a role in the constitutive release of microvesicles in stored platelets (Cauwenberghs et al., 2006). The evidence from our experiments using RFGP56 proposes that outside-in signalling through the GPIIb-IIIa receptor was not involved in pdEV release following stimulation with all agonists. However this observation should be viewed with caution as the experiments were carried out with washed platelets so there would be little or no fibrinogen, which is the main GPIIb-IIIa agonist, present. In a study by Gemmell *et al.* platelets were re-suspended in platelet poor plasma, which contains fibrinogen, rather than calcium supplemented buffer and under these conditions inhibition of GPIIb-IIIa resulted in reduced EV production (Gemmell et al., 1993). Outside-in signalling through GPIIb-IIIa acts through the same PLC-γ pathway as CRP-XL stimulation so it is not surprising that there is evidence for its role in EV production. This suggests that carrying out our experiments in PRP or plasma-supplemented washed platelets may yield different results.

As mentioned previously there were some anomalous results; apyrase did not significantly reduce the number of Annexin-V binding microvesicles detected with flow cytometry and in all

experiments apyrase was only able to achieve a maximal inhibition of ~75%. The minimal changes in Annexin-V positive microvesicles released from platelets inhibited with apyrase and stimulated with PAR1-AP, PAR4-AP and ADP observed by flow cytometric analysis was likely to have been caused by the low numbers of microvesicles generated by these agonists (Figure 2.12). This meant that detecting a reduction on an already small population was challenging and this will have been exacerbated by the limitations of flow cytometry in detecting EV (Gardiner et al., 2015). The other interesting finding was that apyrase was unable to completely inhibit EV release from platelets. It is possible that the apyrase dose was not high enough to cause complete inhibition despite the apyrase being titrated to achieve an optimal dose. An alternative explanation is that platelets release EV constitutively through an ADP-independent mechanism as stated previously. Cauwenberghs *et al.* noted that this release is triggered by GPIIb-IIIa signalling (Cauwenberghs et al., 2006) and the absence of an effect of apyrase on the unstimulated control samples in the inhibitor assays suggests that there are separate mechanisms of constitutive release.

Taken together these results demonstrate that platelets release EV in an agonist-dependent manner that could potentially be explained by signalling through different PLC pathways. We also found that ADP had a clear role to play as a secondary mediator of EV release from platelets. However it was not possible to utilise the differential agonists and inhibitors to produce a completely pure population of exosomes for further study, although signalling with PAR1-AP, PAR4-AP and ADP definitely produced a population which predominantly contained exosomes.

2.5.2 Technical considerations for isolating and characterising EV

Whilst differential EV release in response to different agonists appeared clear from the data, there were a few anomalous results. Firstly, the differences between samples using the flow cytometry assay for Annexin-V binding microvesicles (Figure 2.12) and the thrombotic potential of the samples in the TG assay (Figure 2.14). Both measured the level of PS on the platelet microvesicles and both showed significantly more microvesicles in the CRP-XL stimulated samples. However, the other 3 agonist's pdEV (PAR1-AP, PAR4-AP and ADP) matched the control in the flow cytometry assay but had a significantly greater thrombotic potential than control samples in the TG assay. This is likely to have been caused by the limitations with detecting EV by flow cytometry due to their small size and low refractive index. Estimates suggest that even the best flow cytometers cannot detect vesicles <200nm (Gardiner et al., 2014, van der Pol et al., 2016, Coumans et al., 2014, Varga et al., 2014). This indicated that the flow cytometry assay was only able to see a portion of the procoagulant microvesicles whereas the TG assay measured

the presence of all procoagulant, PS+ve positive microvesicles in the sample, suggesting that the TG assay is more sensitive to microvesicles than flow cytometry.

The samples of EVs released by ADP showed an interesting but insignificant trend towards being smaller in the Nanosight (Figure 2.13B). When this was analysed using the NTA traces (Figure 2.13 C) the presence of smaller particles was clear, as although the ADP trace resembled the others it did not have a single peak. This was likely to have been caused by the detection of out-of-focus particles which cause intensive light scatter that mimics large numbers of small particles rather than a single particle. The sensitivity to small changes in focus means that the NTA measurements of EV are not perfect and in some studies inaccuracies of up to 70% have been reported when NTA is compared to other measures of EV enumeration and characterisation such as flow cytometry and tuned resistive pulse sensing (van der Pol et al., 2014).

A further technical issue in the characterisation of pdEV samples is the lack of a housekeeping protein for western blotting. To date no single marker has been identified that is present at stable levels in all EV or EV subtypes that allows for normalisation of samples. Therefore the strength of CD63 bands could not be interpreted as fully representative of the number of exosomes within the sample. Attempts have been made to compile extensive databases on the markers and content of EV but these are yet to yield a true marker of either exosomes or microvesicles suggesting significant heterogeneity in EV populations (Keerthikumar et al., 2015, Kalra et al., 2012).

While carrying out this work the field of EVs has expanded at a significant rate resulting in advancements in techniques to isolate and characterise EV as well as attempts to remove discrepancies in nomenclature. The low speed differential centrifugation method (2.3.8.1) that was used here has been widely used in EV research and this method has been shown to successfully remove cells and cell debris but retains EV and other soluble factors released from the platelet into the supernatant (Aatonen et al., 2012, Aatonen et al., 2014, Gyorgy et al., 2012, Gardiner et al., 2014, Lacroix et al., 2012). However, this meant that the resulting supernatant used in the EV assays also contained over 300 soluble factors derived from platelet granules as described in several proteomic studies of the platelet-releasate (Coppinger et al., 2004, Kamath et al., 2001).

Conversely the platelet-releasate analysed by Coppinger *et al.* was not devoid of all EV as the maximum centrifugation speed used in their study was 50,000g, so some of the 300 proteins identified by this group could derive from exosomes. An example could be the transmembrane protein CD63, reported by Coppinger *et al.*, which is not a soluble protein and is enriched in the

membranes of exosomes (Conde-Vancells et al., 2008). This suggests that our pdEV samples will have been contaminated with additional soluble proteins, but perhaps not >300 as many of these could be exosome proteins. However, these additional proteins isolated alongside the EV would be unlikely to affect flow cytometry as they are soluble and therefore undetectable. They would not affect the TG assay as the PRP reagent used was dependent upon the PS on the microvesicle surface and western blotting would be unaffected as this was looking at the specific exosomal markers CD63 and HSP70. However there is a possibility that it may affect EV concentration measurements with NTA as protein aggregates can be indistinguishable from EV or lipid accumulations (Webber and Clayton, 2013, Gardiner et al., 2014).

In this study the EV were not isolated using ultracentrifugation which would have provided a mechanism by which it was possible to remove some of the soluble proteins in the samples. Currently ultracentrifugation is the most popular protocol for EV isolation following the initial differential centrifugation steps, normally involving one or more centrifugations at ≥100,000g for up to 16hours (Taylor and Shah, 2015, Taylor et al., 2011, Tauro et al., 2012). There has been considerable debate over whether ultracentrifugation leads to the formation of EV aggregates, causes changes in EV functionality and leads to the co-isolation of other factors such as proteins and lipids (Bard et al., 2004, Gyorgy et al., 2011a, Gyorgy et al., 2011b, van der Pol et al., 2012a). Recent data has shown that this aggregation may be dependent on the cell of origin with pdEV being particularly susceptible to aggregation (Linares et al., 2015, Yuana et al., 2015). This suggests that the use of ultracentrifugation is not ideal for the isolation and subsequent characterisation of pdEV. However, there are other techniques which may improve the purity of the EV preparations.

Size-exclusion chromatography has seen a revival in EV research, it enables researchers to separate EV from contaminating proteins and lipids and has been shown to be particularly useful with plasma samples (Boing et al., 2014, de Menezes-Neto et al., 2015). This technique utilises cross-linked polysaccharide polymers such as sepharose to separate EV from contaminating proteins and lipids. It is a technique that has been previously used to isolate platelets (Zucker et al., 1974, Lages et al., 1975) and through the use of sepharose CL-2B has been shown to successfully isolate EV into fractions separate from contaminants such as high-density lipoprotein (HDL). However this method can result in the loss of EV ~>75nm in size, suggesting that many exosomes will be removed (van der Pol et al., 2016, Boing et al., 2014). It is now possible to purchase commercially mass-produced chromatography columns from Cell-guidance systems (Welton et al., 2015) and iZon Science (Oxford, UK) (Lobb et al., 2015) suitable for isolation of EV populations.

In addition, there has been an increase in the availability of alternative commercial reagents for EV isolation. Exo-Spin columns, available from Cell-guidance systems use a proprietary polymer to precipitate the exosomes from solution, ExoQuick (System Biosciences) uses polyethylene glycol with low speed centrifugation to precipitate exosomes from solution, and Total Exosome Isolation Reagent from Thermo Fisher Scientific uses a proprietary derivative of the above precipitation methods. All of these commercial methods have been compared in studies and found to show poor exosome specificity, low yield and significant contamination, especially when used to isolate exosomes from plasma or serum (Van Deun et al., 2014, Taylor and Shah, 2015, de Menezes-Neto et al., 2015, Lane et al., 2015, Oosthuyzen et al., 2013). In the experiments here the ExoQuick reagent was briefly tested with mixed results, using NTA it appeared to isolate smaller, exosome-like vesicles. But, ExoQuick is a solution containing polyethylene glycol (PEG) 8000 which simply acts to precipitate high molecular weight (MW) proteins and protein complexes from a solution meaning that there is no specificity for exosomes or even EV, and results in contamination with HDL and protein aggregates. The Exo-spin columns were also tested (data not shown) but the result from these was poor with no changes in EV size following exosome isolation with the column, and a large reduction in EV concentration.

Further techniques which have been utilised include immunoaffinity separation and filtration. The immune isolation of exosomes using magnetic beads has been carried out numerous times and with different markers e.g. HER2 for breast cancer EVs (Koga et al., 2005b), EpCAM for colon cancer EVs (Tauro et al., 2012), various HLA antibodies for antigen-presenting cell exosomes (Clayton et al., 2001) and CD63 beads for saliva exosomes (Zlotogorski-Hurvitz et al., 2015). It is evident that a variety of markers have been used, but no single marker can be utilised for all exosomes or microvesicles. Current evidence suggests that any one individual marker is only capable of capturing a subset of EVs and that the diversity between EVs released from single cell lines is vast meaning that there may not even be cell-specific markers for exosomes (Smith et al., 2015, Bobrie et al., 2012).

Filtration has been widely used as a method to isolate EVs but in many cases it has been used alongside other methods, such as ultracentrifugation to remove larger EV e.g. apoptotic bodies using 0.45 and 0.22µm filters (Epple et al., 2012, Azevedo et al., 2007, Lobb et al., 2015). However it has been noted that forcing EV through small pore filters can cause distortion and rupture, resulting in alterations to characteristics and functionality (Witwer et al., 2013). More recently, ultrafiltration with 100kDa molecular weight filters has been used with studies

suggesting that this technique provides a simpler method with comparable yields to ultracentrifugation whilst maintaining functional activity (Lobb et al., 2015, Nordin et al., 2015).

In addition to changes in isolation techniques the field of EV research has built up a wealth of information on EV subtype characteristics, but there is a distinct lack of consistency. As a result the definitions of EV subtypes have become looser rather than more precise in recent years. For example reports from the 2015 ISEV meeting in Washington suggest that exosomes could be up to 250nm in size, that exosomal markers, such as CD63, could be expressed on microvesicles, and that EV with exosome-like characteristics are released directly from the membrane rather than through the endosomal pathway (ISEV, 2015, Booth et al., 2006). These findings are from as yet unpublished work so cannot be explored in detail and the conclusions could be caused by the contamination of microvesicle preparations with exosomes and vice versa. However these results either suggest the need for greater standardisation in methodologies or demonstrate that the differences between microvesicles and exosomes are less distinct than previously believed.

Alongside the changes in EV isolation techniques used, numerous new techniques for their characterisation, such as Raman spectroscopy (Smith et al., 2015, Tatischeff et al., 2012), tuned resistive pulse sensing (van der Pol et al., 2014, Lane et al., 2015, Coumans et al., 2014), cryo-electron microscopy (Arraud et al., 2014, Yuana et al., 2013), proteomics (Pienimaeki-Roemer et al., 2014, Bard et al., 2004) and improved flow cytometry protocols (Pospichalova et al., 2015, Headland et al., 2014) have been developed. These offer opportunities to identify novel characteristics of exosomes such as specific markers or functional attributes which may help with the long term problem of separating the EV sub-populations.

Raman spectroscopy allows for the characterisation of individual vesicles by measuring inelastic light scatter in response to a laser caused by molecular vibrations. This produces a chemical composition fingerprint for individual vesicles that can provide distinguishable characteristics such as phospholipid and cholesterol composition (Tatischeff et al., 2012). Interestingly this technique has identified heterogeneity in vesicle populations from single cell lines and similarities in sub-populations between cell lines (Smith et al., 2015). This technique is in its infancy and more work is needed to explore its possible applications in EV research.

Tuned resistive pulse sensing is a more established technique for EV characterisation and utilises changes in electrical current caused by the passage of EV through a pore to define EV size and concentration. It has been utilised in a very similar way to NTA and produces similar results (van der Pol et al., 2016, Coumans et al., 2014). Cryo-electron microscopy is another technique which

has gained traction in the field of EV research. It has proved very useful because unlike other electron microscopy techniques it does not significantly alter the size and morphology of the EV (Dubochet, 2012). Cryo-electron microscopy has been used to accurately describe the EV populations of the plasma (Arraud et al., 2014, Yuana et al., 2013) and findings from cryo-electron microscopy studies are widely used as the gold-standard for phenotyping EV in heterogeneous populations.

Flow cytometry is the most widely used technique for EV research despite significant shortcomings with regards to lower limits of size detection (Gardiner et al., 2015), swarm detection (whereby multiple EV are simultaneously detected by the flow cytometers laser and treated as a single event) (Harrison and Gardiner, 2012, van der Pol et al., 2012b) and difficulty in determining particle size due to EVs refractive index (van der Pol et al., 2014). However recent advances such as impedance-based flow cytometry, wide angle FSc and the use of UV lasers for FSc detection have improved flow cytometry, meaning it is now possible to observe EV as small as 200nm in size (Pospichalova et al., 2015, van der Pol et al., 2016). In addition techniques that capture EV onto antibody-coated beads that are then run through the flow cytometer with the EV still bound have proved useful in phenotyping EVs as this solves the problem of size and swarm detection (Gyorgy et al., 2012). Another potential improvement in flow cytometry is the use of imaging flow cytometers, these enable the visualisation of each event passing through the laser so it is possible to distinguish single vesicles from those passing through as aggregates (Headland et al., 2014). Flow cytometry currently remains the predominant technique for EV research due to its widespread availability, relative simplicity to use and ability to measure multiple characteristics simultaneously. Improvements in instrumentation that further reduce the size limitations of flow cytometry will enhance its functionality in EV research.

Taken together the improvements in isolation and characterisation represent a real opportunity to separate microvesicles and exosomes and determine whether they are simply on a spectrum of EV subtypes or truly different populations with different implications in health and disease. However evidence suggests that there is significant heterogeneity in EV populations and that there are differences between exosomes in the same samples. There is some evidence for this here; western blotting for the exosomal markers CD63 and HSP70 on identical samples revealed that these markers were differentially affected by apyrase (Figure 2.22 and Figure 2.23). Suggesting that they are perhaps not co-expressed and instead represent different exosome sub-populations.

Having assessed the currently available techniques to both isolate and characterise EV it appears that there is still no method by which it is possible to accurately separate exosomes from microvesicles. However newer techniques such as size-exclusion chromatography are producing preparations of EVs that retain functional activity and are freer from contaminants. Pairing this with new characterisation techniques means that elucidating new unique characteristics which will allow for the separation of microvesicles and exosomes is more feasible. By carrying out our isolations in a closed system and triggering EV release with agonists targeted specifically at platelets we have produced an EV rich supernatant containing both exosomes and microvesicles. Whilst the preparations were likely to contain other soluble factors, these were unlikely to have altered the results of the assays carried out to characterise the EV.

Overall this work observed the production of differential EV populations from platelets using different agonists; microvesicles and exosomes with CRP-XL and predominantly exosomes with PAR1-AP, PAR4-AP and ADP. Further work is required to identify the exact signalling pathways activated in pdEV release but it appears that differential PLC pathways play a critical role in differentiation between exosome and microvesicle release and that ADP is an integral secondary mediator. During this work we were unable to isolate a purely exosomal population for further study and so future work will be carried out comparing the pdEV from all agonists or pdEV generated by PAR1-AP as it produced a predominantly exosomal population with a higher yield than the other GPCR agonists.

Chapter 3

Platelet and platelet-derived
Extracellular Vesicle microRNA

3 Platelet and pdEV microRNA

3.1 Introduction

MicroRNA are a class of small non-coding RNAs responsible for post-transcriptional regulation of mRNA translation. They influence cellular function by targeting the 3'-region of mRNA species leading to altered protein expression. MicroRNA and their associated machinery have strong evolutionary conservation demonstrating that their function is vital in an array of organisms (Ambros et al., 2003, Baek et al., 2008). MicroRNA have been identified throughout the human body, predominantly localised within cells, but a growing body of research has looked at extracellular microRNA particularly within body fluids such as saliva, urine and the blood (Etheridge et al., 2011, Creemers et al., 2012).

Detailed microRNA profiling of the blood has been carried out and these studies have revealed a rich network of functional microRNA species within granulocytes, monocytes and even anucleate platelets (Merkerova et al., 2008). The presence of extracellular RNA in the blood was first suggested in 1972, but was largely disregarded due to the known RNAse activity in plasma (Kamm and Smith, 1972). Recent research has revealed, however, that there is a wealth of cell-free microRNA that is unexpectedly stable over time (Mitchell et al., 2008). Interestingly, exogenous microRNA introduced into the blood did not display the same stability and was degraded, suggesting that extracellular microRNA are normally protected (Tsui et al., 2002). Research suggests that there may be multiple mechanisms that confer this protection including the microRNA forming complexes with RNA binding proteins (e.g. AGO2, NPM1) (Arroyo et al., 2011) and HDL (Vickers et al., 2011) or microRNA localising within EV (El-Hefnawy et al., 2004, Valadi et al., 2007). There is increasing evidence that the majority of extracellular microRNA within the circulation is located within EV (Diehl et al., 2012, Kosaka et al., 2013b, Valadi et al., 2007).

The first suggestion that circulating RNA was protected by EV was in 2003 and was hypothesised following evidence that protection was removed after treatment with detergents (El-Hefnawy et al., 2004). The plasma is known to contain ~40 million EV per mL meaning there is a large amount of genetic material in circulation (Arraud et al., 2014). There is contrasting evidence in the literature over whether the microRNA content of EV is a reflection of the cell of origin or whether there is selective loading. It is suggested that some microRNA are found at higher or lower levels in secreted EV, thereby representing selection (Guduric-Fuchs et al., 2012, Collino et al., 2010, Chen et al., 2010, Ohshima et al., 2010, Pigati et al., 2010). However there is

currently very little understanding of the mechanism by which this occurs and whether there is a functional reason for this selectivity. Alongside the debate on microRNA loading into EV there is a separate question over whether the EV simply contain cellular contents for disposal or functional molecular entities targeted at other cells (Kosaka et al., 2013b).

There is mounting data that indicates that circulating microRNA within EV have an important role to play in intercellular communication. Exosomes have been proposed as the primary source of microRNA, and this was determined by showing that levels of ceramide, which controls exosome secretion, correlated with the level of secreted microRNA (Kosaka et al., 2010). Determining the exact function of microRNA within EVs has proved challenging due to the wealth of circulating microRNA, the 'fine-tuning' nature of microRNA and the additional RNA and protein content within EV. However several studies have shown successful transfer, followed by subsequent functional effects. MicroRNA transfer via EVs has been demonstrated in macrophages (Ismail et al., 2012), from T-cells to antigen presenting cells (Mittelbrunn et al., 2011), between murine dendritic cells (Montecalvo et al., 2012) and from telocytes to cardiac stem cells (Cismasiu and Popescu, 2015). Understanding the processes involved in microRNA transfer via EV in the circulation presents an opportunity for therapeutic intervention via the utilisation of a natural, biological mechanism. Alongside the growing field of functional investigations on microRNA transferred within EV, attempts are being made to utilise EV microRNA as biomarkers of health and disease.

MicroRNA packaged within EV in the blood possess many characteristics that make them ideal for use as biomarkers; they are readily accessed, have a stable profile, are quantifiable and have been shown to be specific (e.g. expression at particular points in development) (Etheridge et al., 2011). Levels of EV are increased in disease due to increased release from affected tissues and this provides an opportunity for detection of disease specific microRNA released from these sites. For example, in the circulation following an MI (Boulanger et al., 2001, Stepien et al., 2012) or a stroke (Simak et al., 2006) and in the blood of patients suffering with diabetes mellitus (Chen et al., 2008, Duan et al., 2014). There are many ongoing studies attempting to use EV as sources of microRNA biomarkers (Quinn et al., 2015)

Research on pdEV in the circulation has already shown that platelets have an exceptionally high microRNA to mRNA ratio (Bray et al., 2013) and that platelets are responsible for up to 50% of circulating EV (Arraud et al., 2014). Platelet-derived EV have been shown to transfer microRNA to other cells and exert functional effects following transfer (Laffont et al., 2013, Laffont et al., 2015). Although there is currently no evidence for biomarker identification in circulating pdEV,

intracellular platelet microRNA is altered in sickle cell anaemia (Jain et al., 2013) and circulating microRNA changes with antiplatelet therapy (Willeit et al., 2013). This makes pdEV potentially important contributors when identifying biomarkers in the circulation.

This information suggests platelets have a large role to play in the production of circulating EV microRNA, however, there is much that we do not yet understand about its value in cell-cell communication and it's potential as a biomarker. In this chapter we looked at the microRNA in platelets, the release of it from platelets into EV and what this meant with regards to circulating EV microRNA.

3.2 Aim

To profile the microRNA content of platelets and pdEV and to identify the effects of using different agonists on the profile of EV microRNA.

To observe how the released pdEV microRNA influences the content of microRNA in plasma and to utilise this information to identify microRNA that could act as a biomarker of platelet activation in blood.

3.3 Materials and methods

The process to investigate the microRNA in all samples followed a simple 4 step method as illustrated in Figure 3.1. Total RNA was extracted, RNA was reverse transcribed in the presence of specific primers and then the cDNA was pre-amplified. Finally, amplified cDNA was utilised in individual TaqMan assays for single microRNA or on microRNA microarrays to identify the microRNA contained within the sample.
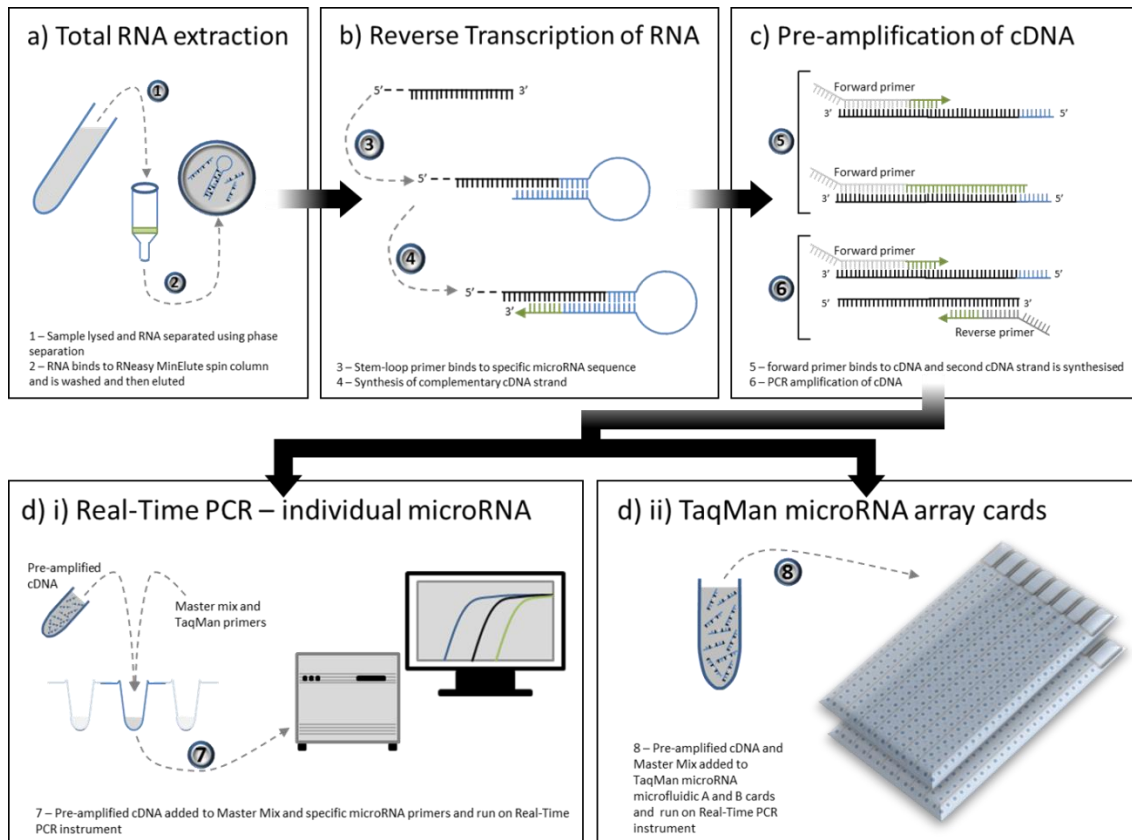
Figure 3.1 – The workflow for analysing the microRNA profiles using TaqMan microRNA microarrays and individual TaqMan assays A step by step overview of the processes used to measure the RNA in samples. Including information on the a) RNA extraction, b) reverse transcription (RTr), c) amplification and measurement using d)i) individual assays and d)ii) TaqMan microRNA microarrays.

3.3.1 RNA extraction

3.3.1.1   miRNeasy micro kit

The miRNeasy micro kit (Qiagen) is an all-in-one kit for total RNA extraction. Briefly, 700μl of Qiazol lysis reagent (containing guanidine salts and phenol) was added to 200μL liquid samples or to cell pellets, which were then mixed by vortexing and incubated at RT for 5 minutes. 140μl of chloroform (>99.5% with 100-200ppm amylenes as stabilisers) was added to the lysed sample and briefly vortexed followed by a 3 minute incubation at RT. Samples were centrifuged at 12000g for 15 minutes at 4°C to separate the sample into 3 phases. The upper aqueous phase (~400μl) was carefully aspirated into a fresh eppendorf and diluted with 1.5x (v/v) 100% ethanol

(~600µl) and mixed by vortexing. The solution was added to RNeasy MinElute spin columns (filter columns which bind RNA) and centrifuged at 13000rpm for 30 seconds, the flow through was discarded. This was followed by 3 separate buffer washes; 700µl RWT buffer (contains guanidine salts and ethanol for washing contaminants from the columns), 500µl RPE buffer (washing buffer for removing salts and phenols from the columns) and 80% ethanol (from 100% molecular-grade ethanol) which were washed through by centrifugation at 13000rpm for 30 seconds, 30 seconds and 2 minutes respectively. The RNeasy MinElute spin columns were then dried by centrifugation at 13000rpm for 5 minutes with no solution in the columns. The total RNA bound to the columns was eluted using 30µl 10mM Tris buffer (10mM Tris, pH8) which was added directly to the membrane in the column, this was washed through by centrifugation at 13000rpm for 1 minute and collected in a fresh eppendorf. The total RNA was measured using a Nanodrop spectrophotometer and stored at -20°C.

3.3.1.2 Cel-miR-39-3p spike-in control

Aliquots of $2x10^{10}$ copies/µL cel-miR-39-3p (ucaccgggguguaaaucagcuug) were thawed on ice and diluted 1 in 5 to a concentration of $4x10^9$ copies/µL and then diluted 1 in 25 to a working concentration of $1.6x10^8$ copies/µL. 3.5µL of this working solution was added to samples undergoing RNA extraction, immediately after lysis with Qiazol and before the addition of chloroform. The RNA extraction then proceeded as described above and cel-miR-39-3p was detected using RT-PCR.

3.3.1.3 Measuring total RNA with the Nanodrop Spectrophotometer

RNA samples were analysed using a Nanodrop 8000 Spectrophotometer (Thermo Fisher Scientific). The instrument was initialised with 2µl deionised RNAse free water and then blanked using 2µl 10mM Tris buffer. A 2µl aliquot of RNA was added to the pedestal and the Nanodrop measured the transmission of light through the sample at specific wavelengths, providing information on the concentration (ng/µl) and purity (based on the 260/280 ratio) of RNA in the sample.

3.3.2 RNA RTr

3.3.2.1 RTr with Megaplex RT primers

Extracted RNA was reverse transcribed to cDNA for downstream applications such as RT-PCR using the TaqMan microRNA RTr kit combined with the TaqMan Megaplex primers Pool A v2.1 and Pool B v3.0 or specific primers for individual microRNA (Thermo Fisher Scientific).

A RTr master mix was made; 0.8µl Megaplex RT primers (either Pool A v2.1 (381 unique microRNA) or Pool B v3.0 (377 unique microRNA) with both containing control probes for U6 snRNA, RNU44, RNU48 and ath-miR-159a), 0.2µl dNTPs (a dNTP mix with dTTP), 1.5µl Multiscribe Reverse Transcriptase (an enzyme from a recombinant moloney murine leukaemia virus), 0.8µl 10x RT buffer (proprietary buffer containing Tris-HCl, KCl and $MgCl_2$), 0.9µl $MgCl_2$, 0.1µl RNAse Inhibitor and 0.2µl nuclease free water, per sample. A 4.5µl aliquot of the master mix was added to 3µl of each RNA sample for a total reaction volume of 7.5µl in a 50µl PCR tube. Tubes were centrifuged and incubated on ice before carrying out the following thermal cycling protocol; 40 cycles [16^oC – 2minutes / 42^oC – 1minute / 50^oC – 1second], 85^oC – 5minutes and then samples were held at 4^oC before storage at -20^oC.

3.3.2.2   RTr with individual microRNA primers

As above replacing the 0.8µl Megaplex RT primer pools with 0.8µl of a single specific TaqMan primer for an individual microRNA (Thermo Fisher Scientific), thereby creating a single cDNA product.

3.3.3   cDNA Pre-amplification

For samples being analysed on the TaqMan microRNA array cards, a higher cDNA concentration was required than provided by RTr reactions alone. Therefore samples were pre-amplified using the same primer pool as the RTr reaction.

3.3.3.1   Pre-amplification with Megaplex pre-amplification primers

Pre-amplification reactions utilised the 2x TaqMan pre-amplification master mix and the Megaplex pre-amplification primers Pool A v2.1 and Pool B v3.0 (Thermo Fisher Scientific). The Megaplex pre-amplification primer pool used for pre-amplification reactions was selected to correspond to the Megaplex RTr primer pools used in the RTr reaction for each sample.

The Pre-amplification reactions used 22.5µl of a master mix, comprising; 12.5µl TaqMan pre-amplification master mix, 2.5µl Megaplex pre-amplification primers (either Pool A v2.1 or Pool B v3.0) and 7.5µl nuclease free water which was added to 2.5µl of cDNA in a 50µl PCR tube. The tubes were briefly centrifuged at 1000g for 1minute and then incubated on ice for 5 minutes before undergoing thermal cycling; 95^oC – 10minutes / 55^oC – 2minutes / 72^oC – 2minutes / 12 cycles [95^oC – 15seconds / 60^oC – 4minutes] / 99.9^oC – 10minutes and then samples were held at 4^oC. The pre-amplified cDNA was diluted in 75µl 10mM Tris buffer and stored at -20^oC.

3.3.4 Individual PCR assays

3.3.4.1 Individual TaqMan primer assays

Individual PCR assays were used to validate findings from the TaqMan microRNA arrays cards and to investigate treatment effects on specific microRNA. TaqMan primers for RTr and RT-PCR reactions were purchased together (Thermo Fisher Scientific). RTr primers were used in the RTr reactions as described in 3.3.2.2 and the resulting cDNA product was used in conjunction with the RT-PCR primers for individual TaqMan primer assays.

Briefly, a master mix of 5µl TaqMan fast master mix, 0.5µl TaqMan RT-PCR primers (detailed in Table 3.1) and 1.5µl nuclease free water per sample was added to 3µl cDNA in a 96-well PCR plate which was then sealed and centrifuged (3000rpm for 1minute) before a 5minute incubation on ice. The plate was then run on a Viia 7 instrument (Applied Biosystems) using the standard fast chemistry protocol; 95°C − 20seconds / 40 cycles of [95°C − 1second / 60°C − 20seconds]. Fluorescence was detected at the end of each cycle and automatically plotted on a logarithmic scale from which the Cycle Threshold (Ct) values were determined for each well, samples were assayed in triplicate and averages calculated. Controls with no template cDNA (nuclease free water was used instead) were run as no template controls to detect non-specific amplification.

Table 3.1 − MicroRNA primers used for RT-PCR A list of the targets of primers used for single RT-PCR including information on the target, target sequence, targets chromosomal location, the product code from Thermo Fisher Scientific and the Megaplex primer pool associated with the target.

microRNA	Mature targets sequence	Chromosomal location	Product code	Megaplex primer pool
hsa-miR-223-3p	UGUCAGUUUGUCAAAUACCCC	Chr.X: 65367812-65367921 [+]	4427975 - 000526	A
hsa-miR-21-5p	UAGCUUAUCAGACUGAUGUUGA	Chr.17: 57918627-57918698 [+]	4427975 - 000397	A
hsa-miR-146a-5p	UGAGAACUGAAUUCCAUGGGUU	Chr.5: 159912359-159912457 [+]	4427975 - 000468	A
hsa-miR-106a-5p	AAAAGUGCUUACAGUGCAGGUAG	Chr.X: 133304228-133304308 [-]	4427975 – 002169	A
U6 snRNA	GTGCTCGCTTCGGCAGCACATATACTA AAATTGGAACGATACAGAGAAGATTA GCATGGCCCCTGCGCAAGGATGACAC GCAAATTCGTGAAGCGTTCCATATTTT	-	4427975 - 001973	A & B
cel-miR-39-3p	UCACCGGGUGUAAAUCAGCUUG	-	4427975 - 000200	-

3.3.5 TaqMan microRNA array cards

3.3.5.1 TaqMan Array Human microRNA A and B card set – version 3.0

Pre-amplified cDNA was run on the TaqMan microRNA array cards (Thermo Fisher Scientific), each sample was reverse transcribed and pre-amplified as previously described. A master mix was made up for each TaqMan array card comprising of 450µl TaqMan fast master mix, 441µl nuclease free water and 9µl pre-amplified cDNA. The master mix was vortexed and 100µl was loaded into each of the 8 reservoirs at the end of the microfluidic microarray card. The array card was then centrifuged at 1200rpm for 2 minutes and sealed using the microarray card sealer. The now empty reservoirs were cut off the card and the microarray was incubated for 5 minutes on ice. Following the incubation the microarray card was loaded into a Viia-7 real-time PCR instrument (Applied Biosystems) and run using the following protocol; $95^{\circ}C$ – 20seconds / 40 cycles of [$95^{\circ}C$ – 1second / $60^{\circ}C$ – 20seconds]. Fluorescence was detected and Ct values determined as with the individual PCR assay.

3.3.6 Analysis of TaqMan microRNA microarray data

After running the TaqMan microRNA microarray cards on the Viia-7 real-time PCR instrument the RUO software analysed the traces from the individual PCR reactions and set thresholds for each probe so that the threshold line crossed the trace during the exponential phase. The point at which the trace crossed the threshold determined the Ct value for that probe as shown in Figure 3.2.
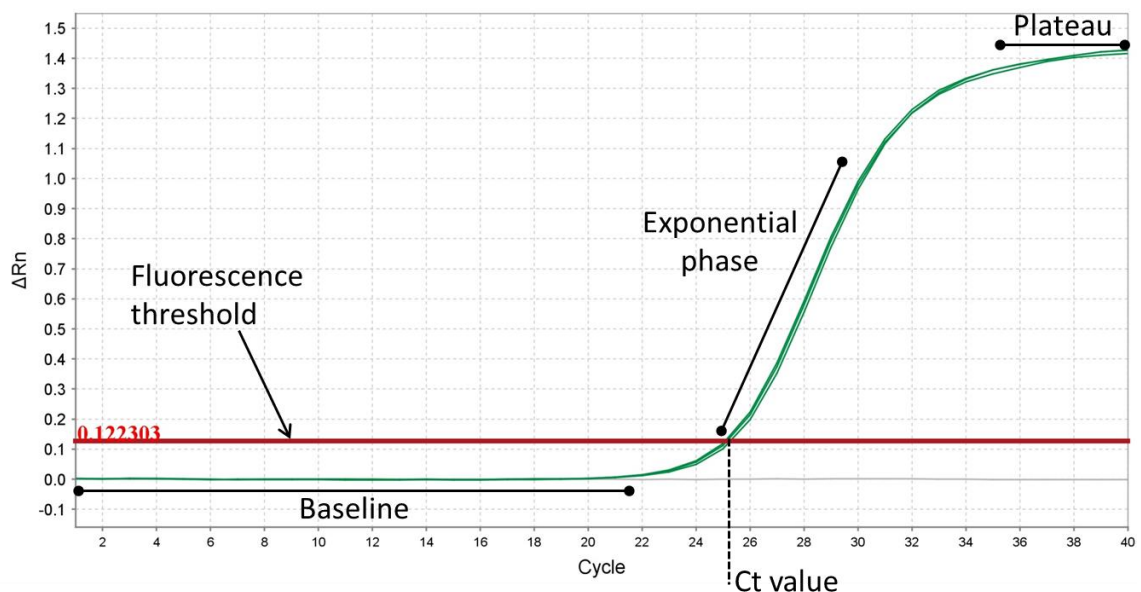
Figure 3.2 – Example RT-PCR trace RT-PCR was used to assess the levels of microRNA in samples, this shows the basic elements of a RT-PCR trace; baseline, exponential and plateau phases and how the Ct value is extracted using the fluorescence threshold. This average Ct value of the triplicates shown here was 25.1256732.

The Viia-7 RUO software exported a data file that listed the Ct values for all of the microRNA probes on that array. The analysis of each array was then carried out to produce a list of expression values for the microRNA in that sample that could be compared to other samples. The steps for this analysis are outlined in Figure 3.3 and are described in detail below.
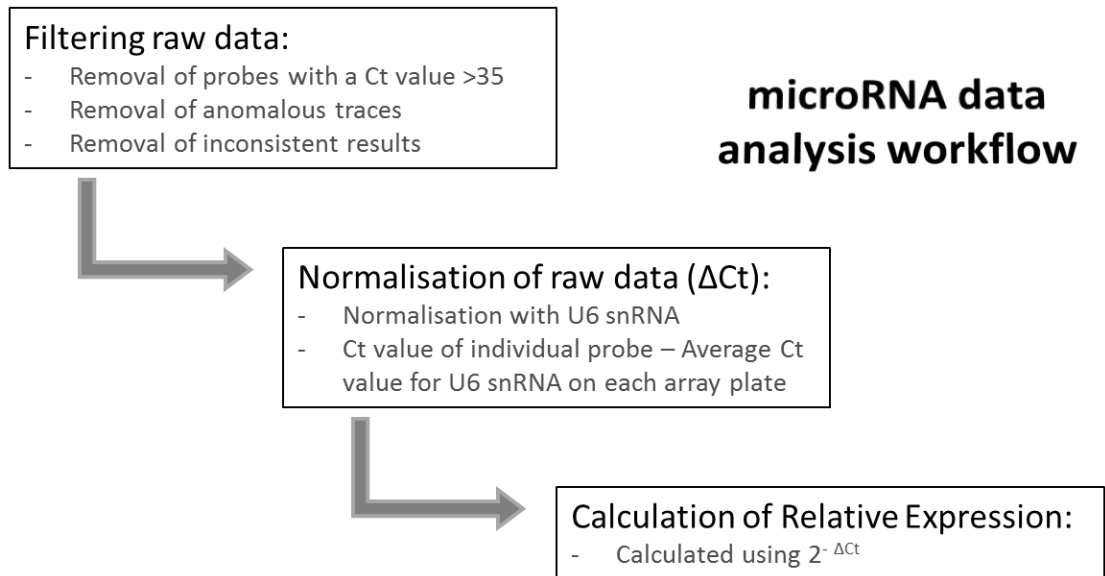
Figure 3.3 – Workflow for analysing the raw data from TaqMan microRNA microarrays *A breakdown of the 3 key steps taken to convert the raw Ct values from the TaqMan microRNA microarrays to relative expression data usable in downstream analyses.*

3.3.6.1 Filtering the raw data for anomalies

Due to the low concentration of the samples and the small size of microRNA the raw data values determined by the software could not be completely relied upon and several checks had to be made to remove potential anomalies. Firstly any probes with raw Ct values over 35 were removed due to low confidence that values this high represented actual detection of the specific microRNA. Secondly traces were manually checked to ensure that the expected baseline, exponential and plateau phases were present. These manual checks were made as the software was unable to tell the difference between anomalous traces which crossed the threshold and a normal trace crossing the threshold. The final filtration step was to remove any microRNA that did not appear in 100% of array replicates carried out on that sample type. This ensured that single instances of microRNA detection were not able to affect the overall results and that the observed microRNA profiles were representative of at least 3 replicates.

3.3.6.2 Normalisation with U6 snRNA

Each TaqMan microRNA microarray card (both A v2.1 and B v3.0) contained a variety of control probes. Each array card had 4 separate wells containing probes for the non-coding small nuclear RNA U6 (U6 snRNA). U6 snRNA has been widely used as a housekeeping gene due to its stability across a wide variety of samples and it was also identified as one of the most stable probes in my datasets using NormFinder (3.3.6.5). Each microarray card was normalised separately using the average Ct value of all 4 U6 snRNA probes on that array. The average Ct value was subtracted from the Ct of the probe of interest and this gave a value termed the ΔΔCt.

3.3.6.3 Calculating relative expression of microRNA

The relative expression (RE) values for each microRNA were calculated using the ΔΔCt value, which was put into the following formula for each probe on all arrays:

$$\textbf{\textit{``2$^{-ΔΔCt}$ / (2 to the power of negative ΔΔCt)''}}$$

This made the RE values reflect the doubling in gene concentration observed with an increase of 1 in Ct value and provided directly comparable expression values.

3.3.6.4 Calculating an average expression profile for pdEV

For the further analyses carried out on the platelet and pdEV microRNA profiles it was useful to summarise all of the separate agonist pdEV microRNA profiles in a single profile. Therefore the average RE expression of all 90 microRNA identified within pdEV was calculated by averaging the expression values for all 4 separate agonist profiles.

3.3.6.5 NormFinder

NormFinder is a Microsoft Excel add-in that was used for identifying normalisation genes. It used an algorithm to assess the stability of all genes across an array (http://moma.dk/normfinder-software Date accessed – 9/7/2014) (Andersen et al., 2004). This method provided an estimation of expression variation, meaning that genes with low variation in expression were the strongest candidates for normalisation.

3.3.6.6 Comparison between platelet microRNA datasets

Whilst the profiling of the microRNA contained within pdEV is novel, investigating the microRNA within platelets has been carried out numerous times (Sondermeijer et al., 2011, Landry et al., 2009, Ple et al., 2012a, Stratz et al., 2012, Xu et al., 2012, Osman and Falker, 2011, Nagalla et al., 2011, Bray et al., 2013). Collating the data from these other datasets provided an opportunity to assess the quality of the data collected through the work carried out here. The previous

datasets were identified through searching PubMed (www.ncbi.nlm.nih.gov/pubmed Date accessed – 9/7/2014) and the GEO datasets database (http://www.ncbi.nlm.nih.gov/gds Date accessed – 9/7/2014) for platelet microRNA profiles. These datasets had all been produced using platelets from healthy donors on a variety of microRNA profiling platforms.

The pre-existing datasets of platelet microRNA were generated using different microRNA profiling platforms. Therefore the first step to allow comparisons was to update all of the platforms' naming nomenclatures to that found in miRbase v20 (http://www.mirbase.org/ Date accessed – 16/3/2015). RE data was obtained for each dataset and this was normalised so that the most highly expressed microRNA was given a value of 1000 and all other microRNA in the dataset were scored relative to the most highly expressed microRNA using the following formula:

"Normalised expression = [RE of gene of interest / RE of most highly expressed gene] x 1000"

The normalised datasets were then directly compared to each other by generating heatmaps and correlations between the datasets calculated using GENE-E (3.3.7.2.1).

3.3.6.7   Comparative analysis with platelets, pdEV and plasma microRNA

A plasma dataset was kindly provided by my co-supervisor, Dr J H Pringle, whose student Dr M I Aslam had carried out the analysis. The dataset was produced using the TaqMan microRNA microarray cards v2.1 and analysed plasma from healthy donors, produced using a 30minute centrifugation at 1800g (RT).

The datasets were sorted so that differences between the v2.1 and v3.0 TaqMan microRNA microarray cards were removed. The raw Ct values were filtered as above to remove anomalous traces and probes with a Ct value above 35. The ΔΔCt was then calculated using U6 snRNA to normalise the cards as described above, 3.3.6.2, and then RE was calculated using the $2^{-\Delta\Delta Ct}$ method. The RE datasets were compared using Venn diagrams (3.3.7.1), scatter plot matrices (3.3.7.3) and correlations were calculated using GraphPad prism (3.3.7.4).

3.3.6.8   Comparative analysis with 40 tissues profiled using TaqMan microRNA microarrays

microRNA profile datasets were collated from Life Technologies who produced the data using their TaqMan microRNA microarray cards (Liang et al., 2007), they profiled 40 different samples using the TaqMan microRNA microarray A card v2.1, which looked for 381 unique microRNA.

The raw Ct values from the platelet, average pdEV and plasma microRNA profiles were compared with the 40 tissues and the microRNA from the different TaqMan microRNA microarray A card versions were aligned. NormFinder (3.3.6.5) was then used to identify a microRNA expressed consistently across all 43 samples; leading to hsa-miR-324-5p being used to normalise all of the samples. The ΔΔCt was calculated as above (3.3.6.2) using hsa-miR-324-5p and then the RE was calculated using the $2^{-\Delta\Delta Ct}$ method.

The RE values were entered into MeV to generate heatmaps with hierarchical clustering (3.3.7.2.2.1) and to identify potential biomarkers using a 2 group t-test (3.3.7.2.2.2). The data were also analysed using GraphPad Prism to show how the different samples correlated (3.3.7.4).

3.3.7 Statistical analysis techniques for comparing microRNA profiles

Once the datasets were normalised and the relative expression calculated it was possible to identify similarities and differences between the groups.

3.3.7.1 Venn diagrams

Venn diagrams were used to show the overlap between different subgroups, they were created using online software provided by a joint enterprise between The Flanders Interuniversity Institute for Biotechnology and The University of Ghent (bioinformatics.psb.ugent/webtools/Venn Date accessed – 10/4/2014). The lists of microRNA were added to the software which calculated the overlap between groups.

3.3.7.2 Microarray analysis software

3.3.7.2.1 GENE-E

GENE-E (Broad Institute, Harvard, USA - http://www.broadinstitute.org/cancer/software/GENE-E/ Date accessed – 27/5/2014) was used to visualise and analyse microarray data. GENE-E was created and developed by Joshua Gould.

3.3.7.2.1.1 Generating Heatmaps with GENE-E

To generate heat maps the RE data was opened with GENE-E which automatically generated heatmaps that could be manipulated aesthetically and analysed using a variety of statistical techniques including hierarchical clustering, ordering, correlation comparisons and filtering. The heat maps were used to display similarities and differences between sample groups

3.3.7.2.1.2 Hierarchical clustering in GENE-E

Hierarchical clustering re-ordered samples based upon their inter-relatedness, which was analysed using Pearson correlation with average linkage.

3.3.7.2.1.3 Analysis of correlation between datasets in GENE-E

All samples within a comparison were analysed to assess their correlation. This used a Pearson correlation calculation to generate r^2 values for each pair of samples and then these values were mapped into a similarity matrix which was colour coded like a heatmap. The samples were also reordered to cluster similar samples.

3.3.7.2.2 Multi-Experiment Viewer (MeV)

MeV is an open source microarray analysis tool, (http://www.tm4.org/ Date accessed – 27/5/2014) which provide a package of microarray analysis tools (Saeed et al., 2003). It was used as well as GENE-E as it provided the ability to perform more detailed analysis between subsets of data.

3.3.7.2.2.1 Hierarchical clustering in MeV

Hierarchical clustering was performed as in GENE-E utilising Pearson correlation with average linkage.

3.3.7.2.2.2 Analysis of differences in individual microRNA across datasets in MeV

A 2 group t-test was performed to compare the microRNA profiles of 40 tissues to platelets, average pdEV and plasma. For the t-test the samples were split into the 40 tissues and the other 3 (platelets, average pdEV and plasma) and equal variance between the samples was assumed. The significance threshold was set at $p < 0.01$ and the results were adjusted for multiple comparisons using standard Bonferroni correction.

3.3.7.3 Scatter plot matrices

Scatter plot matrices were generated using GraphPad prism these allowed for the visualisation of the correlation between sample groups and individual samples.

3.3.7.4 Dataset correlations

Dataset correlations for samples were also carried out using the statistical software GraphPad Prism (GraphPad Software Incorporated, La Jolla, USA). RE values were loaded and a correlation analysis was applied to compute Pearson correlation co-efficients which were represented as r^2 values.

3.4 Results

The results in this chapter focus on obtaining the microRNA profile of platelets, and pdEV and comparing these results to microRNA profiles of plasma, and previously published studies on platelets, and utilising this information to identify potential biomarkers of platelet activation.

3.4.1 RNA extractions from platelets and platelet-derived EV

Platelet and pdEV samples were prepared in two studies; the first used 45mL of blood from 4 healthy donors, the platelets were isolated (2.3.5) and separated into 2 equal volume aliquots, one of which was pelleted and one was activated with thrombin to generate EV that were isolated by differential centrifugation (2.3.8.1), followed by overnight incubation with ExoQuick (2.3.8.2). For the second study, 4 sets of EV samples were prepared; 45mL of blood was collected from 3 different healthy donors and the platelets were isolated by washing. The platelets were then split into 4 aliquots and each was activated by a different agonist to generate EV. The agonists used were; CRP-XL (2µg/mL), PAR1-AP (10µM), PAR4-AP (200µM), thrombin (0.32U/mL) and ADP (50µM) followed by differential centrifugation to produce an EV rich supernatant, as in Chapter 2. Following preparation of the samples, the total RNA was extracted using the miRNeasy micro kit (3.3.1.1) and the quantity and quality of this RNA was measured using a Nanodrop ND8000 spectrophotometer (3.3.1.3), the results of which are shown in Table 3.2.

The concentration of RNA in these samples was low (between 29 and 3ng/µL), but this was unsurprising due to low input volumes. The ratio of absorbance at 260nm and 280nm reflects the purity of samples; a value of 2.00 is deemed as pure for RNA and all of the samples had a value within ±10%. The 260/230 ratio identified the presence of contaminants that absorbed at 230nm (e.g. phenol and guanidine), the expected value was again 2.00 and all of the samples had values within ±17%. The lower values, such as 1.67 for replicate 3 in the PAR1-AP generated EV indicated the sample may have been contaminated with EDTA, carbohydrates or phenols which all absorb at ~230nm. The samples listed in Table 3.2 were used for microRNA profiling with the TaqMan microRNA microarray cards. Before profiling the samples were reverse transcribed, 3.3.2.1, and amplified using the Megaplex Primer pools A and B as described in 3.3.3.1.

Table 3.2 – Information on the RNA samples used for the TaqMan microRNA microarrays *The quality and quantity of RNA extracted from platelets and pdEV was measured using a Nanodrop ND8000 spectrophotometer prior to RTr and amplification for use on the TaqMan microRNA microarrays.*

Sample type	Replicate	Concentration (ng/µl)	Total RNA (ng)	260/280 ratio	260/230 ratio
Platelets	1	29.58	739.50	1.85	1.84
	2	11.18	279.50	1.81	1.68
	3	18.16	454.00	1.92	1.91
	4	9.86	246.62	1.96	1.8
Thrombin generated EV (ExoQuick)	1	14.49	362.25	1.90	1.75
	2	6.59	164.75	1.88	1.88
	3	8.81	220.32	1.89	1.92
	4	6.94	173.70	1.92	1.76
CRP-XL generated EV	1	8.88	177.68	1.95	1.72
	2	6.15	123.18	1.97	1.78
	3	3.26	65.26	1.88	2.07
PAR1-AP generated EV	1	4.12	82.54	1.93	1.77
	2	3.35	67.14	2.08	1.86
	3	3.43	68.78	1.88	1.67
PAR4-AP generated EV	1	3.05	61.18	2.01	1.9
	2	6.88	137.74	1.88	1.77
	3	3.24	64.86	1.90	1.77
ADP generated EV	1	3.61	72.22	1.86	1.71
	2	3.47	69.56	1.91	1.79
	3	3.30	66.08	1.95	1.79

3.4.2 TaqMan microRNA microarray cards

3.4.2.1 Individual sample microarray results

To profile the samples using TaqMan microRNA microarray cards v3.0, as described in 3.3.5.1; 9µL of cDNA was mixed with 450µL TaqMan fast master mix and 441µL MilliQ water, loaded into the TaqMan microRNA microarray cards and run on a Viia7 RT-PCR instrument. The data were filtered to remove anomalous results, normalised to a ΔΔCt value using the average expression of U6 snRNA on each microarray card and then RE was calculated using $2^{-\Delta\Delta Ct}$ (3.3.6). A summary of the results from the microRNA profiling are shown in Table 3.3.

Table 3.3 – Overview of microRNA profiles of platelets and pdEV Details of the results from the TaqMan microRNA microarrays, providing information on each replicate, and the averaging of replicates including total numbers of microRNA and the most abundant microRNA in each sample.

Sample type	Replicate	Number of microRNA	Number of consistently expressed microRNA	Most abundant microRNA
Platelets	1	259		hsa-miR-223-3p
	2	309	220	hsa-miR-223-3p
	3	344		hsa-miR-223-3p
	4	328		hsa-miR-223-3p
Thrombin generated EV (ExoQuick)	1	154		hsa-miR-223-3p
	2	116	62	hsa-miR-223-3p
	3	122		hsa-miR-223-3p
	4	109		hsa-miR-223-3p
CRP-XL generated EV	1	146		hsa-miR-223-3p
	2	123	79	hsa-miR-223-3p
	3	108		hsa-miR-223-3p
PAR1-AP generated EV	1	102		hsa-miR-223-3p
	2	92	66	hsa-miR-223-3p
	3	131		hsa-miR-223-3p
PAR4-AP generated EV	1	100		hsa-miR-223-3p
	2	90	57	hsa-miR-223-3p
	3	92		hsa-miR-223-3p
ADP generated EV	1	99		hsa-miR-223-3p
	2	119	71	hsa-miR-223-3p
	3	127		hsa-miR-223-3p

The number of microRNA identified in the replicates for each sample type was variable with a difference of 85 between replicates 1 and 3 in the platelet samples, representing an increase of 32%. The EV samples showed a similar pattern with the identification of ~40 more microRNA in the largest compared to the smallest profiles for each pdEV sample type, accounting for 25-33% of microRNA identified. When the replicates for each sample type were combined to produce a definitive microRNA profile of consistently identified microRNA, the platelet profile contained 220 microRNA; thrombin generated pdEV; 62, CRP-XL pdEV; 79, PAR1-AP pdEV; 66, PAR4-AP pdEV; 57 and ADP pdEV; 71 (Figure 3.4A). This pattern in the number of microRNA species identified in pdEV closely reflected the concentration of EV produced by the different agonists, as seen in (Figure 2.13).

Overall the number of consistently expressed microRNA in pdEV populations was very similar and the number of microRNA consistently expressed in platelets was significantly greater than detected in EV. Figure 3.4B shows a comparison between the expression profiles of the different samples, the ranked RE levels in all of the pdEV samples follow a very similar pattern with a few microRNA with very low expression (RE=<0.5) and most microRNA having RE levels between 0.5

and 10 and a few highly abundant microRNA (RE=>10). In contrast the platelet profile contained a significant number of low abundance (RE=<0.5) microRNA. The most abundant microRNA in all replicates of all samples was hsa-miR-223-3p, the expression of which, was significantly greater than any other microRNA. The function of this microRNA is explored further in Chapters 4 and 5.
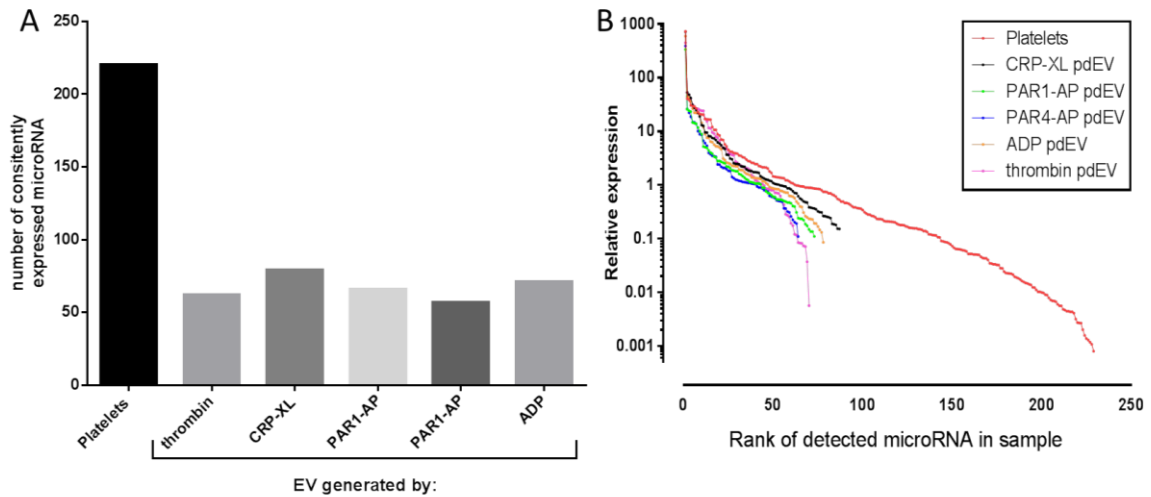
Figure 3.4 – Number and ranked RE of microRNA identified A) Information on the number of consistently identified microRNA in platelets and each pdEV sample type. B) Sigmoid plots comparing the ranked distribution of microRNA RE across the platelet and pdEV samples.

Whilst an initial analysis provided information on the number of microRNA identified and the spread of microRNA expression, a more in depth analysis was required to investigate how the different groups were related. However before this it was important to validate some of the results from the microarrays using single assay RT-PCR.

3.4.2.2   Validation of microarray findings

miR-223-3p and miR-21-5p were selected for validation; miR-223-3p as it was the most abundant microRNA in all samples and miR-21-5p as it was consistently expressed in all samples but had significantly lower expression than miR-223-3p (average pdEV RE = 6.56 vs. 509.63). For validation, 4 new samples were generated for each sample type in exactly the same way as the microarray samples and analysed using a single probe RT-PCR reaction for miR-223-3p and miR-21-5p, as described in 3.3.4. The results of these validation experiments are shown in Figure 3.5.
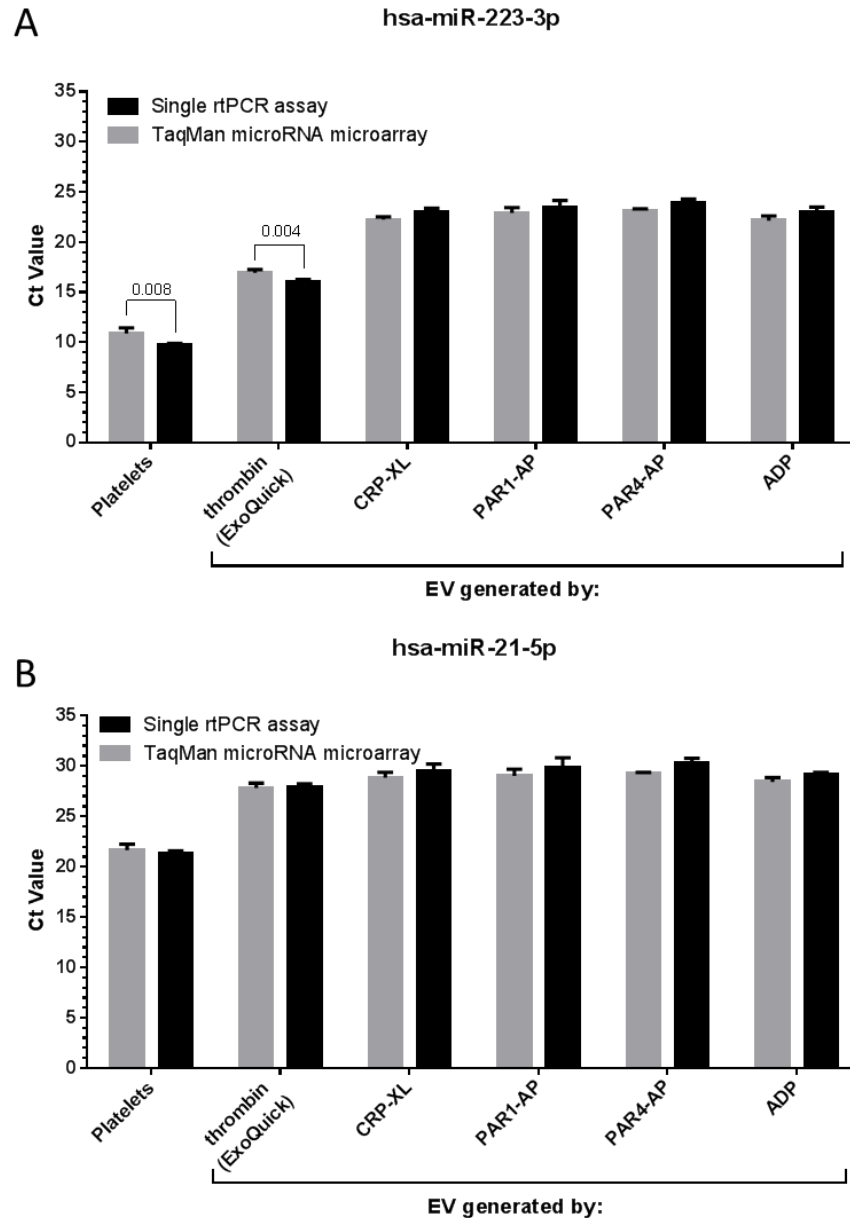
Figure 3.5 – Validation of TaqMan microRNA microarray results *A) hsa-miR-223-3p and B) hsa-miR-21-5p were identified using the TaqMan microRNA microarrays, and these results were validated using individual RT-PCR assays. The graphs compare the Ct values achieved on the microarrays (n=3 or 4±SD) to a separate cohort of samples measuring the same microRNA expression using a single TaqMan microRNA assay (n=4±SD, multiple t-tests with Holm-Sidak correction for multiple comparisons).*

Figure 3.5 shows that the values obtained from single RT-PCR reactions match those obtained from the microarrays. For miR-223-3p, the results of the microarray for the platelet and thrombin generated EV samples are 2 Ct cycles higher than the individual assays (p=0.008 and 0.004 respectively). However all of the other EV generated samples have microarray and single RT-PCR assay results within 1 Ct cycle of each other. When looking at miR-21-5p the results correlate strongly, with all samples except for the PAR4-AP generated EV being within a single Ct cycle of each other. These results suggest that the microarray results are a true reflection of the expression of miR-223-3p and miR-21-5p and it is likely that other results will follow this

pattern. However if further analyses identified microRNA of interest the results were independently verified.

3.4.2.3 Comparison of pdEV microRNA with platelet microRNA

Following the preliminary analysis and verification of the data from the TaqMan microRNA microarrays it was possible to carry out a more in depth analysis.

3.4.2.3.1 Top 10 microRNA – Comparison of expression

The relative expression of the 10 most abundant microRNA were directly compared, these 10 microRNA were identified by averaging the RE of all microRNA across all samples and then taking the 10 most abundant microRNA from this list. This produced a list containing miR-223-3p, miR-146a-5p, miR-19b-3p, miR-24-3p, miR-126-3p, miR-106a-5p, miR-191-5p, miR-17-5p, miR-30c-5p and miR-92a-3p.

Figure 3.6 shows expression levels of these 10 microRNA in all samples. Looking at the expression of miR-223-3p it is clear that it was expressed at a significantly greater level than any other microRNA, with on average a 14-fold greater abundance than the second most abundant microRNA. A comparison of the expression of miR-223-3p across the different sample types shows that it is almost twice as abundant in platelets and CRP-XL generated EV compared to PAR1-AP and PAR4-AP generated EV. The low expression levels in PAR1-AP and PAR4-AP generated EV is consistent across all of the different microRNA species shown. The overall trend of expression appears consistent for all sample types with only one clear anomaly; miR-30c-5p in thrombin generated EV. MiR-30c-5p has significantly higher expression in thrombin generated EV than any other sample; 3 times the expression of platelets and ~10 times the expression in all other EV populations. This suggests that the microRNA profile of thrombin-derived pdEV was different to the other pdEV, although many of the microRNA observed in the thrombin samples (Figure 3.6) correlate strongly with the other samples. This could in turn suggest that there is compartmentalisation of miR-30c-5p through increased incorporation of this microRNA into pdEV generated by thrombin.
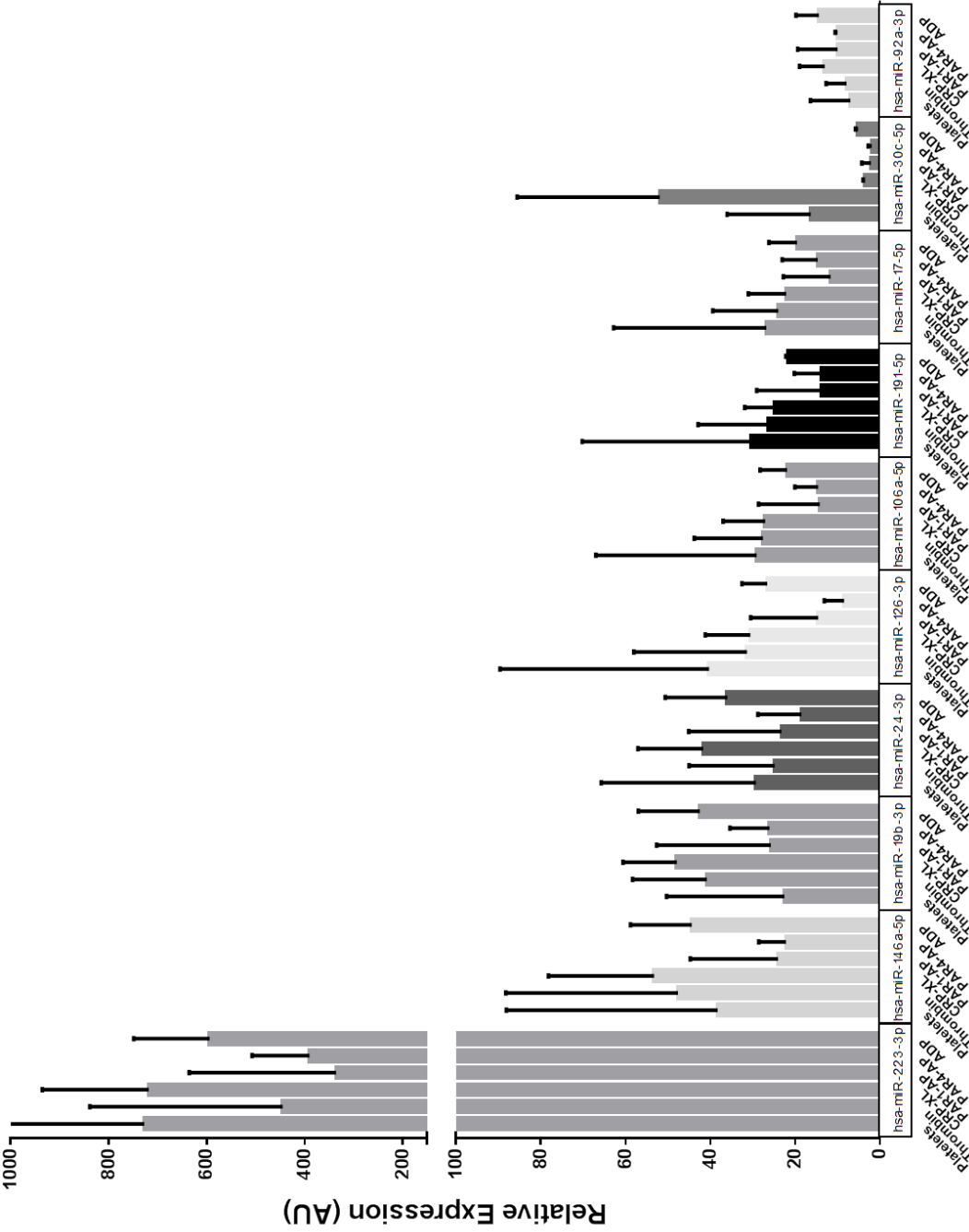
Figure 3.6 – Comparison of the expression of the 10 most abundant microRNA *The 10 most abundant microRNA in platelets and platelet-derived EV were calculated by determining the average relative expression across all samples of all microRNA and then selecting the top 10. The graph here shows the comparison of the relative expression levels of each of these 10 microRNA in all samples (n=3 or 4±SD).*

3.4.2.3.2   Comparison of total microRNA expression profiles

The analysis of the similarities and differences between the microRNA profiles using the highly expressed microRNA revealed few differences and so the analysis was extended to compare complete microRNA profiles. Table 3.3 showed that the full profiles appear very similar, with all pdEV samples having analogous numbers of microRNA and sharing miR-223-3p as the most abundant microRNA. However further techniques were required to enhance the detail of this analysis; the full microRNA profiles were analysed using heatmaps, Venn diagrams, scatter plot matrices and correlation statistics.

The heatmaps in Figure 3.7 were generated using GENE-E (The Broad institute) as described in 3.3.7.2.1.1 using normalised relative expression data. The heatmap was ordered based upon the expression of the microRNA in platelets; microRNA that were not identified in a sample appear grey. The heatmap confirmed the findings in Figure 3.6; it showed that the highly expressed microRNA, particularly the 10 most abundant were expressed at consistent levels in all samples and this trend largely continued for the 35 most abundant microRNA with 3 notable exceptions; miR-484-5p, miR-454-5p and let-7a-5p. These 3 microRNA were detected with high expression in platelets but were not present in any of the pdEV samples suggesting that they are selectively retained in platelets. MiR-484-5p has been implicated in mitochondrial fission (Wang et al., 2012a), miR-454-5p in TGF-β/SMAD signalling (Liu et al., 2013) and let-7a-5p, as part of the let-7 family has roles in cell development and differentiation. All of which could be potential reasons for the retention of these microRNA, although, due to the sequence homology of the let-7 family, the absence of let-7a may be compensated for by the presence of let-7d/e/g (Boyerinas et al., 2010).

The low abundance platelet microRNA were less likely to be identified within pdEV samples, with only 15 of the 110 (14%) least abundant platelet microRNA being observed in any of the pdEV populations. The heatmap clearly shows that beyond the highly expressed microRNA there was more variation in the microRNA profiles with thrombin generated EV being particularly different. 12 of the 62 (19%) microRNA in thrombin pdEV were unique, CRP-XL EV had 6 (7%) unique microRNA, PAR1-AP EV had 1 (miR-744), PAR4-AP EV had no unique microRNA and ADP EV had 5 (7%). Overall this suggested that either all of the low abundance platelet microRNA were selectively retained in platelets or the profiling platform was not sensitive enough to detect them. Taken together the data suggests that there was no clear evidence of selection into pdEV based upon the agonist used.

These differences in overall microRNA profile were explored further in the Venn diagram (Figure 3.8) which clearly shows that all microRNA identified in pdEV were expressed within platelets and from the 5 separate populations of pdEV there was a core group of 36 microRNA expressed in all samples. This Venn diagram adds further evidence to the suggestion that the microRNA profile of thrombin generated EV was significantly different to all other pdEV. There were 12 microRNA unique to thrombin generated pdEV representing almost 20% of the microRNA profile that were completely separate and there were 10 microRNA that were found in all 4 of the other pdEV samples that were not detected in thrombin generated EV. The difference in the observed profile of thrombin generated pdEV is likely to be due to their production in a separate experiment with different donors and the use of an additional isolation step with ExoQuick, as described in 3.4.1, so should not be over-interpreted.

Figure 3.9 added a statistical analysis to the inter-pdEV comparison; the scatter plot matrix on the left showed that the Log2 transformed relative expression values were correlated. From these figures it was clear that the thrombin microRNA profile was very different, as demonstrated by the Pearson correlation coefficients. The other 4 pdEV samples correlated closely with r^2 values of between 0.8902 and 0.9463 (p=<0.0001), whereas the highest correlation coefficient for the thrombin samples was 0.7117 when compared to ADP generated EV and the correlation was as low as 0.5739 when tested against the microRNA profile of PAR4-AP generated EV. However, despite these differences the correlations were still significant (p=<0.0001).

Figure 3.7 – Heatmap comparing microRNA profiles of platelets and pdEV *A heatmap to compare the complete profiles of microRNA in platelets and the EV they release in response to a variety of agonists. The heatmap is split into 2 sections; section 1 on the left is continued from the top of section 2 on the right.*
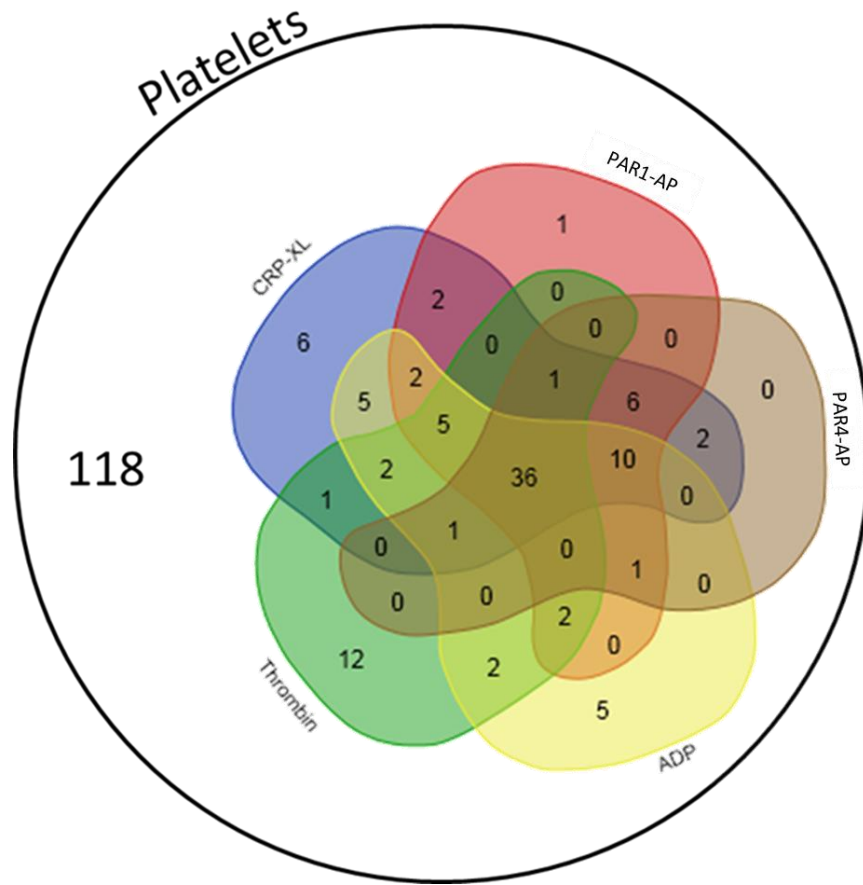
Figure 3.8 – A Venn diagram showing the overlap in microRNA profiles *A Venn diagram to show how many microRNA are shared between whole platelets and the EV they release and between the EV released from platelets in response to different agonists.*
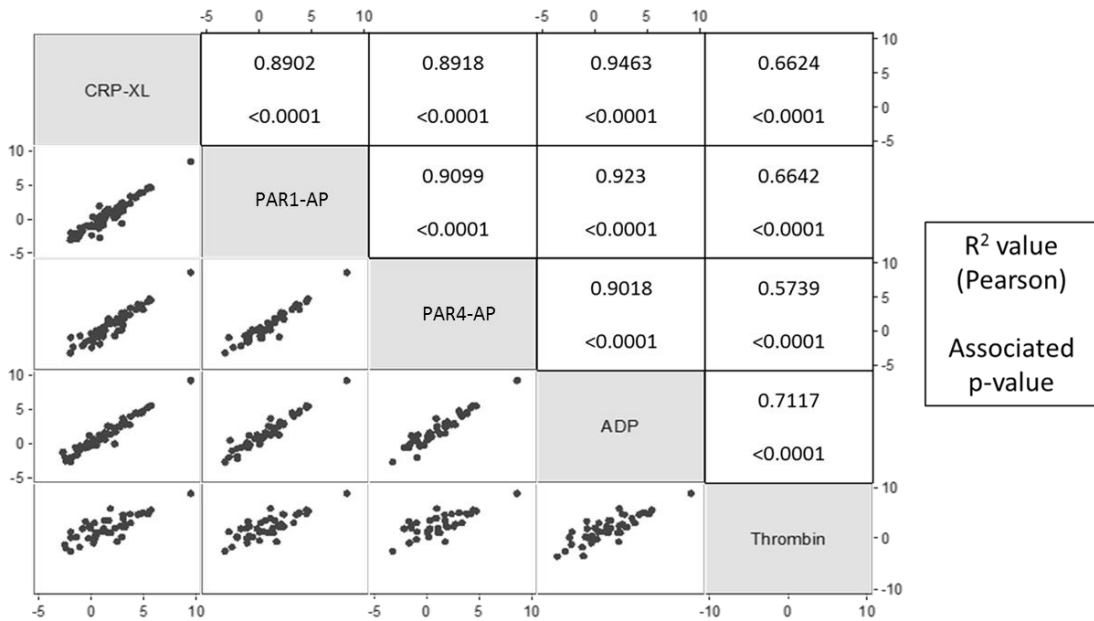
Figure 3.9 – Correlation of EV microRNA profiles *The microRNA profiles of the various EV populations were assessed using a correlation matrix and Pearson correlation statistics in GraphPad prism. The figure shows the correlation between the Log$_2$ RE values of each pair of EV populations as a scatter plot and the associated correlation coefficients.*

Taking the results from Figure 3.7, Figure 3.8 and Figure 3.9 together it was clear that the thrombin generated EV microRNA profile was different to that of CRP-XL, PAR1-AP, PAR4-AP and ADP generated EV. The thrombin pdEV samples were prepared with ExoQuick, which used a polyethylene glycol based approach to prepare a solution containing exosomes and this change in preparation and the use of different donors at a different time suggested that these samples were not directly comparable. Therefore the next section reanalysed the comparison between pdEV and the core microRNA without the results from the thrombin pdEV. The future analyses against other datasets then used an average pdEV microRNA profile, compiled as detailed in 3.3.6.4, from the microRNA profiles of CRP-XL, PAR1-AP, PAR4-AP and ADP generated pdEV.

3.4.2.3.3 Venn diagram comparing platelets and platelet-derived EV microRNA profiles

Figure 3.10 shows the changed dynamic of the overlap in microRNA profiles between platelets and pdEV. The pdEV were made up of 90 unique microRNA, all of which were found in platelets; these 90 made up the average pdEV microRNA profile used in future analyses. With the removal of the thrombin pdEV the 4 remaining pdEV samples have increased overlap, with a core group of 46 microRNA being detected in all samples. The figure also shows that 75 of the 90 microRNA in pdEV were detected in 2 or more populations and 62 in 3 or more, emphasising how closely related the microRNA profiles were, regardless of the agonist used to generate the pdEV. This reflected the results of Figure 3.9 and suggested that the agonist used to stimulate EV release from platelets did not affect the profile of microRNA released. This was an interesting result considering the differential populations of EV released from platelets in response to the same agonists in chapter 2.
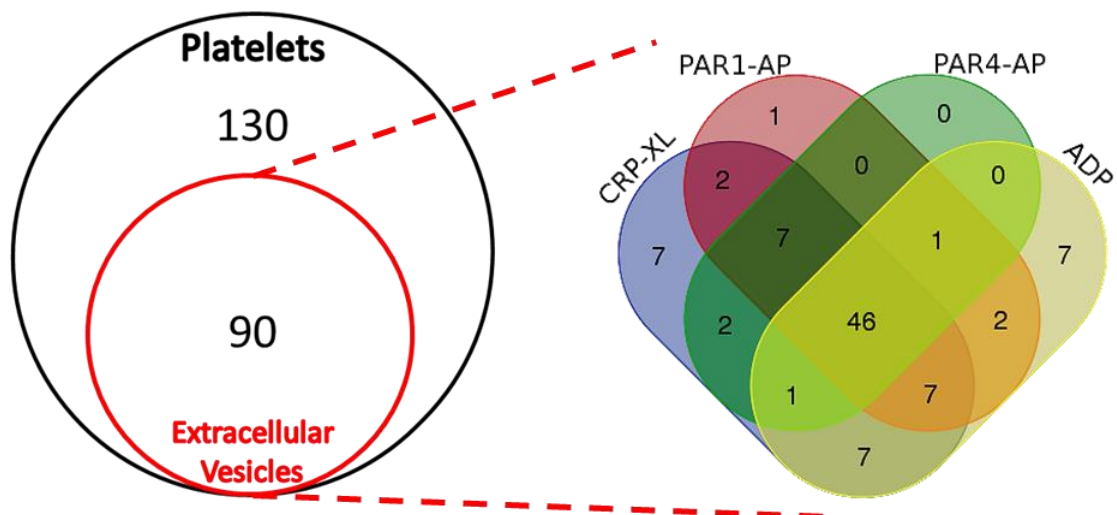
Figure 3.10 – Overlap in microRNA profiles between whole platelets and pdEV *A Venn diagram showing the overlap between the microRNA profiles of whole platelets and pdEV released from platelets through stimulation with CRP-XL, PAR1-AP, PAR4-AP and ADP. The figure is broken into 2 sections; firstly looking at platelets and the average of pdEV and then a breakdown of the overlap between the different EV populations.*

3.4.2.3.4   Analysis of highly expressed microRNA

To further analyse the microRNA profile of platelets and pdEV the 46 microRNA identified as being present in all samples by the Venn diagram in Figure 3.10 were used to generate a heatmap in GENE-E (3.3.7.2.1.1). The resulting heatmap is shown in Figure 3.11 from which several observations can be made; firstly the platelet and pdEV profiles showed high visual similarity with high and low abundance microRNA being the same in almost all samples. However the heatmap does show lower levels of mIR-21-5p and miR-451 in platelets compared to that of the pdEV. Secondly, the commonly researched miR-17/92 cluster and its paralogues miR-106a/b account for 10 of the 46 consistently expressed microRNA. This suggests that these EV may exert functions closely tied to the roles of this cluster of microRNA. The heatmap and Venn diagram provide visual information on the similarities between the sample types, however a statistical analysis was required for validation.
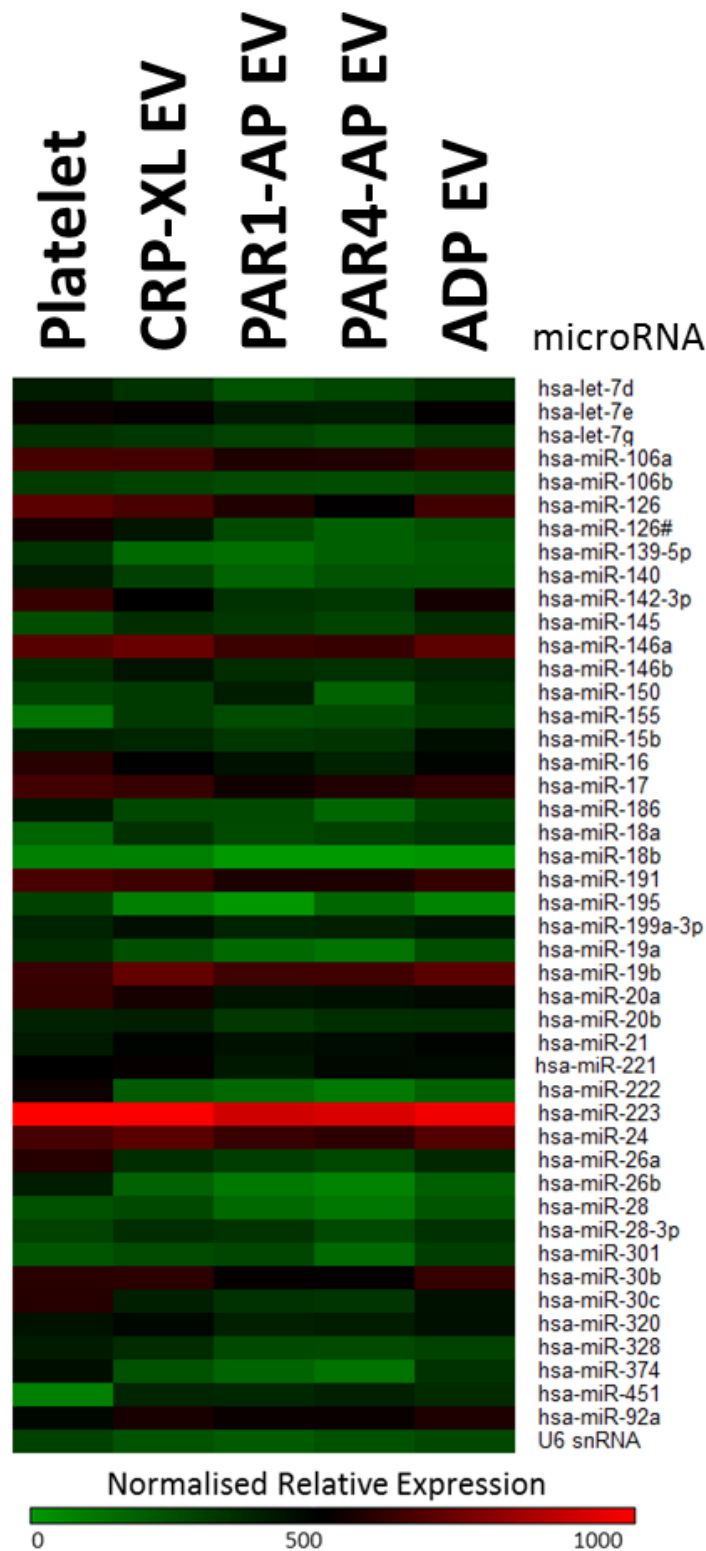
Figure 3.11 – The 46 consistently expressed microRNA in platelets and pdEV *46 microRNA were identified as consistently expressed in all populations of pdEV and in unstimulated whole platelets, these 46 microRNA are visualised here as a heatmap, allowing for comparisons between expression levels in the different EV populations and platelets.*

3.4.2.3.5 Comparison of microRNA expression using gene expression heat-maps

The similarity of expression between the 46 consistently expressed microRNA in pdEV was

measured using the similarity matrix function in GENE-E (3.3.7.2.1.3). In generating the similarity

matrix the software calculated the Pearson correlation coefficients for each pair of pdEV replicates and used these values to generate a heatmap. In addition the samples were clustered using average linkage, showing which samples were most like each other. The results of this analysis are shown in Figure 3.12 which demonstrates that the correlation of the microRNA profiles of pdEV were significantly similar with almost perfect correlation r^2=>0.99 (p=<0.0001).

By assessing each individual replicate it was clear that the expression of these 46 microRNA showed strong inter-individual stability. The hierarchical clustering demonstrated that there was very little to differentiate the donors; only the PAR4-AP EV from donor 3 showed any difference. The consistency of expression of these 46 microRNA suggests that their presence within samples was reliable and that investigating functional effects of these microRNA would be useful in future work. The uniformity of microRNA profile in pdEV, regardless of agonist, indicated that there is possibly only one release mechanism for microRNA from platelets, such as exosomes.

Figure 3.12 – Similarity matrix heatmap comparing the expression of 46 consistently expressed microRNA in all pdEV replicates *Pearson correlation using average linkage was calculated between the microRNA profiles of each individual replicate of pdEV generated using CRP-XL, PAR1-AP, PAR4-AP and ADP. The similarity matrix was clustered using hierarchical clustering to move samples with similar profiles closer to each other.*

3.4.3 Comparison of platelet microRNA datasets

Whilst the profiling of the microRNA contained within pdEV was novel, investigating the microRNA within platelets had been carried out numerous times (Sondermeijer et al., 2011, Landry et al., 2009, Ple et al., 2012a, Stratz et al., 2012, Xu et al., 2012, Osman and Falker, 2011, Nagalla et al., 2011, Bray et al., 2013). Therefore, having profiled the microRNA of platelets, a comparison to the previous datasets provided an opportunity to assess the quality of the data collected here. The previous datasets of platelets from healthy donors were identified as described in 3.3.6.6. To allow comparisons between them the microRNA nomenclature was updated to the current miRbase version and the relative expression data normalised to a comparable scale, as described in 3.3.6.6. The datasets were then aligned and the data was entered into GENE-E to allow for visualisation and comparison.

Table 3.4 shows that all of the previously published profiles used different platforms, although two pairs of these differed only slightly, with the studies of Landry *et al.* and Nagalla *et al.* both using versions of the Exiqon miRcury LNA array. The Osman & Falker dataset used TaqMan microRNA microarrays which was the same as the platform used in the present experiment. The number of microRNA identified varied significantly with Xu *et al*. identifying almost twice as many as Landry *et al*. (389 vs 219), however 4 of the 7 profiles identified between 219 and 233 microRNA. The analysis also looked at the most abundant microRNA in each dataset and found that 4 of the datasets identified miR-223-3p as the most abundant and it was in the top ten of the other 3 datasets. MiR-21-5p, miR-103a-3p and let-7i-5p were the most abundant in the other 3 datasets, whilst these microRNA were expressed in all the other datasets, they were not highly expressed, particularly miR-103a-3p. In the dataset generated for this thesis miR-223-3p was expressed at significantly greater levels than all other microRNA, and for this to be different to 3 of the datasets suggests significant discrepancies between the different platforms and methods.

These inconsistencies were highlighted when the data was visualised as a heatmap in GENE-E (Figure 3.13) in which the microRNA were ordered based upon average expression across all datasets. The most abundant microRNA were listed first and it was apparent that their presence was consistent across all samples, although their level of expression was not always the same. However as the abundance of the microRNA decreased so did the uniformity of microRNA identification between the datasets. Table 3.5 highlights these changes; 513 microRNA were identified between the 7 datasets but only 81 microRNA were identified in all datasets (<25% of

each dataset) and 278 (54% of all the microRNA) were identified in 3 or less of the datasets, although these were predominantly microRNA with lower abundance.

The correlation of the platelet microRNA profiles was analysed using Pearson correlation and the results of this were mapped into a similarity matrix with hierarchical clustering using GENE-E (Figure 3.14). The similarity matrix showed that the correlation between the different datasets was not particularly strong. The two datasets with the strongest correlation were Osman *et al*. and our dataset, with an r^2 value of 0.836, the next strongest correlation was between Landry *et al*. and Nagalla *et al*. (r^2=0.6429). These 2 pairs of strongly correlated microRNA profiles were likely present due to sharing versions of the same microRNA profiling platform. The remaining datasets correlated with r^2 values of between ~0.4 and ~0.6, although correlations with the Sondermeijer *et al*. dataset were weak throughout. This findings demonstrate the challenges of identifying, comparing and interpreting microRNA data from the literature.

Table 3.4 – A comparison of platelet microRNA profiles *The details for the 7 microRNA profiles are compared, providing information on when and how the samples were profiled, information on the samples used and the resulting microRNA profiles.*

Source of array (reference)	Year	Sample	microarray	Number of microRNA identified	Most abundant microRNA
(Landry et al., 2009)	2009	Washed platelets from healthy volunteers with a CD45+ depletion step to remove leukocytes (n=unknown)	Exiqon miRcury LNA Array v8.1, miRbase 8.2	219	hsa-miR-223-3p
(Nagalla et al., 2011)	2011	Washed platelets from healthy volunteers with CD45+ depletion step to remove leukocytes (n=19)	Exiqon miRcury LNA Array v11.0, miRbase 13.0	284	hsa-miR-223-3p
(Xu et al., 2012)	2012	Washed platelets from healthy donors with density centrifugation to remove leukocytes (n=30)	G4470c human microRNA gene chip, miRbase 12.0 (Agilent)	389	hsa-miR-21-5p
(Stratz et al., 2012)	2012	Washed platelets from healthy volunteers with a CD45+ depletion step to remove leukocytes (n=5)	Geniom Biochip miRNA homo sapiens, miRbase 12.0	233	hsa-miR-103a-3p
(Osman and Falker, 2011)	2011	Washed platelets from healthy volunteers with a CD45+ depletion step to remove leukocytes (n=6)	TaqMan human microRNA microarray v2.1	281	hsa-miR-223-3p
(Sondermeijer et al., 2011)	2011	Washed platelets from healthy male volunteers (n=12)	Illumina Human v2 microRNA beadarray, miRbase v12	224	hsa-let-7i-5p
Ambrose	2014	Optimised washed platelet protocol for obtaining platelets from healthy donors without leukocyte contamination (n=4)	TaqMan human microRNA microarray v3.0	220	hsa-miR-223-3p
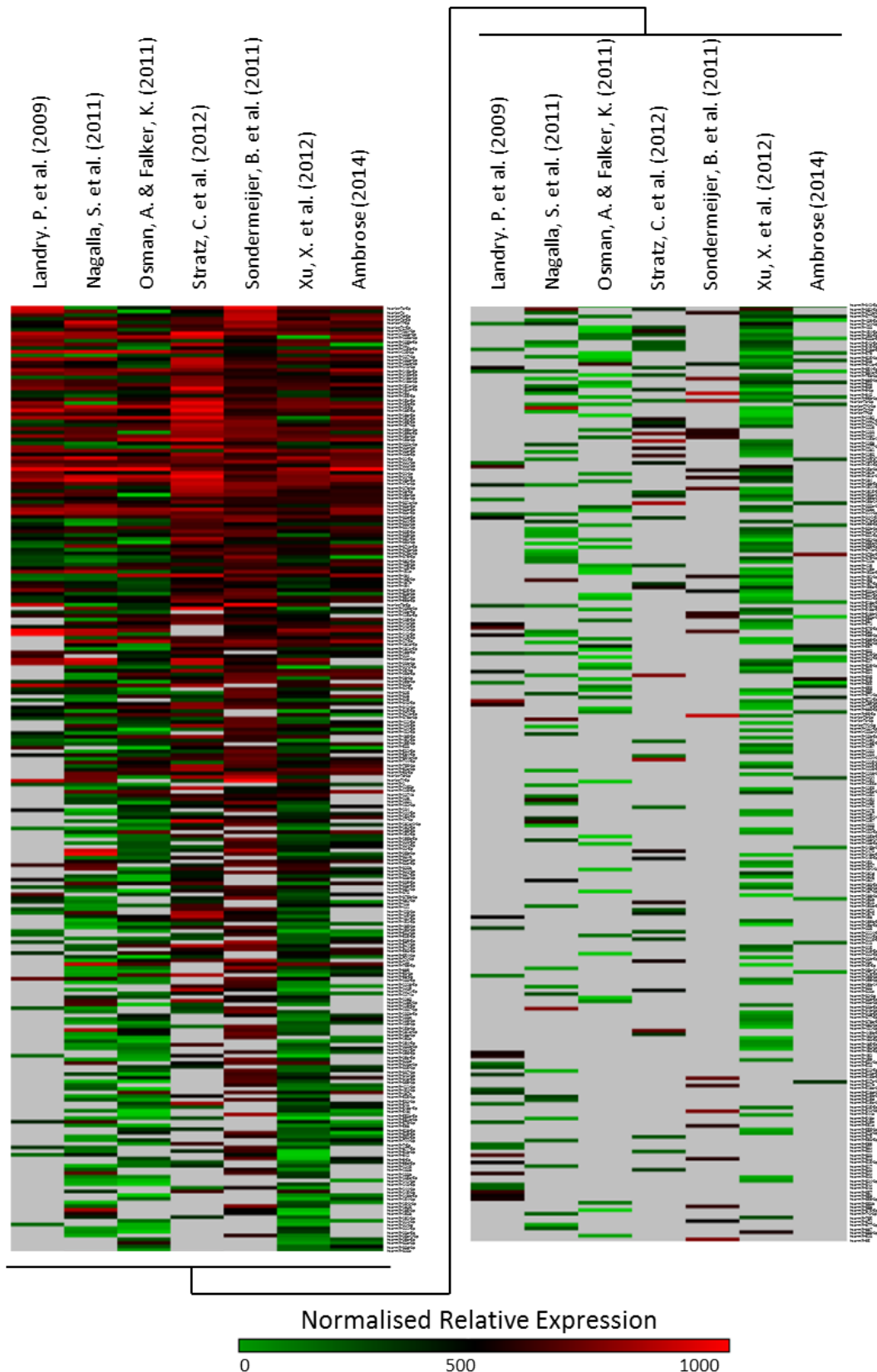
Figure 3.13 – Comparison of platelet microRNA profiles The platelet microRNA profiles identified from the literature were compared using a heatmap. Each sample shows the normalised relative expression of platelet microRNA and provides a comparison between the microRNA profiles identified in each study (Full-resolution image available on included CD). The heatmap is split into 2 sections; section 1 on the left is continued from the top of section 2 on the right.

**Table 3.5 – Overlap in microRNA between different platelet microRNA profiles** *The platelet microRNA profiles from the different sources were analysed using Venn diagram software to identify how many of the microRNA species were shared between the datasets.*

Number of datasets	Number of microRNA
7/7	81
6/7	47
5/7	56
4/7	51
3/7	50
2/7	85
1/7	143
Total	513

Pearson Correlation (average linkage) – r^2
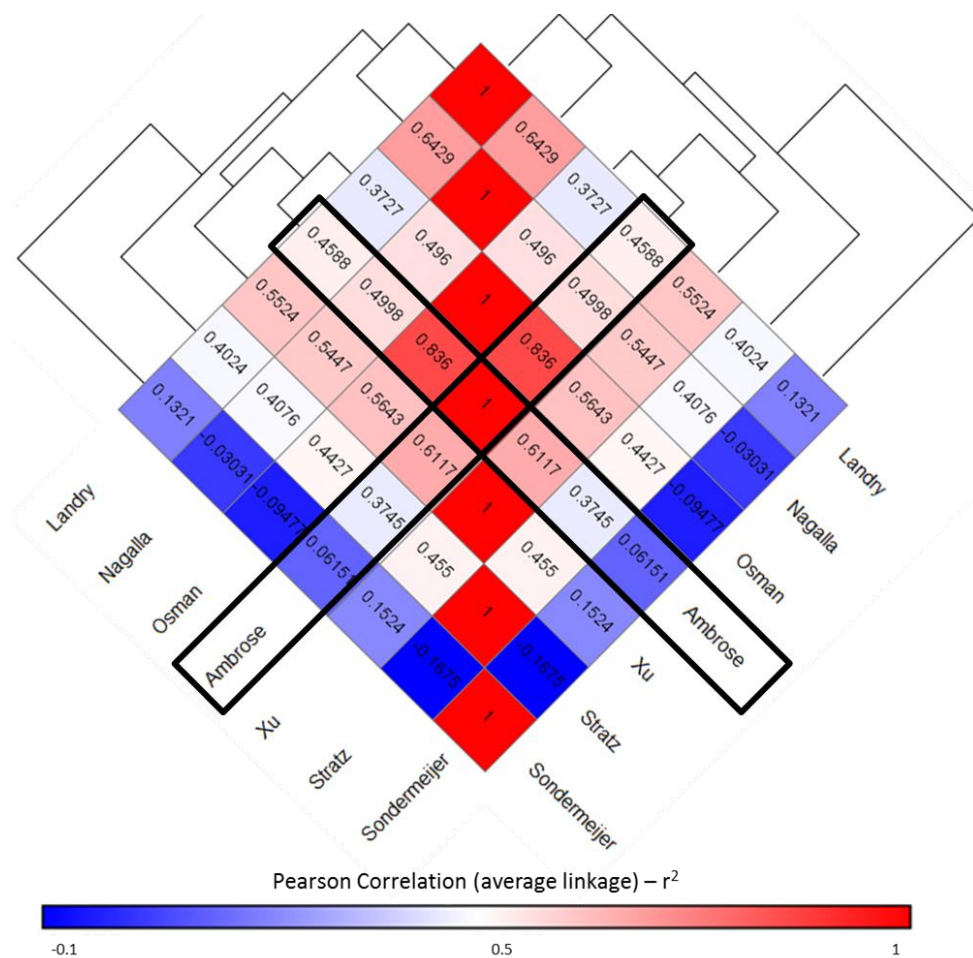
Figure 3.14 – A similarity matrix comparing platelet microRNA profiles *The correlation between the 7 microRNA profiles of platelets were calculated with Pearson correlation using average linkage and the results were mapped into a similarity matrix with hierarchical clustering.*

3.4.4 Comparing platelet and platelet-derived EV microRNA to plasma

Information in the literature suggest that platelets are responsible for up to 50% of the EV in blood (Arraud et al., 2014). Therefore it seemed logical that the microRNA content of the plasma, which contains all EV from the blood, is heavily influenced by the microRNA content of pdEV. Therefore the microRNA profiles of platelets and pdEV were compared to a microRNA profile of plasma. The plasma dataset (3.3.6.7) was generated using the same TaqMan microRNA microarray cards used in the present study allowing for a straightforward analysis. A comparison is shown in Table 3.6 which revealed that platelets and plasma contained similar numbers of unique microRNA species and that the most highly expressed microRNA in plasma was also miR-223-3p.

Table 3.6 – Overview of the microRNA profiles of platelets, pdEV and plasma Information on the microRNA profiles of platelets, platelet-derived EV and plasma identified using TaqMan microRNA microarrays.

Sample	Number of consistently identified microRNA	Most highly expressed microRNA
Platelets	220	hsa-miR-223-3p
Average platelet-derived EV	90	hsa-miR-223-3p
Plasma	234	hsa-miR-223-3p

When the microRNA profiles were analysed for overlap using Venn diagrams (Figure 3.15) it was clear that the overlap between the three groups was significant. All three shared 86 microRNA, which represented 96% of the pdEV microRNA, and left 41 microRNA as exclusive to platelets and 59 only detectable in plasma. This showed that, as predicted, the platelets and pdEV shared a large number of their microRNA with the plasma. Interestingly there were four microRNA that were present in pdEV but not in plasma; miR-374-5p, miR-151-5p, miR-155-5p and miR-320b, but all of these microRNA were expressed at very low levels in pdEV (~1000 fold less than miR-223-3p).
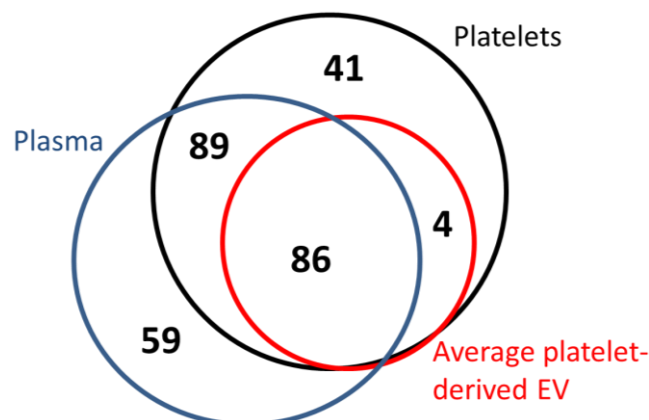
Figure 3.15 – Overlap of the microRNA profiles of platelets, pdEV and plasma The microRNA profiles of platelets, pdEV and plasma were analysed using Venn diagram software to identify the number of overlapping microRNA. This was then visualised as a Venn diagram with the number of microRNA in each group shown.

It was clear that the overlap between the plasma and platelet/pdEV samples was significant and further evidence for this is provided in Figure 3.16, which shows the correlation of each pair of datasets visually and statistically. The scatter plots showed the RE of the shared microRNA species; 175 for platelets vs plasma, 86 for pdEV vs plasma and 90 for platelets vs pdEV. The plots clearly showed a strong correlation in expression between the different samples and this is backed up by the Pearson correlation coefficients which were all >0.98 and all statistically significant (p=<0.0001). This added further evidence to the suggestion that platelets contribute significantly to the microRNA profile of the plasma.
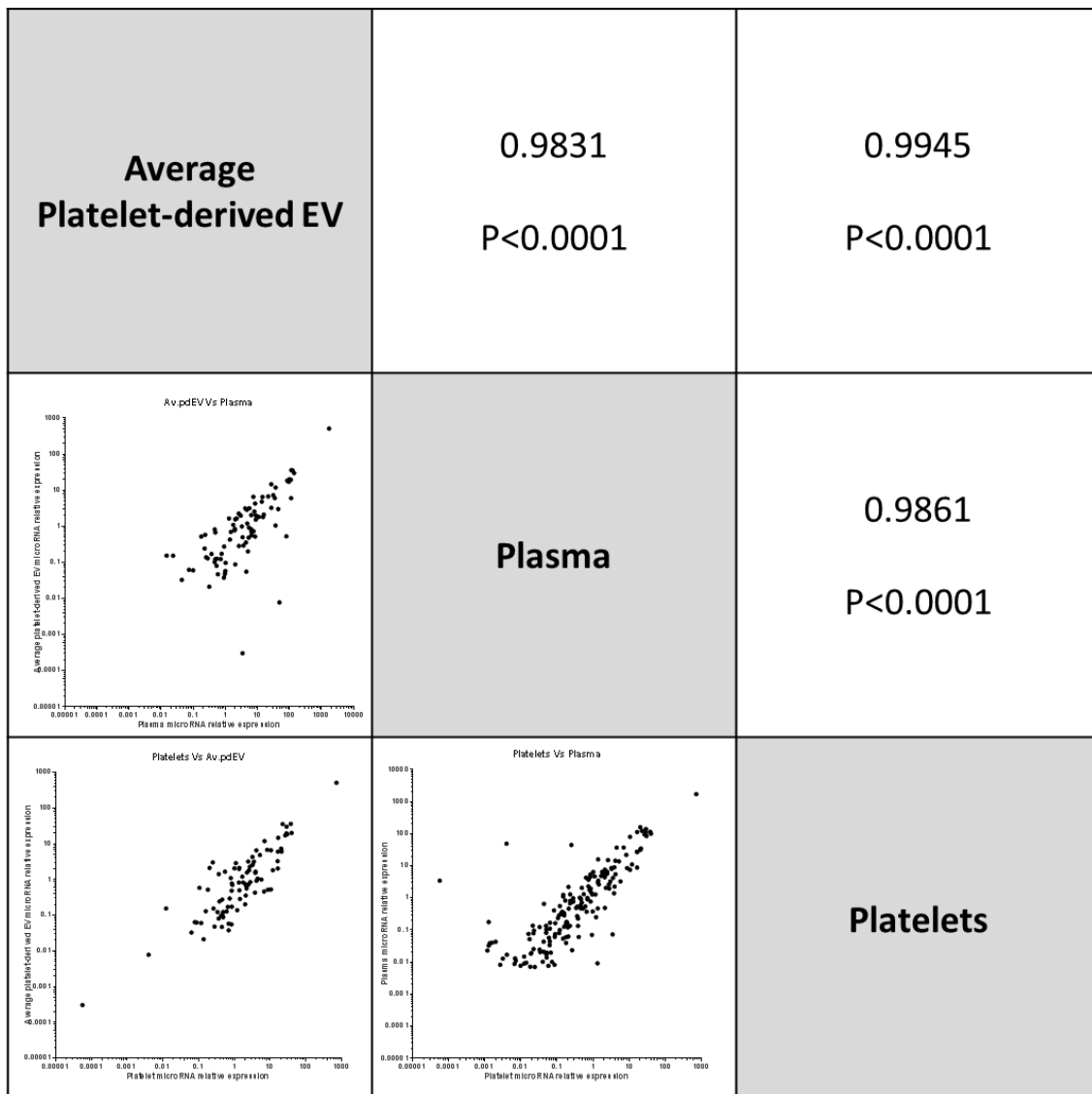
Figure 3.16 – Scatter plot matrix and correlation statistics comparing platelets, pdEV and plasma The microRNA profiles of platelets, pdEV and plasma were analysed using GraphPad prism to show their correlation visually, and statistically using Pearson correlation coefficients.

3.4.5 Identifying a microRNA biomarker of platelet activation

EV are released from platelets, both constitutively and following activation and their microRNA content has a large influence on the microRNA of the plasma (Figure 3.15 and Figure 3.16), suggesting that the pdEV microRNA species could act as a biomarker of platelet activation. Whilst EV and the microRNA in the circulation may come from a variety of sources, pdEV make a significant contribution and may contain specific markers of platelets. To investigate this further a large scale analysis of microRNA profiles from throughout the body was carried out using pre-existing data from 40 tissues profiled using the same TaqMan microRNA microarray platform (Liang et al., 2007). The dataset is described in, 3.3.6.8, and an overview of the findings is shown alongside the information on platelets, pdEV and plasma in Table 3.7. The study used only the A card from the TaqMan microRNA microarrays and so the platelet, pdEV and plasma microRNA profiles were adjusted to show only the microRNA from this card. The table shows that between 120 and 170 microRNA were detected in most of the samples with notable exceptions for the placenta (211) and testes (194/195). In the majority of the samples the most abundant microRNA was miR-26a-5p which is the 14th most abundant in platelets and is not found in the top 25 in pdEV.

To identify a biomarker of platelet activation the data was analysed with the aim of finding a microRNA which displayed unique or increased expression in platelets, pdEV and the plasma compared to the other tissues. To attempt to identify the biomarker all of microRNA profiles were entered into MeV (3.3.7.2.2) following normalisation using the ΔΔCt method (3.3.6.2). Previous data was normalised using the control probe U6 snRNA which was stable in the platelet and pdEV samples (as identified by NormFinder (3.3.6.5)), but U6 snRNA was not stable across this dataset of more diverse cells and tissues and so NormFinder was again used to identify a stable gene. The result from the NormFinder analysis on this dataset are shown in Table 3.8, which revealed that miR-324-3p was the most stable and so was used to normalise the datasets.

Table 3.7 – The microRNA profiles of 43 samples used for analysis *The microRNA of 43 samples was analysed using TaqMan microRNA microarray card A. The results below show the number of microRNA identified and the most abundant microRNA for each sample type.*

Sample	Number of microRNA identified	Most abundant microRNA
Adipose	141	hsa-miR-26a
Adrenal	169	hsa-miR-26a
Bladder	153	hsa-miR-26a
Brain	166	hsa-miR-26a
Breast	175	hsa-miR-26a
Cervix	153	hsa-miR-26a
Distal Colon	161	hsa-miR-26a
Duodenum	159	hsa-miR-26a
Fallopian Tube	149	hsa-miR-26a
Ileum	152	hsa-miR-26a
Jejunum	161	hsa-miR-26a
Kidney	155	hsa-miR-26a
Liver	137	hsa-miR-26a
Lung	148	hsa-miR-26a
Oesophagus	146	hsa-miR-26a
Ovary	151	hsa-miR-26a
Pericardium	157	hsa-miR-26a
Prostate	161	hsa-miR-26a
Proximal Colon	156	hsa-miR-26a
Small Intestine	156	hsa-miR-26a
Spleen	148	hsa-miR-26a
Stomach	168	hsa-miR-26a
Testicle 1	194	hsa-miR-26a
Testicle 2	195	hsa-miR-26a
Thymus	152	hsa-miR-26a
Trachea	149	hsa-miR-26a
Uterus	138	hsa-miR-26a
Vena Cava	150	hsa-miR-26a
Average pdEV	69	hsa-miR-223-3p
Plasma	129	hsa-miR-223-3p
Platelets	124	hsa-miR-223-3p
Pancreas	177	hsa-miR-21
Colon	152	hsa-miR-192
Lymph Node	145	hsa-miR-142-3p
Heart	143	hsa-miR-133b
Left Atrium	149	hsa-miR-133b
Left Ventricle	149	hsa-miR-133b
Right Atrium	150	hsa-miR-133b
Right Ventricle	149	hsa-miR-133b
Skeletal Muscle	147	hsa-miR-133b
Thyroid	147	hsa-miR-133b
PBMC	138	hsa-miR-125b
Placenta	211	hsa-miR-517c

Table 3.8 – Stable genes from the 43 tissues *The data from the TaqMan microRNA microarray A cards were investigated using NormFinder to attempt to identify stable genes within the dataset. All microRNA were assessed and assigned a representative stability value, the 8 most stable are listed here.*

microRNA ID	Stability value
hsa-miR-324-3p	0.019
hsa-miR-361	0.020
hsa-miR-324-5p	0.022
hsa-miR-28	0.022
hsa-miR-101	0.023
hsa-miR-106b	0.025
hsa-miR-345	0.026
hsa-miR-339	0.026

The normalised relative expression datasets were entered into MeV and a heatmap with hierarchical clustering (Pearson correlation using average linkage) was generated (Figure 3.17), the overall pattern showed a large number of consistently expressed microRNA. The hierarchical clustering revealed that platelets, pdEV and plasma clustered separately, suggesting that their microRNA profiles were different, and that identification of a biomarker or biomarker signature may be possible. To analyse this further a correlation matrix was generated (Figure 3.18) which identified the Pearson correlation coefficient values between all samples. This demonstrated the cause of the hierarchical clustering pattern, as all 40 tissues from the research paper correlated with each other with r^2 values >0.65. However the platelets, pdEV and plasma all had r^2 values <0.65 when compared with the other tissues and the maximum correlation of 0.64 was between platelets and the spleen, likely reflecting the abundance of platelets in this organ. This separation of platelets, pdEV and plasma had the potential to aid in the identification of a biomarker but may also represent experimental differences.

The datasets in MeV were tested by comparing each the expression of each microRNA expression in the 40 tissues and their expression in platelets, pdEV and the plasma using a 2 group t-test. The significance threshold was set at <0.01 and t-tests were corrected for multiple comparisons using standard Bonferroni correction (3.3.7.2.2.2). The results from this generated a heatmap, shown in Figure 3.19, and a results table, Table 3.9. The heatmap clearly showed microRNA are differentially expressed between the two groups, and produced 27 potential biomarkers. Of these 13 had reduced expression in platelets, pdEV and plasma compared to the other tissues and 14 were significantly increased. These 14 microRNA therefore have the potential to be utilised as biomarkers of platelet activation. Of the 14, miR-223-3p was selected for further analysis as the difference in expression

between platelets/pdEV/plasma and the other tissue was the greatest and it was the most abundant platelet, pdEV and plasma microRNA. The next choice was miR-106a-5p as it had the second largest difference and third choice was miR-146a, it had the fourth largest difference in expression but a stronger p-value than the third largest difference. The three microRNA are highlighted in the heatmap (Figure 3.19) and their expression in all 43 samples is shown in Figure 3.20. Both of these figures demonstrate their increased expression in platelets/pdEV/plasma compared to the other 40 tissues.
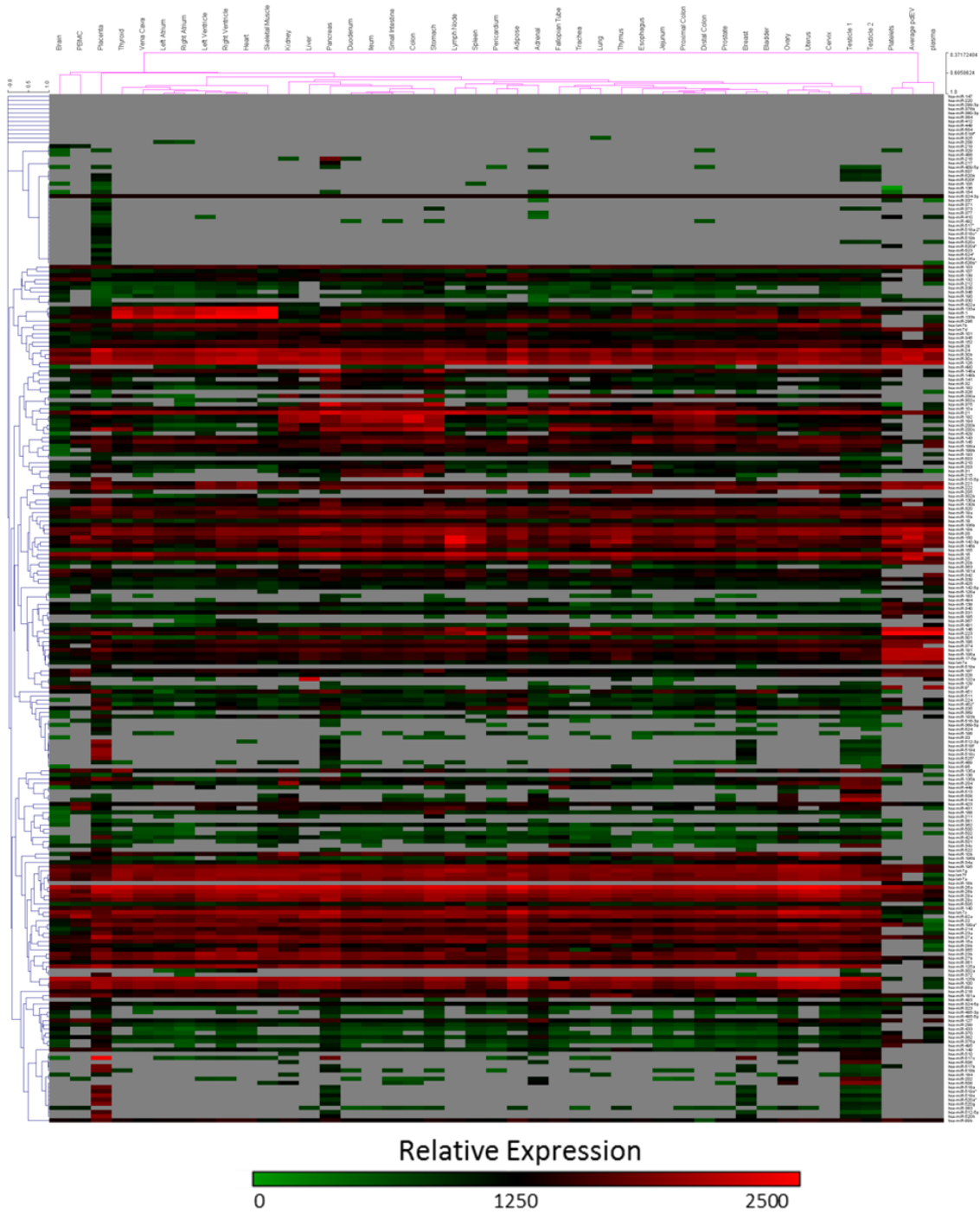
Figure 3.17 – A comparison of microRNA profiles of 43 samples from throughout the body *The relative expression data for the microRNA profiles of 34 different tissues were loaded into MeV and visualised as a heatmap. Hierarchical clustering, using Pearson correlation with average linkage was applied to the samples and microRNA.*
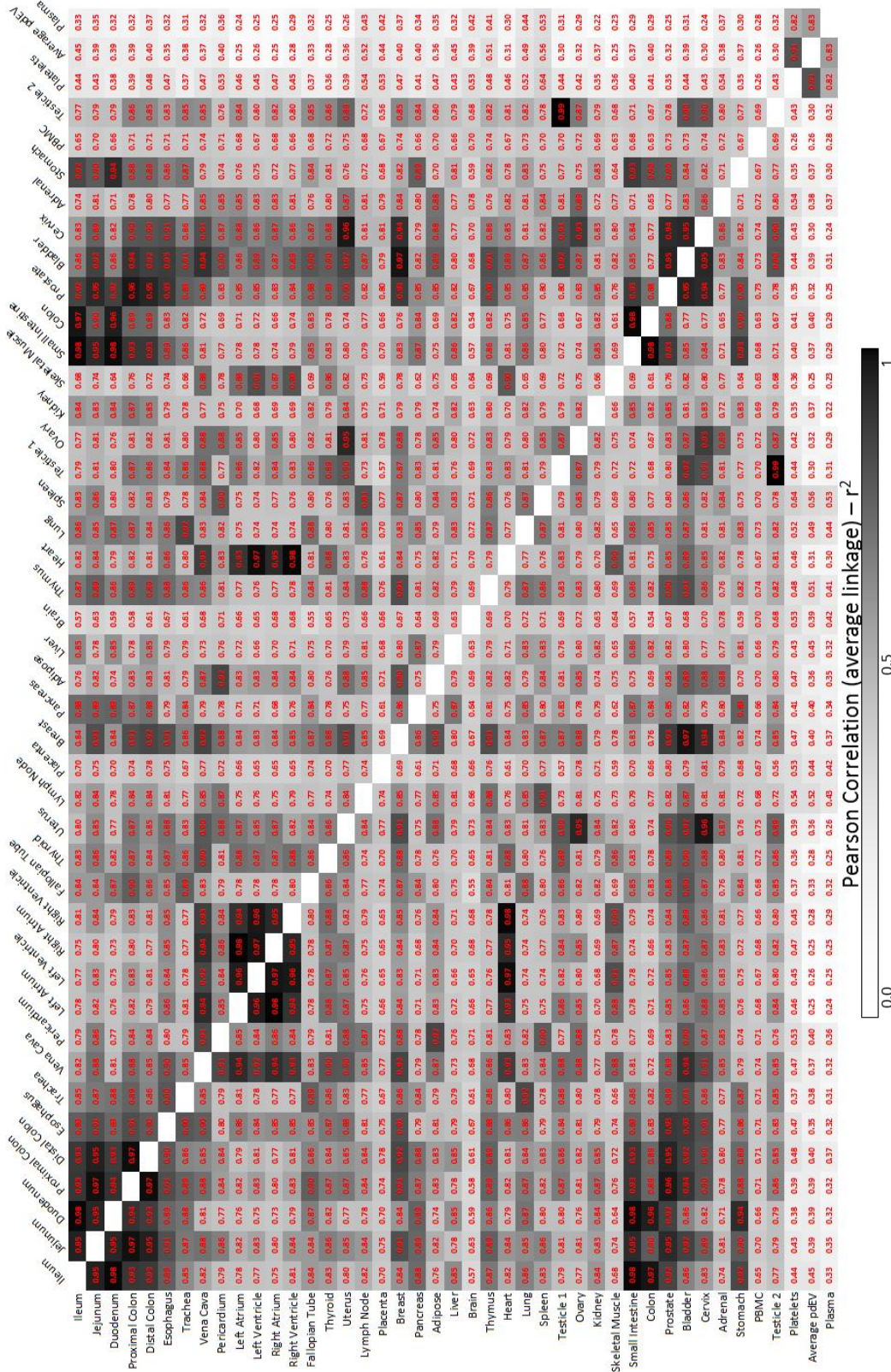
Figure 3.18 – Correlation matrix comparing microRNA profiles of 43 samples from throughout the body *The microRNA profile of all 43 samples was compared to microRNA profile of all the other samples and analysed using Pearson correlation coefficients. These values were then mapped into a matrix to allow for direct comparisons between all of the sample types.*
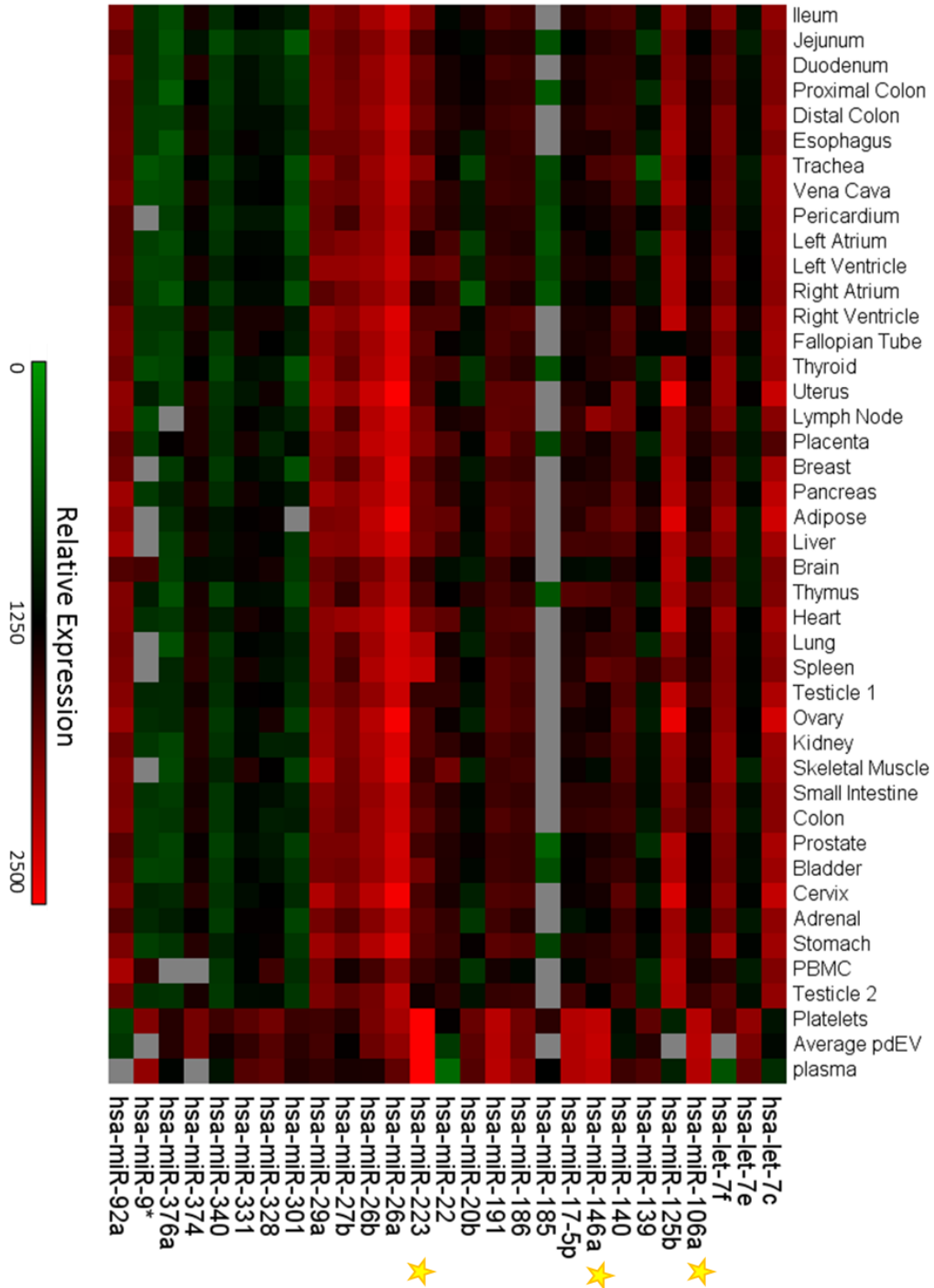
Figure 3.19 – Significantly differentially expressed microRNA – Platelets/pdEV/plasma vs 40 samples *A 2 group t-test was carried out to identify microRNA which were differentially expressed in platelets/pdEV/plasma compared to 40 other tissues that had the potential to act as a biomarker of platelet activation. The microRNA deemed significantly different (p<0.01) by the t-test following standard Bonferroni correction for multiple comparisons are shown. The 3 microRNA selected for further investigation as biomarkers are indicated with yellow stars.*

Table 3.9 – Significantly differentially expressed microRNA – Platelets/pdEV/plasma vs 40 tissues *The significant results from a 2 group t-test comparing microRNA expression in platelets, pdEV and plasma against 40 other samples. Each microRNA was tested individually between the 2 groups and the p-values were corrected using standard Bonferroni correction.*

microRNA ID	40 tissues mean expression	40 tissues SD of expression	Platelet, pdEV and plasma mean expression	Platelet, pdEV and plasma SD of expression	Difference in average group expression	p-value	Corrected p-value
hsa-miR-223-3p	*11.6318*	*2.58471*	*2574.36*	*1.49485*	*2562.73*	*3.56×10^{-12}*	*8.78×10^{-10}*
hsa-miR-146a-5p	*2.82843*	*2.47942*	*198.088*	*1.10957*	*195.26*	*6.69×10^{-10}*	*1.65×10^{-7}*
hsa-miR-106a-5p	*1.87905*	*1.79005*	*147.033*	*1.07177*	*145.154*	*6.66×10^{-16}*	*1.65×10^{-13}*
hsa-miR-17-5p	2.09943	1.85318	130.69	1.04247	128.59	2.64×10^{-14}	6.53×10^{-12}
hsa-miR-191-3p	6.82108	1.67018	134.343	1.04247	127.522	4.78×10^{-13}	1.18×10^{-10}
hsa-miR-9-3p	0.10658	3.16017	43.7133	1.40444	43.6067	2.31×10^{-8}	5.72×10^{-6}
hsa-let-7e-5p	0.54337	1.65864	27.8576	2.00000	27.3143	6.66×10^{-16}	1.65×10^{-13}
hsa-miR-374a-5p	1.8025	1.65864	24.2515	1.00000	22.449	1.39×10^{-8}	3.44×10^{-6}
hsa-miR-186-5p	5.06303	1.72907	26.5382	1.40444	21.4752	7.93×10^{-6}	0.001958
hsa-miR-328-3p	0.68302	2.04202	14.9285	1.47427	14.2455	5.21×10^{-9}	1.29×10^{-6}
hsa-miR-20b-5p	0.42632	3.07375	12.7286	1.31951	12.3023	6.29×10^{-6}	0.001553
hsa-miR-331-3p	0.87661	1.71713	7.6211	1.75321	6.7445	4.71×10^{-8}	1.16×10^{-5}
hsa-miR-139-5p	0.42337	2.71321	6.82108	2.20381	6.39771	2.87×10^{-5}	0.007097
hsa-miR-301a-3p	0.09807	2.42839	3.4822	1.37554	3.38413	2.89×10^{-8}	7.14×10^{-6}
hsa-miR-376a-3p	0.06426	2.32947	1.86607	2.05623	1.80181	5.98×10^{-8}	1.48×10^{-5}
hsa-miR-185-5p	0.02646	1.49485	1.7411	2.41162	1.71464	7.05×10^{-9}	1.74×10^{-6}
hsa-miR-340-5p	0.11266	1.82766	1.59107	3.4822	1.47842	3.28×10^{-8}	8.11×10^{-6}
hsa-miR-22-3p	3.13834	2.36199	0.08839	11.7942	-3.04995	4.86×10^{-7}	1.20×10^{-4}
hsa-miR-140-5p	7.01285	1.76541	1.09429	3.91768	-5.91855	1.42×10^{-5}	0.003509
hsa-miR-27b-3p	18.1261	2.07053	1.90528	1.6245	-16.2209	5.32×10^{-6}	0.001313
hsa-miR-92a-3p	24.4201	1.85318	0.07179	1.33793	-24.3484	4.44×10^{-16}	1.10×10^{-13}
hsa-let-7f-5p	29.8571	1.95884	0.42045	58.4852	-29.4366	1.38×10^{-7}	3.42×10^{-5}
hsa-miR-29a-3p	40.2244	1.7411	5.16941	1.33793	-35.055	1.56×10^{-7}	3.86×10^{-5}
hsa-let-7c-5p	63.5579	2.00000	0.34628	2.34567	-63.2116	1.55×10^{-15}	3.84×10^{-13}
hsa-miR-26b-5p	74.5429	1.94531	10.0561	3.86375	-64.4868	3.35×10^{-5}	0.008286
hsa-miR-125b-5p	88.647	3.01049	0.22531	1.04972	-88.4217	3.10×10^{-9}	7.66×10^{-7}
hsa-miR-26a-5p	288.015	1.89212	42.2243	2.71321	-245.791	1.77×10^{-5}	0.004365
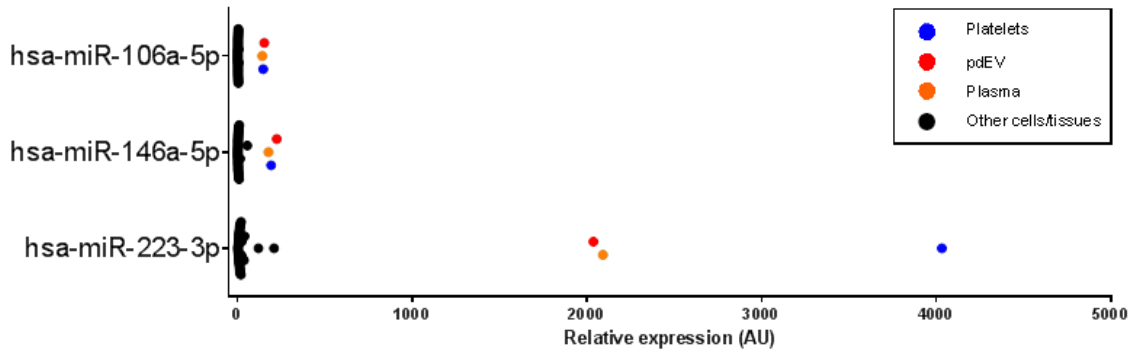
Figure 3.20 – Relative expression of the 3 microRNA selected to test as biomarkers of platelet activation *The relative expression levels of platelets, pdEV, plasma and 40 other samples are shown for the 3 microRNA (miR-106a-5p, miR-146a-5p and miR-223-3p) selected to test as biomarkers of platelet activations*

The 3 microRNA; miR-106a-5p, miR-146a-5p and miR-223-3p were tested as biomarkers of platelet activation by activating platelets in 200µL of PRP with PAR1-AP at a variety of concentrations, and CRP-XL at a maximal dose of 2µg/mL. The activation in these samples was tested by flow cytometry (2.3.9.1) using a P-selectin assay. The results are shown in Figure 3.21, which demonstrates that CRP-XL acts as a strong agonist for platelet with all of the samples achieving over 90% P-selectin expression. The highest dose of PAR1-AP (1×10^{-5}M) also achieved ~90% activation, with the next highest dose (3×10^{-6}M) causing between 72% and 95% activation and the next lower dose (1×10^{-6}M) causing up to 15% activation and lower doses not triggering any activation.
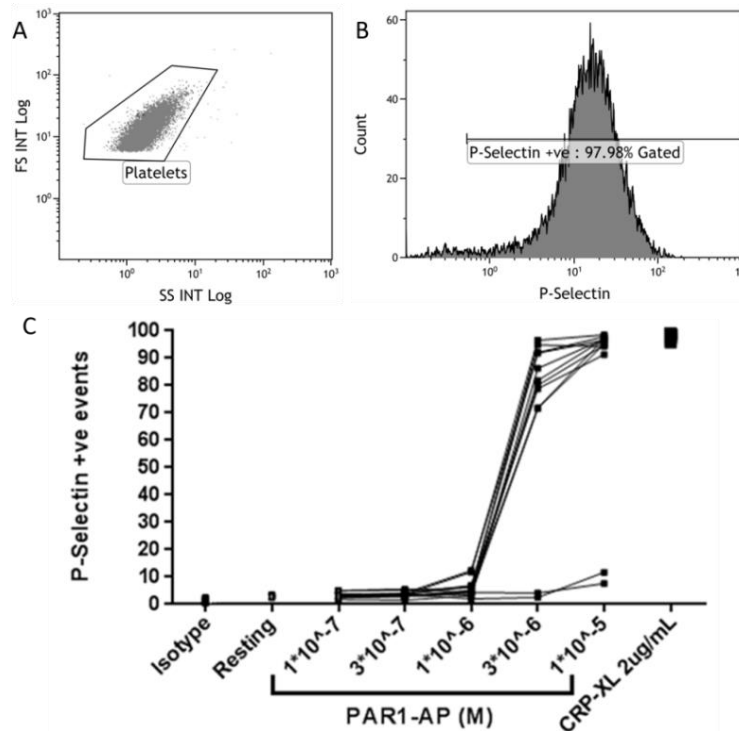
Figure 3.21 – P-selectin expression on platelets activated in whole blood *Platelets were activated with varying doses of PAR1-AP and CRP-XL, or left unstimulated in whole blood. PRP was then isolated using centrifugation and tested for platelet activation using the P-selectin assay on a flow cytometer A) shows the flow cytometry gating for platelets and, B) shows an example histogram for P-selectin. C) Shows the number of P-selectin positive events under each condition (n=12).*

Based on the data from the platelet activation assays, the samples from 2 donors were removed as the platelets were not activated by PAR1-AP at any dose. The 3 highest doses of PAR1-AP activated blood were selected for further analysis alongside an unstimulated sample, the CRP-XL stimulated blood and a serum sample from the 10 remaining healthy donors. Following the activation of whole blood the PRP was isolated as described in (2.3.3) and simultaneously serum was prepared (2.3.4). The RNA was extracted from these samples (3.3.1) and cel-miR-39-3p was spiked in to act as a control (3.3.1.2). A RTr for miR-223-3p, miR-146a-5p, miR-106a-5p and cel-miR-39-3p was carried out (3.3.2) and RT-PCR was used to detect the expression of the 4 microRNA. The results were normalised using spiked-in cel-miR-39-3p to generate $\Delta\Delta$Ct values and from these values the relative expression was calculated for each donor and was compared in Figure 3.22.

The results show that the expression of cel-miR-39-3p was consistent throughout the experiment, as expected for a control microRNA. The analysis of miR-223-3p showed that its expression was significantly increased in serum compared to all other conditions. There was no significant increase with platelet specific stimulation, through CRP-XL and PAR1-AP and no evidence of a dose dependent response. MiR-146a-5p was significantly increased in the serum compared to the low dose PAR1-AP (1×10^{-6}M) sample. The other conditions showed no significant increase beyond the unstimulated sample, although the relative expression of miR-146a-5p in CRP-XL and PAR1-AP (3×10^{-6}M) stimulated plasma was increased. The results were similar for miR-106a-5p, with a significant increase in miR-106a-5p observed in serum samples. There was also a small increase with all platelet agonists and the effects of PAR1-AP did appear to be dose dependent, but these changes were not significant. Taken together these results suggest that these biomarkers are unlikely to be suitable as specific markers of platelet activation as it was not possible to readily detect their increased expression in response to platelet activation. They were all significantly increased in serum samples but this is not solely a reflection of platelet activation.
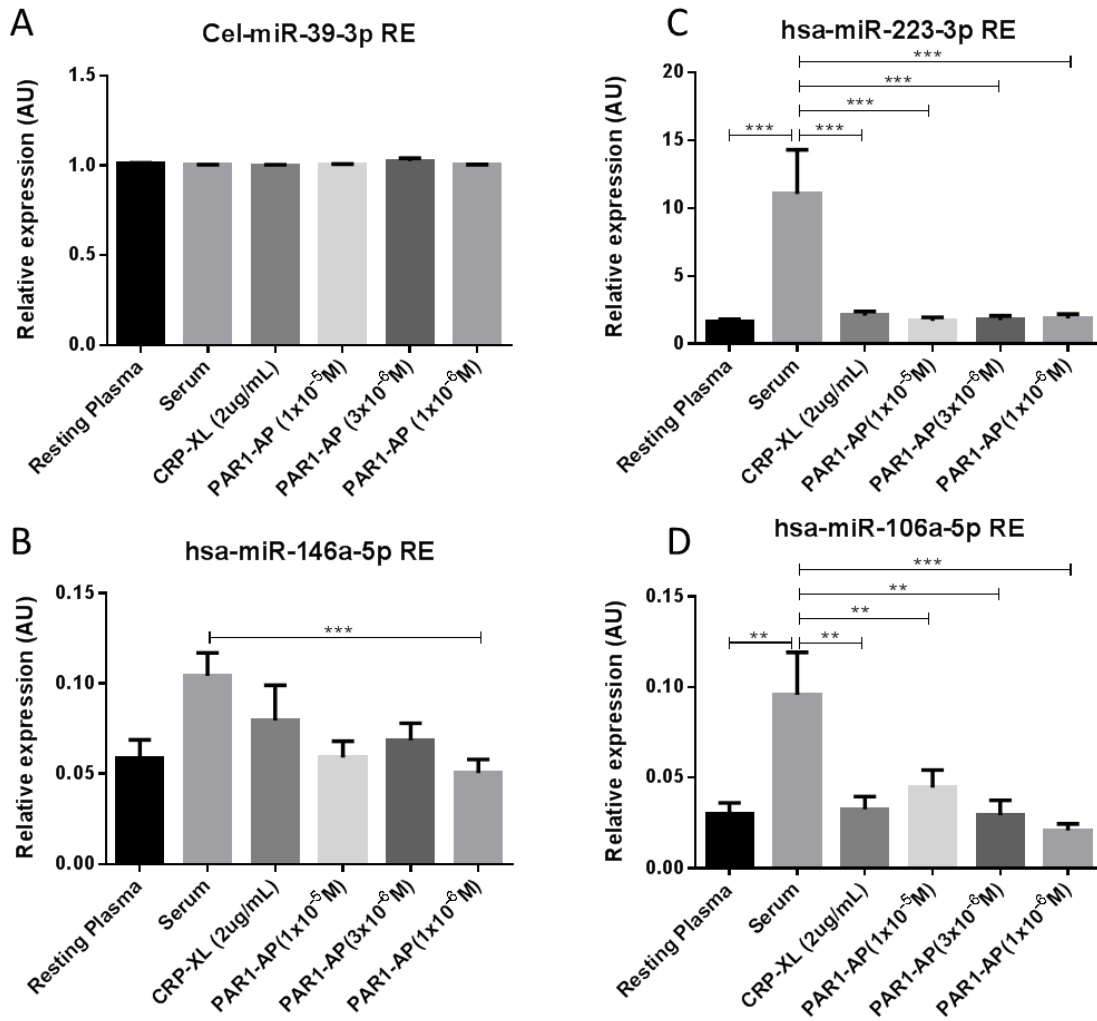
Figure 3.22 – Relative expression of platelet biomarkers following platelet activation in whole blood *The level of expression of miR-223-3p, miR-146a-5p, miR-106a-5p and cel-miR-39-3p (which was spiked-in, to act as an internal control) were assessed in unstimulated plasma, stimulated plasma (3 doses of PAR1-AP and CRP-XL) and in serum of healthy donors using RT-PCR. Relative expression was calculated using the ΔΔCt method with cel-miR-39-3p acting as a control gene, significance was determined using One-way ANOVA with multiple comparisons corrected using Bonferroni correction (n=10).*

3.5 Discussion

MicroRNA are a small, highly conserved species of non-coding RNA that have been shown to play critical roles in the regulation of mRNA translation and therefore protein function (Lee and Ambros, 2001, Winter et al., 2009). Their biological importance is well established, with estimates suggesting that they regulate up to 60% of protein coding genes, however there are still many unknowns with regards to their specific functions (Friedman et al., 2009, Baek et al., 2008, Zhang et al., 2012). MicroRNA are found intracellularly and extracellularly with many cells and body fluids demonstrating specific signatures (Teruel-Montoya et al., 2014, Leidinger et al., 2014, Liang et al., 2007, Landry et al., 2009). Cell-free microRNA have been found in the blood (Fichtlscherer et al., 2010, Chen et al., 2008), cerebrospinal fluid (Quinn et al., 2015), urine (Ramezani et al., 2015) and saliva (Gallo et al., 2012).

Within the blood it has been shown that the extracellular circulating microRNA are resistant to the endogenous RNAse activity and are stable over time (Mitchell et al., 2008). This stability within the circulation, our ease of access to blood in patients and the specific nature of microRNA profiles has led to intense research into the possibility of circulating microRNAs acting as biomarkers of health and disease (Thum and Mayr, 2012, Zampetaki and Mayr, 2012b). Due to the obvious links with the circulation, cardiovascular function and disease has been an area of focus for circulating biomarkers. Increased miR-150 has been implicated in atrial fibrillation in heart failure patients (Goren et al., 2014) and lymphocyte activation (de Candia et al., 2013). Upregulation of miR-192 has been linked to the development of heart failure following MI, miR-208b and miR-499 correlate with myocardial damage (Corsten et al., 2010) while downregulation of miR-223-3p and miR-146a-5p is seen in diabetes mellitus (Duan et al., 2014).

The survival of microRNA in the circulation is considered to be due to the protection conferred on them by incorporation into EV (Laffont et al., 2013, Chen et al., 2010) or HDL (Vickers et al., 2011, Wagner et al., 2013) and argonaute complexes (Arroyo et al., 2011). Although there is conflicting evidence for their predominant location within the circulation, several studies have indicated that EVs are the major source of cell-free circulating microRNA (Diehl et al., 2012, Cheng et al., 2014, Hunter et al., 2008, van der Pol et al., 2016). MicroRNA incorporation into EV rather than HDL or argonaute complexes offers the potential for targeting of microRNA to other cells as a method of intercellular communication (Ismail et al., 2012). This information, in combination with the knowledge that platelets significantly contribute to the EV population of blood (Arraud et al., 2014) makes platelet microRNA and pdEV microRNA potentially important factors in cardiovascular homeostasis (Dangwal and Thum, 2012, Edelstein and Bray, 2011,

Edelstein et al., 2013), disease (Stakos et al., 2012, Duan et al., 2014) and intercellular communication (Aatonen et al., 2012, Setzer et al., 2006, Laffont et al., 2015).

Therefore we aimed to profile the microRNA contained within platelets, the EV that they release following stimulation and then compared these datasets to those of other platelet studies and investigated whether there was an opportunity to use this information for the identification of a biomarker of platelet activation.

3.5.1 Platelet microRNA profile

The microRNA content of platelets and pdEV were successfully profiled using TaqMan microRNA microarrays; 220 species of microRNA were identified in platelets and 79, 66, 57, 71 and 62 microRNA were observed in CRP-XL, PAR1-AP, PAR4-AP, ADP and thrombin generated pdEV respectively (Table 3.3). MiR-223-3p was the most abundant microRNA in all samples, demonstrating expression levels 14-fold greater than the next most abundant microRNA (Table 3.7). The results also showed some evidence of selective loading of microRNA from platelets into pdEV. This phenomenon has been observed with other cell types and here we found miR-21-5p and miR-451 were enriched in pdEV (Guduric-Fuchs et al., 2012).

Profiling of platelets revealed an abundant array of mature microRNA species covering ~6 logs in expression levels. The identification of 220 microRNA was broadly in line with previous studies which identified 219 (Landry et al., 2009), 224 (Sondermeijer et al., 2011) and 233 (Stratz et al., 2012), although some studies have identified significantly more (389 (Xu et al., 2012)) but this is likely due to methodological differences. Platelets predominantly contain mature microRNA which they inherit from their precursor cell, the megakaryocyte (Hussein et al., 2009). Due to their anucleate nature, the microRNA content of platelets is important for regulation of their limited mRNA content and it has been shown that platelet mRNA has lengthened 3'-UTRs to enhance this control (Dittrich et al., 2006). Platelet microRNA have been shown to play roles in normal platelet function and thrombopoiesis, for example miR-223-3p can reduce P2Y12 receptor expression (Landry et al., 2009, Ple et al., 2012a). Platelet microRNA have also been identified as biomarkers of platelet disease, with miR-26b being elevated in the platelets of polycythaemia vera patients (Bruchova et al., 2008).

The platelet profile here found that platelets abundantly expressed miR-223-3p, miR-146a-5p and a variety of the microRNA from the miR-17/92 cluster (CRP-XL; -78% (p=0.0048), PAR1-AP; -86% (p=0.0109), PAR4-AP; -87% (p=0.0030) and ADP; -65% (p=0.00007)(Figure 3.6) with many of these microRNA having been shown to have important functions in health and disease. The

abundance of miR-146a-5p is likely to be carried over from the microRNA content of megakaryocytes, where it has an important function in the negative regulation of megakaryopoeisis through downregulation of CXCR4 (Dahiya et al., 2015, Labbaye et al., 2008, Opalinska et al., 2010). MiR-223-3p also has a role in megakaryopoeisis, where it regulates LMO2, a protein with a central role in haematopoietic lineage differentiation (Felli et al., 2009, Yuan et al., 2009), although this regulation can be achieved in the absence of miR-223-3p (Leierseder et al., 2013). The role of miR-223-3p in regulating the P2Y12 receptor means it has become a potential therapeutic target in cardiovascular medicine (Shi et al., 2013). The miR-17/92 cluster and its paralogues account for a group of 15 microRNA, 13 of which are expressed in platelets. These are the most intensively researched group of microRNA in various cells, and have been heavily linked with central cellular processes such as apoptosis and the cell-cycle regulation (Mogilyansky and Rigoutsos, 2013, O'Donnell et al., 2005). As well as their functions within platelets all of these abundant microRNA have been shown to have roles throughout the body and it is this global role for microRNA which makes their intercellular transfer an intensive area of research.

3.5.2 Comparison of platelet microRNA profiles between studies

The profiling of the microRNA within platelets has been carried out by multiple research groups over the last six years and here we compared six previous datasets generated using a variety of profiling platforms (Table 3.4). The data revealed large differences between the platelet profiles from different studies with 170 more microRNA identified in the largest microRNA profile compared to the smallest (Xu *et al.* vs. Landry *et al.*). There was, however, uniformity for the most abundant microRNA, with 81 of these being identified in all studies. In addition over 50% of the studies identified miR-223-3p as the most abundant platelet microRNA, but similarities between the datasets beyond the abundant microRNA was low with 28% of all microRNA identified being uniquely expressed in one dataset (Table 3.5).

The large differences between the datasets were unexpected as the platelet samples were all prepared from healthy donors using very similar isolation techniques. Even variation in the age, gender and race of participants would be expected to only account for small changes to a select few microRNA (Simon et al., 2014, Edelstein et al., 2013). Based on the information presented there are two likely explanations; the disparate profiling platforms used which cause methodological changes, and the difficulty comparing the available data from the different platforms.

The seven studies (including ours) used five different profiling platforms and even the two pairs of studies using the same platforms used different versions, due to miRbase updates (Kozomara and Griffiths-Jones, 2011). Three of the studies used microarray approaches, and four, including our own, used PCR-based arrays. While two of these four PCR-based arrays show the strongest correlation (r^2=0.836) they did not form a cluster separate to the microarray based approaches (Figure 3.14) suggesting that the differences are not simply caused by the difference between these two technologies. Many studies have compared multiple microRNA profiling platforms with variable results and it is clear that each system has advantages and disadvantages (Chugh and Dittmer, 2012, Zampetaki and Mayr, 2012a, Baker, 2010). Of the techniques used to profile platelets, RT-PCR is believed to offer the greatest specificity and sensitivity with a broad dynamic range (Chen et al., 2005, Jensen et al., 2011). However PCR approaches have been shown to be limited in the recognition of microRNA with low abundance meaning that they are perhaps not the best system for low microRNA input (Jensen et al., 2011, Mestdagh et al., 2014).

Like PCR, the microarrays used have advantages and disadvantages; they are extremely sensitive and frequently offer simple and efficient workflows. However they have a reduced dynamic range and are unable to differentiate between pre- and mature microRNA (Chugh and Dittmer, 2012). The platelet profile of the samples in the Sondermeijer *et al.* study were drastically different to the other studies; one reason for this could be the use of bead based microarrays which require a difficult fractionation step to specifically isolate the smaller microRNA which can introduce significant bias (Liu et al., 2008, Wang et al., 2011).

A large part of the problem with both microarrays and PCR based approaches is that they were designed based upon approaches for mRNA and DNA which are significantly longer, thereby causing problems with accurate probe detection. In addition, due to the requirement for specific probes within these systems they can only detect those microRNAs that have already been identified and documented and this is challenging in an environment where the list of known microRNA is constantly changing (Schopman et al., 2010, Baker, 2010, Mestdagh et al., 2014, Chiang et al., 2010). Further to the unintentional bias that all of these platforms introduce in microRNA detection they also use different sample preparation steps which will manipulate the microRNA in different ways resulting in changes to the prepared samples which are profiled (Mestdagh et al., 2014).

The growing use of next-generation sequencing (NGS) offers an opportunity to overcome these challenges. NGS datasets were not compared in this analysis and early NGS microRNA datasets suffered from bias caused by the restriction endonucleases used in the library preparation

targeting subsets of microRNA due to the presence of their specific recognition site within the microRNA sequence that resulted in the removal of these microRNA for analysis. Attempts to profile microRNA with next-generation sequencing have yielded results similar to those observed here, whereby abundant microRNA are very similar but the lower expressed microRNA are variable (Simon et al., 2014). The technology and costs associated with NGS of microRNA have improved considerably making it a viable alternative, particularly when looking at less abundant microRNA, or when attempting to identify previously uncharacterised microRNA (Eminaga et al., 2013, Pritchard et al., 2012). An interesting platform is the NGS microRNA profiling by HTG Molecular, which generates libraries of only microRNA based on the current miRbase (Gerson et al., 2012).

Beyond the differences between the profiling platforms there was a challenge in directly comparing the datasets. When all datasets are prepared in the same laboratory they can all be analysed using similar techniques (Mestdagh et al., 2014) but these datasets were collected from data repositories where the data was presented as normalised RE values (Tenopir et al., 2011). This meant that different strategies were utilised to generate the values used for the comparison here. Whilst this will have had limited effect on the determination of whether a microRNA is present within the samples it does effect the comparison of relative expression profiles, as carried out in Figure 3.16 and this may significantly affect the correlation analyses. However the values in Table 3.5 still demonstrate that a binary analysis of the microRNA in each sample revealed significant differences, showing that it is not just the enumeration of microRNA concentration but also the absence or presence of them that varies. As the analysis does not alter the thresholds for presence of microRNAs in the sample these differences are likely to be due to the platform differences rather than the analysis conducted.

Ultimately, laboratories will continue to use whichever platform is either readily available to them or, which offers a good compromise between cost, specificity and coverage. Whilst individual laboratories can demonstrate stability in their platform, comparing findings between different platforms in different labs is not reliable, making cross study comparisons challenging (Stratz et al., 2012, Tenopir et al., 2015). These challenges are increased by the depositing of normalised rather than raw data with limited opportunities of reversing the analysis which has been carried out. The aim of this analysis was to determine the quality of the microRNA profiling analysis carried out in this chapter but due to the platform differences this was not truly possible. However, it is clear that there was significant correlation between our data and the other dataset using the same platform suggesting that our experimental work was reliable.

3.5.3 PdEV microRNA profiles

In this study we showed that platelets released microRNA into EV and that the content of these EV was made up entirely of microRNA found in platelets (Figure 3.8). Based on the evidence in the chapter 2 it was suggested that the microRNA was localised in exosomes rather than microvesicles but it was impossible to determine this with complete certainty. There were between 57 and 79 microRNA species in the populations of pdEV generated by different agonists and a core group of 46 of these were consistently expressed in 4 of these subtypes (CRP-XL, PAR1-AP, PAR4-AP and ADP) (Figure 3.11). The expression of these core microRNA within these groups was almost identical, with r^2 values >0.995 (p=<0.0001) (Figure 3.12) suggesting that whilst the agonists triggered the release of disparate EV populations the microRNA contained within them was strikingly similar. The heatmap in Figure 3.7 demonstrated that the microRNA detected in pdEV were predominantly those found at high levels in platelets. This meant that, either only the most abundant microRNA were released from platelets or, that the low levels of microRNA in the pdEV samples prevented the detection of rarer microRNA species due to the level of sensitivity of the microRNA profiling platform (Mestdagh et al., 2014, Van Deun et al., 2014). Despite this, the functional effects of transferred microRNA are likely to be triggered by only the most abundant microRNA, due to their relatively low copy number per EV (Chevillet et al., 2014) and so knowing the identity of abundant microRNA was essential for further study.

Many of the most abundant microRNA in pdEV were found at similar levels in platelets, as shown by Figure 3.6. Several of the most abundant pdEV microRNA have well defined roles which do not directly involve platelets, suggesting that they could be transported from platelets to exert their functions. A study in Zebrafish showed that miR-24-3p (the fourth most abundant pdEV microRNA) triggered endothelial apoptosis through the downregulation of GATA2 and PAK4, resulting in reduced vascular integrity, suggesting that miR-24-3p could be a therapeutic target in diseases associated with ischaemia. MiR-126-3p has a central role in angiogenesis through regulation of the MAPK pathway inhibitor SPRED1 (Fish et al., 2008) and was previously believed to be an endothelial cell specific microRNA (Wang et al., 2008) although evidence from platelets and other haematopoietic lineages have shown this to be incorrect (Osman and Falker, 2011, Teruel-Montoya et al., 2014). MiR-106a-5p and members of the miR-17/92 cluster (10 of which are consistently expressed in pdEV samples) have been shown to play a critical role in monocytopoeisis (Fontana et al., 2007). These functions are all in cells which are potentially targets for pdEV transferred microRNA and there are many studies which have demonstrated the transfer and functional effects of microRNA from pdEV.

One such study demonstrated the transfer of miR-223-3p from platelets to HUVECs in culture and observed the downregulation of FBXW7 protein (Laffont et al., 2013). The same research group also carried out an extensive study looking at pdEV based microRNA transfer to primary human macrophages and observed effects on ATF3, ATP1B1, ATP9A and RAI14, all of which were miR-126-3p targets (Laffont et al., 2015). An important feature of many intercellular communication studies was the transfer of microRNA alongside their functional machinery, such as components of the RISC complex (Laffont et al., 2013, Zhang et al., 2010, Li et al., 2012). The co-transfer of these proteins potentiates the microRNA function once it is transferred to another cell. The confirmed transfer of pdEV microRNA to the endothelium and other cells within the circulation emphasises the importance of understanding the microRNA released from platelets and how this is affected by different agonists.

An interesting finding from the present study was that there was evidence for selective exclusion or enrichment of microRNA from platelets into their EV. MiR-484-5p, miR-454-3p and let-7a-5p were all abundantly expressed in platelets but were not detectable in any of the pdEV samples (Figure 3.7), while conversely miR-21-5p and miR-451 both appeared enriched in pdEV (Figure 3.11). The concept of microRNA compartmentalisation is not novel, with growing evidence that this occurs in several cell types (Creemers et al., 2012, Hulsmans and Holvoet, 2013, Yanez-Mo et al., 2015, Johnsen et al., 2014). The EV released from THP-1 cells and HUVECs in culture have been shown to have significantly different microRNA profiles compared to their parent cells (Diehl et al., 2012) and miR-451 and miR-150-5p were found to be significantly enriched in EV released from HEK293T cells, OEC cells and HMEC cells (Guduric-Fuchs et al., 2012). Mittelbrunn *et al.* found that the microRNA profiles of EV showed poor correlation to their original cells; r^2=0.4 for primary dendritic cells, r^2=0.33 for the J77 cell line (monocyte/macrophage) and r^2=0.5 for the Raji cell line (B-lymphocyte). They also noted that miR-760, miR-632, miR-654-5p and miR-671-5p were significantly enriched in all exosome populations (Mittelbrunn et al., 2011). All of these studies showed clear evidence of the sorting of microRNA into the EV that they release, although this has not yet been investigated in platelets other than in the present study.

The work in this chapter only identified a select few microRNA which were incorporated into or excluded from, pdEV compared to the significant numbers of differentially included microRNA in other studies. Although taken at face-value the data here do suggest that there are >100 microRNA species that are not included in EV released from platelets, however this may be due to the inability of the selected profiling platform to detect microRNA with low abundance from low concentration samples leading to a lack of knowledge on whether those microRNA are enriched or even present in pdEV. Another possibility is that the sorting in platelets is different

to the cells profiled in other studies. As an anucleate cell, platelets are unable to synthesise new microRNA and contain only small amounts of immature microRNA (Landry et al., 2009, Ple et al., 2012a) whereas nucleated cells could readily generate the microRNA required for sorting into released EV.

The mechanism by which the compartmentalisation of microRNA occurs is still yet to be elucidated. There are currently several theories including a neutral SMase2 pathway (Kosaka et al., 2013a), miR-1289 binding sites in the 3' portion of microRNA allowing miR-1289 to act as a chaperone (Bolukbasi et al., 2012) and RISC complex selectivity (Frank et al., 2010). A knockdown of Ago2, a critical component of the RISC complex, resulted in a significant decrease in microRNA within EV, adding evidence for the latter (Guduric-Fuchs et al., 2012). However, the theories all agree that there is a specific element of the microRNAs sequence that contributes to its selective loading into exosomes.

The ability of cells to select microRNA for sorting raised the question of whether the microRNA released are no longer required and are being discarded, or whether they are being released to exert specific functions on other cells (Kosaka et al., 2013b). The microRNA that we observed to be selectively released have been implicated in a variety of functions. MiR-484, which was selectively retained in the platelets has been suggested as a biomarker in the circulation of several cancers (Lu and Lu, 2015, Zearo et al., 2014), suggesting that it is predominantly released under dysfunctional conditions. It also has roles in mitochondrial function which may indicate a reason for its retention (Wang et al., 2012a). MiR-451, which was enriched in pdEVs has previously been found to be enriched in EV released from hepatocellular carcinoma and HEK293T cells (Guduric-Fuchs et al., 2012, Kogure et al., 2011). Its functions have not been widely studied but there are suggestions it may protect against oxidative stress in erythrocytes (Yu et al., 2010). MiR-21-5p was also enriched in EV and is a microRNA that has been implicated as a biomarker in a variety of cancers (Zheng et al., 2014, Yaman Agaoglu et al., 2011, Ouyang et al., 2013) leading to suggestions that it has important roles to play in cancer development via intercellular communication (Kosaka et al., 2013b, Turchinovich et al., 2011). Overall this data suggests that microRNA are specifically sorted into EV, but that the findings in this chapter suggest this is less evident in platelets, perhaps due to their anuclearity.

3.5.4 Thrombin generated pdEV

In this chapter the miR content of EV released from platelets following stimulation with five different agonists was profiled and the analysis indicated that the thrombin dataset was not in line with the other pdEV profiles. This may have been due to differences in the experimental

preparation of this set of samples so the differences could not be definitively attributed to a specific biological variation. There is significant evidence that small changes to sample preparation methods for EV isolation or RNA preparation can lead to changes in RNA profiling (Van Deun et al., 2014, Taylor and Shah, 2015, Taylor et al., 2011). The thrombin generated pdEV were prepared with an additional isolation step using ExoQuick which, as discussed in chapter 2, is unable to selectively isolate exosomes. Van Deun *et al.* found that whilst the EV isolated with ExoQuick were comparable to those prepared with ultracentrifugation and OptiPrep with regards to their protein content, the mRNA profile was distinct. Preparation techniques for other samples such as plasma and serum have also been shown to have significant effects on the detected microRNA profile (Page et al., 2013, Cheng et al., 2013). The thrombin pdEV samples were also prepared from a separate cohort of healthy donors. All of this evidence taken together suggests that the removal of these samples was justified as the observed differences were likely to have been caused by experimental dissimilarities. Whilst the analysis excluded the sample generated with thrombin the receptors targeted by thrombin, PAR1 and PAR4, were individually investigated using the PAR1-AP and PAR4-AP agonists with results that indicated there was no clear difference between the expression profiles of these agonists. It would however have proved interesting to investigate the combined effect of these agonists through the use of thrombin or both agonists simultaneously, but time and cost limitations prevented us from revisiting these experiments.

3.5.5 Localisation of microRNA in pdEV samples

An overriding aim of this study was to determine the localisation of microRNA within the circulation, to attempt to resolve some of the confusions in the literature. The stability of microRNA in the blood is well established (Kamm and Smith, 1972, Stratz et al., 2012, Tsui et al., 2002) and it is known that the survival of microRNA is dependent upon protection from endogenous RNase activity (Valadi et al., 2007, Russo et al., 2012). It has been suggested that this protection is from the microRNAs incorporation into argonaute complexes (Arroyo et al., 2011), HDL complexes (Vickers et al., 2011, Wagner et al., 2013) or internalisation within EV (Cheng et al., 2014, Valadi et al., 2007, Diehl et al., 2012) and it's localisation within EV has opened the debate surrounding whether microRNA is in exosomes or microvesicles. One of the key factors in this confusion is the microRNA profiling of supposedly specific fractions in samples where there is co-isolation of all of these protective complexes together due to the use of techniques such as ultracentrifugation (Yuana et al., 2014)

The evidence against the EV localisation of microRNA is that following size exclusion chromatography fractionation, most microRNA localise within the column rather than the predominant EV fraction, which the authors suggested demonstrated microRNA co-localisation with HDL or argonaute proteins (Boing et al., 2014). However in this study Boing *et al.* found that almost all of the EV >75nm in size, which is the major population of exosomes, was also lost following fractionation, suggesting that the microRNA could have also been localised within exosomes (van der Pol et al., 2016). In addition the localisation of microRNA with argonaute proteins cannot rule out the possibility that these complexes were within EV, as it has previously been shown that microRNA can be bound to Ago2 within EV (Landry et al., 2009, Li et al., 2012, Jaiswal et al., 2012).

HDL have been shown to interact with platelets in the circulation and cause reduced aggregation in response to stimulation, reduced fibrinogen binding and reduced degranulation (Nofer et al., 2010, Nofer et al., 1998). However there is no evidence for the synthesis or release of HDL from platelets and plasma HDLs were removed from this system suggesting that HDLs cannot be the mechanism by which the released microRNA are being protected from RNAse activity. This leaves EV as the likely primary mechanism for microRNA release from platelets in this experimental setup.

As discussed in the previous chapter the methods employed here, as well as all currently available methods are unable to isolate pure populations encompassing the totality of either exosomes or microvesicles. While we found that only CRP-XL generated significant numbers of microvesicles we consistently observed the presence of exosomes in all pdEV samples. While the profile of EVs differed with the different agonists the microRNA profile was consistent regardless of agonist used to stimulate platelets. Therefore, it is plausible that the microRNA are located within the exosomes, since they are present at similar concentrations in all samples. Conversely, whilst all samples contained microvesicles there was no obvious correlation between the microRNA levels and the relative abundance of microvesicles. This suggests, although does not prove, that exosomes were likely to be the main source of microRNA.

3.5.6 Identifying a biomarker of platelet activation

The final section of this chapter attempted to utilise widely available datasets of microRNA profiles to identify a biomarker of platelet activation. Initial studies were carried out that showed the microRNA profile of platelets and pdEV demonstrated significant similarity to the microRNA profile of PPP, suggesting that the microRNA released from platelets in pdEV contributed significantly to the pool of microRNA within the plasma. Our study demonstrated similar findings

to a study by Willeit *et al.* which compared the profiles of platelets to PPP and serum (Willeit et al., 2013). It is known that that microRNA content of platelets is correlated with platelet reactivity and that they can be released in response to activation or disease (Nagalla et al., 2011, Valadi et al., 2007, Ple et al., 2012b). The microRNA content of the plasma is therefore likely to be sensitive to changes in platelet microRNA and in the present study we attempted to utilise this fact to identify a biomarker of platelet activation. In addition to detecting biomarkers in plasma, serum was also investigated as during the preparation of serum, platelets are maximally activated and therefore will release their pdEV containing microRNA.

To identify the microRNA biomarker of platelet activation we compared a wide range of microRNA profiles as cell specific profiles have previously been identified (Merkerova et al., 2008, Liang et al., 2007, Suh et al., 2004, Ruike et al., 2008). However this analysis was limited by available datasets and therefore a group of 40 tissues, profiled using the same TaqMan microRNA array platform as used here, were selected for analysis. The analysis identified several strong potential platelet biomarkers; miR-223-3p, miR-146a-5p and miR-106a-5p. These were tested in the blood of healthy donors but despite clear evidence that the platelets had been activated to the same level as in previous experiments and therefore would have released their microRNA, the results did not demonstrate these microRNA as suitable biomarkers as their detection was not notably altered by specific platelet activation. When copy numbers were calculated using the known values from the cel-miR-39-3p spike-in (data not shown) it was found that PAR1-AP activation (maximal dose) caused an average increase of ~7.5×10^7 copies of miR-223-3p but due to the variability between the 10 donors this was not significant.

The microRNA biomarkers were, however, significantly increased in serum collected from the same individuals. There is strong evidence that serum contains more concentrated microRNA (Wang et al., 2012b) and that some microRNA are actually enriched in serum compared to plasma (Cheng et al., 2013). Although there will have been significant platelet activation in the serum, this is unlikely to have been the sole contributor to the increase in these microRNA and it is to be expected that cell lysis and leukocyte activation will have been important factors, suggesting that these microRNA may not be solely sensitive to platelet activation.

A limitation of the microRNA biomarker selection was that the profiling of the additional tissues had been conducted using only the A card from the TaqMan microRNA microarrays which restricted the profile to ~370 microRNA, all of which were more commonly expressed microRNA. This resulted in attempts to identify uniquely expressed microRNA from a pool of microRNA which were known to be widely expressed. Therefore the selected microRNA may not have

represented the best possible candidates and suggests that an approach where a wider variety of sample types, particularly those from the circulation, were extensively profiled would have yielded better results.

The circulation is known to contain large quantities of circulating cell-free microRNA that is very stable and is built up over time through the release of microRNA from cells (Mitchell et al., 2008, Wang et al., 2012b). It is therefore possible that the acute stimulation in this study was insufficient to cause the build-up of enough of the specific microRNA species for an increase to be detected. Willeit *et al.* were able to demonstrate decreased miR-223-3p, miR-191-5p, miR-126-3p and miR-150-5p in the plasma of healthy individuals taking the anti-platelet agents prasugrel and aspirin every day for a week. Prasugrel blocks the P2Y12 ADP receptor, which as the results in the chapter 2 show would result in a significant reduction in pdEV release in response to platelet activation and as miR-223-3p, miR-191-5p, miR-126-3p and miR-150-5p were all identified in pdEV it is likely that the reduced presence of these specific microRNA was due to a decrease in circulating pdEV.

This group has gone on to demonstrate that plasma levels of miR-223-3p and miR-126-3p correlate with plasma levels of P-selectin, PF4 and other tests of platelet function (Kaudewitz et al., 2016). This data suggests that abundant platelet microRNA, which we have shown to be released from platelets in pdEV have the potential to act as biomarkers of platelet activation. Detection of this change in the study by Kaudewitz *et al.* required microRNA to be observed over a week to allow for a build-up of released microRNA to occur, and cause a significant change.

Overall the data in this chapter demonstrated that platelets release microRNA upon activation with a variety of agonists, that the profile of released microRNA is almost identical regardless of which agonists is used and mirrors that of intact platelets. There is a core group of 46 microRNA that are released following stimulation with CRP-XL, PAR1-AP, PAR4-AP and ADP and the data here suggests, although does not prove that these are predominantly released within exosomes. In addition the microRNA profile of platelets and pdEV is closely related to that of the plasma suggesting the platelets make significant contributions to circulating microRNA. Despite this we were unable to demonstrate microRNA as biomarkers of acute platelet activation, despite other studies showing the profile of these microRNA in the plasma changes in response to prolonged anti-platelet therapy. We also compared the profiling of platelet microRNA using disparate platforms and found significant differences which could predominantly be attributed to the use of the different profiling platforms, suggesting work is needed to make cross-platform comparisons feasible.

Chapter 4

Bioinformatic analysis of microRNA released from platelets in extracellular vesicles

4 Bioinformatic analysis of microRNA released from platelets in extracellular vesicles

4.1 Introduction

In chapter 3, the use of TaqMan microRNA arrays provided information on the range of microRNA released from platelets in response to a variety of agonists. It was relatively easy to interpret these data with regards to numbers of different microRNA, correlation between agonists and their abundance. However, assessing the potential functional role of these microRNA is significantly more challenging but ultimately more important. Our group has had a long term interest in the interaction of platelets and monocytes and these interactions can be split into two types; direct interactions (e.g. P–selectin to PSGL–1) and indirect interactions (e.g. soluble mediators released from platelet granules or EVs). The microRNA released from platelets fall into the latter category and their intercellular transfer within EV has been well documented in a range of different cells (Diehl et al., 2012, Fevrier and Raposo, 2004, Gidlof et al., 2013, Hulsmans and Holvoet, 2013, Hunter et al., 2008, Laffont et al., 2013). This transfer poses a fundamental question; if platelet–derived microRNA is being transferred to monocytes via EV, what biological effects could they have in the target monocytes?

As explained in the introduction to this thesis, each individual species of microRNA can target hundreds of mRNA. Therefore a group of microRNA, such as those released by platelets have the potential to target thousands of mRNA and affect protein expression throughout the cell. Predicting where these changes will occur and whether or not they will be significant is a problem that has been explored extensively (Lewis et al., 2005, Krek et al., 2005, Sethupathy et al., 2006, Pandey et al., 2011). There are now numerous online databases of microRNA–mRNA interactions generated using different target prediction algorithms. These algorithms identify targets through a variety of characteristics such as sequence similarity and cross species conservation. These characteristics are determined from patterns in experimental data from microRNA overexpression or silencing experiments. Approaches used to explore these effects include measuring gene expression using microarrays (Laffont et al., 2015), observing protein expression with proteomics through stable–isotope labelling with amino acids (SILAC) (Baek et al., 2008) and sequencing of microRNA bound mRNA sequences using crosslinking immunoprecipitation (Chi et al., 2009).

Despite the wealth of information available from these high–throughput approaches the microRNA–mRNA interactions are predominantly indirect validations and therefore provide

prediction algorithms with some false patterns and anomalies. Consequently target prediction has a low success rate; experimental evidence suggests that various algorithms produce target lists with 24–51% precision (% = correct/total predictions) and have a sensitivity lower than 20% (total correct predictions/total known specific interactions) (Alexiou et al., 2009, Selbach et al., 2008, Witkos et al., 2011). The authors of these papers suggested that it would be beneficial to utilise the combination of multiple algorithms with differing approaches to target generation. Therefore this approach was taken for predicting microRNA–mRNA interactions in this chapter.

Alongside target prediction algorithms there are repositories containing validated targets from the literature that have been identified through direct scientific evidence. As the field of microRNA research has grown, so has the repository of validated targets. The largest database, miRTarBase, contains data from 4264 published articles detailing 324219 microRNA–mRNA interactions from 2619 human microRNA on 12738 genes meaning that there is almost certainly information on the microRNA(s) of interest (Hsu et al., 2014). Due to the extensive information on microRNA–mRNA interactions, identifying targets for future work is a large task. An easy option would have been to use a single prediction algorithm and select the best match or a target that was already of interest; an approach that has been successful in the past but usually applied when looking at the effects of a single microRNA (Lee et al., 2012, Navarro et al., 2009). When exploring the effects of multiple microRNA, such as those released from platelets, the story is less clear as multiple microRNA can work together to target a single mRNA or pathway (Alexiou et al., 2009, Witkos et al., 2011, Vlachos et al., 2012).

The analysis in this chapter aimed to logically move through the microRNA target identification process and produce a list of targets with strong scientific evidence for further analysis. To identify targets, the prediction algorithms were utilised alongside the databases of validated targets and microarray data from monocyte–platelet interaction experiments.

4.2   Aim

To determine the potential effects of the consistently expressed microRNA released from activated platelets in EVs on monocytes.

4.3   Materials

4.3.1 Monocyte gene expression datasets

To enhance the analysis of pdEV microRNA interactions with monocytes two separate monocyte gene expression datasets were used to identify target genes with mRNA expression in unstimulated monocytes and expression that was altered following an interaction with platelets or platelet-releasate. Both of these datasets were generated from previous students within this lab using the Illumina Whole Genome 6 v2 expression microarrays.

4.3.1.1   Monocyte interaction with CRP–XL activated platelets in whole blood

Monocyte gene expression was analysed at two points; baseline and following 4hour incubation of blood, in which the platelets had been activated with CRP–XL (Figure 4.1). At baseline 8mL of blood was collected from normal healthy donors into EDTA tubes and used for monocyte isolation. For the 4hour activated sample, 15mL of blood was collected into citrate tubes and activated with CRP–XL (1µg/mL) and then incubated for 4hours at 37°C on a tilting plate followed by monocyte isolation. Monocytes were extracted from both samples using CD14 conjugated Dynabeads which utilise an immune magnetic technique to deplete whole blood of CD14+ve monocytes.
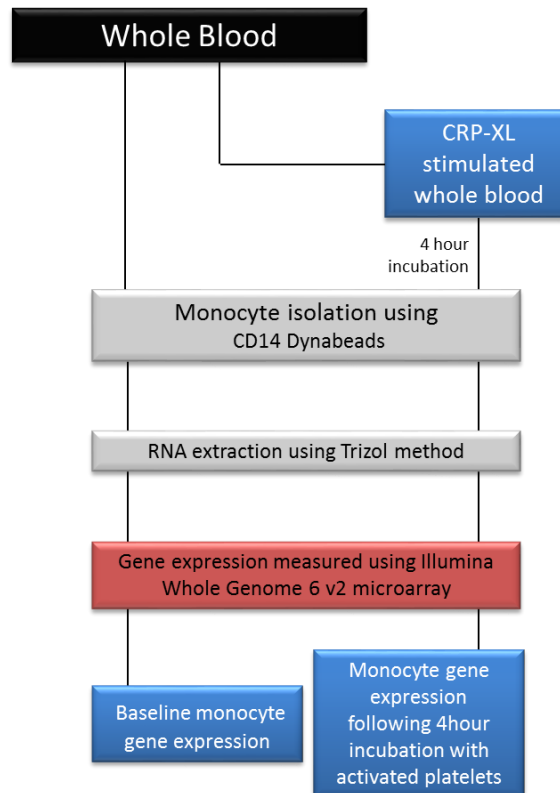
Figure 4.1 – Workflow to measure the effect of platelet activation on monocyte gene expression A pictographic guide explaining the basic steps taken to measure monocyte gene expression before and after 4hour incubations with CRP-XL (1µg/mL) activated platelets in whole blood.

RNA was then extracted from the monocytes using a modified Trizol method from the Dynabead conjugated monocytes, amplified using an in vitro transcription method and then hybridised to the Illumina Whole Genome 6 v2 microarrays. The fluorescent signals from the microarrays were quantified using the Beadarray Reader and then analysed in Bead Studio and R to produce information on which genes were expressed in the samples and their level of expression. The baseline and 4hour CRP–XL stimulated samples were then compared using R to identify the FC in expression, the significance of this change (p–value) and a false discovery rate (FDR) corrected p–value (n=17). This dataset was produced by, and used with the permission of Dr Unni Krishnan (Krishnan, 2012).

4.3.1.2   Monocyte interaction with platelet-releasate

This dataset measured monocyte gene expression before and after incubation with platelet-releasate, which was comprised of all the factors released from platelets following activation (Figure 4.2). Peripheral Blood Mononuclear Cells (PBMC's) were isolated from citrated whole blood using a Lymphoprep method. Briefly, whole blood, collected from normal healthy donors was diluted 1:1 with PBS and then 15mL of blood solution was carefully layered over 10mL of Lymphoprep in a 50mL centrifuge tube. The sample was centrifuged at 1400rpm for 30minutes (RT) and the white PBMC layer was carefully removed using a pastette and transferred to a clean centrifuge tube. The PBMC's were diluted 1:1 in PBS and then centrifuged at 1200rpm for 7minutes (RT), the supernatant was discarded and the cells re-suspended in 3mL of PBS and centrifuged again for 5minutes at 1200rpm (RT). The final pellet was then re-suspended in PPP or platelet-releasate rich plasma which had been prepared simultaneously or for the baseline sample the monocytes were immediately extracted using the CD14 Dynabead method (4.3.1.1).

Platelet-releasate rich plasma was prepared by centrifuging citrated whole blood at 180g for 20minutes (RT), after which the PRP was retained. The PRP was activated with CRP–XL (500ng/mL) for 15minutes at 37°C and then centrifuged at 1800g for 30minutes to pellet cells and cell components; the platelet-releasate rich plasma supernatant was retained. The platelet-releasate rich plasma will contain large numbers of pdEV containing the microRNA described in Chapter 3. PPP was prepared as previously described (2.3.2). The PPP and platelet-releasate rich plasma were incubated with the isolated monocytes for 4hours at 37°C. Monocytes from the 4hour incubated samples were isolated using CD14 Dynabeads and the RNA was extracted and gene expression analysed as before.

To determine the effects of the platelet-releasate the monocytes treated with plasma alone were used as a control and changes in gene expression caused by platelet-releasate rich plasma

were observed as changes greater than those seen with plasma alone (n=6). This dataset was produced by, and used with the permission of Dr Joy Wright (Wright, 2010).
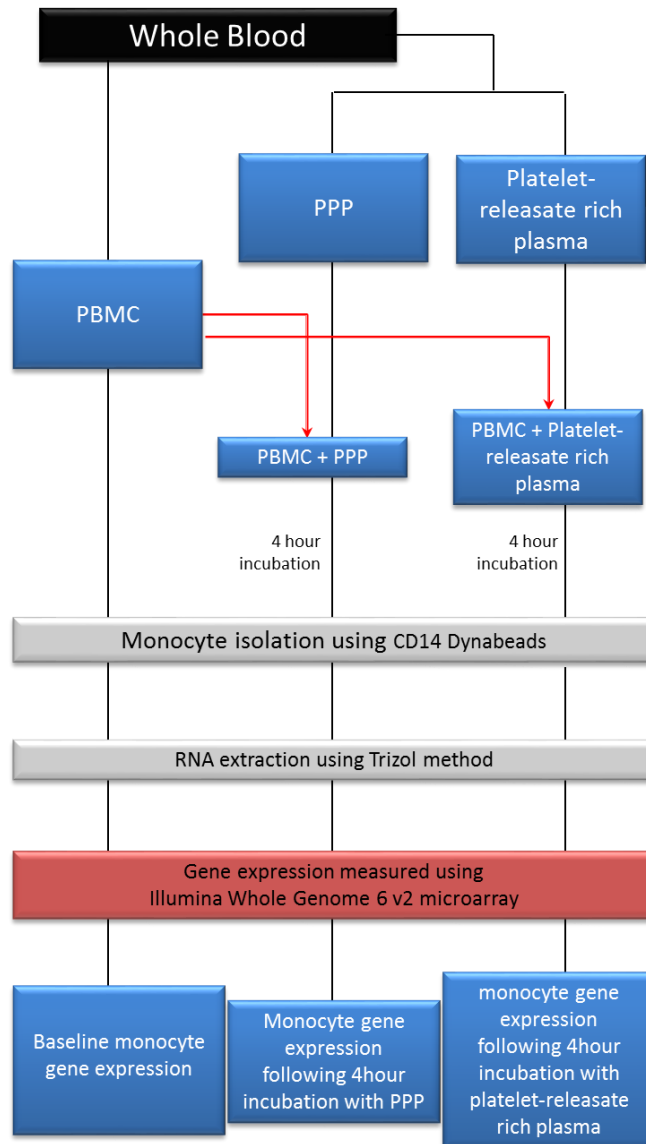
Figure 4.2 – Workflow to measure the effect of platelet-releasate on monocyte gene expression *A pictographic guide explaining the basic steps taken to measure monocyte gene expression before and after 4hour incubations with platelet-releasate rich plasma and PPP.*

4.4 Methods

4.4.1 MicroRNA target identification

The workflow involved in identifying microRNA targets is shown in Figure 4.3. i) MicroRNA targets were identified using either target prediction algorithms or ii) repositories of validated microRNA targets. The predicted targets were obtained using a combination of microRNA.org, miRDB and TargetScan and were iii) filtered to identify those found in all three databases and then iv) merged with the validated targets from miRTarBase.

The data were merged to produce two networks; firstly, a network using the microRNA–mRNA target interactions identified in both the v) Validated AND Predicted datasets and secondly a larger dataset was created containing all of the targets from vi) both groups (Validated PLUS Predicted). vii) This data was then enhanced with monocyte gene expression data at rest and gene fold change (FC) data following 4hour incubation with activated platelets or platelet-releasate. All of these strategies were combined to identify the best targets of pdEV microRNA.
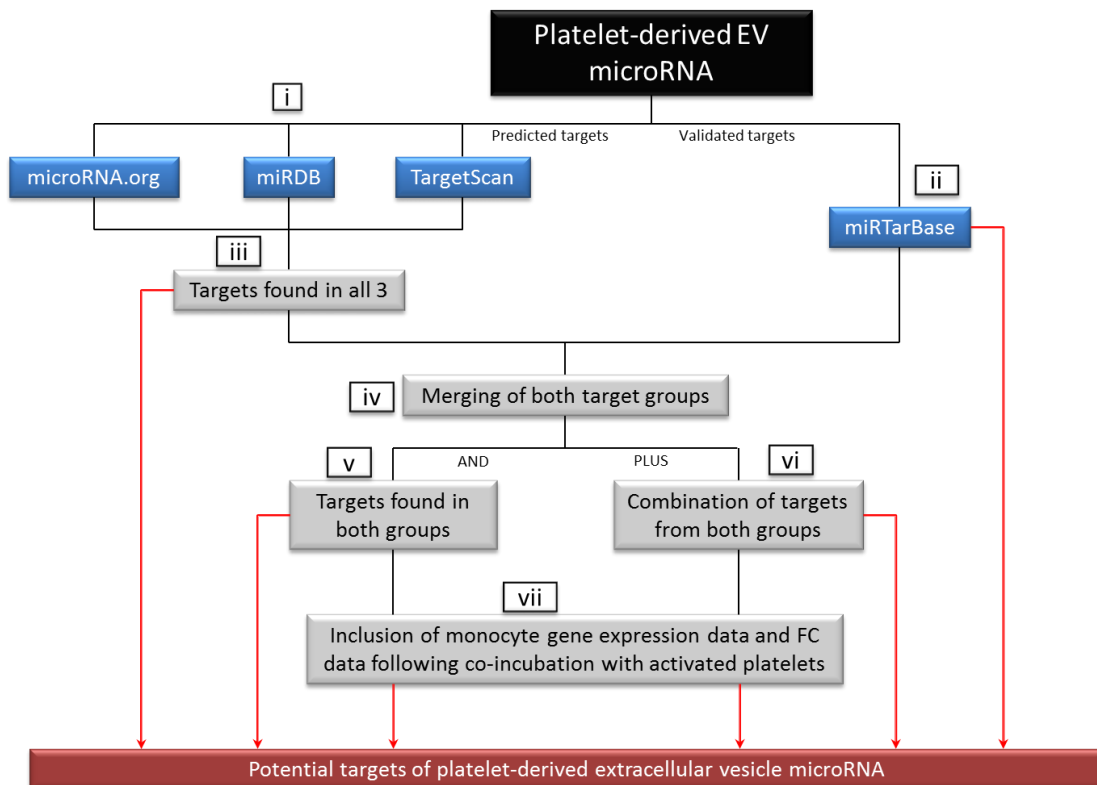
Figure 4.3 – The workflow to identify potential targets of pdEV microRNA The 45 consistently expressed microRNA from pdEV were analysed using three databases to identify predicted targets (microRNA.org, miRDB and TargetScan) and these were retained if found in all three databases and miRTarBase was utilised to find validated targets. These targets were then utilised for network generation. Following this the networks were merged to identify the total cohort of targets and the group of targets that were both validated and predicted. To these new networks the information from monocyte gene expression studies was added. Potential targets for future work were identified at all stages of the process.

4.4.1.1 Predicted targets

Predicted microRNA targets were identified using three separate databases, which utilise different criteria to determine and score targets. The cut–offs and settings for each database were determined to identify targets with high precision:

microRNA.org (August 2010 release) – Used the miRanda target prediction algorithm to produce a mirSVR score; determined by the complementarity of the microRNA sequence to the mRNA transcript, the energy required to allow binding with targets and was filtered based on cross–species conservation. This database contained >16million predicted microRNA binding sites in ~20 thousand human genes.

Targets identified were filtered for a miRSVR score of >1, and where only a specific isoform of a gene contained the microRNA binding site the gene was still retained for further analysis (Betel et al., 2008).

miRDB – Used a 5–fold approach to target prediction; seed–site conservation, quality of match within the seed–site, base composition, accessibility of the binding site and location in the 3'–UTR. This produced a 'target score' between 50 and 100, with a greater number indicating a target was more likely to be real. miRDB contained targets for ~2500 microRNA which were predicted to have almost one million targets in 17925 human genes.

The predicted targets were filtered to ensure that the 'target score' was greater than 60 (Wong and Wang, 2015, Wang, 2010).

TargetScan (Release 7) – Generated a score based upon; complementarity of the seed-site, AU content of the target transcripts 3'–UTR and position within the 3'–UTR. Cross–species conservation was also considered, but was only used to weight the target score. The TargetScan prediction algorithm provided microRNA target information for 19475 human genes.

The results grouped the microRNA into families and identified the transcripts targeted by each family. The data was filtered to allow the inclusion of non–conserved targets with a 'Cumulative weighted context++ score' of ≥–0.5 (Agarwal et al., 2015).

Next the intersection between the three lists was analysed; the lists from each database for each microRNA were analysed using Venn diagram software (The Flanders Interuniversity Institute for Biotechnology and The University of Gent (bioinformatics.psb.ugent/webtools/Venn)). Only the microRNA targets which were detected in all three databases were retained for further analysis. In cases where the information from a single database wasn't available, or there were

less than ten targets, microRNA targets were selected based on their presence in 100% of the remaining databases.

4.4.1.2 Validated targets

miRTarBase (release 6.0) – The largest and most up–to–date validated target database currently available; containing 324219 microRNA–mRNA interactions from 2619 human microRNA on 12738 genes from 4264 published articles.

The process to identify experimentally validated microRNA targets was much simpler. Targets identified through miRTarBase were filtered based upon the strength of the experimental evidence. Only targets which were backed up by strong evidence e.g. reporter assays and western blotting were retained for further analysis. Targets with weaker evidence such as microarray or next generation sequencing (NGS) were discarded due to the indirect nature of these approaches (Hsu et al., 2014).

4.4.2 Network generation

Visualisation of the data was carried out using the network generation tool, Cytoscape 2.8.3 for which the data was organised using Microsoft Office Excel 2010:

Microsoft Office Excel 2010 – Used for data collation and manipulation for further analysis (Elliott et al., 2006). Data was input into Excel from the online microRNA–target identification tools. This data was organised so that every microRNA–target interaction was a separate entity for processing in Cytoscape. Node attribute data, such as gene expression level was also added.

Cytoscape v2.8.3 – microRNA–target interactions were plotted and visualised using the Open Source Software platform Cytoscape v2.8.3 (The Cytoscape Consortium). Used to plot complex networks and to overlay attribute data. MicroRNA–mRNA interactions were plotted as edges between nodes (either a single gene or microRNA) and information such as expression data, strength of interaction and experimentally observed FC were plotted onto the networks (Shannon et al., 2003).

The data from Excel was imported using the 'network from file' option with the data then mapping to nodes (microRNA and targets) and edges (interactions). MicroRNA were mapped as source interactions and the targets as target interactions due to the directional relationship. The network was analysed within Cytoscape to determine the relationships between targets and multiple microRNA allowing for the mapping of characteristics to specific nodes and edges. Networks were then arranged using the Force-directed layout which caused connected nodes

to attract each other whilst repelling all other nodes, thereby forcing nodes that have similar connections close together (microRNA with similar targets will cluster) (Chernobelskiy et al., 2012).

Due to the density of detail within these networks, the figures shown in this thesis are unable to display the data with sufficient resolution, therefore full resolution network images are downloadable from http://tinyurl.com/ashleyambrose.

Once the separate networks for the Validated AND Predicted targets had been created, new networks were created by merging, as described in Figure 4.3. Following this, orphan nodes (nodes with no edges linked to other nodes) were deleted. A final network manipulation was carried out in Cytoscape to overlay monocyte gene expression data (4.3.1). For this the expression and expression change data from Excel were mapped to the target nodes and then utilised to determine the nodes visual appearance (Shannon et al., 2003).

4.4.3 Pathway prediction

Pathway analysis was conducted to determine if any pathways were directly influenced by the Validated AND Predicted targets. This was conducted using the consensus pathway database (CPDB) pathway analyser:

CPDB (release 31) – This was a compilation database that acts to integrate networks of interaction between proteins, genes, metabolites etc. It contained data form 32 different repositories and provided information on 4953 pathways. These pathways were brought together from the INOH, PID, Biocarta, NetPath, Reactome, HumanCyc, KEGG, WikiPathways, SMPDB, PharmGKB, EHMN and SignaLink pathway databases (Kamburov et al., 2013). The analysis utilised hyper-geometric distribution to identify the over–representation of the inputted genes within pathways. This generated a p-value based on the probability of this over–representation occurring by chance, an FDR adjusted p–value was also computed and termed the q–value.

A gene set over–representation analysis was carried out using the microRNA targets HGNC symbols. The 'pathways as defined by pathway databases' analysis was selected with the following settings; all databases selected, minimum overlap with 'input list=10' and a p–value cut–off of 0.01. The results were then filtered to ensure that the q-value (FDR) was <0.01 and any duplicated identical pathways were removed (Kamburov et al., 2013). These thresholds were set to ensure that small pathways with low numbers of genes which focused on very

specific functions did not dominate the analysis. This would have disguised overall themes of the dataset.

4.4.4 Gene Ontology Analysis of microRNA targets

To determine the attributes of the genes identified as potential targets, they were submitted to a gene ontology (GO) analysis using the Panther DB gene list analyser;

Panther DB (version 8) – Protein ANnotation THrough Evolutionary Relationship (PANTHER) is a classification system that contained detailed annotations on almost all genes. The GO terms place genes into groups based upon their molecular function (MF), the biological processes (BP) and the cellular component (CC) where the protein will be found (Mi et al., 2013b, Mi et al., 2013a).

The Gene ID list of the microRNA targets was submitted to the database, the organism was set to 'homo sapiens' and a functional classification analysis was carried out. The analysis results provided information on the level 1 GO terms separated into MF, BP and CC (Mi et al., 2013a, Mi et al., 2013b).

4.5   Results

4.5.1 Analysed microRNA

The scope of this chapter did not allow for the investigation of every microRNA identified in Chapter 3 therefore it focused on the core group of microRNA found to be present in all EVs released from platelets, regardless of the stimulus. This resulted in a group of microRNA that were consistently expressed, but did mean that a couple of relatively abundant microRNA such as miR-409-3p and miR-93 were excluded due to their absence from one or more of the samples. The overlap between the different pdEV populations released from platelets is shown in the Venn diagram in Figure 4.4., which found 90 unique species of microRNA detected in pdEV, but only 46 of these were found in all four of the sample types. These 46 were selected for further analysis.
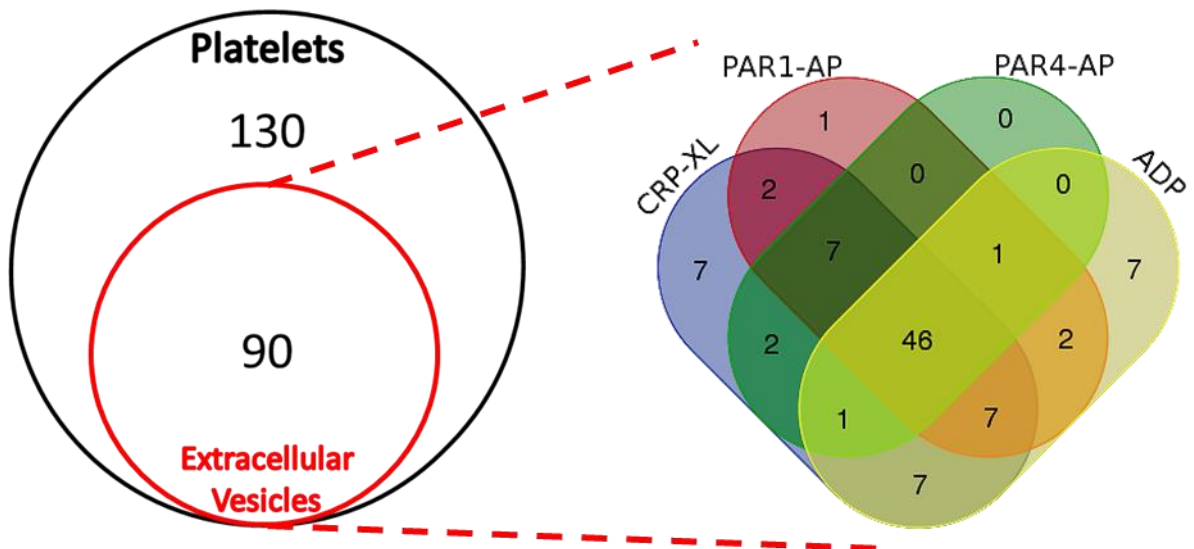
Figure 4.4 – Venn diagram showing the number of shared microRNA between platelets and their vesicles and between the different EV populations MicroRNA from the profiling of platelets and their EV allowed for the identification of overlap between microRNA found in platelets and their EV and then the breaking down of the EV released in response to a variety of agonists.

One of the consistently expressed RNA identified by the TaqMan microRNA microarrays was the control transcript snRNA U6. snRNA U6 is a small nuclear RNA that forms part of a splicesome which is involved in post–translational modifications and so was disregarded for this analysis. The specifics of the remaining 45 microRNA species are detailed in Table 4.1; this includes previous IDs, the sequences, the microRNA family they belong to and their average expression in pdEV.

There are several observations to note from Table 4.1; firstly there was a ~3300–fold spread of expression (AU) from 0.15 (miR–18b–5p) to 509.64 (miR–223–3p), and secondly the miR–17/92

cluster and its two paralogues, miR–106a and miR–106b were highly expressed. The miR–17/92 cluster has been studied in great detail and contains; **miR–17**, **miR–18a**, **miR–19a**, **miR–19b–1**, **miR–20a** and **miR–92a–1** with the paralogue miR–106a cluster containing **miR–106a**, **miR–18b**, **miR–20b**, miR–19b–2, miR–92a–2 and miR–363 and finally the 2nd paralogue miR–106b cluster contains **miR–106b**, miR–93 and miR–25. All those in bold, which represent ten of the fifteen microRNA from this cluster, were found to be consistently expressed in pdEV. The concentration of microRNA from this cluster suggested that it may have a key role in the effect of microRNA transported within pdEV. Research on this cluster indicated that it has strong links to cell death and differentiation (Mogilyansky and Rigoutsos, 2013, Fontana et al., 2007, Bonauer et al., 2009). The targets of these and the other 35 consistently expressed microRNA were thoroughly investigated in this chapter.

Table 4.1 – Details of the 45 consistently expressed microRNA in pdEV Information detailing the ID, alternative IDs, microRNA family, microRNA sequence and the average expression in pdEV (shown numerically and as blue bars in final column) for the 45 microRNA released by platelets in response to all four agonists (CRP–XL, PAR1–AP, PAR4–AP and ADP).

microRNA ID	Alternative microRNA IDs	microRNA family	microRNA sequence	microRNA expression in EV
hsa-let-7d-5p	hsa-let-7d	let-7	agagguaguagguugcauaguu	1.66
hsa-let-7e-5p	hsa-let-7e		ugagguaggagguuguauaguu	6.58
hsa-let-7g-5p	hsa-let-7g		ugagguaguaguuuguacaguu	1.57
hsa-miR-126-3p	hsa-miR-126	miR-126	ucguaccgugaguaauaaugcg	20.11
hsa-miR-126-5p	hsa-miR-126*		cauuauuacuuuugguacgcg	1.82
hsa-miR-301a-5p		miR-130	gcucugacuuuauugcacuacu	1.10
hsa-miR-139-5p	hsa-miR-139	miR-139	ucuacagugcacgugucuccagu	0.56
hsa-miR-140-5p	hsa-miR-140	miR-140	caguggguuuuacccuaugguag	0.92
hsa-miR-142-3p		miR-142	uguaguguuuccuacuuuaugga	6.06
hsa-miR-145-5p	hsa-miR-145	miR-145	guccaguuuucccaggaaucccu	2.05
hsa-miR-146a-5p	hsa-miR-146, hsa-miR-146a	miR-146	ugagaacugaauuccauggguu	36.04
hsa-miR-146b-5p	hsa-miR-146b		ugagaacugaauuccauaggcu	3.19
hsa-miR-15b-5p	hsa-miR-15b	miR-15	uagcagcacaucaugguuuaca	3.16
hsa-miR-16-5p	hsa-miR-16		uagcagcacguaaauauuggcg	6.03
hsa-miR-195-5p	hsa-miR-195		uagcagcacagaaauauuggc	0.29
hsa-miR-150-5p	hsa-miR-150	miR-150	ucucccaacccuuguaccagug	2.11
hsa-miR-155-5p	hsa-miR-155	miR-155	uuaaugcuaaucgugauagggu	1.42
hsa-miR-106a-5p	hsa-miR-106a	miR-17	aaaagugcuuacagugcagguag	19.50
hsa-miR-106b-5p	hsa-miR-106b		uaaagugcugacagugcagau	1.20
hsa-miR-17-5p	hsa-miR-17		caaagugcuuacagugcagguag	17.08
hsa-miR-18a-5p	hsa-miR-18, hsa-miR-18a		uaaggugcaucuagugcagauag	1.65
hsa-miR-18b-5p	hsa-miR-18b		uaaggugcaucuagugcaguuag	0.15
hsa-miR-20a-5p	hsa-miR-20, hsa-miR-20a		uaaagugcuuauagugcagguag	7.32
hsa-miR-20b-5p	hsa-miR-20b		caaagugcucauagugcagguag	2.58
hsa-miR-186-5p	hsa-miR-186	miR-186	caaagaauucuccuuuugggcu	1.05
hsa-miR-19a-3p	hsa-miR-19a	miR-19	ugugcaaaucuaugcaaaacuga	0.71
hsa-miR-19b-3p	hsa-miR-19b		ugugcaaauccaugcaaaacuga	35.61
hsa-miR-191-5p	hsa-miR-191	miR-191	caacggaaucccaaaagcagcug	18.52
hsa-miR-199a-3p	hsa-miR-199a*	miR-199	acaguagucugcacauugguua	4.28
hsa-miR-21-5p	hsa-miR-21	miR-21	uagcuuaucagacugauguuga	6.56
hsa-miR-221-3p	hsa-miR-221	miR-221	agcuacauugucugcuggguuuc	6.72
hsa-miR-222-3p	hsa-miR-222		agcuacaucuggcuacuggu	0.53
hsa-miR-223-3p	hsa-miR-223	miR-223	ugucaguuugucaaauacccca	509.64
hsa-miR-24-3p	hsa-miR-24	miR-24	uggcucaguucagcaggaacag	29.92
hsa-miR-92a-3p	hsa-miR-92, hsa-miR-92a	miR-25	uauugcacuugucccggccugu	11.93
hsa-miR-26a-5p	hsa-miR-26a	miR-26	uucaaguaauccaggauaggcu	2.03
hsa-miR-26b-5p	hsa-miR-26b		uucaaguaauucaggauaggu	0.43
hsa-miR-28-3p		miR-28	cacuagauugugagcuccugga	1.97
hsa-miR-28-5p	hsa-miR-28		aaggagcucacagucuauugag	0.70
hsa-miR-30b-5p	hsa-miR-30b	miR-30	uguaaacauccuacacucagcu	14.67
hsa-miR-30c-5p	hsa-miR-30c		uguaaacauccuacacucucagc	3.25
hsa-miR-320a	hsa-miR-320	miR-320	aaaagcuggguugagagggcga	4.82
hsa-miR-328-3p		miR-328	cuggcccucucugcccuuccgu	1.54
hsa-miR-374a-5p	hsa-miR-374, hsa-miR-374a	miR-374	uuauaauacaaccugauaagug	0.99
hsa-miR-451a	hsa-miR-451	miR-451	aaaccguuaccauuacugaguu	3.01

4.5.2 microRNA target identification

4.5.2.1 miR–223–3p target identification – a worked example

The overall process for microRNA target identification used in this chapter was explained in Figure 4.3 but for clarity a worked example using miR–223–3p is illustrated in Figure 4.5. To identify predicted microRNA targets the microRNA.org, TargetScan and miRDB databases were searched for targets of miR–223–3p and returned 407, 339 and 242 targets respectively. Duplicates were removed from these lists leaving 338 (microRNA.org), 338 (TargetScan) and 242 (miRDB). These were compiled into a Venn diagram to identify the intersection between them; 56 unique targets, listed in Table 4.2. Alongside the identification of predicted targets, validated targets were identified from the miRTarBase, producing the 19 targets shown in Table 4.3.
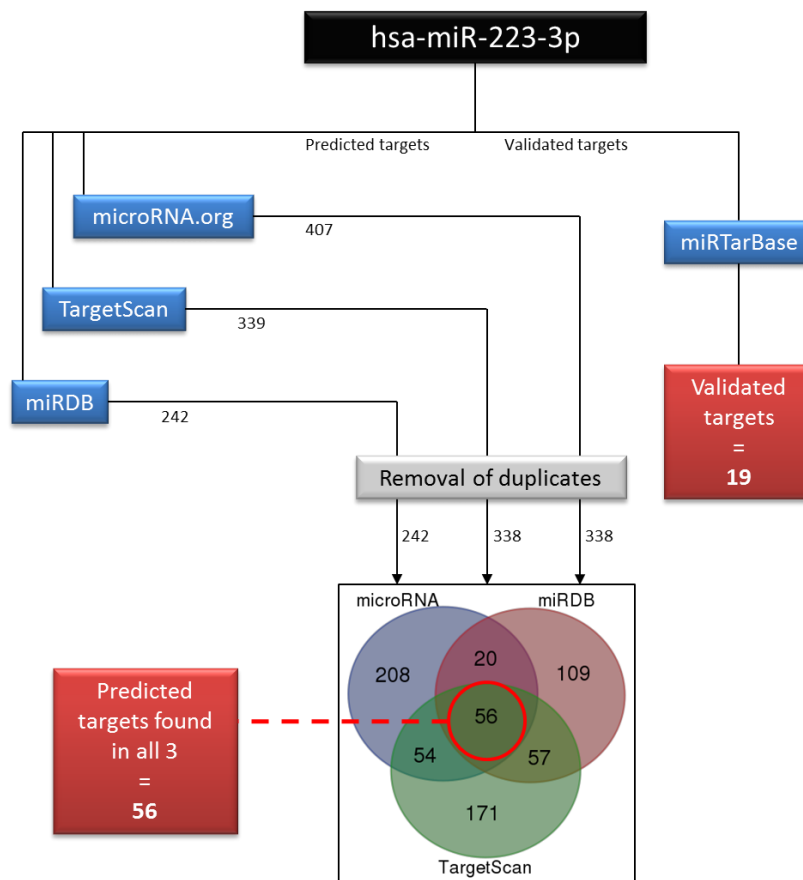
Figure 4.5 – A worked example of the microRNA target identification process used (miR–223–3p) *MiR–223–3p was used as the search term in the microRNA.org, miRDB, TargetScan and miRTarBase databases. The outputs of the predicted target databases were filtered for duplicates and then targets found in all three databases were identified. The number of microRNA identified in each step is shown in the figure.*

By combining the information from multiple databases it increased the likelihood of a predicted target being real due to the multiple algorithms assessing a vast array of criteria (4.4.1.1). This did however result in a significantly reduced number of targets, e.g. for miR–223–3p the three databases produced a combined total of 918 targets. Of these, there were 675 unique targets with only 56 in all three databases, representing a 17% share of each databases targets. The

number of validated targets for miR–223–3p was significantly less than the number of predicted targets and only four targets were shared between the two groups.

Table 4.2 – Predicted targets of miR–223–3p *The predicted targets of miR–223–3p were identified from the microRNA.org, miRDB and TargetScan databases and are listed in the table with those also identified as Validated Targets being highlighted.*

Predicted Targets							
CLSTN1	KPNA3	SRP54	SP3	SEPT10	LYZL6	GTPBP8	RABGAP1L
PAIP1	RERG	ARMCX1	BRMS1L	HARBI1	SLC39A1	TBC1D17	MTPN
CBFB	ARMC1	CDK17	ANKS1B	INPP5B	CEP72	FAM13C	FEZ2
ZNF365	**RHOB**	IL6ST	PTBP2	CRIM1	KIAA1841	ABCD4	CYB5A
NLRP3	TMEM143	ATP7A	RASA1	C8orf22	DUSP10	CLEC14A	CLDN8
FBXO8	TWF1	**HSP90B1**	**LMO2**	TOX	PRDM1	USP16	SEPT6
ACSL3	DCAF12	**FBXW7**	ATP10D	NPY1R	NUP210	C6orf136	ECT2

Table 4.3 – Validated targets of miR–223–3p *The validated targets of miR–223–3p were identified from the miRTarBase database and are listed in the table with those also identified as Predicted Targets being highlighted.*

Validated Targets							
FBXW7	SLC2A4	NFIX	NFIA	CHUK	SP3	ARTN	EPB41L3
FOXO1	**HSP90B1**	SCARB1	PARP1	E2F1	**RHOB**	LIF	IGF1R
MEF2C	STMN1	**LMO2**					

4.5.2.2   MicroRNA target identification overview

The results for target identification for miR–223–3p were representative of the number of targets and percentage of shared targets seen across all of the microRNA (Table 4.4). On average each microRNA had 80 consistently identified targets but this represented a range from 3 to 169 and on average 18% of the targets identified in each database were also found in the other two databases but this ranged from 0.88% to 100%, suggesting significant variation in the overlap. MiR–126–3p presented difficulties (highlighted in Table 4.4) as there was no evidence for targets in the microRNA.org and TargetScan databases, therefore the predicted targets for this microRNA were determined solely by those found in the miRDB database.

On average each microRNA yielded 18 validated targets from miRTarBase with only miR–28–5p having no validated targets. The number of validated targets was always lower than the number of predicted targets with the exceptions of; miR–301a–5p, miR–155–5p and miR–21–5p, where the number of validated targets exceeded the number of predicted targets by 4, 68 and 20 respectively. Overall the process of target identification for the 45 consistently expressed microRNA found 3592 predicted and 811 validated microRNA–mRNA interactions. These data were utilised for network generation, pathway analysis and Gene Ontology analysis.

Table 4.4 – Number of targets identified for each pdEV microRNA Each of the 45 pdEV microRNA found consistently in all samples was submitted to analyses to identify Validated AND Predicted targets as previously describe. This table shows the number of targets identified for each microRNA, the overlap between the different prediction databases and also the total number of Validated AND Predicted targets.

microRNA ID	Predicted targets					Validated targets
	microRNA.org	TargetScan	miRDB	Shared	(%) shared	
let–7d–5p	237	786	438	75	15.40	4
let–7e–5p	251	786	435	76	15.49	4
let–7g–5p	257	786	434	75	15.23	9
miR–106a–5p	628	394	860	149	23.75	13
miR–106b–5p	594	394	855	150	24.42	18
miR–126–3p	0	90	0	90	100.00	23
miR–126–5p	1594	133	644	31	3.92	5
miR–139–5p	318	224	313	66	23.16	2
miR–140–5p	304	325	263	41	13.79	9
miR–142–3p	301	284	192	52	20.08	3
miR–145–5p	527	479	495	84	16.79	81
miR–146a–5p	337	261	224	34	12.41	25
miR–146b–5p	339	261	224	34	12.38	5
miR–150–5p	221	192	224	27	12.72	10
miR–155–5p	662	286	311	62	14.77	130
miR–15b–5p	577	916	1086	164	19.08	7
miR–16–5p	591	916	1088	162	18.73	27
miR–17–5p	628	394	860	149	23.75	39
miR–186–5p	1242	66	886	19	2.60	4
miR–18a–5p	219	379	250	56	19.81	9
miR–18b–5p	238	379	250	56	19.38	2
miR–191–5p	95	152	55	7	6.95	6
miR–195–5p	577	916	1089	161	18.71	18
miR–199a–3p	334	306	287	66	21.36	6
miR–19a–3p	714	559	788	169	24.60	22
miR–19b–3p	651	559	786	166	24.95	12
miR–20a–5p	638	394	847	147	23.47	25
miR–20b–5p	612	394	849	149	24.10	13
miR–21–5p	444	188	240	53	18.23	73
miR–221–3p	426	318	316	70	19.81	16
miR–222–3p	337	318	320	70	21.54	30
miR–223–3p	407	339	242	56	17.00	21
miR–24–3p	163	535	552	58	13.92	19
miR–26a–5p	707	211	515	67	14.03	38
miR–26b–5p	785	211	518	68	13.47	27
miR–28–3p	177	429	281	21	7.10	6
miR–28–5p	268	124	135	17	9.68	0
miR–301a–5p	694	116	216	3	0.88	7
miR–30b–5p	921	455	849	159	21.44	5
miR–30c–5p	943	455	849	158	21.09	5
miR–320a	473	216	581	58	13.70	8
miR–328–3p	87	425	235	17	6.83	7
miR–374a–5p	1746	94	677	36	4.29	5
miR–451a	831	101	23	6	1.88	3
miR–92a–3p	457	389	496	158	35.32	10
Average				79.8	18.0	18.0
Total targets				3592	N/A	811

4.5.2.3 Predicted targets

4.5.2.3.1   Predicted microRNA–target interactions network generation

Figure 4.6 shows the predicted targets of pdEV microRNA visualised into an interaction network. The network shows all of the microRNA (red diamond nodes) and their predicted targets (white square nodes). The size of the target nodes was determined by the number of microRNA interacting with the target, the larger the node the more predicted microRNA interactions.
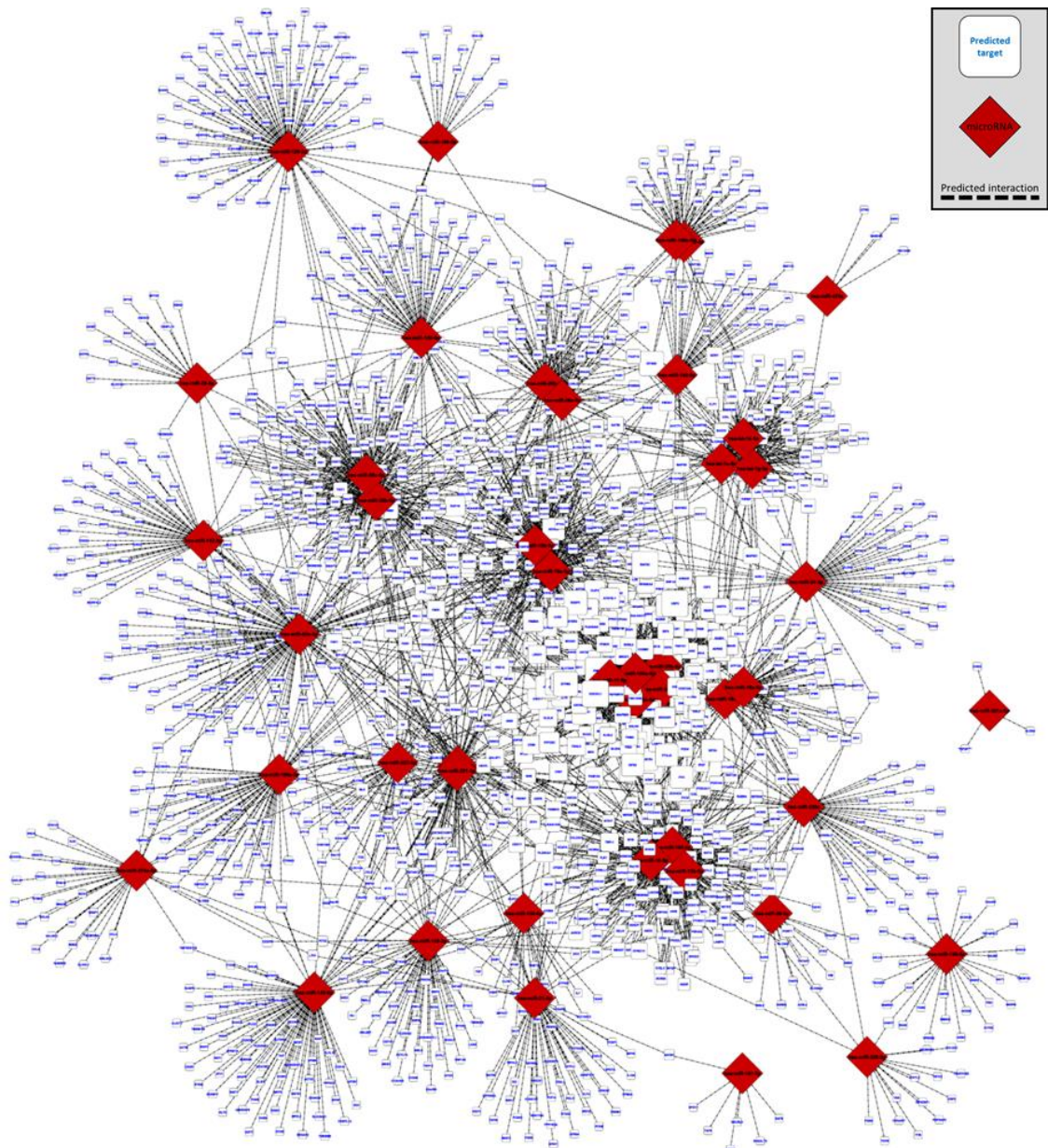
Figure 4.6 – Predicted targets of pdEV microRNA mapped into an interaction network *MicroRNA–target interactions identified through the microRNA.org, TargetScan and miRDB databases for the 45 microRNA consistently found in pdEV were mapped into an interaction network using Cytoscape 2.8.3. MicroRNA were mapped to red diamond source nodes and targets to white square target nodes. These were linked by edges (dashed black line) to indicate predicted interactions. The network was laid out according to a force-directed layout resulting in the clustering of microRNA with similar targets. High resolution image available at http://tinyurl.com/ashleyambrose.*

All of the microRNA except for miR–301a–5p integrated into the network, indicating that they all share targets with other microRNA. Atypically miR–301a–5p, had only three targets (EIF2S2 [*Eukaryotic Translation Initiation Factor 2 Subunit Beta*], HHEX [*Haematopoietically Expressed Homeobox*] and GLRX5 [*Glutaredoxin 5*]) and they were all unique to this microRNA. MiR–301a–5p is one of the lowest expressed microRNA (35th, Table 4.1) and so its effects are likely to be minimal. Of the 44 microRNA integrated into the network, many sat alone on the borders of the network due to the majority of their targets being unique.

There were several microRNA clusters within the network and these were visualised in the network's microRNA map, Figure 4.7. There were four small clusters of microRNA; miR–146a & miR–146b (cluster A), miR–26a & miR–26b (B), miR–19a & miR–19b (C) and miR–30c & miR–30b (D), all of which, as their naming suggests, had closely related sequences (one or two bases difference) (Ambros et al., 2003). In addition to these clusters, there were four larger clusters; the let–7 family of microRNA (E), miR–221/2/3 (F), the miR–15 family (G) and the microRNA associated with the miR–17/92 cluster (H). The three let–7 family microRNA, 7d/e/g, had 75, 76 and 75 predicted targets respectively, with 75 of these being identical across all three (100%, 98.6% and 100% of targets respectively) and only LRRC17 being an additional target for let–7e–5p. This was unsurprising as these three microRNA have >90% sequence homology. The next cluster comprised miR–221–3p, miR–222–3p and miR–223–3p. MiR–221–3p and miR–222–3p both had the same 70 predicted microRNA due to their similar sequences, however the clustering of miR–223–3p was unexpected as only two of the predicted targets for miR–221–3p and miR–222–3p are shared with miR–223–3p. This suggests that the closeness of miR–223–3p to miR–221–3p and miR–222–3p was caused through similar relationships with secondary microRNA nodes. The third cluster was miR-15b–5p, miR–16–5p and miR–195–5p which are all part of the miR–15 family and share 158 targets which represented 96.3%, 97.5% and 98.1% of their total targets respectively.
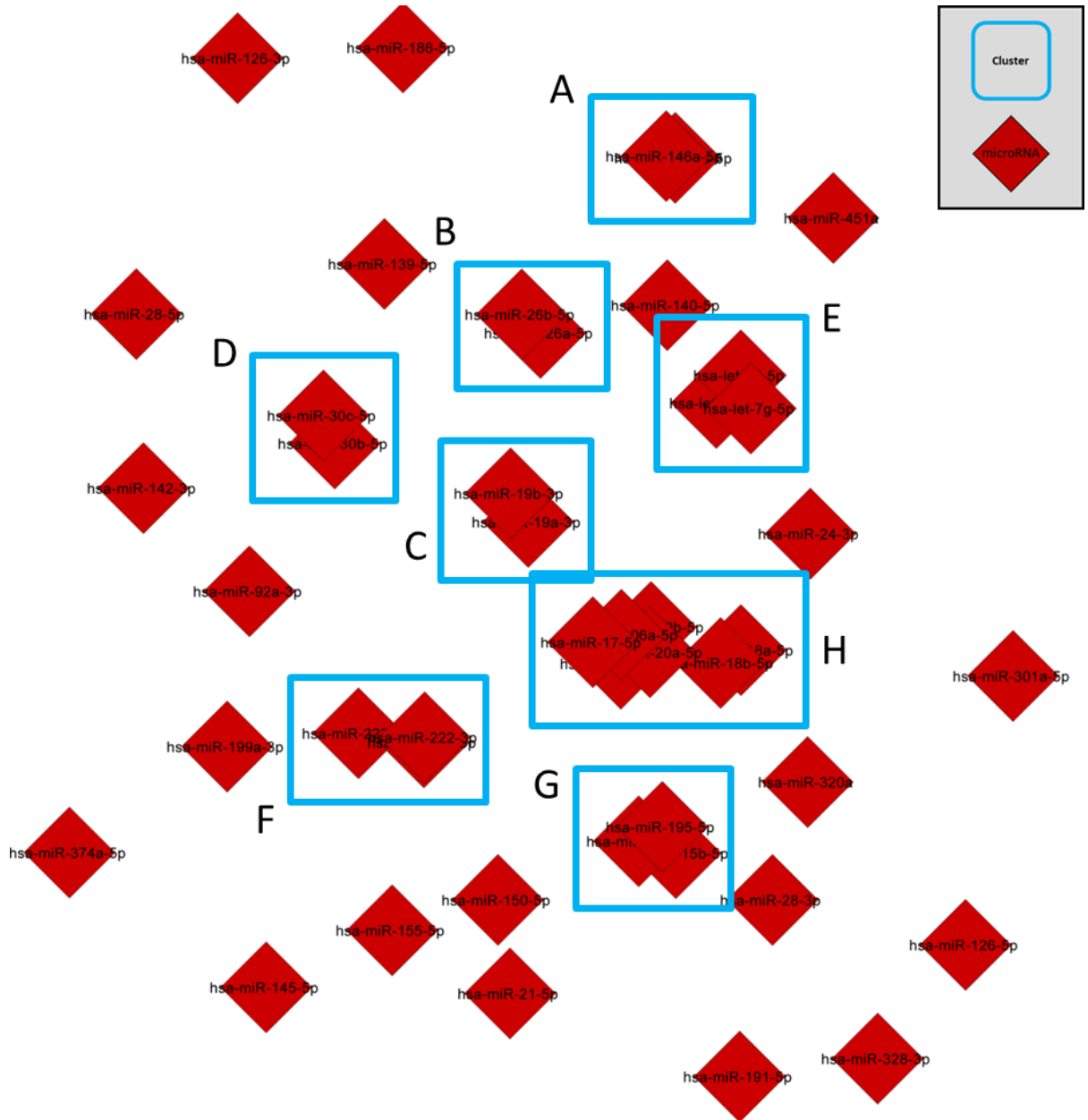
Figure 4.7 – Predicted microRNA targets microRNA map depicting microRNA force–directed layout clustering *An enhanced view of the predicted target network with the targets removed to allow visualisation of microRNA clustering. Clusters identified A) miR–146 family, B) miR–26 family, C) miR–19 family, D) miR–30 family, E) let–7 family, F) miR–221/2/3 family, G) miR–15 family and H) the miR–17/92 cluster. High resolution image available at http://tinyurl.com/ashleyambrose.*

The final and largest cluster of the network was comprised of seven microRNA which were all part of the miR–17/92 cluster and its paralogues (miR–106a and miR–106b). The seven microRNA in this cluster were miR–106b–5p, miR–106a–5p, miR–18b–5p, miR–17–5p, miR–20a–5p, miR–20b–5p and miR–18a–5p. Seven of the ten miR–17/92 cluster that were expressed, and miR–19a and miR–19b were grouped just outside the main cluster but miR–92a was located separately. In total this cluster of seven microRNA had 201 predicted targets and 147 of these were targeted by five or more of them. The network in Figure 4.6 showed that this cluster was integral to the predicted targets of the 45 microRNA and this is explored further in Figure 4.8.
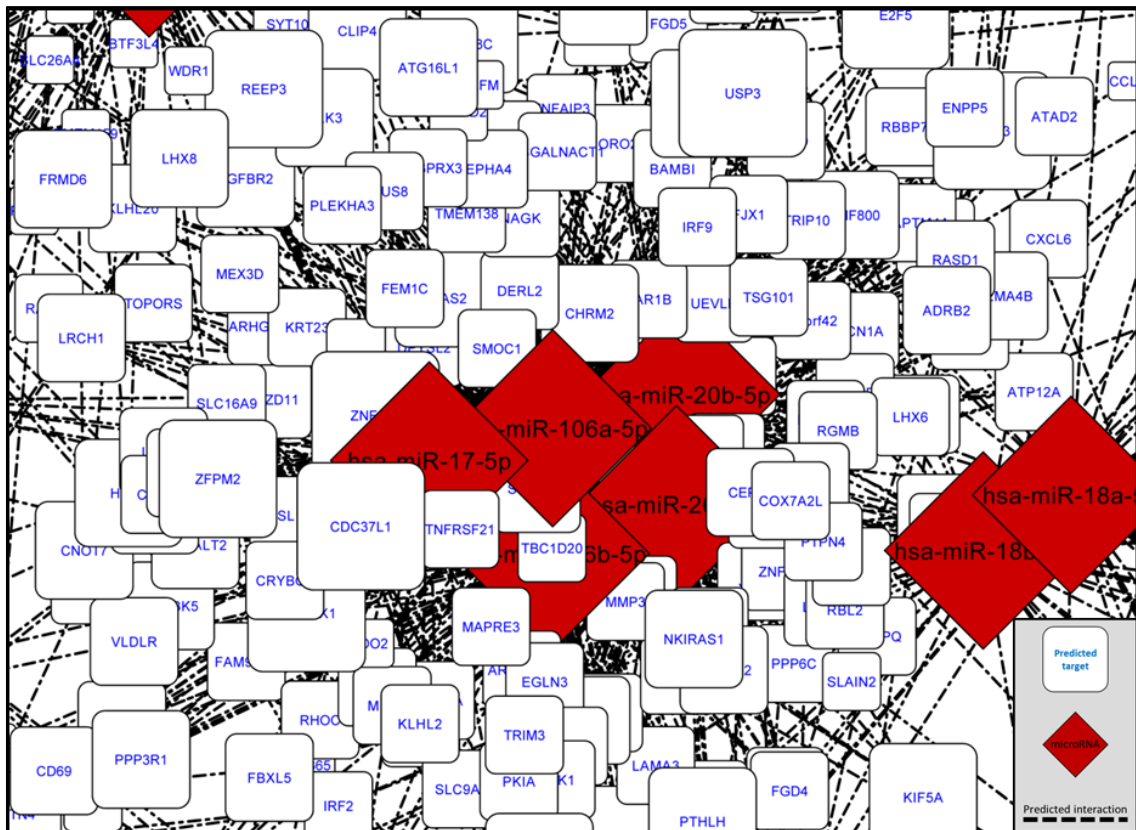
Figure 4.8 – Zoomed section of the predicted target network showing the miR–17 family clustering *Focusing on the miR–17/92 cluster section of the predicted target network. Seven of the ten microRNA from the cluster are shown (miR–17–5p, miR–106a–5p, miR–106b–5p, miR–20a–5p, miR–20b–5p, miR–18a–5p and miR–18b–5p). The targets of these microRNA (white nodes) have increased size in this section as there size is directly proportional to the number of microRNA they interact with. High resolution image available at* http://tinyurl.com/ashleyambrose.

Figure 4.8 shows the zoomed section of the overall predicted target network (Figure 4.6) focusing on the miR–17/92 cluster microRNA (cluster H). It was clear that five of the miR–17/92 cluster shared similar predicted targets and this was confirmed by their sequence homology, with only three (or four in the case of miR–106b–5p), nucleotides being different (Figure 4.9). This also explained why miR–18a/b localised slightly apart from the rest of the cluster as they are six nucleotides different. The size of all target nodes in Figure 4.8 was increased due to them being targets of multiple microRNA. Several stood out due to their node size e.g. CDC37L1 [*Cell Division Cycle 37–Like 1*]*,* USP3 [*Ubiquitin Specific Peptidase 3*], REEP3 [*Receptor Accessory Protein 3*] and ZFPM2 [*Zinc Finger Protein FOG Family Member 2*] which are targeted by nine or ten microRNA making them four of the most commonly targeted transcripts.

```
aaaagugcuuacagugcagguag   -  hsa-miR-106a-5p

uaaaagugcugacagugcagau    -  hsa-miR-106b-5p

caaaagugcuuacagugcagguag  -  hsa-miR-17-5p

uaaaagugcuuauagugcagguag  -  hsa-miR-20a-5p

caaaagugcucauagugcagguag  -  hsa-miR-20b-5p


uaaggugcaucuagugcagauag   -  hsa-miR-18a-5p

uaaggugcaucuagugcaguuag   -  hsa-miR-18b-5p
```
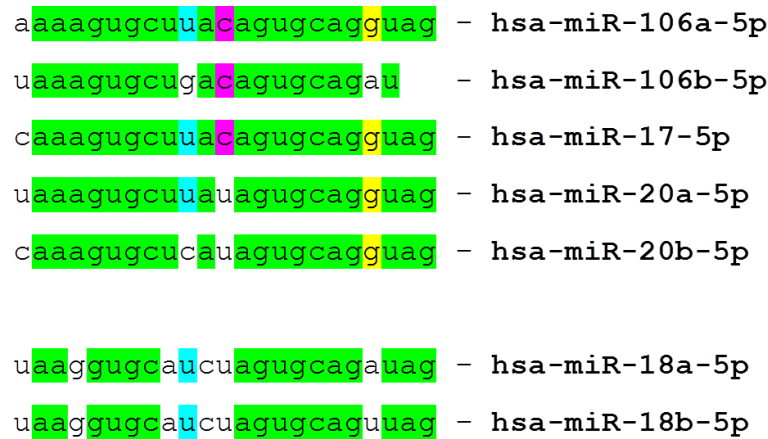
Figure 4.9 – Sequence homology between seven members of the miR–17/92 cluster Alignment of the seven microRNA from the miR–17/92 cluster that group together in the predicted target network. The top five microRNA cluster tightly and have between one and four nucleotides difference in their sequences with miR–106a–5p and miR–17–5p being identical except for the first nucleotide. MiR–18a and miR–18b share slightly less of their sequence with the rest of the cluster but still show strong homology. Green highlighting indicates the base is found in all of the five that cluster tightly and then the other colours show individual bases conserved across the group.

Table 4.5 provides information on the most interesting targets from the analysis of predicted microRNA targets. The targets have predicted interactions with multiple microRNA, often from the miR–17/92 cluster and they have been highlighted because these multiple interactions suggest the target was more likely to be affected by the microRNA in pdEV. In addition to the number of microRNA interacting with a target, the expression level of the microRNA was also important. Targets of miR–223–3p were absent from Table 4.5, yet it was the most highly expressed microRNA in pdEV with relative expression levels 14-fold greater than any other microRNA. Therefore the 56 targets in Table 4.2 are potentially as interesting as the targets in Table 4.5. Together the targets from Table 4.2 and Table 4.5 make up 88 potential targets but at this stage there is not enough information to make an informed decision on the best targets for future work. Despite this, this is often as far as researchers go to identify targets of their microRNA of interest. The next step was to identify validated targets of the 45 microRNA and see if they provided any further insight.

Table 4.5 – Predicted targets targeted by multiple microRNA *The targets with seven or more interacting microRNA are listed in this table alongside the microRNA that they have been predicted to interact with. Targets are ordered based on the number of interacting microRNA and the microRNA were ordered numerically.*

Target	Number of microRNA	Interacting microRNA IDs								
CDC37L1	10	miR–106a–5p	miR–106b–5p	miR–15b–5p	miR–16–5p	miR–17–5p	miR–195–5p	miR–20a–5p	miR–20b–5p	miR–30b–5p	miR–30c–5p
ZNF367	10	miR–106a–5p	miR–106b–5p	miR–17–5p	miR–19a–3p	miR–19b–3p	miR–20a–5p	miR–20b–5p	miR–24–3p	miR–26a–5p	miR–26b–5p
RAP2C	10	miR–106a–5p	miR–106b–5p	miR–146a–5p	miR–146b–5p	miR–15b–5p	miR–16–5p	miR–17–5p	miR–195–5p	miR–20a–5p	miR–20b–5p
USP3	10	miR–106a–5p	miR–106b–5p	miR–17–5p	miR–18a–5p	miR–18b–5p	miR–19a–3p	miR–19b–3p	miR–20a–5p	miR–20b–5p	miR–21–5p
EIF4G2	9	let–7d–5p	let–7e–5p	let–7g–5p	miR–139–5p	miR–140–5p	miR–146a–5p	miR–146b–5p	miR–26a–5p	miR–26b–5p	
HMBOX1	9	miR–106a–5p	miR–106b–5p	miR–17–5p	miR–18a–5p	miR–18b–5p	miR–20a–5p	miR–20b–5p	miR–221–3p	miR–222–3p	
PBX3	9	let–7d–5p	let–7e–5p	let–7g–5p	miR–106a–5p	miR–106b–5p	miR–17–5p	miR–20a–5p	miR–20b–5p	miR–320a	
REEP3	9	miR–106a–5p	miR–106b–5p	miR–17–5p	miR–19a–3p	miR–19b–3p	miR–20a–5p	miR–20b–5p	miR–30b–5p	miR–30c–5p	
ZFPM2	9	miR–106a–5p	miR–106b–5p	miR–17–5p	miR–19a–3p	miR–19b–3p	miR–20a–5p	miR–20b–5p	miR–221–3p	miR–222–3p	
ADAM9	8	miR–106a–5p	miR–106b–5p	miR–126–3p	miR–17–5p	miR–20a–5p	miR–20b–5p	miR–26a–5p	miR–26b–5p		
BTG3	8	miR–106a–5p	miR–106b–5p	miR–139–5p	miR–17–5p	miR–18a–5p	miR–18b–5p	miR–20a–5p	miR–20b–5p		
E2F5	8	let–7d–5p	let–7e–5p	let–7g–5p	miR–106a–5p	miR–106b–5p	miR–17–5p	miR–20a–5p	miR–20b–5p		
HBP1	8	miR–106a–5p	miR–106b–5p	miR–155–5p	miR–17–5p	miR–19a–3p	miR–19b–3p	miR–20a–5p	miR–20b–5p		
KIF23	8	miR–106a–5p	miR–106b–5p	miR–15b–5p	miR–16–5p	miR–17–5p	miR–195–5p	miR–20a–5p	miR–20b–5p		
KIF5A	8	miR–106a–5p	miR–106b–5p	miR–15b–5p	miR–16–5p	miR–17–5p	miR–195–5p	miR–20a–5p	miR–20b–5p		
PLSCR4	8	miR–106a–5p	miR–106b–5p	miR–15b–5p	miR–16–5p	miR–17–5p	miR–195–5p	miR–20a–5p	miR–20b–5p		
PTH	8	miR–106a–5p	miR–106b–5p	miR–15b–5p	miR–16–5p	miR–17–5p	miR–195–5p	miR–20a–5p	miR–20b–5p		
PTHLH	8	miR–106a–5p	miR–106b–5p	miR–15b–5p	miR–16–5p	miR–17–5p	miR–195–5p	miR–20a–5p	miR–20b–5p		
ZBTB4	8	miR–106a–5p	miR–106b–5p	miR–150–5p	miR–17–5p	miR–18a–5p	miR–18b–5p	miR–20a–5p	miR–20b–5p		
ATG16L1	7	miR–106a–5p	miR–106b–5p	miR–17–5p	miR–19a–3p	miR–19b–3p	miR–20a–5p	miR–20b–5p			
CHRM2	7	miR–106a–5p	miR–106b–5p	miR–17–5p	miR–18a–5p	miR–18b–5p	miR–20a–5p	miR–20b–5p			
CLIP4	7	miR–106a–5p	miR–106b–5p	miR–17–5p	miR–19a–3p	miR–19b–3p	miR–20a–5p	miR–20b–5p			
CNOT7	7	miR–106a–5p	miR–106b–5p	miR–17–5p	miR–19a–3p	miR–19b–3p	miR–20a–5p	miR–20b–5p			
COX8C	7	miR–106a–5p	miR–106b–5p	miR–17–5p	miR–19a–3p	miR–19b–3p	miR–20a–5p	miR–20b–5p			
ELK3	7	miR–106a–5p	miR–106b–5p	miR–17–5p	miR–19a–3p	miR–19b–3p	miR–20a–5p	miR–20b–5p			
FRMD6	7	miR–106a–5p	miR–106b–5p	miR–17–5p	miR–20a–5p	miR–20b–5p	miR–30b–5p	miR–30c–5p			
LHX8	7	miR–106a–5p	miR–106b–5p	miR–17–5p	miR–20a–5p	miR–20b–5p	miR–30b–5p	miR–30c–5p			
NKIRAS1	7	miR–106a–5p	miR–106b–5p	miR–17–5p	miR–18a–5p	miR–18b–5p	miR–20a–5p	miR–20b–5p			
NPAS2	7	miR–106a–5p	miR–106b–5p	miR–17–5p	miR–19a–3p	miR–19b–3p	miR–20a–5p	miR–20b–5p			
PPP3R1	7	miR–106a–5p	miR–106b–5p	miR–17–5p	miR–20a–5p	miR–20b–5p	miR–221–3p	miR–222–3p			
RAP1B	7	miR–19a–3p	miR–19b–3p	miR–24–3p	miR–28–5p	miR–30b–5p	miR–30c–5p	miR–92a–3p			
TGFBR2	7	miR–106a–5p	miR–106b–5p	miR–17–5p	miR–19a–3p	miR–19b–3p	miR–20a–5p	miR–20b–5p			

4.5.2.4 Validated Targets

4.5.2.4.1 Validated microRNA–target interactions network generation

Simultaneous to the identification of predicted microRNA–target interactions, validated interactions were identified using miRTarBase. The interactions were loaded into Cytoscape and a network was generated containing 811 microRNA targets (Figure 4.10). Each microRNA had an average of 18 validated targets, but only 44 microRNA were shown in the network; miR–28–5p was absent as it had no validated targets in the database. All of the present microRNA were integrated into the network through shared targets except for miR–142–3p, which was separate due to its three unique targets; RAC1 [*Ras–Related C3 Botulinum Toxin Substrate 1*], ARNTL [*Aryl Hydrocarbon Receptor Nuclear Translocator–Like]* and PROM1 [*Prominin 1*].

There were fewer microRNA on the periphery of the validated target network with 23 microRNA located in the core of the network. This was perhaps due to the lower number of targets for each microRNA, the force-directed layout brought more microRNA towards the centre of the network due to a higher percentage of shared targets. Three microRNA shared a low percentage of their targets with other microRNA; miR–145–5p, miR–155–5p and miR–21–5p share 17.3%, 13.0% and 26% of their targets respectively which was low compared with the average of 44.1%. They also had significantly more validated targets than the other microRNA and this was likely to be responsible for the low percentage overlap with other microRNA. These microRNA highlighted a key issue with identifying targets using validated interaction databases; the information is heavily biased by microRNA or targets that are of interest to specific researchers. The high number of targets for these three microRNA suggested that they had been of interest to researchers in the past and so had been subjected to more extensive investigation.

This phenomenon also affected the clustering of microRNA within the network (Figure 4.11). When analysing predicted targets the clustering was predominantly based upon sequence homology, it now appears to be determined by the targets previously selected for validation. The previous microRNA clusters miR–30b/c, miR–26a/b, miR–146a/b, let–7d/e/g, miR–15b/16/195 and miR–221/222/223–3p no longer form, sharing zero (0%), four (13.8%), three (11.5%), one (6.7%), three (6.5%) and zero (0%) targets between all microRNA in the cluster, respectively. Although many of these microRNA still appear close to each other, this was likely due to increased tightness of the network caused by the reduced number of targets.
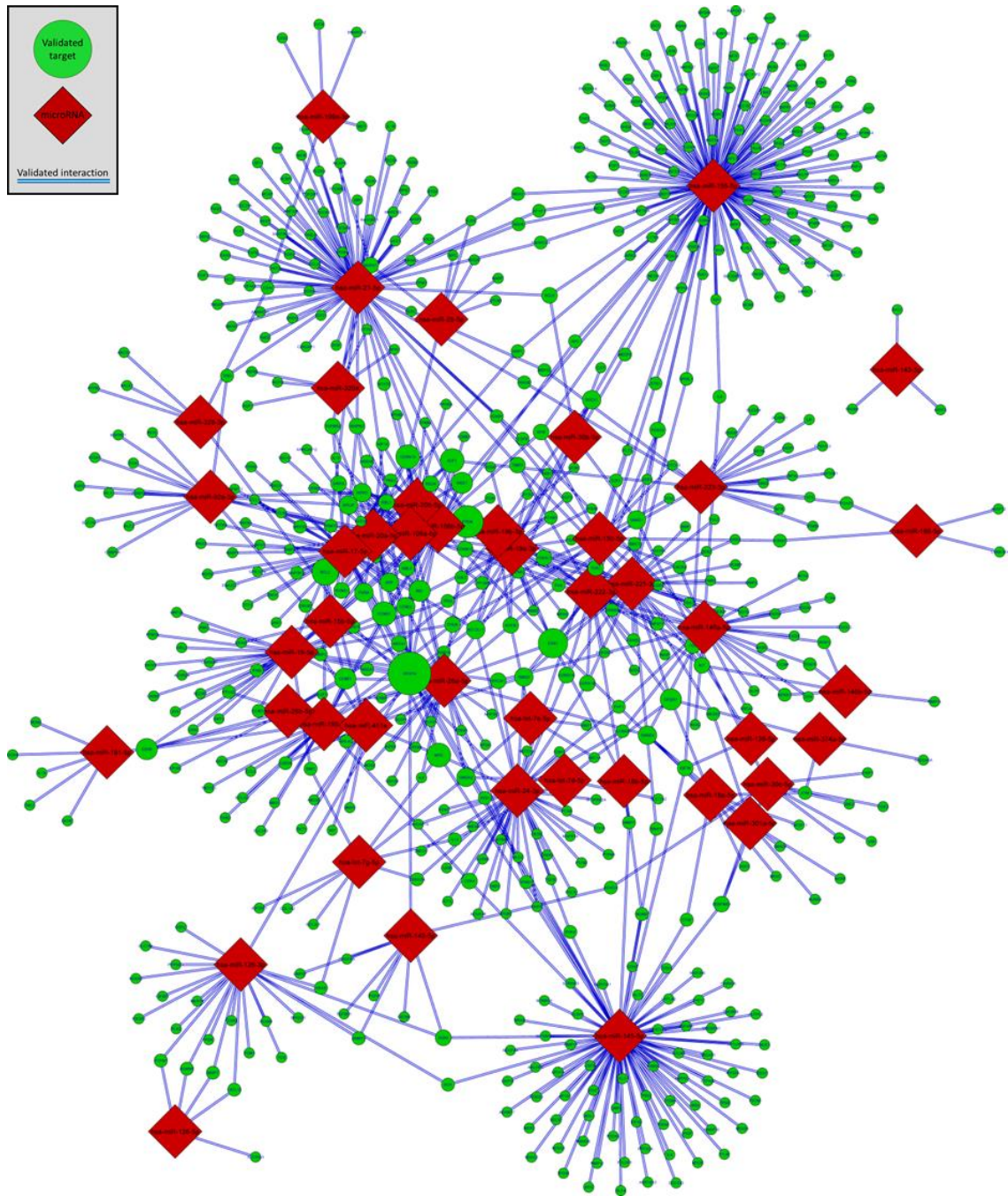
Figure 4.10 – Validated targets of pdEV microRNA mapped into an interaction network *Validated microRNA–target interactions in miRTarBase for the 45 microRNA consistently found in pdEV were mapped into an interaction network using Cytoscape 2.8.3. MicroRNA were mapped to red diamond source nodes and targets to green circle target nodes. These were linked by edges (double blue lines) to indicate validated interactions. The network was laid out according to a force-directed layout resulting in the clustering of microRNA with similar targets. High resolution image available at* http://tinyurl.com/ashleyambrose.

Figure 4.11 – Validated microRNA targets microRNA map depicting microRNA force–directed layout clustering *Target nodes were removed from the network to leave just the microRNA to clearly demonstrate clustering of microRNA. The microRNA nodes were increased in size so only clusters that appear in the actual network are highlighted using the same annotations as previously; Cluster C) miR–19 family, Cluster H) miR–17/92 cluster. High resolution image available at http://tinyurl.com/ashleyambrose.*

Only two clear clusters remained from the predicted target network; miR–19a/b (Cluster C) and the miR–17/92 cluster (H). With the miR–19a/b cluster there were now only eight (30.7%) shared microRNA between them, whereas the overlap was 97.1% of predicted targets. The miR–17/92 cluster remained the largest and dominant cluster in the network. In the predicted network it contained seven of the ten miR–17/92 microRNA, but this was reduced to five, with miR–18a and miR–18b no longer present. The five microRNA (miR–17–5p, miR–20a–5p, miR–

20b–5p, miR–106a–5p and miR–106b–5p) only had two (3.3%) targets that were targeted by all five, but there were 25 (37.3%) targets interacting with two or more of the cluster. This cluster was well researched and it is likely that targets of multiple microRNA within the cluster have been researched together, resulting in this cluster remaining (Bonauer et al., 2009, Fontana et al., 2007, Mogilyansky and Rigoutsos, 2013).
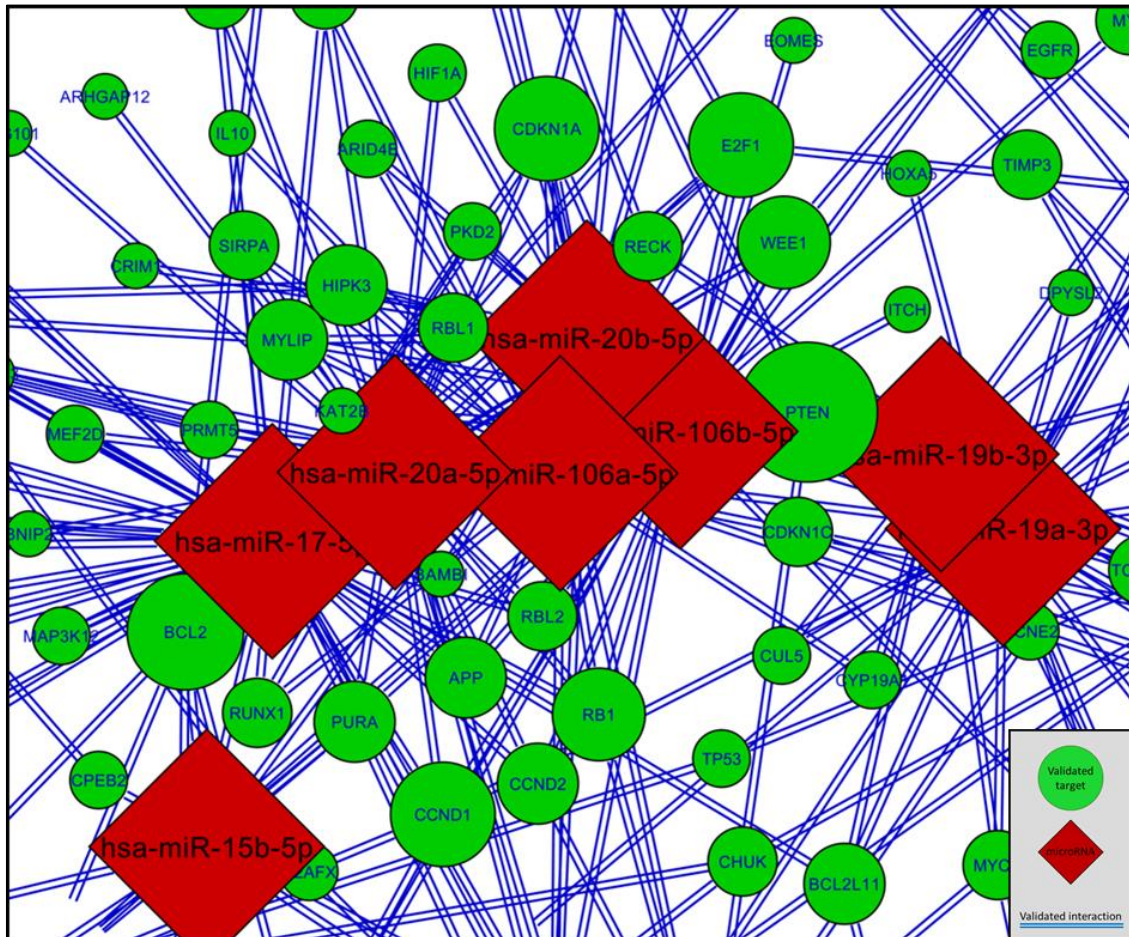
Figure 4.12 – Zoomed section of the predicted target network showing the miR–17/92 family clustering *The clearest cluster in the validated target network was the miR–17/92 cluster. To focus on this network the figure shows a zoomed section of the network containing seven of the miR–17/92 cluster of microRNA. MiR–17–5p, miR–20a–5p, miR–20b–5p, miR–106a–5p and miR–106b–5p are shown alongside miR–19a–3p and miR–19b–3p with their interacting targets. Many of these targets demonstrate increased node size due to their multiple interacting microRNA. High resolution image available at* http://tinyurl.com/ashleyambrose*.*

The five microRNA from the miR–17/92 cluster that remained clustered in the validated target network are shown in detail in Figure 4.12. From the figure it was clear that there were fewer validated targets than predicted targets (Figure 4.8) associated with the miR–17/92 cluster. But as before, many of these targets interacted with multiple microRNA (indicated by increased node size). Figure 4.12 contained many of the most frequently targeted mRNA due to the influence of the miR–17/92 cluster on these targets. This figure suggested at several potentially important targets; CDKN1A [*Cyclin–Dependent Kinase Inhibitor 1A*], PTEN [*Phosphatase and Tensin*

Homolog], E2F1 [*E2F Transcription Factor 1*], BCL2 [*B–Cell CLL/Lymphoma 2*] and CCND1 [*Cyclin D1*], and the most frequently validated targets are listed in Table 4.6. The table listed fewer mRNA with multiple interacting microRNA, but this reflected the lower number of targets identified for each microRNA. Of the targets in Table 4.6 many of them have been frequently researched and have roles in well–known processes such as the cell cycle, demonstrating further evidence of bias in this identification process.

From Table 4.6 it was clear that VEGFA [*Vascular Endothelial Growth Factor A*] had the most validated microRNA–target interactions, with 13 evidence based microRNA interactions. These 13 included the five microRNA from the miR–17/92 cluster and three from the miR–15 family alongside five other microRNA. Despite VEGFA having validated interactions with 13 microRNA from this dataset, the summed expression level of these 13 was still significantly below the expression of miR–223–3p. MiR–223–3p was 5.7 times more abundant and this further illustrated the importance of utilising microRNA expression levels. Of the targets with multiple microRNA interactions shown in Table 4.6, miR–223–3p only interacted with one, E2F1 [*E2F transcription factor 1*], meaning that alongside VEGFA, E2F1 is potentially another important target.

The targets identified through the analysis miRTarBase present many potential targets for further analysis e.g. VEGFA and E2F1. However, as has been alluded to, this approach had several weaknesses in identifying microRNA from databases of information biased by other researchers. Therefore to increase the robustness of the target identification process and to prevent important targets being missed the next step was to merge the Validated AND Predicted target information.

Table 4.6 – Validated targets targeted by multiple microRNA *The targets with the most validated microRNA interactions are shown in this table, they have been ordered so that microRNA with more interactions appear at the top. The microRNA are ordered numerically to allow patterns to be seen.*

Target	Number of microRNA	microRNA IDs								
VEGFA	13	miR–106a–5p miR–195–5p	miR–106b–5p miR–20a–5p	miR–126–3p miR–20b–5p	miR–140–5p miR–21–5p	miR–145–5p	miR–150–5p	miR–15b–5p	miR–16–5p	miR–17–5p
PTEN	9	miR–106b–5p	miR–17–5p	miR–19a–3p	miR–19b–3p	miR–20a–5p	miR–21–5p	miR–221–3p	miR–222–3p	miR–26a–5p
ESR1	8	miR–18a–5p	miR–18b–5p	miR–19a–3p	miR–19b–3p	miR–20b–5p	miR–221–3p	miR–222–3p	miR–26a–5p	
BCL2	7	miR–15b–5p	miR–16–5p	miR–17–5p	miR–195–5p	miR–20a–5p	miR–21–5p	miR–451a		
CCND1	6	miR–106b–5p	miR–16–5p	miR–17–5p	miR–195–5p	miR–19a–3p	miR–20a–5p			
CDKN1A	6	miR–106a–5p	miR–106b–5p	miR–17–5p	miR–20a–5p	miR–20b–5p	miR–28–5p			
E2F1	6	miR–106a–5p	miR–106b–5p	miR–17–5p	miR–20a–5p	miR–21–5p	miR–223–3p			
MYC	6	let–7g–5p	miR–145–5p	miR–17–5p	miR–20a–5p	miR–24–3p	miR–451a			
CCNE1	5	miR–15b–5p	miR–16–5p	miR–195–5p	miR–26a–5p	miR–26b–5p				
CDK6	5	miR–16–5p	miR–191–5p	miR–195–5p	miR–26a–5p	miR–26b–5p				
DICER1	5	let–7d–5p	miR–18a–5p	miR–221–3p	miR–222–3p	miR–374a–5p				
RB1	5	miR–106a–5p	miR–106b–5p	miR–17–5p	miR–20a–5p	miR–26a–5p				
WEE1	5	miR–106b–5p	miR–155–5p	miR–17–5p	miR–195–5p	miR–20a–5p				

4.5.2.5 Merging Validated AND Predicted targets

4.5.2.5.1   Validated PLUS Predicted microRNA–target interactions network
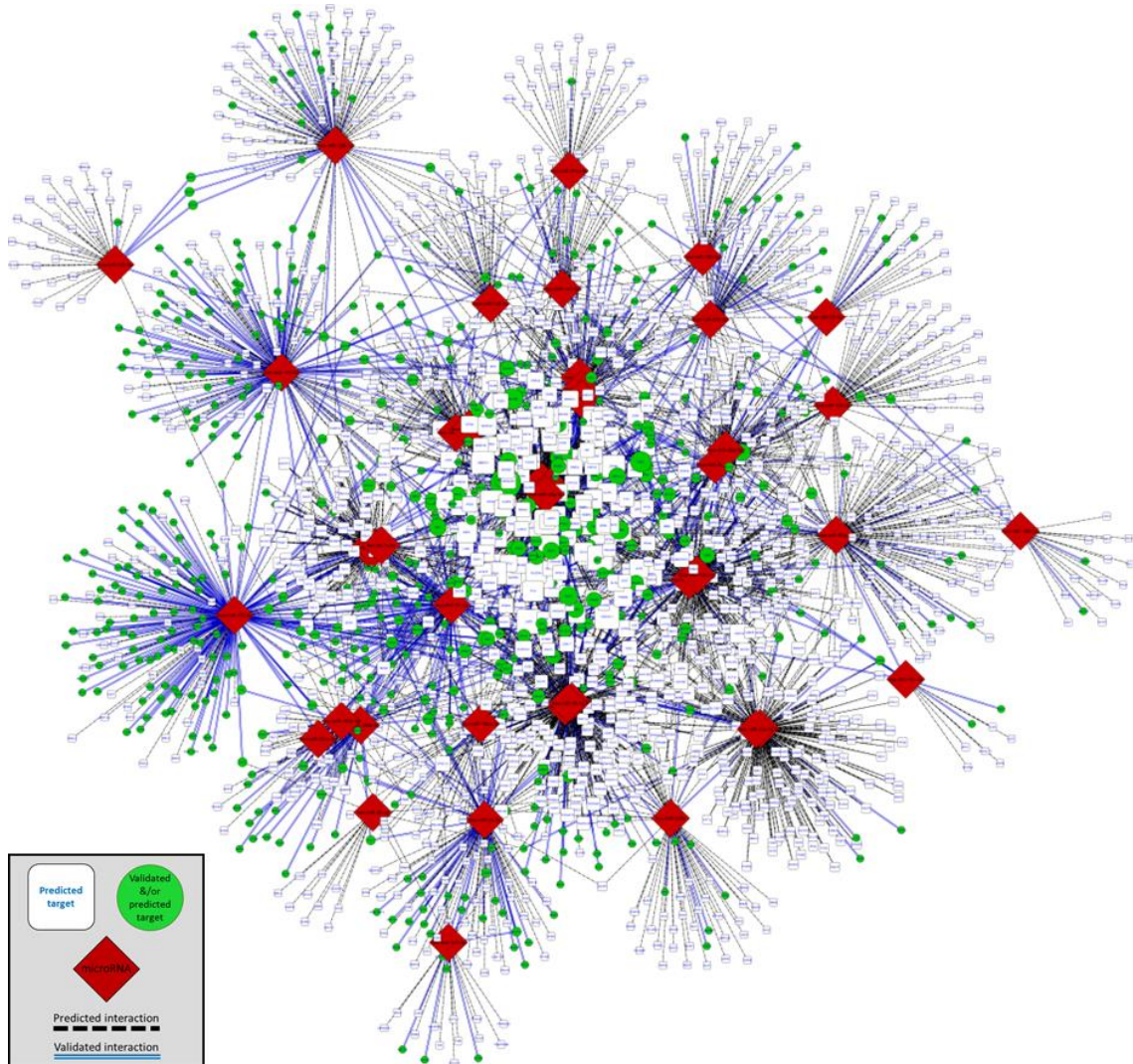
Figure 4.13 – A combination microRNA–target interaction network of the Validated PLUS Predicted microRNA targets *Validated PLUS Predicted microRNA–target interactions from the earlier networks were mapped into an interaction network using Cytoscape 2.8.3. MicroRNA were mapped to red diamond source nodes and targets to green circle target nodes (at least one validated interaction) or white squares (predicted interactions only). These were linked by edges; double blue lines (validated interactions) and black dashed lines (predicted interactions). The network was laid out according to a force-directed layout resulting in the clustering of microRNA with similar targets. High resolution image available at http://tinyurl.com/ashleyambrose.*

As discussed earlier (4.4.1) the Validated AND Predicted target information was merged to create two new networks; predicted targets were added to validated targets to form a network containing all targets (Figure 4.13). Secondly, microRNA–target interactions that were both Validated AND predicted were identified (Figure 4.15). The Validated PLUS Predicted target network shown in Figure 4.13 incorporating all of the information gathered on all targets. The network contains all 45 microRNA and has 2084 target nodes, as before node size indicated the number of interacting microRNA. The node colour indicated the type of interactions; white –

predicted only and green – at least one validated interaction. The edge style showed which microRNA interactions were predicted (black lines) or validated (blue lines).

Again, the most frequently targeted mRNA (larger nodes) were central to the network with close links to the miR–17/92 cluster which contained five of the ten microRNA from the cluster (miR–17–5p, miR–20a–5p, miR–20b–5p, miR–106a–5p and miR–106b–5p). The strength of its influence on the network was shown in the list of most frequently targeted mRNA (Table 4.7). Only one target (EIF4G2) is not targeted by five or more microRNA from the miR–17/92 cluster (miR–17/92 microRNA are underlined).

The network in Figure 4.13 showed that the predicted targets were predominant for most microRNA but there were two notable exceptions; miR–155–5p (62 predicted targets and 130 validated targets) and miR–21–5p (53 predicted and 73 validated). These microRNA have 1252 and 2175 references in PubMed, demonstrating further evidence of the bias in the validated target databases. Despite the abundance of validated targets only fifteen (miR–155–5p) and nine (miR–21–5p) of these were Validated AND Predicted.
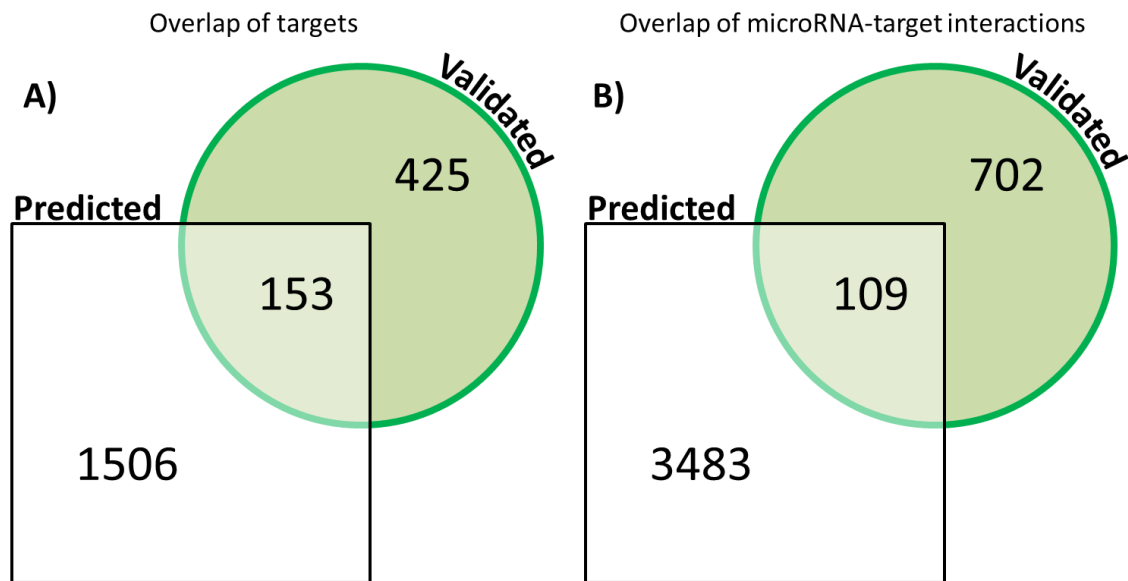
Figure 4.14 – Venn diagrams showing the overlap between the Validated AND Predicted target interactions The interactions between microRNA and the identified Validated AND Predicted targets were analysed for overlap using Venn diagram software. In A) all of the unique targets from the Validated AND Predicted datasets were analysed to show overlap. In B) this analysis was taken further to look at each microRNA to target interaction separately and identify where there was overlap between specific interactions.

The lack of similarity between predicted and validated targets for each microRNA was evident throughout the network and this was analysed in Figure 4.14. Of the 578 validated targets, only 153 (26.5%) were also identified using the predicted target databases. If instead of analysing the presence of a target in both networks we looked at the individual microRNA–mRNA interactions

the overlap is further reduced. There were 811 validated microRNA–target interactions and only 109 (13.4%) were also identified by the predicted databases. ADAM9 [*ADAM Metallopeptidase Domain 9*] is an example of this; it had two validated targets (miR–126–3p and miR–126–5p) and seven predicted interactions (with miR–106a–5p, miR–106b–5p, miR–17–5p, miR–20a–5p, miR–20b–5p, miR–26a–5p and miR–26b–5p). There was no overlap at all between the validated and predicted interactions with this mRNA. Whilst an interaction which is both validated and predicted provided high confidence that it would produce a real effect, the low overlap between the Validated AND Predicted target lists justified the need for the PLUS network alongside the AND network.

By overlapping the networks, mRNA that were targeted by multiple pdEV microRNA in either a predicted or validated interaction could be identified. Table 4.7 showed the targets with the greatest number of microRNA interactions and indicated whether these were predicted, validated or both (highlighted in red). Two targets that showed strong evidence for further investigation at this stage were VEGFA and PTEN, there was validated evidence for more than ten microRNA targeting each and three of these were also predicted for VEGFA and five for PTEN. This approach helped to identify targets with strong evidence for microRNA interactions and prioritised the list of >3000 targets. However there was still not enough information to use these targets within the platelet to monocyte transfer model. To make the data relevant to the effects in monocytes following pdEV microRNA transfer, incorporation of monocyte gene expression data was required. To do this the datasets outlined in 4.3.1.1 (monocyte gene expression changes after 4hour incubation with CRP–XL activated platelets) and 4.3.1.2 (monocyte gene expression changes following incubation with platelet-releasate) were added to the networks.

Table 4.7 – Validated PLUS Predicted targets targeted by multiple microRNA Targets with the most microRNA interactions, including both Validated AND Predicted interactions, are shown ordered by the number of interactions. The microRNA are separated into two sections to denote whether their interaction is validated (left column) or predicted (right). If the interaction was identified as both then it appears in both columns and to show the dominance of the miR–17/92 cluster of microRNA, microRNA species from that cluster are underlined.

Target	# microRNA	microRNA IDs	
		Validated	Predicted
VEGFA	13	*miR–15b–5p, miR–16–5p, miR–195–5p*, miR–106a–5p, miR–106b–5p, miR–126–3p,miR–140–5p, miR–145–5p, miR–150–5p, miR–17–5p, miR–20a–5p, miR–20b–5p,miR–21–5p	*miR–15b–5p, miR–16–5p, miR–195–5p*
PTEN	11	*miR–19a–3p, miR–19b–3p, miR–26a–5p*, miR–106b–5p, miR–17–5p, miR–20a–5p, miR–21–5p, miR–221–3p, miR–222–3p, *miR–26b–5p, miR–92a–3p*	*miR–19a–3p, miR–19b–3p, miR–26a–5p, miR–26b–5p, miR–92a–3p*
CDC37L1	10		miR–106a–5p, miR–106b–5p, miR–15b–5p, miR–16–5p, miR–17–5p, miR–195–5p, miR–20a–5p, miR–20b–5p, miR–30b–5p, miR–30c–5p
RAP2C	10		miR–106a–5p, miR–106b–5p, miR–17–5p, miR–19a–3p, miR–19b–3p, miR–20a–5p, miR–20b–5p, miR–24–3p, miR–26a–5p, miR–26b–5p
USP3	10		miR–106a–5p, miR–106b–5p, miR–146a–5p, miR–146b–5p, miR–15b–5p, miR–16–5p, miR–17–5p, miR–195–5p, miR–20a–5p, miR–20b–5p
ZNF367	10		miR–106a–5p, miR–106b–5p, miR–17–5p, miR–18a–5p, miR–18b–5p, miR–19a–3p, miR–19b–3p, miR–20a–5p, miR–20b–5p, miR–21–5p
ADAM9	9	miR–126–3p, miR–126–5p	miR–106a–5p, miR–106b–5p, miR–17–5p, miR–20a–5p, miR–20b–5p, miR–26a–5p, miR–26b–5p
EIF4G2	9		let–7d–5p, let–7e–5p, let–7g–5p, miR–139–5p, miR–140–5p, miR–146a–5p, miR–146b–5p, miR–26a–5p,miR–26b–5p
HMBOX1	9		miR–106a–5p, miR–106b–5p, miR–17–5p, miR–18a–5p, miR–18b–5p, miR–20a–5p, miR–20b–5p, miR–221–3p, miR–222–3p
PBX3	9		let–7d–5p, let–7e–5p, let–7g–5p, miR–106a–5p, miR–106b–5p, miR–17–5p, miR–20a–5p, miR–20b–5p, miR–320a
REEP3	9		miR–106a–5p, miR–106b–5p, miR–17–5p, miR–19a–3p, miR–19b–3p, miR–20a–5p, miR–20b–5p, miR–30b–5p, miR–30c–5p
ZFPM2	9		miR–106a–5p, miR–106b–5p, miR–17–5p, miR–19a–3p, miR–19b–3p, miR–20a–5p, miR–20b–5p, miR–221–3p, miR–222–3p

4.5.2.5.2 Overlaying monocyte expression data onto Validated PLUS Predicted target network

With the addition of baseline monocyte gene expression data from 4.3.1.1, the network shown in Figure 4.15 reduced in size whilst providing greater information. The reduction was caused by the removal of targets not expressed in baseline monocytes (4.3.1.1) which resulted in the removal of 934 (44.89%) targets from the network. The attributes linked to node size and colour were changed for Figure 4.15; node size showed the level of gene expression in baseline monocytes and node colour provided the Log fold change (LogFC) in expression following 4hour incubation with CRP–XL activated platelets, as described in 4.3.1.1.

Overall the network appeared similar to previous iterations; the microRNA with predominantly unique targets localised at the edge of the network and those working together clustered towards the centre. The miR–17/92 cluster was at the heart of the network, which demonstrated that it remained relevant when the data was focused on the platelet–monocyte interaction. The removal of 934 targets due to their lack of expression in monocytes had a significant effect on many of the previously highlighted targets (Table 4.5, Table 4.6 and Table 4.7). The list of removed targets included; VEGFA, ZNF367 [*Zinc Finger Protein 367*], REEP3, ZFPM2, E2F5 [*E2F Transcription Factor 5*], ESR1 [*Estrogen Receptor 1*], KIF5A [*Kinesin Family Member 5A*], PLSCR4 [*Phospholipid Scramblase 4*], PTH [*Parathyroid Hormone*], PTHLH [*Parathyroid Hormone–Like Hormone*] and E2F1 [*E2F Transcription Factor 1*], all of which had six or more validated and/or predicted microRNA interactions. Based on the previous network (Figure 4.13), VEGFA was a leading target with 13 validated microRNA interactions, three of which were also predicted by all databases. Table 4.8 detailed the top 48 targets ordered based upon their level of expression in monocytes and the summed expression of all interacting microRNA (predicted or validated). Therefore targets with high gene expression and multiple highly expressed interacting microRNA were prioritised. To guide the decision on which targets to investigate further Table 4.8 included all target attributes from Figure 4.15 and a column for 'LogFC after incubation with releasate'. This column used information from the second platelet–monocyte interaction dataset, as described in 4.3.1.2, where monocyte gene expression was measured before and after incubation with platelet-releasate. The sample used to treat monocytes in this second dataset again contained the pdEV microRNA but removed the complication of direct platelet interaction, seen with the first dataset (4.3.1.1) meaning that the responses were perhaps more relevant to the microRNA stimulus.

Ordering the targets in Table 4.8 by their microRNA and target gene expression highlighted the targets of abundant microRNA, such as miR–223–3p. Four targets of miR–223–3p were EPB41L3

[*Erythrocyte Membrane Protein Band 4.1–Like 3*], HSP90B1 [*Heat Shock Protein 90kDa Beta Member 1*], DCAF12 [*DDB1 and CUL4 Associated Factor 12*] and CBFB [*Core–Binding Factor, Beta Subunit*] and these were the top 4 targets in Table 4.8. The gene expression changes of these four targets following monocyte incubation with activated platelets indicated either an increase or no change. However their response to platelet-releasate showed EPB41L3 and HSP90B1 with increased expression, a small decrease with CBFB and a decrease with DCAF12. This would suggest that CBFB and particularly DCAF12 were strong targets for future analysis. However, it is important to consider that there is no information on whether these targets are expressed as proteins or whether the effect of microRNA would be significant as their inclusion is solely reliant on information from the literature.
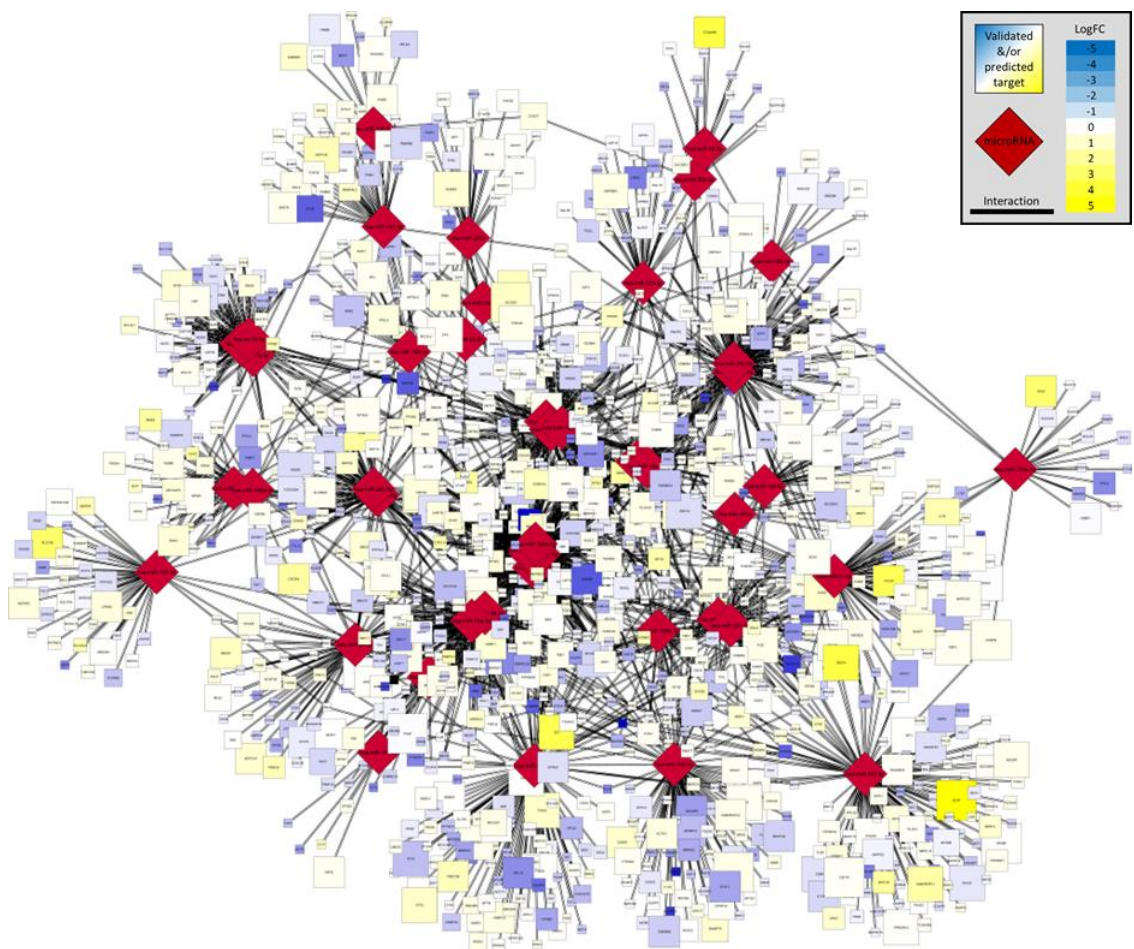
Figure 4.15 – Validated PLUS Predicted microRNA–target interaction network with monocyte gene expression overlay *The Validated PLUS Predicted network was filtered to show only targets which were found to be expressed in monocytes at rest. MicroRNA appear as red diamond source nodes and targets as squares. The target node squares are scaled based on their level of expression in monocytes and coloured to demonstrate the LogFC following interaction with platelets. The microRNA nodes are linked by edges to their targets with no differentiation between validated and predicted targets. The network was laid out according to a force-directed layout. High resolution image available at http://tinyurl.com/ashleyambrose.*

Table 4.8 – MicroRNA–targets expressed in monocytes showing expression levels and expression change following monocyte interaction with platelets/platelet-releasate *Targets from the Validated PLUS Predicted network are displayed alongside information on the number of interacting microRNA, the total expression of these microRNA, the target genes expression in monocytes and the target genes LogFC following incubation with platelets or platelet-releasate. Targets were prioritised for this table based on their expression in monocytes and the sum of their interacting microRNAs expression. (FC colour code (yellow = upregulated/white = no change/blue = downregulated)).*

Target	#microRNA	Sum of microRNA expression	Monocyte Expression (AU)	LogFC after incubation with activated platelets	LogFC after incubation with platelet releasate
EPB41L3	1	509.64	5530.82	0.31	0.70
HSP90B1	1	509.64	5328.42	0.79	0.77
CBFB	2	511.69	4269.31	0.55	-0.14
DCAF12	3	516.89	1622.48	-0.08	-0.61
NLRP3	1	509.64	1457.19	-0.06	0.96
MTPN	1	509.64	1433.12	-0.08	0.47
FEZ2	1	509.64	1421.75	-0.54	-0.19
SIRPA	3	43.90	14477.17	0.34	-0.39
RHOB	4	552.52	1103.61	0.16	-0.39
PRDM1	4	528.47	1092.10	1.78	-0.40
LMO2	1	509.64	1095.39	-1.53	-0.63
USP3	10	96.38	5231.58	0.20	-0.20
HSPA8	5	47.67	10248.73	1.01	-0.14
CHUK	3	515.96	872.43	0.15	0.10
IL8	2	37.46	11733.77	5.13	0.79
SLC39A1	1	509.64	839.95	0.52	-0.42
MEF2C	2	516.20	769.63	-0.57	-0.96
PARP1	1	509.64	778.94	-0.84	-0.69
FBXW7	5	531.04	720.22	0.08	0.21
EIF4G2	9	52.97	6294.17	0.38	0.11
TMBIM6	2	36.32	8889.27	0.06	-0.12
SCARB1	1	509.64	607.11	-1.03	-1.05
NFKB1	2	39.23	6700.56	0.32	0.17
FOXO1	2	510.69	478.68	-0.29	-0.76
C6orf136	1	509.64	469.38	-0.60	-0.85
FAM129A	5	47.67	4984.75	0.54	-0.46
FBXO8	3	545.96	394.63	-0.21	-0.37
PTBP2	1	509.64	391.51	0.51	0.37
KPNA3	1	509.64	391.11	-0.05	0.02
SNX10	3	29.84	6632.23	-0.39	-1.33
IRAK1	2	39.23	4880.55	1.13	0.31
NAGK	5	47.67	3887.36	-1.40	-1.23
SGK1	5	45.79	4014.15	-0.62	-0.80
AHNAK	5	47.67	3784.69	-1.95	-0.75
WDR1	2	36.32	4863.99	0.66	0.16
USP16	1	509.64	341.95	0.05	0.28
PTEN	11	90.11	1912.40	-0.11	-0.07
IRF9	5	47.67	3522.76	0.08	0.35
PPP6C	5	47.67	3279.73	0.07	-0.03
ITM2B	1	11.93	13063.23	0.14	-0.32
TGFBR2	8	90.55	1646.64	0.50	-0.74
NOTCH1	1	29.92	4955.46	1.34	-0.75
TGFBI	1	6.56	21928.71	0.78	-0.01
NUP210	1	509.64	278.49	-0.76	-0.99
YWHAH	4	14.30	9740.17	0.58	-1.06
CXCR4	2	38.15	3558.01	2.72	-0.07
UBE2D3	3	24.48	5430.15	0.21	-0.10
NUMB	2	39.23	3310.31	0.58	0.16

Despite the filtering, prioritising and increase in target attributes, the pool of targets was still large making it difficult to identify ideal candidates for further analysis, especially as the list of targets which were Validated AND Predicted, analysed in 4.5.2.5.4 were yet to be added to the targets in Table 4.8. Therefore further steps to narrow the pool of targets were required and the identification of biological roles was one way to do this. A pathway analysis was carried out to see if microRNA were working in concert on specific pathways, which would strengthen the case for targets within that pathway.

4.5.2.5.3   Pathway analysis of Validated PLUS Predicted targets found in monocytes

The list of mRNA targets from the network in Figure 4.15 were analysed using pathway identification software as described in section 4.4.3. The output identified 413 pathways containing ten or more of the networks targets and with a p–value ≤0.05, Table 4.9 contains the top 33 pathways. These were mainly signalling pathways including those for MAPK, TGF–β, TNF and EGF, many of which appear multiple times. The duplication is due to the use of multiple pathway databases containing similar pathways defined in slightly different ways and containing variations. For example pathways associated with EGF appear three times from the SignalLink, NetPath and WikiPathways databases. By removing exact pathway duplicates but leaving similar pathways there is no bias towards a single database and it highlighted pathways that were significantly altered in a variety of iterations.

The analysis identified the MAPK signalling pathway as the most significantly altered by pdEV microRNA. In the WikiPathways entry, 54 (32.3%) of the 178 genes in the pathway were positive for microRNA–target interactions yielding a p–value of 1.62×10^{-22} and a q–value of 4.63×10^{-20}. These values provide information on the probability of the pathway being affected by chance by the targets from the network and are calculated using hyper-geometric distribution (p–value) and then adjusted for multiple comparisons using FDR (q–value). The MAPK signalling pathway, appeared in Table 4.9 twice more (from the KEGG and BioCarta databases) both of which show significant effects; $p=1.32 \times 10^{-13}$ and $p=1.25 \times 10^{-12}$ respectively. The TGF–β and TNF–α pathways displayed similar changes to the MAPK signalling pathway with 55 (31.8%) and 57 (24.4%) of their genes being affected in the most significantly altered versions of the pathways. In addition to signalling pathways there were three further groups of pathway in Table 4.9; direct miR–targeted gene pathways, apoptosis and cell cycle pathways and a large group of inflammatory/immune related pathways. The two miR–targeted gene pathways from the Wikipathways database were likely to have been generated following a similar process to that in this chapter. Whilst they were targeting lymphocytes and muscle cells and not monocytes it suggests the pdEV microRNA have been shown to have effects in other cell types. It should be

171

noted that there were no entries for miR–targeted genes in monocytes in the Wikipathways database. There were six pathways associated with apoptosis and the cell cycle, suggesting this could be an important area for further investigation particularly as the output for these can be measured. The inflammatory/immune related pathways listed in Table 4.9 were extensive, with 18 of the 33 pathways containing clear links to the inflammatory process. This suggested that inflammatory outcomes, including single key genes, such as NLRP3 and IL8 could play a key role in future experimental work. Therefore when selecting individual targets, those involved in inflammation were of high interest.

Table 4.9 – Pathways involving multiple pdEV microRNA targets filtered for genes expressed in monocytes All of the targets from the Validated PLUS Predicted network were subjected to a pathway analysis using the CPDB. The pathways were filtered so that each pathway contained ≥10 targets and had a p–value ≤0.05. Exact duplicates were removed from the resulting list of pathways and then the 32 pathways which were most significantly affected (as determined by p–value) were displayed below alongside information detailing the number of genes in that pathway, the number of validated targets within that pathway genes, the significance of the effect (p–value), the significance after correction for FDR and the database the pathway was sourced from.

Pathway name	#Genes in pathway	#Validated targets	p–value	q–value (FDR)	Pathway source
MAPK Signalling Pathway	168	54 (32.3%)	1.62×10^{-22}	4.63×10^{-20}	Wikipathways
TGF_beta_Receptor	174	55 (31.8%)	1.63×10^{-22}	4.63×10^{-20}	NetPath
Hepatitis B – Homo sapiens (human)	146	47 (32.2%)	1.18×10^{-19}	2.24×10^{-17}	KEGG
TGF beta Signalling Pathway	132	44 (33.3%)	3.86×10^{-19}	5.48×10^{-17}	Wikipathways
Regulation of nuclear SMAD2/3 signalling	78	33 (42.9%)	1.62×10^{-18}	1.83×10^{-16}	PID
EGF–Core	105	37 (35.6%)	2.32×10^{-17}	2.19×10^{-15}	Signalink
TNFalpha	234	57 (24.4%)	3.46×10^{-17}	2.81×10^{-15}	NetPath
Pathways in cancer – Homo sapiens (human)	398	75 (18.8%)	1.56×10^{-15}	1.11×10^{-13}	KEGG
FoxO signalling pathway – Homo sapiens (human)	134	39 (29.3%)	5.50×10^{-15}	3.47×10^{-13}	KEGG
miR–targeted genes in lymphocytes – TarBase	480	83 (17.3%)	7.83×10^{-15}	4.23×10^{-13}	Wikipathways
TNF signalling pathway – Homo sapiens (human)	110	35 (31.8%)	8.87×10^{-15}	4.23×10^{-13}	KEGG
AGE–RAGE pathway	66	27 (40.9%)	8.94×10^{-15}	4.23×10^{-13}	Wikipathways
EGF–EGFR Signalling Pathway	162	43 (26.5%)	1.13×10^{-14}	4.92×10^{-13}	Wikipathways
Structural Pathway of Interleukin 1 (IL–1)	44	22 (50.0%)	1.63×10^{-14}	6.59×10^{-13}	Wikipathways
IL1	55	24 (43.6%)	4.90×10^{-14}	1.74×10^{-12}	NetPath
EGFR1	453	78 (17.3%)	6.08×10^{-14}	2.03×10^{-12}	NetPath
MAPK signalling pathway – Homo sapiens (human)	257	54 (21.2%)	1.32×10^{-13}	4.17×10^{-12}	KEGG
Chronic myeloid leukaemia – Homo sapiens (human)	73	27 (37.0%)	1.69×10^{-13}	5.05×10^{-12}	KEGG
Measles – Homo sapiens (human)	134	37 (27.6%)	2.21×10^{-13}	6.26×10^{-12}	KEGG
Activated TLR4 signalling	110	33 (30.0%)	3.43×10^{-13}	9.26×10^{-12}	Reactome
Chagas disease (American trypanosomiasis) – Homo sapiens (human)	104	32 (30.8%)	3.60×10^{-13}	9.29×10^{-12}	KEGG
miR–targeted genes in muscle cell – TarBase	394	69 (17.5%)	9.23×10^{-13}	2.28×10^{-11}	Wikipathways
EPO signalling	185	43 (23.5%)	1.10×10^{-12}	2.61×10^{-11}	INOH
Apoptosis	84	28 (33.3%)	1.20×10^{-12}	2.62×10^{-11}	Wikipathways
Direct p53 effectors	141	37 (26.2%)	1.22×10^{-12}	2.62×10^{-11}	PID
mapkinase signalling pathway	57	23 (40.4%)	1.25×10^{-12}	2.62×10^{-11}	BioCarta
Integrated Pancreatic Cancer Pathway	170	41 (24.1%)	1.51×10^{-12}	3.05×10^{-11}	Wikipathways
Epstein–Barr virus infection – Homo sapiens (human)	201	45 (22.5%)	1.66×10^{-12}	3.25×10^{-11}	KEGG
IL6	74	26 (35.1%)	1.92×10^{-12}	3.62×10^{-11}	NetPath
DNA Damage Response (only ATM dependent)	110	32 (29.1%)	2.00×10^{-12}	3.65×10^{-11}	Wikipathways
Regulation of retinoblastoma protein	64	24 (37.5%)	2.68×10^{-12}	4.75×10^{-11}	PID
Toll Like Receptor 4 (TLR4) Cascade	119	33 (27.7%)	3.91×10^{-12}	6.72×10^{-11}	Reactome

4.5.2.5.4   Validated AND Predicted microRNA–target interactions network

Focussing on a network containing only Validated AND Predicted microRNA–target interactions significantly reduced the network size; only 31 of the 45 microRNA were present and these had 109 interactions with 86 different targets. Of the 31 microRNA, ten only had one target and twelve only had targets unique to themselves. Clustering in this network was non–existent but there were instead some sub–networks. Three of the miR–17/92 cluster were linked but only shared a couple of targets and three of the miR–15 family were also linked. Only fifteen targets interacted with multiple microRNA, of which only four had three interactions; RBL2 [*Retinoblastoma–Like 2*], VEGFA, PTEN and CCNE1 [*Cyclin E1*]. These significantly reduced numbers were a reflection of the smaller network and as these interactions were both validated and predicted they were the strongest candidates for further analysis. The next step was to overlay the monocyte gene expression data.
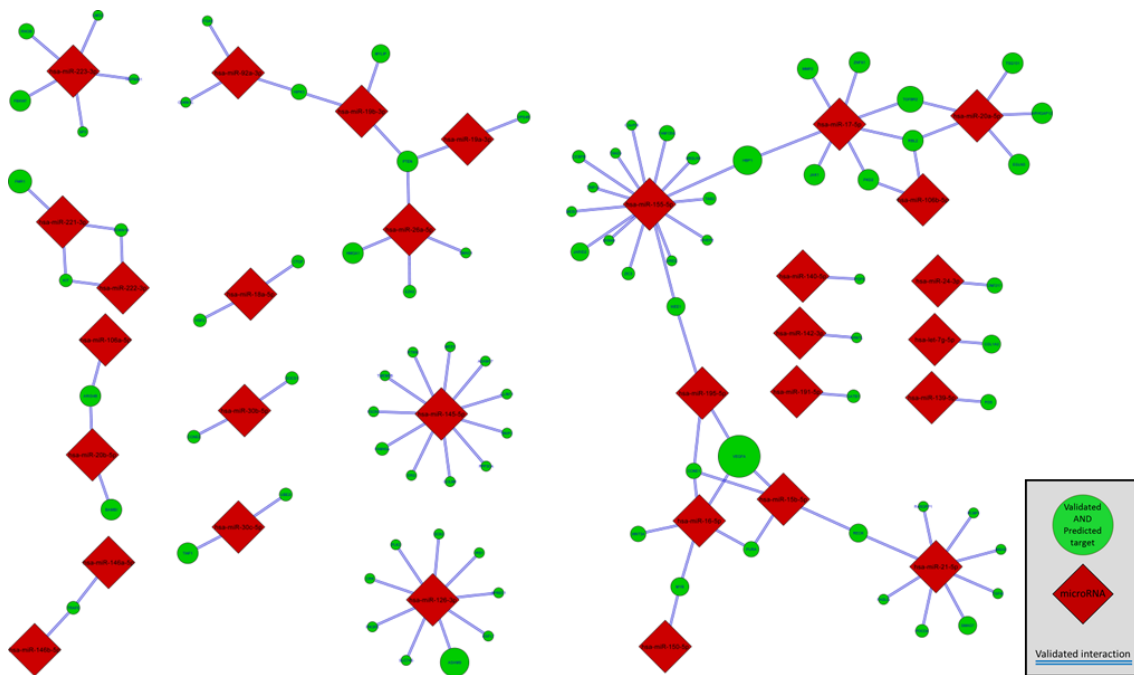
Figure 4.16 – A microRNA–target interaction network of the Validated AND Predicted microRNA targets *Validated microRNA–target interactions from miRTarBase that were also predicted in the microRNA.org, TargetScan and miRDB databases for the 45 microRNA consistently found in pdEV were mapped into an interaction network using Cytoscape 2.8.3. MicroRNA were mapped to red diamond source nodes and targets to green circle target nodes, node size indicates the number of microRNA with either predicted or validated interactions to the target but only interactions which are both Validated AND Predicted are shown with links. MicroRNA are linked to targets by edges (double blue lines) to indicate interactions which were both validated AND predicted and the network was laid out according to a force-directed layout. High resolution image available at http://tinyurl.com/ashleyambrose.*

4.5.2.5.5   Overlaying monocyte expression data onto Validated AND Predicted target network

The result of incorporating the monocyte gene expression data into the Validated AND Predicted network can be seen in Figure 4.17. This was the most selective network produced and included information to demonstrate the level of each genes expression (node size) and the LogFC following 4hour incubation with stimulated platelets (node colour).
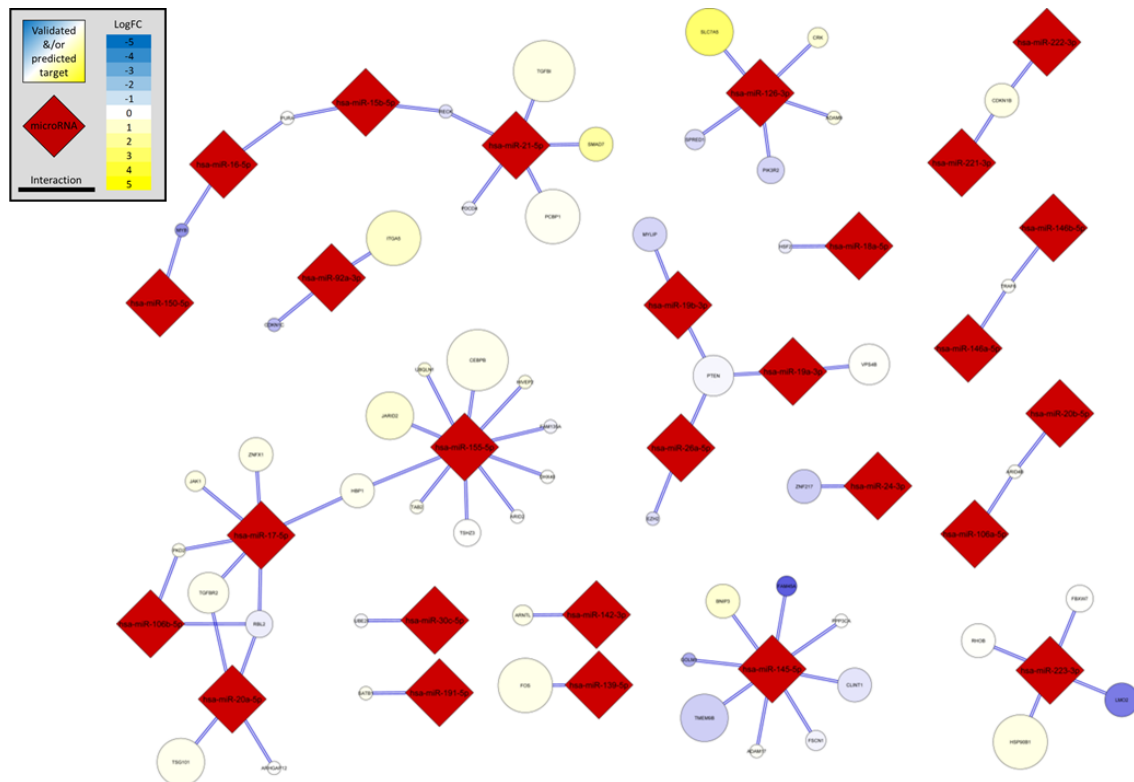
Figure 4.17 – A network showing Validated AND Predicted microRNA–target interactions overlaid with monocyte gene expression data The Validated AND Predicted microRNA–target network was filtered for targets with monocyte gene expression. MicroRNA were mapped to red diamond source nodes and targets to coloured circle nodes. The size of the node was determined by the level of that genes expression in resting monocytes and the colour indicated the change in gene expression following interaction with platelets. The network was laid out according to a force-directed layout resulting in the clustering of microRNA with similar targets. High resolution image available at http://tinyurl.com/ashleyambrose.

The network consisted of 27 microRNA targeting 54 unique mRNA through 69 interactions. To create this network, 32 (37.21%) of the targets in the Validated AND Predicted network (Figure 4.16) were removed due to absence of expression in monocytes. The new network contained nine targets with two interacting microRNA and only two that interacted with three microRNA; PTEN and RBL2. Both PTEN and RBL2 mRNA showed down regulation after incubation with stimulated platelets or platelet-releasate and of all 56 targets; 20 in monocytes stimulated by intact platelets and 31 induced by incubation with platelet-releasate showed a decrease, albeit with only three and four of these decreasing by >50%. These subtle changes in expression are

consistent with the known function of microRNA in fine tuning expression rather than causing complete inhibition.

Both PTEN and RBL2 stood out from the above network because they had the most interacting microRNA, but it was important not to overlook the targets of miR–223–3p due to the abundance of this microRNA. In the Validated AND Predicted network overlaid with monocyte expression, miR–223–3p had four unique targets; HSP90B1, LMO2 [*LIM Domain Only 2*], FBXW7 [*F–Box and WD Repeat Domain Containing 7*] and RHOB [*Ras Homolog Family Member B*]. LMO2 mRNA was downregulated after incubation with platelets and with platelet-releasate while RHOB was down regulated only after incubation with releasate. Table 4.10 lists all of the targets from the Validated AND Predicted network (Figure 4.17) and is weighted to highlight targets with high gene expression in monocytes and high abundance of interacting microRNA, an analysis that results in all of the miR–223–3p targets moving to the top of the list.

All of the targets in Table 4.10 were both Validated AND Predicted and expressed in monocytes so had strong cases for further study. Additional information on the FC of gene expression following stimulation of monocytes with platelets was then used to narrow the list down to a manageable number of potential targets. Additional information was added through a pathway analysis of the targets (4.5.2.5.6) to identify important target themes and then the remaining targets were filtered to form a final list (4.5.2.6).

Table 4.10 – Validated AND Predicted targets of pdEV microRNA expressed in monocytes Targets from the Validated AND Predicted network which had been filtered for genes expressed in monocytes at rest are shown. They are alongside data detailing the number of microRNA targeting the gene, the sum of the expression of those microRNA, the genes expression in monocytes and the genes LogFC following 4hour incubation with activated platelets or the releasate from platelets. Genes are ordered to prioritise targets of highly expressed microRNA with high gene expression in monocytes. (FC colour coding (yellow = upregulated/white = no change/blue = downregulated)).

Target	#microRNA	Sum of microRNA expression	Monocyte Expression (AU)	LogFC after incubation with activated platelets	LogFC after incubation with platelet releasate
HSP90B1	1	509.64	5328.42	0.79	0.77
RHOB	1	509.64	1103.61	0.16	-0.39
LMO2	1	509.64	1095.39	-1.53	-0.63
FBXW7	1	509.64	720.22	0.08	0.21
TGFBI	1	6.56	21928.71	0.78	-0.01
PCBP1	1	6.56	12493.80	0.34	-0.12
PTEN	3	38.34	1912.40	-0.11	-0.07
ITGA5	1	11.93	5988.68	1.57	0.45
SLC7A5	1	20.11	2533.73	4.28	1.44
MYLIP	1	35.61	1370.60	-0.48	-1.01
TGFBR2	2	24.40	1646.64	0.50	-0.74
ZNF217	1	29.92	1151.02	-0.58	-0.03
CEBPB	1	1.42	23792.48	0.55	-0.01
ZNFX1	1	17.08	1157.65	0.67	0.41
RBL2	3	25.59	754.17	-0.21	-0.74
PIK3R2	1	20.11	882.39	-0.50	-0.76
TSG101	1	7.32	2014.48	0.54	0.05
CRK	1	20.11	505.49	1.15	0.29
CDKN1B	2	7.25	1317.03	0.77	0.06
SPRED1	1	20.11	462.05	-0.44	-0.78
JAK1	1	17.08	511.49	0.81	0.29
SMAD7	1	6.56	1225.37	2.73	-0.09
TRAF6	2	39.23	185.89	0.24	0.13
JARID2	1	1.42	4125.71	1.20	0.81
TMEM9B	1	2.05	2344.97	-0.57	-0.65
PKD2	2	18.28	226.74	0.59	0.80
ARNTL	1	6.06	620.23	0.70	-0.53
FOS	1	0.56	6281.52	0.67	-1.08
ARID4B	2	22.08	152.31	0.32	0.14
BNIP3	1	2.05	1356.41	1.33	1.17
CDKN1C	1	11.93	229.28	-0.81	-0.29
SATB1	1	18.52	137.86	0.54	0.14
CLINT1	1	2.05	1166.69	-0.32	-0.12
PURA	2	9.19	223.70	0.09	-0.15
MYB	2	8.14	203.52	-1.25	-1.11
PDCD4	1	6.56	215.58	-0.17	-0.32
VPS4B	1	0.71	1730.51	0.15	-0.29
FSCN1	1	2.05	592.87	-0.13	-1.12
ARHGAP12	1	7.32	159.76	0.05	-0.44
FAM45A	1	2.05	564.83	-1.89	-0.54
TSHZ3	1	1.42	717.22	0.06	-0.66
RECK	2	9.72	86.33	-0.37	-0.33
PPP3CA	1	2.05	263.57	0.03	-0.32
HSF2	1	1.65	297.25	-0.23	-0.03
UBQLN1	1	1.42	255.23	0.99	0.11
TAB2	1	1.42	217.08	0.52	0.32
HIVEP2	1	1.42	204.22	0.79	0.35
ARID2	1	1.42	195.73	0.03	-0.33
UBE2I	1	3.25	80.55	-0.09	-0.22
ADAM17	1	2.05	123.08	0.30	0.51
DHX40	1	1.42	154.67	0.17	0.47
GOLM1	1	2.05	94.91	-0.96	-0.17
EZH2	1	2.03	92.18	-0.37	0.21
FAM135A	1	1.42	111.72	-0.16	-0.16

4.5.2.5.6 Pathway analysis of Validated PLUS Predicted targets found in monocytes

The pathway analysis of the Validated AND Predicted targets was carried out as previously described and the results are shown in Table 4.11. As there were only 56 targets and the threshold for the number of targets genes in a pathway was >10 (as detailed in 4.4.3) the list of identified pathways was small. The four pathways that were identified retained two of the previous themes from Table 4.9; two pathways fell into the miR–targeted genes group and two into the inflammation/immune system grouping. In this instance the effect of the microRNA were deemed more significant on the miR–targeted pathways although the overall percentage of genes involved was low; 2.9% and 3.4%. This pattern was the same for the inflammatory/immune pathways and was likely caused by the large overall size of these pathways along with the small target pool. The overlap with the previous pathway analysis suggested immune and inflammatory related genes were good targets, whilst the inclusion of the miR targeted pathways did not provide much information as the analysis was based on microRNA targeted genes.

Table 4.11 – Pathways affected by targets in the Validated AND Predicted network that are expressed in monocytes
Targets from the Validated AND Predicted network which had expression in monocytes at rest were analysed using the CPDB pathway analysis tool. The pathways which involved 10 or more of the targets and had a p–value ≤0.05 are displayed in the table below with information on the number of genes in the pathway, the number of those genes that are Validated AND Predicted targets, the significance of the association with the pathway (p–value), the significance following correction for false discovery (q–value) and finally the database where that pathway originated.

Pathway name	#Genes in pathway	#Validated targets	p–value	q–value (FDR)	Pathway source
miR–targeted genes in lymphocytes – TarBase	480	14 (2.9%)	5.46x10–9	2.73x10–8	Wikipathway
MicroRNAs in cancer – Homo sapiens (human)	297	10 (3.4%)	3.22x10–7	8.05x10–7	KEGG
Innate Immune System	709	11 (1.6%)	0.000123	0.000205	Reactome
Immune System	1174	13 (1.1%)	0.000757	0.000947	Reactome

4.5.2.6 Key targets of pdEV microRNA

This chapter started with 45 microRNA and aimed to identify their potential targets following their transfer via pdEV from platelets to monocytes. The processes described in this chapter led to the identification of 4403 potential targets, which following target filtering, generated two networks made up of 2084 and 86 potential targets. These targets were identified as having either predicted or validated interactions with the 45 microRNA and were also expressed in monocytes. The flowchart in Figure 4.18 shows the steps taken to narrow these down to a final list from which targets for future work were selected.

The workflow shown in Figure 4.18 demonstrated how the targets from the PLUS and AND networks shown in Figure 4.13 and Figure 4.16 were combined with monocyte gene expression data to give the 34 targets in Table 4.12. The nine steps were; i) Generation of networks from the predicted and the validated microRNA targets ii) Filtering of networks to remove genes not expressed in monocytes (Figure 4.15 and Figure 4.17) iii) Prioritising of Targets in Figure 4.15 to select targets with the high gene expression and abundant interacting microRNA; iv) Lists from the PLUS and AND network were merged and duplicates identified, highlighted (bold in Table 4.12) and then removed; v) Genes then had their protein function characterised and any with uncharacterised protein functions were removed; vi) For the observable change in the target to be viable it required the level of microRNA acting on the target to be significant. Therefore any targets where the sum of microRNA expression (AU) was below a value of '2' were removed. vii) The same process was applied to the level of target gene expression (AU) in monocytes; here a cut–off of '500' was applied. iix) A ratio of the sum of microRNA expression (AU) to the target gene expression (AU) was calculated, any target where the ratio was less than 0.01 (1%) was removed, thereby removing any targets where the microRNA was likely to be insufficient to elicit an effect. ix) A final list of 34 targets, shown in Table 4.12, was generated. This list was small enough to work through manually to identify definitive candidates for future investigation.

In Table 4.12 the remaining targets were ordered based upon their LogFC following incubation with platelet-releasate (the closest stimulus to pdEV microRNA available). They were displayed with gene names and the protein functions alongside the information on microRNA number, microRNA expression, mRNA expression in monocytes and the ratio of expression. Any targets from both the PLUS network and the AND network appear in bold as there was clearly strong evidence for these targets. In this list 16 (47%) were targeted by miR–223–3p and nine by five or more of the miR–17/92 cluster reflecting the continually emphasised importance of these microRNA, in addition over half had predicted or validated interactions with multiple microRNA.

179

When we looked at the gene expression of these targets following monocyte incubation with platelet-releasate 24 were downregulated which would correlate with the decrease in gene expression that microRNA frequently, but not always, cause (Baek et al., 2008).
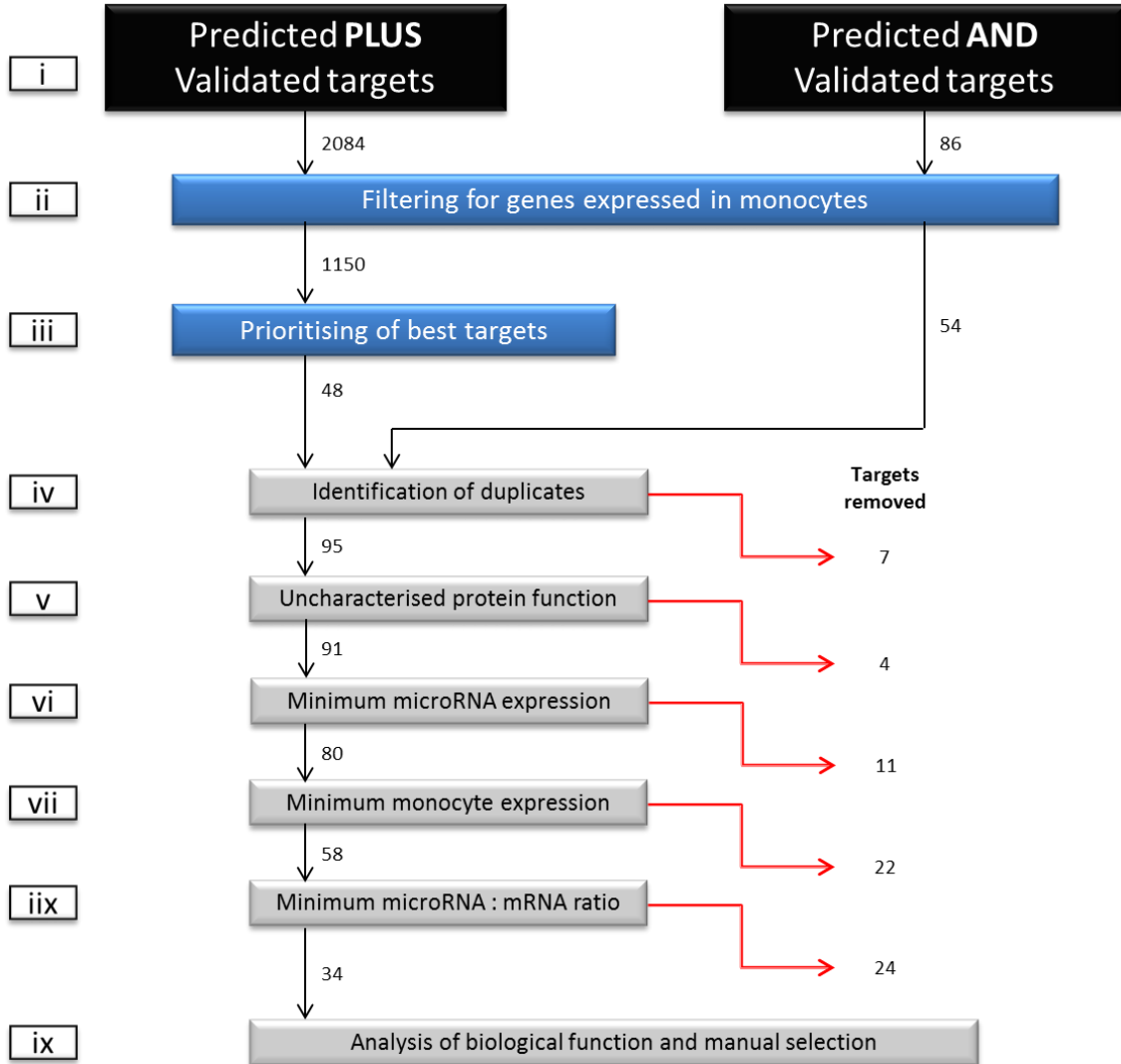
Figure 4.18 – Flowchart showing the selection of a final list of targets for future experiments *Following the identification of targets that are strong candidate from the Validated PLUS Predicted network and all of the targets from the Validated AND Predicted network they were filtered and sorted to provide a final list of targets. Initially the Validated PLUS Predicted targets were prioritised using the sum of microRNA and monocyte gene expression. These targets were then amalgamated with those which were Validated AND Predicted; overlap between the two groups was identified and the duplicate removed. Protein functions were identified and any uncharacterised proteins were removed, the minimum sum of interacting microRNA expression was then set at two and the minimum monocyte expression was set at 500. Once targets that did not meet these thresholds were removed a final filtration step, utilising the microRNA:mRNA expression ratio was set. Any target with a ratio <0.01 was also removed.*

Table 4.12 – The final 34 targets identified in the analysis Following the extensive filtration and analysis of the microRNA targets the final list in this table was produced. These targets are listed alongside the essential information required for informing a decision on which targets to pursue. The targets are listed alongside their full names, the number of interacting microRNA (predicted and/or validated), the sum of microRNA and the monocyte gene expression, the ratio of these expressions and the LogFC following incubation with platelet or platelet-releasate. (Fold change is colour coded (yellow = upregulated/white = no change/blue = downregulated)).

Target	Name	Protein Function	#miRs	Sum of microRNA expression (AU)	Monocyte Expression (AU)	miR:monocyte expression ratio	Target LogFC after incubation with activated platelets	LogFC after incubation with platelet release
NAGK	N-Acetylglucosamine Kinase	Involved in the Neu5Gc degradation pathway	5	47.67	3887.36	0.012	-1.40	-1.23
SCARB1	Scavenger Receptor Class B Member 1	Facilitates the uptake of cholesteryl esters from HDL	1	509.64	607.11	0.839	-1.03	-1.05
MYLIP	Myosin regulatory light chain interacting protein	Ubiquinates LDL receptors in endosomes and sends them for degradation	1	35.61	1370.6	0.026	-0.48	-1.01
MEF2C	Myocyte-specific enhancer factor 2C	Cardiac morphogenesis & myogenesis and vascular development	2	516.20	769.63	0.671	-0.57	-0.96
SGK1	Serum Glucocorticoid Regulated Kinase 1	Regulation of transport, hormone release, neuroexcitability, inflammation, cell proliferation and apoptosis	5	45.79	4014.15	0.011	-0.62	-0.80
PIK3R2	Phosphoinositide-3-Kinase Regulatory Subunit 2	Phosphorylates PtdIns(4,5)P2 to generate PIP3 (involved in cell growth etc.)	1	20.11	882.39	0.023	-0.5	-0.76
AHNAK	AHNAK Nucleoprotein	Neuronal cell differentiation	5	47.67	3784.69	0.013	-1.95	-0.75
RBL2	Retinoblastoma-Like 2	Key regulator of entry into cell division	3	25.59	754.17	0.034	-0.21	-0.74
TGFBR2	Transforming growth factor, β receptor II	Binds TGF-β in a heterodimeric complex -> transcription of cell proliferation genes	8	90.55	1646.64	0.055	0.50	-0.74
PARP1	Poly [ADP-ribose] polymerase 1	Differentiation % proliferation/(Ab)Normal recovery from DNA damage	1	509.64	778.94	0.654	-0.84	-0.69
LMO2	LIM domain only 2	Central role in hematopoietic development	1	509.64	1095.39	0.465	-1.53	-0.63
DCAF12	DDB1 And CUL4 Associated Factor 12	Interacts with the COP9 signalosome	3	516.89	1622.48	0.319	-0.08	-0.61
ARNTL	Aryl Hydrocarbon Receptor Nuclear Translocator-Like	Transcriptional activator/Component of the circadian clock	1	6.06	620.23	0.010	0.7	-0.53
FAM129A	Family With Sequence Similarity 129, Member A	Regulates phosphorylation of proteins involved in translation regulation	5	47.67	4984.75	0.010	0.54	-0.46
SLC39A1	Zinc transporter ZIP1	Responsible for the active transport of zinc into prostate cells.	1	509.64	839.95	0.607	0.52	-0.42
PRDM1	PR domain zinc finger protein 1	Repressor of β-IFN gene expression	4	528.47	1092.10	0.484	1.78	-0.40
RHOB	Ras homolog gene family, member B	Mediates apoptosis after DNA damage/Affects cell adhesion and GF signaling/Negative role in tumorigenesis/Intracellular protein trafficking	4	552.52	1103.61	0.501	0.16	-0.39
USP3	Ubiquitin Specific Peptidase 3	Deubiquitinates proteins/Progression through S phase and mitotic entry/DNA damage response.	10	96.38	5231.58	0.018	0.20	-0.20
FEZ2	Fasciculation and elongation protein zeta-2	Normal axonal bundling and elongation within axon bundles.	1	509.64	1421.75	0.358	-0.54	-0.19
CBFB	Core-binding factor subunit β	β subunit of TF which regulates hematopoiesis and osteogenesis genes	2	511.69	4269.31	0.120	0.55	-0.14
PTEN	Phosphatase and tensin homolog	Negatively regulates internal levels of PIP3/Negatively regulatingAkt/PKB signaling	11	90.11	1912.40	0.047	-0.11	-0.07
CXCR4	C-X-C chemokine receptor type 4	α-chemokine receptor specific for CXCL12	2	38.15	3558.01	0.011	2.72	-0.07
PPP6C	Protein Phosphatase 6, Catalytic Subunit	Subunit of PP6 which regulates cell cycle progression in response to IL2.	5	47.67	3279.73	0.015	0.07	-0.03
ZNF217	Zinc finger protein 217	Attenuation of apoptotic signals resulting from telomere dysfunction	1	29.92	1151.02	0.026	-0.58	-0.03
CHUK	Conserved Helix-Loop-Helix Ubiquitous Kinase	Part of the IκB kinase complex that regulates the NF-κB TF	3	515.96	872.43	0.591	0.15	0.10
NUMB	Protein numb homolog	Determination of cell fates during development	2	39.23	3310.31	0.012	0.58	0.16
FBXW7	F-box/WD repeat-containing protein 7	Mediates ubiquitination & degradation of target proteins	5	531.04	720.22	0.737	0.08	0.21
CRK	V-Crk Avian Sarcoma Virus CT10 Oncogene Homolog	MAPK8 activation, membrane ruffling and cell motility	1	20.11	505.49	0.040	1.15	0.29
JAK1	Janus kinase 1	Transduces signals by IFN-α/β and γ interferons and IL-10 family.	1	17.08	511.49	0.033	0.81	0.29
IRF9	Interferon Regulatory Factor 9	TF that mediates signaling by type I IFNs	5	47.67	3522.76	0.014	0.08	0.35
MTPN	Myotrophin	Regulates NF-kappa-B TF activity/Promotes growth of cardiomyocytes	1	509.64	1433.12	0.356	-0.08	0.47
EPB41L3	Erythrocyte membrane protein band 4.1-like 3	Interact with YWHAB, YWHAH, YWHAG and Cell adhesion molecule 1.	1	509.64	5530.82	0.092	0.31	0.70
HSP90B1	Heat shock protein 90kDa β1 / Endoplasmin	Folding proteins such as TLRs and integrins/Immune chaperone to regulate innate and adaptive immunity	1	509.64	5328.42	0.096	0.79	0.77
NLRP3	NOD-like receptor family, pyrin domain containing 3	Part of the inflammasome in macrophages, leads to production of IL-1β/18	1	509.64	1457.19	0.350	-0.06	0.96

Almost all of the targets in Table 4.12 would have made sensible targets for future work but through manual examination SCARB1 and LMO2 were selected as the first two targets to investigate:

SCARB1 [*Scavenger Receptor Class B Member 1*] – Was a validated target of miR–223–3p which was featured frequently in networks and top target tables throughout the chapter (Figure 4.10, Figure 4.13, Figure 4.15, Table 4.3 and Figure 4.8. In this analysis a predicted interaction was not identified, however, there are predicted interactions for miR–223–3p with SCARB1 in both the microRNA.org and TargetScan databases but these fall below the thresholds used to identify targets and there was no predicted target in miRDB. The validated interaction corresponded to entry 'MIRT035551' in miRTarBase which detailed the regulation of SCARB1 (referred to as SR–B1 in the article) by miR–223–3p in HepG2 cells (a human liver carcinoma line). The evidence for this interaction in the paper was a ~55% decrease in SCARB1 mRNA, a ~15% decrease in cell surface expression accompanied by a decrease in overall protein expression following HepG2 incubation with a miR–223–3p mimic. The authors also briefly investigated the effects of this microRNA on SCARB1 mRNA expression in PMA stimulated THP–1 cells and found a slight decrease (Wang et al., 2013).

In addition to the evidence from the literature the evidence for this interaction from the analysis in this chapter was very strong. MiR–223–3p was the most abundant microRNA in pdEV making targets of this miRNA strong candidates. The level of SCARB1 gene expression in monocytes was above the gene expression threshold of 500, but had one of the lowest expression levels of the remaining targets. This significantly improved the ratio of microRNA to mRNA but also meant there was likely to be small amounts of protein. Another factor favouring SCARB1 as a target was that the gene expression decreased following monocyte incubation with either CRP–XL activated platelets or platelet-releasate. Taken together, these factors made SCARB1 a logical and strong target. In addition, its function in taking up cholesterol from HDL-cholesterol (HDL-C) and its known presence in atherosclerotic plaques made it of biological and clinical relevance (Hirano et al., 1999, Chinetti et al., 2000).

LMO2 [*LIM Domain Only 2*] – Is another target of miR–223–3p with both validated and predicted interactions. The evidence for a validated interaction (MIRT000130) came from two separate papers, both of which had shown the direct interaction of miR–223–3p with LMO2 via a variety of techniques. Yuan *et al.* demonstrated a significant reduction in LMO2 protein and mRNA (up to 80%) in K562 cells following enforced expression of miR–223–3p and a 50% reduction in luciferase activity from a vector containing the 3'–UTR of LMO2 co–transfected into NIH–3T3

cells with pre–miR–223. Felli *et al.* found that LMO2 and miR–223–3p expression were inversely correlated in a variety of haematopoietic cell lineages, including monocytes. During monocytic differentiation there was a marked decrease in LMO2 but the authors did not follow this up, so a direct link with miR–223–3p in this cell type was not established. They did however identify the direct interaction between miR–223–3p and LMO2 with a Luciferase assay in HeLa cells, observing a 50% reduction in activity (Felli et al., 2009, Yuan et al., 2009).

As with SCARB1 the evidence for LMO2 as a target in this chapter was strong. Table 4.12 showed that the expression of the interacting microRNA was high, the level of gene expression in monocytes was high and the ratio of microRNA to mRNA was suggestive that a strong effect could be observed. The LogFC in LMO2 gene expression of –1.53 and –0.63 following stimulation of monocytes with platelets or releasate respectively was strongly suggestive of a potential interaction. Finally the central role of this target in haematopoietic cell development indicated that it may be relevant in the interaction between platelets and monocytes.

4.5.3 Gene Ontology Analysis Comparison

The targets from the predicted targets (Figure 4.6), validated targets (Figure 4.10), Validated PLUS Predicted targets with monocyte expression (Figure 4.15) and Validated AND Predicted targets with monocyte expression (Figure 4.17) networks were subjected to a GO analysis. This aimed to identify the functions, processes and cellular components within the networks and to compare these across the networks to identify changes occurring to the changing list of targets. The GO analysis was split into three sections; Molecular function (MF), biological processes (BP) and cellular components (CC). All four of the networks resulting from the selection described above were analysed for GO terms linked to each. The GO database annotations are extensive, therefore the analysis only looked at GO terms directly linked to the searched ontology section e.g. MF. The results are shown in Figure 4.19, Figure 4.20 and Figure 4.21; pie charts for each network show the distribution of GO terms and the bar charts provided direct comparisons between the networks.

4.5.3.1 Gene Ontology – Molecular Function

Figure 4.19 investigated the MF GO terms; overall the pie charts for each network were closely matched and this was confirmed in the bar graph. When the GO terms were ranked by percentage (high to low) then all networks, except the Validated AND Predicted with monocyte expression network had the same order. There was little variation between each network within the individual terms with the biggest difference in the 'Binding' term where the predicted network had 20.9% less than the Validated AND Predicted with monocyte expression network. The only other notable difference was that the 'protein binding transcription factor activity', 'channel regulator activity' and 'antioxidant activity' GO terms were all lost from the Validated AND Predicted with monocyte expression network. This was only a minor change as they only represented 1.2%, 0.2% and 0.3% at their peak in the other networks. Despite these small differences the overall trend remained consistent between the networks regardless of the various stages of data manipulation. In addition to assessing correlation between networks, the GO terms provided information on the roles of the targets. The majority of MF terms involved interacting with another molecule ('binding') and then exerting an effect e.g. enzyme catalysis or nucleic transcription factors.
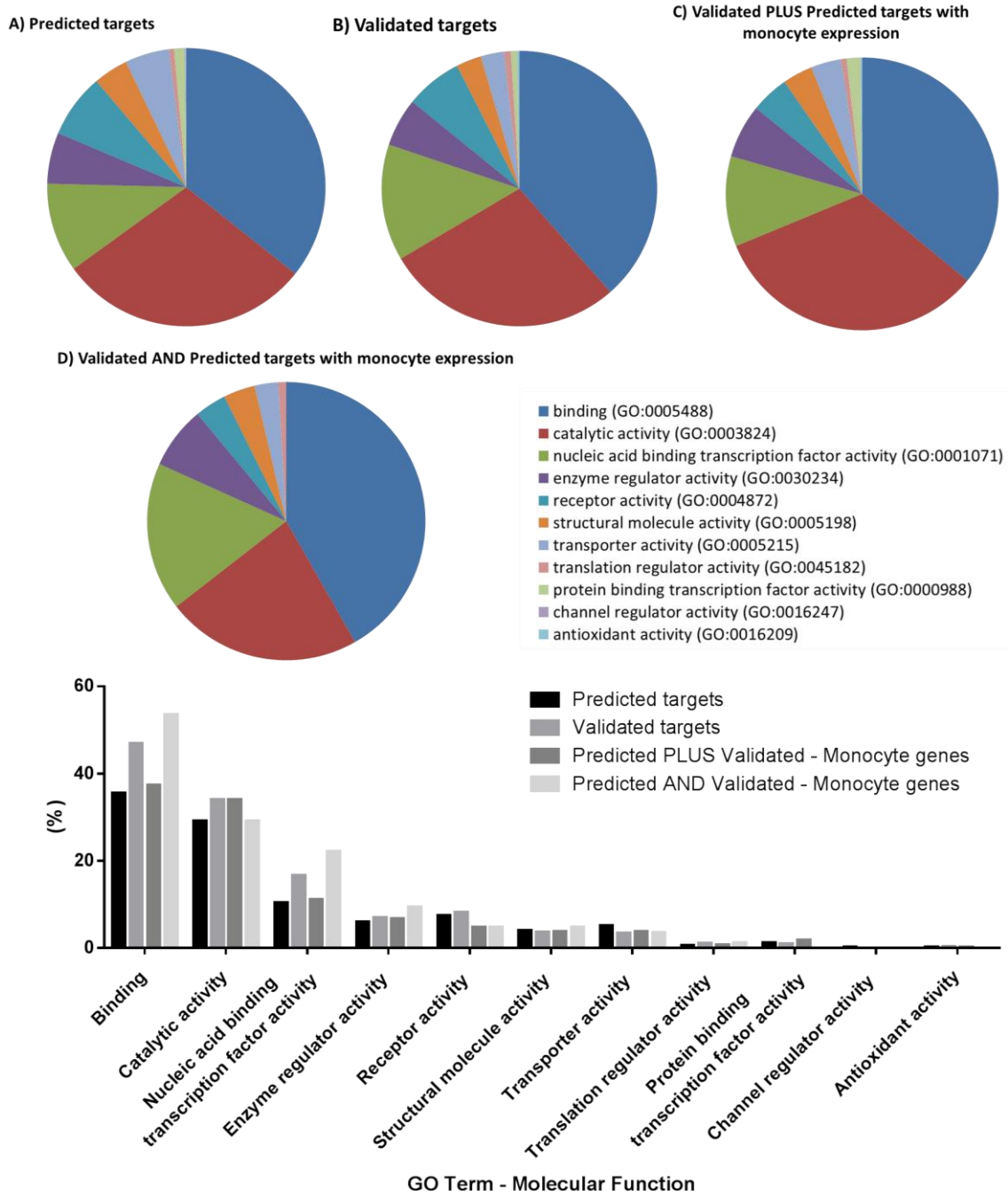
Figure 4.19 – Comparison of Gene Ontology Annotations for Molecular Function between microRNA–target networks *A Gene Ontology analysis was completed for the targets in the Predicted, Validated, Validated PLUS Predicted filtered for monocyte genes and the Validated AND Predicted filtered for monocyte genes networks. All the targets from each network were input into the PANTHER DB GO term analyser and terms directly related to Molecular Function were identified. Pie charts were produced showing the distribution of these terms in each network and a bar chart to allow for direct comparisons between the four networks.*

4.5.3.2 Gene Ontology – Biological Processes

In Figure 4.20 the BP family of GO terms was explored and the pattern of expression between the different networks was similar again despite small changes in the order. The largest single percentage difference was in the 'biological regulation' term where the highest and lowest varied by 16.5%. The GO terms mapped to this sections targets were predominantly general cell processes such as metabolism and movement. This suggested that the microRNA were not acting to target specific BP on a large scale. But as these GO terms were broad there may be secondary GO terms which provide more insight into the effects of pdEV microRNA on monocytes.
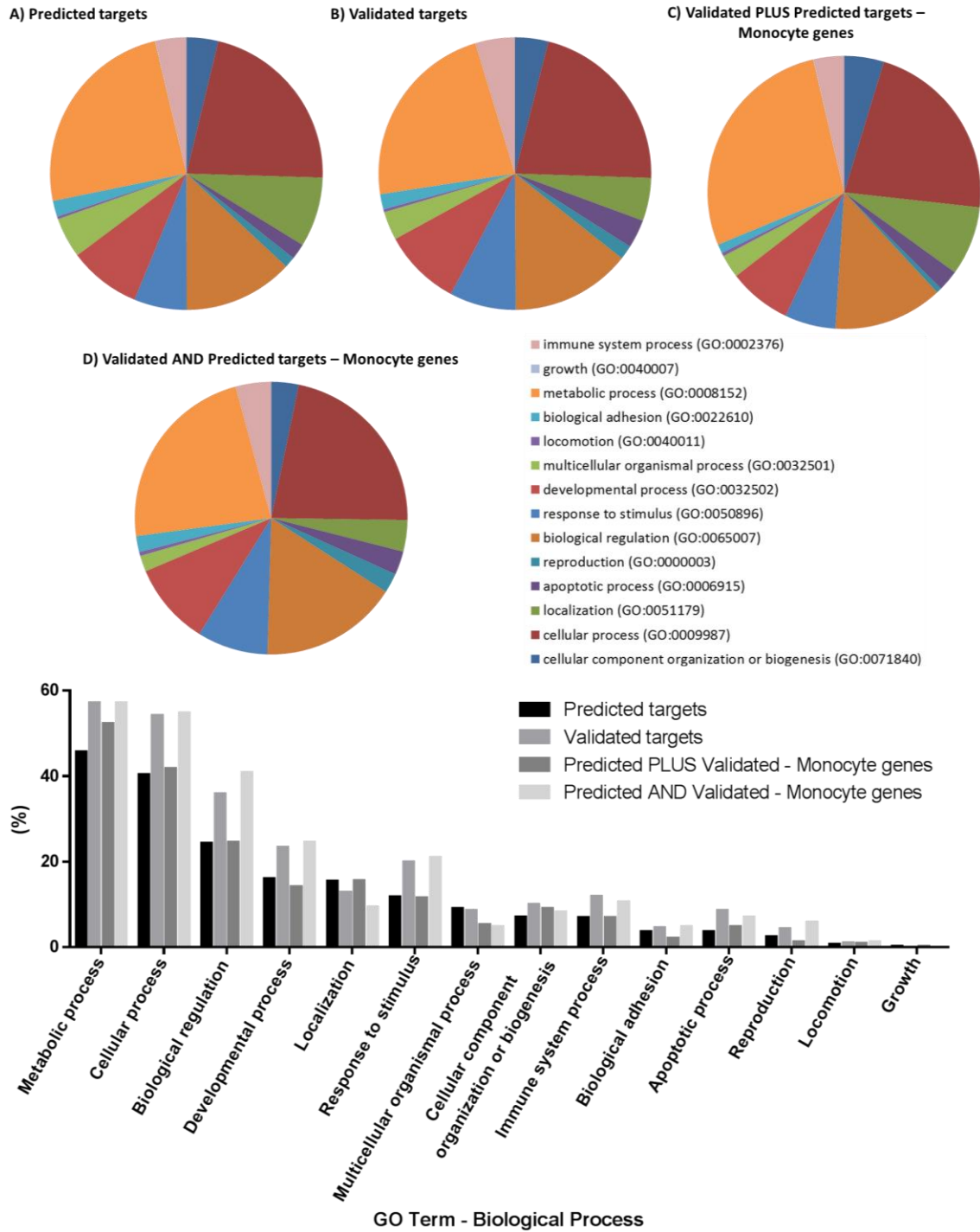
Figure 4.20 – Comparison of Gene Ontology Annotations for Biological Processes between microRNA–target networks A Gene Ontology analysis was completed for the targets in the Predicted, Validated, Validated PLUS Predicted filtered for monocyte genes and the Validated AND Predicted filtered for monocyte genes networks. All the targets from each network were input into the PANTHER DB GO term analyser and terms directly related to Biological Processes were identified. Pie charts were produced showing the distribution of these terms in each network and a bar chart to allow for direct comparisons between the four networks.

4.5.3.3 Gene Ontology – Cellular Components

The trend of consistency between the networks continued for the CC sub–section of GO terms. Six of the eight terms identified from the networks were found in all four and these six were consistently in the same order of abundance. The 'cell junction' and 'synapse' terms were lost from the validated network, but these had the lowest abundance and only represented the loss of two targets. It was again the case that the individual GO terms could not describe specific effects of pdEV microRNA and whether they were likely to be targeting a precise part of the cell, but the components of the membrane and extracellular regions appeared less targeted than those of intracellular parts or organelles. This may suggest that the microRNA were internalised, rather than acting directly at the membrane.
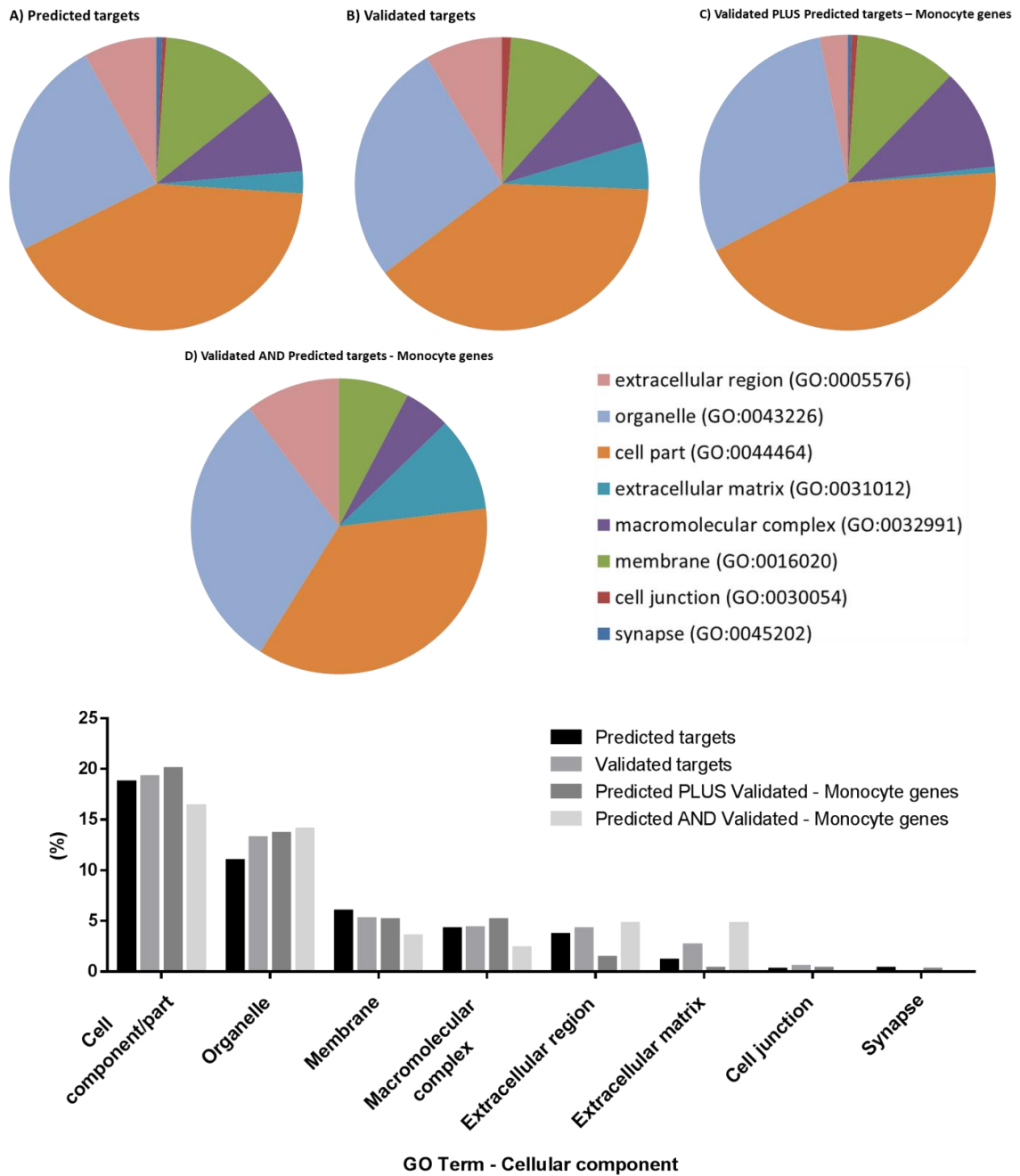
Figure 4.21 – Comparison of Gene Ontology Annotations for Cellular Component between microRNA–target networks *A Gene Ontology analysis was completed for the targets in the Predicted, Validated, Validated PLUS Predicted filtered for monocyte genes and the Validated AND Predicted filtered for monocyte genes networks. All the targets from each network were input into the PANTHER DB GO term analyser and terms directly related to the Cellular Component for each target were identified. Pie charts were produced showing the distribution of these terms in each network and a bar chart to allow for direct comparisons between the four networks.*

4.6   Discussion

The ability of microRNA to regulate protein expression through post-transcriptional control of mRNA is a highly conserved mechanism that effects up to 60% of vertebrate mRNA (Bartel, 2004, Friedman et al., 2009, Mendell and Olson, 2012). The binding of microRNA to complimentary target sequences within the 3'-UTRs of mRNA leads to a reduction in translation and in some cases complete mRNA degradation (Zhang et al., 2012). These interactions cause a fine-tuning of protein expression instead of complete inhibition and this modulatory rather than all-or-nothing response makes understanding and utilising microRNA for therapeutic applications an intensive area of research (Ambros et al., 2003, Lee and Ambros, 2001). The first microRNAs are currently undergoing clinical trials such as a miR-103/107 inhibitor (AZD4076) in phase I trials for the treatment of non-alcoholic steatohepatitis in diabetics and pre-diabetics (Trajkovski et al., 2011, ClinicalTrials.gov, 2016).

Whilst microRNA are clearly showing therapeutic potential, our knowledge of their specific function is still limited and elucidating their precise effects has proved challenging due to the ability of individual microRNA to target several hundred mRNA and the identification of >1000 separate microRNA species (Witkos et al., 2011, Ritchie and Rasko, 2014, Afonso-Grunz and Muller, 2015, Krek et al., 2005). Each microRNA is ~22 nucleotides long and this is made up of a seed region of between 6 and 8 nucleotides at the 5' end and a secondary binding site between nucleotides 13 and 16 in the non-seed region (Lai, 2002, Lewis et al., 2005). The seed region requires almost 100% complementarity and is critical to the determination of targets and so the sequence of this region of microRNA is used as the basis for predicting microRNA targets (Baek et al., 2008, Selbach et al., 2008).

Target identification utilises patterns identified from the results of previous experiments that have used high-throughput techniques to characterise microRNA-mRNA interactions (Ritchie and Rasko, 2014). These patterns are then applied to microRNA which have not been experimentally investigated to identify their potential targets. This has resulted in the availability of a multitude of microRNA prediction databases that use a variety of features in addition to the seed region complementarity to generate predicted targets. These extra features include, but are not limited to, sequence conservation across species which demonstrates an evolution-driven requirement for that binding site (Friedman et al., 2009), the thermodynamic stability of the microRNA-mRNA interaction (Betel et al., 2010), the availability of the microRNAs binding site based on knowledge of the mRNAs secondary structure (Grimson et al., 2007) and the number of target sites for a microRNA within the 3'-UTR of an mRNA (Betel et al., 2008).

Current techniques often result in the prediction of false positives and are readily applied across all cell types and experimental systems, regardless of where the initial data was validated (Ritchie and Rasko, 2014, Seitz, 2009). This results in wasted time and money investigating interactions which may not have observable functional outcomes. For this reason we investigated the targets of multiple microRNA using data from a variety of target databases and incorporated information from platelet-monocyte interaction datasets to identify targets which we had high confidence could be validated in proceeding experiments.

4.6.1 microRNA target prediction

The analysis carried out in this chapter utilised a range of resources resulting in the identification of a list of 34 targets. There were strong cases to suggest that pdEV microRNA could significantly influence the protein expression of each target in monocytes. The final list contained 16 targets of miR-223-3p, reflecting the strong influence of the most abundant pdEV microRNA, and also contained 9 targets of the miR-17/92 cluster. Two targets, LMO2 and SCARB1 were selected for validation and further analysis as they were both targeted by miR-223-3p and experimental data showed that interactions with platelets caused downregulation of their gene expression. In addition the interactions were predicted to be based upon a match of 8 nucleotides in the microRNAs seed region with conservation across a wide variety of species.

The strength of the microRNAs seed complementarity and the conservation of the binding site across species are 2 of the strongest indicators of likely microRNA-mRNA interactions and form the basis for prediction software. In plants, target prediction is straightforward with almost all interactions being based on perfect complementarity between the microRNA and mRNA (Voinnet, 2009). However the interactions in vertebrates have been shown to be significantly more complex and so target prediction must utilise far more than just seed complementarity (Sethupathy et al., 2006), and this has led to the development of a multitude of microRNA target prediction databases (Kozomara and Griffiths-Jones, 2014, Wong and Wang, 2015, Betel et al., 2008). Unfortunately these are designed based on differing original datasets and so prioritise different interaction characteristics leading to the prediction of inconsistent targets for the same microRNA. In addition these databases produce extensive lists of potential targets with very little indication of any potential impacts on the interaction in an environment different to that where the pattern of interaction was determined.

Understanding each of these limitations lead to the development of the method used for microRNA target identification in the present study. Whilst the individual databases are extremely useful tools they are often built upon potentially erroneous concepts that used

indirect experimental data to extrapolate patterns of interaction. For example the overexpression of a specific microRNA followed by observations of the effects on gene or protein expression with high-throughput mass spectrometry or microarrays. However, this frequently only involves a single time point, in a specific cell type (often cultured cells) and cannot account for the secondary and indirect effects on genes and proteins downstream of the actual target (Linsley et al., 2007, Wang, 2010, Loeb et al., 2012). The databases then assimilate data for multiple experiments and use machine learning to identify the patterns and whilst the predictions are not based upon single datasets it is still difficult to apply the findings ubiquitously and leads to the identification of many false positives (Witkos et al., 2011).

Due to the large number of false positives caused by the differential approaches to target prediction there is low overlap between target lists generated by different databases. A study by Sethupathy *et al.* found that some databases only predicted 10% of the known, experimentally validated interactions, and no algorithm was able to identify more than 50% of the experimentally validated targets, demonstrating that these databases produce large numbers of potential targets with many false positives, but also miss many real targets (Sethupathy et al., 2006). This suggests that no single target prediction system can successfully identify all of the true targets and a contributing factor is the specific milieu in which the microRNA is acting (Baek et al., 2008, Alexiou et al., 2009, Seitz, 2009, Morozova et al., 2012).

For these reasons we elected to use three databases; miRDB, microRNA.org (miRanda) and TargetScan to identify predicted targets of pdEV microRNA. These three databases used different target prediction approaches, as described in 4.4.1.1, and by only retaining targets present in all databases this provided a stringent target identification analysis. The overlap from these three databases clearly demonstrated the disparity caused by the separate approaches. Here we found that on average there was only 18% intersection between all three approaches and this dropped as low as 0.88% for the low abundance miR-301a-5p. This did lead to significantly reduced numbers of potential targets with 3592 targets carried forward from the initial analysis which yielded 62328 potential microRNA-target interactions (Table 4.4). This demonstrates that this approach was able to simply and effectively reduce the number of potential targets, even beyond that which a single database approach would have yielded (~20000) whilst avoiding bias from using a single prediction algorithm. This is an approach that has been used successfully before (Pandey et al., 2011) but the analysis here incorporated further data to improve the likelihood of predicting a strong target.

The next inclusion was of microRNA-target interactions which had been validated with strong, direct experimental evidence such as reporter assays and western blotting. The ability to utilise this approach has only recently become truly useful. 10 years ago this database only contained 130 microRNA-target interactions for mammals and only 84 of these were for experiments where strong evidence had been found (Sethupathy et al., 2006). However this database now contains over 300000 microRNA-target interactions. The addition of data from miRTarBase significantly reduced the number of targets, but again demonstrated the disparity between prediction and validation with only ~2.5% of the combined predicted and validated microRNA-mRNA interactions being both validated and predicted (Hsu et al., 2014). This did however mean that the targets we were analysing had significant evidence for their interaction.

Whilst miRTarBase offered a method of significantly narrowing the analysis and simultaneously increasing the evidence for each remaining target, the information from this database must be used with caution. Entries into this database are based on literature mining and so the microRNA and mRNA which are investigated are heavily biased by research focuses, such as cancer biology. This results in lots of entries for some microRNA and very little information on others, meaning that this approach is suitable when used in tandem with others as steps needed to be taken to explore the full potential of a microRNAs targets without solely relying on previously investigated microRNA-mRNA interactions (Hsu et al., 2014).

4.6.2 Alternative target identification approaches

In-silico approaches were utilised to identify potential targets but as shown above even the stringent analysis used here could not produce a list of targets that showed significant overlap with the experimentally validated targets. The utilisation of multiple datasets did however allow for the identification of microRNA-mRNA interactions that were backed by substantial evidence. However, there are alternatives to computational approaches for the identification of microRNA targets such as the use of immunoprecipitation and quantitative proteomics (Thomson et al., 2011).

The RISC is a ribonucleoprotein which incorporates microRNA and then recognises and binds their complementary mRNA (Winter et al., 2009). Several elements of the RISC have been utilised in immunoprecipitation experiments to pull out bound mRNA transcripts. In these studies cells were transfected with epitope tagged components of RISC and following incubation or stimulation of the cells RNA was cross-linked to RNA-binding proteins, such as Ago2, using UV irradiation. The cells were then lysed and the complexes immunoprecipitated and the mRNA within the transcripts was analysed allowing for the precise identification of the mRNA

sequences that are being targeted by microRNA seed regions (Moore et al., 2014). Interestingly this approach has identified microRNA binding sites in the coding regions and 5'-UTR of mRNAs (Chi et al., 2009). The most advanced version of this method is called photoactivatable-ribonucleoside-enhanced crosslinking and immunoprecipitation (PAR-CLIP); this has been used alongside the transfection of microRNA mimics to enhance the identification of a specific microRNAs targets by overloading the system with a single microRNA which will displace other microRNA from the RISC complex (Thomson et al., 2011, Hafner et al., 2010, Hafner et al., 2012). A further variation is the use of biotin tagged microRNA where cells are transfected with biotinylated microRNA. Following incubation the cells are lysed and the microRNA with target mRNA bound is pulled out using streptavidin and then the mRNA is sequenced to identify the targets of the specifically biotinylated microRNA (Orom and Lund, 2007).

In addition to the immunoprecipitation approaches, quantitative proteomics has been widely used. As microRNA have greater effects on protein, measuring proteins rather than genes provides a more precise analysis of the effects of a microRNA. One proteomics approach that could be used is stable isotope labelling with amino-acids in cell culture (SILAC) (Schwanhausser et al., 2009). In this technique cells are transfected with a specific microRNA and simultaneously a stable isotope labelled amino acid is added to the cultures. This means that de novo synthesised proteins will incorporate the labelled amino acid and the exact effects of the microRNA on protein synthesis can then be analysed in these new, isotope labelled proteins compared to a control (Selbach et al., 2008, Kaller et al., 2014). There is however limitations with the depth of coverage of proteomics compared to genomics approaches and all potential targets would still require individual variation as it is impossible to distinguish the direct effects of the microRNA from secondary outcomes (Thomson et al., 2011, Alexiou et al., 2009).

These experimental approaches enable the investigation of microRNA of interest in the investigators cell or model of interest. However the cell needs to be capable of being transfected with high efficiency to generate measurable changes. In addition the effects of labelling the components involved in the microRNA-mRNA interaction are unclear and may cause modifications to the interactions suggesting that the results should be interpreted with care (Easow et al., 2007). In addition, only a single microRNA can be investigated in each experiment so researchers must be certain of which microRNA they want to investigate. These techniques require detailed knowledge of the biology involved which makes them challenging and they also generate lots of data which then involves an analysis at least as complex as using an in-silico approach (Alexiou et al., 2009).

The large databases of microRNA targets that are currently available provide powerful tools for researchers attempting to identify microRNA targets. They can be utilised to interpret the targets of sets of microRNA and provide a good starting point for future work. Up to this point many researchers have often looked at only one database, but approaches similar to that used here and by Pandey *et al.* demonstrate that a more detailed approach can yield better results. Experimental approaches can also produce good results but all of the caveats listed above must be considered when deciding which approach is best. For the work here, it is clear that a computational approach was superior due to the number of microRNA involved and the difficulty of using monocytes for the techniques.

4.6.3 Incorporation of platelet-monocyte interaction gene expression datasets

In addition to using both validated and predicted microRNA targets from multiple databases this analysis also utilised gene expression microarrays to further refine the microRNA targets. Online microRNA-mRNA interaction databases simply list all of the possible combinations found using their algorithm (Wang, 2008, Wong and Wang, 2015) and this does not take into consideration that no single cell simultaneously expresses all of the genes in the human genome and so only a portion of the identified targets are therefore possible within the cell of interest. Here we explored the effects of the pdEV microRNA on monocytes and so monocyte gene expression arrays were used to filter the total list of microRNA targets.

This analysis resulted in the removal of ~45% of the potential targets because they weren't expressed in monocytes, demonstrating that this step was extremely valuable in the narrowing of the list of potential targets. In addition, the datasets added to the analysis provided information on the changes in these genes following incubation with platelets and platelet-releasate and detailed the relative amounts of each mRNA which could be targeted by the microRNA. Both of these mRNA attributes were informative and focused the target search onto the most promising targets.

The mRNA expression at baseline in the platelet-monocyte interaction dataset was used to filter the targets and determine relative ratios of microRNA to mRNA expected in experiments. This helped to determine whether a specific microRNA was present in sufficient abundance to exert an effect on a target mRNA, with low abundance mRNA targeted by abundant microRNA being more likely to be significantly affected (Mukherji et al., 2011). Analysing the relative levels of microRNA and mRNA as a ratio to determine the potential strength of a target is a technique which, to my knowledge, has not previously been used. Due to the two datasets (microRNA and

mRNA) being generated separately it is unlikely that the ratio reflects the true relationship between them in monocytes. However it did function as an effective bioinformatic tool and experimental validation of this approach could be utilised for the development of better microRNA target prediction algorithms.

The level of a targets expression within a cell has been a commonly overlooked factor in microRNA target analysis and it has been suggested that this is the critical feature causing the discrepancy between predicted targets and the experimentally observed microRNA-mRNA interactions (Seitz, 2009). Seitz suggests that many microRNA target sites simply act to bind excess microRNA and that the small changes in protein expression this causes are below the level of functional significance. Therefore identifying targets that are susceptible to small change in an environment, where the microRNA of interest is not sequestered and therefore remains in high enough quantities to have an effect, is critical to the identification of true targets. In addition there are non-coding circular RNA, which act as "microRNA sponges" which would have a similar effect to that of the mRNA in Seitz's theory (Hansen et al., 2013, Memczak et al., 2013). This hypothesis is yet to be proven, and to determine its actual effects would require detailed study, so whilst it is a potentially important factor it was not considered here but may well prove valid as part of microRNA target identification workflows in the future.

As well as utilising the platelet-monocyte interaction datasets for the analysis of which genes were or were not present to be targets, the monocyte genes FC from baseline following co-incubation with platelet or platelet-releasate were used to inform target selection. When microRNA interact with mRNA they lead to downregulation and sometimes degradation of mRNA meaning that changes in gene expression can be indicative of microRNA function (Wang and Wang, 2006, Bagga et al., 2005). Therefore genes that were downregulated following platelet/platelet-releasate interaction were prioritised as potential targets.

This step in the workflow helped to streamline the list of targets but was carried out with several caveats. Firstly that the changes used were in gene expression and not the ultimate microRNA target, protein expression. But there is strong evidence to suggest that changes in mRNA expression can be caused by microRNA and are therefore potentially good indicators of microRNA function (Bagga et al., 2005, Baek et al., 2008, Ruike et al., 2008). Secondly, the change in gene expression was measured at a single time point, 4hours in both datasets, so this data must be interpreted with caution as the time taken for pdEV to transfer microRNA to monocytes and trigger changes was not yet known. Thirdly the stimulus used was not identical as neither was looking at either an isolated population of pdEV or just the effects of microRNA. Therefore

there was a lot of opportunity for the observed changes to have been caused by alternatives such as direct cell contact, soluble mediators or the direct transfer of mRNA.

Despite these caveats these datasets helped to identify potential targets and the inclusion of this data was beneficial for this analysis. If the datasets had been acquired from a single model then this would have significantly enhanced their contribution to the analysis and these co-expression profiles have previously been used to good effect for target identification (Landgraf et al., 2007, Girardi et al., 2012, Nagalla et al., 2011, Simon et al., 2014). Alongside the addition of the genomic dataset, the use of proteomics in a pdEV treated monocyte system, to observe the expected changes caused by microRNA would have proved extremely useful.

4.6.4 Analysis of affected pathways and identification of associated GO terms

As part of this analysis the effect of the group of pdEV microRNA on common cellular pathways was tested and the GO terms of the target genes was analysed. Pathway analysis has been an integral part of the in-silico analysis of microRNA targets in many studies due to its ability to incorporate multiple microRNA and look at how they may work synergistically (Afonso-Grunz and Muller, 2015, Wang, 2010, Mogilyansky and Rigoutsos, 2013, Stather et al., 2013). The pathway analysis carried out here did not provide significant levels of information with which the list of targets could be further enhanced. Godard and van Eyll investigated the effect of using random sets of microRNA on the output from miRPath and found that several pathways, especially those related to cancer, almost always appeared in the results suggesting that this approach lacks specificity and demonstrates clear bias (Godard and van Eyll, 2015, Bleazard et al., 2015).

This bias could be due to the wealth of research on cancer pathways as the pathway databases were only able to provide information on the research that had been carried out, so the results are heavily biased by the curation of the pathways within the database (Mork et al., 2014). For example, the Predicted PLUS Validated dataset contained 98 proteins that map to the GO term 'Endocytosis' (data not shown) such as TSG101 and several of the Vacuolar Protein Sorting (VPS) proteins e.g. VPS4A/B, VPS13 and VPS18 but the endocytosis pathway does not appear in the list of targeted pathways (Hislop et al., 2004). In addition to this the pathway analysis does not provide information on whether the overall effect on the pathway will be up or down regulation, whether it is relevant in your cell of interest or what is the most suitable point to measure the effect on the pathway. It is also impossible to tell whether there is redundancy in the pathway to prevent any functional effect and the analysis treats every microRNA as equal despite their

differential expression (Godard and van Eyll, 2015, Khatri et al., 2012). Taken together this suggests that the current pathway analysis tools do not suit the needs of microRNA and so their results do not significantly enhance our ability to select targets (Bleazard et al., 2015).

Alongside the pathway analysis the GO terms of the microRNA targets were analysed at each stage of the target identification process. This was predominantly to demonstrate that there was no bias in the filtering steps resulting in the removal of specific subsets of targets associated with specific GO terms. However this was a simple analysis of overarching GO terms and it is possible that a more in-depth analysis may have provided further detail which the pathway analysis was not able to offer (Roubelakis et al., 2009).

4.6.5 Specific target identification

The overall aim of the work in this chapter was to identify targets of pdEV microRNA in monocytes that could be investigated experimentally. From the analysis it was determined that LMO2 and SCARB1 were the strongest potential targets and that the effect of miR-223-3p on their expression in monocytes would be investigated. Interestingly both of these targets were identified at the very beginning of the analysis (Table 4.2 and Table 4.3) by simply using the predicted and validated targets of miR-223-3p. However at this stage there was no evidence demonstrating their expression in monocytes, no indication that they would be modulated by interactions with platelets, no suggestion of how strong this interaction would be or whether other microRNA targeted these mRNA. Therefore the subsequent analyses confirmed their potential as targets of interest to study.

Both of the selected targets are associated with miR-223-3p, and whilst the analysis looked at all 45 consistently expressed microRNA the strongest targets were likely to interact with miR-223-3p due to its significantly greater abundance. The delivery of miR-223-3p has been shown before; from platelets to the A549 lung cancer cell line (Liang et al., 2015), from platelets to endothelial cells (Pan et al., 2014) and between macrophages (Ismail et al., 2012). In addition it has been implicated in a variety of cellular processes including reducing the inflammatory response of macrophages (Zhuang et al., 2012), the regulation of haematopoietic stem cell fate (Yuan et al., 2009) and as a biomarker of platelet reactivity (Zhang et al., 2013, Shi et al., 2013). Taken together this evidence shows that miR-223-3p has many roles in the circulation and its abundance in platelets positions them as a central controller of this activity, potentially via pdEV.

Alongside miR-223-3p this analysis was dominated by microRNA from the miR-17/92 cluster. This cluster of microRNA has important roles including monocytopoiesis (Fontana et al., 2007)

and angiogenesis (Sato, 2013, Mogilyansky and Rigoutsos, 2013) but none of the targets associated with this cluster were selected for further analysis. This was due to the lower abundance of these microRNA, even when their expression was combined, and experimental difficulties in attempting to look at the effects of multiple microRNA simultaneously. The drawbacks of the miR-17/92 cluster strengthened the case for using miR-223-3p targets and ultimately led to the selection of LMO2 and SCARB1.

The interaction of both of these targets with miR-223-3p has previously been validated experimentally. Wang *et al*. observed that miR-223-3p significantly reduced SCARB1 protein and gene expression in the HEPG2 hepatocyte cell line but not in the monocytic/macrophage THP-1 cell line. It is possible that the mRNA environment in these 2 cell types caused the differential effects or that the high endogenous expression of miR-223-3p generated in THP-1 cells treated with high doses of PMA (as used in their study) rendered any further effects of additional miR-223-3p added to the cells undetectable. Transformation of THP-1 cells with PMA induces a macrophage-like phenotype (Daigneault et al., 2010) and this analysis focuses on monocytes that have lower endogenous levels of miR-223-3p, which would potentially allow for pdEV delivered miR-223-3p to cause reduced SCARB1 expression. Direct interactions have been shown between miR-223-3p and LMO2 in the K562 erythroleukaemia cell line but so far this link has only been inferred in monocytes using indirect correlation of LMO2 protein western blotting and RT-PCR quantification of miR-223-3p expression (Felli et al., 2009). The role of LMO2 in haematopoiesis is well documented but the function of its continued expression in circulating monocytes is unclear. However its downregulation following interaction with platelets suggests that it may have roles to play beyond haematopoiesis.

Overall the bioinformatic analysis in this chapter has yielded several promising targets of pdEV microRNA in monocytes and helped to tease apart the roles which pdEV microRNA may play in monocyte function. The process utilised all of the available resources to provide a workflow which conducted a comprehensive analysis of multiple microRNA. It suggests that an online algorithm that also contains information on gene expression in specific cell types would prove useful for microRNA prediction and a particularly useful advancement would be to understand the role the mRNA environment of a cell plays on microRNA function. Therefore a microRNA target prediction platform which contained details on the transcriptome of baseline mRNA, or the ability to input baseline mRNA data, with a method of calculating the effects of all the targets on a microRNA to help determine the truly important targets would be a powerful tool for the furthering of microRNA research. Ultimately the success of the work in this chapter will not be quantified until experiments into the identified interactions have been carried out.

Chapter 5

Functional effects of platelet-derived
Extracellular vesicles

5 Functional effects of platelet-derived extracellular vesicles

5.1 Introduction

A number of studies have now demonstrated intercellular communication via EVs (Montecalvo et al., 2012, Cabrera-Fuentes et al., 2015, Cai et al., 2015, Guduric-Fuchs et al., 2012), including the transfer of nucleic acids (Cismasiu and Popescu, 2015, Hulsmans and Holvoet, 2013, Mittelbrunn et al., 2011) and proteins (Losche et al., 2004) as well as observing genetic (Valadi et al., 2007, Yanez-Mo et al., 2015) and phenotypic changes (Cabrera-Fuentes et al., 2015, Kapustin et al., 2015, Dalli et al., 2013, Ismail et al., 2012). These intercellular EV interactions work alongside and supplement other cell communication methods and provide clear evidence that EV have a role to play in cell-cell communication, and demonstrate that understanding their function could be beneficial for the development of therapeutic targets (Kosaka et al., 2013b, Tushuizen et al., 2011, Record et al., 2011).

The ability of EV to enter other cells makes them an attractive part of the intercellular communication pathway to study. They are an important component of the complex intercellular signalling networks that occur in the circulation and offer the opportunity for targeted bulk cargo delivery (Kwekkeboom et al., 2014). The makeup of the EV membranes could play a critical role in their targeting to specific cell types and studies are currently underway to elucidate EV uptake, release and cargo selection mechanisms. Current evidence suggests that EV are actively taken up through endocytic mechanisms and that their cargo, such as microRNA are specifically selected (Duchez et al., 2015, Bolukbasi et al., 2012, Kosaka et al., 2013a, Kosaka et al., 2010, Mulcahy et al., 2014). There is likely to be significant undiscovered complexity to the EV signalling network due to the potential separation of EV beyond simply microvesicles or exosomes (Smith et al., 2015).

It is known that exosomes are enriched for tetraspanins such as CD63 and CD81 although this varies from cell-to-cell and not all exosomes from a specific cell with have the same tetraspanin characteristics (Belov et al., 2016). Tetraspanins are fusogenic proteins that have been shown to play roles in phagocytosis, oocyte-spermatozoa fusion and cellular entry by viruses (Rubinstein et al., 2006a, Takeda et al., 2003, Li et al., 2014). The abundance of tetraspanins on exosomes suggests their importance in the transfer of messages between cells, and the specific make-up of these may play a role in the specific targeting of the EV. As well as variation in the membrane, the cargo of EVs has been shown to vary significantly (Diehl et al., 2012) and paired with the

knowledge that even the EV subtypes; exosomes and microvesicles, have their own distinct subsets containing disparate cargoes suggests that each EV may be released for a specific function (Ohshima et al., 2010, Bolukbasi et al., 2012). The targeting of EV is poorly understood; many studies have investigated the relationship between EV populations from a single cell interacting with a specific cell in isolation, whilst others have added EV to an animal model where uptake measurement resolution was insufficient to provide specifics, other than to identify the target organ (Rana et al., 2012, Zech et al., 2012). These studies have therefore been unable to provide much new information beyond demonstrating a cells ability to take up EV and their cargo.

Due to the abundance of pdEV in the circulation and their significant influence on the circulating profile of microRNA their role in intercellular communication has been widely investigated (Arraud et al., 2014, Willeit et al., 2013). PdEV have been shown to deliver microRNA to endothelial cells and reduce expression of FBXW7 protein (Laffont et al., 2013) and transfer mRNA, such as that for the γ-globulins HGB1/2 to THP-1 cells (Risitano et al., 2012). The relationship between platelets and leukocytes is of particular interest due to the known role of platelets in the progression of atherosclerosis and the interactions of these cells in inflammation (Kaplan and Jackson, 2011, Koyama and Nishizawa, 2005, Gawaz et al., 2005, Gawaz et al., 2008, Linden and Jackson, 2010).

Platelets interact with leukocytes in a variety of ways (Li et al., 2000) and these interactions have been shown to be important for monocyte recruitment into thrombi (von Bruhl et al., 2012, Freedman and Loscalzo, 2002, Kirchhofer et al., 1997) and recruitment to sites of inflammation (Alard et al., 2015, Vieira-de-Abreu et al., 2012, Langer et al., 2007). Direct contact between the cells initially occurs through P-selectin/PSGL-1 interactions (Cerletti et al., 1999) and this leads to the formation of further attachments, signals are also sent via chemokines and cytokines, such as PF4 which is released from platelet granules (Baltus et al., 2005, Coppinger et al., 2004). Indirect effects of pdEV on monocytes have been observed, with microvesicles recruiting monocytes to the endothelium through the transfer of RANTES to endothelial cells (Mause et al., 2005, Barry et al., 1998). However, there is limited direct work on interactions between pdEV and monocytes and the current body of work has mainly been carried out using cell lines.

pdEV uptake has been observed in the monocytic cell line, THP-1, but a question remains over primary human monocytes (PriMo) as THP-1 cells do not precisely reflect their primary counterparts, particularly when treated with PMA which induces a macrophage-like rather than a monocyte-like phenotype (Risitano et al., 2012, Daigneault et al., 2010, Maess et al., 2014).

Studies have also shown that pdEV induce differential gene expression in the monocytic cell line MonoMac6, with clear changes in the mRNA and activity levels of sphingosine kinase 1 (Setzer et al., 2006). Risitano *et al.* looked at the effects of pdEV on PBMCs gene expression in a mouse model and observed an increase in multiple genes which they believed had been transferred from pdEV. However, the controls in the experiment did not preclude the option for the RNA transfer to be an artefact of leukocyte-platelet aggregates in the circulation which occur following activation, as observed in their study (Risitano et al., 2012, Barnard et al., 2003, Furman et al., 1998). Investigations in cell lines do not consider the competitive, multicellular environment of the circulation which leaves many unknown factors about this interaction. However, these experiments do suggest that pdEV have an important role to play in platelet-leukocyte crosstalk that is yet to be fully elucidated.

In the previous chapter the microRNA content of pdEV was investigated to identify potential targets using an in-depth bioinformatics approach. From this analysis we identified several promising targets, that led to the effects of miR-223-3p on LMO2 and SCARB1 expression in PriMo and THP-1 cells being investigated in this final chapter.

5.2 Aim

To identify whether pdEV are taken up by primary monocytes in an ex-vivo whole blood system, and by cultured THP-1 cells. To determine whether pdEV uptake by these cells allows the transfer of the pdEVs microRNA cargo and to explore the effects of miR-223-3p on LMO2 and SCARB1 gene and protein expression.

5.3 Materials and methods

All reagents were purchased from Sigma-Aldrich unless otherwise stated.

5.3.1 Isolation of peripheral blood mononuclear cells (PBMCs)

Blood was collected into citrated tubes, as previously described (2.3.1) and centrifuged at 160g for 20minutes to isolate PRP (2.3.5). The remaining isolation steps were carried out under sterile conditions, in a Class II cabinet. PRP was carefully removed and either retained to isolate platelets or discarded. The remaining blood was then mixed with sterile PBS/EDTA (0.01M phosphate buffer and 0.154M sodium chloride with 5mM EDTA) to make it back to the original blood volume. All samples were then pooled into 50mL falcons and diluted 1:1 with sterile PBS/EDTA.

Separately, 50mL falcon tubes were prepared containing 15mL of lymphoprep (9.1% w/v Sodium diatrizoate, 5.7% w/v polysaccharide, Axis-Shield, Dundee, UK)) and 22.5mL of the blood with sterile PBS/EDTA mixture was carefully overlaid on top of the lymphoprep. This was then centrifuged at 800g for 30minutes at RT, with a slow brake, to separate the PBMCs from the rest of the blood. The PBMCs were carefully aspirated using a Pasteur pipette into a new 50mL falcon and the volume was made up to 50mL with sterile PBS/EDTA. The tubes were centrifuged at 200g for 15minutes (RT), the supernatant was discarded and the pellet re-suspended in 30mL PBS/EDTA. The cells were then pelleted again (200g-15minutes (RT)) and re-suspended in 2mL PBS/EDTA. The number of PBMCs was counted using an Ac·T diff automated cell counter (Beckmann Coulter) and 13mL of PBS/EDTA was added to the PBMCs, which were re-pelleted at 400g for 15minutes.

The supernatant was discarded and the cells re-suspended in a volume that produced a concentration of 1.25×10^8 PBMCs/mL. To this CD61 microbeads (Miltenyi Biotec, Bergisch Gladbach, Germany) were added at a ratio of 20µL per 1×10^7 PBMCs, followed by an incubation at 4°C for 15minutes. The mixture was then diluted with 1mL of PBS/EDTA and magnetic separation was performed using an AutoMACS Pro (Miltenyi Biotec) using the "depletes" programme which produced a CD61+ve fraction (platelets) and a CD61-ve platelet-free PBMC preparation. The PBMCs were then pelleted by centrifugation at 400g for 10minutes and re-suspended in RPMI-1640 for culture (Sterile media with L-glutamine (0.3g/L), phenol red (0.0053g/L) and sodium bicarbonate (2g/L)).

5.3.2 Cell Culture

5.3.2.1   THP-1 cells

THP-1 cells are a human monocyte cell line derived from an acute monocytic leukaemia patient (American Type Culture Collection, Manassas, Virginia, USA). These cells were cultured in T75 flasks in an incubator at 37°C with 5% CO_2 in RPMI-1640 media supplemented with 10% Foetal Bovine Serum (FBS) (Thermo Fisher Scientific) and Penicillin-streptomycin (Penicillin-100IU (base/mL) / streptomycin-100µg/mL, PAA laboratories ltd, Yeovil, UK). The cells were cultured in ~50mL of media that was changed 3 times a week; 50% of the medium was removed and exchanged for an equal volume of pre-heated fresh medium. Cells were counted at each passage; 10µL of sample was mixed with 10µL of 0.4% Trypan blue and then 10µL of the total mix was pipetted under the coverslip of a haemocytometer. Four large grids of 16 squares on the haemocytometer were counted and an average calculated, this value was multiplied by 20000 to give the number of cells/mL. Cultures were maintained at a density of between $2.0x10^5$/mL and $6.0x10^5$/mL and when the density exceeded this the cells were passaged.

Aliquots of early passage cells were stored in liquid nitrogen, cells were counted and concentrated by centrifugation at 1000rpm for 7minutes to produce a pellet containing between $3-5x10^6$ cells/mL. This pellet was then re-suspended in 1mL of freezing media (8mL normal media supplemented with 1mL DMSO and 1mL FBS), placed inside a cool cell at -80°C overnight and then transferred to liquid nitrogen. To bring cultures from liquid nitrogen, the cells were rapidly defrosted in a 37°C water bath and then added to 9mL of pre-warmed RPMI-1640. This mixture was then centrifuged at 1000rpm for 7minutes to pellet the cells, the supernatant was aspirated and the cells re-suspended in 20mL of pre-warmed RPMI-1640 and cultured until the cells were at $~2x10^6$/mL.

THP-1 cells required differentiation to obtain monocyte-like characteristics. To achieve this THP-1 cells were cultured with either Phorbol 12-Myristate 13-Acetate (PMA) or 1α,25-Dihydroxyvitamin-D3 (VitaminD3), optimisation of this process is shown in the results (5.4.1).

5.3.2.2   Primary human monocytes

Following isolation of platelet-depleted PBMCs (5.3.1) the cells were plated in 24 well plates at a density of $1x10^6$ cells/well in 1mL of un-supplemented RPMI-1640. These plates were incubated at 37°C in 5% CO_2 for 2hours, during which time the PriMo become adherent. The cells were then washed twice with pre-heated RPMI-1640 and then incubated in RPMI-1640 at 37°C in 5% CO_2 for experimental use.

5.3.3 Staining of extracellular vesicles

To generate stained EV, isolated platelets were treated with the general lipid membrane fluorescent cell linker dye, PKH67 (excitation (ex)-490nm and emission (em)-502nm) and then stimulated to release EV which were isolated as previously described (2.3.8.1). To stain platelets with PKH67, PGI$_2$ (200ng/mL) was added to isolated platelets which were then pelleted at 600g for 5minutes at RT. This pellet was then re-suspended in 250µL diluent C (iso-osmotic labelling vehicle) and was added to a solution of 246µL diluent C with 4µL PKH67 dye. The samples were incubated at 37°C on a rotating mixer for 5minutes and then 50µL of 10% Bovine Serum Albumin (BSA) (Fisher Scientific–10450141) was added and incubated for 5minutes in the dark at RT. Samples were then supplemented with PGI$_2$ to a final concentration of (200ng/mL) and washed twice by centrifugation at 600g for 5minutes at RT, removal of the supernatant and then re-suspension in 1mL HBS. The cells were pelleted again at 600g for 5minutes at RT and re-suspended in 500µL HBS.Ca. The platelets were left at RT for 20minutes to allow the effects of the PGI$_2$ to decay and then the platelets were activated with PAR1-AP (10µM) for 10minutes at 37°C to generate EV, which were isolated as previously described (2.3.8.1). Stained EV were then added to THP-1 cells, PriMo cultures or whole blood at a concentration that reflected the ratio of platelets used to generate the EV to PriMo found in whole blood (~1000 platelets:1 PriMo /µL).

5.3.4 Microscopy

Fluorescence and confocal microscopy was used to observe pdEV transfer to, and transfection of, THP-1 cells and PriMo.

5.3.4.1   Microscopy preparation for observing EV transfer

Single wells of a 24 well plate containing 1x10^6 THP-1 cells that had been incubated for 20hours with PKH67-stained, or unstained, pdEV were aspirated into Eppendorf tubes and then centrifuged at 600g for 5minutes to pellet the cells. The cells were washed once with HBS and pelleted at 600g for 5minutes. Simultaneously a solution of 4% Paraformaldehyde (PFA) (4g PFA in 100mL PBS) with 300nM 4',6-Diamidino-2-Phenylindole (DAPI) (ex-[357/44]/em-[447/60]) (Thermo Fisher Scientific) for nuclear staining and 5µg/mL Wheat Germ Agglutinin (WGA), Texas Red-X conjugate [ex-595nm/em-615nm] (Thermo Fisher Scientific) for cell membrane staining was prepared. The supernatant was discarded and the pelleted cells were re-suspended in 500µL 4% PFA + 300nM DAPI + 5µg/mL WGA and incubated in the dark for 60minutes. The cells were then centrifuged at 600g for 5minutes and the pellet re-suspended in 500µL 0.2%FS. Aliquots (100µL) of the THP-1 suspension was loaded into Cytospin funnels (Fisher Scientific)

and centrifuged at 600rpm for 2minutes. The Cytospin apparatus was disassembled and Prolong AntiFade Gold (Thermo Fisher Scientific) was added to the slides, which were sealed with a coverslip.

For PriMo, $1x10^6$ PBMCs were seeded in a single well of a Nunc™ Lab-Tek™ II CC2™ 8 well Chamber Slide System (Thermo Fisher Scientific) in serum free RPMI-1640 which resulted in ~$2x10^5$/well PriMo after washing to remove lymphocytes (5.3.1). The cells were incubated with PKH67-stained or unstained pdEV for 20hours. The media was aspirated, the cells were washed with 200µL HBS and then incubated in 200µL 4% PFA with 300nM DAPI + 5µg/mL WGA for 1hour. The solution was then aspirated and the cells washed with 200µL HBS, which was then aspirated. The Chamber slides were disassembled and Prolong AntiFade Gold was added to the slides, followed by a coverslip.

Prepared slides were imaged on either an EVOS FL imaging system microscope using separate filters for DAPI (nucleus staining - ex-[357/44]/em-[447/60]), GFP (for PKH67 stained pdEV - ex-[470/22]/em-[510/42]) and RFP (for WGA membrane staining - ex-[531/40]/em-[593/40]) or using an Olympus FV1000 confocal microscope (4 lasers and 5 separate detectors for imaging fluorescence and 3D z-stacks). Confocal microscopy was carried out in the Advanced Imaging Facility with the assistance of Dr Kees Straatman (University of Leicester, Leicester) and images were processed using FIJI (Schindelin et al., 2012).

5.3.4.2   Microscopy preparation for observation of transfection

To observe transfection of PriMo, the medium was aspirated from transfected cells in 24 well plates, which were washed once with 500µL HBS and then 500µL 4% PFA was added. The plate was then imaged directly on the EVOS FL imaging system microscope.

To observe transfection of THP-1 cells, the cells were aspirated from the well, pelleted via centrifugation at 600g for 5minutes at RT and the supernatant was discarded. The cells were re-suspended in 500µL PBS and then centrifuged again at 600g for 5minutes followed by re-suspension in 300µL 4% PFA and then Cytospin slides were prepared (5.3.4.1) for imaging on the EVOS FL imaging system microscope.

5.3.5 Flow cytometry

Flow cytometry experiments were carried out essentially as described previously (2.3.9). However the specific protocols for preparing the THP-1/PriMo for analysis of CD14, CD68, LMO2 and SCARB1 are described below.

5.3.5.1   Detection of CD14 and CD68 on THP-1 cells

Cells from 1 well of a 24 well plate (1×10^6 cells) were aspirated and centrifuged at 600g for 5minutes. Cells were then re-suspended in 400µL of HBS and 50µL was added to a tube containing 2µL CD14-VioBlue (Miltenyi Biotec) [130-098-05 – Clone: TÜK4], 3µL of CD68-FITC (Miltenyi Biotec) [130-100-299 – Clone: Y1/82A] and 45µL HBS and then incubated at RT in the dark for 20minutes. For control experiments the samples were incubated with isotype antibodies Mouse IgG2a-VioBlue (Miltenyi Biotec) [130-098-898 - Clone: S43.10] and Mouse IgG2b-FITC isotype (Miltenyi Biotec) [130-099-119 – Cloe: IS6-11E5.11]. The samples were then diluted with 200µL 0.2%FS (v/v) and incubated at RT in the dark for a further 20minutes before analysis with the Gallios Flow Cytometer.

5.3.5.2   Measuring pdEV uptake into cells

Uptake of pdEV into THP-1 cells was measured using flow cytometry, following co-incubation of THP-1 cells with PKH67 stained pdEV for up to 24hours the cells were washed twice by pelleting at 600g for 5minutes and then re-suspending in 500µL HBS. After the second wash 50µL of the solution was added to a separate tube and 2µL of CD14-VioBlue was added and incubated for 30minutes at RT. The solution was then diluted with 450µL of 0.2%FS and pdEV uptake was measured by gating THP-1 cells and measuring the PKH67 fluorescence in the FL1 channel.

PdEV uptake was also measured in leukocytes in whole blood using flow cytometry; pKH67 stained pdEV were co-incubated with whole blood at 37°C on a rotor for up to 24hours. 10µL aliquots were added to 38µL of HBS and 2µL of CD14-VioBlue and incubated at RT for 30minutes. The sample was then diluted with 1mL of VersaLyse (Beckmann Coulter) to lyse the red blood cells, briefly vortexed and incubated at RT for 30minutes. The samples were analysed on the flow cytometer; lymphocytes, monocytes and neutrophils were separated using FSc vs. CD14 plot and the uptake of pdEV into each separate population was measured on the FL1 channel.

5.3.5.3   Flow cytometric analysis of LMO2 and SCARB1 in THP-1 cells

Cells from 1 well of a 6 well plate (1×10^6 cells) were aspirated and pelleted at 600g for 5minutes (RT). The supernatant was discarded and the cells were re-suspended in 500µL 4% PFA and incubated at RT for 10minutes. The cells were pelleted by centrifugation at 600g for 5minutes (RT) and the supernatant discarded, and the cells re-suspended in 500µL 0.2% PBS-tween (PBS with 0.2% Tween-20) and incubated for 20minutes. The sample was then centrifuged at 600g for 5minutes (RT) and the supernatant removed followed by re-suspension in 200µL flow buffer (PBS + 10% goat serum + 0.3M Glycine) and addition of 1µL of Rabbit monoclonal primary antibodies, either Anti-LMO2 (Abcam, Cambridge, UK) [ab91652 – Clone: EP3257, 1.26µg/mL]

or Anti-Scavenging Receptor SR-B1 (Abcam) [ab52629 - clone: EP1556Y, 1.155µg/mL] and was then incubated in the dark for 30minutes. 1µL of the goat anti-rabbit secondary antibody (Abcam) [ab150079, 0.975µg/mL] was added and incubated for 30minutes in the dark; control samples only contained the secondary antibody. The final sample was then centrifuged at 600g for 5minutes (RT) and the pellet re-suspended in 400µL PBS and run on the Gallios flow cytometer.

5.3.5.4 Flow cytometric analysis of LMO2 and SCARB1 in PriMo

These incubations were carried out as described above, except the cells remained attached to the bottom of the wells of a 6 well plate throughout staining, therefore any centrifugation steps were replaced with simply aspirating the solution from the well and adding the next solution. Once the cells were in the flow buffer they were scraped using the rubber plunger from a sterile 2mL syringe and then the cell suspension was aspirated. Antibodies were then added and incubated in an eppendorf tube prior to centrifugation and re-suspension in PBS.

5.3.6 RT-PCR

RT-PCR for microRNA was carried out as previously described (3.3.4) using the primers in Table 5.1. Actinomycin-D (10nM) was used in RT-PCR experiment sample preparation as a control to inhibit de novo transcription. Cells were treated with Actinomycin-D for 5minutes prior to treatment with pdEV. MiR-125b was used to normalise data as it was unaffected by addition of pdEV to samples, due to its absence from platelets or by addition of Actinomycin-D, as shown in Figure 5.1.

Table 5.1 – RT-PCR microRNA primers Details, including sequences of primers used for the detection of miR-126-3p and miR-125b-3p.

microRNA	Mature targets sequence	Chromosomal location	Product code	Megaplex primer pool
hsa-miR-126-3p	UCGUACCGUGAGUAAUAAUGC	Chr .9: 136670602-136670686 [+]	4427975 - 000450	A
hsa-miR-125b-5p	UCCCUGAGACCCUAACUUGUGA	Chr.11: 121970465 – 121970552 [-]	4427975 - 000449	A
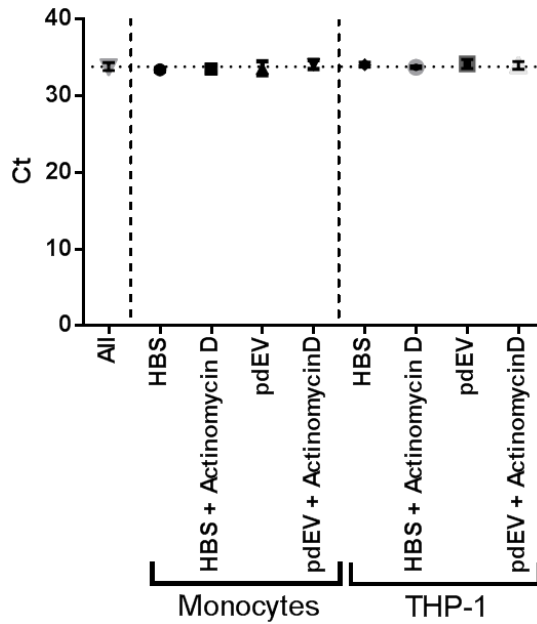
Figure 5.1 – Stability of miR-125b in monocyte and THP-1 samples MiR-125b was used to normalise PCR results, this shows that its Ct values were stable across a variety of sample types and cell types (n=5±SD).

5.3.7 Transfection

Both THP-1 cells and PriMo were transfected in culture using a forward transfection protocol with Viromer GREEN (Lipocalyx, Halle (Saale), Germany). Cells were transfected with either microRNA mimics or transfection controls, as detailed in Table 5.2. Mimics and transfection controls were purchased from Dharmacon (Dharmacon Inc., Lafayette, Colorado, USA) and were reconstituted in microRNA mimic buffer (300mM KCl, 30mM HEPES and 1.2mM $MgCl_2$) at 20µM (verified by Nanodrop).

Table 5.2 – MicroRNA mimics and microRNA mimic controls Details of the microRNA mimics and controls transfected into THP-1 cells and PriMo.

microRNA	Oligo sequence	Product code
miRIDIAN microRNA mimic hsa-miR-223-3p	UGUCAGUUUGUCAAAUACCCCA	C-300580-07-0002
miRIDIAN microRNA Mimic Negative Control 1	UCACAACCUCCUAGAAAGAGUAGA	CN-001000-01-05
SiGlo Green (Transfection control labelled with a FAM dye)	UCACAACCUCCUAGAAAGAGUAGA	D-001630-01-05

To transfect the cells they were seeded in 6 well plates in 2mL serum free RPMI-1640 media at either ~2.5×10^6 PBMCs to yield 5×10^5 PriMo, or 2.5×10^6 THP-1 cells. PriMo were transfected immediately following their isolation (5.3.1) while THP-1 cells were first transformed with 50nM VitaminD$_3$ for 60hours prior to transfection (5.4.1).

Two separate transfection solutions were prepared (volumes are per well); i) 8.4µL of 20µM microRNA mimic/scrambled control and/or transfection control was diluted in 51.6µL buffer GREEN (pH7.2 solution) to provide a total RNA concentration of 75nM/well, and mixed by pipetting and ii) 6µL of Viromer GREEN was diluted with 540µL of buffer GREEN and then vortexed for 5seconds. The solution containing Viromer GREEN was then added to the microRNA/transfection control solution, mixed by pipetting, and then incubated for 15minutes in the dark at RT. 550µL of the transfection solution was then added to each well and incubated for 24hours at 37°C and 5% CO_2 in the dark.

Experiments were carried out to optimise the transfection of PriMo and THP-1 cells. The optimisation experiments looked at the effects of cell density, volume of media, transfection time and oligonucleotide concentration. Figure 5.2 shows the final optimisation step which investigated the effects of transfecting with increasing doses of SiGlo. A concentration of 75nM was optimal for both THP-1 cells and PriMo, although the THP-1 cells transfected with significantly greater efficiency (95% vs. 36%). Figure 5.2 also shows the appearance of the positively transfected cells in the flow cytometer. Due to the low transfection efficiency of the PriMo in experiments using the microRNA mimic the mimic was co-transfected with the SiGlo to allow for selection of transfected cells via this gating strategy.

THP-1 Cells
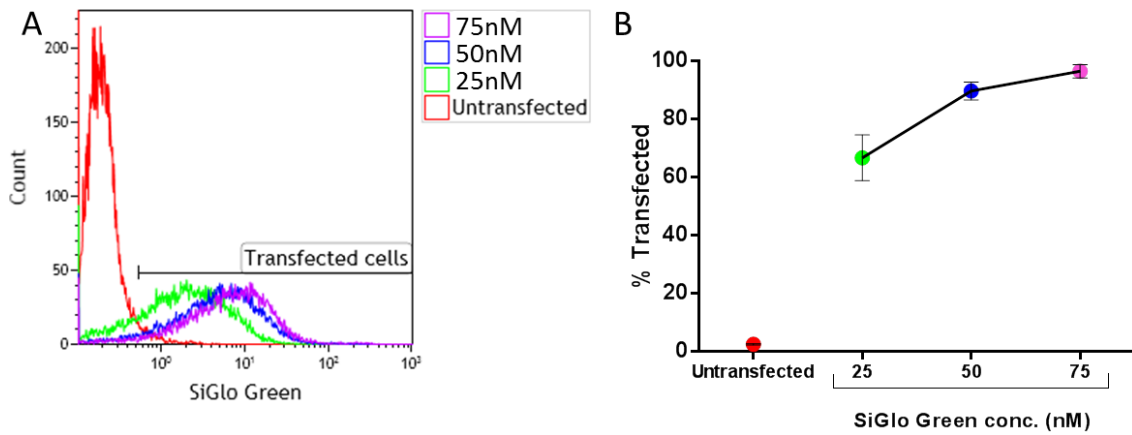
Primary human monocytes
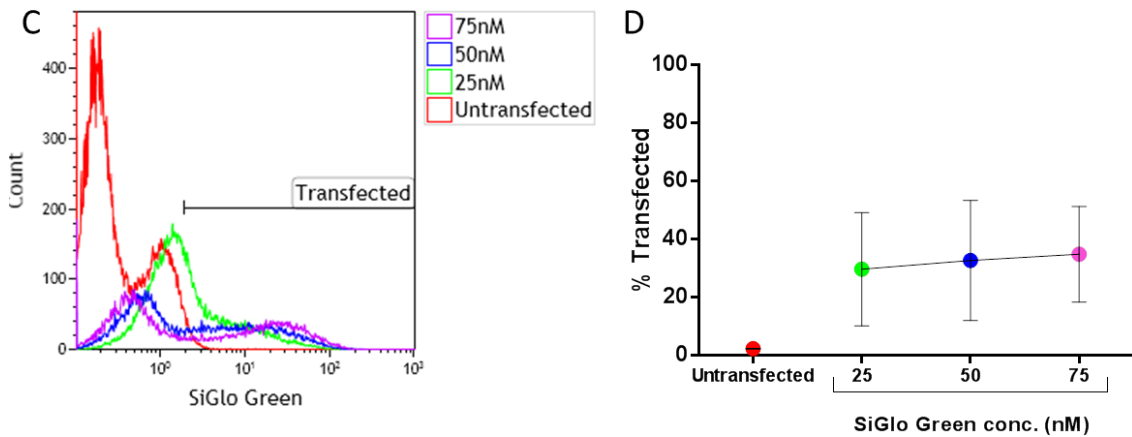
Figure 5.2 – Optimising the transfection of THP-1 cells and PriMo Cells were transfected with SiGlo using Viromer GREEN transfection reagents and then cultured at 37ºC in 5% CO_2 for 24hours before transfection efficiency was tested using flow cytometry. Cells were either left untransfected or transfected with SiGlo to produce final concentrations of 25nM, 50nM or 75nM. A) Histograms showing the level of transfection in untransfected or transfected THP-1 cells at 24hours, B) the percentage of transfected THP-1 cells (n=3). C) Histogram of untransfected and transfected PriMo and D) the percentage of positively transfected PriMo in each condition (n=3).

5.4 Results

5.4.1 Transformation of THP-1 cells

THP-1 cells are an acute monocytic leukaemia cell line that has been used widely in research into monocytes and macrophages. PriMo are challenging to extract in large quantities, undergo phenotypic changes and do not survive for more than a week in culture, unlike the THP-1 cell line which provides researchers with more consistent responses. Normally THP-1 cells exhibit pre-monocytic characteristics and therefore require differentiation before they exhibit monocytic characteristics (Daigneault et al., 2010, Maess et al., 2014). Both PMA and VitaminD3 have been widely used to differentiate THP-1 cells to macrophage and monocytic cell states respectively, but the specific use of these agents to transform the cells is not universal. Therefore guided by the work of Daigneault *et al.* we tested varying doses of these agents, to observe the differentiation of THP-1 cells to monocytes and macrophages.

It was expected that monocytes would express CD14, remain in suspension and have a rounded morphology lacking granules, whereas macrophages would be CD68 positive, adhere to the culture plate, have an increased cytoplasm relative to the nucleus and greater granularity. THP-1 cells were therefore cultured with PMA and VitaminD3 for 4 days and the levels of CD14 and CD68 were measured by flow cytometry every 12hours (5.3.5.1) (Figure 5.3 and Figure 5.4), morphology and adherence was observed every 24hours (Figure 5.5) using microscopy.

Figure 5.3 shows that prior to treatment the THP-1 cells did not express CD14 and that following 24hours there was no change in CD14 expression with either treatment. After 36hours ~30% of THP-1 cells treated with VitaminD3 (50nM or 100nM) displayed a significant increase in CD14 (p=<0.0001). At consecutive time points there was a steady increase in CD14 following treatment with VitaminD3 which peaked at 80% after 60hours and decreased to ~50% by 72hours; possibly caused by exhaustion of the medium. THP-1 cells that were either untreated, or treated with PMA (50, 100 and 150nM) displayed no change in CD14 expression over the 4 days.

The expression of CD68 showed a very different pattern to that of CD14 (Figure 5.4), VitaminD3 caused no change in CD68 expression over the 4days and matched the untreated control. However, treatment with PMA induced a significant increase in CD68 expression after 36hours compared to the control and VitaminD3 samples (p=<0.01). This increase continued throughout the 4days with a maximal CD68 expression of ~12% with both 100nM and 150nM PMA at 96hours (p=<0.0001).
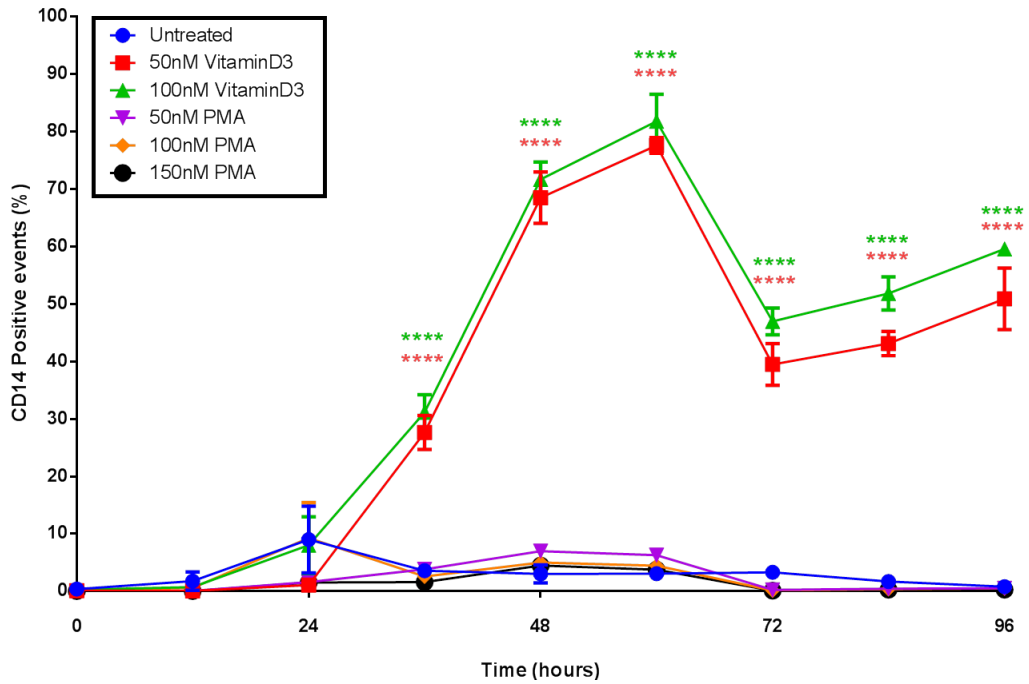
Figure 5.3 – CD14 expression changes on transformed THP-1 cells *THP-1 cells were cultured for 4days after treatment with VitaminD3 (50nM and 100nM) and PMA (50nM, 100nM and 150nM). Levels of CD14 expression were tested using flow cytometry every 12hours (n=3±SD, Repeated measures 2-way ANOVA with Tukey's multiple comparison test, each VitaminD3 condition vs. control and all PMA conditions).*
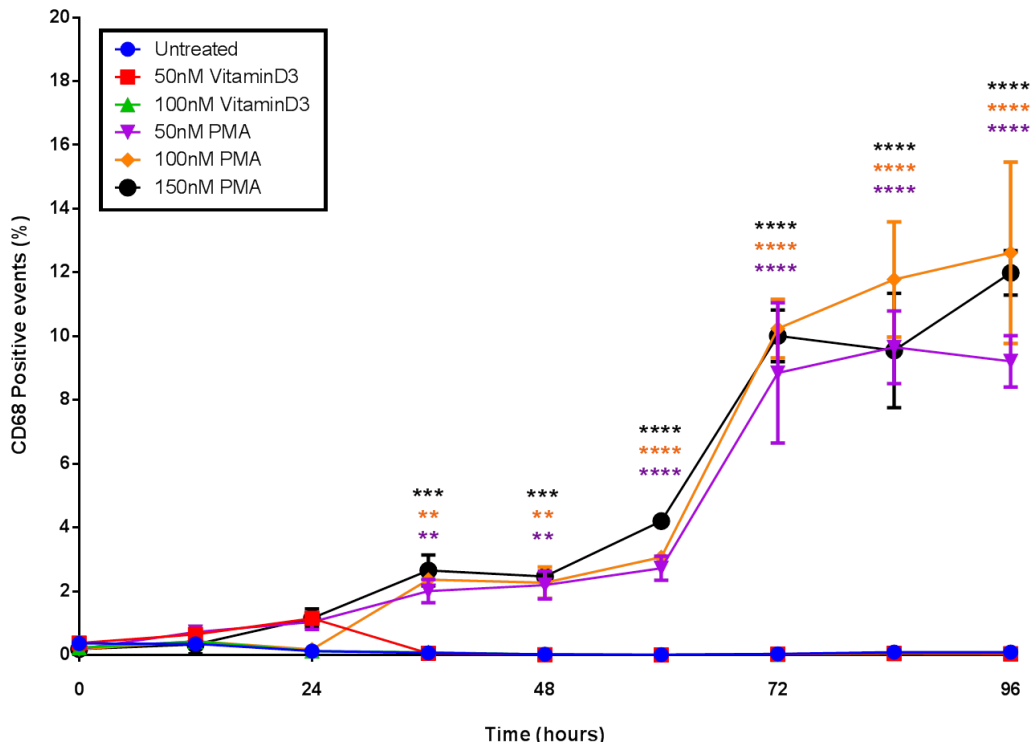
Figure 5.4 – CD68 expression on transformed THP-1 cells *THP-1 cells were cultured for 4days after treatment with VitaminD3 (50nM and 100nM) and PMA (50nM, 100nM and 150nM). Levels of CD68 expression were tested using flow cytometry every 12hours (n=3±SD, Repeated measures 2-way ANOVA with Tukey's multiple comparison test, each PMA condition vs. control and all VitaminD3 conditions).*

The morphological changes observed by microscopy showed that the cells treated with VitaminD3 (50/100nM) were not significantly different to the untreated control whereas the

cells treated with PMA (50/100/150nM) were larger, more granular and overgrew each other (Figure 5.5). In addition while THP-1 cells treated with VitaminD3 displayed similar adherence to the untreated control almost all cells treated with PMA became adherent, this is shown in the zoomed sections of Figure 5.5, where the VitaminD3 cells clearly appear more rounded and detached compared to the flattened morphology of the cells treated with PMA.
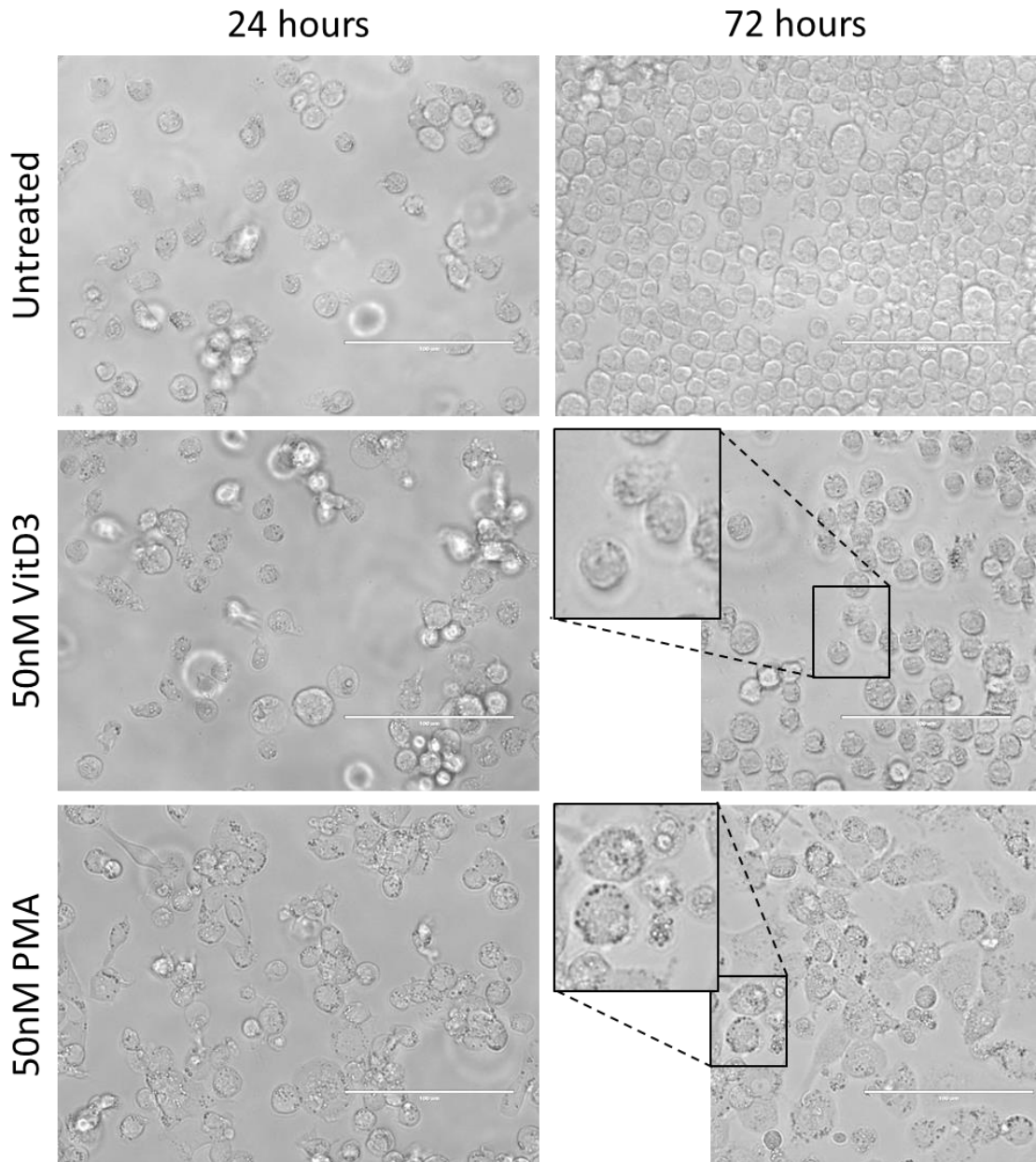
Figure 5.5 – THP-1 cell morphology following treatment *THP-1 cells were imaged using a light microscope with a 40x objective every 24hours. Images are representative of multiple images from 3 separate repeats (scale bars represent 100μm).*

Taken together these experiments showed that without treatment THP-1 cells were pre-monocytic but treatment with VitaminD3 (50/100nM) resulted in a monocytic phenotype with

the cells being rounded, non-granular and non-adherent and expressing CD14 but not CD68. However following treatment with PMA (50/100/150nM) the cells became more granular and adherent, did not express CD14 but became positive for CD68, consistent with a macrophage-like phenotype. These changes were reproducible as shown by the close correlation between the data from different experiments. Since the aim of the experiments in this chapter was to investigate the interactions of pdEV with monocytes, treatment of THP-1 with 50nM VitaminD3 for 60hours was selected as producing the most monocytic-like phenotype; the higher concentration (100nM) of VitaminD3 gave no greater effect and the expression of CD14 peaked at 60hours.

5.4.2 Transfer of pdEV to monocytes

5.4.2.1 Generation of fluorescent pdEV

Platelets were stained with PKH67 and then activated to generate pdEV with fluorescent membranes (5.3.3). Figure 5.6 demonstrates PKH67-stained platelets observed with the EVOS FL imaging system, the stained pdEV that they release and an image of unstained pdEV. These samples were then analysed using the Gallios flow cytometer to determine their relative fluorescence. The histogram in Figure 5.6 demonstrates that the platelets were effectively stained with PKH67 and that all of the detectable pdEV they released were also fluorescent. The lower level of fluorescence of the pdEVs probably reflects their smaller size.
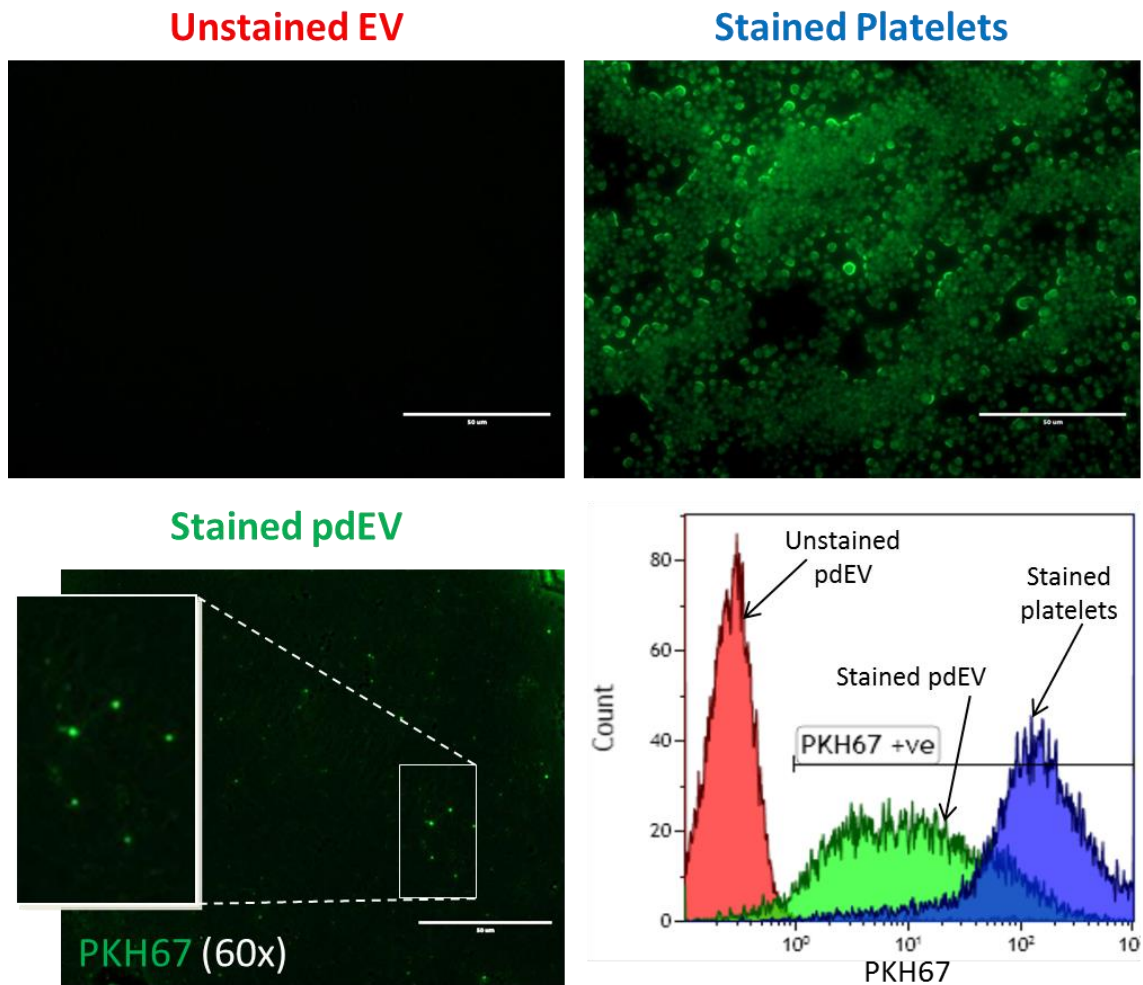
Figure 5.6 – Staining of pdEV with PKH67 To observe transfer of pdEV they were stained with PKH67. Platelets were treated with PKH67 and then stimulated to trigger pdEV release, followed by centrifugation to isolate them. The images show the fluorescence of unstained pdEV, PKH67 stained platelets and PKH67 stained pdEV viewed through a 60x objective (scale bars represent 50µm). The fluorescence from unstained pdEV (red), stained platelets (blue) and stained pdEV (green) was also detected using flow cytometry on the FL1 channel.

5.4.2.2 Microscopy to analyse pdEV uptake into THP-1 cells and PriMo

Fluorescent pdEV were incubated with THP-1 cells or PriMo for 16-24hours and uptake was observed using the EVOS FL Imaging system (Figure 5.7) and an Olympus FV1000 confocal microscope (Figure 5.8/Figure 5.9/Figure 5.10). PdEV were added to cells at a ratio that reflected that of platelets and monocytes in peripheral blood (~1000 platelets:1 monocyte). The images from the EVOS FL imaging system (Figure 5.7) showed that the pdEV were associated with the THP-1 cells. However, what was not clear was whether the pdEV were inside the cells or attached to the outside, therefore higher resolution confocal microscopy was employed to investigate the positioning of the pdEV. Cells were co-stained with DAPI and WGA-Texas red to identify the cell nuclei and membrane respectively.
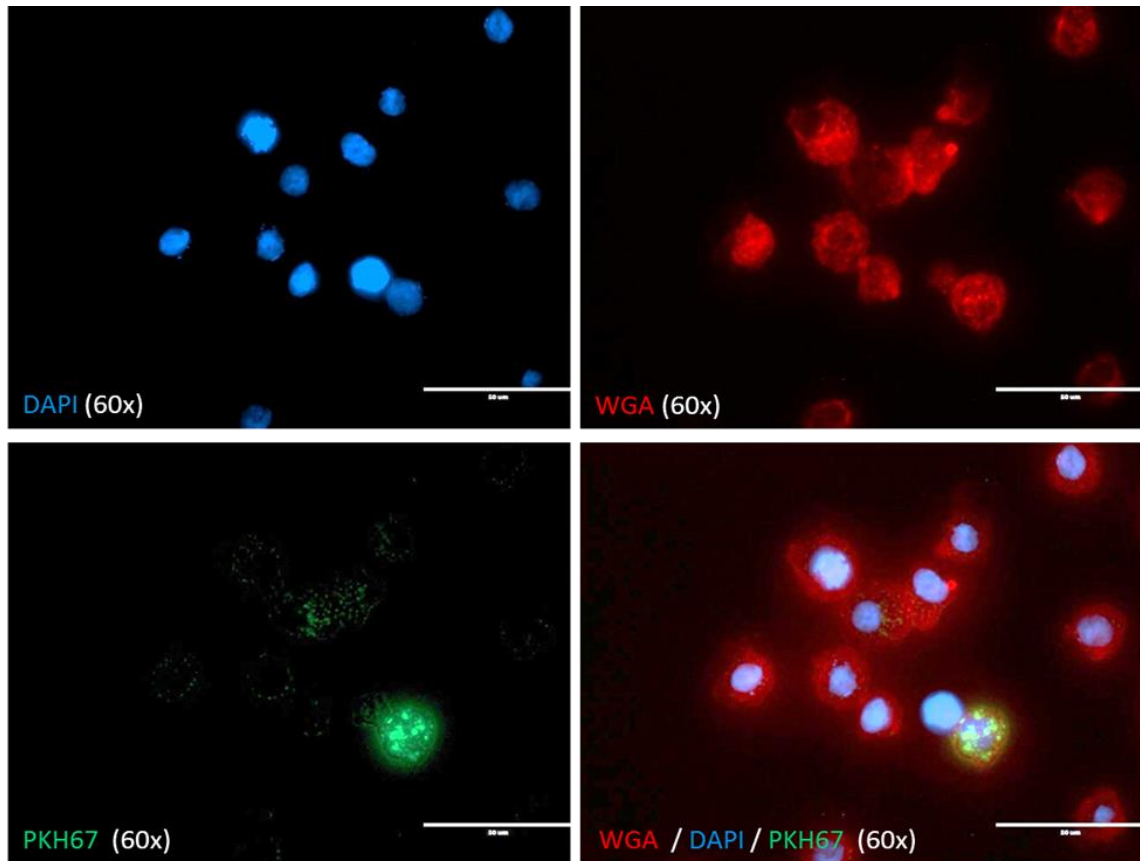
Figure 5.7 – PdEV uptake into THP-1 cells *THP-1 cells transformed with 50nM VitaminD3 for 60hours were incubated with pdEV stained with PKH67 for 16hours and then stained with DAPI and WGA and then imaged using an EVOS FL imaging system microscope using a 60x objective. A) DAPI stained cells, B) WGA staining, C) PKH67 staining and D) an overlay of the other 3 fluorescent images (scale bar represents 50µM).*
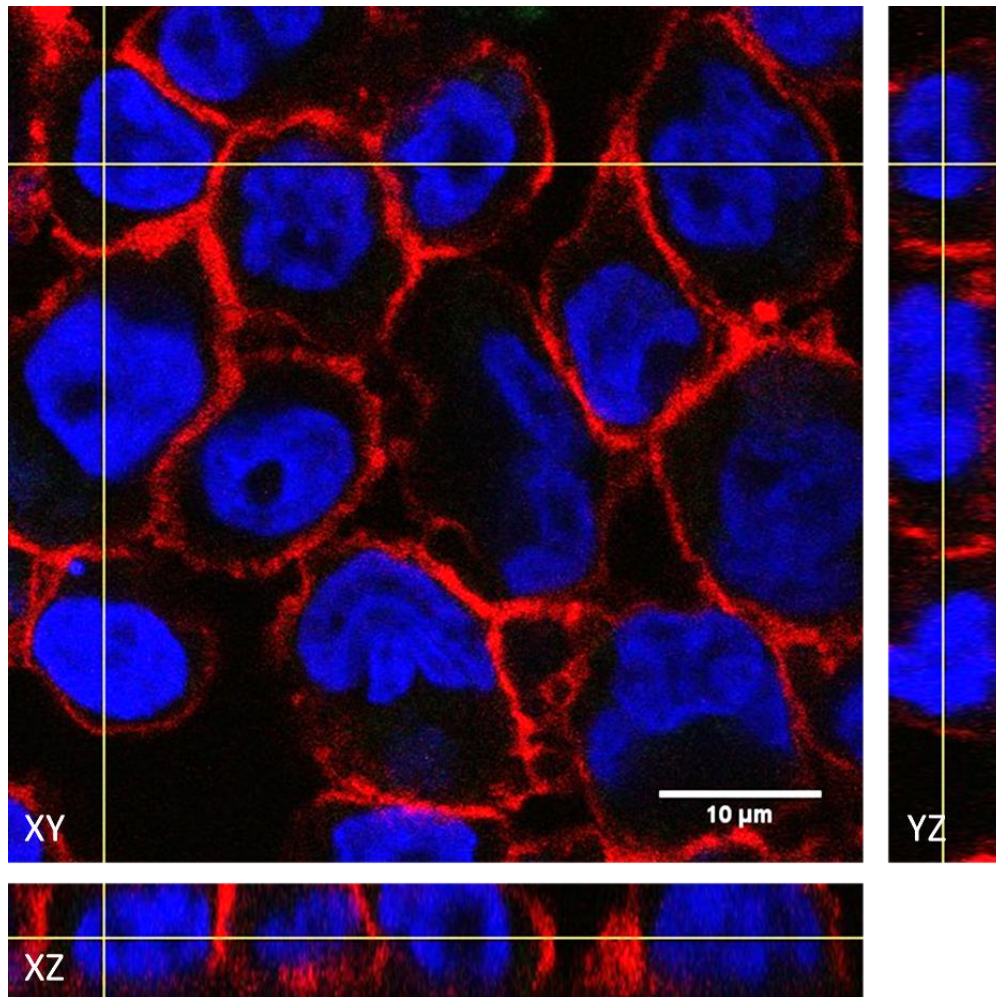
Figure 5.8 – Confocal microscopy orthogonal slices of THP-1 cells supplemented with unstained pdEV *THP-1 cells were incubated with unstained pdEV for 16hours, cells were then washed, fixed and stained with DAPI and WGA (Texas-red) and microscopy slides were prepared by cytospinning the fixed cells. Z stacks of the sample were obtained using an Olympus FV1000 confocal microscope and a single Z-axis slice of the XY stack is shown alongside orthogonal slices in the YZ (right) and XZ (bottom) axis. Images were taken on a 60x objective with 4x zoom.*

The confocal microscopy images showed that there was no detection of pdEV within THP-1 cells in the control when unstained pdEV were added (Figure 5.8). In the images taken with stained pdEV (Figure 5.9) it was clear that the pdEV were located within the cell cytoplasm. The Figure 5.9 YZ-orthogonal slice clearly showed the presence of pdEV within the cytoplasm of 5 separate cells and the same was seen for 3 cells on the XZ-orthogonal slice. These experiments were repeated in PriMo (Figure 5.10) which demonstrated that the PriMo internalised pdEV in a similar pattern to the THP-1 cells.
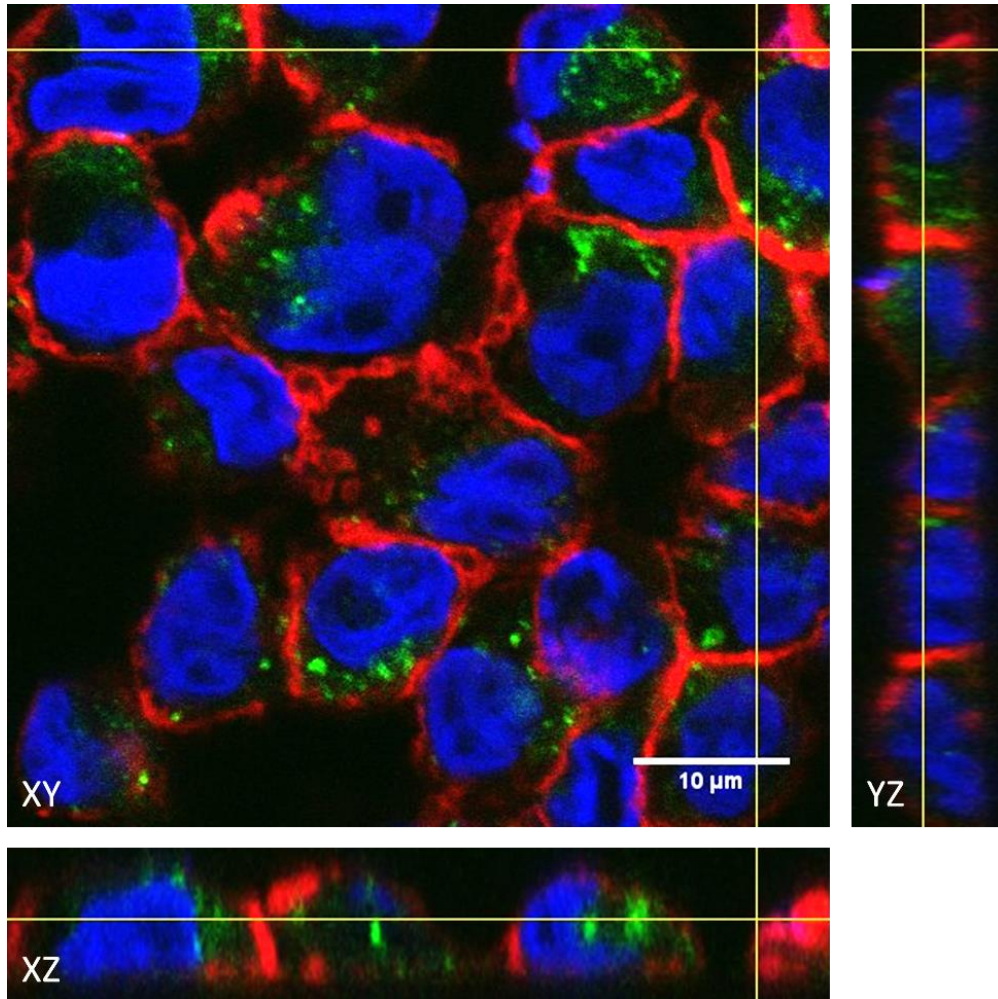
Figure 5.9 – Confocal microscopy orthogonal slices of THP-1 cells supplemented with PKH67 stained pdEV *THP-1 cells were incubated with PKH67 stained pdEV for 16hours, cells were then washed, fixed and stained with DAPI and WGA (Texas-red). Microscopy slides were prepared by cytospinning the fixed cells and Z stacks of the sample were obtained using an Olympus FV1000 confocal microscope and a single Z-axis slice of the XY stack is shown alongside orthogonal slices in the YZ (right) and XZ (bottom) axis. Images were taken on a 60x objective with 4x zoom.*
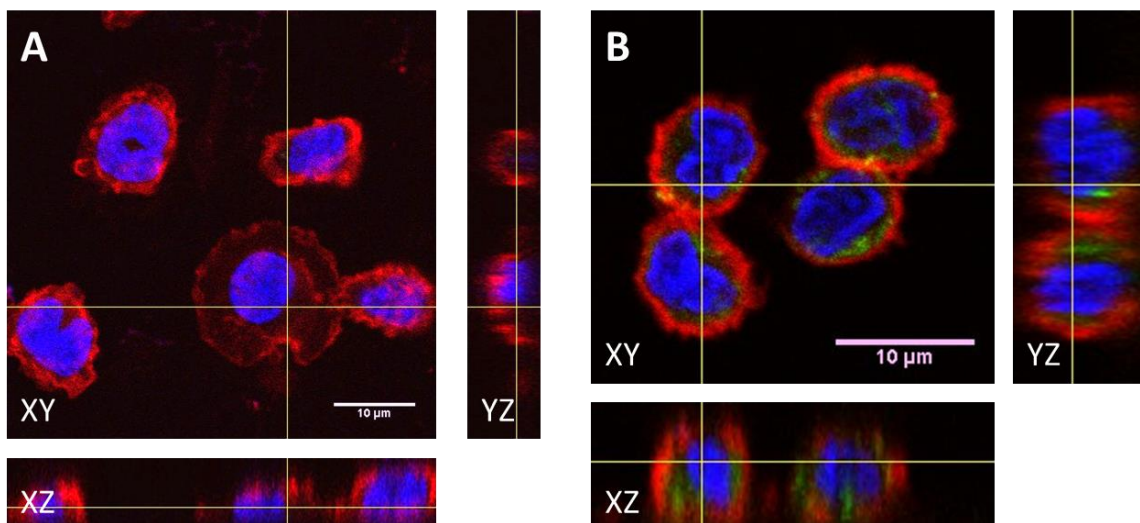
Figure 5.10 – Confocal microscopy orthogonal slices of PriMo treated with pdEV *PriMo were incubated with A) unstained pdEV or B) PKH67 stained pdEV for 16hours on cell culture chamber slides. Cells were then washed, fixed and stained with DAPI and WGA (Texas-red) and then Z stacks of the sample were obtained using an Olympus FV1000 confocal microscope and a single Z-axis slice of the XY stack is shown alongside orthogonal slices in the YZ (right) and XZ (bottom) axis. Images were taken on a 60x objective with 4x zoom.*

220

5.4.2.3   Measurement of pdEV uptake into THP-1 cells and whole blood leukocytes

The confocal images provided visual confirmation that pdEV were being taken up by monocytes, however this was in culture and only a few cells could be imaged at a time. Therefore flow cytometry was used to observe the uptake of fluorescent pdEV in whole blood and THP-1 cells. Cells were treated with pdEV, again maintaining the platelet:monocyte ratio of peripheral blood, for 24hours and pdEV uptake was assessed every 4hours.

In THP-1 cells the uptake steadily increased over 24hours with pdEV being detected in ~85% of cells after 24hours (Figure 5.11A). In whole blood the monocytes were labelled with CD14, which, when combined with FSc allowed for their discrimination from the other leukocyte populations (Figure 5.11B). The fluorescence was then measured in the lymphocyte, monocyte and neutrophil populations at each time point (Figure 5.11C). There were lower levels of uptake over the first 2hours, but after 4hours the uptake was in monocytes significantly greater than both neutrophils and lymphocytes (p=<0.0001) and this difference continued over the 24hours with peak uptake being observed at ~80% after 20hours. The uptake in both neutrophils and lymphocytes, was limited, suggesting that monocytes were the main target for pdEV. When the uptake profile of THP-1 cells was compared to whole blood monocytes (Figure 5.11D) the pattern was almost identical, apart from PriMo showing a slight and insignificant increase in uptake after 4hours.
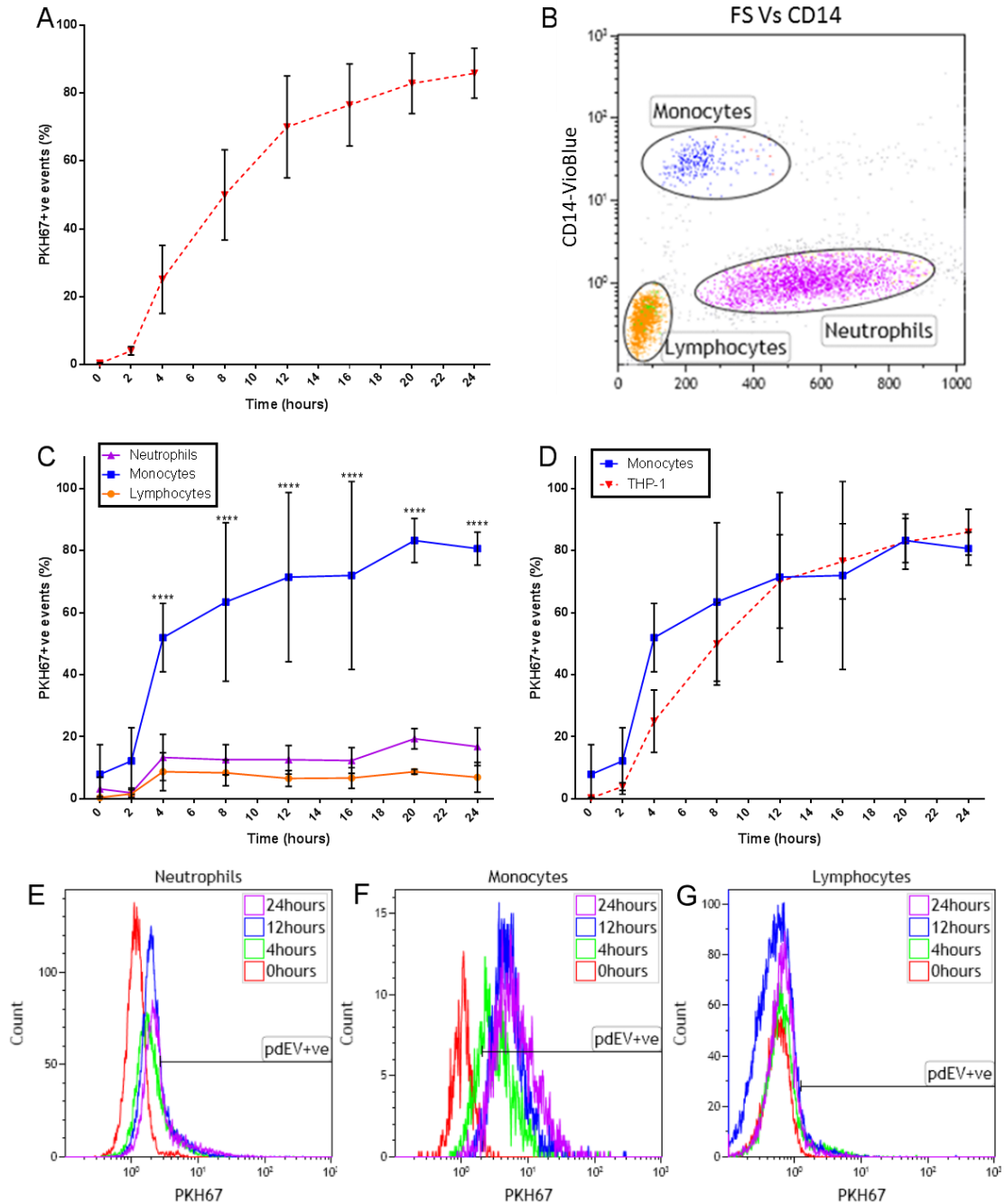
Figure 5.11 – PKH67 stained pdEV uptake into THP-1 cells and whole blood *Cells were incubated with PKH67 stained pdEV for 24hours and uptake was observed at 0, 2, 4, 8, 12, 16, 20 and 24hours using flow cytometry. A) Uptake in THP-1 cell cultures (n=3±SD), B) The gating strategy used on the flow cytometer for separating the leukocyte populations in whole blood, the blood was incubated with a CD14 antibody to allow for the separation of monocytes and the other populations were selected based on FSc C) Uptake in whole blood, comparing monocytes, lymphocytes and neutrophils (n=3±SD, 2 way ANOVA with Tukey's Multiple comparison test) and C) uptake comparison between THP-1 cells in culture and monocytes in whole blood (n=3±SD, Multiple t-tests with Holm-Sidak multiple correction). Histograms showing the increase in uptake at 0hours, 4hours, 12hours and 24hours are shown from E) neutrophils, F) monocytes and G) lymphocytes.*

5.4.2.4 Transfer of pdEV microRNA to monocytes

PriMo and THP-1 cells were co-incubated with pdEV for 16hours, with and without Actinomycin-D, to prevent results being confounded by de-novo transcription. The cells were washed twice

with PBS and lysed with Qiazol, the RNA was extracted using the miRNeasy kit (3.3.1.1) and reverse transcribed (3.3.2). MiR-223-3p, miR-126-3p and miR-125b were measured by RT-PCR; miR-223-3p and miR-126-3p were analysed to determine their transfer between the cells in pdEV and miR-125b was used as a control due to its absence from pdEV and stability following cellular treatment with Actinomycin-D as shown previously (Figure 5.1) (Laffont et al., 2015).

5.4.2.4.1   PdEV microRNA transfer to THP-1 cells

Figure 5.12 shows the transfer of miR-223-3p and miR-126-3p to THP-1 cells via pdEV with the relative expression calculated using the $2^{-\Delta\Delta Ct}$ method (3.3.6.3), and relative FC, calculated for each individual sample compared to the HBS control. THP-1 cells showed increased relative expression of miR-223-3p following treatment with pdEV, and this increase was not affected by the addition of Actinomycin-D, demonstrating that the increase was due to transfer rather than de-novo transcription. The increase in miR-223-3p was clearer when assessed by relative FC, showing a ~1.8-fold increase (p=0.0490) which was more significant in the presence of Actinomycin-D (p=0.0051).
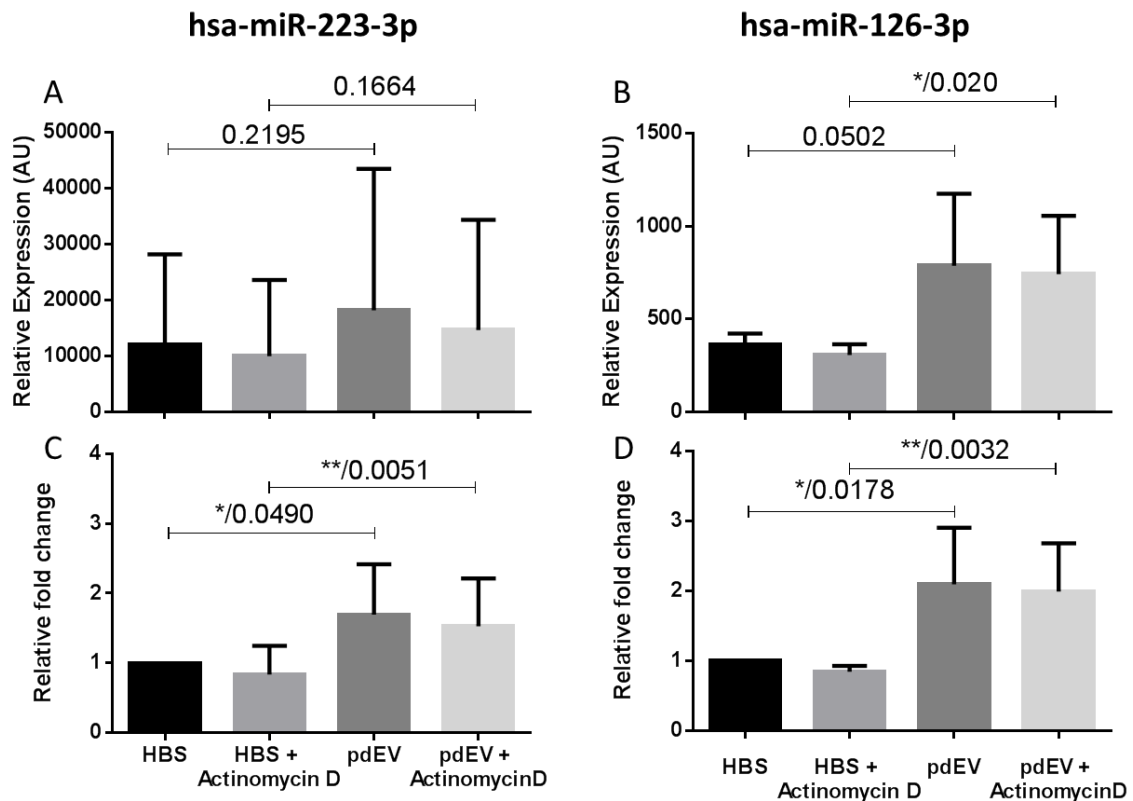
Figure 5.12 – Transfer of microRNA to THP-1 cells from platelets via pdEV THP-1 cells were incubated with HBS or pdEV in the presence or absence of Actinomycin-D for 16hours, the cells were washed, harvested and the RNA extracted. MiR-223-3p and hsa-miR-126-3p were measured in all samples and normalised using hsa-miR-125b. A) Shows the change in relative expression of hsa-miR-223-3p and B) Shows the change in relative expression of hsa-miR-126-3p (n=5±SD paired t-tests). C) Shows the relative FC compared to the control HBS samples for each replicate for hsa-miR-223-3p and D) Shows the relative FC for hsa-miR-126-3p (n=5±SD ratio paired t-test).

The results also showed an increase in miR-126-3p in THP-1 cells treated with pdEV; the relative expression showed consistent increases, and this was statistically significant in the presence of Actinomycin-D (p=0.02). The significance was greater when the relative FC was assessed, with ~2-fold changes being seen in both sets of conditions (p=0.0178 without Actinomycin-D and p=0.0032 with Actinomycin-D). Both these sets of results provide strong evidence that pdEV shuttle microRNA to THP-1 cells.

5.4.2.4.2   pdEV microRNA transfer to PriMo

The same experiment was repeated using PriMo in place of THP-1 cells. The relative expression results for miR-223-3p showed that following incubation with pdEV the PriMo also showed increased expression that was significant in the presence of Actinomycin-D (p=0.0163), however when the relative FC was analysed these results did not quite reach statistical significance; a reflection of the greater variability in the change between donors compared to the variability between experiments with the THP-1 cells (p=0.0651 without Actinomycin-D and p=0.0581 with Actinomycin-D). The results for miR-126-3p again showed stronger changes, with relative expression increases being significant both in the presence and absence of Actinomycin-D (p=0.0056 and p=0.0161 respectively). The significance of this increase was best shown by looking at the relative FC, where a ~4-fold change was observed in the absence of Actinomycin-D (p=0.0054) and a ~3-fold change was observed in PriMo treated with Actinomycin-D (p=0.0022). Overall these results demonstrate that pdEV were able to transfer microRNA to PriMo in culture and that there was a significant increase in both miR-223-3p and miR-126-3p.

hsa-miR-223-3p
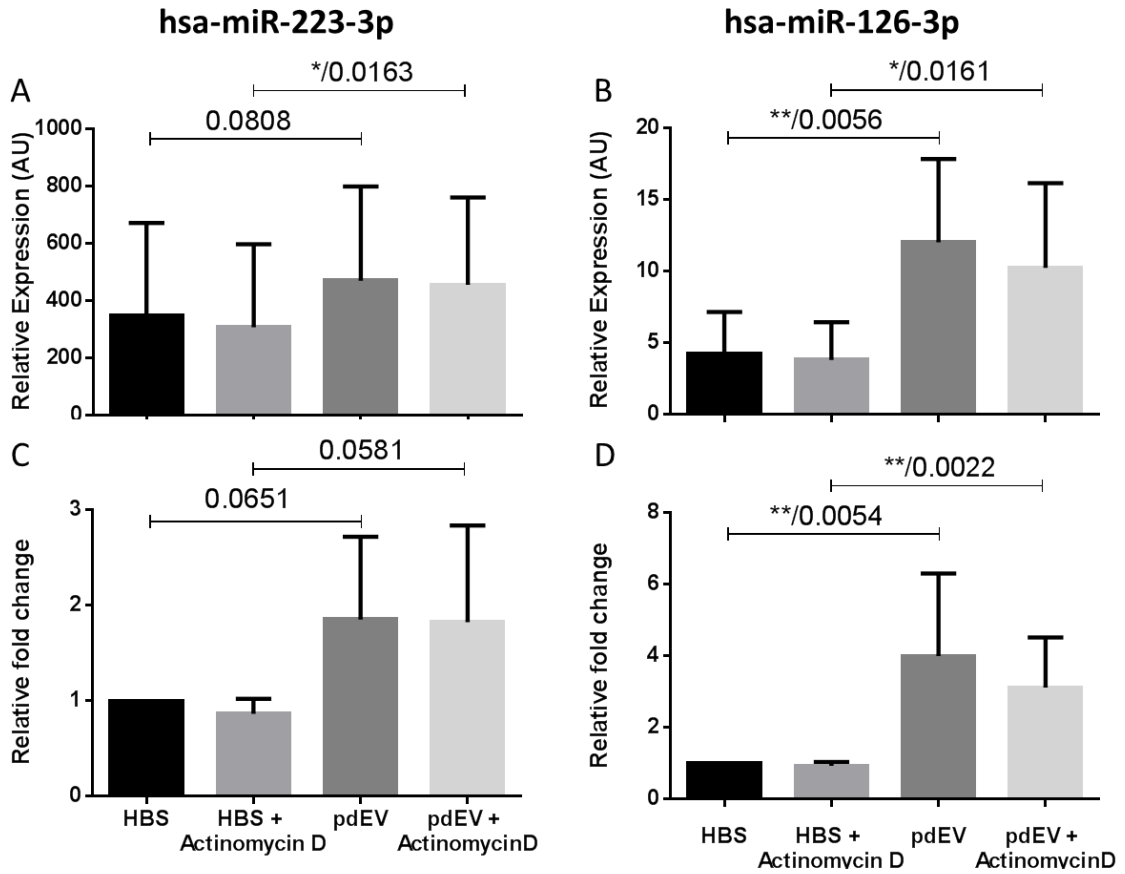
hsa-miR-126-3p

Figure 5.13 – Transfer of microRNA to PriMo from platelets via pdEV *PriMo were incubated with HBS or pdEV in the presence or absence of Actinomycin-D for 16hours, the cells were washed, harvested and the RNA extracted. MiR-223-3p and hsa-miR-126-3p were measured in all samples and normalised using hsa-miR-125b. A) Shows the change in relative expression of hsa-miR-223-3p and B) Shows the change in relative expression of hsa-miR-126-3p (n=5±SD paired t-tests). C) Shows the relative FC compared to the control HBS samples for each replicate for hsa-miR-223-3p and D) Shows the relative FC for hsa-miR-126-3p (n=5±SD ratio paired t-test).*

5.4.3 Effect of miR-223-3p on SCARB1 and LMO2

Due to the low transfection efficiency in PriMo, as shown earlier (Figure 5.2) microRNA mimics were co-transfected with SiGlo to allow for the selection of positively transfected cells. While the earlier experiments optimised the transfection protocol they did not indicate the optimal conditions for causing and observing functional effects of miR-223-3p following transfection into cells. Therefore the time period (Figure 5.14) and dosage required (Figure 5.15) to trigger LMO2 and SCARB1 protein expression changes were investigated.

5.4.3.1 Effect of miR-223-3p on SCARB1 and LMO2 - Timecourse

THP-1 cells were simultaneously transfected with SiGlo (37.5nM) and miR-223-3p mimic/Scrambled control (37.5nM) and then incubated for 24/48hours at 37°C in 5% CO_2 (5.3.7). The cells were then fixed, permeabilised and stained with antibodies for SCARB1 and LMO2 according to the protocol outlined in 5.3.5.3.

The time course demonstrated that 24hours was the optimal time point for changes in both proteins in THP-1 cells. The percentage of LMO2+ve cells (Figure 5.14A) and the median fluorescence intensity (MFI) (Figure 5.14C) was reduced by miR-223-3p after 24hours compared to the scrambled microRNA control. However, after 48hours the LMO2 expression in response to the miR-223-3p mimic was above that of the control, perhaps suggesting a compensation for the earlier reduction. SCARB1 expression was reduced at both 24 and 48hours by the miR-223-3p mimic compared to the scrambled control, this change was evident looking at both the percentage of positive cells (Figure 5.14B) and the median fluorescence intensity (Figure 5.14D). Therefore 24hours was selected as the optimal time period for further examination of the effects of miR-223-3p on LMO2 and SCARB1 protein expression.
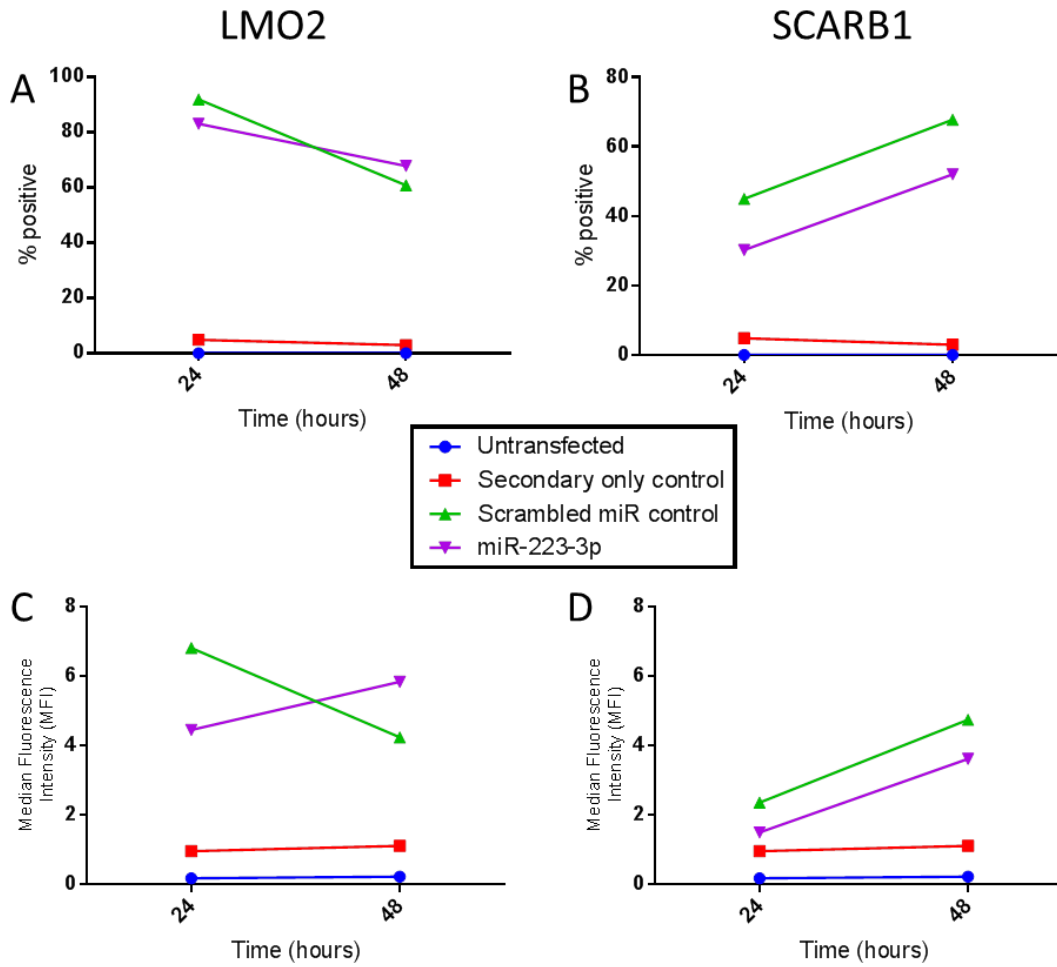
Figure 5.14 – Optimisation of time point for detecting effects of miR-223-3p mimic *2.5x10^6 THP-1 cells were plated into 6 well tissue culture dish and transfected with a mixture of SiGlo (37.5nM) and miR-223-3p mimic/scrambled microRNA control (37.5nM) and then incubated for 24 or 48hours at 37°C in 5% CO$_2$. Cells were then fixed, permeabilised and stained with antibodies for LMO2 and SCARB1 and protein expression detected using flow cytometry, cells were gated for positive transfection using the SiGlo (FAM) and then LMO2 and SCARB1 expression was measured in the positively transfected population (Alex Fluor 647). The percentage of LMO2 (A) and SCARB1 (B) positive cells and the median fluorescence intensity of LMO2 (C) and SCARB1 (D) was measured after 24 and 48hours in all conditions (n=2).*

5.4.3.2   Effect of miR-223-3p on SCARB1 and LMO2 – Dose response

The concentration of miR-223-3p mimic added was also varied to determine if this would increase the change in protein expression after 24hours. THP-1 cells were prepared as before and transfected with 30, 60 or 90nM of the miR-223-3p mimic or 90nM of the scrambled control and the effect on LMO2 and SCARB1 expression at 24hours was analysed as before. The results in Figure 5.15 demonstrate that for LMO2 there was no clear effect of increasing the dose, with the percentage of positive cells reducing by similar amounts with all three mimic concentrations. The changes in MFI were varied but had no pattern to suggest a dose dependent response. With SCARB1 the increase in microRNA mimic surprisingly resulted in an increase in the number of positive cells and MFI. Therefore for subsequent experiments the mimics were used at a dose of 37.5nM and the SiGlo concentration was also set at 37.5nM. For both LMO2 and SCARB1 the level of expression was unaffected by the presence of the Scrambled miR control or miR-223-3p mimic (data not shown).
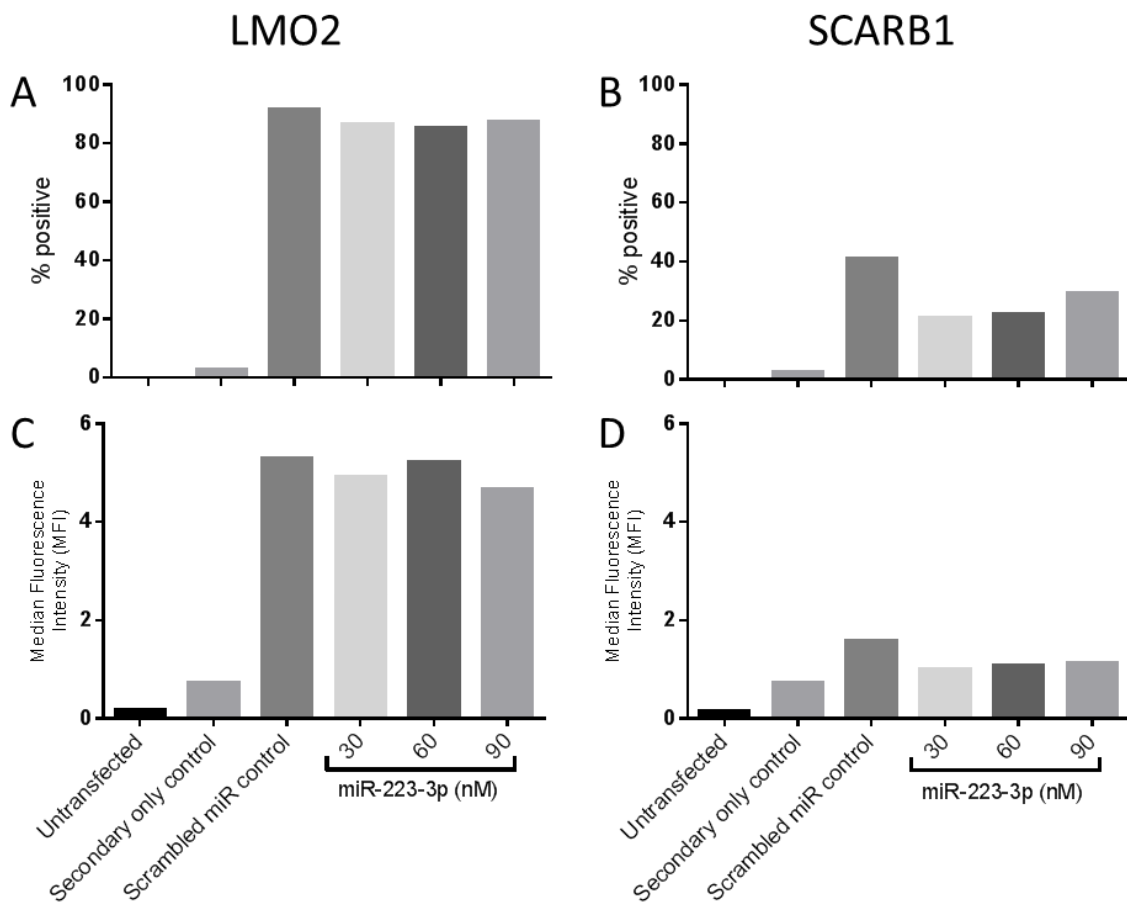
Figure 5.15 – Optimisation of miR-223-3p concentration *2.5x10^6 THP-1 cells were plated into 6 well tissue culture dish and transfected with a mixture of SiGlo (37.5nM) and miR-223-3p mimic (30/60/90nM) or scrambled microRNA control (90nM) and then incubated for 24hours at 37°C in 5% CO$_2$. Cells were then fixed, permeabilised and stained with antibodies for LMO2 and SCARB1 and protein expression detected using flow cytometry, cells were gated for positive transfection using the SiGlo (FAM) and then LMO2 and SCARB1 expression was measured in the positively transfected population (Alex Fluor 647). The percentage of LMO2 (A) and SCARB1 (B) positive cells and the median fluorescence intensity of LMO2 (C) and SCARB1 (D) was measured after 24 and 48hours in all conditions (n=2).*

5.4.3.3 Effect of miR-223-3p on SCARB1 and LMO2 in THP-1 cells

Following the optimisation of the miR-223-3p mimic the experiment was repeated using the optimal conditions in five separate THP-1 cultures and the effect on both LMO2 and SCARB1 was measured. Figure 5.16 and Figure 5.17 indicate that miR-223-3p was able to trigger the downregulation of both LMO2 and SCARB1. The relative amount of cells positive for LMO2 expression was significantly decreased by ~10% by the miR-223-3p mimic (p=0.0043) (Figure 5.16A) and a decrease was also observed in MFI (p=0.1169) (Figure 5.16B). Figure 5.16 shows the shift in the cell populations fluorescence caused by the miR-223-3p mimic observed on the flow cytometer (C) and the localisation of LMO2 staining within the cell (D).
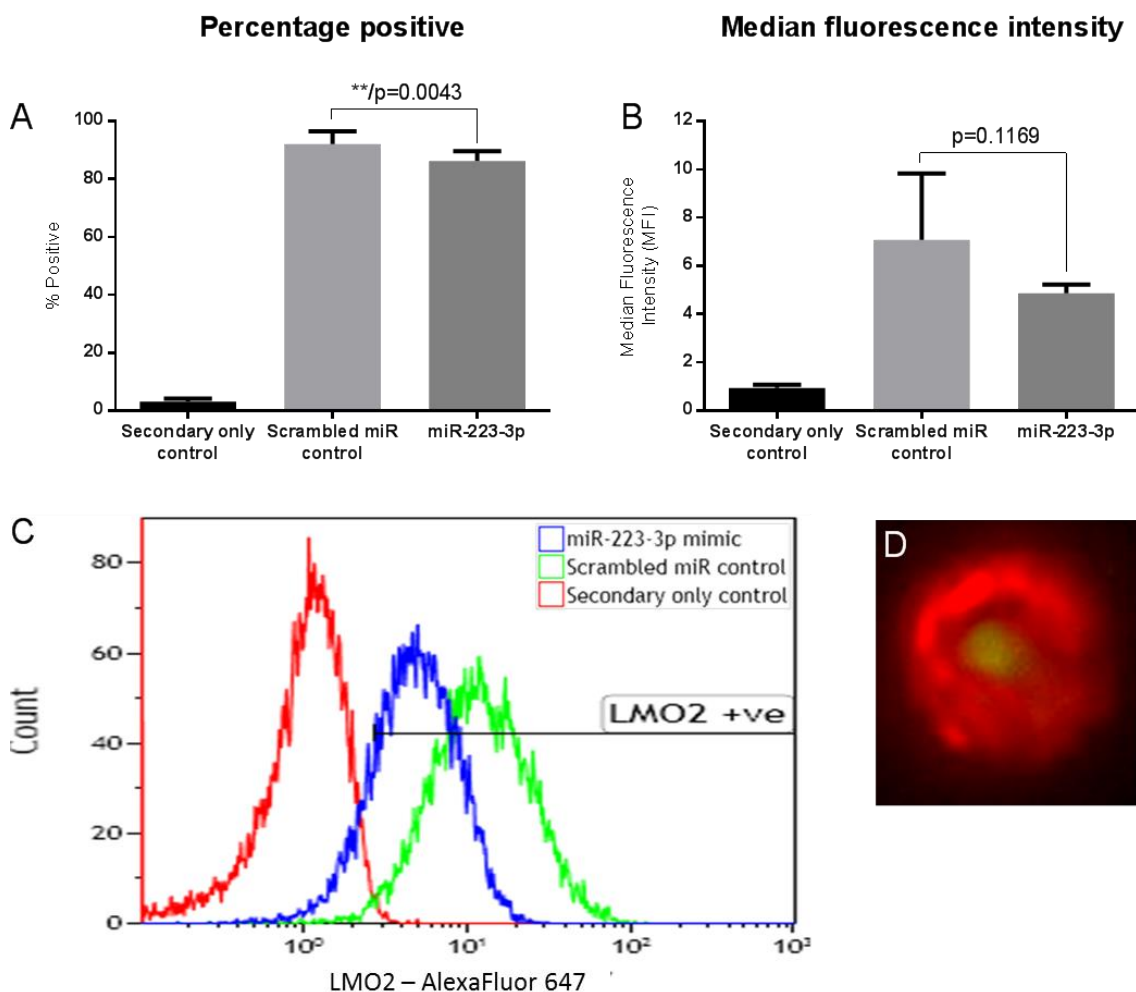
Figure 5.16 – LMO2 expression changes in response to miR-223-3p mimic in THP-1 cells *2.5x10⁶ THP-1 cells were plated into 6 well tissue culture dish and transfected with a mixture of SiGlo (37.5nM) and miR-223-3p mimic/scrambled microRNA control (37.5nM) and then incubated for 24hours at 37ºC in 5% CO_2. Cells were then fixed, permeabilised and stained with antibodies for LMO2 and protein expression detected using flow cytometry. Cells were gated for positive transfection using the SiGlo (FAM) and then LMO2 expression was measured in the positively transfected population (Alex Fluor 647). A) The number of cells positive for LMO2 following treatment with miR-223-3p compared to the scrambled control (n=5±SD paired t-test). B) The change in MFI following treatment with miR-223-3p compared to the scrambled control (n=5±SD paired t-test). C) An example of overlaid histogram traces from a signal donor and D) an example of LMO2 staining in a single THP-1 cell using fluorescence microscopy (60x objective).*

229

Figure 5.17 shows the effects of the miR-223-3p mimic on SCARB1 expression, there was a significant reduction in cells positive for SCARB1 and this was quantified as a decrease of 46% (p=0.0085) (Figure 5.17A) and the MFI was also significantly reduced by ~25% (p=0.0317) (Figure 5.17B). An example histogram is shown in (C) which demonstrates the changes in MFI and percentage positive and D shows the localisation of SCARB1 in THP-1 cells. The microscopy image corresponds to its known localisation to caveolae which are small invaginated lipid rafts in cellular plasma membranes (Babitt et al., 1997). Whilst there was a significant decrease in the amount of SCARB1 expression, only ~40% of THP-1 cells positively expressed the protein. However, taken together, the results in Figure 5.16 and Figure 5.17 indicate that miR-223-3p can control the protein levels of both LMO2 and SCARB1 in THP-1 cells.
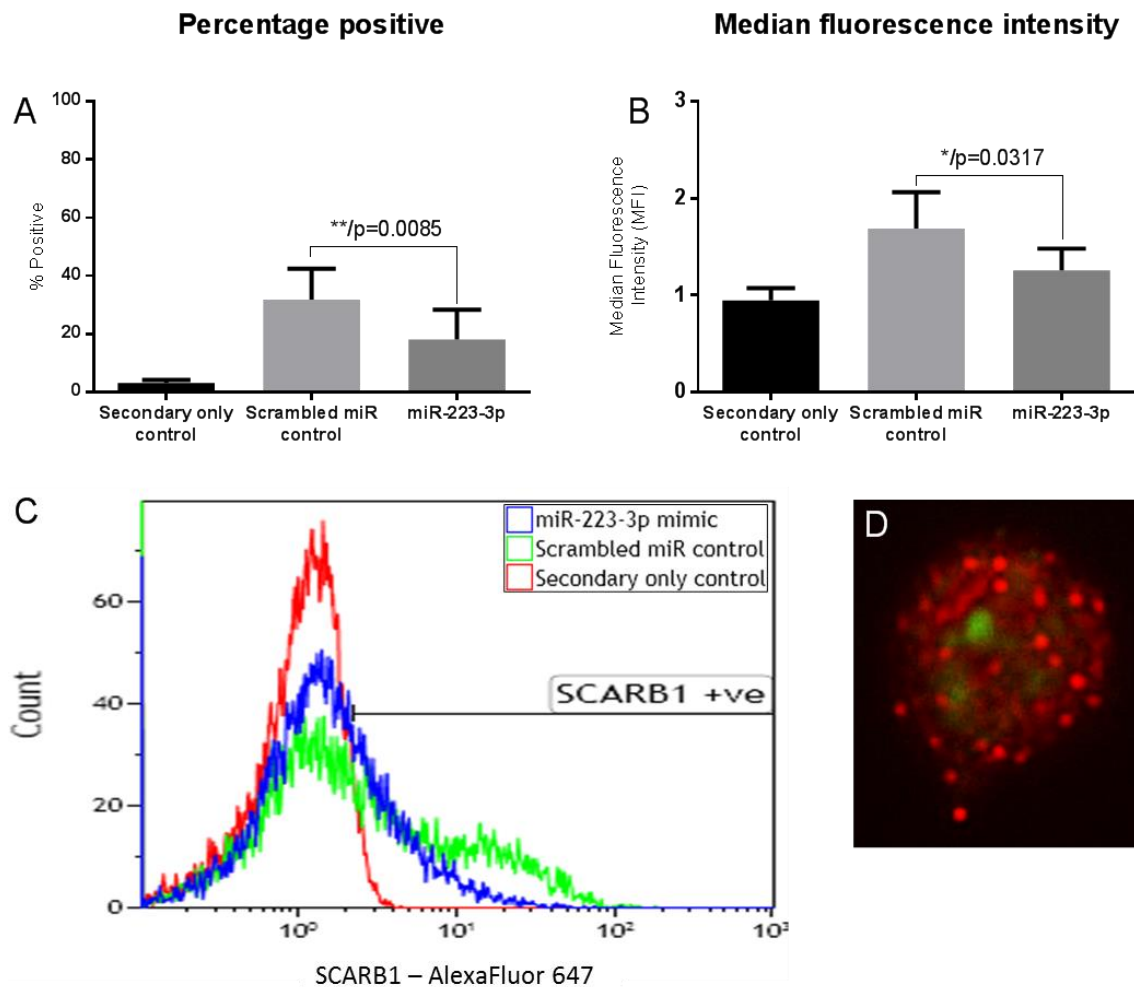
Figure 5.17 – SCARB1 expression changes in response to miR-223-3p mimic in THP-1 cells *2.5x10^6 THP-1 cells were plated into 6 well tissue culture dish and transfected with a mixture of SiGlo (37.5nM) and miR-223-3p mimic/scrambled microRNA control (37.5nM) and then incubated for 24hours at 37°C in 5% CO$_2$. Cells were then fixed, permeabilised and stained with antibodies for SCARB1 and protein expression detected using flow cytometry, cells were gated for positive transfection using the SiGlo (FAM) and then SCARB1 was measured in the positively transfected population (Alex Fluor 647). A) The change in cells positive for SCARB1 following treatment with miR-223-3p compared to the scrambled control (n=5±SD paired t-test). B) The change in MFI following treatment with miR-223-3p compared to the scrambled control (n=5±SD paired t-test). C) An example of overlaid histogram traces from a signal donor and D) an example of LMO2 staining in a THP-1 cell using a fluorescent microscope using a 60x objective.*

5.4.3.4 Effect of miR-223-3p on SCARB1 and LMO2 in PriMo

The previous experiment (5.4.3.3) was repeated in PriMo; the results in Figure 5.18 show that the miR-223-3p mimic caused a 100% increase in the number of cells positively expressing LMO2 (A) and a significant increase in the MFI of LMO2 (B, p=0.0441). However the miR-223-3p mimic did decrease the number of SCARB1 positive cells by ~40%, albeit causing no change in MFI. It should be noted, however, that only 6% of the PriMo were positive for SCARB1 and 20% for LMO2 compared to 40% and 92% of THP-1 cells, respectively.
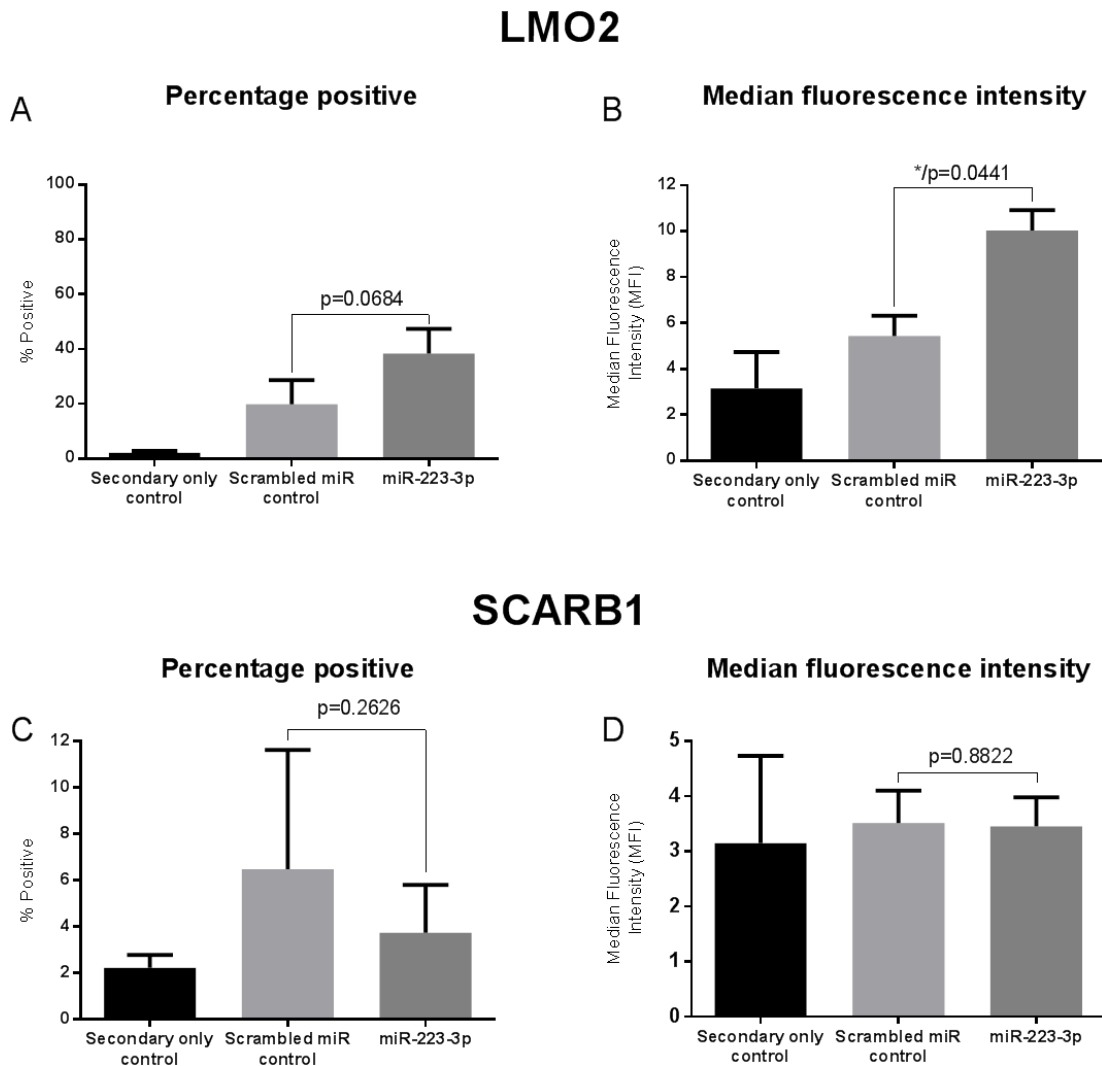
Figure 5.18 – LMO2 and SCARB1 expression changes in response to miR-223-3p mimic in PriMo $5x10^5$ PriMo were plated into 6 well tissue culture dish and transfected with a mixture of SiGlo (37.5nM) and miR-223-3p mimic/scrambled microRNA control (37.5nM) and then incubated for 24hours at 37^oC in 5% CO_2. Cells were then fixed, permeabilised and stained with antibodies for SCARB1 and LMO2 and protein expression detected using flow cytometry, cells were gated for positive transfection using the SiGlo (FAM) and then LMO2/SCARB1 was measured in the positively transfected population (Alex Fluor 647). A) The change in cells positive for LMO2 following treatment with miR-223-3p compared to the scrambled control (n=3±SD paired t-test). B) The change in LMO2 MFI following treatment with miR-223-3p compared to the scrambled control (n=3±SD paired t-test). C) The change in cells positive for SCARB1 following treatment with miR-223-3p compared to the scrambled control (n=3±SD paired t-test). D) The change in SCARB1 MFI following treatment with miR-223-3p compared to the scrambled control (n=3±SD paired t-test).

5.4.3.5   Effect of pdEV on SCARB1 and LMO2 in THP-1 cells

THP-1 cells were incubated with pdEV for 24hours and LMO2 and SCARB1 protein expression was measured. Figure 5.19 shows very similar results to Figure 5.16 and Figure 5.17 with both LMO2 and SCARB1 expression decreasing by roughly the same amount as observed with the microRNA mimic, LMO2 by ~10% (p=0.0655) and SCARB1 by ~50% (p=0.1592). These results demonstrate that the pdEV have a similar functional affect to the direct transfer of miR-223-3p which directly targets LMO2 and SCARB1 in THP-1 cells.
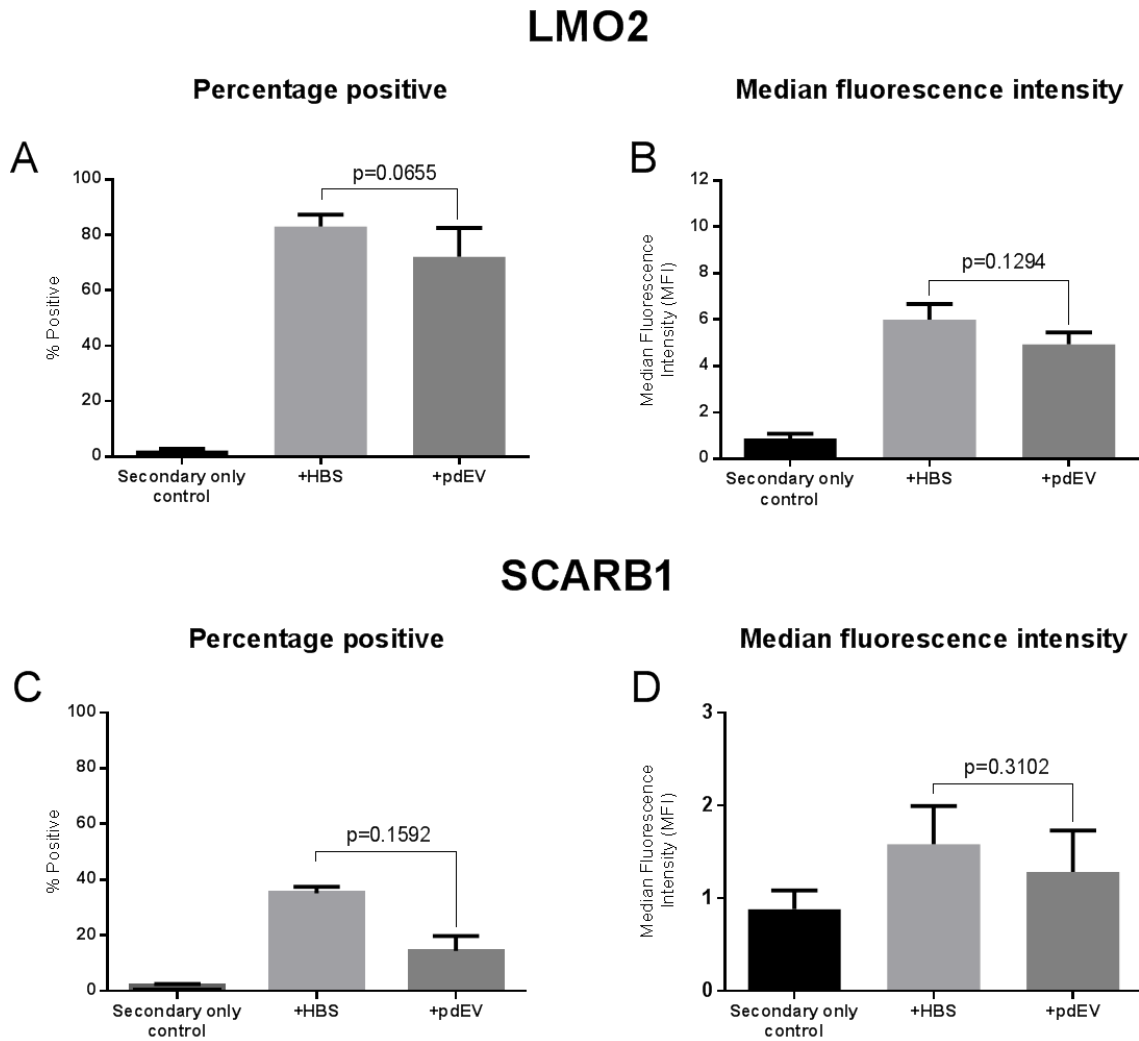

Figure 5.19 – LMO2 and SCARB1 expression changes in response to pdEV in THP-1 cells *2.5x10^6 THP-1 cells were plated into 6 well tissue culture dish and then incubated with pdEV for 24hours at 37°C in 5% CO$_2$. Cells were then fixed, permeabilised and stained with antibodies for SCARB1 and protein expression detected using flow cytometry, cells were gated for positive transfection using the SiGlo (FAM) and then LMO2/SCARB1 was measured (Alex Fluor 647). A) The change in cells positive for LMO2 following treatment with pdEV compared to HBS (n=4±SD paired t-test). B) The change in LMO2 MFI following treatment with pdEV compared to HBS (n=4±SD paired t-test). C) The change in cells positive for SCARB1 following treatment with pdEV compared to HBS (n=4±SD paired t-test). D) The change in SCARB1 MFI following treatment with pdEV compared to HBS (n=4±SD paired t-test).*

5.5 Discussion

The work in Chapters 2 and 3 indicated that platelets release EV containing microRNA and that this microRNA has a multitude of targets in monocytes of which LMO2 and SCARB1 were selected for further investigation. This was based on information from databases of predicted and validated targets as well as changes in gene expression in monocytes treated with platelets and platelet-releasate. The aim of the work in this chapter was to observe the transfer of pdEV to monocytes, to determine whether the microRNA cargo was delivered and to investigate whether this microRNA then affected the protein expression of the selected targets. The pdEV used in this chapter were generated using PAR1-AP on the assumption that this would be a predominantly exosomal population which would contain the microRNA as suggested by the evidence in Chapter 2 and 3.

The intercellular delivery of cargo via EV has been established as an important mechanism of cell-cell communication, and the scale of EV release and uptake in the circulation suggests that it has an important role (Loyer et al., 2014, Vickers et al., 2011, Clancy and Freedman, 2013). Here the work focused on the interaction between platelets and monocytes which has been shown to contribute to thrombus and atherosclerotic plaque development (Freedman and Loscalzo, 2002, von Bruhl et al., 2012, Alard et al., 2015). This interaction utilises many mechanisms such as direct contact and soluble mediators but the contributions of pdEV are yet to be elucidated (Cerletti et al., 1999, Li et al., 2000, Laffont et al., 2015).

5.5.1 Targeting and uptake of pdEV

The data in this chapter was able to demonstrate the uptake and internalisation of pdEV into THP-1 cells and PriMo and that monocytes were the preferred leukocyte target for pdEV in the circulation. The uptake of EV into cells has been widely documented for EV derived from an array of different cells to numerous target cells (Montecalvo et al., 2012, Cabrera-Fuentes et al., 2015, Cai et al., 2015, Guduric-Fuchs et al., 2012). What is not yet clear are the mechanisms by which the EV are taken into the cells or what is required for targeted delivery. There are currently many theories on the mechanisms of EV uptake and this process can be separated into 2 elements; the membrane interactions involved in the triggering and targeting of EV uptake and the mechanism by which uptake occurs (Mulcahy et al., 2014).

Evidence suggests that there are several groups of EV membrane components that could contribute to EV uptake including tetraspanins, proteoglycans, integrins and lectins. In preliminary investigations we found that interrupting the P-selectin-PSGL-1 interaction between

platelets and monocytes in whole blood significantly reduced but did not abolish EV uptake (p=0.003) (Figure 5.20B).
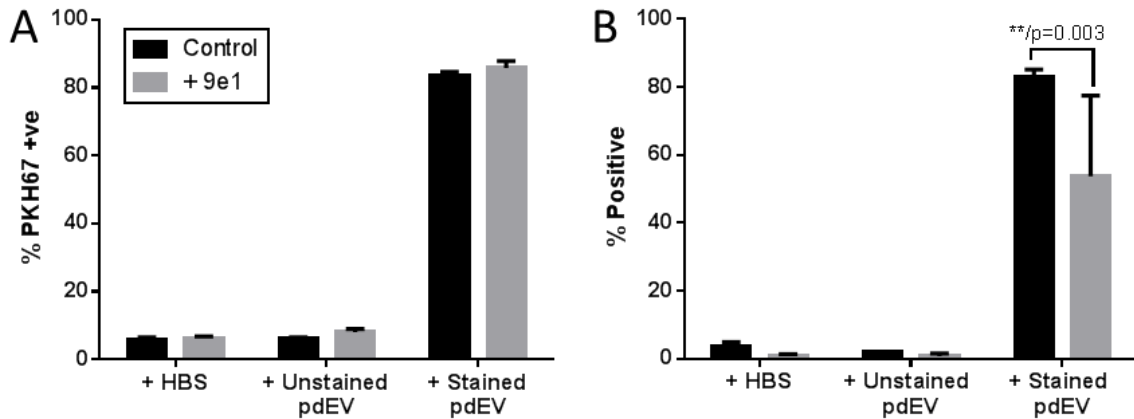
Figure 5.20 – Effects of a P-selectin blocking monoclonal antibody on pdEV uptake *THP-1 cells and whole blood was incubated with the P-selectin blocking antibody 9E1 and then treated with HBS, unstained pdEV and PKH67 stained pdEV. Uptake was assessed after 20hours using flow cytometry in THP-1 cells (A) and whole blood monocytes (B) which were separated out using CD14 expression and SSc (n=3±SD paired t-test).*

We also observed the expression of the tetraspanin, CD63, in platelet-derived exosomes (Figure 2.15). Tetraspanins have been shown to play a key role in the fusion of spermatozoa and oocytes as well as being important for virus entry and replication within cells (Rubinstein et al., 2006a, Rubinstein et al., 2006b, Li et al., 2014, Thali, 2009) and are enriched on exosome membranes. Tetraspanins are found in microdomains that have been shown to play a role in cell and vesicular fusion (Hemler, 2005). The role of tetraspanins CD9 and CD81 in EV uptake has been explored by Morelli *et al.*, using antibodies that block their function, who showed a reduction in bone marrow-derived EV uptake into dendritic cells (Morelli et al., 2004).

Integrins and proteoglycans have also been implicated in EV-cell interactions which lead to uptake. For example the interaction between ICAM-1 and the integrin CD11a has been shown to be involved in dendritic cell EV uptake, and the T-cell receptor CD28 interacts with lymphocyte function-associated antigen 1 (LFA-1) for EV uptake in naïve T-cells, demonstrating the importance of for EV uptake in immune cells (Hwang et al., 2003, Morelli et al., 2004). Proteoglycans are used by viral particles and lipoproteins to gain cellular entry and studies that blocked the heparin sulphate proteoglycans with heparin sulphate mimics reduced glioblastoma cell EV uptake into glioblastoma cells (Shukla et al., 1999, Christianson et al., 2013). A further study demonstrated that negatively charged PS may be critical for the uptake of microvesicles as blocking with Annexin-V reduced overall EV uptake into macrophages (Yuyama et al., 2012). This study suggests that there may potentially be different uptake mechanisms for exosomes and microvesicles, which may lead to them having different fate and functions within target cells. With so many potential mechanisms all seeming to contribute to EV uptake it appears that

it is involves multiple membrane proteins and that these may act simultaneously or function individually in different scenarios.

One important variable in understanding EV uptake are the cell from which the EV have originated and the cell they enter. The work here demonstrated that pdEV were predominantly interacting with monocytes in the circulation which suggests that there is at least an element of specific targeting occurring. Previous studies have shown that certain cell lines more readily take up EV, but each cell line was investigated in isolation (Zech et al., 2012). Rana *et al.* investigated selective uptake in rats and found that EV expressing TSPAN8-alpha4 complexes were targeted to the endothelium and pancreas (Rana et al., 2012). However, to our knowledge the present work was the first study which identified selective EV uptake in the multicellular and competitive environment of human blood. A caveat is that the experiment was conducted ex-vivo and so uptake into the endothelium was not taken into account. Since this is possibly an important target for pdEV (Boulanger et al., 2001, Cai et al., 2015, Diehl et al., 2012, Gambim et al., 2007, Mause et al., 2005) there may be competition in-vivo that limits the update by peripheral blood leukocytes.

The mechanism by which the pdEV were targeted to the monocytes is yet to be elucidated but the P-selectin/PSGL-1 interaction may play a role in monocytes in whole blood but not THP-1 cells (Figure 5.20). It is know that platelet microvesicles can express P-selectin, so this could contribute to microvesicle uptake into monocytes, although the P-selectin ligand PSGL-1 is expressed on a variety of leukocytes so would not necessarily contribute to the preferential targeting of pdEV to monocytes (van der Zee et al., 2006, Lok et al., 2007). The pdEV population used here was presumed to be predominantly exosomal and the expression of P-selectin on exosomes is unknown. It is possible that the reduced uptake caused by blocking P-selectin/PSGL-1 only targeted microvesicles, but further work would be required to determine whether EV sub-populations relied on differential uptake mechanisms.

Flow cytometry indicated that pdEV were mainly associated with monocytes but did not indicate whether the EV were simply bound to, or internalised within the cells. However confocal microscopy confirmed that pdEV were internalised by both PriMo and THP-1 cells, a control experiment using trypsin to dissociate membrane bound pdEV could have been used to further demonstrate the internalisation. As with the understanding of the method for EV-cell interactions, the mechanism of uptake is keenly debated, and whilst several studies have identified endocytosis as a critical mechanism, this is simply an umbrella term which describes many separate pathways; macropinocytosis (Fitzner et al., 2011), clathrin-mediated endocytosis

(Escrevente et al., 2011), caveolin-dependent endocytosis (Nanbo et al., 2013) and phagocytosis (Feng et al., 2010), all of which have been implicated in endocytic EV uptake.

Another alternative is cell membrane fusion, whereby the EV contents are released directly into the cytoplasm and the pdEV membrane becomes part of the cells membrane (Montecalvo et al., 2012). The data here suggests that this mechanism is unlikely, as the pdEV membranes were stained and the PKH67 staining was identified within the monocytes rather than becoming incorporated as part of the plasma membranes of the target cells. However since this observation was only made at a single time point it is possible that membrane fusion could occur within the endosomes following EV endocytosis, resulting in the release of EV cargo into the cytosol. Membrane fusion has been associated with the tetraspanins on the membrane of exosomes, so has potential as an uptake mechanism but requires further study. Interestingly, it was proposed that the PKH67 dye itself could alter uptake mechanisms but many studies have used a multitude of fluorescent dyes and seen similar results suggesting that the dye has little if any effect (Mulcahy et al., 2014). Establishing whether EV uptake is specifically through one, or all of these pathways is challenging due to their overlapping mechanisms, however what has been confirmed is that it is not a passive process as it requires calcium (Barres et al., 2010), does not occur in fixed cells (Fitzner et al., 2011) and is inhibited by the presence of the metabolic inhibitor azide (Simms et al., 2013).

As monocytes are phagocytes it seems plausible that phagocytosis could be an EV uptake mechanism into monocytes, but the lack of uptake in neutrophils would suggest that phagocytosis was a selective process for EV uptake. To date the use of inhibitors to block specific endocytic pathways has yielded mixed results and it appears that there may be redundancy between the different pathways. Due to our inability to resolve the heterogeneity of EV populations we are unable to see whether there are separate pathways for EV subtypes and specific trans-cellular targeting (Mulcahy et al., 2014). While the work here is unable to determine the molecules and pathways involved it does suggest an area for further direction and particularly investigating whether there are cell and EV subtype specific pathways.

In addition to the undetermined targeting and uptake mechanisms it was also unclear where the pdEV are localised once inside the cells. The present studies using confocal microscopy indicated that they were localised to the cytoplasm but it was impossible to tell whether they were associated with internal structures or organelles. If the pdEV were taken up through an endocytic pathway then it is likely that they may be located within endosomes, but investigation of this would require microscopy with significantly greater resolution. As the delivered

microRNA were able to exert an effect on their microRNA targets it suggests that their localisation is conducive to their functionality and that they are not simply being degraded.

5.5.2 Transfer and functional effects of pdEV microRNA

The transfer of functional microRNA to monocytes via pdEV was shown in both THP-1 cells and PriMo with miR-223-3p showing a ~2-fold increase and miR-126-3p showing a 2- to 4-fold increase. Transfer of microRNA is a widely studied phenomenon which was first reported by Valadi *et al.* in 2007 , since then the transfer of genetic material via EV has been implicated in a wide variety of processes and species (Stoorvogel, 2012, Montecalvo et al., 2012, Diehl et al., 2012, Guduric-Fuchs et al., 2012, Cai et al., 2015). Establishing the physiological relevance of microRNA shuttling is proving to be a complex process but it is generally agreed that the effects of pdEV are likely to be important due to their abundance in the circulation and the ability of their cargo, such as microRNA, to exert functional effects.

PdEV uptake has been observed in stimulated HUVECs and THP-1 cells (Risitano et al., 2012) and pdEV have been shown to deliver miR-223-3p to HUVECs (Laffont et al., 2013) and miR-126-3p to monocyte-derived macrophages (Laffont et al., 2015). Importantly this delivered microRNA has then been shown to downregulate mRNA and protein levels of the miR-223-3p targets FBXW7 and EFNA1 in HUVECs (Laffont et al., 2013) and mRNA of the miR-126-3p targets, ATP9A and RAI14 and both the mRNA and protein of ATF3 and ATP1B1 in monocyte-derived macrophages (Laffont et al., 2015). However investigations into these targets did not explore whether there were any functional effect on cellular activity. While the study by Laffont *et al.* did observe decreased cytokine and chemokine release in response to pdEV treatment of monocyte-derived macrophages (Laffont et al., 2015) it did not establish a direct role of microRNA in this response.

In this chapter we were able to observe the effect of miR-223-3p on its predicted targets LMO2 and SCARB1 in both THP-1 cells and PriMo. There were contrasting results in the two cell types; THP-1 cells exhibited reduced protein expression for both targets in response to the microRNA mimic, however in the PriMo only SCARB1 was reduced. This may reflect the levels of expression of the targets in the two cells types; ~90% and ~40% of THP-1 cells were positive while only ~20% and 6% of PriMo expressed LMO2 and SCARB1 respectively. Until that point the THP-1 cells treated with VitaminD3 had appeared to be a good model for PriMo with almost identical EV uptake profiles, similar uptake viewed using the confocal microscopy and matching changes in microRNA expression following treatment with pdEV. However this potential discrepancy in gene expression highlights the challenges of using immortalised cell lines to replicate the

responses of primary cells. THP-1 cells have been shown to require specific differentiation protocols to mimic monocyte characteristics and these protocols often result in the expression of other characteristics which do not reflect monocytes, therefore results in these cells need to be validated in primary cells (Daigneault et al., 2010, Qin, 2012).

The low expression of LMO2 and SCARB1 in PriMo was unexpected as preliminary experiments to optimise the flow cytometry protocols for detecting LMO2 and SCARB1 indicated that untransfected PriMo expressed the proteins at levels similar to those of THP-1 cells 72% for LMO2 and ~19% for SCARB1. Figure 5.21 shows these results, PBMCs were isolated (5.3.1) and PriMo selected for by attachment, and then incubated for 24hours in RPMI-1640 medium and then probed for LMO2 and SCARB1 as described previously (5.3.5.4) using flow cytometry. Therefore this suggests that either these initial experiments yielded incorrect results or that the transfection procedure lead to altered protein expression in the PriMo. Unfortunately these experiments were unable to be repeated due to time pressures, however preliminary investigations suggest that the transfection procedure may lead to increased cell death in the PriMo and therefore altered levels of auto-fluorescence and may have altered expression of the target proteins.
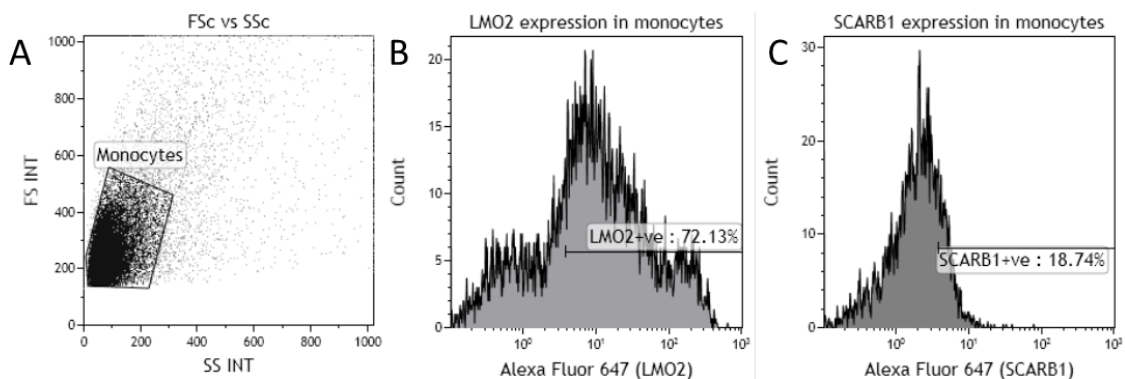
Figure 5.21 – LMO2 and SCARB1 expression on PriMo in preliminary experiments *Isolated PriMo were incubated for 24hours and then LMO2 and SCARB1 expression was assessed by flow cytometry to determine if the flow cytometry protocol was suitable for measuring these proteins. A) The FSc vs SSc plot used to gate the monocytes B) the expression of LMO2 and C) expression of SCARB1 (n=1).*

In chapter 4, targets that had low mRNA expression were intentionally selected as this provided a stronger microRNA to mRNA ratio, meaning that any microRNA effect observed was likely to be greater. However this risked selecting targets that had little or no protein expression; the transcriptome array data did not provide information on protein levels, and online databases did not provide definitive answers.

In addition the experimental conditions for evaluating the effect of the microRNA mimic were optimised using the THP-1 cells and then applied to experiments using both THP-1 cells and

PriMo. This could have resulted in conditions that were sub-optimal for the PriMo. The concentration of the microRNA mimic could have been particularly important, as the amount of microRNA mimic was the same in all conditions and so could have altered the protein expression in all experiments. Because these experiments were conducted with PriMo the number of cells treated in the PriMo experiments was only 20% of those in the THP-1 cell experiments and so the dose of microRNA mimic each cell received would have been ~5 times higher. This could impact on the experiment as high doses of microRNA mimics have been shown to have negative effects on cells (Jin et al., 2015). Taken together these factors suggest that the experiments in the PriMo need to be repeated and adjusted to determine whether the current results are correct or due to experimental issues, with particular care being taken to further optimise transfection conditions to prevent cell death and to determine the best experimental conditions in PriMo rather than simply using the THP-1 conditions.

The data shown in Chapter 2 from NTA analysis suggest that platelets stimulated with PAR1-AP release ~1EV/platelet (Figure 2.13) and based on the microRNA data from the biomarker experiments the copy number of miR-223-3p is ~0.5copies/EV (Figure 3.22). This means that in the pdEV experiments each monocyte received a dose of EV that equated to ~500 copies of miR-223-3p, however in the microRNA mimic experiments the monocytes were treated with ~200,000 copies per monocyte (calculated by utilising Avogadro's constant [6.022×10^{23}]). This suggests that the level of microRNA mimic is ~4000-fold higher than that found physiologically, which would indicate that either the number of mimic copies that could be successfully transfected and incorporated into the RISC complex would be very low (<0.025%). It is also important to acknowledge that pdEV do not solely deliver microRNA to monocytes and so other factors, such as mRNA, proteins and membrane receptors could contribute to the effects on LMO2 and SCARB1 in THP-1 cells.

An experiment that could answer this question would be to transfect the cells with a microRNA inhibitor, which would prevent the miR-223-3p from having any effect and then treat them with pdEV. This would determine whether the effect of the pdEV was due to the transfer of miR-223-3p or other factors associated with the pdEV. The use of a microRNA inhibitor would not be perfect however, as the inhibitor would also prevent the activity of the endogenous miR-223-3p in the cells in addition to the newly delivered miR-223-3p.

If the results from the THP-1 cells are looked at in isolation, due to the limitations of the studies with the PriMo, an important question remains; is the effect on the protein expression of LMO2 and SCARB1 physiologically relevant? LMO2 is an enigmatic protein, it has been implicated in

haematopoietic development (Felli et al., 2009, Yuan et al., 2009), angiogenesis (Yamada et al., 2002) and oncogenesis (Nam and Rabbitts, 2006) but as a protein which acts as a scaffold for protein complexes it has many unknown functions (Chambers and Rabbitts, 2015). In addition, the level of effect of miR-223-3p and pdEV on LMO2 expression, while significant, was only small. The ~10% decrease suggests that LMO2 is either being slightly fine-tuned, as has been proposed for microRNA function, or as suggested by the Seitz and colleagues LMO2 could simply act to bind and remove excess miR-223-3p expression within the cell without adversely affecting its function (Seitz, 2009). When the full range of functions for LMO2 are revealed it may become a target of high importance, but at this point in time it's regulation by pdEV requires further investigation.

The observed effect on SCARB1 was much greater than on LMO2, which could indicate that the interaction is likely to produce a significant and important functional effect. The role of SCARB1 as a HDL-C uptake receptor is well established (Valacchi et al., 2011, de Villiers and Smart, 1999, Van Eck et al., 2003) and its importance in the control of circulating HDL-C levels was recently highlighted in humans (Zanoni et al., 2016). Traditionally circulating HDL has been viewed as protective in CVD when it is present at a high ratio compared to LDL (Castelli et al., 1992). Contrary to this, loss-of-function mutations in SCARB1 are associated with increased circulating HDL-C and result in an increased risk of CAD (odds ratio = 1.79) (Zanoni et al., 2016).

These results match findings in mice where SCARB1 overexpression reduced circulating HDL-C and reduced atherosclerosis (Kozarsky et al., 1997) whereas SCARB1 KO increased both circulating HDL-C and atherosclerotic burden (Van Eck et al., 2003). However, the mechanism by which SCARB1 expression is associated with atherosclerosis is yet to be fully elucidated, particularly when analysing the effect on SCARB1 throughout the body as it also has central roles in the liver and steroidogenic cells (Connelly and Williams, 2003). Van Eck *et al.* suggest a bimodal response where reduced SCARB1 expression causes cholesterol accumulation in the arterial wall whilst causing increased HDL-C accumulation in the circulation due to impaired delivery to the liver (Van Eck et al., 2003).

It has been suggested that reduced SCARB1 expression in macrophages results in less reverse cholesterol transport (RCT) from the macrophage (de Villiers and Smart, 1999, Zhang et al., 2005). This suggests that control of SCARB1 function through pdEV-delivered miR-223-3p could be important in controlling monocyte/macrophage RCT and cholesterol efflux, which may lead to increased foam cell formation and associated CAD (Rosenson et al., 2012, Van Eck et al., 2003). Whilst the expression of SCARB1 in PriMo is low, the effect of pdEV on monocytes could

potentially trigger reduced SCARB1 expression in monocytes as they mature into macrophages. A scenario in which this could happen is outlined in Figure 5.22, briefly, endothelial damage attracts platelets which then become activated and released pdEV, and monocytes are then recruited and take up the released pdEV. This increases the miR-223-3p expression in monocytes, which then reduces SCARB1 expression, and this is sustained in the resultant macrophages that mature from the monocytes once they have entered the intima. These macrophages may then have impaired RCT, resulting in an imbalance in cholesterol homeostasis and thereby enhancing the development of atherosclerosis.
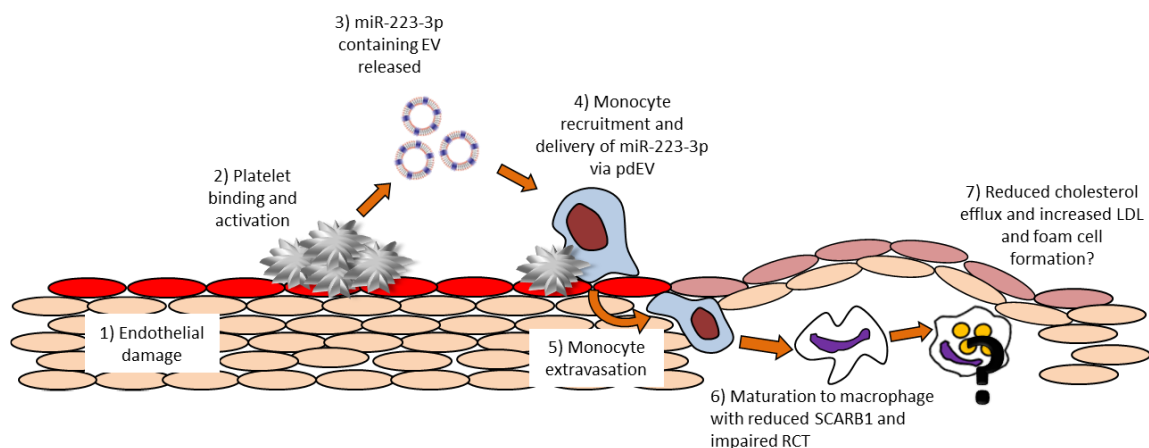
Figure 5.22 – A schematic detailing a potential scenario where pdEV target monocytes and contribute to atherosclerotic development *Due to endothelial damage (1) platelets are attracted and activated (2) causing the release of pdEV (3) which are taken up by the recruited monocytes (4) leading to miR-223-3p delivery and reduced SCARB1 expression in monocytes which extravasiate into the vessel wall (5) and become macrophages with impaired RCT (6).*

This potential mechanism for the regulation of SCARB1 in monocytes, and the implications of this in atherosclerosis, are speculative and would require extensive further investigations to determine its importance. Whilst the functional effect on HDL-C uptake and RCT in THP-1 cells caused by the downregulation of SCARB1 through pdEV-delivered miR-223-3p was not explored in this work, the use of cholesterol uptake and efflux assays could determine the functional effects of this interaction.

Cholesterol uptake and efflux is a process that is important in a variety cells, therefore investigating the effects of pdEV delivered miR-223-3p on SCARB1 in macrophages (Chinetti et al., 2000), the endothelium (Armstrong et al., 2015) and the liver (Zhang et al., 2005) could provide further insights into atherosclerosis. SCARB1 also has roles in LDL transcytosis (Armstrong et al., 2015), pathogen recognition (Schafer et al., 2009) and lipid soluble vitamin E uptake (Reboul et al., 2006) as well as being implicated in diseases such as chronic obstructive pulmonary disease (Valacchi et al., 2015) and female infertility due to its influence on steroidogenesis (Christianson and Yates, 2012). Taken together these factors suggest a complex

and multifaceted role for SCARB1 in which pdEV delivered miR-223-3p could play a controlling role. For example pdEV are known to communicate with the endothelium (Laffont et al., 2013), and in doing so they could directly affect cholesterol uptake and LDL transcytosis, thereby contributing to atherosclerosis. Alternatively the pdEV could target the liver, where reduced SCARB1 expression has significant implications in the clearance of circulating HDL-C, particularly that from macrophage RCT (Zhang et al., 2005, Van Eck et al., 2003).

These interactions need to be studied in detail, although particular care needs to be taken when attempting to transfer findings from mice to humans. The work here has, however, demonstrated the concept that pdEV can deliver microRNA that is controlling protein levels, and thus function in monocytes, and suggests that SCARB1 may be a target of interest. Further experiments, detailed here, could provide greater insights into the relevance of this mechanism. In addition, the other targets described in the chapter 4 demonstrate the potential scope of platelet-monocyte interactions via EV.

Chapter 6

General discussion

6 General discussion

Research into EV continues to grow, with investigations relating to almost all aspects of health and disease. EV have proved to be valuable as biomarkers, functional intercellular signallers and are predicted to become pivotal in the development of targeted therapeutics (Kwekkeboom et al., 2014, van der Pol et al., 2016, van der Pol et al., 2012a, Danielson and Das, 2014). Their role in communication is only just beginning to be unravelled and there are several factors that require intensive study, namely their cargo, how the cargo is selected, their functional effects once delivered, the mechanisms by which they are taken up and how/if they are specifically targeted (Mulcahy et al., 2014). Through the work in this thesis we aimed to characterise the EVs released from platelets in terms of their phenotype and cargo of microRNA, demonstrate that they were able to transfer this to monocytes and in doing so alter their protein expression.

6.1 Platelet-derived EV

We first looked at the profiles of EV released from platelets following stimulation with different agonists. This identified 2 clear groups of agonists; CRP-XL which was the most potent agonist and triggered the generation of both exosomes and substantial numbers of procoagulant microvesicles whilst PAR1-AP, PAR4-AP and ADP stimulated the release of predominantly exosomal populations. Interestingly the separation of these agonists matched the difference in their PLC signalling pathways; PLC-γ for CRP-XL and PLC–β for the GPCR agonists PAR1-AP, PAR4-AP and ADP (Jackson and Schoenwaelder, 2003). These agonists are already known to play different roles in platelet activation, aggregation and degranulation and the release of different EV profiles would complement these differences (Heemskerk et al., 2002, Versteeg et al., 2013).

These different patterns of EV release are likely to contribute and alter platelet functions; therefore it is worth considering how differential release might occur within the architecture of a thrombus (Figure 6.1B). Collagen (substituted in experiments here with CRP-XL) is immobile and located within the sub-endothelial matrix, thrombin is predominantly generated within the thrombus core and is confined by its interactions with its target proteins and inhibitors, whereas ADP is freely diffusible within the thrombus (Welsh et al., 2014). Procoagulant microvesicles are well known to be important for the rapid development of a thrombus as originally demonstrated by Chargaff and West in 1946 who demonstrated slower clotting in microvesicle depleted plasma (Chargaff and West, 1946).
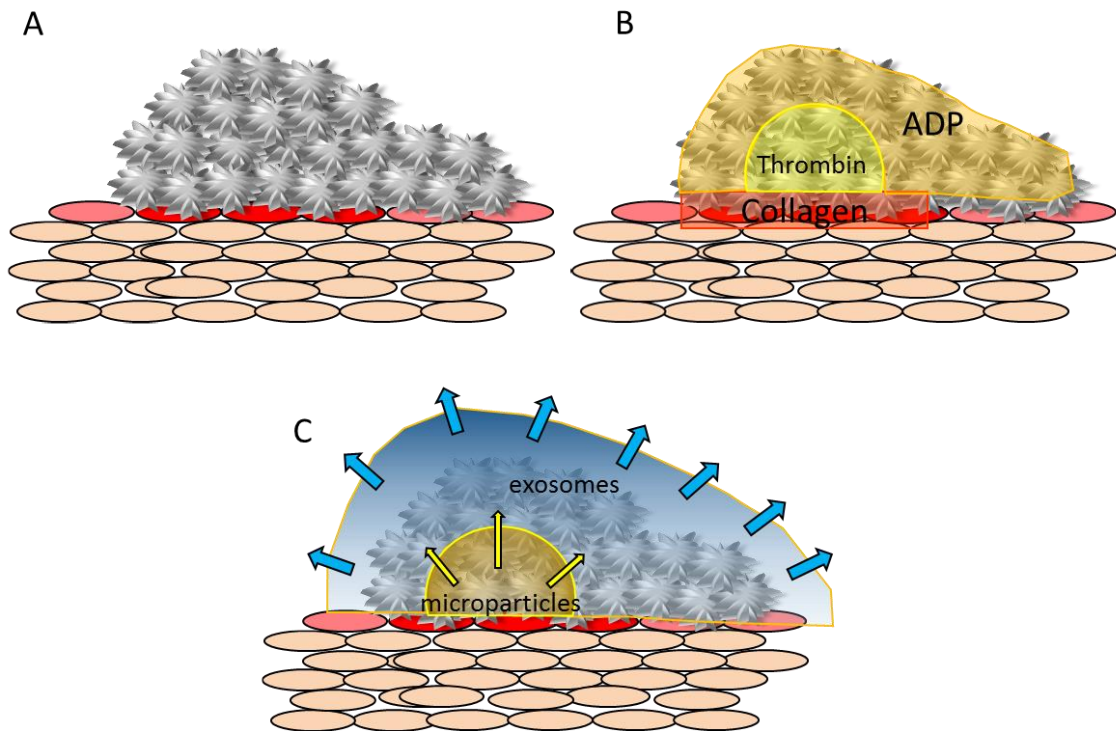
Figure 6.1 – Procoagulant microvesicle production in thrombi *Illustrating the production of microvesicles within a thrombus due to the localisation of agonists within specific regions of the thrombus. A) A thrombus formed from platelets, B) the localisation of collagen, thrombin and ADP within the thrombus' architecture and C) the predicted localisation of microvesicles and exosomes within the thrombus due to agonist localisation.*

Therefore microvesicle production following stimulation of platelets, through GPVI, by collagen directly adjacent to the endothelium, is important for platelet activation and the early growth of thrombi (Figure 6.1C). The microvesicles released can diffuse through the thrombus and the negatively charged PS on their surface promotes coagulation, supporting the assembly of clotting cascade components into the tenase (FVa•FIIa) and prothrombinase (FIXa•FVIIIa) complexes (Owens and Mackman, 2011, Heemskerk et al., 2002). The prothrombinase complex on microvesicles enables the production of thrombin in the thrombus core and this activates adjacent platelets triggering degranulation and the release of a predominantly exosomal population of EV. Platelet degranulation within the thrombus causes ADP release from dense granules which can diffuse throughout the thrombus. The ADP activates platelets through P2Y receptors causing further exosome release from the shell of the thrombus. The released exosomes are able to deliver their cargo to, and communicate with cells within the thrombus and the vasculature such as monocytes and the endothelium.

Studies have demonstrated that pdEV increase the adhesiveness of the endothelium through the delivery of RANTES and PF4 leading to the recruitment of monocytes and therefore triggering pro-inflammatory signalling increasing the development of conditions such as

atherosclerosis (Rautou et al., 2011a, Rautou et al., 2011b, Baltus et al., 2005, Mause et al., 2005, Nomura et al., 2001).

Based on this work it has been postulated that the pdEV binding to monocytes could also increase the levels of pro-inflammatory platelet-monocyte aggregates in the circulation, which are associated with diseases such as CAD, MI and stroke (Furman et al., 1998, Michelson et al., 2001, Smout et al., 2009, Passacquale et al., 2011). A recent study also suggested that platelet activation through thrombin and collagen leads to increased pro-inflammatory cytokine loading into pdEV, which could promote the development of atherosclerosis through interactions with the endothelium (Goetzl et al., 2016). However, in contrast to these studies there have been reports that pdEV trigger an anticoagulant response and reduce platelet aggregation. PdEV caused reduced lipid loading and platelet coagulation through reduced macrophage and platelet CD36 expression, respectively, due to increased CD36 ubiquitination resulting in its degradation (Srikanthan et al., 2014). In addition, Gidlof *et al.* found that pdEV delivered miR-320 to the endothelium, reducing ICAM-1 expression and associated leukocyte infiltration and inflammation (Gidlof et al., 2013). Taken together, these studies exhibit opposing views on the role of pdEV. It is likely that the conflicting evidence is due to the differential separation of microvesicles and exosomes in these studies. But further work would be required to identify their separate contributions to pro- and anti-inflammatory responses.

Due to the differential EV populations seen with the different agonists, our data suggested that there could be separate signalling pathways causing the release of exosomes and microvesicles. Collagen/CRP-XL has previously been shown to be a potent trigger for procoagulant microvesicle production from platelets (Heemskerk et al., 1997, Ilveskero et al., 2001), but the role of the other agonists in the mechanisms of pdEV release are less well studied (Aatonen et al., 2014). However, due to the involvement of many secondary mediators in platelet signalling and activation the individual agonists were unable to provide sufficient specificity to identify separate microvesicle and exosome release pathways. Therefore anti-platelet agents were utilised to understand the effects of secondary signalling through ADP, thromboxane, thrombin and the GPIIb-IIIa receptor. Whilst none of the experiments identified a mechanisms by which platelets released only exosomes, they did demonstrate the importance of secondary ADP signalling in the production of pdEV. ADP signalling is already known to be critical for the propagation of platelet signalling in clot formation and is important for the shape change and degranulation associated with platelet activation (Atkinson et al., 2001, Gachet, 2008, Murugappa and Kunapuli, 2006).

ADP signalling is targeted clinically through the P2Y12 receptor with antagonists such as clopidogrel, ticagrelor and prasugrel (Wijeyeratne and Heptinstall, 2011, Jackson and Schoenwaelder, 2003). These drugs provide antithrombotic therapy by reducing sustained platelet activation and in so doing they will also reduce microvesicle production, which may contribute to their antithrombotic effects. Previous work had demonstrated that ADP was critical for microvesicle production and through the work here we demonstrated that secondary ADP signalling also played a crucial role in exosome release (Heemskerk et al., 2002, Takano et al., 2004). Therefore drugs such as clopidogrel and ticagrelor would affect the function of platelet-derived exosomes as well as the procoagulant microvesicles. But, to date, no study has investigated the direct effect of ADP antagonists on exosome production from platelets and the consequences on intercellular communication.

An indirect study looked at the plasma levels of microRNA, such as miR-223-3p that is released in pdEV and found that it was reduced in the circulation of healthy subjects taking clopidogrel (Willeit et al., 2013). This reduction could be attributed to reduced exosome release. In addition these drugs have been linked with reduced inflammation which may be due to reduced delivery of pro-inflammatory signals via pdEV (Nylander and Schulz, 2016, Thomas and Storey, 2015). However, as detailed above there is clear evidence for both pro- and anti-inflammatory effects of pdEV and so further investigation into the effects of ADP antagonists on pdEV release and the associated platelet-monocyte cross-talk are required. These studies would add more detail to this mechanism and identify whether there are any side effects of long term treatment with ADP antagonists.

One of the initial aims of the project was to see if it was possible to separate the release of microvesicles from exosomes to determine the keenly debated location of microRNA within the circulation. As detailed above, the use of agonists and inhibitors was insufficient to achieve this goal and more traditional techniques such as ultracentrifugation which attempt to separate EV subsets have problems with aggregates and determining suitable centrifugal forces to allow for the differential fractionation of microvesicles and exosomes (Linares et al., 2015, Lane et al., 2015, Lobb et al., 2015). Alternative approaches could be exploited in future experiments to isolate pdEV, such as immune selection and size exclusion chromatography. However both of these techniques come with significant caveats; size exclusion chromatography can separate EV from contaminants but it does not have the ability to distinguish microvesicles from exosomes and has been shown to lose EV smaller than 75nm (Boing et al., 2014, van der Pol et al., 2016). While, immune selection requires the selection of an exosomal marker but to date no single universal marker has been identified therefore the use of a single marker may only isolate a

fraction of all exosomes (Zlotogorski-Hurvitz et al., 2015, Koga et al., 2005b). However, immune-selection represents the best opportunity for specific separation of EV subsets but further work is needed to identify suitable EV markers. The identification of markers which can discriminate the subsets is the biggest challenge facing the field of EV research at this time.

The main metric used to differentiate microvesicles and exosomes in this thesis was the known procoagulant activity of microvesicles, which occurs due to the surface exposure of negatively-charged plasma membrane phospholipids, predominantly PS (Aye et al., 2009, Pegtel, 2014). However, comparing this data to previous work in the field is challenging due to the variety of characteristics used to define the EV subsets and the inconsistent application of terminology (van der Pol et al., 2016, van der Pol et al., 2012a). Based on the issues with isolation, characterisation and changeable nomenclature there has been a call to simply use the umbrella term 'extracellular vesicles' (EV) to describe total populations of exosomes and microvesicles where there is no clear evidence of subset isolation.

This appears to be a sensible way forward until a consensus is reached, however, this may in fact slow progress in the field. Even with the current confusion it is clear that there are separate roles for exosomes and microvesicles (Raposo and Stoorvogel, 2013, Andreu and Yanez-Mo, 2015). In addition, data now suggests that there are likely to be several different populations of exosomes with differential enrichment for specific tetraspanins and surface receptors (Smith et al., 2015, Bobrie et al., 2012). These differences would provide a potential mechanism for exosome targeting to recipient cells and the loading of specific cargo, although it is not yet clear whether there are distinct subsets or a spectrum of exosomes with different surface protein and cargo expression (Andreu and Yanez-Mo, 2015, Mulcahy et al., 2014). Together, these factors demonstrate that further studies into the diversity and characteristics of EV are required to uncover the complexity of this intercellular communication network.

6.2 Platelet-derived microRNA

Following characterisation of pdEV and the effects of various inhibitors on their production we profiled the pdEV microRNA content. The intercellular shuttling of EV cargo has been widely investigated as a method of targeted cell-cell communication and the identification of microRNA in these vesicles provided a direct method by which the EV could control the protein function of target cells (Lee and Ambros, 2001, Valadi et al., 2007). Our research indicated that platelets released their most abundant microRNA into EV and that the profile of this microRNA was remarkably stable between the different agonists used to generate the EV. The stable microRNA

profiles suggest that the microRNA are released through a consistent mechanism, which we postulated to be exosomes.

Whilst not definitive, this hypothesis was generated for three reasons; firstly, exosomes were identified at comparable levels in all of the agonist-generated pdEV samples, which matched the consistent microRNA profiles and this clear correlation was strongly suggestive that the exosomes carried the microRNA. Secondly, the microRNA require protection from RNAse in the circulation and the other widely reported mechanism of protection, HDL, was not present in this experimental system. Thirdly, there is now a growing body of evidence in the literature which demonstrates exosomes as a microRNA transport vehicle with multiple mechanisms shown to load microRNA into exosomes (Kosaka et al., 2013a, Bolukbasi et al., 2012, Cheng et al., 2014, Zhang et al., 2015a, Mittelbrunn et al., 2011, Gallo et al., 2012). While the evidence here suggests that exosomes were the primary release mechanism for microRNA from platelets in these experiments, this may not be applicable in all cells or reflect platelets in the circulation where the contribution of interacting cells and factors in the blood could play a role.

With respect to the experiments carried out here, the localisation of microRNA released from platelets is not the most significant factor. If the microRNA in our samples was present in microvesicles or attached to HDL it would not change the fact that it was delivered to monocytes and altered protein expression. However, understanding the localisation of microRNA would be beneficial for understanding the mechanisms which control selective microRNA release and how the released microRNA interacts with target cells (Raposo and Stoorvogel, 2013, Weber, 2013). It has been demonstrated that in conditions such as CAD the profile of microRNA in the circulation associated with EV, HDL and other factors changes, and that this significantly reduces the ability of circulating microRNA to be delivered to endothelial cells (Finn et al., 2013). Whilst the separation of these fractions from the circulation still presents technical challenges, there is significant evidence for microRNA transport in EV, HDL and other mechanisms, suggesting that microRNA is transported via multiple pathways simultaneously (Boon and Vickers, 2013). If this is the case, then questions remain over the relative contribution of different cell types to the separate mechanisms, how microRNA are selectively incorporated into the different complexes and what is the fate of the microRNA within the different transport mechanisms

These different mechanisms present opportunities for differential targeting and functions for the microRNA. But determining the importance of each mechanism and the triggers for their release is essential to furthering our understanding of the complexities of intercellular microRNA signalling and for the identification of potential therapeutic targets in disease. These therapies

could target the transport mechanisms, if, for example, EV transported microRNA were determined to specifically contribute to a disease or target the effects of a particular microRNA associated with pathology progression. The targeting of specific microRNA is a strategy that is already being used for the treatment of conditions such as non-alcoholic steatohepatitis in diabetics (Trajkovski et al., 2011, ClinicalTrials.gov, 2016). Alongside these mechanisms being targetable by therapeutics, attempts are also being made to exploit them for therapeutic delivery, and this is another area which would benefit from greater understanding of the intricacies of the loading and targeting of microRNA transport mechanisms (Ailawadi et al., 2015, Kwekkeboom et al., 2014).

6.3 MicroRNA biomarkers

An area of circulating microRNA research which has progressed at a much faster rate is the identification of disease biomarkers. Circulating microRNA present an opportunity for readily accessible, sensitive and specific biomarkers. Most work has focused on the identification of biomarkers from the total RNA within the circulation, but the evidence above suggests that assessment of the different microRNA transport mechanisms may offer a more sensitive metric (Finn et al., 2013, Jakobsen et al., 2015, Quinn et al., 2015). However, this increases the challenges of applying a biomarker within the clinical setting as it would significantly increase the complexity of the assessment. As demonstrated by several studies, slight variations in the preparation of microRNA for assessment or as demonstrated here, the technique used to quantify the microRNA have a significant impact on the identification and quantification of a microRNA (Page et al., 2013, Jensen et al., 2011, Grasedieck et al., 2013). Therefore for microRNA biomarkers to be applied in a clinical setting there would need to be rigorous protocol standardisation.

Here we attempted to identify a biomarker of platelet activation; miR-223-3p, miR-146a-5p and miR-106a-5p were selected for assessment, because when compared to a variety of tissues from throughout the body they were determined to have a significant association with platelets and the microRNA they release into the circulation following activation. The results here indicated that they were not suitable as markers of acute platelet activation as there expression was not significantly raised in response to a variety of agonists. However, this assessment was in a very specific, ex-vivo experiment and required rapid accumulation of the biomarker. A more realistic test would be to investigate the effect of sustained platelet activation, and the subsequent long term accumulation of these microRNA in-vivo. Conversely, the effect of dual anti-platelet therapy (aspirin and clopidogrel) on these three microRNA found that all three were significantly

reduced in PPP after 48hours (miR-223-3p p=<0.001, miR-146a-5p p=0.025 and miR-106a-5p p=0.008) (Willeit et al., 2013). This work suggests that microRNA could act as a robust biomarkers for the assessment of anti-platelet treatment in patients, particularly as platelets make such a significant contribution to the microRNA content of the plasma (Willeit et al., 2013, Kaudewitz et al., 2016).

Whilst the work here was unable to identify a biomarker of platelet activation, the overall consensus is that microRNA show promise as biomarkers of the activation state of platelets. However, further work is needed to determine the best markers, and to develop methods that provide a simple indication of an individual's platelet activity and reactivity to therapy. In addition, investigations into the long-term implications of reduced circulating platelet microRNA are needed as many patients are on long-term dual anti-platelet therapy (Kaudewitz et al., 2016, Thomas and Storey, 2015).

6.4 MicroRNA target identification

Following the profiling of platelet and pdEV microRNA, the targets of pdEV microRNA were identified using a detailed and novel bioinformatic approach. The majority of current target identification methods are relatively simple; selecting a single microRNA of interest, searching online databases for its targets and then investigating whether overexpression of the microRNA has any effect on the predicted targets (Ritchie and Rasko, 2014, Thomson et al., 2011). However this fails to take into account factors such as the abundance of the mRNA target and the ratio of this to the microRNAs expression. Studies frequently use a single target prediction database, resulting in a biased approach with many false positives due to the specific algorithm which does not take into account the specific environment where the microRNA is expressed (Seitz, 2009). In addition the incorporation of mRNA expression changes following interactions with stimuli that include pdEV in our analysis enabled a more targeted approach. Ultimately the success of this approach was dependent on the results from experiments trying to validate the identified targets.

Based on the data in chapter 4, the identification of LMO2 and SCARB1 as targets of miR-223-3p was validated in THP-1 cells. Simultaneous experiments in PriMo lead to inconclusive results; LMO2 expression increased after treatment with a miR-223-3p mimic and SCARB1 expression was reduced but overall protein expression was at significantly lower levels than expected in all conditions. Further examination of these experiments suggests this may have been due to reduced cell viability in response to transfection with Viromer GREEN. Alongside LMO2 and SCARB1 the microRNA target analysis also identified a large number of potential targets, many

of which could be investigated in future work. For example the myosin regulatory light chain interacting protein (MYLIP) that has been shown to be involved in LDL receptor degradation or N-Acetylglucosamine Kinase (NAGK) that was predicted to be targeted by 5 separate pdEV microRNA. The successful validation of both LMO2 and SCARB1 as targets for miR-223-3p demonstrated that a more incorporated approach was superior to traditional techniques for the identification of functional microRNA-mRNA interactions. The wealth of data included in the target identification process enabled the selection of targets which not only met the criteria of the prediction algorithms, but also matched with gene expression from relative datasets and therefore were targets relevant in the pdEV to monocyte transfer scenario explored in this study. In addition the process ensured that the microRNA were weighted based on their relative expression, ensuring that targets of microRNA with greater abundance were assessed to have greater significance.

Due to publication bias, meaning negative data is often not reported, it is impossible to know how frequently predicted microRNA targets are unable to be validated. However, large scale experiments that have been conducted suggest ~50% of the targets in microRNA target prediction databases do not translate to functional interactions (Sethupathy et al., 2006, Wang, 2010, Witkos et al., 2011). Therefore an online resource which allows researchers to utilise freely available datasets to approach microRNA target identification using the same process as here would allow researchers to approach microRNA research with greater confidence of identifying important functional interactions. This could be achieved through the incorporation of data from multiple prediction algorithms, utilisation of online repositories of baseline cellular gene expression data and through allowing inclusion of the researchers own genetic or proteomic data whilst weighting the targets based on microRNA abundance.

Whilst work on improving microRNA target prediction algorithms continues, greater collaboration between laboratory-based and in-silico approaches is required to further the development of these resources (Agarwal et al., 2015). The computer algorithms can readily be modified to improve sensitivity and specificity by 1 or 2% in response to new findings but there are still fundamental elements of microRNA-mRNA interactions that are poorly understood and this results in falsely predicted targets. The idea outlined by Seitz, that some microRNA targets act to mop-up excess microRNA expression without a significant effect on function has merit and deserves further investigation (Seitz, 2009). In addition to this, data has suggested cell-specific functions for some microRNA and so furthering our understanding of the effects of specific cellular and mRNA environments is needed to improve target prediction (Liu and Abraham, 2013).

6.5 Platelet-derived EV communication with monocytes

Incubation of pdEV with THP-1 cells and PriMo resulted in the transfer of miR-223-3p and miR-126-3p with the expression of both increasing ~2-fold. What was not clear from these results was whether these microRNA were delivered to the same cells or whether some cells experienced significant increases in just miR-223-3p, miR-126-3p, both or neither of the microRNA. Fluorescent tracking of these 2 microRNA could reveal whether they are delivered together or separately and this may work in combination with specific EV subsets, revealing further information on intercellular targeting.

The 2-fold change observed is small compared to the large gene expression changes that can occur in cells following stimulation and suggests that functional changes caused by the microRNAs transfer are likely to fit with the described 'fine-tuning' role of microRNA (Baek et al., 2008). As both miR-223-3p and miR-126-3p were already expressed in monocytes the observed effect on SCARB1 and LMO2 may have been limited (Bidzhekov et al., 2012). The monocytes endogenous miR-223-3p and miR-126-3p are likely to have already been suppressing expression of LMO2 and SCARB1 and so the pdEV delivered microRNA could only supplement this effect. Therefore, future investigations could take this factor into account and look at targets of pdEV microRNA which are not expressed in the target cells, or microRNA which would see a large increase in expression. This information could also be incorporated into bioinformatic analyses of targets to provide further evidence for microRNA-mRNA interactions.

One of the most surprising findings of this body of work was the clear difference in pdEV uptake between leukocyte subsets. The data convincingly demonstrated that monocytes preferentially take up pdEV compared to lymphocytes and neutrophils, suggesting that there may be a mechanism by which pdEV are targeted to monocytes. Although, as explained in the discussion to chapter 5, very little is known about the mechanisms of targeting and there are likely to be multiple targets of EV from a single cell type. The tetraspanin and receptor rich membranes of EV provide the opportunity for specific targeting and the likely heterogeneity of EVs from a single source suggests that there is an integrated network of EV communication that must be teased apart to further our understanding of its role in health and disease (Zhang et al., 2015a).

The changes that were observed in LMO2 and SCARB1 suggested that microRNA from pdEV are able to reduce the expression of these proteins in monocytes, and that communication between platelets and monocytes via EV has a functional significance which is worth exploring further. In particular, the interaction of miR-223-3p with SCARB1 appears significant and could have implications in cholesterol homeostasis. This leads to questions over whether pdEV are able to

deliver miR-223-3p and influence SCARB1 expression in other cell types where cholesterol balance is important in health and disease. For example, reduced SCARB1 in the liver of mice results in increased circulating HDL-C and has been associated with increased incidence of atherosclerosis and patients with loss-of-function mutations in this gene also have increased risk of CAD (Zanoni et al., 2016, Van Eck et al., 2003). Therefore platelet activation and the subsequent release of miR-223-3p containing pdEV could play an important role in global SCARB1 expression, with implications for cholesterol homeostasis and associated cardiovascular pathologies.

Whilst the evidence presented here strongly infers that pdEV delivery of miR-223-3p to monocytes triggers the down-regulation of SCARB1 and LMO2, the mechanism has not been definitively proven. Alongside their microRNA cargo pdEV are known to transport a variety of other protein and RNA which could potentially exert these functional effects. EV have been shown to cause functional changes in other cells, through interactions with membrane receptors. For example, breast cancer tumour-derived exosomes triggered pro-inflammatory activity in macrophages through activation of the NF-κB pathway by interacting with the TLR4 receptor on the cells surface (Chow et al., 2014). Work with microRNA inhibitors could demonstrate that the effect on LMO2 and SCARB1 was due to the delivery of miR-223-3p.

An interesting observation from the experiments looking at the effects of miR-223-3p on LMO2 and SCARB1 was that transfection of a microRNA mimic at levels 4000x higher than those found in pdEV did not have a greater effect. This suggests that whilst transfection is frequently an inefficient technique, the pdEV are able to deliver large concentrations of microRNA to target cells. Whilst this could be partially explained by the existence of unmeasured miR-223-3p precursor in the pdEV it still suggests that pdEV are an extremely efficient delivery mechanism for their cargo. This efficiency suggests that the considerable interest in applying EV as delivery vehicles for therapeutics is justifiable. However, as already discussed, there are many questions which need to be addressed before EV can be utilised for drug delivery. Many of these problems have been outlined here and include; cargo selection, as well as de-selection to prevent transfer of unwanted EV contents, EV targeting and generation of methods for large-scale production of EV.

Whilst the work here supports a role for microRNA in the control of protein expression, the importance of this role was unclear and requires characterisation of the functional effects of the reduced expression of these proteins. However, the global significance of microRNA is still unclear. MicroRNA knockouts in C. elegans demonstrated that less than 10% of microRNA

caused embryonic lethality or obvious phenotypes and even specifically knocking out microRNA with known functions in mice has led to no observable phenotype (Park et al., 2010, Miska et al., 2007, Jin et al., 2009). For example, miR-223-3p has been demonstrated to play an important role in haematopoietic development and is the most abundant microRNA in megakaryocytes and platelets, yet without it platelets function normally and there are only minor effects on their production (Leierseder et al., 2013). This suggests that due to the numerous different microRNA species and their ability to target an array of different mRNA that there is a significant level of redundancy in the microRNA network. This increases the challenge that researchers face to identify the roles of microRNA and suggests that the function of individual microRNA may only be important under the stressful conditions induced by disease.

6.6 Future work

The work here has been able to demonstrate the targeted intercellular transfer of microRNA from platelets to monocytes, resulting in the modulation of identified target protein expression. However, it has left several questions unanswered, which recent advances in EV-associated techniques may present an opportunity to investigate further.

Firstly, by what method is EV released from platelets? Here the evidence suggested that exosomes were the predominant release strategy for microRNA from platelets but the results were not definitive. The use of techniques such as size-exclusion chromatography to separate EV from contaminants (e.g. proteins and lipoproteins) followed by immune-selection to isolate exosomes and microvesicles and possibly subsets of these populations would enable the separation of fractions capable of transporting the microRNA. These fractions could then undergo extensive characterisation to determine their precise separation from the other fractions. The microRNA content of these samples could then be profiled using techniques with greater sensitivity than the RT-PCR arrays used here such as microRNA sequencing. Answering this question using platelets would provide significant insight into the situation in the circulation due to the contribution platelets make to the circulating microRNA profile.

In conjunction with the above work, the detailed characterisation of EV subsets released from platelets and other cells is required. It is clear that platelets release both microvesicles and exosomes, but it is not known whether they release a single homogenous population of microvesicles and a single population of exosomes. Answering this question is still very challenging using current techniques as it is not possible to resolve the expression of markers on a single EV. To carry out this work would require further advancement of technologies, e.g. improving flow cytometry to allow EV as small as 30-40nm to be viewed, although this would be

extremely challenging. Alternatively, the simultaneous visualisation of multiple fluorescent markers on individual EV through improved NTA instrumentation or the application of techniques such as single-cell proteomics to individual EV may prove suitable. Resolving EV on a single vesicle basis is essential to unravelling the complexities of EV functions and will become possible as technology advances.

A further key area of investigation is understanding how EV are targeted and taken up by specific cells. The work here identified a clear directional transfer of EV from platelets to monocytes and demonstrated that the P-selectin/PSGL-1 interaction may play a role. Further work in this area could be carried out using a variety of inhibitors to cell-surface receptors on EV and their cells to block interactions. This approach could be guided by the further characterisation of EV detailed previously. In addition, detailed investigations into the fate of EV in more complex scenarios, such as whole animal models, or experiments which flow whole blood over cultured endothelial cells could identify whether monocytes are the sole target of pdEV. In addition, specific tagging of EV, using fluorescent proteins such as CD63, P-selectin, CD81 etc. could reveal whether all EV are targeted together. Testing EV from other cells in this scenario would also prove useful to see if the monocytes are specifically targeted by pdEV or simply acting in a clearance capacity, whereby they phagocytose circulating EV.

Finally, the interaction of pdEV with monocytes needs to be explored further. This work has suggested that the transferred microRNA may have an important influence on monocyte protein expression, but this mechanism of control needs to be proven with microRNA inhibitors to demonstrate its specificity. If the interaction proves to be specific, then identifying the functional implications through investigations into the effects on cholesterol homeostasis are essential. Further to this, demonstrating its importance in a physiological setting could be critical for the development of therapies to slow the progression of atherosclerosis.

At present, research into EV takes a broad view of their role in intercellular communication. The recommendations to treat EV as a single population rather than separating microvesicles and exosomes may provide clarity in future literature. However, this is likely to slow research into the specific functions of EV subsets, particularly as it appears that microvesicles and exosomes may work antagonistically in situations such as inflammation. EV and their cargo form part of a highly complex and integrated intercellular communication network and studies have only just begun to unravel the breadth of its function. Current EV isolation approaches only allow us to measure the total effect of all EV or crude isolations of microvesicles or exosomes which are frequently contaminated with other EV populations, protein aggregates and lipoproteins.

Combination techniques such as size-exclusion chromatography with immune-selection provide an opportunity to assess the roles of precise sub-populations. This approach could help dissect the EV signalling networks and identify the roles of distinct subsets of exosomes and/or microvesicles, the messages they convey and whether this represents clinically targetable processes. Investigations into the utilisation of EV as delivery vehicles for therapeutics is a rapidly expanding area, but considerations need to be made as to how best to utilise this mechanism and whether there are any significant implications for adding therapeutics alongside other cargo with unknown functional effects.

7 References

AATONEN, M., GRONHOLM, M. & SILJANDER, P. R. 2012. Platelet-derived microvesicles: multitalented participants in intercellular communication. *Semin Thromb Hemost,* 38**,** 102-13.

AATONEN, M. T., OHMAN, T., NYMAN, T. A., LAITINEN, S., GRONHOLM, M. & SILJANDER, P. R. 2014. Isolation and characterization of platelet-derived extracellular vesicles. *J Extracell Vesicles,* 3.

AFONSO-GRUNZ, F. & MULLER, S. 2015. Principles of miRNA-mRNA interactions: beyond sequence complementarity. *Cell Mol Life Sci,* 72**,** 3127-41.

AGARWAL, V., BELL, G. W., NAM, J. W. & BARTEL, D. P. 2015. Predicting effective microRNA target sites in mammalian mRNAs. *Elife,* 4.

AILAWADI, S., WANG, X., GU, H. & FAN, G. C. 2015. Pathologic function and therapeutic potential of exosomes in cardiovascular disease. *Biochim Biophys Acta,* 1852**,** 1-11.

ALARD, J. E., ORTEGA-GOMEZ, A., WICHAPONG, K., BONGIOVANNI, D., HORCKMANS, M., MEGENS, R. T., LEONI, G., FERRARO, B., ROSSAINT, J., PAULIN, N., NG, J., IPPEL, H., SUYLEN, D., HINKEL, R., BLANCHET, X., GAILLARD, F., D'AMICO, M., VON HUNDELSHAUSEN, P., ZARBOCK, A., SCHEIERMANN, C., HACKENG, T. M., STEFFENS, S., KUPATT, C., NICOLAES, G. A., WEBER, C. & SOEHNLEIN, O. 2015. Recruitment of classical monocytes can be inhibited by disturbing heteromers of neutrophil HNP1 and platelet CCL5. *Sci Transl Med,* 7**,** 317ra196.

ALBERTS, B., WILSON, J. H. & HUNT, T. 2008. *Molecular biology of the cell,* New York, Garland Science.

ALEXIOU, P., MARAGKAKIS, M., PAPADOPOULOS, G. L., RECZKO, M. & HATZIGEORGIOU, A. G. 2009. Lost in translation: an assessment and perspective for computational microRNA target identification. *Bioinformatics,* 25**,** 3049-55.

ALONSO-LEBRERO, J. L., SERRADOR, J. M., DOMINGUEZ-JIMENEZ, C., BARREIRO, O., LUQUE, A., DEL POZO, M. A., SNAPP, K., KANSAS, G., SCHWARTZ-ALBIEZ, R., FURTHMAYR, H., LOZANO, F. & SANCHEZ-MADRID, F. 2000. Polarization and interaction of adhesion molecules P-selectin glycoprotein ligand 1 and intercellular adhesion molecule 3 with moesin and ezrin in myeloid cells. *Blood,* 95**,** 2413-9.

AMBROS, V., BARTEL, B., BARTEL, D. P., BURGE, C. B., CARRINGTON, J. C., CHEN, X., DREYFUSS, G., EDDY, S. R., GRIFFITHS-JONES, S., MARSHALL, M., MATZKE, M., RUVKUN, G. & TUSCHL, T. 2003. A uniform system for microRNA annotation. *RNA,* 9**,** 277-9.

ANDERSEN, C. L., JENSEN, J. L. & ORNTOFT, T. F. 2004. Normalization of real-time quantitative reverse transcription-PCR data: a model-based variance estimation approach to identify genes suited for normalization, applied to bladder and colon cancer data sets. *Cancer Res,* 64**,** 5245-50.

ANDREU, Z. & YANEZ-MO, M. 2015. Tetraspanins in extracellular vesicle formation and function. *Frontiers in Immunology,* 5.

ARMSTRONG, S. M., SUGIYAMA, M. G., FUNG, K. Y., GAO, Y., WANG, C., LEVY, A. S., AZIZI, P., ROUFAIEL, M., ZHU, S. N., NECULAI, D., YIN, C., BOLZ, S. S., SEIDAH, N. G.,

CYBULSKY, M. I., HEIT, B. & LEE, W. L. 2015. A novel assay uncovers an unexpected role for SR-BI in LDL transcytosis. *Cardiovasc Res,* 108**,** 268-77.

ARRAUD, N., LINARES, R., TAN, S., GOUNOU, C., PASQUET, J. M., MORNET, S. & BRISSON, A. R. 2014. Extracellular Vesicles from Blood Plasma:Determination of their morphology, size, phenotype and concentration. *J Thromb Haemost***,** 614-627.

ARROYO, J. D., CHEVILLET, J. R., KROH, E. M., RUF, I. K., PRITCHARD, C. C., GIBSON, D. F., MITCHELL, P. S., BENNETT, C. F., POGOSOVA-AGADJANYAN, E. L., STIREWALT, D. L., TAIT, J. F. & TEWARI, M. 2011. Argonaute2 complexes carry a population of circulating microRNAs independent of vesicles in human plasma. *Proc Natl Acad Sci U S A,* 108**,** 5003-8.

ASAKURA, T. & KARINO, T. 1990. Flow patterns and spatial distribution of atherosclerotic lesions in human coronary arteries. *Circ Res,* 66**,** 1045-66.

ASHCROFT, B. A., DE SONNEVILLE, J., YUANA, Y., OSANTO, S., BERTINA, R., KUIL, M. E. & OOSTERKAMP, T. H. 2012. Determination of the size distribution of blood microparticles directly in plasma using atomic force microscopy and microfluidics. *Biomed Microdevices,* 14**,** 641-9.

ASHIRU, O., BOUTET, P., FERNANDEZ-MESSINA, L., AGUERA-GONZALEZ, S., SKEPPER, J. N., VALES-GOMEZ, M. & REYBURN, H. T. 2010. Natural killer cell cytotoxicity is suppressed by exposure to the human NKG2D ligand MICA*008 that is shed by tumor cells in exosomes. *Cancer Res,* 70**,** 481-9.

ASSELIN, J., GIBBINS, J. M., ACHISON, M., LEE, Y. H., MORTON, L. F., FARNDALE, R. W., BARNES, M. J. & WATSON, S. P. 1997. A collagen-like peptide stimulates tyrosine phosphorylation of syk and phospholipase C gamma2 in platelets independent of the integrin alpha2beta1. *Blood,* 89**,** 1235-42.

ASSELIN, J., KNIGHT, C. G., FARNDALE, R. W., BARNES, M. J. & WATSON, S. P. 1999. Monomeric (glycine-proline-hydroxyproline)10 repeat sequence is a partial agonist of the platelet collagen receptor glycoprotein VI. *Biochem J,* 339 (Pt 2)**,** 413-8.

ATKINSON, B. T., STAFFORD, M. J., PEARS, C. J. & WATSON, S. P. 2001. Signalling events underlying platelet aggregation induced by the glycoprotein VI agonist convulxin. *Eur J Biochem,* 268**,** 5242-8.

AYE, I. L., SINGH, A. T. & KEELAN, J. A. 2009. Transport of lipids by ABC proteins: interactions and implications for cellular toxicity, viability and function. *Chem Biol Interact,* 180**,** 327-39.

AZEVEDO, L. C., JANISZEWSKI, M., PONTIERI, V., PEDRO MDE, A., BASSI, E., TUCCI, P. J. & LAURINDO, F. R. 2007. Platelet-derived exosomes from septic shock patients induce myocardial dysfunction. *Crit Care,* 11**,** R120.

BABITT, J., TRIGATTI, B., RIGOTTI, A., SMART, E. J., ANDERSON, R. G., XU, S. & KRIEGER, M. 1997. Murine SR-BI, a high density lipoprotein receptor that mediates selective lipid uptake, is N-glycosylated and fatty acylated and colocalizes with plasma membrane caveolae. *J Biol Chem,* 272**,** 13242-9.

BAEK, D., VILLEN, J., SHIN, C., CAMARGO, F. D., GYGI, S. P. & BARTEL, D. P. 2008. The impact of microRNAs on protein output. *Nature,* 455**,** 64-71.

BAGGA, S., BRACHT, J., HUNTER, S., MASSIRER, K., HOLTZ, J., EACHUS, R. & PASQUINELLI, A. E. 2005. Regulation by let-7 and lin-4 miRNAs results in target mRNA degradation. *Cell,* 122**,** 553-63.

BAKER, M. 2010. MicroRNA profiling: separating signal from noise. *Nat Methods,* 7**,** 687-92.

BALTUS, T., VON HUNDELSHAUSEN, P., MAUSE, S. F., BUHRE, W., ROSSAINT, R. & WEBER, C. 2005. Differential and additive effects of platelet-derived chemokines on monocyte arrest on inflamed endothelium under flow conditions. *J Leukoc Biol,* 78**,** 435-41.

BARD, M. P., HEGMANS, J. P., HEMMES, A., LUIDER, T. M., WILLEMSEN, R., SEVERIJNEN, L. A., VAN MEERBEECK, J. P., BURGERS, S. A., HOOGSTEDEN, H. C. & LAMBRECHT, B. N. 2004. Proteomic analysis of exosomes isolated from human malignant pleural effusions. *Am J Respir Cell Mol Biol,* 31**,** 114-21.

BARNARD, M. R., KRUEGER, L. A., FRELINGER, A. L., 3RD, FURMAN, M. I. & MICHELSON, A. D. 2003. Whole blood analysis of leukocyte-platelet aggregates. *Curr Protoc Cytom,* Chapter 6**,** Unit 6 15.

BARRES, C., BLANC, L., BETTE-BOBILLO, P., ANDRE, S., MAMOUN, R., GABIUS, H. J. & VIDAL, M. 2010. Galectin-5 is bound onto the surface of rat reticulocyte exosomes and modulates vesicle uptake by macrophages. *Blood,* 115**,** 696-705.

BARROGA, C. F., PHAM, H. & KAUSHANSKY, K. 2008. Thrombopoietin regulates c-Myb expression by modulating micro RNA 150 expression. *Exp Hematol,* 36**,** 1585-92.

BARRY, O. P., PRATICO, D., SAVANI, R. C. & FITZGERALD, G. A. 1998. Modulation of monocyte-endothelial cell interactions by platelet microparticles. *J Clin Invest,* 102**,** 136-44.

BARTEL, D. P. 2004. MicroRNAs: genomics, biogenesis, mechanism, and function. *Cell,* 116**,** 281-97.

BARTEL, D. P. 2009. MicroRNAs: target recognition and regulatory functions. *Cell,* 136**,** 215-33.

BASU, D. & KULKARNI, R. 2014. Overview of blood components and their preparation. *Indian J Anaesth,* 58**,** 529-37.

BATTINELLI, E. M., MARKENS, B. A. & ITALIANO, J. E., JR. 2011. Release of angiogenesis regulatory proteins from platelet alpha granules: modulation of physiologic and pathologic angiogenesis. *Blood,* 118**,** 1359-69.

BELOV, L., MATIC, K. J., HALLAL, S., BEST, O. G., MULLIGAN, S. P. & CHRISTOPHERSON, R. I. 2016. Extensive surface protein profiles of extracellular vesicles from cancer cells may provide diagnostic signatures from blood samples. *J Extracell Vesicles,* 5.

BERCKMANS, R. J., NIEUWLAND, R., BOING, A. N., ROMIJN, F. P., HACK, C. E. & STURK, A. 2001. Cell-derived microparticles circulate in healthy humans and support low grade thrombin generation. *Thromb Haemost,* 85**,** 639-46.

BETEL, D., KOPPAL, A., AGIUS, P., SANDER, C. & LESLIE, C. 2010. Comprehensive modeling of microRNA targets predicts functional non-conserved and non-canonical sites. *Genome Biol,* 11**,** R90.

BETEL, D., WILSON, M., GABOW, A., MARKS, D. S. & SANDER, C. 2008. The microRNA.org resource: targets and expression. *Nucleic Acids Res,* 36**,** D149-53.

BHATNAGAR, S., SHINAGAWA, K., CASTELLINO, F. J. & SCHOREY, J. S. 2007. Exosomes released from macrophages infected with intracellular pathogens stimulate a proinflammatory response in vitro and in vivo. *Blood,* 110**,** 3234-44.

BIDZHEKOV, K., GAN, L., DENECKE, B., ROSTALSKY, A., HRISTOV, M., KOEPPEL, T. A., ZERNECKE, A. & WEBER, C. 2012. microRNA expression signatures and parallels

between monocyte subsets and atherosclerotic plaque in humans. *Thromb Haemost,* 107**,** 619-25.

BLEAZARD, T., LAMB, J. A. & GRIFFITHS-JONES, S. 2015. Bias in microRNA functional enrichment analysis. *Bioinformatics,* 31**,** 1592-8.

BOBRIE, A., COLOMBO, M., KRUMEICH, S., RAPOSO, G. & THERY, C. 2012. Diverse subpopulations of vesicles secreted by different intracellular mechanisms are present in exosome preparations obtained by differential ultracentrifugation. *J Extracell Vesicles,* 1.

BOILARD, E., DUCHEZ, A. C. & BRISSON, A. 2015. The diversity of platelet microparticles. *Curr Opin Hematol,* 22**,** 437-44.

BOING, A. N., VAN DER POL, E., GROOTEMAAT, A. E., COUMANS, F. A., STURK, A. & NIEUWLAND, R. 2014. Single-step isolation of extracellular vesicles by size-exclusion chromatography. *J Extracell Vesicles,* 3.

BOLUKBASI, M. F., MIZRAK, A., OZDENER, G. B., MADLENER, S., STROBEL, T., ERKAN, E. P., FAN, J. B., BREAKEFIELD, X. O. & SAYDAM, O. 2012. miR-1289 and "Zipcode"-like Sequence Enrich mRNAs in Microvesicles. *Mol Ther Nucleic Acids,* 1**,** e10.

BONAUER, A., CARMONA, G., IWASAKI, M., MIONE, M., KOYANAGI, M., FISCHER, A., BURCHFIELD, J., FOX, H., DOEBELE, C., OHTANI, K., CHAVAKIS, E., POTENTE, M., TJWA, M., URBICH, C., ZEIHER, A. M. & DIMMELER, S. 2009. MicroRNA-92a controls angiogenesis and functional recovery of ischemic tissues in mice. *Science,* 324**,** 1710-3.

BOON, R. A. & VICKERS, K. C. 2013. Intercellular Transport of MicroRNAs. *Arteriosclerosis, Thrombosis, and Vascular Biology,* 33**,** 186-192.

BOOTH, A. M., FANG, Y., FALLON, J. K., YANG, J. M., HILDRETH, J. E. & GOULD, S. J. 2006. Exosomes and HIV Gag bud from endosome-like domains of the T cell plasma membrane. *J Cell Biol,* 172**,** 923-35.

BOULANGER, C. M., SCOAZEC, A., EBRAHIMIAN, T., HENRY, P., MATHIEU, E., TEDGUI, A. & MALLAT, Z. 2001. Circulating microparticles from patients with myocardial infarction cause endothelial dysfunction. *Circulation,* 104**,** 2649-52.

BOYERINAS, B., PARK, S. M., HAU, A., MURMANN, A. E. & PETER, M. E. 2010. The role of let-7 in cell differentiation and cancer. *Endocr Relat Cancer,* 17**,** F19-36.

BRAY, P. F., MCKENZIE, S. E., EDELSTEIN, L. C., NAGALLA, S., DELGROSSO, K., ERTEL, A., KUPPER, J., JING, Y., LONDIN, E., LOHER, P., CHEN, H. W., FORTINA, P. & RIGOUTSOS, I. 2013. The complex transcriptional landscape of the anucleate human platelet. *BMC Genomics,* 14**,** 1.

BROWN, M. S., HO, Y. K. & GOLDSTEIN, J. L. 1980. The cholesteryl ester cycle in macrophage foam cells. Continual hydrolysis and re-esterification of cytoplasmic cholesteryl esters. *J Biol Chem,* 255**,** 9344-52.

BRUCHOVA, H., MERKEROVA, M. & PRCHAL, J. T. 2008. Aberrant expression of microRNA in polycythemia vera. *Haematologica,* 93**,** 1009-16.

BURGER, D., MONTEZANO, A. C., NISHIGAKI, N., HE, Y., CARTER, A. & TOUYZ, R. M. 2011. Endothelial microparticle formation by angiotensin II is mediated via Ang II receptor type I/NADPH oxidase/ Rho kinase pathways targeted to lipid rafts. *Arterioscler Thromb Vasc Biol,* 31**,** 1898-907.

CABRERA-FUENTES, H. A., LOPEZ, M. L., MCCURDY, S., FISCHER, S., MEILER, S., BAUMER, Y., GALUSKA, S. P., PREISSNER, K. T. & BOISVERT, W. A. 2015. Regulation of

monocyte/macrophage polarisation by extracellular RNA. *Thromb Haemost,* 113**,** 473-81.

CAI, J., GUAN, W., TAN, X., CHEN, C., LI, L., WANG, N., ZOU, X., ZHOU, F., WANG, J., PEI, F., CHEN, X., LUO, H., WANG, X., HE, D., ZHOU, L., JOSE, P. A. & ZENG, C. 2015. SRY Gene Transferred by Extracellular Vesicles Accelerates Atherosclerosis by Promotion of Leukocyte Adherence to Endothelial Cells. *Clin Sci (Lond)***,** 259-269.

CAMPBELL, C. L., SMYTH, S., MONTALESCOT, G. & STEINHUBL, S. R. 2007. Aspirin dose for the prevention of cardiovascular disease: a systematic review. *JAMA,* 297**,** 2018-24.

CASTELLI, W. P., ANDERSON, K., WILSON, P. W. & LEVY, D. 1992. Lipids and risk of coronary heart disease. The Framingham Study. *Ann Epidemiol,* 2**,** 23-8.

CAUWENBERGHS, S., FEIJGE, M. A., HARPER, A. G., SAGE, S. O., CURVERS, J. & HEEMSKERK, J. W. 2006. Shedding of procoagulant microparticles from unstimulated platelets by integrin-mediated destabilization of actin cytoskeleton. *FEBS Lett,* 580**,** 5313-20.

CERLETTI, C., EVANGELISTA, V. & DE GAETANO, G. 1999. P-selectin-beta 2-integrin cross-talk: a molecular mechanism for polymorphonuclear leukocyte recruitment at the site of vascular damage. *Thromb Haemost,* 82**,** 787-93.

CHAMBERS, J. & RABBITTS, T. H. 2015. LMO2 at 25 years: a paradigm of chromosomal translocation proteins. *Open Biol,* 5**,** 150062.

CHARGAFF, E. & WEST, R. 1946. The biological significance of the thromboplastic protein of blood. *J Biol Chem,* 166**,** 189-97.

CHEN, C., RIDZON, D. A., BROOMER, A. J., ZHOU, Z., LEE, D. H., NGUYEN, J. T., BARBISIN, M., XU, N. L., MAHUVAKAR, V. R., ANDERSEN, M. R., LAO, K. Q., LIVAK, K. J. & GUEGLER, K. J. 2005. Real-time quantification of microRNAs by stem-loop RT-PCR. *Nucleic Acids Res,* 33**,** e179.

CHEN, T. S., LAI, R. C., LEE, M. M., CHOO, A. B., LEE, C. N. & LIM, S. K. 2010. Mesenchymal stem cell secretes microparticles enriched in pre-microRNAs. *Nucleic Acids Res,* 38**,** 215-24.

CHEN, W. F., LEE, J. J., CHANG, C. C., LIN, K. H., WANG, S. H. & SHEU, J. R. 2013. Platelet protease-activated receptor (PAR)4, but not PAR1, associated with neutral sphingomyelinase responsible for thrombin-stimulated ceramide-NF-kappaB signaling in human platelets. *Haematologica,* 98**,** 793-801.

CHEN, X., BA, Y., MA, L., CAI, X., YIN, Y., WANG, K., GUO, J., ZHANG, Y., CHEN, J., GUO, X., LI, Q., LI, X., WANG, W., ZHANG, Y., WANG, J., JIANG, X., XIANG, Y., XU, C., ZHENG, P., ZHANG, J., LI, R., ZHANG, H., SHANG, X., GONG, T., NING, G., WANG, J., ZEN, K., ZHANG, J. & ZHANG, C. Y. 2008. Characterization of microRNAs in serum: a novel class of biomarkers for diagnosis of cancer and other diseases. *Cell Res,* 18**,** 997-1006.

CHENG, H. H., YI, H. S., KIM, Y., KROH, E. M., CHIEN, J. W., EATON, K. D., GOODMAN, M. T., TAIT, J. F., TEWARI, M. & PRITCHARD, C. C. 2013. Plasma Processing Conditions Substantially Influence Circulating microRNA Biomarker Levels. *PLoS One,* 8**,** e64795.

CHENG, L., SHARPLES, R. A., SCICLUNA, B. J. & HILL, A. F. 2014. Exosomes provide a protective and enriched source of miRNA for biomarker profiling compared to intracellular and cell-free blood. *J Extracell Vesicles,* 3.

CHENG, Y., TAN, N., YANG, J., LIU, X., CAO, X., HE, P., DONG, X., QIN, S. & ZHANG, C. 2010. A translational study of circulating cell-free microRNA-1 in acute myocardial infarction. *Clin Sci (Lond),* 119**,** 87-95.

CHERNOBELSKIY, R., CUNNINGHAM, K. I., GOODRICH, M. T., KOBOUROV, S. G. & TROTT, L. 2012. Force-Directed Lombardi-Style Graph Drawing. *Graph Drawing,* 7034**,** 320-331.

CHESNEY, J., BACHER, M., BENDER, A. & BUCALA, R. 1997. The peripheral blood fibrocyte is a potent antigen-presenting cell capable of priming naive T cells in situ. *Proc Natl Acad Sci U S A,* 94**,** 6307-12.

CHEVILLET, J. R., KANG, Q., RUF, I. K., BRIGGS, H. A., VOJTECH, L. N., HUGHES, S. M., CHENG, H. H., ARROYO, J. D., MEREDITH, E. K., GALLICHOTTE, E. N., POGOSOVA-AGADJANYAN, E. L., MORRISSEY, C., STIREWALT, D. L., HLADIK, F., YU, E. Y., HIGANO, C. S. & TEWARI, M. 2014. Quantitative and stoichiometric analysis of the microRNA content of exosomes. *Proc Natl Acad Sci U S A,* 111**,** 14888-93.

CHI, S. W., ZANG, J. B., MELE, A. & DARNELL, R. B. 2009. Argonaute HITS-CLIP decodes microRNA-mRNA interaction maps. *Nature,* 460**,** 479-486.

CHIANG, H. R., SCHOENFELD, L. W., RUBY, J. G., AUYEUNG, V. C., SPIES, N., BAEK, D., JOHNSTON, W. K., RUSS, C., LUO, S., BABIARZ, J. E., BLELLOCH, R., SCHROTH, G. P., NUSBAUM, C. & BARTEL, D. P. 2010. Mammalian microRNAs: experimental evaluation of novel and previously annotated genes. *Genes Dev,* 24**,** 992-1009.

CHINETTI, G., GBAGUIDI, F. G., GRIGLIO, S., MALLAT, Z., ANTONUCCI, M., POULAIN, P., CHAPMAN, J., FRUCHART, J. C., TEDGUI, A., NAJIB-FRUCHART, J. & STAELS, B. 2000. CLA-1/SR-BI is expressed in atherosclerotic lesion macrophages and regulated by activators of peroxisome proliferator-activated receptors. *Circulation,* 101**,** 2411-2417.

CHOW, A., ZHOU, W., LIU, L., FONG, M. Y., CHAMPER, J., VAN HAUTE, D., CHIN, A. R., REN, X., GUGIU, B. G., MENG, Z., HUANG, W., NGO, V., KORTYLEWSKI, M. & WANG, S. E. 2014. Macrophage immunomodulation by breast cancer-derived exosomes requires Toll-like receptor 2-mediated activation of NF-kappaB. *Sci Rep,* 4**,** 5750.

CHRISTIANSON, H. C., SVENSSON, K. J., VAN KUPPEVELT, T. H., LI, J. P. & BELTING, M. 2013. Cancer cell exosomes depend on cell-surface heparan sulfate proteoglycans for their internalization and functional activity. *Proc Natl Acad Sci U S A,* 110**,** 17380-5.

CHRISTIANSON, M. S. & YATES, M. 2012. Scavenger receptor class B type 1 gene polymorphisms and female fertility. *Curr Opin Endocrinol Diabetes Obes,* 19**,** 115-20.

CHRONOS, N. A., GOODALL, A. H., WILSON, D. J., SIGWART, U. & BULLER, N. P. 1993. Profound platelet degranulation is an important side effect of some types of contrast media used in interventional cardiology. *Circulation,* 88**,** 2035-44.

CHUGH, P. & DITTMER, D. P. 2012. Potential pitfalls in microRNA profiling. *Wiley Interdiscip Rev RNA,* 3**,** 601-16.

CHUNG, I. & LIP, G. Y. 2003. Virchow's triad revisited: blood constituents. *Pathophysiol Haemost Thromb,* 33**,** 449-54.

CISMASIU, V. B. & POPESCU, L. M. 2015. Telocytes transfer extracellular vesicles loaded with microRNAs to stem cells. *J Cell Mol Med,* 19**,** 351-8.

CLANCY, L. & FREEDMAN, J. E. 2013. New paradigms in thrombosis: novel mediators and biomarkers platelet RNA transfer. *J Thromb Thrombolysis***,** 12-16.

CLAYTON, A., COURT, J., NAVABI, H., ADAMS, M., MASON, M. D., HOBOT, J. A., NEWMAN, G. R. & JASANI, B. 2001. Analysis of antigen presenting cell derived exosomes, based on immuno-magnetic isolation and flow cytometry. *J Immunol Methods,* 247**,** 163-74.

CLINICALTRIALS.GOV. 2016. *Identifier - NCT02612662; A Study to Assess the Safety and Tolerability of Single Doses of AZD4076 in Healthy Male Subjects* [Online]. Available: https://clinicaltrials.gov/ct2/show/NCT02612662 [Accessed 26th February 2016].

COLLINO, F., DEREGIBUS, M. C., BRUNO, S., STERPONE, L., AGHEMO, G., VILTONO, L., TETTA, C. & CAMUSSI, G. 2010. Microvesicles derived from adult human bone marrow and tissue specific mesenchymal stem cells shuttle selected pattern of miRNAs. *PLoS One,* 5**,** e11803.

CONDE-VANCELLS, J., RODRIGUEZ-SUAREZ, E., EMBADE, N., GIL, D., MATTHIESEN, R., VALLE, M., ELORTZA, F., LU, S. C., MATO, J. M. & FALCON-PEREZ, J. M. 2008. Characterization and comprehensive proteome profiling of exosomes secreted by hepatocytes. *J Proteome Res,* 7**,** 5157-66.

CONNELLY, M. A. & WILLIAMS, D. L. 2003. SR-BI and cholesterol uptake into steroidogenic cells. *Trends Endocrinol Metab,* 14**,** 467-72.

COPPINGER, J. A., CAGNEY, G., TOOMEY, S., KISLINGER, T., BELTON, O., MCREDMOND, J. P., CAHILL, D. J., EMILI, A., FITZGERALD, D. J. & MAGUIRE, P. B. 2004. Characterization of the proteins released from activated platelets leads to localization of novel platelet proteins in human atherosclerotic lesions. *Blood,* 103**,** 2096-104.

COPPINGER, J. A., O'CONNOR, R., WYNNE, K., FLANAGAN, M., SULLIVAN, M., MAGUIRE, P. B., FITZGERALD, D. J. & CAGNEY, G. 2007. Moderation of the platelet releasate response by aspirin. *Blood,* 109**,** 4786-92.

CORSTEN, M. F., DENNERT, R., JOCHEMS, S., KUZNETSOVA, T., DEVAUX, Y., HOFSTRA, L., WAGNER, D. R., STAESSEN, J. A., HEYMANS, S. & SCHROEN, B. 2010. Circulating MicroRNA-208b and MicroRNA-499 reflect myocardial damage in cardiovascular disease. *Circ Cardiovasc Genet,* 3**,** 499-506.

COUMANS, F. A., VAN DER POL, E., BOING, A. N., HAJJI, N., STURK, G., VAN LEEUWEN, T. G. & NIEUWLAND, R. 2014. Reproducible extracellular vesicle size and concentration determination with tunable resistive pulse sensing. *J Extracell Vesicles,* 3.

CREAGER, M. A., LUSCHER, T. F., COSENTINO, F. & BECKMAN, J. A. 2003. Diabetes and vascular disease: pathophysiology, clinical consequences, and medical therapy: Part I. *Circulation,* 108**,** 1527-32.

CREEMERS, E. E., TIJSEN, A. J. & PINTO, Y. M. 2012. Circulating microRNAs: novel biomarkers and extracellular communicators in cardiovascular disease? *Circ Res,* 110**,** 483-95.

D'ALESSANDRA, Y., DEVANNA, P., LIMANA, F., STRAINO, S., DI CARLO, A., BRAMBILLA, P. G., RUBINO, M., CARENA, M. C., SPAZZAFUMO, L., DE SIMONE, M., MICHELI, B., BIGLIOLI, P., ACHILLI, F., MARTELLI, F., MAGGIOLINI, S., MARENZI, G., POMPILIO, G. & CAPOGROSSI, M. C. 2010. Circulating microRNAs are new and sensitive biomarkers of myocardial infarction. *Eur Heart J,* 31**,** 2765-73.

D'ALESSANDRA, Y., POMPILIO, G. & CAPOGROSSI, M. C. 2012. MicroRNAs and myocardial infarction. *Curr Opin Cardiol,* 27**,** 228-35.

DAHIYA, N., SARACHANA, T., VU, L., BECKER, K. G., WOOD, W. H., 3RD, ZHANG, Y. & ATREYA, C. D. 2015. Platelet MicroRNAs: An Overview. *Transfus Med Rev,* 29**,** 215-9.

DAIGNEAULT, M., PRESTON, J. A., MARRIOTT, H. M., WHYTE, M. K. & DOCKRELL, D. H. 2010. The identification of markers of macrophage differentiation in PMA-stimulated THP-1 cells and monocyte-derived macrophages. *PLoS One,* 5**,** e8668.

DALLI, J., MONTERO-MELENDEZ, T., NORLING, L. V., YIN, X., HINDS, C., HASKARD, D., MAYR, M. & PERRETTI, M. 2013. Heterogeneity in neutrophil microparticles reveals distinct proteome and functional properties. *Mol Cell Proteomics,* 12**,** 2205-19.

DANGWAL, S. & THUM, T. 2012. MicroRNAs in platelet biogenesis and function. *Thromb Haemost,* 108**,** 599-604.

DANIELSON, K. M. & DAS, S. 2014. Extracellular Vesicles in Heart Disease: Excitement for the Future ? *Exosomes Microvesicles,* 2.

DE CANDIA, P., TORRI, A., GORLETTA, T., FEDELI, M., BULGHERONI, E., CHERONI, C., MARABITA, F., CROSTI, M., MORO, M., PARIANI, E., ROMANO, L., ESPOSITO, S., MOSCA, F., ROSSETTI, G., ROSSI, R. L., GEGINAT, J., CASORATI, G., DELLABONA, P., PAGANI, M. & ABRIGNANI, S. 2013. Intracellular modulation, extracellular disposal and serum increase of MiR-150 mark lymphocyte activation. *PLoS One,* 8**,** e75348.

DE MENEZES-NETO, A., SAEZ, M. J., LOZANO-RAMOS, I., SEGUI-BARBER, J., MARTIN-JAULAR, L., ULLATE, J. M., FERNANDEZ-BECERRA, C., BORRAS, F. E. & DEL PORTILLO, H. A. 2015. Size-exclusion chromatography as a stand-alone methodology identifies novel markers in mass spectrometry analyses of plasma-derived vesicles from healthy individuals. *J Extracell Vesicles,* 4.

DE VILLIERS, W. J. & SMART, E. J. 1999. Macrophage scavenger receptors and foam cell formation. *J Leukoc Biol,* 66**,** 740-6.

DEATON, C., FROELICHER, E. S., WU, L. H., HO, C., SHISHANI, K. & JAARSMA, T. 2011. The global burden of cardiovascular disease. *J Cardiovasc Nurs,* 26**,** S5-14.

DENZER, K., VAN EIJK, M., KLEIJMEER, M. J., JAKOBSON, E., DE GROOT, C. & GEUZE, H. J. 2000. Follicular dendritic cells carry MHC class II-expressing microvesicles at their surface. *J Immunol,* 165**,** 1259-65.

DI VIZIO, D., MORELLO, M., DUDLEY, A. C., SCHOW, P. W., ADAM, R. M., MORLEY, S., MULHOLLAND, D., ROTINEN, M., HAGER, M. H., INSABATO, L., MOSES, M. A., DEMICHELIS, F., LISANTI, M. P., WU, H., KLAGSBRUN, M., BHOWMICK, N. A., RUBIN, M. A., D'SOUZA-SCHOREY, C. & FREEMAN, M. R. 2012. Large oncosomes in human prostate cancer tissues and in the circulation of mice with metastatic disease. *Am J Pathol,* 181**,** 1573-84.

DIEHL, P., FRICKE, A., SANDER, L., STAMM, J., BASSLER, N., HTUN, N., ZIEMANN, M., HELBING, T., EL-OSTA, A., JOWETT, J. B. & PETER, K. 2012. Microparticles: major transport vehicles for distinct microRNAs in circulation. *Cardiovasc Res,* 93**,** 633-44.

DIMMELER, S. & ZEIHER, A. M. 2010. Circulating microRNAs: novel biomarkers for cardiovascular diseases? *Eur Heart J,* 31**,** 2705-7.

DITTRICH, M., BIRSCHMANN, I., PFRANG, J., HERTERICH, S., SMOLENSKI, A., WALTER, U. & DANDEKAR, T. 2006. Analysis of SAGE data in human platelets: features of the transcriptome in an anucleate cell. *Thromb Haemost,* 95**,** 643-51.

DUAN, X., ZHAN, Q., SONG, B., ZENG, S., ZHOU, J., LONG, Y., LU, J., LI, Z., YUAN, M., CHEN, X., YANG, Q. & XIA, J. 2014. Detection of platelet microRNA expression in patients with diabetes mellitus with or without ischemic stroke. *J Diabetes Complications,* 28**,** 705-10.

DUBOCHET, J. 2012. Cryo-EM--the first thirty years. *J Microsc,* 245**,** 221-4.

DUCHEZ, A. C., BOUDREAU, L. H., BOLLINGER, J., BELLEANNEE, C., CLOUTIER, N., LAFFONT, B., MENDOZA-VILLARROEL, R. E., LEVESQUE, T., ROLLET-LABELLE, E., ROUSSEAU, M., ALLAEYS, I., TREMBLAY, J. J., POUBELLE, P. E., LAMBEAU, G., POULIOT, M., PROVOST, P., SOULET, D., GELB, M. H. & BOILARD, E. 2015. Platelet microparticles are internalized in neutrophils via the concerted activity of 12-lipoxygenase and secreted phospholipase A2-IIA. *Proc Natl Acad Sci U S A,* 112**,** E3564-73.

EASOW, G., TELEMAN, A. A. & COHEN, S. M. 2007. Isolation of microRNA targets by miRNP immunopurification. *RNA,* 13**,** 1198-204.

EDELSTEIN, L. C. & BRAY, P. F. 2011. MicroRNAs in platelet production and activation. *Blood,* 117**,** 5289-96.

EDELSTEIN, L. C., SIMON, L. M., MONTOYA, R. T., HOLINSTAT, M., CHEN, E. S., BERGERON, A., KONG, X., NAGALLA, S., MOHANDAS, N., COHEN, D. E., DONG, J. F., SHAW, C. & BRAY, P. F. 2013. Racial differences in human platelet PAR4 reactivity reflect expression of PCTP and miR-376c. *Nat Med,* 19**,** 1609-16.

EGAN, K., CROWLEY, D., SMYTH, P., O'TOOLE, S., SPILLANE, C., MARTIN, C., GALLAGHER, M., CANNEY, A., NORRIS, L., CONLON, N., MCEVOY, L., FFRENCH, B., STORDAL, B., KEEGAN, H., FINN, S., MCENEANEY, V., LAIOS, A., DUCREE, J., DUNNE, E., SMITH, L., BERNDT, M., SHEILS, O., KENNY, D. & O'LEARY, J. 2011. Platelet adhesion and degranulation induce pro-survival and pro-angiogenic signalling in ovarian cancer cells. *PLoS One,* 6**,** e26125.

EL-HEFNAWY, T., RAJA, S., KELLY, L., BIGBEE, W. L., KIRKWOOD, J. M., LUKETICH, J. D. & GODFREY, T. E. 2004. Characterization of amplifiable, circulating RNA in plasma and its potential as a tool for cancer diagnostics. *Clin Chem,* 50**,** 564-73.

ELLIOTT, A. C., HYNAN, L. S., REISCH, J. S. & SMITH, J. P. 2006. Preparing data for analysis using microsoft Excel. *J Investig Med,* 54**,** 334-41.

EMINAGA, S., CHRISTODOULOU, D. C., VIGNEAULT, F., CHURCH, G. M. & SEIDMAN, J. G. 2013. Quantification of microRNA expression with next-generation sequencing. *Curr Protoc Mol Biol,* Chapter 4**,** Unit 4 17.

EPPLE, L. M., GRIFFITHS, S. G., DECHKOVSKAIA, A. M., DUSTO, N. L., WHITE, J., OUELLETTE, R. J., ANCHORDOQUY, T. J., BEMIS, L. T. & GRANER, M. W. 2012. Medulloblastoma exosome proteomics yield functional roles for extracellular vesicles. *PLoS One,* 7**,** e42064.

ESCREVENTE, C., KELLER, S., ALTEVOGT, P. & COSTA, J. 2011. Interaction and uptake of exosomes by ovarian cancer cells. *BMC Cancer,* 11**,** 108.

ETHERIDGE, A., LEE, I., HOOD, L., GALAS, D. & WANG, K. 2011. Extracellular microRNA: a new source of biomarkers. *Mutat Res,* 717**,** 85-90.

EULALIO, A., MANO, M., DAL FERRO, M., ZENTILIN, L., SINAGRA, G., ZACCHIGNA, S. & GIACCA, M. 2012. Functional screening identifies miRNAs inducing cardiac regeneration. *Nature,* 492**,** 376-81.

FELLI, N., PEDINI, F., ROMANIA, P., BIFFONI, M., MORSILLI, O., CASTELLI, G., SANTORO, S., CHICARELLA, S., SORRENTINO, A., PESCHLE, C. & MARZIALI, G. 2009. MicroRNA 223-dependent expression of LMO2 regulates normal erythropoiesis. *Haematologica,* 94**,** 479-86.

FENG, D., ZHAO, W. L., YE, Y. Y., BAI, X. C., LIU, R. Q., CHANG, L. F., ZHOU, Q. & SUI, S. F. 2010. Cellular internalization of exosomes occurs through phagocytosis. *Traffic,* 11**,** 675-87.

FESKE, S., GWACK, Y., PRAKRIYA, M., SRIKANTH, S., PUPPEL, S. H., TANASA, B., HOGAN, P. G., LEWIS, R. S., DALY, M. & RAO, A. 2006. A mutation in Orai1 causes immune deficiency by abrogating CRAC channel function. *Nature,* 441**,** 179-85.

FEVRIER, B. & RAPOSO, G. 2004. Exosomes: endosomal-derived vesicles shipping extracellular messages. *Curr Opin Cell Biol,* 16**,** 415-21.

FICHTLSCHERER, S., DE ROSA, S., FOX, H., SCHWIETZ, T., FISCHER, A., LIEBETRAU, C., WEBER, M., HAMM, C. W., ROXE, T., MULLER-ARDOGAN, M., BONAUER, A., ZEIHER, A. M. & DIMMELER, S. 2010. Circulating microRNAs in patients with coronary artery disease. *Circ Res,* 107**,** 677-84.

FICHTLSCHERER, S., ZEIHER, A. M. & DIMMELER, S. 2011. Circulating microRNAs: biomarkers or mediators of cardiovascular diseases? *Arterioscler Thromb Vasc Biol,* 31, 2383-90.

FIEDLER, J., JAZBUTYTE, V., KIRCHMAIER, B. C., GUPTA, S. K., LORENZEN, J., HARTMANN, D., GALUPPO, P., KNEITZ, S., PENA, J. T., SOHN-LEE, C., LOYER, X., SOUTSCHEK, J., BRAND, T., TUSCHL, T., HEINEKE, J., MARTIN, U., SCHULTE-MERKER, S., ERTL, G., ENGELHARDT, S., BAUERSACHS, J. & THUM, T. 2011. MicroRNA-24 regulates vascularity after myocardial infarction. *Circulation,* 124**,** 720-30.

FINN, N. A., EAPEN, D., MANOCHA, P., AL KASSEM, H., LASSEGUE, B., GHASEMZADEH, N., QUYYUMI, A. & SEARLES, C. D. 2013. Coronary heart disease alters intercellular communication by modifying microparticle-mediated microRNA transport. *FEBS Lett,* 587**,** 3456-63.

FISH, J. E., SANTORO, M. M., MORTON, S. U., YU, S., YEH, R. F., WYTHE, J. D., IVEY, K. N., BRUNEAU, B. G., STAINIER, D. Y. & SRIVASTAVA, D. 2008. miR-126 regulates angiogenic signaling and vascular integrity. *Dev Cell,* 15**,** 272-84.

FITZNER, D., SCHNAARS, M., VAN ROSSUM, D., KRISHNAMOORTHY, G., DIBAJ, P., BAKHTI, M., REGEN, T., HANISCH, U. K. & SIMONS, M. 2011. Selective transfer of exosomes from oligodendrocytes to microglia by macropinocytosis. *J Cell Sci,* 124**,** 447-58.

FLAUMENHAFT, R., DILKS, J. R., RICHARDSON, J., ALDEN, E., PATEL-HETT, S. R., BATTINELLI, E., KLEMENT, G. L., SOLA-VISNER, M. & ITALIANO, J. E., JR. 2009. Megakaryocyte-derived microparticles: direct visualization and distinction from platelet-derived microparticles. *Blood,* 113**,** 1112-21.

FONTANA, L., PELOSI, E., GRECO, P., RACANICCHI, S., TESTA, U., LIUZZI, F., CROCE, C. M., BRUNETTI, E., GRIGNANI, F. & PESCHLE, C. 2007. MicroRNAs 17-5p-20a-106a control monocytopoiesis through AML1 targeting and M-CSF receptor upregulation. *Nat Cell Biol,* 9**,** 775-87.

FRANK, F., SONENBERG, N. & NAGAR, B. 2010. Structural basis for 5'-nucleotide base-specific recognition of guide RNA by human AGO2. *Nature,* 465**,** 818-22.

FREEDMAN, J. E. & LOSCALZO, J. 2002. Platelet-monocyte aggregates: bridging thrombosis and inflammation. *Circulation,* 105**,** 2130-2.

FRENCH, D. L. & SELIGSOHN, U. 2000. Platelet glycoprotein IIb/IIIa receptors and Glanzmann's thrombasthenia. *Arterioscler Thromb Vasc Biol,* 20**,** 607-10.

FRIEDMAN, R. C., FARH, K. K., BURGE, C. B. & BARTEL, D. P. 2009. Most mammalian mRNAs are conserved targets of microRNAs. *Genome Res,* 19**,** 92-105.

FURCHGOTT, R. F. & ZAWADZKI, J. V. 1980. The obligatory role of endothelial cells in the relaxation of arterial smooth muscle by acetylcholine. *Nature,* 288**,** 373-6.

FURMAN, M. I., BENOIT, S. E., BARNARD, M. R., VALERI, C. R., BORBONE, M. L., BECKER, R. C., HECHTMAN, H. B. & MICHELSON, A. D. 1998. Increased platelet reactivity and circulating monocyte-platelet aggregates in patients with stable coronary artery disease. *J Am Coll Cardiol,* 31**,** 352-8.

GACEB, A., MARTINEZ, M. C. & ANDRIANTSITOHAINA, R. 2014. Extracellular vesicles: New players in cardiovascular diseases. *International Journal of Biochemistry & Cell Biology,* 50**,** 24-28.

GACHET, C. 2006. Regulation of platelet functions by P2 receptors. *Annu Rev Pharmacol Toxicol,* 46**,** 277-300.

GACHET, C. 2008. P2 receptors, platelet function and pharmacological implications. *Thromb Haemost,* 99**,** 466-72.

GACHET, C., LEON, C. & HECHLER, B. 2006. The platelet P2 receptors in arterial thrombosis. *Blood Cells Mol Dis,* 36**,** 223-7.

GALLO, A., TANDON, M., ALEVIZOS, I. & ILLEI, G. G. 2012. The majority of microRNAs detectable in serum and saliva is concentrated in exosomes. *PLoS One,* 7**,** e30679.

GAMBIM, M. H., DO CARMO ADE, O., MARTI, L., VERISSIMO-FILHO, S., LOPES, L. R. & JANISZEWSKI, M. 2007. Platelet-derived exosomes induce endothelial cell apoptosis through peroxynitrite generation: experimental evidence for a novel mechanism of septic vascular dysfunction. *Crit Care,* 11**,** R107.

GARCIA, B. A., SMALLEY, D. M., CHO, H., SHABANOWITZ, J., LEY, K. & HUNT, D. F. 2005. The platelet microparticle proteome. *J Proteome Res,* 4**,** 1516-21.

GARDINER, C., FERREIRA, Y. J., DRAGOVIC, R. A., REDMAN, C. W. & SARGENT, I. L. 2013. Extracellular vesicle sizing and enumeration by nanoparticle tracking analysis. *J Extracell Vesicles,* 2.

GARDINER, C., HARRISON, P., BELTING, M., BOING, A., CAMPELLO, E., CARTER, B. S., COLLIER, M. E., COUMANS, F., ETTELAIE, C., VAN ES, N., HOCHBERG, F. H., MACKMAN, N., RENNERT, R. C., THALER, J., RAK, J. & NIEUWLAND, R. 2015. Extracellular vesicles, tissue factor, cancer and thrombosis - discussion themes of the ISEV 2014 Educational Day. *J Extracell Vesicles,* 4.

GARDINER, C., SHAW, M., HOLE, P., SMITH, J., TANNETTA, D., REDMAN, C. W. & SARGENT, I. L. 2014. Measurement of refractive index by nanoparticle tracking analysis reveals heterogeneity in extracellular vesicles. *J Extracell Vesicles,* 3.

GARZON, R., PICHIORRI, F., PALUMBO, T., IULIANO, R., CIMMINO, A., AQEILAN, R., VOLINIA, S., BHATT, D., ALDER, H., MARCUCCI, G., CALIN, G. A., LIU, C. G., BLOOMFIELD, C. D., ANDREEFF, M. & CROCE, C. M. 2006. MicroRNA fingerprints during human megakaryocytopoiesis. *Proc Natl Acad Sci U S A,* 103**,** 5078-83.

GAWAZ, M., LANGER, H. & MAY, A. E. 2005. Platelets in inflammation and atherogenesis. *J Clin Invest,* 115**,** 3378-84.

GAWAZ, M., STELLOS, K. & LANGER, H. F. 2008. Platelets modulate atherogenesis and progression of atherosclerotic plaques via interaction with progenitor and dendritic cells. *J Thromb Haemost,* 6**,** 235-42.

GEBUHRER, V., MURPHY, J. F., BORDET, J. C., RECK, M. P. & MCGREGOR, J. L. 1995. Oxidized low-density lipoprotein induces the expression of P-selectin (GMP140/PADGEM/CD62) on human endothelial cells. *Biochem J,* 306 (Pt 1)**,** 293-8.

GEMMELL, C. H., SEFTON, M. V. & YEO, E. L. 1993. Platelet-derived microparticle formation involves glycoprotein IIb-IIIa. Inhibition by RGDS and a Glanzmann's thrombasthenia defect. *J Biol Chem,* 268**,** 14586-9.

GERSON, K. D., MADDULA, V. S., SELIGMANN, B. E., SHEARSTONE, J. R., KHAN, A. & MERCURIO, A. M. 2012. Effects of beta4 integrin expression on microRNA patterns in breast cancer. *Biol Open,* 1**,** 658-66.

GIDLOF, O., VAN DER BRUG, M., OHMAN, J., GILJE, P., OLDE, B., WAHLESTEDT, C. & ERLINGE, D. 2013. Platelets activated during myocardial infarction release functional miRNA, which can be taken up by endothelial cells and regulate ICAM1 expression. *Blood,* 121**,** 3908-17.

GIMBRONE, M. A., JR., NAGEL, T. & TOPPER, J. N. 1997. Biomechanical activation: an emerging paradigm in endothelial adhesion biology. *J Clin Invest,* 100**,** S61-5.

GIRARDI, C., DE PITTA, C., CASARA, S., SALES, G., LANFRANCHI, G., CELOTTI, L. & MOGNATO, M. 2012. Analysis of miRNA and mRNA expression profiles highlights alterations in ionizing radiation response of human lymphocytes under modeled microgravity. *PLoS One,* 7**,** e31293.

GODARD, P. & VAN EYLL, J. 2015. Pathway analysis from lists of microRNAs: common pitfalls and alternative strategy. *Nucleic Acids Res,* 43**,** 3490-7.

GOETZL, E. J., GOETZL, L., KARLINER, J. S., TANG, N. & PULLIAM, L. 2016. Human plasma platelet-derived exosomes: effects of aspirin. *FASEB J***,** 2058-2063.

GOLDSTEIN, J. L. & BROWN, M. S. 1985. Familial hypercholesterolemia: a genetic receptor disease. *Hosp Pract (Off Ed),* 20**,** 35-41, 45-6.

GOREN, Y., MEIRI, E., HOGAN, C., MITCHELL, H., LEBANONY, D., SALMAN, N., SCHLIAMSER, J. E. & AMIR, O. 2014. Relation of reduced expression of MiR-150 in platelets to atrial fibrillation in patients with chronic systolic heart failure. *Am J Cardiol,* 113**,** 976-81.

GRASEDIECK, S., SORRENTINO, A., LANGER, C., BUSKE, C., DOHNER, H., MERTENS, D. & KUCHENBAUER, F. 2013. Circulating microRNAs in hematological diseases: principles, challenges, and perspectives. *Blood,* 121**,** 4977-84.

GRIMSON, A., FARH, K. K., JOHNSTON, W. K., GARRETT-ENGELE, P., LIM, L. P. & BARTEL, D. P. 2007. MicroRNA targeting specificity in mammals: determinants beyond seed pairing. *Mol Cell,* 27**,** 91-105.

GUDURIC-FUCHS, J., O'CONNOR, A., CAMP, B., O'NEILL, C. L., MEDINA, R. J. & SIMPSON, D. A. 2012. Selective extracellular vesicle-mediated export of an overlapping set of microRNAs from multiple cell types. *BMC Genomics,* 13**,** 357.

GUPTA, S. K., BANG, C. & THUM, T. 2010. Circulating microRNAs as biomarkers and potential paracrine mediators of cardiovascular disease. *Circ Cardiovasc Genet,* 3**,** 484-8.

GYORGY, B., MODOS, K., PALLINGER, E., PALOCZI, K., PASZTOI, M., MISJAK, P., DELI, M. A., SIPOS, A., SZALAI, A., VOSZKA, I., POLGAR, A., TOTH, K., CSETE, M., NAGY, G., GAY, S., FALUS, A., KITTEL, A. & BUZAS, E. I. 2011a. Detection and isolation of cell-derived microparticles are compromised by protein complexes resulting from shared biophysical parameters. *Blood,* 117**,** e39-48.

GYORGY, B., SZABO, T. G., PASZTOI, M., PAL, Z., MISJAK, P., ARADI, B., LASZLO, V., PALLINGER, E., PAP, E., KITTEL, A., NAGY, G., FALUS, A. & BUZAS, E. I. 2011b. Membrane vesicles, current state-of-the-art: emerging role of extracellular vesicles. *Cell Mol Life Sci,* 68**,** 2667-88.

GYORGY, B., SZABO, T. G., TURIAK, L., WRIGHT, M., HERCZEG, P., LEDECZI, Z., KITTEL, A., POLGAR, A., TOTH, K., DERFALVI, B., ZELENAK, G., BOROCZ, I., CARR, B., NAGY, G., VEKEY, K., GAY, S., FALUS, A. & BUZAS, E. I. 2012. Improved flow cytometric assessment reveals distinct microvesicle (cell-derived microparticle) signatures in joint diseases. *PLoS One,* 7**,** e49726.

HAFNER, M., LANDTHALER, M., BURGER, L., KHORSHID, M., HAUSSER, J., BERNINGER, P., ROTHBALLER, A., ASCANO, M., JR., JUNGKAMP, A. C., MUNSCHAUER, M., ULRICH, A., WARDLE, G. S., DEWELL, S., ZAVOLAN, M. & TUSCHL, T. 2010. Transcriptome-wide identification of RNA-binding protein and microRNA target sites by PAR-CLIP. *Cell,* 141**,** 129-41.

HAFNER, M., LIANOGLOU, S., TUSCHL, T. & BETEL, D. 2012. Genome-wide identification of miRNA targets by PAR-CLIP. *Methods,* 58**,** 94-105.

HANSEN, T. B., JENSEN, T. I., CLAUSEN, B. H., BRAMSEN, J. B., FINSEN, B., DAMGAARD, C. K. & KJEMS, J. 2013. Natural RNA circles function as efficient microRNA sponges. *Nature,* 495**,** 384-388.

HANSSON, G. K. 2005. Inflammation, atherosclerosis, and coronary artery disease. *N Engl J Med,* 352**,** 1685-95.

HARRISON, P. & GARDINER, C. 2012. Invisible vesicles swarm within the iceberg. *J Thromb Haemost,* 10**,** 916-8.

HE, Y., ZHANG, L., LI, Z., GAO, H., YUE, Z., LIU, Z., LIU, X., FENG, X. & LIU, P. 2015. RIP140 triggers foam-cell formation by repressing ABCA1/G1 expression and cholesterol efflux via liver X receptor. *FEBS Lett,* 589**,** 455-60.

HEADLAND, S. E., JONES, H. R., D'SA, A. S., PERRETTI, M. & NORLING, L. V. 2014. Cutting-edge analysis of extracellular microparticles using ImageStream(X) imaging flow cytometry. *Sci Rep,* 4**,** 5237.

HEEMSKERK, J. W., BEVERS, E. M. & LINDHOUT, T. 2002. Platelet activation and blood coagulation. *Thromb Haemost,* 88**,** 186-93.

HEEMSKERK, J. W., VUIST, W. M., FEIJGE, M. A., REUTELINGSPERGER, C. P. & LINDHOUT, T. 1997. Collagen but not fibrinogen surfaces induce bleb formation, exposure of phosphatidylserine, and procoagulant activity of adherent platelets: evidence for regulation by protein tyrosine kinase-dependent Ca2+ responses. *Blood,* 90**,** 2615-25.

HEIJNEN, H. F., SCHIEL, A. E., FIJNHEER, R., GEUZE, H. J. & SIXMA, J. J. 1999. Activated platelets release two types of membrane vesicles: microvesicles by surface shedding and exosomes derived from exocytosis of multivesicular bodies and alpha-granules. *Blood,* 94**,** 3791-9.

HEMLER, M. E. 2005. Tetraspanin functions and associated microdomains. *Nat Rev Mol Cell Biol,* 6**,** 801-11.

HIRANO, K., YAMASHITA, S., NAKAGAWA, Y., OHYA, T., MATSUURA, F., TSUKAMOTO, K., OKAMOTO, Y., MATSUYAMA, A., MATSUMOTO, K., MIYAGAWA, J. & MATSUZAWA, Y. 1999. Expression of human scavenger receptor class B type I in cultured human monocyte-derived macrophages and atherosclerotic lesions. *Circ Res,* 85**,** 108-16.

HISLOP, J. N., MARLEY, A. & VON ZASTROW, M. 2004. Role of mammalian vacuolar protein-sorting proteins in endocytic trafficking of a non-ubiquitinated G protein-coupled receptor to lysosomes. *J Biol Chem,* 279**,** 22522-31.

HJEMDAHL, P., CHRONOS, N. A., WILSON, D. J., BOULOUX, P. & GOODALL, A. H. 1994. Epinephrine sensitizes human platelets in vivo and in vitro as studied by fibrinogen binding and P-selectin expression. *Arterioscler Thromb,* 14**,** 77-84.

HOWARD, G., WAGENKNECHT, L. E., BURKE, G. L., DIEZ-ROUX, A., EVANS, G. W., MCGOVERN, P., NIETO, F. J. & TELL, G. S. 1998. Cigarette smoking and progression of atherosclerosis: The Atherosclerosis Risk in Communities (ARIC) Study. *JAMA,* 279**,** 119-24.

HOY, A. M. & BUCK, A. H. 2012. Extracellular small RNAs: what, where, why? *Biochem Soc Trans,* 40**,** 886-90.

HSU, S. D., TSENG, Y. T., SHRESTHA, S., LIN, Y. L., KHALEEL, A., CHOU, C. H., CHU, C. F., HUANG, H. Y., LIN, C. M., HO, S. Y., JIAN, T. Y., LIN, F. M., CHANG, T. H., WENG, S. L., LIAO, K. W., LIAO, I. E., LIU, C. C. & HUANG, H. D. 2014. miRTarBase update 2014: an information resource for experimentally validated miRNA-target interactions. *Nucleic Acids Res,* 42**,** D78-85.

HUBER, H. J. & HOLVOET, P. 2015. Exosomes: emerging roles in communication between blood cells and vascular tissues during atherosclerosis. *Curr Opin Lipidol,* 26**,** 412-9.

HUGEL, B., MARTINEZ, M. C., KUNZELMANN, C. & FREYSSINET, J. M. 2005. Membrane microparticles: two sides of the coin. *Physiology (Bethesda),* 20**,** 22-7.

HULSMANS, M. & HOLVOET, P. 2013. MicroRNA-containing microvesicles regulating inflammation in association with atherosclerotic disease. *Cardiovasc Res,* 100**,** 7-18.

HUNTER, M. P., ISMAIL, N., ZHANG, X., AGUDA, B. D., LEE, E. J., YU, L., XIAO, T., SCHAFER, J., LEE, M. L., SCHMITTGEN, T. D., NANA-SINKAM, S. P., JARJOURA, D. & MARSH, C. B. 2008. Detection of microRNA expression in human peripheral blood microvesicles. *PLoS One,* 3**,** e3694.

HUO, Y., SCHOBER, A., FORLOW, S. B., SMITH, D. F., HYMAN, M. C., JUNG, S., LITTMAN, D. R., WEBER, C. & LEY, K. 2003. Circulating activated platelets exacerbate atherosclerosis in mice deficient in apolipoprotein E. *Nat Med,* 9**,** 61-7.

HUSSEIN, K., THEOPHILE, K., DRALLE, W., WIESE, B., KREIPE, H. & BOCK, O. 2009. MicroRNA expression profiling of megakaryocytes in primary myelofibrosis and essential thrombocythemia. *Platelets,* 20**,** 391-400.

HWANG, I., SHEN, X. & SPRENT, J. 2003. Direct stimulation of naive T cells by membrane vesicles from antigen-presenting cells: distinct roles for CD54 and B7 molecules. *Proc Natl Acad Sci U S A,* 100**,** 6670-5.

ILVESKERO, S., SILJANDER, P. & LASSILA, R. 2001. Procoagulant activity on platelets adhered to collagen or plasma clot. *Arterioscler Thromb Vasc Biol,* 21**,** 628-35.

INOUE, O., SUZUKI-INOUE, K., DEAN, W. L., FRAMPTON, J. & WATSON, S. P. 2003. Integrin alpha2beta1 mediates outside-in regulation of platelet spreading on

collagen through activation of Src kinases and PLCgamma2. *J Cell Biol,* 160, 769-80.

ISEV 2015. The Fourth International Meeting of ISEV, ISEV2015. *J Extracell Vesicles,* 4.

ISMAIL, N., WANG, Y., DAKHLALLAH, D., MOLDOVAN, L., AGARWAL, K., BATTE, K., SHAH, P., WISLER, J., EUBANK, T. D., TRIDANDAPANI, S., PAULAITIS, M. E., PIPER, M. G. & MARSH, C. B. 2012. Macrophage microvesicles induce macrophage differentiation and miR-223 transfer. *Blood,* 121, 984-995.

JACKSON, S. P. 2011. Arterial thrombosis--insidious, unpredictable and deadly. *Nat Med,* 17, 1423-36.

JACKSON, S. P. & SCHOENWAELDER, S. M. 2003. Antiplatelet therapy: In search of the 'magic bullet'. *Nature Reviews Drug Discovery,* 2, 775-789.

JACOBY, R. C., OWINGS, J. T., HOLMES, J., BATTISTELLA, F. D., GOSSELIN, R. C. & PAGLIERONI, T. G. 2001. Platelet activation and function after trauma. *J Trauma,* 51, 639-47.

JAIN, S., KAPETANAKI, M. G., RAGHAVACHARI, N., WOODHOUSE, K., YU, G., BARGE, S., CORONNELLO, C., BENOS, P. V., KATO, G. J., KAMINSKI, N. & GLADWIN, M. T. 2013. Expression of regulatory platelet microRNAs in patients with sickle cell disease. *PLoS One,* 8, e60932.

JAISWAL, R., LUK, F., GONG, J., MATHYS, J. M., GRAU, G. E. & BEBAWY, M. 2012. Microparticle conferred microRNA profiles--implications in the transfer and dominance of cancer traits. *Mol Cancer,* 11, 37.

JAKOBSEN, K. R., PAULSEN, B. S., BAEK, R., VARMING, K., SORENSEN, B. S. & JORGENSEN, M. M. 2015. Exosomal proteins as potential diagnostic markers in advanced non-small cell lung carcinoma. *J Extracell Vesicles,* 4.

JANDROT-PERRUS, M., LAGRUE, A. H., OKUMA, M. & BON, C. 1997. Adhesion and activation of human platelets induced by convulxin involve glycoprotein VI and integrin alpha2beta1. *J Biol Chem,* 272, 27035-41.

JANES, S. L., WILSON, D. J., COX, A. D., CHRONOS, N. A. & GOODALL, A. H. 1994. ADP causes partial degranulation of platelets in the absence of aggregation. *Br J Haematol,* 86, 568-73.

JANISZEWSKI, M., DO CARMO, A. O., PEDRO, M. A., SILVA, E., KNOBEL, E. & LAURINDO, F. R. 2004. Platelet-derived exosomes of septic individuals possess proapoptotic NAD(P)H oxidase activity: A novel vascular redox pathway. *Crit Care Med,* 32, 818-25.

JANOWSKA-WIECZOREK, A., WYSOCZYNSKI, M., KIJOWSKI, J., MARQUEZ-CURTIS, L., MACHALINSKI, B., RATAJCZAK, J. & RATAJCZAK, M. Z. 2005. Microvesicles derived from activated platelets induce metastasis and angiogenesis in lung cancer. *Int J Cancer,* 113, 752-60.

JENSEN, S. G., LAMY, P., RASMUSSEN, M. H., OSTENFELD, M. S., DYRSKJOT, L., ORNTOFT, T. F. & ANDERSEN, C. L. 2011. Evaluation of two commercial global miRNA expression profiling platforms for detection of less abundant miRNAs. *BMC Genomics,* 12, 435.

JIN, H. Y., GONZALEZ-MARTIN, A., MILETIC, A. V., LAI, M., KNIGHT, S., SABOURI-GHOMI, M., HEAD, S. R., MACAULEY, M. S., RICKERT, R. C. & XIAO, C. 2015. Transfection of microRNA Mimics Should Be Used with Caution. *Front Genet,* 6, 340.

JIN, M., DRWAL, G., BOURGEOIS, T., SALTZ, J. & WU, H. M. 2005. Distinct proteome features of plasma microparticles. *Proteomics,* 5, 1940-52.

JIN, Z. B., HIROKAWA, G., GUI, L., TAKAHASHI, R., OSAKADA, F., HIURA, Y., TAKAHASHI, M., YASUHARA, O. & IWAI, N. 2009. Targeted deletion of miR-182, an abundant retinal microRNA. *Mol Vis,* 15**,** 523-33.

JOHNSEN, K. B., GUDBERGSSON, J. M., SKOV, M. N., PILGAARD, L., MOOS, T. & DUROUX, M. 2014. A comprehensive overview of exosomes as drug delivery vehicles - endogenous nanocarriers for targeted cancer therapy. *Biochim Biophys Acta,* 1846**,** 75-87.

JOHNSTONE, R. M., ADAM, M., HAMMOND, J. R., ORR, L. & TURBIDE, C. 1987. Vesicle formation during reticulocyte maturation. Association of plasma membrane activities with released vesicles (exosomes). *J Biol Chem,* 262**,** 9412-20.

JONES, C. I., BRAY, S., GARNER, S. F., STEPHENS, J., DE BONO, B., ANGENENT, W. G., BENTLEY, D., BURNS, P., COFFEY, A., DELOUKAS, P., EARTHROWL, M., FARNDALE, R. W., HOYLAERTS, M. F., KOCH, K., RANKIN, A., RICE, C. M., ROGERS, J., SAMANI, N. J., STEWARD, M., WALKER, A., WATKINS, N. A., AKKERMAN, J. W., DUDBRIDGE, F., GOODALL, A. H., OUWEHAND, W. H. & BLOODOMICS, C. 2009. A functional genomics approach reveals novel quantitative trait loci associated with platelet signaling pathways. *Blood,* 114**,** 1405-16.

JOUTSI-KORHONEN, L., SMETHURST, P. A., RANKIN, A., GRAY, E., M, I. J., ONLEY, C. M., WATKINS, N. A., WILLIAMSON, L. M., GOODALL, A. H., DE GROOT, P. G., FARNDALE, R. W. & OUWEHAND, W. H. 2003. The low-frequency allele of the platelet collagen signaling receptor glycoprotein VI is associated with reduced functional responses and expression. *Blood,* 101**,** 4372-9.

JUNG, C., SORENSSON, P., SALEH, N., ARHEDEN, H., RYDEN, L. & PERNOW, J. 2012. Circulating endothelial and platelet derived microparticles reflect the size of myocardium at risk in patients with ST-elevation myocardial infarction. *Atherosclerosis,* 221**,** 226-31.

KADOGLOU, N. P., ILIADIS, F., ANGELOPOULOU, N., PERREA, D., LIAPIS, C. D. & ALEVIZOS, M. 2008a. Beneficial effects of rosiglitazone on novel cardiovascular risk factors in patients with Type 2 diabetes mellitus. *Diabet Med,* 25**,** 333-40.

KADOGLOU, N. P., ILIADIS, F. & LIAPIS, C. D. 2008b. Exercise and carotid atherosclerosis. *Eur J Vasc Endovasc Surg,* 35**,** 264-72.

KAHN, M. L., ZHENG, Y. W., HUANG, W., BIGORNIA, V., ZENG, D., MOFF, S., FARESE, R. V., JR., TAM, C. & COUGHLIN, S. R. 1998. A dual thrombin receptor system for platelet activation. *Nature,* 394**,** 690-4.

KAHNER, B. N., DORSAM, R. T. & KUNAPULI, S. P. 2008. Role of P2Y receptor subtypes in platelet-derived microparticle generation. *Front Biosci,* 13**,** 433-9.

KALLER, M., OELJEKLAUS, S., WARSCHEID, B. & HERMEKING, H. 2014. Identification of microRNA targets by pulsed SILAC. *Methods Mol Biol,* 1188**,** 327-49.

KALRA, H., SIMPSON, R. J., JI, H., AIKAWA, E., ALTEVOGT, P., ASKENASE, P., BOND, V. C., BORRAS, F. E., BREAKEFIELD, X., BUDNIK, V., BUZAS, E., CAMUSSI, G., CLAYTON, A., COCUCCI, E., FALCON-PEREZ, J. M., GABRIELSSON, S., GHO, Y. S., GUPTA, D., HARSHA, H. C., HENDRIX, A., HILL, A. F., INAL, J. M., JENSTER, G., KRAMER-ALBERS, E. M., LIM, S. K., LLORENTE, A., LOTVALL, J., MARCILLA, A., MINCHEVA-NILSSON, L., NAZARENKO, I., NIEUWLAND, R., NOLTE-'T HOEN, E. N., PANDEY, A., PATEL, T., PIPER, M. G., PLUCHINO, S., PRASAD, T. S., RAJENDRAN, L., RAPOSO, G., RECORD, M., REID, G. E., SANCHEZ-MADRID, F., SCHIFFELERS, R. M., SILJANDER, P., STENSBALLE, A., STOORVOGEL, W., TAYLOR, D., THERY, C.,

VALADI, H., VAN BALKOM, B. W., VAZQUEZ, J., VIDAL, M., WAUBEN, M. H., YANEZ-MO, M., ZOELLER, M. & MATHIVANAN, S. 2012. Vesiclepedia: a compendium for extracellular vesicles with continuous community annotation. *PLoS Biol,* 10**,** e1001450.

KAMATH, S., BLANN, A. D. & LIP, G. Y. 2001. Platelet activation: assessment and quantification. *Eur Heart J,* 22**,** 1561-71.

KAMBUROV, A., STELZL, U., LEHRACH, H. & HERWIG, R. 2013. The ConsensusPathDB interaction database: 2013 update. *Nucleic Acids Res,* 41**,** D793-800.

KAMM, R. C. & SMITH, A. G. 1972. Nucleic acid concentrations in normal human plasma. *Clin Chem,* 18**,** 519-22.

KANNAN, M., MOHAN, K. V., KULKARNI, S. & ATREYA, C. 2009. Membrane array-based differential profiling of platelets during storage for 52 miRNAs associated with apoptosis. *Transfusion,* 49**,** 1443-50.

KAPLAN, J. E. & SABA, T. M. 1978. Platelet removal from the circulation by the liver and spleen. *Am J Physiol,* 235**,** H314-20.

KAPLAN, Z. S. & JACKSON, S. P. 2011. The role of platelets in atherothrombosis. *Hematology Am Soc Hematol Educ Program,* 2011**,** 51-61.

KAPUSTIN, A. N., CHATROU, M. L., DROZDOV, I., ZHENG, Y., DAVIDSON, S. M., SOONG, D., FURMANIK, M., SANCHIS, P., DE ROSALES, R. T., ALVAREZ-HERNANDEZ, D., SHROFF, R., YIN, X., MULLER, K., SKEPPER, J. N., MAYR, M., REUTELINGSPERGER, C. P., CHESTER, A., BERTAZZO, S., SCHURGERS, L. J. & SHANAHAN, C. M. 2015. Vascular smooth muscle cell calcification is mediated by regulated exosome secretion. *Circ Res,* 116**,** 1312-23.

KAUDEWITZ, D., SKROBLIN, P., BENDER, L. H., BARWARI, T., WILLEIT, P., PECHLANER, R., SUNDERLAND, N. P., WILLEIT, K., MORTON, A. C., ARMSTRONG, P. C., CHAN, M. V., LU, R., YIN, X., GRACIO, F., DUDEK, K., LANGLEY, S. R., ZAMPETAKI, A., DE RINALDIS, E., YE, S., WARNER, T. D., SAXENA, A., KIECHL, S., STOREY, R. F. & MAYR, M. 2016. Association of MicroRNAs and YRNAs With Platelet Function. *Circ Res,* 118**,** 420-32.

KEERTHIKUMAR, S., CHISANGA, D., ARIYARATNE, D., AL SAFFAR, H., ANAND, S., ZHAO, K., SAMUEL, M., PATHAN, M., JOIS, M., CHILAMKURTI, N., GANGODA, L. & MATHIVANAN, S. 2015. ExoCarta: A Web-Based Compendium of Exosomal Cargo. *J Mol Biol***,** 688-692.

KELLER, S., SANDERSON, M. P., STOECK, A. & ALTEVOGT, P. 2006. Exosomes: from biogenesis and secretion to biological function. *Immunol Lett,* 107**,** 102-8.

KELLY, B. B., NARULA, J. & FUSTER, V. 2012. Recognizing global burden of cardiovascular disease and related chronic diseases. *Mt Sinai J Med,* 79**,** 632-40.

KHATRI, P., SIROTA, M. & BUTTE, A. J. 2012. Ten years of pathway analysis: current approaches and outstanding challenges. *PLoS Comput Biol,* 8**,** e1002375.

KHVOROVA, A., REYNOLDS, A. & JAYASENA, S. D. 2003. Functional siRNAs and miRNAs exhibit strand bias. *Cell,* 115**,** 209-16.

KING, S. M., MCNAMEE, R. A., HOUNG, A. K., PATEL, R., BRANDS, M. & REED, G. L. 2009. Platelet dense-granule secretion plays a critical role in thrombosis and subsequent vascular remodeling in atherosclerotic mice. *Circulation,* 120**,** 785-91.

KIRCHHOFER, D., RIEDERER, M. A. & BAUMGARTNER, H. R. 1997. Specific accumulation of circulating monocytes and polymorphonuclear leukocytes on platelet thrombi in a vascular injury model. *Blood,* 89**,** 1270-8.

KOGA, H., SUGIYAMA, S., KUGIYAMA, K., WATANABE, K., FUKUSHIMA, H., TANAKA, T., SAKAMOTO, T., YOSHIMURA, M., JINNOUCHI, H. & OGAWA, H. 2005a. Elevated levels of VE-cadherin-positive endothelial microparticles in patients with type 2 diabetes mellitus and coronary artery disease. *J Am Coll Cardiol,* 45**,** 1622-30.

KOGA, K., MATSUMOTO, K., AKIYOSHI, T., KUBO, M., YAMANAKA, N., TASAKI, A., NAKASHIMA, H., NAKAMURA, M., KUROKI, S., TANAKA, M. & KATANO, M. 2005b. Purification, characterization and biological significance of tumor-derived exosomes. *Anticancer Res,* 25**,** 3703-7.

KOGURE, T., LIN, W. L., YAN, I. K., BRACONI, C. & PATEL, T. 2011. Intercellular nanovesicle-mediated microRNA transfer: a mechanism of environmental modulation of hepatocellular cancer cell growth. *Hepatology,* 54**,** 1237-48.

KONDKAR, A. A., BRAY, M. S., LEAL, S. M., NAGALLA, S., LIU, D. J., JIN, Y., DONG, J. F., REN, Q., WHITEHEART, S. W., SHAW, C. & BRAY, P. F. 2010. VAMP8/endobrevin is overexpressed in hyperreactive human platelets: suggested role for platelet microRNA. *J Thromb Haemost,* 8**,** 369-78.

KOSAKA, N., IGUCHI, H., HAGIWARA, K., YOSHIOKA, Y., TAKESHITA, F. & OCHIYA, T. 2013a. Neutral sphingomyelinase 2 (nSMase2)-dependent exosomal transfer of angiogenic microRNAs regulate cancer cell metastasis. *J Biol Chem,* 288**,** 10849-59.

KOSAKA, N., IGUCHI, H., YOSHIOKA, Y., TAKESHITA, F., MATSUKI, Y. & OCHIYA, T. 2010. Secretory mechanisms and intercellular transfer of microRNAs in living cells. *J Biol Chem,* 285**,** 17442-52.

KOSAKA, N., YOSHIOKA, Y., HAGIWARA, K., TOMINAGA, N., KATSUDA, T. & OCHIYA, T. 2013b. Trash or Treasure: extracellular microRNAs and cell-to-cell communication. *Front Genet,* 4**,** 173.

KOYAMA, H. & NISHIZAWA, Y. 2005. Platelet in progression of atherosclerosis: a potential target in diabetic patients. *Curr Diabetes Rev,* 1**,** 159-65.

KOZARSKY, K. F., DONAHEE, M. H., RIGOTTI, A., IQBAL, S. N., EDELMAN, E. R. & KRIEGER, M. 1997. Overexpression of the HDL receptor SR-BI alters plasma HDL and bile cholesterol levels. *Nature,* 387**,** 414-7.

KOZEK-LANGENECKER, S. A., SPISS, C. K., MICHALEK-SAUBERER, A., FELFERNIG, M. & ZIMPFER, M. 2003. Effect of prostacyclin on platelets, polymorphonuclear cells, and heterotypic cell aggregation during hemofiltration. *Crit Care Med,* 31**,** 864-8.

KOZOMARA, A. & GRIFFITHS-JONES, S. 2011. miRBase: integrating microRNA annotation and deep-sequencing data. *Nucleic Acids Res,* 39**,** D152-7.

KOZOMARA, A. & GRIFFITHS-JONES, S. 2014. miRBase: annotating high confidence microRNAs using deep sequencing data. *Nucleic Acids Res,* 42**,** D68-73.

KREK, A., GRUN, D., POY, M. N., WOLF, R., ROSENBERG, L., EPSTEIN, E. J., MACMENAMIN, P., DA PIEDADE, I., GUNSALUS, K. C., STOFFEL, M. & RAJEWSKY, N. 2005. Combinatorial microRNA target predictions. *Nat Genet,* 37**,** 495-500.

KRISHNAN, U. 2012. *Identification of Novel Genes Involved In Coronary Atherothrombosis by Blood Cell Transcriptome Profiling.* PhD Thesis, University of Leicester.

KROL, J., LOEDIGE, I. & FILIPOWICZ, W. 2010. The widespread regulation of microRNA biogenesis, function and decay. *Nat Rev Genet,* 11**,** 597-610.

KUCKLEBURG, C. J., YATES, C. M., KALIA, N., ZHAO, Y., NASH, G. B., WATSON, S. P. & RAINGER, G. E. 2011. Endothelial cell-borne platelet bridges selectively recruit monocytes in human and mouse models of vascular inflammation. *Cardiovasc Res,* 91**,** 134-41.

KUKREJA, R. C., YIN, C. & SALLOUM, F. N. 2011. MicroRNAs: new players in cardiac injury and protection. *Mol Pharmacol,* 80**,** 558-64.

KWEKKEBOOM, R. F., LEI, Z., DOEVENDANS, P. A., MUSTERS, R. J. & SLUIJTER, J. P. 2014. Targeted delivery of miRNA therapeutics for cardiovascular diseases: opportunities and challenges. *Clin Sci (Lond),* 127**,** 351-65.

LABBAYE, C., SPINELLO, I., QUARANTA, M. T., PELOSI, E., PASQUINI, L., PETRUCCI, E., BIFFONI, M., NUZZOLO, E. R., BILLI, M., FOA, R., BRUNETTI, E., GRIGNANI, F., TESTA, U. & PESCHLE, C. 2008. A three-step pathway comprising PLZF/miR-146a/CXCR4 controls megakaryopoiesis. *Nat Cell Biol,* 10**,** 788-801.

LACROIX, R., JUDICONE, C., PONCELET, P., ROBERT, S., ARNAUD, L., SAMPOL, J. & DIGNAT-GEORGE, F. 2012. Impact of pre-analytical parameters on the measurement of circulating microparticles: towards standardization of protocol. *J Thromb Haemost,* 10**,** 437-46.

LAFFONT, B., CORDUAN, A., PLE, H., DUCHEZ, A. C., CLOUTIER, N., BOILARD, E. & PROVOST, P. 2013. Activated platelets can deliver mRNA regulatory Ago2*microRNA complexes to endothelial cells via microparticles. *Blood,* 122**,** 253-61.

LAFFONT, B., CORDUAN, A., ROUSSEAU, M., DUCHEZ, A. C., LEE, C. H., BOILARD, E. & PROVOST, P. 2015. Platelet microparticles reprogram macrophage gene expression and function. *Thromb Haemost,* 115**,** 311-323.

LAGES, B., SCRUTTON, M. C. & HOLMSEN, H. 1975. Studies on gel-filtered human platelets: isolation and characterization in a medium containing no added Ca2+, Mg2+, or K+. *J Lab Clin Med,* 85**,** 811-25.

LAI, E. C. 2002. Micro RNAs are complementary to 3 ' UTR sequence motifs that mediate negative post-transcriptional regulation. *Nature Genetics,* 30**,** 363-364.

LAN, Y. F., CHEN, H. H., LAI, P. F., CHENG, C. F., HUANG, Y. T., LEE, Y. C., CHEN, T. W. & LIN, H. 2012. MicroRNA-494 Reduces ATF3 Expression and Promotes AKI. *J Am Soc Nephrol,* 23**,** 2012-23.

LANDGRAF, P., RUSU, M., SHERIDAN, R., SEWER, A., IOVINO, N., ARAVIN, A., PFEFFER, S., RICE, A., KAMPHORST, A. O., LANDTHALER, M., LIN, C., SOCCI, N. D., HERMIDA, L., FULCI, V., CHIARETTI, S., FOA, R., SCHLIWKA, J., FUCHS, U., NOVOSEL, A., MULLER, R. U., SCHERMER, B., BISSELS, U., INMAN, J., PHAN, Q., CHIEN, M., WEIR, D. B., CHOKSI, R., DE VITA, G., FREZZETTI, D., TROMPETER, H. I., HORNUNG, V., TENG, G., HARTMANN, G., PALKOVITS, M., DI LAURO, R., WERNET, P., MACINO, G., ROGLER, C. E., NAGLE, J. W., JU, J., PAPAVASILIOU, F. N., BENZING, T., LICHTER, P., TAM, W., BROWNSTEIN, M. J., BOSIO, A., BORKHARDT, A., RUSSO, J. J., SANDER, C., ZAVOLAN, M. & TUSCHL, T. 2007. A mammalian microRNA expression atlas based on small RNA library sequencing. *Cell,* 129**,** 1401-14.

LANDRY, P., PLANTE, I., OUELLET, D. L., PERRON, M. P., ROUSSEAU, G. & PROVOST, P. 2009. Existence of a microRNA pathway in anucleate platelets. *Nat Struct Mol Biol,* 16**,** 961-6.

LANE, R. E., KORBIE, D., ANDERSON, W., VAIDYANATHAN, R. & TRAU, M. 2015. Analysis of exosome purification methods using a model liposome system and tunable-resistive pulse sensing. *Sci Rep,* 5**,** 7639.

LANGER, H. F., DAUB, K., BRAUN, G., SCHONBERGER, T., MAY, A. E., SCHALLER, M., STEIN, G. M., STELLOS, K., BUELTMANN, A., SIEGEL-AXEL, D., WENDEL, H. P., AEBERT, H., ROECKEN, M., SEIZER, P., SANTOSO, S., WESSELBORG, S., BROSSART, P. & GAWAZ, M. 2007. Platelets recruit human dendritic cells via Mac-1/JAM-C interaction and modulate dendritic cell function in vitro. *Arterioscler Thromb Vasc Biol,* 27**,** 1463-70.

LATRONICO, M. V., CATALUCCI, D. & CONDORELLI, G. 2007. Emerging role of microRNAs in cardiovascular biology. *Circ Res,* 101**,** 1225-36.

LEE, E. J., BAEK, M., GUSEV, Y., BRACKETT, D. J., NUOVO, G. J. & SCHMITTGEN, T. D. 2008. Systematic evaluation of microRNA processing patterns in tissues, cell lines, and tumors. *RNA,* 14**,** 35-42.

LEE, M. R., PRASAIN, N., CHAE, H. D., KIM, Y. J., MANTEL, C., YODER, M. C. & BROXMEYER, H. E. 2012. Epigenetic regulation of NANOG by miR-302 cluster-MBD2 completes induced pluripotent stem cell reprogramming. *Stem Cells,* 31**,** 666-81.

LEE, R. C. & AMBROS, V. 2001. An extensive class of small RNAs in Caenorhabditis elegans. *Science,* 294**,** 862-4.

LEIDINGER, P., BACKES, C., DAHMKE, I. N., GALATA, V., HUWER, H., STEHLE, I., BALS, R., KELLER, A. & MEESE, E. 2014. What makes a blood cell based miRNA expression pattern disease specific?--a miRNome analysis of blood cell subsets in lung cancer patients and healthy controls. *Oncotarget,* 5**,** 9484-97.

LEIERSEDER, S., PETZOLD, T., ZHANG, L., LOYER, X., MASSBERG, S. & ENGELHARDT, S. 2013. MiR-223 is dispensable for platelet production and function in mice. *Thromb Haemost,* 110**,** 1207-14.

LEON, C., RAVANAT, C., FREUND, M., CAZENAVE, J. P. & GACHET, C. 2003. Differential involvement of the P2Y1 and P2Y12 receptors in platelet procoagulant activity. *Arterioscler Thromb Vasc Biol,* 23**,** 1941-7.

LEWIS, B. P., BURGE, C. B. & BARTEL, D. P. 2005. Conserved seed pairing, often flanked by adenosines, indicates that thousands of human genes are microRNA targets. *Cell,* 120**,** 15-20.

LEY, K., MILLER, Y. I. & HEDRICK, C. C. 2011. Monocyte and macrophage dynamics during atherogenesis. *Arterioscler Thromb Vasc Biol,* 31**,** 1506-16.

LI, G., ENDSLEY, M. A., SOMASUNDERAM, A., GBOTA, S. L., MBAKA, M. I., MURRAY, J. L. & FERGUSON, M. R. 2014. The dual role of tetraspanin CD63 in HIV-1 replication. *Virol J,* 11**,** 23.

LI, L., ZHU, D., HUANG, L., ZHANG, J., BIAN, Z., CHEN, X., LIU, Y., ZHANG, C. Y. & ZEN, K. 2012. Argonaute 2 complexes selectively protect the circulating microRNAs in cell-secreted microvesicles. *PLoS One,* 7**,** e46957.

LI, N., HU, H., LINDQVIST, M., WIKSTROM-JONSSON, E., GOODALL, A. H. & HJEMDAHL, P. 2000. Platelet-leukocyte cross talk in whole blood. *Arterioscler Thromb Vasc Biol,* 20**,** 2702-8.

LI, N., WALLEN, N. H., LADJEVARDI, M. & HJEMDAHL, P. 1997. Effects of serotonin on platelet activation in whole blood. *Blood Coagul Fibrinolysis,* 8**,** 517-23.

LI, Y., JIANG, Z., XU, L., YAO, H., GUO, J. & DING, X. 2011. Stability analysis of liver cancer-related microRNAs. *Acta Biochim Biophys Sin (Shanghai),* 43**,** 69-78.

LIANG, H., YAN, X., PAN, Y., WANG, Y., WANG, N., LI, L., LIU, Y., CHEN, X., ZHANG, C. Y., GU, H. & ZEN, K. 2015. MicroRNA-223 delivered by platelet-derived microvesicles promotes lung cancer cell invasion via targeting tumor suppressor EPB41L3. *Mol Cancer,* 14**,** 58.

LIANG, Y., RIDZON, D., WONG, L. & CHEN, C. 2007. Characterization of microRNA expression profiles in normal human tissues. *BMC Genomics,* 8**,** 166.

LIAO, J. K. 2013. Linking endothelial dysfunction with endothelial cell activation. *J Clin Invest,* 123**,** 540-1.

LIBBY, P. 2001. Current concepts of the pathogenesis of the acute coronary syndromes. *Circulation,* 104**,** 365-72.

LINARES, R., TAN, S., GOUNOU, C., ARRAUD, N. & BRISSON, A. R. 2015. High-speed centrifugation induces aggregation of extracellular vesicles. *J Extracell Vesicles,* 4.

LINDEMANN, S., TOLLEY, N. D., DIXON, D. A., MCINTYRE, T. M., PRESCOTT, S. M., ZIMMERMAN, G. A. & WEYRICH, A. S. 2001. Activated platelets mediate inflammatory signaling by regulated interleukin 1beta synthesis. *J Cell Biol,* 154**,** 485-90.

LINDEN, M. D. & JACKSON, D. E. 2010. Platelets: pleiotropic roles in atherogenesis and atherothrombosis. *Int J Biochem Cell Biol,* 42**,** 1762-6.

LINSLEY, P. S., SCHELTER, J., BURCHARD, J., KIBUKAWA, M., MARTIN, M. M., BARTZ, S. R., JOHNSON, J. M., CUMMINS, J. M., RAYMOND, C. K., DAI, H., CHAU, N., CLEARY, M., JACKSON, A. L., CARLETON, M. & LIM, L. 2007. Transcripts targeted by the microRNA-16 family cooperatively regulate cell cycle progression. *Mol Cell Biol,* 27**,** 2240-52.

LIU, C. G., CALIN, G. A., VOLINIA, S. & CROCE, C. M. 2008. MicroRNA expression profiling using microarrays. *Nat Protoc,* 3**,** 563-78.

LIU, G. & ABRAHAM, E. 2013. MicroRNAs in Immune Response and Macrophage Polarization. *Arterioscler Thromb Vasc Biol,* 33**,** 170-7.

LIU, L., NIE, J., CHEN, L., DONG, G., DU, X., WU, X., TANG, Y. & HAN, W. 2013. The oncogenic role of microRNA-130a/301a/454 in human colorectal cancer via targeting Smad4 expression. *PLoS One,* 8**,** e55532.

LOBB, R. J., BECKER, M., WEN, S. W., WONG, C. S., WIEGMANS, A. P., LEIMGRUBER, A. & MOLLER, A. 2015. Optimized exosome isolation protocol for cell culture supernatant and human plasma. *J Extracell Vesicles,* 4.

LOEB, G. B., KHAN, A. A., CANNER, D., HIATT, J. B., SHENDURE, J., DARNELL, R. B., LESLIE, C. S. & RUDENSKY, A. Y. 2012. Transcriptome-wide miR-155 binding map reveals widespread noncanonical microRNA targeting. *Mol Cell,* 48**,** 760-70.

LOK, C. A., NIEUWLAND, R., STURK, A., HAU, C. M., BOER, K., VANBAVEL, E. & VANDERPOST, J. A. 2007. Microparticle-associated P-selectin reflects platelet activation in preeclampsia. *Platelets,* 18**,** 68-72.

LOPEZ, A. D., MATHERS, C. D., EZZATI, M., JAMISON, D. T. & MURRAY, C. J. 2006. Global and regional burden of disease and risk factors, 2001: systematic analysis of population health data. *Lancet,* 367**,** 1747-57.

LOSCHE, W., SCHOLZ, T., TEMMLER, U., OBERLE, V. & CLAUS, R. A. 2004. Platelet-derived microvesicles transfer tissue factor to monocytes but not to neutrophils. *Platelets,* 15**,** 109-15.

LOYER, X., VION, A. C., TEDGUI, A. & BOULANGER, C. M. 2014. Microvesicles as cell-cell messengers in cardiovascular diseases. *Circ Res,* 114**,** 345-53.

LOZANO, R., NAGHAVI, M., FOREMAN, K., LIM, S., SHIBUYA, K., ABOYANS, V., ABRAHAM, J., ADAIR, T., AGGARWAL, R., AHN, S. Y., ALVARADO, M., ANDERSON, H. R., ANDERSON, L. M., ANDREWS, K. G., ATKINSON, C., BADDOUR, L. M., BARKER-COLLO, S., BARTELS, D. H., BELL, M. L., BENJAMIN, E. J., BENNETT, D., BHALLA, K., BIKBOV, B., BIN ABDULHAK, A., BIRBECK, G., BLYTH, F., BOLLIGER, I., BOUFOUS, S., BUCELLO, C., BURCH, M., BURNEY, P., CARAPETIS, J., CHEN, H., CHOU, D., CHUGH, S. S., COFFENG, L. E., COLAN, S. D., COLQUHOUN, S., COLSON, K. E., CONDON, J., CONNOR, M. D., COOPER, L. T., CORRIERE, M., CORTINOVIS, M., DE VACCARO, K. C., COUSER, W., COWIE, B. C., CRIQUI, M. H., CROSS, M., DABHADKAR, K. C., DAHODWALA, N., DE LEO, D., DEGENHARDT, L., DELOSSANTOS, A., DENENBERG, J., DES JARLAIS, D. C., DHARMARATNE, S. D., DORSEY, E. R., DRISCOLL, T., DUBER, H., EBEL, B., ERWIN, P. J., ESPINDOLA, P., EZZATI, M., FEIGIN, V., FLAXMAN, A. D., FOROUZANFAR, M. H., FOWKES, F. G., FRANKLIN, R., FRANSEN, M., FREEMAN, M. K., GABRIEL, S. E., GAKIDOU, E., GASPARI, F., GILLUM, R. F., GONZALEZ-MEDINA, D., HALASA, Y. A., HARING, D., HARRISON, J. E., HAVMOELLER, R., HAY, R. J., HOEN, B., HOTEZ, P. J., HOY, D., JACOBSEN, K. H., JAMES, S. L., JASRASARIA, R., JAYARAMAN, S., JOHNS, N., KARTHIKEYAN, G., KASSEBAUM, N., KEREN, A., KHOO, J. P., KNOWLTON, L. M., KOBUSINGYE, O., KORANTENG, A., KRISHNAMURTHI, R., LIPNICK, M., LIPSHULTZ, S. E., OHNO, S. L., et al. 2013. Global and regional mortality from 235 causes of death for 20 age groups in 1990 and 2010: a systematic analysis for the Global Burden of Disease Study 2010. *Lancet,* 380**,** 2095-128.

LU, X. & LU, J. 2015. The significance of detection of serum miR-423-5p and miR-484 for diagnosis of colorectal cancer. *Clin Lab,* 61**,** 187-90.

LUBSCZYK, B., KOLLARS, M., HRON, G., KYRLE, P. A., WELTERMANN, A. & GARTNER, V. 2010. Low dose acetylsalicylic acid and shedding of microparticles in vivo in humans. *Eur J Clin Invest,* 40**,** 477-82.

LUDWIG, A. K. & GIEBEL, B. 2012. Exosomes: small vesicles participating in intercellular communication. *Int J Biochem Cell Biol,* 44**,** 11-5.

MAESS, M. B., WITTIG, B., CIGNARELLA, A. & LORKOWSKI, S. 2014. Reduced PMA enhances the responsiveness of transfected THP-1 macrophages to polarizing stimuli. *J Immunol Methods,* 402**,** 76-81.

MARCHESE, P., SALDIVAR, E., WARE, J. & RUGGERI, Z. M. 1999. Adhesive properties of the isolated amino-terminal domain of platelet glycoprotein Ibalpha in a flow field. *Proc Natl Acad Sci U S A,* 96**,** 7837-42.

MATHERS, C. D. & LONCAR, D. 2006. Projections of global mortality and burden of disease from 2002 to 2030. *PLoS Med,* 3**,** e442.

MATHIVANAN, S., JI, H. & SIMPSON, R. J. 2010. Exosomes: extracellular organelles important in intercellular communication. *J Proteomics,* 73**,** 1907-20.

MAUSE, S. F., VON HUNDELSHAUSEN, P., ZERNECKE, A., KOENEN, R. R. & WEBER, C. 2005. Platelet microparticles: a transcellular delivery system for RANTES promoting monocyte recruitment on endothelium. *Arterioscler Thromb Vasc Biol,* 25**,** 1512-8.

MAXFIELD, F. R. & TABAS, I. 2005. Role of cholesterol and lipid organization in disease. *Nature,* 438**,** 612-21.

MCDONALD, M. K., CAPASSO, K. E. & AJIT, S. K. 2013. Purification and microRNA profiling of exosomes derived from blood and culture media. *J Vis Exp,* 76**,** e50294.

MCMANUS, D. D. & FREEDMAN, J. E. 2015. MicroRNAs in platelet function and cardiovascular disease. *Nat Rev Cardiol,* 12**,** 711-717.

MELO, S. A., LUECKE, L. B., KAHLERT, C., FERNANDEZ, A. F., GAMMON, S. T., KAYE, J., LEBLEU, V. S., MITTENDORF, E. A., WEITZ, J., RAHBARI, N., REISSFELDER, C., PILARSKY, C., FRAGA, M. F., PIWNICA-WORMS, D. & KALLURI, R. 2015. Glypican-1 identifies cancer exosomes and detects early pancreatic cancer. *Nature,* 523**,** 177-82.

MEMCZAK, S., JENS, M., ELEFSINIOTI, A., TORTI, F., KRUEGER, J., RYBAK, A., MAIER, L., MACKOWIAK, S. D., GREGERSEN, L. H., MUNSCHAUER, M., LOEWER, A., ZIEBOLD, U., LANDTHALER, M., KOCKS, C., LE NOBLE, F. & RAJEWSKY, N. 2013. Circular RNAs are a large class of animal RNAs with regulatory potency. *Nature,* 495**,** 333-338.

MENDELL, J. T. & OLSON, E. N. 2012. MicroRNAs in stress signaling and human disease. *Cell,* 148**,** 1172-87.

MERKEROVA, M., BELICKOVA, M. & BRUCHOVA, H. 2008. Differential expression of microRNAs in hematopoietic cell lineages. *Eur J Haematol,* 81**,** 304-10.

MESTDAGH, P., HARTMANN, N., BAERISWYL, L., ANDREASEN, D., BERNARD, N., CHEN, C., CHEO, D., D'ANDRADE, P., DEMAYO, M., DENNIS, L., DERVEAUX, S., FENG, Y., FULMER-SMENTEK, S., GERSTMAYER, B., GOUFFON, J., GRIMLEY, C., LADER, E., LEE, K. Y., LUO, S., MOURITZEN, P., NARAYANAN, A., PATEL, S., PEIFFER, S., RUBERG, S., SCHROTH, G., SCHUSTER, D., SHAFFER, J. M., SHELTON, E. J., SILVERIA, S., ULMANELLA, U., VEERAMACHANENI, V., STAEDTLER, F., PETERS, T., GUETTOUCHE, T., WONG, L. & VANDESOMPELE, J. 2014. Evaluation of quantitative miRNA expression platforms in the microRNA quality control (miRQC) study. *Nat Methods,* 11**,** 809-15.

MEYER, S. U., KAISER, S., WAGNER, C., THIRION, C. & PFAFFL, M. W. 2012. Profound effect of profiling platform and normalization strategy on detection of differentially expressed microRNAs--a comparative study. *PLoS One,* 7**,** e38946.

MI, H., MURUGANUJAN, A., CASAGRANDE, J. T. & THOMAS, P. D. 2013a. Large-scale gene function analysis with the PANTHER classification system. *Nat Protoc,* 8**,** 1551-66.

MI, H., MURUGANUJAN, A. & THOMAS, P. D. 2013b. PANTHER in 2013: modeling the evolution of gene function, and other gene attributes, in the context of phylogenetic trees. *Nucleic Acids Res,* 41**,** D377-86.

MICHELSON, A. D. 2007. *Platelets,* Amsterdam ; Boston, Academic Press/Elsevier.

MICHELSON, A. D., BARNARD, M. R., KRUEGER, L. A., VALERI, C. R. & FURMAN, M. I. 2001. Circulating monocyte-platelet aggregates are a more sensitive marker of in vivo platelet activation than platelet surface P-selectin: studies in baboons, human coronary intervention, and human acute myocardial infarction. *Circulation,* 104**,** 1533-7.

MISKA, E. A., ALVAREZ-SAAVEDRA, E., ABBOTT, A. L., LAU, N. C., HELLMAN, A. B., MCGONAGLE, S. M., BARTEL, D. P., AMBROS, V. R. & HORVITZ, H. R. 2007. Most Caenorhabditis elegans microRNAs are individually not essential for development or viability. *PLoS Genet,* 3**,** e215.

MITCHELL, P. S., PARKIN, R. K., KROH, E. M., FRITZ, B. R., WYMAN, S. K., POGOSOVA-AGADJANYAN, E. L., PETERSON, A., NOTEBOOM, J., O'BRIANT, K. C., ALLEN, A., LIN, D. W., URBAN, N., DRESCHER, C. W., KNUDSEN, B. S., STIREWALT, D. L., GENTLEMAN, R., VESSELLA, R. L., NELSON, P. S., MARTIN, D. B. & TEWARI, M. 2008. Circulating microRNAs as stable blood-based markers for cancer detection. *Proc Natl Acad Sci U S A,* 105**,** 10513-8.

MITTELBRUNN, M., GUTIERREZ-VAZQUEZ, C., VILLARROYA-BELTRI, C., GONZALEZ, S., SANCHEZ-CABO, F., GONZALEZ, M. A., BERNAD, A. & SANCHEZ-MADRID, F. 2011. Unidirectional transfer of microRNA-loaded exosomes from T cells to antigen-presenting cells. *Nat Commun,* 2**,** 282.

MOGILYANSKY, E. & RIGOUTSOS, I. 2013. The miR-17/92 cluster: a comprehensive update on its genomics, genetics, functions and increasingly important and numerous roles in health and disease. *Cell Death Differ,* 20**,** 1603-14.

MOKDAD, A. H., BOWMAN, B. A., FORD, E. S., VINICOR, F., MARKS, J. S. & KOPLAN, J. P. 2001. The continuing epidemics of obesity and diabetes in the United States. *Jama-Journal of the American Medical Association,* 286**,** 1195-1200.

MONTECALVO, A., LARREGINA, A. T., SHUFESKY, W. J., STOLZ, D. B., SULLIVAN, M. L., KARLSSON, J. M., BATY, C. J., GIBSON, G. A., ERDOS, G., WANG, Z., MILOSEVIC, J., TKACHEVA, O. A., DIVITO, S. J., JORDAN, R., LYONS-WEILER, J., WATKINS, S. C. & MORELLI, A. E. 2012. Mechanism of transfer of functional microRNAs between mouse dendritic cells via exosomes. *Blood,* 119**,** 756-66.

MOORE, K. J. & TABAS, I. 2011. Macrophages in the pathogenesis of atherosclerosis. *Cell,* 145**,** 341-55.

MOORE, M. J., ZHANG, C., GANTMAN, E. C., MELE, A., DARNELL, J. C. & DARNELL, R. B. 2014. Mapping Argonaute and conventional RNA-binding protein interactions with RNA at single-nucleotide resolution using HITS-CLIP and CIMS analysis. *Nat Protoc,* 9**,** 263-93.

MOREL, O., JESEL, L., FREYSSINET, J. M. & TOTI, F. 2011. Cellular mechanisms underlying the formation of circulating microparticles. *Arterioscler Thromb Vasc Biol,* 31**,** 15-26.

MORELLI, A. E., LARREGINA, A. T., SHUFESKY, W. J., SULLIVAN, M. L. G., STOLZ, D. B., PAPWORTH, G. D., ZAHORCHAK, A. F., LOGAR, A. J., WANG, Z. L., WATKINS, S. C., FALO, L. D. & THOMSON, A. W. 2004. Endocytosis, intracellular sorting, and processing of exosomes by dendritic cells. *Blood,* 104**,** 3257-3266.

MORK, S., PLETSCHER-FRANKILD, S., PALLEJA CARO, A., GORODKIN, J. & JENSEN, L. J. 2014. Protein-driven inference of miRNA-disease associations. *Bioinformatics,* 30**,** 392-7.

MOROI, M., ONITSUKA, I., IMAIZUMI, T. & JUNG, S. M. 2000. Involvement of activated integrin alpha2beta1 in the firm adhesion of platelets onto a surface of immobilized collagen under flow conditions. *Thromb Haemost,* 83**,** 769-76.

MOROZOVA, N., ZINOVYEV, A., NONNE, N., PRITCHARD, L. L., GORBAN, A. N. & HAREL-BELLAN, A. 2012. Kinetic signatures of microRNA modes of action. *RNA,* 18**,** 1635-55.

MORTON, L. F., HARGREAVES, P. G., FARNDALE, R. W., YOUNG, R. D. & BARNES, M. J. 1995. Integrin alpha 2 beta 1-independent activation of platelets by simple collagen-like peptides: collagen tertiary (triple-helical) and quaternary

(polymeric) structures are sufficient alone for alpha 2 beta 1-independent platelet reactivity. *Biochem J,* 306 (Pt 2)**,** 337-44.

MUKHERJI, S., EBERT, M. S., ZHENG, G. X., TSANG, J. S., SHARP, P. A. & VAN OUDENAARDEN, A. 2011. MicroRNAs can generate thresholds in target gene expression. *Nat Genet,* 43**,** 854-9.

MULCAHY, L. A., PINK, R. C. & CARTER, D. R. 2014. Routes and mechanisms of extracellular vesicle uptake. *J Extracell Vesicles,* 3.

MURUGAPPA, S. & KUNAPULI, S. P. 2006. The role of ADP receptors in platelet function. *Front Biosci,* 11**,** 1977-86.

MUSTARD, J. F. & PACKHAM, M. A. 1970. Factors influencing platelet function: adhesion, release, and aggregation. *Pharmacol Rev,* 22**,** 97-187.

NAGALLA, S., SHAW, C., KONG, X., KONDKAR, A. A., EDELSTEIN, L. C., MA, L., CHEN, J., MCKNIGHT, G. S., LOPEZ, J. A., YANG, L., JIN, Y., BRAY, M. S., LEAL, S. M., DONG, J. F. & BRAY, P. F. 2011. Platelet microRNA-mRNA coexpression profiles correlate with platelet reactivity. *Blood,* 117**,** 5189-97.

NAM, C. H. & RABBITTS, T. H. 2006. The role of LMO2 in development and in T cell leukemia after chromosomal translocation or retroviral insertion. *Mol Ther,* 13**,** 15-25.

NANBO, A., KAWANISHI, E., YOSHIDA, R. & YOSHIYAMA, H. 2013. Exosomes derived from Epstein-Barr virus-infected cells are internalized via caveola-dependent endocytosis and promote phenotypic modulation in target cells. *J Virol,* 87**,** 10334-47.

NAVARRO, F., GUTMAN, D., MEIRE, E., CACERES, M., RIGOUTSOS, I., BENTWICH, Z. & LIEBERMAN, J. 2009. miR-34a contributes to megakaryocytic differentiation of K562 cells independently of p53. *Blood,* 114**,** 2181-92.

NIESWANDT, B., BERGMEIER, W., ECKLY, A., SCHULTE, V., OHLMANN, P., CAZENAVE, J. P., ZIRNGIBL, H., OFFERMANNS, S. & GACHET, C. 2001a. Evidence for cross-talk between glycoprotein VI and Gi-coupled receptors during collagen-induced platelet aggregation. *Blood,* 97**,** 3829-35.

NIESWANDT, B., BRAKEBUSCH, C., BERGMEIER, W., SCHULTE, V., BOUVARD, D., MOKHTARI-NEJAD, R., LINDHOUT, T., HEEMSKERK, J. W., ZIRNGIBL, H. & FASSLER, R. 2001b. Glycoprotein VI but not alpha2beta1 integrin is essential for platelet interaction with collagen. *EMBO J,* 20**,** 2120-30.

NIESWANDT, B. & WATSON, S. P. 2003. Platelet-collagen interaction: is GPVI the central receptor? *Blood,* 102**,** 449-61.

NOFER, J. R., BRODDE, M. F. & KEHREL, B. E. 2010. High-density lipoproteins, platelets and the pathogenesis of atherosclerosis. *Clin Exp Pharmacol Physiol,* 37**,** 726-35.

NOFER, J. R., WALTER, M., KEHREL, B., WIERWILLE, S., TEPEL, M., SEEDORF, U. & ASSMANN, G. 1998. HDL3-mediated inhibition of thrombin-induced platelet aggregation and fibrinogen binding occurs via decreased production of phosphoinositide-derived second messengers 1,2-diacylglycerol and inositol 1,4,5-tris-phosphate. *Arterioscler Thromb Vasc Biol,* 18**,** 861-9.

NOMURA, S., TANDON, N. N., NAKAMURA, T., CONE, J., FUKUHARA, S. & KAMBAYASHI, J. 2001. High-shear-stress-induced activation of platelets and microparticles enhances expression of cell adhesion molecules in THP-1 and endothelial cells. *Atherosclerosis,* 158**,** 277-87.

NONNE, C., LENAIN, N., HECHLER, B., MANGIN, P., CAZENAVE, J. P., GACHET, C. & LANZA, F. 2005. Importance of platelet phospholipase Cgamma2 signaling in arterial thrombosis as a function of lesion severity. *Arterioscler Thromb Vasc Biol,* 25**,** 1293-8.

NORDIN, J. Z., LEE, Y., VADER, P., MAGER, I., JOHANSSON, H. J., HEUSERMANN, W., WIKLANDER, O. P., HALLBRINK, M., SEOW, Y., BULTEMA, J. J., GILTHORPE, J., DAVIES, T., FAIRCHILD, P. J., GABRIELSSON, S., MEISNER-KOBER, N. C., LEHTIO, J., SMITH, C. I., WOOD, M. J. & EL ANDALOUSSI, S. 2015. Ultrafiltration with size-exclusion liquid chromatography for high yield isolation of extracellular vesicles preserving intact biophysical and functional properties. *Nanomedicine,* 11**,** 879-83.

NYLANDER, S. & SCHULZ, R. 2016. Effects of P2Y12 receptor antagonists beyond platelet inhibition - comparison of ticagrelor with thienopyridines. *Br J Pharmacol,* 173**,** 1163-78.

O'DONNELL, K. A., WENTZEL, E. A., ZELLER, K. I., DANG, C. V. & MENDELL, J. T. 2005. c-Myc-regulated microRNAs modulate E2F1 expression. *Nature,* 435**,** 839-43.

OFFERMANNS, S. 2006. Activation of platelet function through G protein-coupled receptors. *Circ Res,* 99**,** 1293-304.

OFFERMANNS, S., LAUGWITZ, K. L., SPICHER, K. & SCHULTZ, G. 1994. G proteins of the G12 family are activated via thromboxane A2 and thrombin receptors in human platelets. *Proc Natl Acad Sci U S A,* 91**,** 504-8.

OHSHIMA, K., INOUE, K., FUJIWARA, A., HATAKEYAMA, K., KANTO, K., WATANABE, Y., MURAMATSU, K., FUKUDA, Y., OGURA, S., YAMAGUCHI, K. & MOCHIZUKI, T. 2010. Let-7 microRNA family is selectively secreted into the extracellular environment via exosomes in a metastatic gastric cancer cell line. *PLoS One,* 5**,** e13247.

OOSTHUYZEN, W., SIME, N. E., IVY, J. R., TURTLE, E. J., STREET, J. M., POUND, J., BATH, L. E., WEBB, D. J., GREGORY, C. D., BAILEY, M. A. & DEAR, J. W. 2013. Quantification of human urinary exosomes by nanoparticle tracking analysis. *J Physiol,* 591**,** 5833-42.

OPALINSKA, J. B., BERSENEV, A., ZHANG, Z., SCHMAIER, A. A., CHOI, J., YAO, Y., D'SOUZA, J., TONG, W. & WEISS, M. J. 2010. MicroRNA expression in maturing murine megakaryocytes. *Blood,* 116**,** e128-38.

OROM, U. A. & LUND, A. H. 2007. Isolation of microRNA targets using biotinylated synthetic microRNAs. *Methods,* 43**,** 162-5.

OSMAN, A. & FALKER, K. 2011. Characterization of human platelet microRNA by quantitative PCR coupled with an annotation network for predicted target genes. *Platelets,* 22**,** 433-41.

OUYANG, L., LIU, P., YANG, S., YE, S., XU, W. & LIU, X. 2013. A three-plasma miRNA signature serves as novel biomarkers for osteosarcoma. *Med Oncol,* 30**,** 340.

OWENS, A. P., 3RD & MACKMAN, N. 2011. Microparticles in hemostasis and thrombosis. *Circ Res,* 108**,** 1284-97.

PAGE, K., GUTTERY, D. S., ZAHRA, N., PRIMROSE, L., ELSHAW, S. R., PRINGLE, J. H., BLIGHE, K., MARCHESE, S. D., HILLS, A., WOODLEY, L., STEBBING, J., COOMBES, R. C. & SHAW, J. A. 2013. Influence of plasma processing on recovery and analysis of circulating nucleic acids. *PLoS One,* 8**,** e77963.

PALMER, R. M., FERRIGE, A. G. & MONCADA, S. 1987. Nitric oxide release accounts for the biological activity of endothelium-derived relaxing factor. *Nature,* 327**,** 524-6.

PAN, Y., LIANG, H., LIU, H., LI, D., CHEN, X., LI, L., ZHANG, C. Y. & ZEN, K. 2014. Platelet-Secreted MicroRNA-223 Promotes Endothelial Cell Apoptosis Induced by Advanced Glycation End Products via Targeting the Insulin-like Growth Factor 1 Receptor. *J Immunol,* 192**,** 437-46.

PANDEY, P., QIN, S., HO, J., ZHOU, J. & KREIDBERG, J. A. 2011. Systems biology approach to identify transcriptome reprogramming and candidate microRNA targets during the progression of polycystic kidney disease. *BMC Syst Biol,* 5**,** 56.

PARK, C. Y., CHOI, Y. S. & MCMANUS, M. T. 2010. Analysis of microRNA knockouts in mice. *Hum Mol Genet,* 19**,** R169-75.

PASSACQUALE, G., VAMADEVAN, P., PEREIRA, L., HAMID, C., CORRIGALL, V. & FERRO, A. 2011. Monocyte-Platelet Interaction Induces a Pro-Inflammatory Phenotype in Circulating Monocytes. *Plos One,* 6.

PEGTEL, D. M. 2014. The Biogenesis of Exosomes. *Extracellular Vesicles in Health and Disease.* Pan Stanford Publishing.

PENG, W. M., YU, C. F., KOLANUS, W., MAZZOCCA, A., BIEBER, T., KRAFT, S. & NOVAK, N. 2011. Tetraspanins CD9 and CD81 are molecular partners of trimeric FcvarepsilonRI on human antigen-presenting cells. *Allergy,* 66**,** 605-11.

PFISTER, S. L. 2004. Role of platelet microparticles in the production of thromboxane by rabbit pulmonary artery. *Hypertension,* 43**,** 428-33.

PICCIN, A., MURPHY, W. G. & SMITH, O. P. 2007. Circulating microparticles: pathophysiology and clinical implications. *Blood Rev,* 21**,** 157-71.

PIENIMAEKI-ROEMER, A., KUHLMANN, K., BOTTCHER, A., KONOVALOVA, T., BLACK, A., ORSO, E., LIEBISCH, G., AHRENS, M., EISENACHER, M., MEYER, H. E. & SCHMITZ, G. 2014. Lipidomic and proteomic characterization of platelet extracellular vesicle subfractions from senescent platelets. *Transfusion***,** 507-521.

PIGATI, L., YADDANAPUDI, S. C., IYENGAR, R., KIM, D. J., HEARN, S. A., DANFORTH, D., HASTINGS, M. L. & DUELLI, D. M. 2010. Selective release of microRNA species from normal and malignant mammary epithelial cells. *PLoS One,* 5**,** e13515.

PLE, H., LANDRY, P., BENHAM, A., COARFA, C., GUNARATNE, P. H. & PROVOST, P. 2012a. The Repertoire and Features of Human Platelet microRNAs. *PLoS One,* 7**,** e50746.

PLE, H., MALTAIS, M., CORDUAN, A., ROUSSEAU, G., MADORE, F. & PROVOST, P. 2012b. Alteration of the platelet transcriptome in chronic kidney disease. *Thromb Haemost,* 108**,** 605-15.

POSPICHALOVA, V., SVOBODA, J., DAVE, Z., KOTRBOVA, A., KAISER, K., KLEMOVA, D., ILKOVICS, L., HAMPL, A., CRHA, I., JANDAKOVA, E., MINAR, L., WEINBERGER, V. & BRYJA, V. 2015. Simplified protocol for flow cytometry analysis of fluorescently labeled exosomes and microvesicles using dedicated flow cytometer. *J Extracell Vesicles,* 4.

PRITCHARD, C. C., CHENG, H. H. & TEWARI, M. 2012. MicroRNA profiling: approaches and considerations. *Nat Rev Genet,* 13**,** 358-69.

QIN, Z. 2012. The use of THP-1 cells as a model for mimicking the function and regulation of monocytes and macrophages in the vasculature. *Atherosclerosis,* 221**,** 2-11.

QUINN, J. F., PATEL, T., WONG, D., DAS, S., FREEDMAN, J. E., LAURENT, L. C., CARTER, B. S., HOCHBERG, F., VAN KEUREN-JENSEN, K., HUENTELMAN, M., SPETZLER, R.,

KALANI, M. Y., ARANGO, J., ADELSON, P. D., WEINER, H. L., GANDHI, R., GOILAV, B., PUTTERMAN, C. & SAUGSTAD, J. A. 2015. Extracellular RNAs: development as biomarkers of human disease. *J Extracell Vesicles,* 4.

QUINTON, T. M., OZDENER, F., DANGELMAIER, C., DANIEL, J. L. & KUNAPULI, S. P. 2002. Glycoprotein VI-mediated platelet fibrinogen receptor activation occurs through calcium-sensitive and PKC-sensitive pathways without a requirement for secreted ADP. *Blood,* 99**,** 3228-34.

RAMEZANI, A., DEVANEY, J. M., COHEN, S., WING, M. R., SCOTT, R., KNOBLACH, S., SINGHAL, R., HOWARD, L., KOPP, J. B. & RAJ, D. S. 2015. Circulating and urinary microRNA profile in focal segmental glomerulosclerosis: a pilot study. *Eur J Clin Invest,* 45**,** 394-404.

RANA, S., YUE, S., STADEL, D. & ZOLLER, M. 2012. Toward tailored exosomes: the exosomal tetraspanin web contributes to target cell selection. *Int J Biochem Cell Biol,* 44**,** 1574-84.

RAPOSO, G., NIJMAN, H. W., STOORVOGEL, W., LIEJENDEKKER, R., HARDING, C. V., MELIEF, C. J. & GEUZE, H. J. 1996. B lymphocytes secrete antigen-presenting vesicles. *J Exp Med,* 183**,** 1161-72.

RAPOSO, G. & STOORVOGEL, W. 2013. Extracellular vesicles: exosomes, microvesicles, and friends. *J Cell Biol,* 200**,** 373-83.

RASCHE, H. 2001. Haemostasis and thrombosis: an overview. *European Heart Journal Supplements,* 3**,** Q3-Q7.

RAUTOU, P. E., LEROYER, A. S., RAMKHELAWON, B., DEVUE, C., DUFLAUT, D., VION, A. C., NALBONE, G., CASTIER, Y., LESECHE, G., LEHOUX, S., TEDGUI, A. & BOULANGER, C. M. 2011a. Microparticles from human atherosclerotic plaques promote endothelial ICAM-1-dependent monocyte adhesion and transendothelial migration. *Circ Res,* 108**,** 335-43.

RAUTOU, P. E., VION, A. C., AMABILE, N., CHIRONI, G., SIMON, A., TEDGUI, A. & BOULANGER, C. M. 2011b. Microparticles, vascular function, and atherothrombosis. *Circ Res,* 109**,** 593-606.

REBOUL, E., KLEIN, A., BIETRIX, F., GLEIZE, B., MALEZET-DESMOULINS, C., SCHNEIDER, M., MARGOTAT, A., LAGROST, L., COLLET, X. & BOREL, P. 2006. Scavenger receptor class B type I (SR-BI) is involved in vitamin E transport across the enterocyte. *J Biol Chem,* 281**,** 4739-45.

RECORD, M., SUBRA, C., SILVENTE-POIROT, S. & POIROT, M. 2011. Exosomes as intercellular signalosomes and pharmacological effectors. *Biochem Pharmacol,* 81**,** 1171-82.

RENDU, F. & BROHARD-BOHN, B. 2001. The platelet release reaction: granules' constituents, secretion and functions. *Platelets,* 12**,** 261-73.

RISITANO, A., BEAULIEU, L. M., VITSEVA, O. & FREEDMAN, J. E. 2012. Platelets and platelet-like particles mediate intercellular RNA transfer. *Blood,* 119**,** 6288-95.

RITCHIE, W. & RASKO, J. E. 2014. Refining microRNA target predictions: sorting the wheat from the chaff. *Biochem Biophys Res Commun,* 445**,** 780-4.

RO, S., PARK, C., YOUNG, D., SANDERS, K. M. & YAN, W. 2007. Tissue-dependent paired expression of miRNAs. *Nucleic Acids Res,* 35**,** 5944-53.

ROBERTS, H. R., MONROE, D. M. & ESCOBAR, M. A. 2004. Current concepts of hemostasis: implications for therapy. *Anesthesiology,* 100**,** 722-30.

ROGER, V. L., GO, A. S., LLOYD-JONES, D. M., BENJAMIN, E. J., BERRY, J. D., BORDEN, W. B., BRAVATA, D. M., DAI, S., FORD, E. S., FOX, C. S., FULLERTON, H. J., GILLESPIE, C., HAILPERN, S. M., HEIT, J. A., HOWARD, V. J., KISSELA, B. M., KITTNER, S. J., LACKLAND, D. T., LICHTMAN, J. H., LISABETH, L. D., MAKUC, D. M., MARCUS, G. M., MARELLI, A., MATCHAR, D. B., MOY, C. S., MOZAFFARIAN, D., MUSSOLINO, M. E., NICHOL, G., PAYNTER, N. P., SOLIMAN, E. Z., SORLIE, P. D., SOTOODEHNIA, N., TURAN, T. N., VIRANI, S. S., WONG, N. D., WOO, D., TURNER, M. B., AMERICAN HEART ASSOCIATION STATISTICS, C. & STROKE STATISTICS, S. 2012. Heart disease and stroke statistics--2012 update: a report from the American Heart Association. *Circulation,* 125**,** e2-e220.

ROSENSON, R. S., BREWER, H. B., JR., DAVIDSON, W. S., FAYAD, Z. A., FUSTER, V., GOLDSTEIN, J., HELLERSTEIN, M., JIANG, X. C., PHILLIPS, M. C., RADER, D. J., REMALEY, A. T., ROTHBLAT, G. H., TALL, A. R. & YVAN-CHARVET, L. 2012. Cholesterol efflux and atheroprotection: advancing the concept of reverse cholesterol transport. *Circulation,* 125**,** 1905-19.

ROSS, R. 1999. Atherosclerosis--an inflammatory disease. *N Engl J Med,* 340**,** 115-26.

ROUBELAKIS, M. G., ZOTOS, P., PAPACHRISTOUDIS, G., MICHALOPOULOS, I., PAPPA, K. I., ANAGNOU, N. P. & KOSSIDA, S. 2009. Human microRNA target analysis and gene ontology clustering by GOmir, a novel stand-alone application. *BMC Bioinformatics,* 10 Suppl 6**,** S20.

RUBINSTEIN, E., ZIYYAT, A., PRENANT, M., WROBEL, E., WOLF, J. P., LEVY, S., LE NAOUR, F. & BOUCHEIX, C. 2006a. Reduced fertility of female mice lacking CD81. *Dev Biol,* 290**,** 351-8.

RUBINSTEIN, E., ZIYYAT, A., WOLF, J. P., LE NAOUR, F. & BOUCHEIX, C. 2006b. The molecular players of sperm-egg fusion in mammals. *Semin Cell Dev Biol,* 17**,** 254-63.

RUIKE, Y., ICHIMURA, A., TSUCHIYA, S., SHIMIZU, K., KUNIMOTO, R., OKUNO, Y. & TSUJIMOTO, G. 2008. Global correlation analysis for micro-RNA and mRNA expression profiles in human cell lines. *J Hum Genet,* 53**,** 515-23.

RUIZ, F. A., LEA, C. R., OLDFIELD, E. & DOCAMPO, R. 2004. Human platelet dense granules contain polyphosphate and are similar to acidocalcisomes of bacteria and unicellular eukaryotes. *J Biol Chem,* 279**,** 44250-7.

RUSSO, F., DI BELLA, S., NIGITA, G., MACCA, V., LAGANA, A., GIUGNO, R., PULVIRENTI, A. & FERRO, A. 2012. miRandola: Extracellular Circulating MicroRNAs Database. *PLoS One,* 7**,** e47786.

SABRKHANY, S., GRIFFIOEN, A. W. & OUDE EGBRINK, M. G. 2011. The role of blood platelets in tumor angiogenesis. *Biochim Biophys Acta,* 1815**,** 189-96.

SACHAIS, B. S., KUO, A., NASSAR, T., MORGAN, J., KARIKO, K., WILLIAMS, K. J., FELDMAN, M., AVIRAM, M., SHAH, N., JARETT, L., PONCZ, M., CINES, D. B. & HIGAZI, A. A. 2002. Platelet factor 4 binds to low-density lipoprotein receptors and disrupts the endocytic machinery, resulting in retention of low-density lipoprotein on the cell surface. *Blood,* 99**,** 3613-22.

SADALLAH, S., EKEN, C., MARTIN, P. J. & SCHIFFERLI, J. A. 2011. Microparticles (ectosomes) shed by stored human platelets downregulate macrophages and modify the development of dendritic cells. *J Immunol,* 186**,** 6543-52.

SAEED, A. I., SHAROV, V., WHITE, J., LI, J., LIANG, W., BHAGABATI, N., BRAISTED, J., KLAPA, M., CURRIER, T., THIAGARAJAN, M., STURN, A., SNUFFIN, M., REZANTSEV,

A., POPOV, D., RYLTSOV, A., KOSTUKOVICH, E., BORISOVSKY, I., LIU, Z., VINSAVICH, A., TRUSH, V. & QUACKENBUSH, J. 2003. TM4: a free, open-source system for microarray data management and analysis. *Biotechniques,* 34**,** 374-8.

SARLON-BARTOLI, G., BENNIS, Y., LACROIX, R., PIERCECCHI-MARTI, M. D., BARTOLI, M. A., ARNAUD, L., MANCINI, J., BOUDES, A., SARLON, E., THEVENIN, B., LEROYER, A. S., SQUARCIONI, C., MAGNAN, P. E., DIGNAT-GEORGE, F. & SABATIER, F. 2013. Plasmatic level of leukocyte-derived microparticles is associated with unstable plaque in asymptomatic patients with high-grade carotid stenosis. *J Am Coll Cardiol,* 62**,** 1436-41.

SATO, Y. 2013. Is histone deacetylase-9-MicroRNA-17~92 cluster a novel axis for angiogenesis regulation? *Arterioscler Thromb Vasc Biol,* 33**,** 445-6.

SAUNDERSON, S. C., SCHUBERTH, P. C., DUNN, A. C., MILLER, L., HOCK, B. D., MACKAY, P. A., KOCH, N., JACK, R. W. & MCLELLAN, A. D. 2008. Induction of exosome release in primary B cells stimulated via CD40 and the IL-4 receptor. *J Immunol,* 180**,** 8146-52.

SAVAGE, B., SALDIVAR, E. & RUGGERI, Z. M. 1996. Initiation of platelet adhesion by arrest onto fibrinogen or translocation on von Willebrand factor. *Cell,* 84**,** 289-97.

SCHAFER, G., GULER, R., MURRAY, G., BROMBACHER, F. & BROWN, G. D. 2009. The role of scavenger receptor B1 in infection with Mycobacterium tuberculosis in a murine model. *PLoS One,* 4**,** e8448.

SCHEUERER, B., ERNST, M., DURRBAUM-LANDMANN, I., FLEISCHER, J., GRAGE-GRIEBENOW, E., BRANDT, E., FLAD, H. D. & PETERSEN, F. 2000. The CXC-chemokine platelet factor 4 promotes monocyte survival and induces monocyte differentiation into macrophages. *Blood,* 95**,** 1158-66.

SCHINDELIN, J., ARGANDA-CARRERAS, I., FRISE, E., KAYNIG, V., LONGAIR, M., PIETZSCH, T., PREIBISCH, S., RUEDEN, C., SAALFELD, S., SCHMID, B., TINEVEZ, J. Y., WHITE, D. J., HARTENSTEIN, V., ELICEIRI, K., TOMANCAK, P. & CARDONA, A. 2012. Fiji: an open-source platform for biological-image analysis. *Nat Methods,* 9**,** 676-82.

SCHOPMAN, N. C., HEYNEN, S., HAASNOOT, J. & BERKHOUT, B. 2010. A miRNA-tRNA mix-up: tRNA origin of proposed miRNA. *RNA Biol,* 7**,** 573-6.

SCHWANHAUSSER, B., GOSSEN, M., DITTMAR, G. & SELBACH, M. 2009. Global analysis of cellular protein translation by pulsed SILAC. *Proteomics,* 9**,** 205-9.

SEITZ, H. 2009. Redefining microRNA targets. *Curr Biol,* 19**,** 870-3.

SELBACH, M., SCHWANHAUSSER, B., THIERFELDER, N., FANG, Z., KHANIN, R. & RAJEWSKY, N. 2008. Widespread changes in protein synthesis induced by microRNAs. *Nature,* 455**,** 58-63.

SEMPLE, J. W., ITALIANO, J. E., JR. & FREEDMAN, J. 2011. Platelets and the immune continuum. *Nat Rev Immunol,* 11**,** 264-74.

SENZEL, L., GNATENKO, D. V. & BAHOU, W. F. 2009. The platelet proteome. *Curr Opin Hematol,* 16**,** 329-33.

SETHUPATHY, P., MEGRAW, M. & HATZIGEORGIOU, A. G. 2006. A guide through present computational approaches for the identification of mammalian microRNA targets. *Nat Methods,* 3**,** 881-6.

SETZER, F., OBERLE, V., BLASS, M., MOLLER, E., RUSSWURM, S., DEIGNER, H. P., CLAUS, R. A., BAUER, M., REINHART, K. & LOSCHE, W. 2006. Platelet-derived

microvesicles induce differential gene expression in monocytic cells: a DNA microarray study. *Platelets,* 17**,** 571-6.

SHANNON, P., MARKIEL, A., OZIER, O., BALIGA, N. S., WANG, J. T., RAMAGE, D., AMIN, N., SCHWIKOWSKI, B. & IDEKER, T. 2003. Cytoscape: a software environment for integrated models of biomolecular interaction networks. *Genome Res,* 13**,** 2498-504.

SHATTIL, S. 2006. Platelet tectonics: Unearthing secrets of integrin signaling. *Matrix Biology,* 25**,** S6-S6.

SHATTIL, S. J. 1999. Signaling through platelet integrin alpha IIb beta 3: Inside-out, outside-in, and sideways. *Thromb Haemost,* 82**,** 318-325.

SHI, R., GE, L., ZHOU, X., JI, W. J., LU, R. Y., ZHANG, Y. Y., ZENG, S., LIU, X., ZHAO, J. H., ZHANG, W. C., JIANG, T. M. & LI, Y. M. 2013. Decreased platelet miR-223 expression is associated with high on-clopidogrel platelet reactivity. *Thromb Res,* 131**,** 508-13.

SHTAM, T. A., KOVALEV, R. A., VARFOLOMEEVA, E. Y., MAKAROV, E. M., KIL, Y. V. & FILATOV, M. V. 2013. Exosomes are natural carriers of exogenous siRNA to human cells in vitro. *Cell Commun Signal,* 11**,** 88.

SHUKLA, D., LIU, J., BLAIKLOCK, P., SHWORAK, N. W., BAI, X., ESKO, J. D., COHEN, G. H., EISENBERG, R. J., ROSENBERG, R. D. & SPEAR, P. G. 1999. A novel role for 3-O-sulfated heparan sulfate in herpes simplex virus 1 entry. *Cell,* 99**,** 13-22.

SIMAK, J., GELDERMAN, M. P., YU, H., WRIGHT, V. & BAIRD, A. E. 2006. Circulating endothelial microparticles in acute ischemic stroke: a link to severity, lesion volume and outcome. *J Thromb Haemost,* 4**,** 1296-302.

SIMMS, P., FRANZEN, C., VOLGINA, C. & GUPTA, G. 2013. Detecton of Internalized Exosomes by Tumor Cells Using Amnis ImageStreamX. *Poster presented at CYTO 2013,* B129.

SIMON, L. M., EDELSTEIN, L. C., NAGALLA, S., WOODLEY, A. B., CHEN, E. S., KONG, X., MA, L., FORTINA, P., KUNAPULI, S., HOLINSTAT, M., MCKENZIE, S. E., DONG, J. F., SHAW, C. A. & BRAY, P. F. 2014. Human platelet microRNA-mRNA networks associated with age and gender revealed by integrated plateletomics. *Blood,* 123**,** e37-45.

SMALLEY, D. M., SHEMAN, N. E., NELSON, K. & THEODORESCU, D. 2008. Isolation and identification of potential urinary microparticle biomarkers of bladder cancer. *J Proteome Res,* 7**,** 2088-96.

SMITH, J. B. 1981. Prostaglandins and platelet aggregation. *Acta Med Scand Suppl,* 651**,** 91-9.

SMITH, Z. J., LEE, C., ROJALIN, T., CARNEY, R. P., HAZARI, S., KNUDSON, A., LAM, K., SAARI, H., IBANEZ, E. L., VIITALA, T., LAAKSONEN, T., YLIPERTTULA, M. & WACHSMANN-HOGIU, S. 2015. Single exosome study reveals subpopulations distributed among cell lines with variability related to membrane content. *J Extracell Vesicles,* 4.

SMOUT, J., DYKER, A., CLEANTHIS, M., FORD, G., KESTEVEN, P. & STANSBY, G. 2009. Platelet function following acute cerebral ischemia. *Angiology,* 60**,** 362-9.

SMYTH, S. S., MCEVER, R. P., WEYRICH, A. S., MORRELL, C. N., HOFFMAN, M. R., AREPALLY, G. M., FRENCH, P. A., DAUERMAN, H. L., BECKER, R. C. & PLATELET COLLOQUIUM, P. 2009. Platelet functions beyond hemostasis. *J Thromb Haemost,* 7**,** 1759-66.

SNAPP, K. R., HEITZIG, C. E. & KANSAS, G. S. 2002. Attachment of the PSGL-1 cytoplasmic domain to the actin cytoskeleton is essential for leukocyte rolling on P-selectin. *Blood,* 99**,** 4494-502.

SONDERMEIJER, B. M., BAKKER, A., HALLIANI, A., DE RONDE, M. W., MARQUART, A. A., TIJSEN, A. J., MULDERS, T. A., KOK, M. G., BATTJES, S., MAIWALD, S., SIVAPALARATNAM, S., TRIP, M. D., MOERLAND, P. D., MEIJERS, J. C., CREEMERS, E. E. & PINTO-SIETSMA, S. J. 2011. Platelets in patients with premature coronary artery disease exhibit upregulation of miRNA340* and miRNA624*. *PLoS One,* 6**,** e25946.

SOULET, C., HECHLER, B., GRATACAP, M. P., PLANTAVID, M., OFFERMANNS, S., GACHET, C. & PAYRASTRE, B. 2005. A differential role of the platelet ADP receptors P2Y1 and P2Y12 in Rac activation. *J Thromb Haemost,* 3**,** 2296-306.

SRIKANTHAN, S., LI, W., SILVERSTEIN, R. L. & MCINTYRE, T. M. 2014. Exosome poly-ubiquitin inhibits platelet activation, downregulates CD36 and inhibits pro-atherothombotic cellular functions. *J Thromb Haemost,* 12**,** 1906-17.

SRIVASTAVA, A., FILANT, J., MOXLEY, K. M., SOOD, A., MCMEEKIN, S. & RAMESH, R. 2015. Exosomes: a role for naturally occurring nanovesicles in cancer growth, diagnosis and treatment. *Curr Gene Ther,* 15**,** 182-92.

STAKOS, D. A., GATSIOU, A., STAMATELOPOULOS, K., TSELEPIS, A. D. & STELLOS, K. 2012. Platelet microRNAs: From platelet biology to possible disease biomarkers and therapeutic targets. *Platelets,* 24**,** 579-589.

STANCU, C. & SIMA, A. 2001. Statins: mechanism of action and effects. *J Cell Mol Med,* 5**,** 378-87.

STATHER, P. W., SYLVIUS, N., WILD, J. B., CHOKE, E., SAYERS, R. D. & BOWN, M. J. 2013. Differential microRNA expression profiles in peripheral arterial disease. *Circ Cardiovasc Genet,* 6**,** 490-7.

STEPIEN, E., STANKIEWICZ, E., ZALEWSKI, J., GODLEWSKI, J., ZMUDKA, K. & WYBRANSKA, I. 2012. Number of microparticles generated during acute myocardial infarction and stable angina correlates with platelet activation. *Arch Med Res,* 43**,** 31-5.

STOORVOGEL, W. 2012. Functional transfer of microRNA by exosomes. *Blood,* 119**,** 646-8.

STOORVOGEL, W., KLEIJMEER, M. J., GEUZE, H. J. & RAPOSO, G. 2002. The biogenesis and functions of exosomes. *Traffic,* 3**,** 321-30.

STRATZ, C., NUHRENBERG, T. G., BINDER, H., VALINA, C. M., TRENK, D., HOCHHOLZER, W., NEUMANN, F. J. & FIEBICH, B. L. 2012. Micro-array profiling exhibits remarkable intra-individual stability of human platelet micro-RNA. *Thromb Haemost,* 107**,** 634-41.

SUH, M. R., LEE, Y., KIM, J. Y., KIM, S. K., MOON, S. H., LEE, J. Y., CHA, K. Y., CHUNG, H. M., YOON, H. S., MOON, S. Y., KIM, V. N. & KIM, K. S. 2004. Human embryonic stem cells express a unique set of microRNAs. *Dev Biol,* 270**,** 488-98.

SUZUKI-INOUE, K., YATOMI, Y., ASAZUMA, N., KAINOH, M., TANAKA, T., SATOH, K. & OZAKI, Y. 2001. Rac, a small guanosine triphosphate-binding protein, and p21-activated kinase are activated during platelet spreading on collagen-coated surfaces: roles of integrin alpha(2)beta(1). *Blood,* 98**,** 3708-3716.

SZUMILO, M. & RAHDEN-STARON, I. 2008. Phosphoinositide-specific phospholipase C in mammalian cells: structure, properties, and function. *Postepy Hig Med Dosw (Online),* 62**,** 47-54.

TABAS, I. 2010. Macrophage death and defective inflammation resolution in atherosclerosis. *Nat Rev Immunol,* 10**,** 36-46.

TABAS, I., TALL, A. & ACCILI, D. 2010. The impact of macrophage insulin resistance on advanced atherosclerotic plaque progression. *Circ Res,* 106**,** 58-67.

TAKANO, K., ASAZUMA, N., SATOH, K., YATOMI, Y. & OZAKI, Y. 2004. Collagen-induced generation of platelet-derived microparticles in whole blood is dependent on ADP released from red blood cells and calcium ions. *Platelets,* 15**,** 223-9.

TAKEDA, Y., TACHIBANA, I., MIYADO, K., KOBAYASHI, M., MIYAZAKI, T., FUNAKOSHI, T., KIMURA, H., YAMANE, H., SAITO, Y., GOTO, H., YONEDA, T., YOSHIDA, M., KUMAGAI, T., OSAKI, T., HAYASHI, S., KAWASE, I. & MEKADA, E. 2003. Tetraspanins CD9 and CD81 function to prevent the fusion of mononuclear phagocytes. *J Cell Biol,* 161**,** 945-56.

TATISCHEFF, I., LARQUET, E., FALCON-PEREZ, J. M., TURPIN, P. Y. & KRUGLIK, S. G. 2012. Fast characterisation of cell-derived extracellular vesicles by nanoparticles tracking analysis, cryo-electron microscopy, and Raman tweezers microspectroscopy. *J Extracell Vesicles,* 1.

TAURO, B. J., GREENING, D. W., MATHIAS, R. A., JI, H., MATHIVANAN, S., SCOTT, A. M. & SIMPSON, R. J. 2012. Comparison of ultracentrifugation, density gradient separation, and immunoaffinity capture methods for isolating human colon cancer cell line LIM1863-derived exosomes. *Methods,* 56**,** 293-304.

TAURO, B. J., GREENING, D. W., MATHIAS, R. A., MATHIVANAN, S., JI, H. & SIMPSON, R. J. 2013. Two distinct populations of exosomes are released from LIM1863 colon carcinoma cell-derived organoids. *Mol Cell Proteomics,* 12**,** 587-98.

TAYLOR, D. D. & SHAH, S. 2015. Methods of isolating extracellular vesicles impact down-stream analyses of their cargoes. *Methods,* 87**,** 3-10.

TAYLOR, D. D., ZACHARIAS, W. & GERCEL-TAYLOR, C. 2011. Exosome isolation for proteomic analyses and RNA profiling. *Methods Mol Biol,* 728**,** 235-46.

TENOPIR, C., ALLARD, S., DOUGLASS, K., AYDINOGLU, A. U., WU, L., READ, E., MANOFF, M. & FRAME, M. 2011. Data sharing by scientists: practices and perceptions. *PLoS One,* 6**,** e21101.

TENOPIR, C., DALTON, E. D., ALLARD, S., FRAME, M., PJESIVAC, I., BIRCH, B., POLLOCK, D. & DORSETT, K. 2015. Changes in Data Sharing and Data Reuse Practices and Perceptions among Scientists Worldwide. *PLoS One,* 10**,** e0134826.

TERUEL-MONTOYA, R., KONG, X., ABRAHAM, S., MA, L., KUNAPULI, S. P., HOLINSTAT, M., SHAW, C. A., MCKENZIE, S. E., EDELSTEIN, L. C. & BRAY, P. F. 2014. MicroRNA Expression Differences in Human Hematopoietic Cell Lineages Enable Regulated Transgene Expression. *PLoS One,* 9**,** e102259.

THALI, M. 2009. The roles of tetraspanins in HIV-1 replication. *Curr Top Microbiol Immunol,* 339**,** 85-102.

THERY, C., AMIGORENA, S., RAPOSO, G. & CLAYTON, A. 2006. Isolation and characterization of exosomes from cell culture supernatants and biological fluids. *Curr Protoc Cell Biol,* Chapter 3**,** Unit 3 22.

THERY, C., OSTROWSKI, M. & SEGURA, E. 2009. Membrane vesicles as conveyors of immune responses. *Nat Rev Immunol,* 9**,** 581-93.

THOMAS, D. W., MANNON, R. B., MANNON, P. J., LATOUR, A., OLIVER, J. A., HOFFMAN, M., SMITHIES, O., KOLLER, B. H. & COFFMAN, T. M. 1998. Coagulation defects

and altered hemodynamic responses in mice lacking receptors for thromboxane A2. *Journal of Clinical Investigation,* 102**,** 1994-2001.

THOMAS, M. R. & STOREY, R. F. 2015. Effect of P2Y12 inhibitors on inflammation and immunity. *Thromb Haemost,* 114**,** 490-7.

THOMSON, D. W., BRACKEN, C. P. & GOODALL, G. J. 2011. Experimental strategies for microRNA target identification. *Nucleic Acids Res,* 39**,** 6845-53.

THON, J. N. & ITALIANO, J. E. 2010. Platelet formation. *Semin Hematol,* 47**,** 220-6.

THON, J. N., MONTALVO, A., PATEL-HETT, S., DEVINE, M. T., RICHARDSON, J. L., EHRLICHER, A., LARSON, M. K., HOFFMEISTER, K., HARTWIG, J. H. & ITALIANO, J. E., JR. 2010. Cytoskeletal mechanics of proplatelet maturation and platelet release. *J Cell Biol,* 191**,** 861-74.

THUM, T. & MAYR, M. 2012. Review focus on the role of microRNA in cardiovascular biology and disease. *Cardiovasc Res,* 93**,** 543-4.

TOUSOULIS, D., DAVIES, G., STEFANADIS, C., TOUTOUZAS, P. & AMBROSE, J. A. 2003. Inflammatory and thrombotic mechanisms in coronary atherosclerosis. *Heart,* 89**,** 993-7.

TRAJKOVIC, K., HSU, C., CHIANTIA, S., RAJENDRAN, L., WENZEL, D., WIELAND, F., SCHWILLE, P., BRUGGER, B. & SIMONS, M. 2008. Ceramide triggers budding of exosome vesicles into multivesicular endosomes. *Science,* 319**,** 1244-7.

TRAJKOVSKI, M., HAUSSER, J., SOUTSCHEK, J., BHAT, B., AKIN, A., ZAVOLAN, M., HEIM, M. H. & STOFFEL, M. 2011. MicroRNAs 103 and 107 regulate insulin sensitivity. *Nature,* 474**,** 649-53.

TSUI, N. B., NG, E. K. & LO, Y. M. 2002. Stability of endogenous and added RNA in blood specimens, serum, and plasma. *Clin Chem,* 48**,** 1647-53.

TURCHINOVICH, A., WEIZ, L., LANGHEINZ, A. & BURWINKEL, B. 2011. Characterization of extracellular circulating microRNA. *Nucleic Acids Res,* 39**,** 7223-33.

TUSHUIZEN, M. E., DIAMANT, M., STURK, A. & NIEUWLAND, R. 2011. Cell-derived microparticles in the pathogenesis of cardiovascular disease: friend or foe? *Arterioscler Thromb Vasc Biol,* 31**,** 4-9.

VALACCHI, G., MAIOLI, E., STICOZZI, C., CERVELLATI, F., PECORELLI, A., CERVELLATI, C. & HAYEK, J. 2015. Exploring the link between scavenger receptor B1 expression and chronic obstructive pulmonary disease pathogenesis. *Ann N Y Acad Sci,* 1340**,** 47-54.

VALACCHI, G., STICOZZI, C., LIM, Y. & PECORELLI, A. 2011. Scavenger receptor class B type I: a multifunctional receptor. *Ann N Y Acad Sci,* 1229**,** E1-7.

VALADI, H., EKSTROM, K., BOSSIOS, A., SJOSTRAND, M., LEE, J. J. & LOTVALL, J. O. 2007. Exosome-mediated transfer of mRNAs and microRNAs is a novel mechanism of genetic exchange between cells. *Nat Cell Biol,* 9**,** 654-9.

VAN DER POL, E., BOING, A. N., GOOL, E. L. & NIEUWLAND, R. 2016. Recent developments in the nomenclature, presence, isolation, detection and clinical impact of extracellular vesicles. *J Thromb Haemost,* 14**,** 48-56.

VAN DER POL, E., BOING, A. N., HARRISON, P., STURK, A. & NIEUWLAND, R. 2012a. Classification, functions, and clinical relevance of extracellular vesicles. *Pharmacol Rev,* 64**,** 676-705.

VAN DER POL, E., COUMANS, F. A., GROOTEMAAT, A. E., GARDINER, C., SARGENT, I. L., HARRISON, P., STURK, A., VAN LEEUWEN, T. G. & NIEUWLAND, R. 2014. Particle size distribution of exosomes and microvesicles determined by transmission

electron microscopy, flow cytometry, nanoparticle tracking analysis, and resistive pulse sensing. *J Thromb Haemost,* 12**,** 1182-92.

VAN DER POL, E., VAN GEMERT, M. J., STURK, A., NIEUWLAND, R. & VAN LEEUWEN, T. G. 2012b. Single vs. swarm detection of microparticles and exosomes by flow cytometry. *J Thromb Haemost,* 10**,** 919-30.

VAN DER ZEE, P. M., BIRO, E., KO, Y., DE WINTER, R. J., HACK, C. E., STURK, A. & NIEUWLAND, R. 2006. P-selectin- and CD63-exposing platelet microparticles reflect platelet activation in peripheral arterial disease and myocardial infarction. *Clin Chem,* 52**,** 657-64.

VAN DEUN, J., MESTDAGH, P., SORMUNEN, R., COCQUYT, V., VERMAELEN, K., VANDESOMPELE, J., BRACKE, M., DE WEVER, O. & HENDRIX, A. 2014. The impact of disparate isolation methods for extracellular vesicles on downstream RNA profiling. *J Extracell Vesicles,* 3.

VAN ECK, M., TWISK, J., HOEKSTRA, M., VAN RIJ, B. T., VAN DER LANS, C. A., BOS, I. S., KRUIJT, J. K., KUIPERS, F. & VAN BERKEL, T. J. 2003. Differential effects of scavenger receptor BI deficiency on lipid metabolism in cells of the arterial wall and in the liver. *J Biol Chem,* 278**,** 23699-705.

VAN GILS, J. M., ZWAGINGA, J. J. & HORDIJK, P. L. 2009. Molecular and functional interactions among monocytes, platelets, and endothelial cells and their relevance for cardiovascular diseases. *J Leukoc Biol,* 85**,** 195-204.

VARGA, Z., YUANA, Y., GROOTEMAAT, A. E., VAN DER POL, E., GOLLWITZER, C., KRUMREY, M. & NIEUWLAND, R. 2014. Towards traceable size determination of extracellular vesicles. *J Extracell Vesicles,* 3.

VERSTEEG, H. H., HEEMSKERK, J. W., LEVI, M. & REITSMA, P. H. 2013. New fundamentals in hemostasis. *Physiol Rev,* 93**,** 327-58.

VICKERS, K. C., PALMISANO, B. T., SHOUCRI, B. M., SHAMBUREK, R. D. & REMALEY, A. T. 2011. MicroRNAs are transported in plasma and delivered to recipient cells by high-density lipoproteins. *Nat Cell Biol,* 13**,** 423-33.

VIEIRA-DE-ABREU, A., CAMPBELL, R. A., WEYRICH, A. S. & ZIMMERMAN, G. A. 2012. Platelets: versatile effector cells in hemostasis, inflammation, and the immune continuum. *Semin Immunopathol,* 34**,** 5-30.

VINE, A. K. 2009. Recent advances in haemostasis and thrombosis. *Retina,* 29**,** 1-7.

VIRMANI, R., BURKE, A. P. & FARB, A. 1999. Plaque rupture and plaque erosion. *Thromb Haemost,* 82 Suppl 1**,** 1-3.

VLACHOS, I. S., KOSTOULAS, N., VERGOULIS, T., GEORGAKILAS, G., RECZKO, M., MARAGKAKIS, M., PARASKEVOPOULOU, M. D., PRIONIDIS, K., DALAMAGAS, T. & HATZIGEORGIOU, A. G. 2012. DIANA miRPath v.2.0: investigating the combinatorial effect of microRNAs in pathways. *Nucleic Acids Res,* 40**,** W498-504.

VLASSOV, A. V., MAGDALENO, S., SETTERQUIST, R. & CONRAD, R. 2012. Exosomes: current knowledge of their composition, biological functions, and diagnostic and therapeutic potentials. *Biochim Biophys Acta,* 1820**,** 940-8.

VOINNET, O. 2009. Origin, biogenesis, and activity of plant microRNAs. *Cell,* 136**,** 669-87.

VON BRUHL, M. L., STARK, K., STEINHART, A., CHANDRARATNE, S., KONRAD, I., LORENZ, M., KHANDOGA, A., TIRNICERIU, A., COLETTI, R., KOLLNBERGER, M., BYRNE, R. A., LAITINEN, I., WALCH, A., BRILL, A., PFEILER, S., MANUKYAN, D., BRAUN, S., LANGE, P., RIEGGER, J., WARE, J., ECKART, A., HAIDARI, S., RUDELIUS, M.,

SCHULZ, C., ECHTLER, K., BRINKMANN, V., SCHWAIGER, M., PREISSNER, K. T., WAGNER, D. D., MACKMAN, N., ENGELMANN, B. & MASSBERG, S. 2012. Monocytes, neutrophils, and platelets cooperate to initiate and propagate venous thrombosis in mice in vivo. *J Exp Med,* 209**,** 819-35.

WAGNER, J., RIWANTO, M., BESLER, C., KNAU, A., FICHTLSCHERER, S., ROXE, T., ZEIHER, A. M., LANDMESSER, U. & DIMMELER, S. 2013. Characterization of levels and cellular transfer of circulating lipoprotein-bound microRNAs. *Arterioscler Thromb Vasc Biol,* 33**,** 1392-400.

WANG, B., WANG, X. F. & XI, Y. 2011. Normalizing bead-based microRNA expression data: a measurement error model-based approach. *Bioinformatics,* 27**,** 1506-12.

WANG, K., LONG, B., JIAO, J. Q., WANG, J. X., LIU, J. P., LI, Q. & LI, P. F. 2012a. miR-484 regulates mitochondrial network through targeting Fis1. *Nat Commun,* 3**,** 781.

WANG, K., YUAN, Y., CHO, J. H., MCCLARTY, S., BAXTER, D. & GALAS, D. J. 2012b. Comparing the MicroRNA spectrum between serum and plasma. *PLoS One,* 7**,** e41561.

WANG, L., JIA, X. J., JIANG, H. J., DU, Y., YANG, F., SI, S. Y. & HONG, B. 2013. MicroRNAs 185, 96, and 223 Repress Selective High-Density Lipoprotein Cholesterol Uptake through Posttranscriptional Inhibition. *Molecular and Cellular Biology,* 33**,** 1956-1964.

WANG, S., AURORA, A. B., JOHNSON, B. A., QI, X., MCANALLY, J., HILL, J. A., RICHARDSON, J. A., BASSEL-DUBY, R. & OLSON, E. N. 2008. The endothelial-specific microRNA miR-126 governs vascular integrity and angiogenesis. *Dev Cell,* 15**,** 261-71.

WANG, X. 2008. miRDB: a microRNA target prediction and functional annotation database with a wiki interface. *RNA,* 14**,** 1012-7.

WANG, X. 2010. Computational prediction of microRNA targets. *Methods Mol Biol,* 667**,** 283-95.

WANG, X. & WANG, X. 2006. Systematic identification of microRNA functions by combining target prediction and expression profiling. *Nucleic Acids Res,* 34**,** 1646-52.

WATKINS, N. A., SMETHURST, P. A., ALLEN, D., SMITH, G. A. & OUWEHAND, W. H. 2002. Platelet alphaIIbbeta3 recombinant autoantibodies from the B-cell repertoire of a post-transfusion purpura patient. *Br J Haematol,* 116**,** 677-85.

WEBBER, J. & CLAYTON, A. 2013. How pure are your vesicles? *J Extracell Vesicles,* 2.

WEBER, C. 2013. MicroRNAs: from basic mechanisms to clinical application in cardiovascular medicine. *Arterioscler Thromb Vasc Biol,* 33**,** 168-9.

WELSH, J. D., STALKER, T. J., VORONOV, R., MUTHARD, R. W., TOMAIUOLO, M., DIAMOND, S. L. & BRASS, L. F. 2014. A systems approach to hemostasis: 1. The interdependence of thrombus architecture and agonist movements in the gaps between platelets. *Blood,* 124**,** 1808-15.

WELTON, J. L., WEBBER, J. P., BOTOS, L. A., JONES, M. & CLAYTON, A. 2015. Ready-made chromatography columns for extracellular vesicle isolation from plasma. *J Extracell Vesicles,* 4.

WEYRICH, A. S., ELSTAD, M. R., MCEVER, R. P., MCINTYRE, T. M., MOORE, K. L., MORRISSEY, J. H., PRESCOTT, S. M. & ZIMMERMAN, G. A. 1996. Activated platelets signal chemokine synthesis by human monocytes. *J Clin Invest,* 97**,** 1525-34.

WEYRICH, A. S., MCINTYRE, T. M., MCEVER, R. P., PRESCOTT, S. M. & ZIMMERMAN, G. A. 1995. Monocyte tethering by P-selectin regulates monocyte chemotactic protein-1 and tumor necrosis factor-alpha secretion. Signal integration and NF-kappa B translocation. *J Clin Invest,* 95**,** 2297-303.

WIJEYERATNE, Y. D. & HEPTINSTALL, S. 2011. Anti-platelet therapy: ADP receptor antagonists. *Br J Clin Pharmacol,* 72**,** 647-57.

WILLEIT, P., ZAMPETAKI, A., DUDEK, K., KAUDEWITZ, D., KING, A. S., KIRKBY, N. S., CROSBY-NWAOBI, R., PROKOPI, M., DROZDOV, I., LANGLEY, S., SIVAPRASAD, S., MARKUS, H. S., MITCHELL, J. A., WARNER, T., KIECHL, S. & MAYR, M. 2013. Circulating MicroRNAs as Novel Biomarkers for Platelet Activation. *Circ Res,* 112**,** 595-600.

WILLIAMS, R. L. 1999. Mammalian phosphoinositide-specific phospholipase C. *Biochim Biophys Acta,* 1441**,** 255-67.

WINTER, J., JUNG, S., KELLER, S., GREGORY, R. I. & DIEDERICHS, S. 2009. Many roads to maturity: microRNA biogenesis pathways and their regulation. *Nat Cell Biol,* 11**,** 228-34.

WITKOS, T. M., KOSCIANSKA, E. & KRZYZOSIAK, W. J. 2011. Practical Aspects of microRNA Target Prediction. *Curr Mol Med,* 11**,** 93-109.

WITWER, K. W., BUZAS, E. I., BEMIS, L. T., BORA, A., LASSER, C., LOTVALL, J., NOLTE-'T HOEN, E. N., PIPER, M. G., SIVARAMAN, S., SKOG, J., THERY, C., WAUBEN, M. H. & HOCHBERG, F. 2013. Standardization of sample collection, isolation and analysis methods in extracellular vesicle research. *J Extracell Vesicles,* 2.

WOLF, P. 1967. The nature and significance of platelet products in human plasma. *Br J Haematol,* 13**,** 269-88.

WONG, N. & WANG, X. 2015. miRDB: an online resource for microRNA target prediction and functional annotations. *Nucleic Acids Res,* 43**,** D146-52.

WRIGHT, J. 2010. *Variation in the Haemostatic Response and Thrombotic Risk: Interplay Between Haemostatic Factors, Platelets and Monocytes.* PhD Thesis, University of Leicester.

XIAO, H., JEPKORIR, C. J., HARVEY, K. & REMICK, D. G. 2002. Thrombin-induced platelet microparticles improved the aggregability of cryopreserved platelets. *Cryobiology,* 44**,** 179-88.

XU, X., GNATENKO, D. V., JU, J., HITCHCOCK, I. S., MARTIN, D. W., ZHU, W. & BAHOU, W. F. 2012. Systematic analysis of microRNA fingerprints in thrombocythemic platelets using integrated platforms. *Blood***,** 3575-3585.

YAMADA, Y., PANNELL, R., FORSTER, A. & RABBITTS, T. H. 2002. The LIM-domain protein Lmo2 is a key regulator of tumour angiogenesis: a new anti-angiogenesis drug target. *Oncogene,* 21**,** 1309-15.

YAMAN AGAOGLU, F., KOVANCILAR, M., DIZDAR, Y., DARENDELILER, E., HOLDENRIEDER, S., DALAY, N. & GEZER, U. 2011. Investigation of miR-21, miR-141, and miR-221 in blood circulation of patients with prostate cancer. *Tumour Biol,* 32**,** 583-8.

YANEZ-MO, M., SILJANDER, P. R., ANDREU, Z., ZAVEC, A. B., BORRAS, F. E., BUZAS, E. I., BUZAS, K., CASAL, E., CAPPELLO, F., CARVALHO, J., COLAS, E., CORDEIRO-DA SILVA, A., FAIS, S., FALCON-PEREZ, J. M., GHOBRIAL, I. M., GIEBEL, B., GIMONA, M., GRANER, M., GURSEL, I., GURSEL, M., HEEGAARD, N. H., HENDRIX, A., KIERULF, P., KOKUBUN, K., KOSANOVIC, M., KRALJ-IGLIC, V., KRAMER-ALBERS, E. M., LAITINEN, S., LASSER, C., LENER, T., LIGETI, E., LINE, A., LIPPS, G., LLORENTE,

A., LOTVALL, J., MANCEK-KEBER, M., MARCILLA, A., MITTELBRUNN, M., NAZARENKO, I., NOLTE-'T HOEN, E. N., NYMAN, T. A., O'DRISCOLL, L., OLIVAN, M., OLIVEIRA, C., PALLINGER, E., DEL PORTILLO, H. A., REVENTOS, J., RIGAU, M., ROHDE, E., SAMMAR, M., SANCHEZ-MADRID, F., SANTAREM, N., SCHALLMOSER, K., OSTENFELD, M. S., STOORVOGEL, W., STUKELJ, R., VAN DER GREIN, S. G., VASCONCELOS, M. H., WAUBEN, M. H. & DE WEVER, O. 2015. Biological properties of extracellular vesicles and their physiological functions. *J Extracell Vesicles,* 4.

YU, D., DOS SANTOS, C. O., ZHAO, G., JIANG, J., AMIGO, J. D., KHANDROS, E., DORE, L. C., YAO, Y., D'SOUZA, J., ZHANG, Z., GHAFFARI, S., CHOI, J., FRIEND, S., TONG, W., ORANGE, J. S., PAW, B. H. & WEISS, M. J. 2010. miR-451 protects against erythroid oxidant stress by repressing 14-3-3zeta. *Genes Dev,* 24**,** 1620-33.

YUAN, J. Y., WANG, F., YU, J., YANG, G. H., LIU, X. L. & ZHANG, J. W. 2009. MicroRNA-223 reversibly regulates erythroid and megakaryocytic differentiation of K562 cells. *J Cell Mol Med,* 13**,** 4551-9.

YUANA, Y., BOING, A. N., GROOTEMAAT, A. E., VAN DER POL, E., HAU, C. M., CIZMAR, P., BUHR, E., STURK, A. & NIEUWLAND, R. 2015. Handling and storage of human body fluids for analysis of extracellular vesicles. *J Extracell Vesicles,* 4.

YUANA, Y., KONING, R. I., KUIL, M. E., RENSEN, P. C., KOSTER, A. J., BERTINA, R. M. & OSANTO, S. 2013. Cryo-electron microscopy of extracellular vesicles in fresh plasma. *J Extracell Vesicles,* 2.

YUANA, Y., LEVELS, J., GROOTEMAAT, A., STURK, A. & NIEUWLAND, R. 2014. Co-isolation of extracellular vesicles and high-density lipoproteins using density gradient ultracentrifugation. *J Extracell Vesicles,* 3.

YUYAMA, K., SUN, H., MITSUTAKE, S. & IGARASHI, Y. 2012. Sphingolipid-modulated exosome secretion promotes clearance of amyloid-beta by microglia. *J Biol Chem,* 287**,** 10977-89.

ZAMPETAKI, A. & MAYR, M. 2012a. Analytical challenges and technical limitations in assessing circulating miRNAs. *Thromb Haemost,* 108**,** 592-8.

ZAMPETAKI, A. & MAYR, M. 2012b. MicroRNAs in vascular and metabolic disease. *Circ Res,* 110**,** 508-22.

ZAMPETAKI, A., WILLEIT, P., TILLING, L., DROZDOV, I., PROKOPI, M., RENARD, J. M., MAYR, A., WEGER, S., SCHETT, G., SHAH, A., BOULANGER, C. M., WILLEIT, J., CHOWIENCZYK, P. J., KIECHL, S. & MAYR, M. 2012. Prospective study on circulating MicroRNAs and risk of myocardial infarction. *J Am Coll Cardiol,* 60**,** 290-9.

ZAND, T., HOFFMAN, A. H., SAVILONIS, B. J., UNDERWOOD, J. M., NUNNARI, J. J., MAJNO, G. & JORIS, I. 1999. Lipid deposition in rat aortas with intraluminal hemispherical plug stenosis. A morphological and biophysical study. *Am J Pathol,* 155**,** 85-92.

ZANONI, P., KHETARPAL, S. A., LARACH, D. B., HANCOCK-CERUTTI, W. F., MILLAR, J. S., CUCHEL, M., DEROHANNESSIAN, S., KONTUSH, A., SURENDRAN, P., SALEHEEN, D., TROMPET, S., JUKEMA, J. W., DE CRAEN, A., DELOUKAS, P., SATTAR, N., FORD, I., PACKARD, C., MAJUMDER, A., ALAM, D. S., DI ANGELANTONIO, E., ABECASIS, G., CHOWDHURY, R., ERDMANN, J., NORDESTGAARD, B. G., NIELSEN, S. F., TYBJAERG-HANSEN, A., SCHMIDT, R. F., KUULASMAA, K., LIU, D. J., PEROLA, M., BLANKENBERG, S., SALOMAA, V., MANNISTO, S., AMOUYEL, P., ARVEILER, D., FERRIERES, J., MULLER-NURASYID, M., FERRARIO, M., KEE, F., WILLER, C. J.,

SAMANI, N., SCHUNKERT, H., BUTTERWORTH, A. S., HOWSON, J. M., PELOSO, G. M., STITZIEL, N. O., DANESH, J., KATHIRESAN, S., RADER, D. J., CONSORTIUM, C. H. D. E., CONSORTIUM, C. A. E. & GLOBAL LIPIDS GENETICS, C. 2016. Rare variant in scavenger receptor BI raises HDL cholesterol and increases risk of coronary heart disease. *Science,* 351**,** 1166-71.

ZEARO, S., KIM, E., ZHU, Y., ZHAO, J. T., SIDHU, S. B., ROBINSON, B. G. & SOON, P. 2014. MicroRNA-484 is more highly expressed in serum of early breast cancer patients compared to healthy volunteers. *BMC Cancer,* 14**,** 200.

ZECH, D., RANA, S., BUCHLER, M. W. & ZOLLER, M. 2012. Tumor-exosomes and leukocyte activation: an ambivalent crosstalk. *Cell Commun Signal,* 10**,** 37.

ZERNECKE, A., BIDZHEKOV, K., NOELS, H., SHAGDARSUREN, E., GAN, L., DENECKE, B., HRISTOV, M., KOPPEL, T., JAHANTIGH, M. N., LUTGENS, E., WANG, S., OLSON, E. N., SCHOBER, A. & WEBER, C. 2009. Delivery of microRNA-126 by apoptotic bodies induces CXCL12-dependent vascular protection. *Sci Signal,* 2**,** ra81.

ZHANG, C. & YANG, Y. 2012. Microparticles are the basic storage units for different proteins in platelet granules. *Blood*.

ZHANG, J., LI, S., LI, L., LI, M., GUO, C., YAO, J. & MI, S. 2015a. Exosome and exosomal microRNA: trafficking, sorting, and function. *Genomics Proteomics Bioinformatics,* 13**,** 17-24.

ZHANG, W., DENG, W., ZHOU, L., XU, Y., YANG, W., LIANG, X., WANG, Y., KULMAN, J. D., ZHANG, X. F. & LI, R. 2015b. Identification of a juxtamembrane mechanosensitive domain in the platelet mechanosensor glycoprotein Ib-IX complex. *Blood,* 125**,** 562-9.

ZHANG, Y., DA SILVA, J. R., REILLY, M., BILLHEIMER, J. T., ROTHBLAT, G. H. & RADER, D. J. 2005. Hepatic expression of scavenger receptor class B type I (SR-BI) is a positive regulator of macrophage reverse cholesterol transport in vivo. *J Clin Invest,* 115**,** 2870-4.

ZHANG, Y., LIU, D., CHEN, X., LI, J., LI, L., BIAN, Z., SUN, F., LU, J., YIN, Y., CAI, X., SUN, Q., WANG, K., BA, Y., WANG, Q., WANG, D., YANG, J., LIU, P., XU, T., YAN, Q., ZHANG, J., ZEN, K. & ZHANG, C. Y. 2010. Secreted monocytic miR-150 enhances targeted endothelial cell migration. *Mol Cell,* 39**,** 133-44.

ZHANG, Y. Y., ZHOU, X., JI, W. J., SHI, R., LU, R. Y., LI, J. L., YANG, G. H., LUO, T., ZHANG, J. Q., ZHAO, J. H., JIANG, T. M. & LI, Y. M. 2013. Decreased circulating microRNA-223 level predicts high on-treatment platelet reactivity in patients with troponin-negative non-ST elevation acute coronary syndrome. *J Thromb Thrombolysis,* 38**,** 65-72.

ZHANG, Z., QIN, Y. W., BREWER, G. & JING, Q. 2012. MicroRNA degradation and turnover: regulating the regulators. *Wiley Interdiscip Rev RNA,* 3**,** 593-600.

ZHENG, Q., PESKOE, S. B., RIBAS, J., RAFIQI, F., KUDROLLI, T., MEEKER, A. K., DE MARZO, A. M., PLATZ, E. A. & LUPOLD, S. E. 2014. Investigation of miR-21, miR-141, and miR-221 expression levels in prostate adenocarcinoma for associated risk of recurrence after radical prostatectomy. *Prostate,* 74**,** 1655-62.

ZHU, G. Z., MILLER, B. J., BOUCHEIX, C., RUBINSTEIN, E., LIU, C. C., HYNES, R. O., MYLES, D. G. & PRIMAKOFF, P. 2002. Residues SFQ (173-175) in the large extracellular loop of CD9 are required for gamete fusion. *Development,* 129**,** 1995-2002.

ZHUANG, G., MENG, C., GUO, X., CHERUKU, P. S., SHI, L., XU, H., LI, H., WANG, G., EVANS, A. R., SAFE, S., WU, C. & ZHOU, B. 2012. A novel regulator of macrophage

activation: miR-223 in obesity-associated adipose tissue inflammation. *Circulation,* 125**,** 2892-903.

ZIMMERMAN, G. A., ELSTAD, M. R., LORANT, D. E., MCLNTYRE, T. M., PRESCOTT, S. M., TOPHAM, M. K., WEYRICH, A. S. & WHATLEY, R. E. 1996. Platelet-activating factor (PAF): signalling and adhesion in cell-cell interactions. *Adv Exp Med Biol,* 416**,** 297-304.

ZLOTOGORSKI-HURVITZ, A., DAYAN, D., CHAUSHU, G., KORVALA, J., SALO, T., SORMUNEN, R. & VERED, M. 2015. Human saliva-derived exosomes: comparing methods of isolation. *J Histochem Cytochem,* 63**,** 181-9.

ZUCKER, W. H., SHERMER, R. W. & RG, M. A. 1974. Ultrastructural comparison of human platelets separated from blood by various means. *Am J Pathol,* 77**,** 255-67.